frontiers | Research Topics

Interactive effects of plant growth-promoting microbes and nanoparticles on the physiology, growth, and yield of crops

Edited by
Waheed Akram, Aqeel Ahmad and
Nasim Ahmad Yasin

Published in
Frontiers in Plant Science

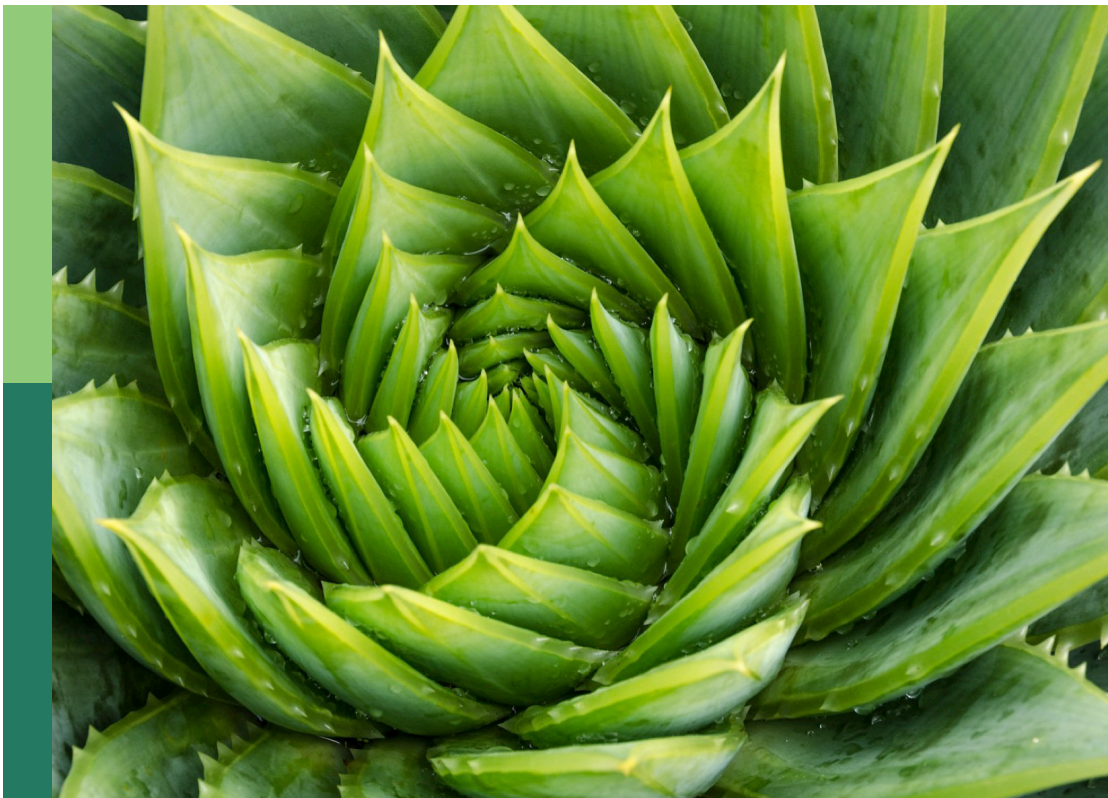

ISSN 1664-8714
ISBN 978-2-8325-4624-6
DOI 10.3389/978-2-8325-4624-6

About Frontiers

Frontiers is more than just an open access publisher of scholarly articles: it is a pioneering approach to the world of academia, radically improving the way scholarly research is managed. The grand vision of Frontiers is a world where all people have an equal opportunity to seek, share and generate knowledge. Frontiers provides immediate and permanent online open access to all its publications, but this alone is not enough to realize our grand goals.

Frontiers journal series

The Frontiers journal series is a multi-tier and interdisciplinary set of open-access, online journals, promising a paradigm shift from the current review, selection and dissemination processes in academic publishing. All Frontiers journals are driven by researchers for researchers; therefore, they constitute a service to the scholarly community. At the same time, the *Frontiers journal series* operates on a revolutionary invention, the tiered publishing system, initially addressing specific communities of scholars, and gradually climbing up to broader public understanding, thus serving the interests of the lay society, too.

Dedication to quality

Each Frontiers article is a landmark of the highest quality, thanks to genuinely collaborative interactions between authors and review editors, who include some of the world's best academicians. Research must be certified by peers before entering a stream of knowledge that may eventually reach the public - and shape society; therefore, Frontiers only applies the most rigorous and unbiased reviews. Frontiers revolutionizes research publishing by freely delivering the most outstanding research, evaluated with no bias from both the academic and social point of view. By applying the most advanced information technologies, Frontiers is catapulting scholarly publishing into a new generation.

What are Frontiers Research Topics?

Frontiers Research Topics are very popular trademarks of the *Frontiers journals series*: they are collections of at least ten articles, all centered on a particular subject. With their unique mix of varied contributions from Original Research to Review Articles, Frontiers Research Topics unify the most influential researchers, the latest key findings and historical advances in a hot research area.

Find out more on how to host your own Frontiers Research Topic or contribute to one as an author by contacting the Frontiers editorial office: frontiersin.org/about/contact

Interactive effects of plant growth-promoting microbes and nanoparticles on the physiology, growth, and yield of crops

Topic editors

Waheed Akram — University of the Punjab, Pakistan

Aqeel Ahmad — University of Florida, United States

Nasim Ahmad Yasin — University of the Punjab, Pakistan

Citation

Akram, W., Ahmad, A., Yasin, N. A., eds. (2024). *Interactive effects of plant growth-promoting microbes and nanoparticles on the physiology, growth, and yield of crops*. Lausanne: Frontiers Media SA. doi: 10.3389/978-2-8325-4624-6

Table of contents

frontiers | Frontiers in Plant Science

TYPE Editorial
PUBLISHED 07 March 2024
DOI 10.3389/fpls.2024.1338470

OPEN ACCESS

EDITED BY
Vijay Singh Meena,
CIMMYT-Borlaug Institute for South Asia (BISA), India

REVIEWED BY
Debasis Mitra,
Graphic Era University, India
Abdul Gafur,
SMF Corporate R&D Advisory Board, Indonesia

*CORRESPONDENCE
Nasim Ahmad Yasin
nasimhort@gmail.com

RECEIVED 14 November 2023
ACCEPTED 21 February 2024
PUBLISHED 07 March 2024

CITATION
Ahmad A, Akram W, Sardar R and Yasin NA (2024) Editorial: Interactive effects of plant growth-promoting microbes and nanoparticles on the physiology, growth, and yield of crops.
Front. Plant Sci. 15:1338470.
doi: 10.3389/fpls.2024.1338470

Editorial: Interactive effects of plant growth-promoting microbes and nanoparticles on the physiology, growth, and yield of crops

Aqeel Ahmad[1], Waheed Akram[2], Rehana Sardar[3] and Nasim Ahmad Yasin[4*]

[1]Institute of Geographic Sciences and Natural Resources Research / University of Chinese Academy of Sciences, CAS, Beijing, China, [2]Department of Plant Pathology, Faculty of Agricultural Sciences, University of the Punjab, Lahore, Pakistan, [3]Institute of Botany, University of the Punjab, Lahore, Pakistan, [4]RO-II Office, University of the Punjab, Lahore, Pakistan

KEYWORDS

PGPM, NPS, plant nutrition, plant growth, sustainable crop production

Editorial on the Research Topic
Interactive effects of plant growth-promoting microbes and nanoparticles on the physiology, growth, and yield of crops

Continuous demand of plant-based nutritious food from the ever-growing population has become an alarming issue throughout the world. Inorganic, organic and hybrid nanoparticles (NPs) having 1-100 nm size have enormous potential to improve crop yield and assure sustainability. Nanoparticles are essential for plant development and quality enhancement because they boost photosynthetic activity, improve metabolism, and increase nutritional content. Yield and quality of agricultural crops may be enhanced through the judicious application of nano techniques which increases effectiveness of inputs and reduces related losses. Nanotechnology assists in preserving stability of pathogen-free food items. Nanomaterials have been used to develop pesticides, fertilizers and other plant growth promoting products. An enormous quantity of various fertilizers is required for the improvement of soil fertility leading to higher crop yield. However, the recurrently applied higher quantity of fertilizers negatively affects soil health and fertility. A large quantity of conventional fertilizer persists in the rhizosphere or may leach down causing environmental contamination that injures the adjacent fauna and flora. Hence, the appropriate administration of fertilizer is a tricky task for the development of sustainable agriculture. Nano fertilizers not only mitigate nutrient deficiency but also release nutrients according to the needs of the crop. Therefore, higher fertilizer use efficiency by applying nano fertilizers enables farmers to obtain better crop yield without polluting the ecosystem.

Plant growth-promoting microbes (PGPM) may improve plant stress tolerance, fertilizer use efficiency and nutrient uptake potential of assisted plants. Such microbes live in plant tissues or within rhizospheric area and sustain plant growth by several mechanisms including enhancement of hormonal synthesis, phytostimulation,

augmentation of stress tolerance besides improvement of nutrients availability and uptake. Hence, application of PGPM should be examined to decrease the dependance on synthetic agrochemicals to enhance crop yield. *In vitro* studies, under controlled and ideal environments, have shown beneficial effects of PGPM inoculation on various crops. Nevertheless, further field experimentations especially under environmental extremes seems mandatory to evaluate the effects of plant microbe cross talk to advance growth and yield of inoculated plants.

Keeping in view the importance of nanoparticles and PGPM, the Guest Editors of the Research Topic made a call for research manuscripts through Frontiers in Plant Science. Guest Editors encouraged scientists to submit their manuscript regarding crucial aspects related to beneficial effects of PGPM and NPs on the physiology, growth, and yield of crop plants. It is expected that this Research Topic will be very productive to trigger a quest in researchers to find the dynamic potential of NPs and PGPM to increase plant growth. Research articles for this Research Topic come from various continents. Scientists applied numerous physiological, biochemical, molecular procedures to elucidate the interaction among NPs, PGPM and plants.

In this Research Topic 27 manuscripts were received. However only 10 manuscripts having the better quality were accepted for publication following peer-review. Adoko et al. found that PGPR-based bio stimulants combined with mineral fertilizer enhanced growth, yield and nutritional status of maize. Ahmad et al. reported that differentially expressed genes of *Cymbidium ensifolium*, *C. goeringii* and *C. sinense* were mainly related to bacterial secretion systems (*FLS2, CNGCs* and *EFR*) which adjust hypersensitive response, stomatal movement and defense induction. Ali et al. revealed that growth promoting *Bacillus* strain NMTD17 improves the activity of antioxidative enzymes and stress tolerance of rice plants under saline conditions. Mirza et al. demonstrated that application of bio-fabricated graphene oxide nanoparticles enhances growth and seed yield of *Vigna radiata*.

Sehar et al. found that combined application of *Serendipita indica* and phosphorus alleviate the arsenic stress in rice through genotype-dependent modulations. Microbes may enhance the medicinal value of associated plants. Zhang et al. observed the role of *Cercospora* inoculation on growth and active ingredients of *Polygonum hydropiper* sp. Sohail and Chen proposed a systematic approach on assessment of sustainable agriculture in climate change particularly in floods. Zhou et al. concluded that intercropping improved soil health, microbial community, plant growth and biomass production in tobacco. Salehi et al. concluded that manganese nanoparticles improved seed germination, photosynthetic activity, antioxidative activity and plant growth in *Artemisia annua.* Jalal et al. observed synergistic effects of nano-Zn and *B. subtilis* and *Pseudomonas fluorescens* in improving wheat plant growth and nutrition.

In general, the manuscripts selected for this Research Topic divulge the importance of interaction among NPs, PGPM and plants. However, further studies at the transcriptomics, metabolomics, proteomics and genomics level are required to identify and demonstrate beneficial and harmful interactions among NPs, PGPM and plants to continue sustainable crop production under normal and harsh environmental conditions. Conclusively, this Research Topic includes valuable research articles which enables scientists and community workers to acquire the basic information about NPs, PGPM and plant communication.

Author contributions

AA: Conceptualization, Writing – review & editing. WA: Conceptualization, Writing – original draft, Writing – review & editing. NY: Conceptualization, Writing – original draft, Writing – review & editing. RS: Validation, Writing – review & editing.

Acknowledgments

The Guest Editors would like to thank Editorial Board and Staff Members of the Frontiers in Plant Science, Authors and Reviewers for their positive contribution for the successful completion and publication of this Research Topic.

Conflict of interest

The authors declare that the research was conducted in the absence of any commercial or financial relationships that could be construed as a potential conflict of interest.

The author(s) declared that they were an editorial board member of Frontiers, at the time of submission. This had no impact on the peer review process and the final decision.

Publisher's note

frontiers | Frontiers in Plant Science

TYPE Original Research
PUBLISHED 25 August 2022
DOI 10.3389/fpls.2022.990785

OPEN ACCESS

EDITED BY
Aqeel Ahmad,
University of Florida, United States

REVIEWED BY
Sidra Sohail,
Pakistan Institute of Development Economics, Pakistan
Ifeanyichukwu Anthony Ogueji,
University of Ibadan, Nigeria
Muzammil Khurshid,
University of the Punjab, Pakistan

*CORRESPONDENCE
Shaoming Chen
chensm@gcu.edu.cn

SPECIALTY SECTION
This article was submitted to Plant Symbiotic Interactions, a section of the journal Frontiers in Plant Science

RECEIVED 10 July 2022
ACCEPTED 01 August 2022
PUBLISHED 25 August 2022

CITATION
Sohail MT and Chen S (2022) A systematic PLS-SEM approach on assessment of indigenous knowledge in adapting to floods; A way forward to sustainable agriculture. *Front. Plant Sci.* 13:990785. doi: 10.3389/fpls.2022.990785

A systematic PLS-SEM approach on assessment of indigenous knowledge in adapting to floods; A way forward to sustainable agriculture

Muhammad Tayyab Sohail[1,2] and Shaoming Chen[3]*

[1]School of Public Administration, Xiangtan University, Xiangtan, Hunan, China, [2]South Asia Research Center, School of Public Administration, Xiangtan University, Xiangtan, Hunan, China, [3]International Business School, Guangzhou City University of Technology, Guangzhou, China

The present study was conducted in one of the major agriculture areas to check farmers indigenous knowledge about the impacts of floods on their farming lives, food security, sustainable development, and risk assessment. In the current study, primary data was used to analyze the situation. A semi-structured questionnaire was distributed among farmers. We have collected a cross-sectional dataset and applied the PLS-SEM dual-stage hybrid model to test the proposed hypotheses and rank the social, economic, and technological factors according to their normalized importance. Results revealed that farmers' knowledge associated with adaption strategies, food security, risk assessment, and livelihood assets are the most significant predictors. Farmers need to have sufficient knowledge about floods, and it can help them to adopt proper measurements. A PLS-SEM dual-stage hybrid model was used to check the relationship among all variables, which showed a significant relationship among DV, IV, and control variables. PLS-SEM direct path analysis revealed that AS (b = −0.155; *p* 0.001), FS (b = 0.343; *p* 0.001), LA (b = 0.273; *p* 0.001), RA (b = 0.147; *p* 0.006), and for FKF have statistically significant values of beta, while SD (b = −0.079NS) is not significant. These results offer support to hypotheses H1 through H4 and H5 being rejected. On the other hand, age does not have any relationship with farmers' knowledge of floods. Our study results have important policy suggestions for governments and other stakeholders to consider in order to make useful policies for the ecosystem. The study will aid in the implementation of effective monitoring and public policies to promote integrated and sustainable development, as well as how to minimize the impacts of floods on farmers' lives and save the ecosystem and food.

KEYWORDS

farmer, PLS-SEM, climate change, floods, South Punjab, Pakistan

Introduction

In recent decades, more people have become aware of the effects of climate change on the entire world. Climate change is a worldwide problem that would disproportionately affect low-income countries (Rosenzweig et al., 2001; Adger et al., 2003; Thornton et al., 2014). Due to climate change, natural disasters like floods, droughts, tsunamis, storms, and tornadoes commonly occur (Abid et al., 2016; Khan et al., 2020). Patt and Schröter (2008) stated that this phenomenon (climate change) may result in shifting climatic zones, altered rainfall patterns, and rising sea levels. The frequency of floods that are mostly caused by excessive rainfall or occur from the unintended release of water storage, such as dams, snow, or tides, is one of the most often observed effects of climate change (Kavvada and Held, 2018; Samu and Kentel, 2018). Due to low incomes and limited adaptations, impoverished agricultural and rural residents in developing countries are extremely concerned about climate change (Thornton et al., 2014; Sohail et al., 2014b; Sohail et al., 2019b). Emerging economies are more vulnerable to climate hazards than industrialized ones, and Pakistan is one of the areas most affected by climate change (Ali and Erenstein, 2017). Floods and droughts are the most prevalent natural disasters that seriously endanger humanity's economic and social well-being, especially in developing nations with little capacity for adaptation and vulnerable populations (Strömberg, 2007; Muhammad et al., 2014; Shahab et al., 2016; Mahfooz et al., 2017, 2019, 2020; Rasool et al., 2017; Lu and Sohail, 2022; Mustafa et al., 2022a). High rates of urbanization in flood-prone locations, a huge number of sub-customary buildings, changes in land use, an increase in population density, and especially global warming, have all had a substantial impact on flooding. The intensification of extreme weather events, which also contribute to global warming and present another barrier to sustainable growth, will result in food shortages and a decline in poverty. Land use, particularly management, urban planning, and the development of flood control technologies, has a substantial impact on flood damage (Luino et al., 2018). Implementing acceptable and effective adaptation measures (such as disaster risk reduction measures) into management plans and strategies can help to minimize the impacts of natural disasters (Thomalla et al., 2006; Begum et al., 2014). Pakistan is one of the countries most susceptible to natural calamities. One of the most important environmental problems caused by global climate change is flooding, as Pakistan has experienced over the past 6–7 years (Webster, 2011; Azam and Mariani, 2012; Surminski and Oramas-Dorta, 2014; Yen et al., 2017, 2021; Sohail et al., 2020; Zinda et al., 2021; Wang and Sohail, 2022). Natural disasters, such as floods, droughts, scorching temperatures, and high rates of pests and disease, have been more frequent and severe in the United States over the previous 10 years (Smit and Skinner, 2002). In 2010, 2011, 2012, and 2015, Pakistan was ranked seventh for climate change and the hazards it poses, and sixteenth for flood vulnerability (Kreft et al., 2013; Abid et al., 2016; Khan et al., 2020). The deterioration of these weather patterns will hasten global warming and introduce fresh barriers to sustainable development, increasing poverty and causing a food shortage (Sohail et al., 2017; Luino et al., 2018; Yat et al., 2018; Yasar et al., 2019; Sohail et al., 2021a; Sohail et al., 2021a; Sohail et al., 2021a). It is envisaged that developing countries can minimize natural hazards and dangers connected with extreme climate change by incorporating appropriate and effective adaptation measures (including disaster risk reduction measures) into their management plans and strategies (Hoanh et al., 2006; Thomalla et al., 2006; Atta-ur-Rahman et al., 2010; Azam and Mariani, 2012; Begum et al., 2014; Jiang et al., 2021). In the previous 10 years, the freuqency and intensity of natural disasters in the nation have increased. Examples include floods, droughts, painful heat, and high rates of pests and diseases (Smit and Skinner, 2002). According to Abid et al. (2016) and Khan et al. (2020), Pakistan was seventh among the countries most vulnerable to the risks associated with climate change, while it was ranked seventeenth most vulnerable to floods in 2010, 2011, 2012, and 2015, respectively (Kreft et al., 2013). These analyses make a strong argument for the creation of a specialized, market-based flood insurance policy as a climate change adaptation measure. It is crucial to research the factors that affect farmers' willingness to pay for flood insurance before starting a program in order to reduce their flood risk, regardless of whether they accept it. Along with risk attitudes and subjective estimates of the risk of flooding, they also include social and geographic factors. Farmers' flood risk behaviors, in particular their risk perception and attitude, may be crucial when considering willingness to pay for flood insurance. Their decisions about agricultural productivity, investments, and farm management may also be impacted by this (Champonnois and Erdlenbruch, 2021). At the moment, it's thought that managing flood risk necessitates using subjective risk assessment, including risk perception (Lechowska, 2018). The farmer's risk aversion, however, affects their economic behavior and the coping mechanisms they use to decrease the effects of numerous disaster-related threats (Saqib et al., 2016; Zhao et al., 2019, 2022a,b; Sohail et al., 2021b,d). In this study, the influence of various factors on farmers' perceptions of floods and their potential consequences on their farming practices were assessed. Floods won't have much of an impact on farmers' regular activities provided they have the equipment and knowledge to handle such disasters. Based on the literature that is already available, the following questions have been raised: Global warming-related over-melting of the Karakoram glacier is expected to rise by 50% in the first half of the century before falling by 40% by the end of the century (Rees and Collins, 2006). There is significant geographical variation in the amount of precipitation and air temperature along the Indus basin tributaries that flow out of Punjab, Pakistan (Saqib et al., 2016). These spatial and temporal variations in temperature and

TABLE 1 Flood in Pakistan (1950–2019).

Sr. No.	Period	Floods (Numbers)	Economics (Loss the US $)	Population (Affected)	Deaths (Numbers)
1	2010–2019	30	18113000	36495066	4,713
2	2000–2009	33	706148	9574150	2,265
3	1990–1999	14	1092230	18148606	4,180
4	1980–1989	7	1367000	1304900	519
5	1970–1979	5	1166500	13637200	2,066
6	1960–1969	2	3300	224427	32
7	1950–1959	6	1719000	36954	3,691

Khan et al. (2021).

precipitation have a direct impact on the hydrological cycles and climatic extremes in the area. Floods are the worst of all-natural disasters that hurt humans; they can cause a large number of fatalities and put populations at risk of economic and social loss (Ali et al., 2013). Data from the past shows that floods in Pakistan have increased in frequency, size, and duration during the past few decades. The flood history of Pakistan from 1950 to 2019 is presented in **Table 1**. However, the floods that hit Pakistan in 2010, 2011, 2012, and 2014 are typical examples that significantly impacted both the GDP and the lives of the populace (Mustafa and Wescoat, 1997; Abid et al., 2016). Future forecasts of potentially catastrophic events like earthquakes, floods, and droughts are important to estimate the losses caused by natural disasters like earthquakes. In this study, we examined the impending floods in Pakistan and their consequences on GDP, impacted populations, and urban damage. A detailed literature review was conducted to find out more about Pakistan's vulnerability to floods and previous flood disasters. To assess the potential harm that flooding could cause, look into the prospective effects on GDP, and illustrate the long-term effects, various flood prevention measures were used based on the literature research. These are some main research questions on the basis of literature. What are the influences of farmers' knowledge about floods to minimize the impacts of natural disasters (floods) on their daily lives? What is the stabilized importance of adaptation strategies against floods in South Punjab, Pakistan? Does gender play a moderating role in farmers' knowledge and adaptation strategies against floods? The main purposes of this study are (1) to analyze the influences of farmers' knowledge about floods to minimize the impacts of farmers on their daily lives and food security livelihood assets; (2) to determine the possible causes of floods and estimate future flood-related risks in the country; (3) Farmers' views about floods and adaption strategies against them, and (4) How can we minimize the impacts of floods on farmers' lives and safe ecosystems and foods?

To expand, preserve self-sufficiency, and guarantee access to enough food, the agricultural sector needs to implement effective climate change adaptation measures, particularly in the wake of natural disasters like floods (Ferdushi et al., 2019). Sharing information/knowledge and understanding about adaptation is one of these and is crucial for boosting the agricultural sector's resilience in Bangladesh since it will help protect farmers' livelihoods and agricultural sustainability (Budhathoki et al., 2020). In this regard, smallholder farmers who are already feeling the effects of climate change have begun to apply a range of agricultural approaches (Alam et al., 2017; Manoj, 2017). The opinions, knowledge, and awareness of climate change among farmers are necessary for adaptation strategies. Therefore, farmers need to have a thorough awareness of climate change to use the most effective adaptation strategies and methods (Somda et al., 2017). One of the best and most important risk management techniques for natural catastrophes is the employment of dependable strategies. It has also been suggested as one of the adaptation strategies for climate change (Goodwin and Smith, 1995; Goodwin and Mahul, 2004). Farmers that are aware of natural disasters can utilize good management to prevent them (Di Falco et al., 2014; Jian et al., 2021; Sohail et al., 2021a, Sohail et al., 2022a; Lan et al., 2022; Li et al., 2022a,b). Over the years, crop insurance has been employed in numerous ways and for numerous purposes in numerous countries, with variable degrees of success (Vandeveer, 2001; Enjolras et al., 2012; Parvin et al., 2016; Mustafa et al., 2021). Food security depends on agriculture and farmers managing natural disasters effectively and using the right techniques to minimize their effects on food production (Yang et al., 2015). Due to the increased frequency of natural disasters like droughts and flooding, global warming harms agricultural production (Gong et al., 2003; Sun et al., 2005; Zhao et al., 2009; Zhang et al., 2011). Due to the climate, some farmers, particularly smallholder farmers, are vulnerable and lose their livelihoods (Sen, 1981; Valdivia et al., 2010). Climate change exacerbates global inequality because those most affected are also the least to blame for it (Barnett, 2006; Roberts and Parks, 2007). Vulnerable households employ their limited resources to deal with a changing range of stressors, such as social, economic, political, and environmental stress (Mortimore and Adams, 2001; Sohail et al., 2014a; Sohail et al., 2015; Sohail et al., 2019a; Liu N. et al., 2022; Liu Y. et al., 2022; Sohail et al., 2022a; Sohail et al., 2022a). It is believed that natural disasters are mostly to blame for the recent increases in undernourishment and food insecurity around the world, particularly in developing countries where farmers' livelihoods are more exposed to and vulnerable to calamities brought on by climate change. Furthermore, it is widely established that natural catastrophes reduce smallholder farmers' resistance to threats, shocks, and pressures while increasing the vulnerability of their livelihoods. Despite being a worry on a global scale, the implications of human-caused climate change vary depending on the location, system, family, and community. Because of this, the susceptibility of each object varies (Adger and Kelly, 1999;

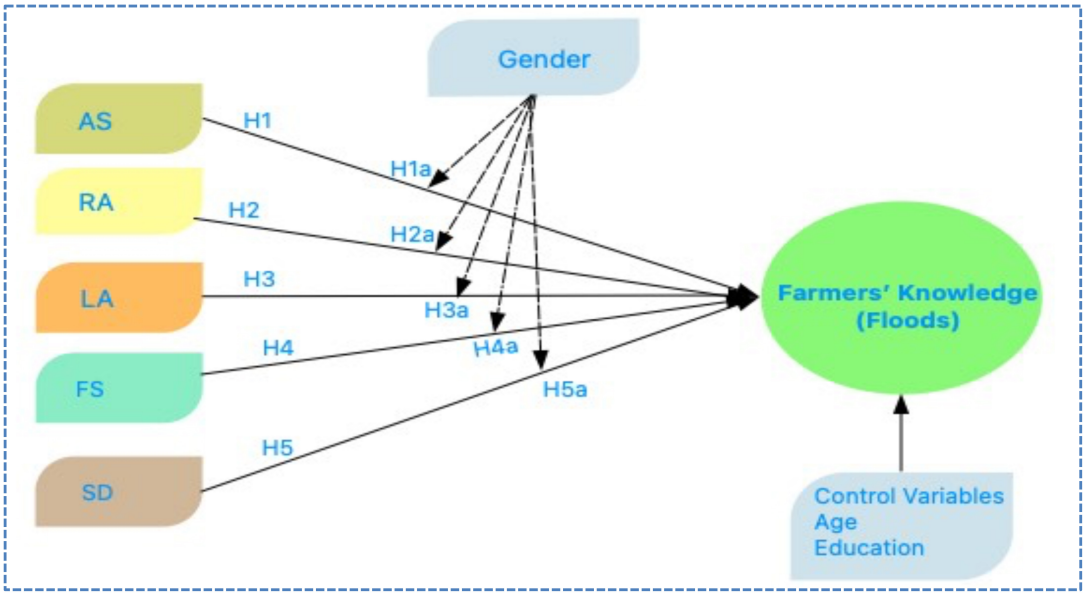

FIGURE 1
Research model.

Adger et al., 2004, 2006; Zahid and Khurshid, 2018; Zahid et al., 2022a,b). This has led some researchers to advocate using local assessments to gauge a region's vulnerability to climate change (Deressa et al., 2009; Below et al., 2012). Understanding the vulnerability of rural households' livelihoods is essential to establishing adaptation strategies and practical solutions/policies for decreasing climate-related risks and strengthening their resilience, particularly in countries that are heavily dependent on agriculture. By encouraging landowners to invest in long-term soil remediation, land tenure rights are thought to improve sustainable natural resource management and ensure the livelihoods of nearby households (Jakobsen et al., 2007). This investigation led us to develop the following research proposal: H1: Adaption strategies (AS) against floods are positively associated with farmers' knowledge of floods. H2: The Risk Assessment (RA) against floods is positively associated with farmers' knowledge of floods. H3: Livelihood Assets (LA) of farmers (which help) against floods are positively associated with the farmer's knowledge of floods. H4: Impacts of floods on food production. Food security (FS) against floods is positively associated with farmers' knowledge (floods). H5: Floods' impacts on the sustainable development (SD) of a specific area are positively associated with farmers' knowledge (floods). The explanatory variables are linked by age, gender, and educational attainment as significant modiators (Mustafa et al., 2022a,b,c). Men and women approach decision-making with very diverse perspectives on the surrounding environment. There are numerous ways in which the world appears extremely different when viewed through the eyes of a man as opposed to a woman. According to Pakistani studies (Mustafa et al., 2022d), environmental knowledge has a significant impact on men's intentions but has a minimal effect on women's. Mustafa, Tengyue, Jamil, et al. argue that there are differences in the way that the relationships between different factors hold across sexes (2022e). Because of the observed pattern of gender differences, we can predict that male and female farmers will have quite different preferences for adapting to their environment. As a result, it is assumed there is a strong relationship between farmers' knowledge of AS, RA, LA, FS, and SD (H1a-H5a), all of which are strongly affected by their gender (floods) **Figure 1**.

Materials and methods

Study area

Punjab is the most populated area with five rivers. Most of the people from this province work in farming. The Khyber Pukhtunkhwa Province and the federal capital region of Islamabad are located north of Punjab. The Indian Punjab and Rajasthan are to the south-east, Sindh is to the south-west, Baluchistan and the Federally Administered Tribal Areas are to the west, and Azad Kashmir is to the north-east (FATA). Although the province is predominantly flat, the extreme north and south-west contain some hilly areas. In addition, Cholistan is a desert belt in the south-eastern region, and the Potohar plateau is a plateau adjacent to the mountains. This province is traversed by all five of the country's major rivers: the Indus, Jhelum, Chenab, and Ravi, in addition to the Sutlej. They originate in the Himalayas and travel from north to south.

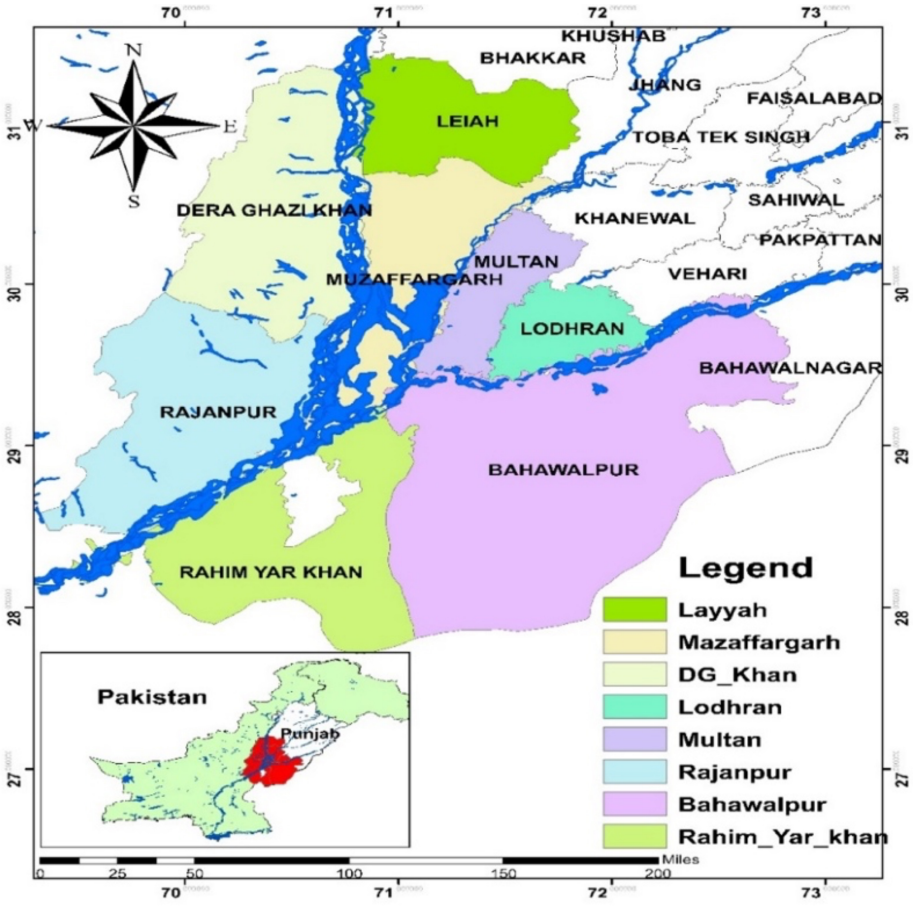

FIGURE 2
Study area.

They are primitive, and during monsoon rains in the summer, the water level rises, causing occasional flooding. Punjab is the province with the largest population in Pakistan. As of the 1998 Census, the province had a population of 7,258,500 people. It includes Lahore, Faisalabad, Rawalpindi, Multan, and Gujranwala, which are some of the most populous cities in the country (Figure 2).

Data sources and data preparation

This study was carried out in Punjab province, based on farmers' experiences with flooding, climate change, and adaption measures (Sohail et al., 2021a, 2022a). This area of Pakistan is primarily agricultural, making it particularly susceptible to natural disasters, including riverbank erosion, floods, and droughts. Floods are mostly caused by the Indus rivers, making this area highly vulnerable to natural disasters. A systematic questionnaire was used to conduct in-depth interviews with farm households that had experienced flooding to gather primary data (Figure 2). To analyze the relationship between farmers' knowledge about floods to minimize their impacts on their daily lives and to determine the possible causes of floods; estimate future flood-related risks in the country; famers' views about floods and adaption strategies against them; and how to minimize impacts of floods on farmers' lives and safe ecosystems and foods. Eight districts in the Punjab province were selected based on the degree of previous flood damage, flooding history, vulnerability, and agricultural significance. A semi-structured questionnaire adapted from a previous study was used to gather information from eight districts in South Punjab, Pakistan (Sohail, 2013; Sohail et al., 2013; Fahad and Wang, 2020; Sohail et al., 2022a). To gather information from farmers in South Punjab, Pakistan. We informed farmers about climate change as well as information about the study's objective. Data was entered into SPSS 25 and Smart-PLS for further analysis after data collection. The information was examined using statistical techniques. Because PLS-SEM is one of the most efficient methods for predicting outcomes, PLS-SEM was used to analyze the data in our study to check the relationship between

DV and IV variables. PLS-SEM is the method that is most often recommended for predicting and evaluating explained variables in order to account for the most possible differences.

Results and discussion

For this study, 1,200 farmers from Pakistan's Punjab Province were interviewed. **Table 1** includes numerous internal variables that may influence a farmer's response and adaptability, including personal characteristics, unique conditions, and farming practices (Bryan et al., 2013). Deressa et al. (2009) found that a farmer's awareness is positively associated with their farming background and education. Existing research indicates that farmers' perceptions of climate change and its implications are influenced by the features of farmland and farmers' demographic assets (Singh et al., 2017). Previous research supports the importance of farmers' socioeconomic and demographic characteristics in the implementation of climate change adaptation techniques on their farms.

Figure 3 elaborates the main reasons for the floods in South Punjab, Pakistan. Without a doubt, the effects of climate change have become more apparent over the last few decades (Patt and Schröter, 2008). The main indicators which were encompassed to check perception were lack of proper management, lack of dams, lack of policy implications, climate change, heavy rainfall, deforestation, inadequate maintenance of drainage facilities, and overflowing of rivers and settlements in flood plains. According to farmer responses about a lack of proper management in Layyah 80%, Muzaffargarh 85%, DG Khan 75%, Lodhran 65%, Multan 50%, Rajanpur 64%, Bahawalpur 53%, and Rahim_Yar_Khan 76%, respectively, flooding could be the main threat to farmers in that area due to the Indus River provided sufficient evidence of the impacts of temperature stress and floods on farmers' lives (Maheen and Hoban, 2017). Farmers in Layyah responded 71%, Muzaffargarh 88%, DG Khan 90%, Lodhran 69%, Multan 55%, Rajanpur 83%, Bahawalpur 89%, and Rahim_Yar_Khan 90% to a lack of policy implications. Both short-term and long-term actions are essential to effectively managing the losses caused by floods. When undertaking rational decision-and risk analysis regarding catastrophic events, the gathering of information is a key stage. Making more informed decisions can be aided by the capacity to draw from a sizable body of knowledge from prior decisions and safety measures put in place in disaster zones. With a solid conceptual framework, it can be simpler to understand perspectives on fair procedures and results. A standardized model makes data collection simpler and can aid in the development of a knowledge base that various model instances can use. This article explores the trends in national flood control as well as flooding in the major basins. Flooding in the Indus Basin is mostly brought on by monsoon precipitation, whereas flooding in the Kharan Basin and Makran Coastal Area is brought on by Mediterranean waves and cyclones that occur over the Arabian Sea. Floods in the Indus Basin have caused substantial financial harm. Since Pakistan's founding in 1947, the government has allotted a sizeable percentage of its budget toward relief efforts and flood relief projects. Several provincial and federal laws, regulations, agreements, and treaties influence the nation's flood policy. The institutional setting for flood hazard and disaster management has evolved. However, data does not show a material drop in the flood-to-damage ratio. Examining and maximizing the interactions between structural and non-structural measures is necessary for more effective flood management. All rivers in Pakistan's transboundary rivers flow *via* India, and upstream activities mostly determine the shape of a flood wave's shape. Layyah, Muzaffargarh, DG Khan, Lodhran, Multan, Rajanpur, Bahawalpur, and Rahim Yar Khan all received 100% farmer feedback on the lack of a dam. Farmers in Layyah, Muzaffargarh, DG Khan, Lodhran, Multan, Rajanpur, Bahawalpur, and Rahim Yar Khan are concerned about climate change. Recent environmental degradation in Pakistan caused floods in 2010 and 2011. In the future, more disasters are expected. Changing environmental conditions like urbanization, population increase, etc., threaten Pakistan's ecosystem and biodiversity. According to the Federal Bureau of Statistics, the forest area declined by 3% between 2000 and 2005. Overgrazing, farming methods, and rural wood consumption create this. Northern Pakistan's rising temperatures are due to deforestation. In the past 50 years, both the risky area's population and human settlement vulnerability have increased. Human choices and investments enhance catastrophic losses (Benson and Clay, 2004). According to Jamshed et al. (2019), Pakistan's socioeconomic basis has been undermined by flooding. The country is one of the most flood-prone in the world, with frequency and intensity rising (Hirabayashi et al., 2013). The 2010 floods alone inundated 2.1 million acres of standing crops and harmed nearly 400,000 animals. Khyber-Pakhtunkhwa (KP) remains highly vulnerable to flooding and its catastrophic impacts. Pakistan is a growing nation attempting to advance in many areas, but a large portion of the population, especially farmers in rural disaster zones, lives in poor conditions (Fahad et al., 2020). In 2010, 2011, and 2014, Pakistan witnessed devastating floods in several places that devastated forestry, cattle, fisheries, infrastructure, fertilizers, animal barns, and more than 250,000 farmhouses on 1 million acres of cultivated land (NDMA, 2014). Crop failure, low yields, and livestock fatalities can result from these disasters (Harvey, 2014).

The present study also included adaptation techniques against floods; these parameters were: creating runoff pools; stopping cutting trees; planting trees; buying insurance; canal cleaning; and information before floods (**Figure 4**). It is very common for many farmers to choose different techniques to deal with livelihood risks (Kuang et al., 2020). It is reported

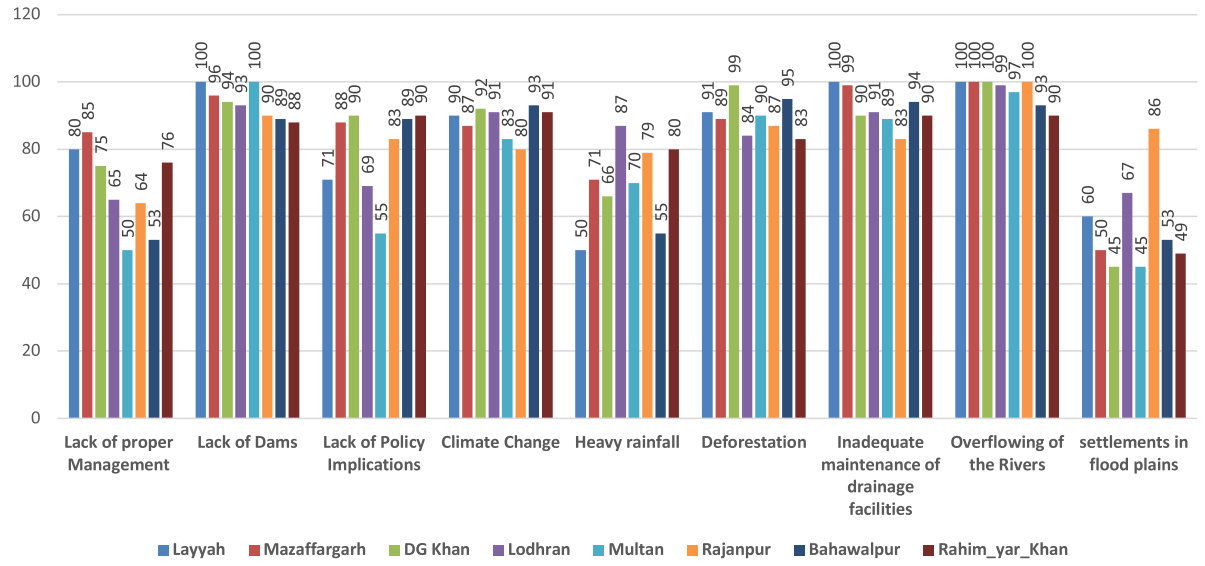

FIGURE 3
Main reasons for overflooding in South Punjab Pakistan (%).

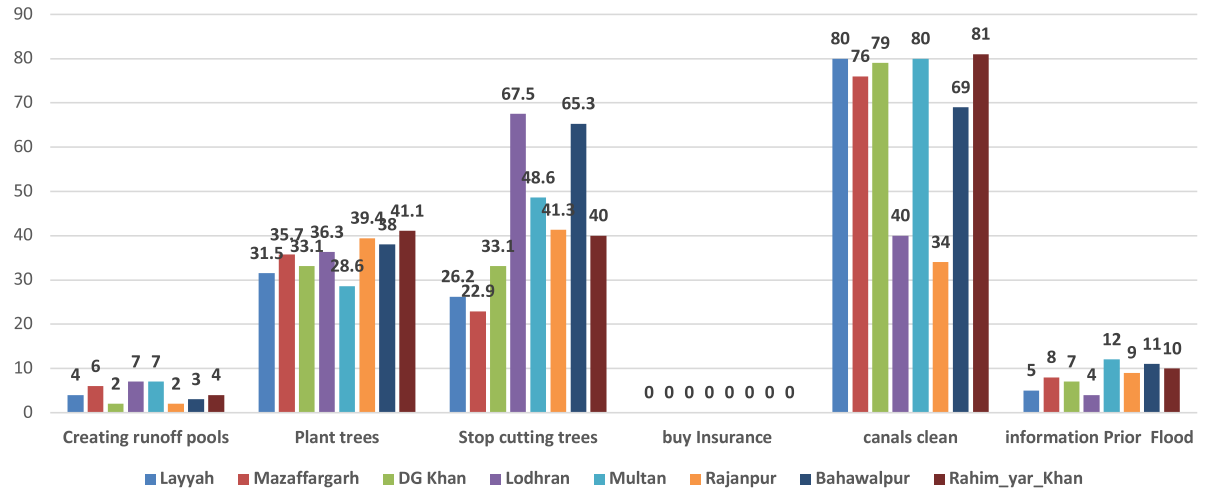

FIGURE 4
Adaption strategies/measures (%) against floods by farmers in South Punjab Pakistan.

that similar kinds of adaptation measures like changing planting trees, cleaning canals with the government, and other techniques are adopted by farmers in Pakistan (Gorst et al., 2015). According to research, small farmers are more likely than large farms to have problems responding to climate change (Jamshidi et al., 2019). Additionally, the effect of climatic threats on farmers' income, family food, and security was even more pronounced for farmers with limited access to resources (Shukla et al., 2019). Researchers discovered that the first step in responding to climate change was to modify how people thought about it in another study conducted in Africa (Trinh et al., 2018). Farmers must be aware of the threats posed by the climate and how to adapt to them. They can do this to boost agricultural productivity and reduce risk (Fahad and Wang, 2020). The physical, natural, and social resources of farmers aid in the adoption of adaptation techniques (Kuang et al., 2020). The percentage of farmers who claimed they wished to create runoff pools was 4% in Layyah, 6% in Muzaffargarh, 2% in DG Khan, 93% in Lodhran, 100% in Multan, 90% in Rajanpur, 89.9% in Bahawalpur, and 88% in Rahim-Yar-Khan. City life can be severely disrupted by runoff flooding. As a result, runoff flooding should not be a problem for a city. The study of ecology

TABLE 2 Demographic information of participants (%).

		Layyah	Muzaffargarh	DG Khan	Lodhran	Multan	Rajanpur	Bahawalpur	Rahim_yar_Khan
Gender	Male	85.4	81.4	73.8	75	77.1	71.6	74	72.2
	Female	14.6	18.6	26.2	25	22.9	28.4	26	22.8
Age (Years)	18–25	17.7	13.6	13.8	15	19.3	23.2	22.7	20.6
	26–35	37.7	20.7	37.2	33.1	32.9	34.8	33.3	26.7
	36–45	28.5	43.6	26.2	40.6	32.1	28.4	32.7	41.1
	Above 45	16.2	22.1	22.8	11.3	15.7	13.5	11.3	11.7
Education (Years)	Primary School	31.1	23.6	25.5	45.6	52.1	49	39.3	30.6
	High School	43.1	50	54.5	40.6	39.3	41.3	34.7	38.9
	College Level	14.6	15.7	11	9.4	5	7.7	18.7	21.1
	University level	9.2	10.7	9	4.4	3.6	1.9	7.3	9.4
Farming present land (Years)	1–5	26.2	35	46.2	45	53.6	49	54	61.7
	6–10	50	32.9	28.3	31.9	20.7	36.1	28.7	28.9
	11–15	10	21.4	18.6	15.6	22.1	9	12.7	5.6
	16-above	13.8	10.7	6.9	7.5	3.6	5.8	4.7	3.9
Plowing per year	Once	16.9	3.6	4.1	6.9	8.6	5.8	8	5
	Twice	70	78.6	80.7	61.3	63.6	56.8	45.3	45
	Three-more	31.1	17.9	15.2	31.9	27.9	37.4	46.7	50

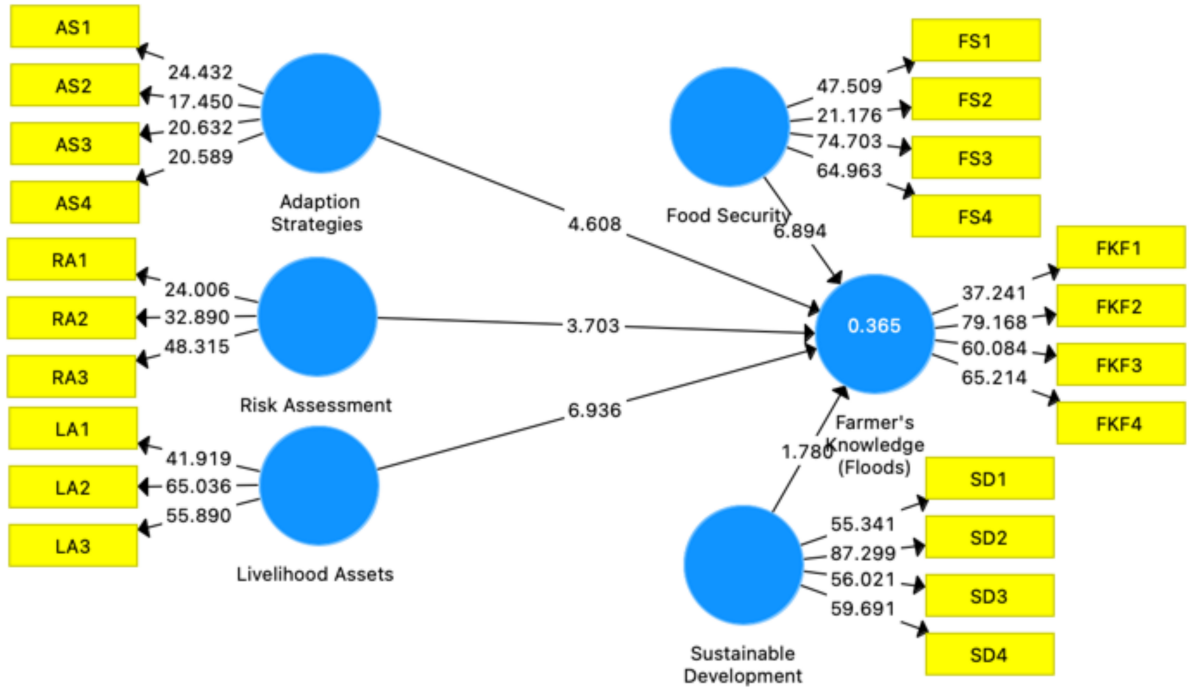

FIGURE 5
Measurement model.

gave rise to the concept of resilience. A system's resilience is its capacity to handle external changes while maintaining its identity, structure, and functions (Holling, 1973). A system that has resilience can adjust to stress and become less vulnerable. The socio-ecological system is utilized in conjunction with the emerging concept of ecological resilience as a comprehensive

human-in-nature perspective (Berkes and Folke, 1998). Dam failure disasters are a major concern around the world, especially in poorer nations where dam safety hasn't received much attention (WB, 1990; Dam, 2011). Numerous organizations from around the world are looking for tools and strategies to improve the situation, such as increased data collection, performance measurement, and rankings, as a result of the development of water infrastructure in developing countries and the deterioration and poor management of older infrastructure (Berg). (Bryan et al., 2009). 31.5 percent of farmers in Layyah said they would plant trees; 35.7 percent in Muzaffargarh; 33.1 percent in DG Khan; 28.6 percent in Lodhran; 39.4 percent in Multan; 41.1 percent in Rajanpur; and 41.1 percent in Rahim-Yar-Khan. There is some evidence that, at least occasionally, clearing a landscape of trees increases the likelihood of flooding (Bruijnzeel, 1990, 2004). According to the postulated process, less vegetation is thought to increase runoff because less rainfall is captured and less water evaporates from the tree canopy. This makes it more difficult for water to seep into the soil, which is associated with a decrease in the hydraulic conductivity (infiltration rate) of soils (Clark et al., 2021). So, the idea that the loss of natural habitat increases the danger and severity of catastrophic floods, as well as the harm they bring to people and their property, has arisen as a result of the rapid rate at which forests are currently being chopped down (Achard et al., 2002; Laurance, 2004; Clark et al., 2021). According to what farmers in Layyah, Muzaffargarh, DG Khan, Lodhran, Bahawalpur, and Rahim Yar Khan said regarding not cutting down trees, 26.2 percent, 22.9 percent, 33.1 percent, 33.1 percent, 67.5 percent, 48.6 percent, 41.3 percent, 65.5 percent, and 40 percent, respectively, said they would refrain from doing so. According to farmer opinions on purchasing insurance against natural catastrophes, 0% of farmers in Layyah, 0% in Muzaffargarh, 0% in DG Khan, 0% in Lodhran, 0% in Multan, 0% in Rajanpur, 0% in Bahawalpur, and 0% in Rahim-Yar-Khan purchased insurance. One of the most significant methods of risk transmission is insurance. By eliminating or lowering the financial risks, it can assist in managing the flood risk before it occurs (Surminski and Oramas-Dorta, 2013). Although this kind of policy is uncommon in underdeveloped nations, many industrialized nations use flood insurance as a non-structural method of dealing with flooding (Champonnois and Erdlenbruch, 2021). Even if structural adjustments can prevent actual property damage and fatalities, flood insurance can significantly reduce economic losses, especially in low-income nations that are prone to floods (Aliagha et al., 2014). People have observed that small and medium-sized farmers have had an extremely difficult time recovering the money they lost due to the floods (Wedawatta and Ingirige, 2012). Small farmers in Bangladesh may therefore find flood insurance to be a wise investment because it enables them to adapt to climate change by covering insured losses in the event of a flood disaster. According to Hossain et al. (2019), climate-related floods, heavy rain, drought, cyclones, and storms have a severe impact on agricultural output as well as on buildings, dams, and other architectural structures in underdeveloped developing nations. The impact on rural income and food security is significant. As a result, the poorest nations in South and Southeast Asia will be severely harmed (Vinke et al., 2017). Extreme weather events have increased in frequency and severity during the past few decades (Hossain et al., 2019). One of the most dangerous natural calamities that individuals might experience is flooding. They might result in numerous fatalities as well as social and economic issues (Ali et al., 2013; Mondal et al., 2020).

TABLE 3 Validity and reliability analysis.

Variables	Items	Loadings	VIF	T Statistics	α	CR	AVE
Adaption Strategies	AS1	0.778***	1.511	24.354	0.740	0.753	0.555
	AS2	0.721***	1.555	17.598			
	AS3	0.743***	1.520	20.741			
	AS4	0.736***	1.511	21.012			
Risk Assessment	RA1	0.749***	1.315	24.599	0.880	0.833	0.736
	RA2	0.803***	1.530	32.982			
	RA3	0.852***	1.511	48.756			
Food Security	FS1	0.830***	1.726	46.442	0.847	0.874	0.686
	FS2	0.696***	1.479	21.405			
	FS3	0.891***	2.873	74.845			
	FS4	0.882***	2.897	64.785			
Livelihood Assets	LA1	0.846***	1.844	41.425	0.829	0.831	0745
	LA2	0.880***	2.092	65.747			
	LA3	0.863***	1.826	56.130			
Sustainable Development	SD1	0.854**	2.285	55.681	0.725	0.743	0.644
	SD2	0.892**	2.538	88.514			
	SD3	0.857**	2.380	56.166			
	SD4	0.868**	2.438	58.923			
Farmer's Knowledge (Floods)	FKF1	0.811***	1.870	37.581	0.891	0.901	0.753
	FKF2	0.885***	2.616	81.021			
	FKF3	0.866***	2.300	59.459			
	FKF4	0.869***	2.372	66.316			

$\alpha > 0.7$; CR > 0.7; AVE > 0.5; VIF < 5; ***Significant at $p < 0.001$.

PLS-SEM and multivariate assumptions

One of the most effective methods for predicting outcomes and explanatory variables is PLS-SEM to examine relationships between variables (Hair et al., 2020). PLS-SEM generates more accurate results with smaller sample sizes. Internal and external processing of every model is possible simultaneously.

TABLE 4 Fornell–Larcker criterion.

	STDEV	Mean	AS	FKF	FS	LA	RA	SD
AS	0.024	0.551	**0.745**					
FKF	0.019	0,735	0.341	**0.858**				
FS	0.016	0.685	0.225	0.436	**0.828**			
LA	0.019	0.744	0.313	0.473	0.297	**0.863**		
RA	0.019	0.642	0.366	0.419	0.347	0.446	**0.803**	
SD	0.015	0.752	0.332	0.324	0.660	0.320	0.380	**0.868**

Bold diagonal values are the square root of AVE.
AS, adaption strategies; FKF, farmer's knowledge (floods); FS, food security; LA, livelihood Assets; RA, risk assessment; SD, sustainable development: STDEV, standard deviation.

Complex route models can be studied using this data collection (Hair et al., 2021; Mustafa and Wen, 2022; Mustafa et al., 2022e). The non-linear account interactions in the model necessitate a two-stage analysis. A PLS-based route modeling method is verified twice to ensure accuracy and dependability. Analyze the validity, reliability, and convergent validity of a structural model before developing an inner model or link between latent components. According to academics, multivariate assumptions need to be verified before an investigation (Mustafa and Wen, 2022; Mustafa et al., 2022e). Data assumptions include linearity, multicollinearity, and homoscedasticity. A Kolmogorov-Smirnov analysis was used to determine whether the data set was normal. There are both linear and non-linear interactions between the explanatory variables and the exploratory variables. Finally, we examined the VIF of the model for collinearity. In **Table 2**, all variables have VIF values under 5. When VIF is less than 5, according to them, dataset collinearity isn't a concern.

Convergent and discriminant validity should be examined when evaluating measurement models. To determine if the concept indicators accurately assessed the research variables, we evaluated the instrument's dependability using item loading and Cronbach's alpha. The average variance extracted (AVE) and composite reliability (CR) show how much the hidden construct offsets indicator variance. The reliability of each item is assessed using factor loadings on linked structures (**Figure 3** and **Table 2**). For a component to be deemed significant, its outer loading must be at least 0.6 (Hair et al., 2020). To boost confidence, Cronbach's alpha should be higher than or close to 0.7 for all conditions. According to Werts et al. (1974), this improves reliability. Composite reliability (CR), as well as Cronbach's alpha, were measured. The conventional method was replaced by this (Werts et al., 1974). Strong dependability ratings (>0.7) support these conclusions, and convergent validity estimates above 0.50 are shown in **Table 2** (Hair et al., 2020). **Figure 5** displays computations of the PLS algorithmic measurements model for all variables and DV/IV variables (**Figure 5**).

The discriminant validity of the proposed model is evaluated using the Fornell-Larcker criterion and heterotrait-monotrait (HTMT) ratios (Hair et al., 2020, Hair et al., 2021). The strongest significant correlation of variables in each column in **Table 3** demonstrates that the Fornell-Larcker criteria have been utilized to demonstrate discriminant validity (Fornell and Larcker, 1981; Henseler et al., 2015). The values of the Fornell-Larcker criterion, the standard deviation, and the mean of all the variables are shown in **Table 3**. Even if it was adequate for measuring discriminant validity, the Fornell-Larcker criteria couldn't distinguish between its lack and presence, they said. This led to the use of the HTMT to test discriminant validity. **Table 4** shows the HTMT values for each of the research criteria. As per requirement, values of HTMT must be below 0.90 to prove data validity, and in this research, HTMT values were below 0.90, which showed this research data was valid (Henseler, Ringle, Sarstedt) (**Table 4**).

Structural model research is the second phase of PLS-SEM evaluation. Examine the predictive relevance, multicollinearity, empirical significance, and confidence of the structural path model. Evaluation of the structural route model's dependability. This study used data guidelines from Hair et al. (2021) to analyze the structural model. To determine how various factors impact FKF (**Figure 6** and **Table 5**) elaborate on the real situation of structural model research. As per the beta value and significance of this study, H1-H4 were significant and showed a relationship with IV, while H5 was insignificant. Under this research, H1-H4 hypotheses were approved while H5 was rejected. R2 and adjusted R2 are 0.379 and 0.372, respectively **Table 6**. This study found that control variables (gender and education) showed a significant direct relationship with DV. This study found that farmers' awareness of flooding and their capacity to cope with natural disasters are influenced by their gender and education (**Table 5**). To test the validity of the hypotheses that had been put forward previously, we began by examining the causal relationships that were already known to exist between the different variables. Following that, we carried out a bootstrapping test using 5,000 replicates to evaluate the degree to which our findings were consistent with the hypothesis (Mustafa and Wen, 2022; Mustafa et al., 2022e). PLS-SEM direct path analysis rveealed that AS (b = −0.155; *p* 0.001), FS (b = 0.343; *p* 0.001), LA (b = 0.273; *p* 0.001), RA (b = 0.147; *p* 0.006), and for FKF have statistically significant values of beta, while SD (b = −0.079NS) is not significant. These results offer support to hypotheses H1 through H4 and H5 being rejected. We have also looked at the levels of education and gender of the respondents as control variables have a significant relationship with the dependent variable. On the other hand, age does not have any relationship with farmers' knowledge of floods (**Figure 6** and **Table 5**).

Conclusion

This research was carried out in one of the important agricultural regions of Pakistan to check farmers' knowledge about the impacts of floods on their farming lives, food

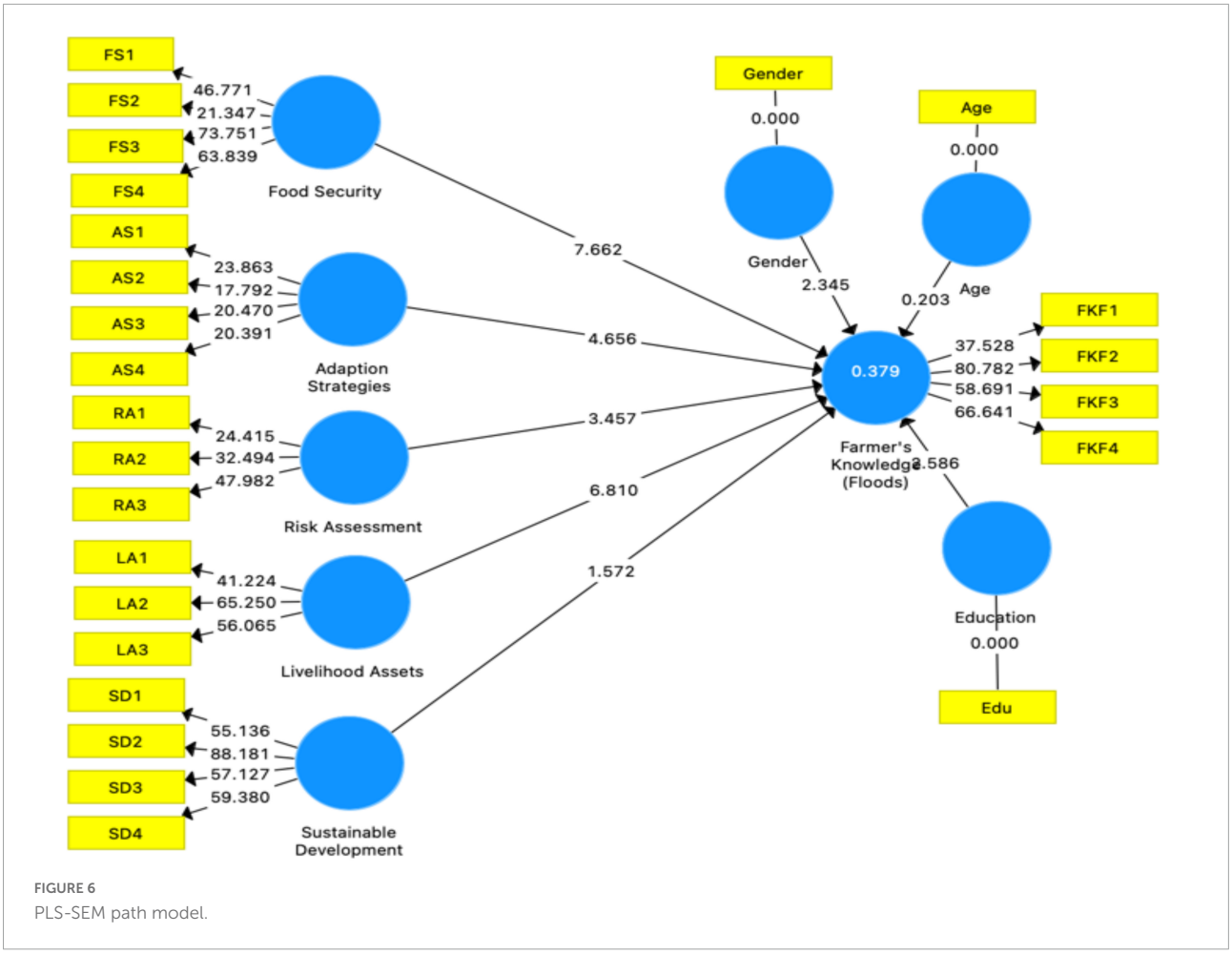

FIGURE 6
PLS-SEM path model.

TABLE 5 HTMT ratio.

Variables	*AS*	*FKF*	*FS*	*LA*	*RA*	*SD*
AS						
FKF	0.401					
FS	0.260	0.492				
LA	0.390	0.552	0.344			
RA	0.480	0.519	0.445	0.569		
SD	0.387	0.361	0.767	0.369	0.468	

AS, adaption strategies; FKF, farmer's knowledge (floods); FS, food security; LA, livelihood assets; RA, risk assessment; SD, sustainable development.

TABLE 6 Path analysis (PLS-SEM).

Statistical Paths	*Beta (β)*	*Std. Dev*	*T-Value*
AS - > FKF	0.155***	0.033	4.655
FS - > FKF	0.343***	0.044	7.662
LA - > FKF	0.273***	0.040	6.809
RA - > FKF	0.147***	0.042	3.457
SD - > FKF	−0.079^{NS}	0.050	1.572
Control Variables			
Age - > FKF	−0.000^{NS}	0.029	0.202
EDU - > FKF	0.074***	0.028	2.586
Gender- > FKF	0.078***	0.033	2.345
R^2		0.379	
Adjusted R^2		0.372	

***Significant at $p < 0.001$, NS, not supported; AS, adaption strategies; FKF, farmer's knowledge (floods); FS, food security; LA, livelihood assets; RA, risk assessment; SD, sustainable development; STDEV, standard deviation.

security, sustainable development, and risk assessment. Floods are very common in this study area, which has very adverse effects on farmers' lives and food security. Flood types vary considerably across the country because of differences in physiographic, climatic, hydrologic, demographic, and socioeconomic features. A PLS-SEM dual-stage hybrid model was used to check the relationship among all variables, which showed a significant relationship among DV, IV, and control variables. Following that, we carried out a bootstrapping test using 5,000 replicates to evaluate the degree to which our findings were consistent with the hypothesis. PLS-SEM direct path analysis revealed that AS,

FS, LA, RA, and FKF had statistically significant beta () while SD was not significant. These results offer support to hypotheses H1 through H4 and H5 being rejected. As control variables, we also looked at how much education the respondents had and what gender they were. Both of these things have a strong relationship with the dependent variable. On the other hand, age does not have any relationship with farmers' knowledge of floods. This study can help policymakers and government officials to make suitable policies for this study area, and it can help farmers to get more knowledge about floods.

Data availability statement

The original contributions presented in the study are included in the article/supplementary material, further inquiries can be directed to the corresponding author.

Ethics statement

Ethics review and approval/written informed consent was not required as per local legislation and institutional requirements.

Author contributions

MS: conceptualization, methodology, software, and writing–original draft, supervision and final draft approval, data collection and analyzing, editing, and data collection. SC: visualization and investigation. Both authors contributed to the article and approved the submitted version.

Conflict of interest

The authors declare that the research was conducted in the absence of any commercial or financial relationships that could be construed as a potential conflict of interest.

Publisher's note

All claims expressed in this article are solely those of the authors and do not necessarily represent those of their affiliated organizations, or those of the publisher, the editors and the reviewers. Any product that may be evaluated in this article, or claim that may be made by its manufacturer, is not guaranteed or endorsed by the publisher.

References

Abid, M., Scheffran, J., Schneider, U. A., and Ashfaq, M. (2016). Climate change vulnerability, adaptation, and risk perceptions at farm level in Punjab, Pakistan. *Sci. Total Environ.* 547, 447–460. doi: 10.1016/j.scitotenv.2015.11.125

Achard, F., Eva, H. D., Stibig, H. J., Mayaux, P., Gallego, J., Richards, T., et al. (2002). Determination of deforestation rates of the world's humid tropical forests. *Science* 297, 999–1002. doi: 10.1126/science.1070656

Adger, W. N., and Kelly, P. M. (1999). Social vulnerability to climate change and the architecture of entitlements. *Mitig. Adapt. Strateg. Glob. Chang.* 4, 253–266. doi: 10.1023/A:1009601904210

Adger, W. N., Brooks, N., Bentham, G., Agnew, M. D., and Eriksen, S. H. (2004). *New Indicators Of Vulnerability And Adaptive Capacity*. Norwich: Tyndall Centre for Climate Change Research.

Adger, W. N., Huq, S., Brown, K., Conway, D., and Hulme, M. (2003). Adaptation to climate change in the developing world. *Prog. Dev. Stud.* 3, 179–195. doi: 10.1191/1464993403ps060oa

Adger, W. N., Paavola, J., and Huq, S. (2006). "Toward justice in adaptation to climate change," in *Fairness in Adaptation to Climate Change*, eds W. N. Adger, J. Paavola, S. Huq, and M. J. Mace (Cambridge: The MIT Press), 1–19. doi: 10.7551/mitpress/2957.001.0001

Alam, G. M. M., Alam, K., and Mushtaq, S. (2017). Climate Change Perceptions and Local Adaptation Strategies of Hazard-Prone Rural Households in Bangladesh. *Clim. Risk Manag.* 17, 52–63. doi: 10.1016/j.crm.2017.06.006

Ali, A., and Erenstein, O. (2017). Assessing farmer use of climate change adaptation practices and impacts on food security and poverty in Pakistan. *Clim. Risk Manag.* 16, 183–194. doi: 10.1016/j.crm.2016.12.001

Ali, F., Omar, R., and Amin, M. (2013). An examination of the relationships between physical environment, perceived value, image and behavioural Intentions: A SEM approach towards Malaysian resort hotels. *J. Hotel Tour. Manag.* 27, 9–26.

Aliagha, U. G., Jin, T. E., Choong, W. W., Nadzri Jaafar, M., and Ali, H. M. (2014). Factors affecting flood insurance purchase in residential properties in Johor, Malaysia. *Nat. Hazards Earth Syst. Sci.* 14, 3297–3310. doi: 10.5194/nhess-14-3297-2014

Atta-ur-Rahman, A. U. R., Hareem, S., Choudhary, M., Sener, B., Abbaskhan, A., Siddiqui, H., et al. (2010). New and known constituents from iris unguicularis and their antioxidant activity. *Heterocycles* 82, 813–824. doi: 10.3987/COM-10-S(E)6

Azam, S. E., and Mariani, S. (2012). Dual estimation of partially observed nonlinear structural systems: A particle filter approach. *Mech. Res. Commun.* 46, 54–61. doi: 10.1016/j.mechrescom.2012.08.006

Barnett, J. (2006). "Climate change, insecurity, and injustice," in *Fairness in Adaptation to Climate Change*, eds W. N. Adger, J. Paavola, S. Huq, and M. J. Mace (Cambridge: The MIT Press), 115–130.

Begum, H., Reddy, M. T., Malathi, S., Reddy, B. P., Narshimulu, G., Nagaraju, J., et al. (2014). Morphological and microsatellite analysis of intravarietal heterogeneity in 'Beneshan'mango (*Mangifera indica L.*). *Int. J. Agric. Food Res.* 3, 1–18. doi: 10.24102/ijafr.v3i2.498

Below, T. B., Mutabazi, K. D., Kirschke, D., Franke, C., Sieber, S., Siebert, R., et al. (2012). Can farmers' adaptation to climate change be explained by socio-economic household-level variables? *Glob. Environ. Change* 22, 223–235. doi: 10.1016/j.gloenvcha.2011.11.012

Benson, C., and Clay, E. J. (2004). *Understanding The Economic And Financial Impacts Of Natural Disasters*. Washington, DC: World Bank Publications. doi: 10.1596/0-8213-5685-2

Berkes, F., and Folke, C. (1998). "*Linking social and ecological systems: management practices and social IOP Conf. Series: Earth and Environmental Science*," in *Linking Social And Ecological Systems For Resilience And Sustainability*, eds F. Berkes, C. Folke, and J. Colding (Cambridge: Cambridge University Press).

Bruijnzeel, L. A. (1990). *Hydrology Of Moist Tropical Forests And Effects Of Conversion: A State Of Knowledge Review*. Paris: UNESCO.

Bruijnzeel, L. A. (2004). Hydrological functions of tropical forests: Not seeing the soil for the trees? *Agric. Ecosyst. Environ.* 104, 185–228. doi: 10.1016/j.agee.2004.01.015

Bryan, E., Deressa, T. T., Gbetibouo, G. A., and Ringler, C. (2009). Adaptation to limate change in Ethiopia and South Africa: Options and constraints. *Environ. Sci. Policy* 12, 413–426. doi: 10.1016/j.envsci.2008.11.002

Bryan, E., Ringler, C., Okoba, B., Roncoli, C., Silvestri, S., and Herrero, M. (2013). Adapting agriculture to climate change in Kenya: Household strategies and determinants. *J. Environ. Manag.* 114, 26–35. doi: 10.1016/j.jenvman.2012.10.036

Budhathoki, N. K., Paton, D., Lassa, J. A., Bhatta, G. D., and Zander, K. K. (2020). Heat, cold, and floods: Exploring farmers' motivations to adapt to extreme weather events in the Terai region of Nepal. *Nat. Hazards* 103, 3213–3237. doi: 10.1007/s11069-020-04127-0

Champonnois, V., and Erdlenbruch, K. (2021). Willingness of households to reduce flood risk in southern France. *J. Flood Risk Manag.* 14:e12696. doi: 10.1111/jfr3.12696

Clark, B., DeFries, R., and Krishnaswamy, J. (2021). India's commitments to increase tree and forest cover: Consequences for water supply and agriculture production within the central Indian Highlands. *Water* 13:959. doi: 10.3390/w13070959

Deressa, T. T., Hassan, R. M., Ringler, C., Alemu, T., and Yesuf, M. (2009). Determinants of farmers' choice of adaptation methods to climate change in the Nile Basin of Ethiopia. *Glob. Environ. Change* 19, 248–255. doi: 10.1016/j.gloenvcha.2009.01.002

Di Falco, S., Adinolfi, F., Bozzola, M., and Capitanio, F. (2014). Hedging against extreme events: Crop insurance as a strategy to adapt to climate change. *J. Agric. Econ.* 65, 485–504. doi: 10.1111/1477-9552.12053

Enjolras, G., Capitanio, F., and Adinolfi, F. (2012). The demand for crop insurance: Combined approaches for France and Italy. *Agric. Econ. Rev.* 13, 5–22. doi: 10.2139/ssrn.1836798

Fahad, S., and Wang, J. (2020). Climate change, vulnerability, and its impacts in rural Pakistan: A review. *Environ. Sci. Pollut. Res.* 27, 1334–1338. doi: 10.1007/s11356-019-06878-1

Fahad, S., Inayat, T., Wang, J., Dong, L., Hu, G., Khan, S., et al. (2020). Farmers' awareness level and their perceptions of climate change: A case of Khyber Pakhtunkhwa province, Pakistan. *Land Use Policy* 96:104669. doi: 10.1016/j.landusepol.2020.104669

Ferdushi, K. F., Ismail, M. T., and Kamil, A. A. (2019). Perceptions, knowledge and adaptation about climate change: A Study on farmers of Haor areas after a flash flood in Bangladesh. *Climate* 7:85. doi: 10.3390/cli7070085

Fornell, C., and Larcker, D. F. (1981). Structural equation models with unobservable variables and measurement error: Algebra and statistics. *J. Mark. Res.* 18, 382–388. doi: 10.1177/002224378101800313

Gong, Y., Lu, W. S., and Tao, L. (2003). Spatial and temporal distribution of anomalous temperature/precipitation in spring and summer as well as their relationships to drought/flood in Northeast of China. *J. Nanjing Inst. Meteorol.* 26, 349–357.

Goodwin, B. K., and Mahul, O. (2004). *Risk Modeling Concepts Relating To The Design And Rating Of Agricultural Insurance Contracts*. Washington, DC: World Bank Publications. doi: 10.1596/1813-9450-3392

Goodwin, B. K., and Smith, V. H. (1995). *The Economics Of Crop Insurance And Disaster Aid*. Washington, DC: AEI Press.

Gorst, C., Kwok, C. S., Aslam, S., Buchan, I., Kontopantelis, E., Myint, P. K., et al. (2015). Long-term glycemic variability and risk of adverse outcomes: A systematic review and meta-analysis. *Diabet. Care* 38, 2354–2369. doi: 10.2337/dc15-1188

Hair, J. F., Hult, T. M., Ringle, C. M., and Sarstedt, M. (2021). *A Primer On Partial Least Squares Structural Equation Modeling (Pls-Sem)*. Thousand Oaks: Sage publications. doi: 10.1007/978-3-030-80519-7

Hair, Jr. J. F, Howard, M. C., and Nitzl, C. (2020). Assessing measurement model quality in PLS-SEM using confirmatory composite analysis. *J. Bus. Res.* 109, 101–110. doi: 10.1016/j.jbusres.2019.11.069

Harvey, D. (2014). *Seventeen Contradictions And The End Of Capitalism*. Oxford: Oxford University Press.

Henseler, J., Ringle, C. M., and Sarstedt, M. (2015). "A new criterion for assessing discriminant validity in variance-based structural equation modeling". *J. Acad. Mark. Sci.* 43, 115–135. doi: 10.1007/s11747-014-0403-8

Hirabayashi, Y., Mahendran, R., Koirala, S., Konoshima, L., Yamazaki, D., Watanabe, S., et al. (2013). Global flood risk under climate change. *Nat. Clim. Change* 3, 816–821. doi: 10.1038/nclimate1911

Hoanh, C. T., Tuong, T. P., and John, W. G. (2006). *Environment and Livelihoods in Tropical Coastal Zones: Managing Agriculture-fishery- Quaculture Conflicts*. Wallingford: CABI. doi: 10.1079/9781845931070.0000

Holling, C. (1973). Resilience and stability of ecological systems. *Ann. Rev. Ecol. Syst.* 4, 1–23. doi: 10.1146/annurev.es.04.110173.000245

Hossain, M. A., Zahid, A. M., Arifunnahar, M., and Siddique, M. N. A. (2019). Effect of brick kiln on arable land degradation, environmental pollution and consequences on livelihood of Bangladesh. *J. Sci. Technol. Environ. Inform.* 6, 474–488. doi: 10.18801/jstei.060219.50

Jakobsen, J., Rasmussen, K., Leisz, S., Folving, R., and Nguyen, V. Q. (2007). The effects of land tenure policy on rural livelihoods and food sufficiency in the upland village of Que, North Central Vietnam. *Agric. Syst.* 94, 309–319. doi: 10.1016/j.agsy.2006.09.007

Jamshed, A., Rana, I. A., Mirza, U. M., and Birkmann, J. (2019). Assessing relationship between vulnerability and capacity: An empirical study on rural flooding in Pakistan. *Int. J. Disaster Risk Reduct.* 36:101109. doi: 10.1016/j.ijdrr.2019.101109

Jamshidi, O., Asadi, A., Kalantari, K., Azadi, H., and Scheffran, J. (2019). Vulnerability to climate change of smallholder farmers in the Hamadan province, Iran. *Clim. Risk Manag.* 23, 146–159. doi: 10.1016/j.crm.2018.06.002

Jian, L., Sohail, M. T., Ullah, S., and Majeed, M. T. (2021). Examining the role of non-economic factors in energy consumption and CO2 emissions in China: Policy options for the green economy. *Environ. Sci. Pollut. Res.* 28, 67667–67676. doi: 10.1007/s11356-021-15359-3

Jiang, A., Cao, Y., Sohail, M. T., Majeed, M. T., and Sohail, S. (2021). Management of green economy in China and India: Dynamics of poverty and policy drivers. *Environ. Sci. Pollut. Res.* 28, 55526–55534. doi: 10.1007/s11356-021-14753-1

Kavvada, A., and Held, A. (2018). "Analysis-ready earth observation data and the united nations sustainable development goals," in *IGARSS 2018-2018 IEEE International Geoscience and Remote Sensing Symposium*, (Piscataway: IEEE), 434–436. doi: 10.1109/IGARSS.2018.8519405

Khan, I., Lei, H., Shah, A. A., Khan, I., and Muhammad, I. (2021). Climate change impact assessment, flood management, and mitigation strategies in Pakistan for sustainable future. *Environ. Sci. Pollut. Res.* 28, 29720–29731. doi: 10.1007/s11356-021-12801-4

Khan, N. A., Gao, Q., and Abid, M. (2020). Public institutions' capacities regarding climate change adaptation and risk management support in agriculture: The case of Punjab Province, Pakistan. *Sci. Rep.* 10:14111. doi: 10.1038/s41598-020-71011-z

Kreft, S., Eckstein, D., and Melchior, I. (2013). *Global climate risk index 2014. Who suffers most from extreme weather events*. Bonn: Germanwatch.

Kuang, F., Jin, J., He, R., Ning, J., and Wan, X. (2020). Farmers' livelihood risks, livelihood assets and adaptation strategies in Rugao City, China. *J. Environ. Manag.* 264:110463. doi: 10.1016/j.jenvman.2020.110463

Lan, H., Cheng, C., and Sohail, M. T. (2022). Asymmetric determinants of CO2 emissions in China: Do government size and economic size matter? *Environ. Sci. Pollut. Res.* 29, 47225–47232. doi: 10.1007/s11356-022-19096-z

Laurance, W. F. (2004). Forest-climate interactions in fragmented tropical landscapes. *Philos. Trans. R. Soc. Lond. Series B* 359, 345–352. doi: 10.1098/rstb.2003.1430

Lechowska, E. (2018). What determines flood risk perception? A review of factors of flood risk perception and relations between its basic elements. *Nat. Hazards* 94, 1341–1366. doi: 10.1007/s11069-018-3480-z

Li, Y., Chen, J., and Sohail, M. T. (2022a). Does education matter in China? Myths about financial inclusion and energy consumption. *Environ. Sci. Pollut. Res.* [Epub ahead of print]. doi: 10.1007/s11356-022-21011-5

Li, Y., Chen, J., and Sohail, M. T. (2022b). Financial inclusion and their role in renewable energy and non-renewable energy consumption in China: Exploring the transmission channels. *Res. Sq.* [Preprint]. doi: 10.21203/rs.3.rs-1355688/v1

Liu, N., Hong, C., and Sohail, M. T. (2022). Does financial inclusion and education limit CO2 emissions in China? A new perspective. *Environ. Sci. Pollut. Res.* 29, 18452–18459. doi: 10.1007/s11356-021-17032-1

Liu, Y., Sohail, M. T., Khan, A., and Majeed, M. T. (2022). Environmental benefit of clean energy consumption: Can BRICS economies achieve environmental sustainability through human capital? *Environ. Sci. Pollut. Res.* 29, 6766–6776. doi: 10.1007/s11356-021-16167-5

Lu, F., and Sohail, M. T. (2022). Exploring the Effects of Natural Capital Depletion and Natural Disasters on Happiness and Human Wellbeing: A Study in China. *Front. Psychol.* 13:870623. doi: 10.3389/fpsyg.2022.870623

Luino, F., Turconi, L., Paliaga, G., Faccini, F., and Marincioni, F. (2018). Torrential floods in the upper Soana Valley (NW Italian Alps): Geomorphological processes and risk-reduction strategies. *Int. J. Disaster Risk Reduct.* 27, 343–354. doi: 10.1016/j.ijdrr.2017.10.021

Maheen, H., and Hoban, E. (2017). Rural women's experience of living and giving birth in relief camps in Pakistan. *PLoS Curr.*

9:ecurrents.dis.7285361a16eefbeddacc8599f326a1dd. doi: 10.1371/currents.dis.7285361a16eefbeddacc8599f326a1dd

Mahfooz, Y., Yasar, A., Guijian, L., Yousaf, B., Sohail, M. T., Khan, S., et al. (2020). An assessment of wastewater pollution, treatment efficiency and management in a semi-arid urban area of Pakistan. *Desalination Water Treat.* 177, 167–175. doi: 10.5004/dwt.2020.24949

Mahfooz, Y., Yasar, A., Sohail, M. T., Tabinda, A. B., Rasheed, R., Irshad, S., et al. (2019). Investigating the drinking and surface water quality and associated health risks in a semi-arid multi-industrial metropolis (Faisalabad), Pakistan. *Environ. Sci. Pollut. Res.* 26, 20853–20865. doi: 10.1007/s11356-019-05367-9

Mahfooz, Y., Yasar, A., Tabinda, A. B., Sohail, M. T., Siddiqua, A., and Mahmood, S. (2017). Quantification of the River Ravi pollution load and oxidation pond treatment to improve the drain water quality. *Desalination Water Treat.* 85, 132–137. doi: 10.5004/dwt.2017.21195

Manoj, M. (2017). Smallholder Agriculture and Climate Change Adaptation in Bangladesh: Questioning the Technological Optimism. *Clim. Dev.* 9, 337–347. doi: 10.1080/17565529.2016.1145101

Mondal, P., Anweshan, A., and Purkait, M. K. (2020). Green synthesis and environmental application of iron-based nanomaterials and nanocomposite: A review. *Chemosphere* 259:127509. doi: 10.1016/j.chemosphere.2020.127509

Mortimore, M. J., and Adams, W. M. (2001). Farmer adaptation, change and 'crisis' in the Sahel. *Glob. Environ. Change* 11, 49–57. doi: 10.1016/S0959-3780(00)00044-3

Muhammad, A. M., Zhonghua, T., Dawood, A. S., and Sohail, M. T. (2014). A Study to Investigate and Compare Groundwater Quality in Adjacent Areas of Landfill Sites in Lahore City. *Nat. Environ. Pollut. Technol.* 13, 1–10.

Mustafa, D., and Wescoat, Jr. J. L (1997). Development of flood hazards policy in the Indus River Basin of Pakistan, 1947–1996. *Water Int.* 22, 238–244. doi: 10.1080/02508069708686712

Mustafa, S., and Wen, Z. (2022). How to achieve maximum participation of users in technical versus non-technical online q&a communities? *Int. J. Electron. Commer.* 26.

Mustafa, S., Qiao, Y., Yan, X., Anwar, A., Tengyue, H., and Rana, S. (2022a). Digital students' satisfaction with and intention to use online teaching modes, role of big five personality traits. *Front. Psychol.* 13:956281. doi: 10.3389/fpsyg.2022.956281

Mustafa, S., Sohail, M. T., Alroobaea, R., Rubaiee, S., Anas, A., Othman, A. M., et al. (2022b). Éclaircissement to understand consumers' decision-making psyche and gender effects, a fuzzy set qualitative comparative analysis. *Front. Psychol.* 13920594. doi: 10.3389/fpsyg.2022.920594

Mustafa, S., Tengyue, H., Jamil, K., Qiao, Y., and Nawaz, M. (2022c). Role of eco-friendly products in the revival of developing countries' economies & achieving a sustainable green economy. *Front. Environ. Sci.* 10:955245. doi: 10.3389/fenvs.2022.955245

Mustafa, S., Tengyue, H., Qiao, Y., Sha, S. K., and Sun, R. (2022d). How a successful implementation and sustainable growth of e-commerce can be achieved in developing countries; a pathway towards green economy. *Front. Environ. Sci.* 10, doi: 10.3389/fenvs.2022.940659

Mustafa, S., Wen, Z., and Naveed, M. M. (2022e). What motivates online community contributors to contribute consistently? A case study on stackoverflow netizens. *Curr. Psychol.* [Epub ahead of print]. doi: 10.1007/s12144-022-03307-4

Mustafa, S., Zhang, W., Shehzad, M. U., Anwar, A., and Rubakula, G. (2022f). Does health consciousness matter to adopt new technology? An integrated model of utaut2 with sem-fsqca approach. *Front. Psychol.* 13:836194. doi: 10.3389/fpsyg.2022.836194

Mustafa, S., Zhang, W., and Li, R. (2021). "Does environmental awareness play a role in ev adoption? A value-based adoption model analysis with sem-ann approach," in *IEEE/WIC/ACM International Conference on Web Intelligence and Intelligent Agent Technology*, (Melbourne: Association for Computing Machinery), 433–440. doi: 10.1145/3498851.3498992

NDMA (2014). *Pakistan Floods 2014: Recovery Needs Assessment and Action Framework 2014-16*. Islamabad: NDMA.

Parvin, G. A., Shimi, A. C., Shaw, R., and Biswas, C. (2016). Flood in a changing climate: The impact on livelihood and how the rural poor cope in Bangladesh. *Climate* 4:60. doi: 10.3390/cli4040060

Patt, A. G., and Schröter, D. (2008). Perceptions of climate risk in Mozambique: Implications for the success of adaptation strategies. *Glob. Environ. Change* 18, 458–467. doi: 10.1016/j.gloenvcha.2008.04.002

Rasool, A., Jundong, H., and Sohail, M. T. (2017). Relationship of intrinsic and extrinsic rewards on job motivation and job satisfaction of expatriates in China. *J. Appl. Sci.* 17, 116–125. doi: 10.3923/jas.2017.116.125

Rees, H. G., and Collins, D. N. (2006). Regional differences in response of flow in glacier-fed Himalayan rivers to climatic warming. *Hydrol. Process.* 20, 2157–2169. doi: 10.1002/hyp.6209

Roberts, T. J., and Parks, B. C. (2007). *A Climate of Injustice: Global Inequality, North-South Politics, and Climate Policy*. Cambridge.: MIT Press.

Rosenzweig, C., Iglesius, A., Yang, X. B., Epstein, P. R., and Chivian, E. (2001). Climate change and extreme weather events-Implications for food production, plant diseases, and pests. *Glob. Change Hum. Health* 2, 90–104. doi: 10.1023/A:1015086831467

Samu, R., and Kentel, A. S. (2018). An analysis of the flood management and mitigation measures in Zimbabwe for a sustainable future. *Int. J. Disaster Risk Reduct.* 31, 691–697. doi: 10.1016/j.ijdrr.2018.07.013

Saqib, S., Ahmad, M. M., Panezai, S., and Ali, U. (2016). Factors influencing farmers' adoption of agricultural credit as a risk management strategy: The case of Pakistan. *Int. J. Disaster Risk Reduct.* 17, 67–76. doi: 10.1016/j.ijdrr.2016.03.008

Sen, A. (1981). *Poverty and Famines: An Essay on Entitlement and Deprivation*. Oxford: Clarendon Press.

Shahab, A., Shihua, Q., Rashid, A., Hasan, F. U., and Sohail, M. T. (2016). Evaluation of Water Quality for Drinking and Agricultural Suitability in the Lower Indus Plain in Sindh Province, Pakistan. *Pol. J. Environ. Stud.* 25, 2563–2574. doi: 10.15244/pjoes/63777

Shukla, R., Agarwal, A., Sachdeva, K., Kurths, J., and Joshi, P. K. (2019). Climate change perception: An analysis of climate change and risk perceptions among farmer types of Indian Western Himalayas. *Clim. Change* 152, 103–119. doi: 10.1007/s10584-018-2314-z

Singh, R. K., Zander, K. K., Kumar, S., Singh, A., Sheoran, P., Kumar, A. et al. (2017). Perceptions of climate variability and livelihood adaptations relating to gender and wealth among the Adi community of the eastern Indian Himalayas. *Appl. Geogr.* 86, 41–52. doi: 10.1016/j.apgeog.2017.06.018

Smit, B., and Skinner, M. W. (2002). Adaptation options in agriculture to climate change: A typology. *Mitig. Adapt. Strateg. Glob. Chang.* 7, 85–114. doi: 10.1023/A:1015862228270

Sohail, M. T., (2013). Job satisfaction surrounded by academic staff: A case study of job satisfaction of academic staff of the GCUL, Pakistan. *Interdiscip. J. Contemp. Res. Bus.* 4, 126–137.

Sohail, M. T., Aftab, R., Mahfooz, Y., Yasar, A., Yen, Y., Shaikh, S. A., et al. (2019a). Estimation of water quality, management and risk assessment in Khyber Pakhtunkhwa and Gilgit-Baltistan, Pakistan. *Desalination Water Treat.* 171, 105–114. doi: 10.5004/dwt.2019.24925

Sohail, M. T., Mahfooz, Y., Azam, K., Yen, Y., Genfu, L., and Fahad, S. (2019b). Impacts of urbanization and land cover dynamics on underground water in Islamabad, Pakistan. *Desalination Water Treat.* 159, 402–411. doi: 10.5004/dwt.2019.24156

Sohail, M. T., Delin, H., and Siddiq, A. (2014a). Indus basin waters a main resource of water in Pakistan: An analytical approach. *Curr. World Environ.* 9, 670–685. doi: 10.12944/CWE.9.3.16

Sohail, M. T., Delin, H., Talib, M. A., Xiaoqing, X., and Akhtar, M. M. (2014b). An analysis of environmental law in Pakistan-policy and conditions of implementation. *Res. J. Appl. Sci. Eng. Technol.* 8, 644–653. doi: 10.19026/rjaset.8.1017

Sohail, M. T., Delin, H., Siddiq, A., Idrees, F., and Arshad, S. (2015). Evaluation of historic Indo-Pak relations, water resource issues and its impact on contemporary bilateral affairs. *Asia Pac. J. Multidiscip. Res.* 3, 48–55.

Sohail, M. T., Ehsan, M., Riaz, S., Elkaeed, E. B., Awwad, N. S., and Ibrahium, H. A. (2022a). Investigating the Drinking Water Quality and Associated Health Risks in Metropolis Area of Pakistan. *Front. Mater.* 9:864254. doi: 10.3389/fmats.2022.864254

Sohail, M. T., Elkaeed, E. B., Irfan, M., Acevedo-Duque, Á, and Mustafa, S. (2022b). Determining Farmers' awareness about climate change mitigation and wastewater irrigation: A pathway towards green and sustainable development. *Front. Environ. Sci.* 10:193.

Sohail, M. T., Majeed, M. T., Shaikh, P. A., and Andlib, Z. (2022c). Environmental costs of political instability in Pakistan: Policy options for clean energy consumption and environment. *Environ. Sci. Pollut. Res.* 29, 25184–25193. doi: 10.1007/s11356-021-17646-5

Sohail, M. T., Mustafa, S., Ma, M., and Riaz, S. (2022d). Agricultural communities' risk assessment and the effects of climate change: A pathway toward green productivity and sustainable development. *Front. Environ. Sci.* 10:948016.

Sohail, M. T., Huang, D., Bailey, E., Akhtar, M. M., and Talib, M. A. (2013). Regulatory framework of mineral resources sector in Pakistan and investment

proposal to Chinese companies in Pakistan. *Am. J. Ind. Bus. Manag.* 3, 514–524. doi: 10.4236/ajibm.2013.35059

Sohail, M. T., Lin, X., Lizhi, L., Rizwanullah, M., Nasrullah, M., Xiuyuan, Y., et al. (2021a). Farmers' awareness about impacts of reusing wastewater, risk perception and adaptation to climate change in Faisalabad District, Pakistan. *Pol. J. Environ. Stud.* 30, 4663–4675. doi: 10.15244/pjoes/134292

Sohail, M. T., Xiuyuan, Y., Usman, A., Majeed, M. T., and Ullah, S. (2021d). Renewable energy and non-renewable energy consumption: Assessing the asymmetric role of monetary policy uncertainty in energy consumption. *Environ. Sci. Pollut. Res.* 28, 31575–31584. doi: 10.1007/s11356-021-12867-0

Sohail, M. T., Ullah, S., Majeed, M. T., and Usman, A. (2021b). Pakistan management of green transportation and environmental pollution: A nonlinear ARDL analysis. *Environ. Sci. Pollut. Res.* 28, 29046–29055. doi: 10.1007/s11356-021-12654-x

Sohail, M. T., Ullah, S., Majeed, M. T., Usman, A., and Andlib, Z. (2021c). The shadow economy in South Asia: Dynamic effects on clean energy consumption and environmental pollution. *Environ. Sci. Pollut. Res.* 28, 29265–29275. doi: 10.1007/s11356-021-12690-7

Sohail, M. T., Mahfooz, Y., Hussain, S., Khan, M. B., and Hadi, N. U. (2017). Impacts of Landfill Sites on Groundwater Quality In Lahore, Pakistan. *Abasyn J. Soc. Sci.* 10.

Sohail, M. T., Mahfoozb, Y., Aftabc, R., Yend, Y., Talibe, M. A., and Rasoolf, A. (2020). Water quality and health risk of public drinking water sources: A study of filtration plants installed in Rawalpindi and Islamabad, Pakistan. *Desalination Water Treat.* 181, 239–250. doi: 10.5004/dwt.2020.25119

Somda, J., Zougmore, R., Sawadogo, I., Buah, S., and Abasse, T. (2017). "Adaptation Processes in Agriculture and Food Security: Insights from Evaluating Behavioral Changes in West Africa," in *Evaluating Climate Change Action for Sustainable Development*, eds J. Uitto, J. Puri, and R. van den Berg (Berlin: Springer), 255–269. doi: 10.1007/978-3-319-43702-6_14

Strömberg, D. (2007). Natural disasters, economic development, and humanitarian aid. *J. Econ. Perspect.* 21, 199–222. doi: 10.1257/jep.21.3.199

Sun, F., Yang, S., and Chen, P. (2005). Climatic warming-drying trend in Northeastern China during the last 44 years and its effects. *Chin. J. Ecol.* 24, 751–755.

Surminski, S., and Oramas-Dorta, D. (2013). *Do Flood Insurance Schemes In Developing Countries Provide Incentives To Reduce Physical Risks?*. London: Grantham Research Institute on Climate Change and the Environment.

Surminski, S., and Oramas-Dorta, D. (2014). Flood insurance schemes and climate adaptation in developing countries. *Int. J. Disaster Risk Reduct.* 7, 154–164. doi: 10.1016/j.ijdrr.2013.10.005

Thomalla, F., Downing, T., Spanger-Siegfried, E., Han, G., and Rockström, J. (2006). Reducing hazard vulnerability: Towards a common approach between disaster risk reduction and climate adaptation. *Disasters* 30, 39–48. doi: 10.1111/j.1467-9523.2006.00305.x

Thornton, P. K., Ericksen, P. J., Herrero, M., and Challinor, A. J. (2014). Climate variability and vulnerability to climate change: A review. *Glob. Change Biol.* 20, 3313–3328. doi: 10.1111/gcb.12581

Trinh, T. Q., Rañola, Jr. R. F., Camacho, L. D., and Simelton, E. (2018). Determinants of farmers' adaptation to climate change in agricultural production in the central region of Vietnam. *Land Use Policy* 70, 224–231. doi: 10.1016/j.landusepol.2017.10.023

Valdivia, C., Seth, A., Gilles, J. L., Garcıʿa, M., Jimeʿnez, E., Cusicanqui, J., et al. (2010). Adapting to climate change in Andean ecosystems: landscapes, capitals, and perceptions shaping rural livelihood strategies and linking knowledge systems. *Ann. Assoc. Am. Geogr.* 100, 818–834. doi: 10.1080/00045608.2010.500198

Vandeveer, M. L. (2001). Demand for area crop insurance among litchi producers in northern Vietnam. *Agric. Econ.* 26, 173–184. doi: 10.1111/j.1574-0862.2001.tb00061.x

Vinke, K., Martin, M. A., Adams, S., Baarsch, F., Bondeau, A., Coumou, D., et al. (2017). Climatic risks and impacts in South Asia: Extremes of water scarcity and excess. *Reg. Environ. Change* 17, 1569–1583. doi: 10.1007/s10113-015-0924-9

Wang, Z., and Sohail, M. T. (2022). Short-and Long-Run Influence of Education on Subjective Well-Being: The Role of Information and Communication Technology in China. *Front. Psychol.* 13:927562. doi: 10.3389/fpsyg.2022.927562

Webster, M. A. (2011). Adaptation and visual coding. *J. Vis.* 11:3. doi: 10.1167/11.5.3

Wedawatta, G., and Ingirige, B. (2012). Resilience and adaptation of small and medium-sized enterprises to flood risk. *Disaster Prev. Manag.* 21, 474–488. doi: 10.1108/09653561211256170

Werts, C. E., Linn, R. L., and Jöreskog, K. G. (1974). "Intraclass Reliability Estimates: Testing Structural Assumptions". *Educ. Psychol. Meas.* 34, 25–33. doi: 10.1177/001316447403400104

Yang, X., Liu, Y., Bai, W., and Liu, B. (2015). Evaluation of the crop insurance management for soybean risk of natural disasters in Jilin Province, China. *Nat. Hazards* 76, 587–599. doi: 10.1007/s11069-014-1510-z

Yasar, A., Farooqa, T., Tabindaa, A. B., Sohailb, M. T., Mahfooza, Y., and Malika, A. (2019). Macrophytes as potential indicator of heavy metals in river water. *Desalination Water Treat.* 142, 272–278. doi: 10.5004/dwt.2019.23433

Yat, Y. E. N., Yumin, S. H. I., and Bunly Soeung, R. S. (2018). Victimization of the substance abuse and sexual behaviors among junior high school students in Cambodia. *Iran. J. Public Health* 47:357.

Yen, Y., Wang, Z., Shi, Y., Xu, F., Soeung, B., Sohail, M. T., et al. (2017). The predictors of the behavioral intention to the use of urban green spaces: The perspectives of young residents in Phnom Penh, Cambodia. *Habitat Int.* 64, 98–108. doi: 10.1016/j.habitatint.2017.04.009

Yen, Y., Zhao, P., and Sohail, M. T. (2021). The morphology and circuity of walkable, bikeable, and drivable street networks in Phnom Penh, Cambodia. *Environ. Plann. B* 48, 169–185. doi: 10.1177/2399808319857726

Zahid, R. A., and Khurshid, M. (2018). Impact Of Safta On Capital Market Integration Of South Asia: Evidence From Cointegration Analysis. *Rev. Econ. Bus. Stud.* 11, 79–96. doi: 10.1515/rebs-2018-0065

Zahid, R. A., Khurshid, M., and Khan, W. (2022a). Do chief executives matter in corporate financial and social responsibility performance nexus? A dynamic model analysis of Chinese firms. *Front. Psychol.* 13:897444. doi: 10.3389/fpsyg.2022.897444

Zahid, R. M., Khurshid, M., Waheed, M., and Sanni, T. (2022b). Impact of Environmental Fluctuations on Stock Markets: Empirical Evidence from South Asia. *J. Environ. Public Health* 2022:7692086. doi: 10.1155/2022/7692086

Zhang, S., Zhang, Y., Ji, R., Cai, F., and Wu, J. (2011). Analysis of spatio-temporal characteristics of drought for maize in Northeast China. *Agric. Res. Arid. Areas* 29, 231–236.

Zhao, C. Y., Ren, G. Y., and Zhang, Y. F. (2009). Climate change of the Northeast China over the past 50 years. *J. Arid. Land. Resour. Environ.* 23, 25–30.

Zhao, P., Yen, Y., Bailey, E., and Sohail, M. T. (2019). Analysis of urban drivable and walkable street networks of the ASEAN Smart Cities Network. *ISPRS Int. J. Geo-Inf.* 8:459. doi: 10.3390/ijgi8100459

Zhao, W., Chang, M., Yu, L., and Sohail, M. T. (2022a). Health and Human Wellbeing in China: Do Environmental Issues and Social Change Matter? *Front. Psychol.* 13:860321. doi: 10.3389/fpsyg.2022.860321

Zhao, W., Huangfu, J., Yu, L., Li, G., Chang, Z., and Sohail, M. T. (2022b). Analysis on Price Game and Supervision of Natural Gas Pipeline Tariff under the Background of Pipeline Network Separation in China. *Pol. J. Environ. Stud.* 31, 2961–2972. doi: 10.15244/pjoes/145603

Zinda, J. A., Williams, L. B., Kay, D. L., and Alexander, S. M. (2021). Flood risk perception and responses among urban residents in the northeastern United States. *Int. J. Disaster Risk Reduct.* 64:102528. doi: 10.1016/j.ijdrr.2021.102528

frontiers | Frontiers in Plant Science

TYPE Original Research
PUBLISHED 02 September 2022
DOI 10.3389/fpls.2022.994902

OPEN ACCESS

EDITED BY
Aqeel Ahmad,
University of Florida,
United States

REVIEWED BY
Wajid Zaman,
Yeungnam University,
South Korea
Weimeng Song,
South China Agricultural University, China
Iqra Shahzadi,
Wuhan University,
China

*CORRESPONDENCE
Xuewen Gao
gaoxw@njau.edu.cn

SPECIALTY SECTION
This article was submitted to Plant Symbiotic Interactions, a section of the journal Frontiers in Plant Science

RECEIVED 15 July 2022
ACCEPTED 10 August 2022
PUBLISHED 02 September 2022

CITATION
Ali Q, Ayaz M, Mu G, Hussain A, Yuanyuan Q, Yu C, Xu Y, Manghwar H, Gu Q, Wu H and Gao X (2022) Revealing plant growth-promoting mechanisms of *Bacillus* strains in elevating rice growth and its interaction with salt stress. *Front. Plant Sci.* 13:994902. doi: 10.3389/fpls.2022.994902

Revealing plant growth-promoting mechanisms of *Bacillus* strains in elevating rice growth and its interaction with salt stress

Qurban Ali[1], Muhammad Ayaz[1], Guangyuan Mu[2], Amjad Hussain[3], Qiu Yuanyuan[1], Chenjie Yu[1], Yujiao Xu[1], Hakim Manghwar[4], Qin Gu[1], Huijun Wu[1] and Xuewen Gao[1]*

[1]Key Laboratory of Integrated Management of Crop Diseases and Pests, Department of Plant Pathology, College of Plant Protection, The Sanya Institute of Nanjing Agricultural University, Nanjing Agricultural University, Nanjing, China, [2]Shenzhen Batian Ecotypic Engineering Co., Ltd., Shenzhen, China, [3]National Key Laboratory of Crop Genetic Improvement, Huazhong Agricultural University, Wuhan, China, [4]Lushan Botanical Garden, Chinese Academy of Sciences, Jiujiang, China

Soil salinity is a major environmental stress that has been negatively affecting the growth and productivity of rice. However, various salt-resistant plant growth-promoting rhizobacteria (PGPR) have been known to promote plant growth and alleviate the damaging effects of salt stress *via* mitigating physio-biochemical and molecular characteristics. This study was conducted to examine the salt stress potential of *Bacillus* strains identified from harsh environments of the Qinghai-Tibetan plateau region of China. The *Bacillus* strains NMTD17, GBSW22, and FZB42 were screened for their response under different salt stress conditions (1, 4, 7, 9, 11, 13, and 16%). The screening analysis revealed strains NMTD17, GBSW22, and FZB42 to be high-salt tolerant, moderate-salt tolerant, and salt-sensitive, respectively. The NMTD17 strain produced a strong biofilm, followed by GBSW22 and FZB42. The expression of salt stress-related genes in selected strains was also analyzed through qPCR in various salt concentrations. Further, the *Bacillus* strains were used in pot experiments to study their growth-promoting ability and antioxidant activities at various concentrations (0, 100, 150, and 200mmol). The analysis of growth-promoting traits in rice exhibited that NMTD17 had a highly significant effect and GSBW22 had a moderately significant effect in comparison with FZB42. The highly resistant strain NMTD17 that stably promoted rice plant growth was further examined for its function in the composition of rhizobacterial communities. The inoculation of NMTD17 increased the relative abundance and richness of rhizobacterial species. These outcomes propose that NMTD17 possesses the potential of PGPR traits, antioxidants enzyme activities, and reshaping the rhizobacterial community that together mitigate the harmful effects of salinity in rice plants.

KEYWORDS

rice, cell physiology, cellular interactions, antioxidant enzymes, PGPR, biofilm

Introduction

Rice (*Oryza sativa* L.) is a vital staple food and feed crop that provides nutrition to billions of people around the world. It is usually cultivated as a staple crop in tropical regions (Abbas et al., 2019). Soil salinity is one of the major limiting factors of abiotic stress that decreases rice production. Due to the rising level of soil salinization, crop productivity is limited in many regions of the world (Kumar et al., 2020a). Because of salinity stress, plants can undergo many metabolic, molecular, and physiological changes (Wang et al., 2019; Kumar et al., 2020b, 2021). Salt stress triggers ionic toxicity, osmotic stress, ion imbalance, and decreased water potential, which severely affects plant physiology and metabolism. It mainly affects physiological, morphological, and biochemical processes of plant development and growth (Bistgani et al., 2019). The level of global soil salinization is increasing year by year, and it is estimated that 50% of agricultural land will be affected by salinization by 2050 (Ansari et al., 2019).

Salinity stress affects various aspects of plant development that eventually results in an overall reduction in crop production. For example, it affects seed germination, plant growth and development, spike development, and reproductive growth (Ke et al., 2020; Korenblum et al., 2020). Plant growth and metabolism are severely affected by salt stress because of ion (Na^+ and K^+) accumulation. High salt concentrations in soil accumulate simultaneously as Cl^- and Na^+; nonetheless, their impact differs (Abbas et al., 2019; Mengistu, 2020). Increased Na^+ levels alter soil qualities, such as aeration, water conductivity, and porosity (Compant et al., 2019; Mukherjee et al., 2020). In addition, the cell walls activate osmotic stress and cause cell death in plants with the increase of sodium ions. The chlorophyll content in the leaf is reduced by drought and salinity stresses, which results in reducing the rate of photosynthesis. Stomatal conductance, leaf area, and photosynthetic efficacy may possibly be disturbed by high salinity (Stassen et al., 2020; Hassan et al., 2021; Solangi et al., 2021).

For the sustainable development of agriculture, enhancing the cadmium and salt stress tolerance of plants is therefore of high practical importance (Ali et al., 2022). To overcome this problem, chemical fertilizers and pesticides are widely used in modern agriculture, gradually altering the supply of nutrients, reducing microbial activity, diversity, and deteriorating soil health (Etesami and Glick, 2020; Ali et al., 2021a,b). However, in the natural environment, many microorganisms, including plant growth-promoting bacteria (PGPB) inhabit plants. Plants are exposed to billions of microbes in nature, which form colonies and occupy various compartments of plants, such as endosphere, rhizoplane, rhizosphere, and phyllosphere, which are thus regarded as the secondary genome of plants (Dubey et al., 2019; Kumar et al., 2019). In general, the interaction between plants and microorganisms in the rhizosphere/root zone is essential for plant nutrient acquisition, resistance to various stresses, and plant development (Hubbard et al., 2019; Kong et al., 2021). For in-plant resistance to abiotic stresses, plant relationship with beneficial microorganisms plays an important role (Liu et al., 2020; Sun et al., 2021; Ali et al., 2022). Several studies have evaluated the potential of microorganisms to enhance the growth of host plants under salt stress. A number of studies have reported that beneficial plant bacteria have a complex regulatory mechanism that promote growth and improve host plant damage to salt stress. Plant growth-promoting rhizobacteria (PGPR) increase plant development directly or indirectly by producing growth-promoting traits, for example, 1-aminocyclopropane-1-carboxylate (ACC) deaminase production, and nitrogen fixation (Sarkar et al., 2018; Kumar et al., 2020a).

In addition, rhizosphere bacteria increase plant resistance to salt stress by controlling the effectiveness of photosynthesis, ion homeostasis, osmotic regulation, secondary metabolite accumulation, and plant hormone gene expression signaling pathways (Hassan et al., 2021; Manghwar et al., 2022). Furthermore, various plants possess the natural capability to change soil salinity through metabolism, gene expression, and signal pathway regulation (Daliakopoulos et al., 2016). Salt toxicity is mediated by the formation of antioxidants and the suppression of the generation of reactive oxygen species (ROS) (Abbas et al., 2019). In the natural environment, several crops are recurrently affected by salt stress because it interrupts ecological relations between plants and microorganisms in the soil and inhibits the proliferation of microorganisms in the surrounding environment (Barnawal et al., 2014; Trivedi et al., 2020).

Research has revealed that the bacteria isolated from saline soil, such as *Enterobacter*, *Pseudomonas*, *Arthrobacter*, *Bacillus*, *Chryseobacterium*, *Achromobacter*, and *Ochrobactrum* can enhance plant growth under saline conditions (Sarkar et al., 2018; Kumar et al., 2021). PGPR can help crops survive adverse environments by increasing their development and growth (Kumar and Verma, 2019; Zubair et al., 2019). PGPR are a unique set of microbes that settle/colonize the surrounding plant rhizosphere and promote plant growth in stressful conditions (Kumar and Verma, 2018; Singh et al., 2020). Plant–microbe interactions play a vital role in maintaining soil properties, microbial diversity, and crop productivity under abiotic stresses, including high salinity (Zubair et al., 2019; Kumar et al., 2020b). Several PGPR have been reported worldwide to improve plant growth and development in salt and natural environments (Mukherjee et al., 2019).

The current study aimed to conduct genetic screening and expression analysis to better understand the genetic potential and physiological characteristics of *Bacillus* spp., which enable them to tolerate salt stress. The *Bacillus* spp. were used in the present study to evaluate their potential in alleviating the

Abbreviations: ACC, 1-Aminocyclopropane-1-carboxylate; APX, Ascorbate peroxidase; CAT, Catalase; DCFH-DA, Sichloro-dihydro-fluorescein diacetate; DEGs, Differentially expressed genes; LB, Luria Bertani; OD, Optical density; PBS, Phosphate buffered solution; PCoA, Principal coordinate analysis; PCR, Polymerase chain reaction; PGP, Plant growth promotion; PGPB, Plant growth-promoting bacteria; PGPR, Plant growth-promoting rhizobacteria; POD, Peroxidase; ROS, Reactive oxygen species; SOD, Superoxide dismutase.

unfavorable effects of salt stress in rice plants, which showed resistance by regulating their metabolic process under salt stress conditions. The *Bacillus* strains NMTD17 and GBSW22 were found to have a significant PGP ability that enhanced growth and alleviated salt stress on rice plants by regulating salt stress response and plant growth hormones under stress environment. Furthermore, the analysis of relative clusters and structural composition of rhizosphere bacterial clusters through 16S rRNA gene sequencing revealed that the NMTD17 inoculation increased the relative abundance and richness of rhizobacterial species.

Materials and methods

Screening of bacterial strains under salt stress

The *Bacillus* strains used in this study were isolated in our laboratory from rhizosphere soil of different plants collected from the Qinghai–Tibetan Plateau, China (Wu et al., 2019). Four strains, *Bacillus* spp. NMTD17, *Bacillus safensis* GBSW22, *Bacillus pumilus* NMSW10, and *Bacillus velezensis* GBSW11 were tested for their growth promotion and salt resistance potential along with model biocontrol strain *B. velezensis* FZB42 as a control on Luria Bertani (LB) agar plates containing various salt (NaCl) concentrations, i.e., 1, 4, 7, 9, 11, 13, and 16%, maintained at 37°C for 4 days (d). The selected strains were then grown in liquid culture to determine their growth pattern *via* the spectrophotometer in terms of optical density (OD_{600}) at different time intervals at 37°C for 4 days. The growth curves at various time intervals were used to determine the growth pattern of each strain. The experiment trial was repeated three times.

Biofilm formation assay under salt stress

The formation of biofilm by microorganisms is an essential feature from which it is possible to analyze their binding to the surface of roots for different functions in their community (Chaves et al., 2020). The selected strains were grown on LB liquid culture in order to know the effect of various salt concentrations on biofilm formation. To achieve an $OD_{600} = 1.0$, 4 µl, the selected salt-tolerant strains were grown in 20 ml flasks at 37°C. Each bacterial strain was cultured in LB with various salt concentrations, and the resulting mixture was poured onto cluster plates of costar® sterile 12-well cell culture. The cluster plates were tightly closed with parafilm and kept at 37°C for 4 days. A confocal laser scanning microscope (Confocal Microscope Zeiss LSM 780, Japan) was used to evaluate the influence of various salt concentrations on the biofilm formation of each strain. Further, the reactive oxygen species (ROS) were also analyzed under the same conditions (see details in Supplementary material).

RNA extraction and qPCR

The RNA isolation kit (OMEGA Bio-tek, Inc. Norcross, GA, United States) was used to extract the RNA from different samples as described in (Supplementary material). The sequence of each gene was taken from NCBI, followed by designing primers *via* the primer Quest tool listed in Supplementary Table S1. The *rpsJ* gene was used as a housekeeping gene in *Bacillus* strains, as previously used by Zubair et al. (2019). The cDNA of each sample was used in qPCR to check the gene expression profile. The expression profile of these genes (Supplementary Table S1) in salt-tolerant strains was measured through qPCR [Quant Studio Real-Time Thermocycler (Thermo Fisher Scientific, San Jose, CA, United States)]. The qPCR was programmed with the initial temperature of denaturation 95°C for 30 s, including 40 cycles of 95°C for 5 and 34 s for 60°C. The relative expression levels of the genes were calculated by the method of $2^{-\Delta\Delta CT}$ as reported by (Ayaz et al., 2021).

Vigor index and root morphology analysis under salt stress

The effect of salt stress on the germination and growth of rice seedlings was calculated by measuring the vigor index as the formula described by Rasul et al. (2019). The seedlings were then removed from each treatment to measure different root parameters to study the root morphology. The rhizoscanner (EPSON Perfection V700 Photo, Epson America, Long Beach, CA, United States) and WinRHIZO software given by Regent Instruments Co (Sainte-Foy, Quebec, Canada) were used to measure root morphological parameters as described by Rasul et al. (2019). (Detailed description in Supplementary material).

Salt stress alleviation and plant growth promotion by *Bacillus* strains

The soil was sterilized at 180°C for 30 min and stored in a controlled cold room at 4°C for further use. Seven days old rice seedlings were transplanted into similar-sized pots filled with sterilized soil and kept in a controlled environment in the greenhouse. The PGPR cell cultures [NMTD17, GBSW22, and FZB42 grown overnight to OD_{600} of 1.0 (1×107 cfu/ml)] were added into the respective pots. After 1 day, 20 ml salt solutions with various concentrations (0, 100, 150, and 200 mmol) were applied to inoculated PGPR strains and un-inoculated only salt in rice plants. The simple ddH_2O was used for plants grown as a control (CK). Each treatment was performed in triplicate with three rice seedlings in each pot. After 9 days of inoculation, the effect of salt stress was observed for each treatment. The growth parameters, i.e., fresh/dry weights were measured, and the root morphological parameters were analyzed. The data were used as an indication of growth promotion traits. (See details in Supplementary material).

Determination of antioxidant enzyme activity

Various stress response parameters were analyzed for bacterial inoculated and control plants in the salt stress environments, for example, catalase (CAT), peroxidase (POD), ascorbate peroxidase (APX), and superoxide dismutase (SOD) 9 days of post-inoculation (dpi) followed by the method of Ayaz et al. (2021). Briefly, fresh leaf samples of 0.3 g were ground in a phosphate buffered solution (PBS) of pH 7.8 and 1 mM EDTA in an ice bath, followed by centrifugation for 30 min and 12,000 rpm at 4°C. Enzyme extracts were made from the supernatant using ddH_2O as a control. The absorbance activity was recorded at 240 nm for CAT, 470 nm for POD, 560 nm for SOD, and 290 nm for APX, and ddH_2O was used as a control. The commercial kit (Nanjing Jiancheng Bioengineering Institute, China) was used to determine the APX concentrations.

RNA extraction and gene expression analysis

To find the relative expression of the above salt stress response parameters, the genes *Ossamdc2*, *Osdreb1f*, *Oserebp2*, *Oslea3-1*, *Oserf104*, and *Oscyp89g1*, and the actin gene *OS03G0836000* were used. For this, the selected gene sequences were taken from NCB1, followed by designing primers through the PrimerQuest tool; primers are listed in Supplementary Table S2. For RNA extraction, the fresh leaves of plants were harvested from PGPR inoculated plants grown in a salt environment for 7 days using the TRizole method. The Applied Biological Materials Inc. (abm®, Beijing, China) 5× All-In-One RT Master Mix (with AccuRT Genomic DNA Removal Kit) kit was used for cDNA synthesis. The qPCR was performed to analyze the expression profile of selected genes in rice plants through Quant Studio Real-Time Thermocycler (Thermo Fisher Scientific, San Jose, CA, United States). The PCR machine was programmed using the following steps: i.e., initial denaturation at 95°C for 30 s, including 40 cycles of 95°C for 5 s, and 34 s at 60°C. Finally, relative quantification was performed according to the comparative C method of $2^{-\Delta\Delta CT}$ as described by (Liang et al., 2022).

DNA extraction, 16Sr DNA gene sequencing, and bioinformatics analyses

Rhizosphere soil samples were collected from PGPR inoculated and un-inoculated rice plants grown under various salt treatments (0, 100, 150, and 200 mmol). The genomic DNA was isolated using the applied protocol TIANamp Soil DNA Kit [TIANGEN Biotech (Beijing) Co., Ltd.]. The V5–V7 bacterial portions of the 16S rRNA gene were amplified using primers (799F: AACMGGATTAGATACCCKG, and 1193R: ACGTCATCCCCACCTTCC), as described in Supplementary material. The refined amplicon was combined in equimolar amounts and sequenced with an Illumina MiSeq platform following paired-end pairing (2 × 300) according to Meige Biotechnology Co., Ltd. (Guangzhou, China) standard protocols (Illumina, San Diego, CA, United States). The fastq-formatted sequences were processed and analyzed using QIIME2 (ver. 2022.01). Sequence read quality, denoising, and filtering were examined by following the procedure of Han et al. (2020). Briefly, fastq-formatted sequences with primers, quality scores < 28, and read length < 300 bp were removed. The diversity metrics of within-sample (alpha-diversity; Observed, Shannon, Chao1, ACE, and Simpson index) and between samples (β-diversity; Bray-Curtis matrix) were calculated using the R package vegan (version 2.1). Spearman's correlation coefficients were used to find correlations among the bacterial community at the genus level with growth promotion and plant antioxidant activity parameters.

Statistical analyses

All the experiments were carried out in a completely randomized design. The data were expressed in ± standard deviations (SD) of three replicates ($n = 3$). The means were calculated using Tukey's HSD test at $p \leq 0.05$ after ANOVA. IBM SPSS Statistics 21.0 was used to conduct all statistical analyses of the data. The graphical illustrations were made with Origin graphical and analysis software (Version 2022, OriginLab Corporation, Northamptom, MA, United States).

Results

Bacterial growth screening under various salt concentrations

The PGPR strains isolated from harsh environments were screened for their growth potential under different salt concentrations (1, 4, 7, 9, 11, 13, and 16%) on LB medium along with a known salt-sensitive *B. venzelisis* FZB42 strain. Most of the strains, including FZB42 and GBSW22 were able to grow on LB medium containing up to 11% salt concentration. The strain NMTD17 was able to grow up to 13 and 16%, showing the highest resistance under salt stress conditions compared to control (Figure 1). All three strains were then grown in LB liquid medium containing the same salt concentrations (1–16%) as mentioned above, and the growth pattern of each strain was evaluated through OD_{600} calculation at 600 nm by using a spectrophotometer. The OD_{600} was calculated at different time intervals, and growth parameters were noted, which showed that the growth curve for strain NMTD17 continuously increased in a linear method up to 96 h (Figure 1). The salt-tolerant strain NMTD17 exhibited the highest growth at 16% salt treatment, followed by GBSW22. In comparison, the growth curve of FZB42 showed a non-significant growth pattern at 16% post-inoculation up to 96 h.

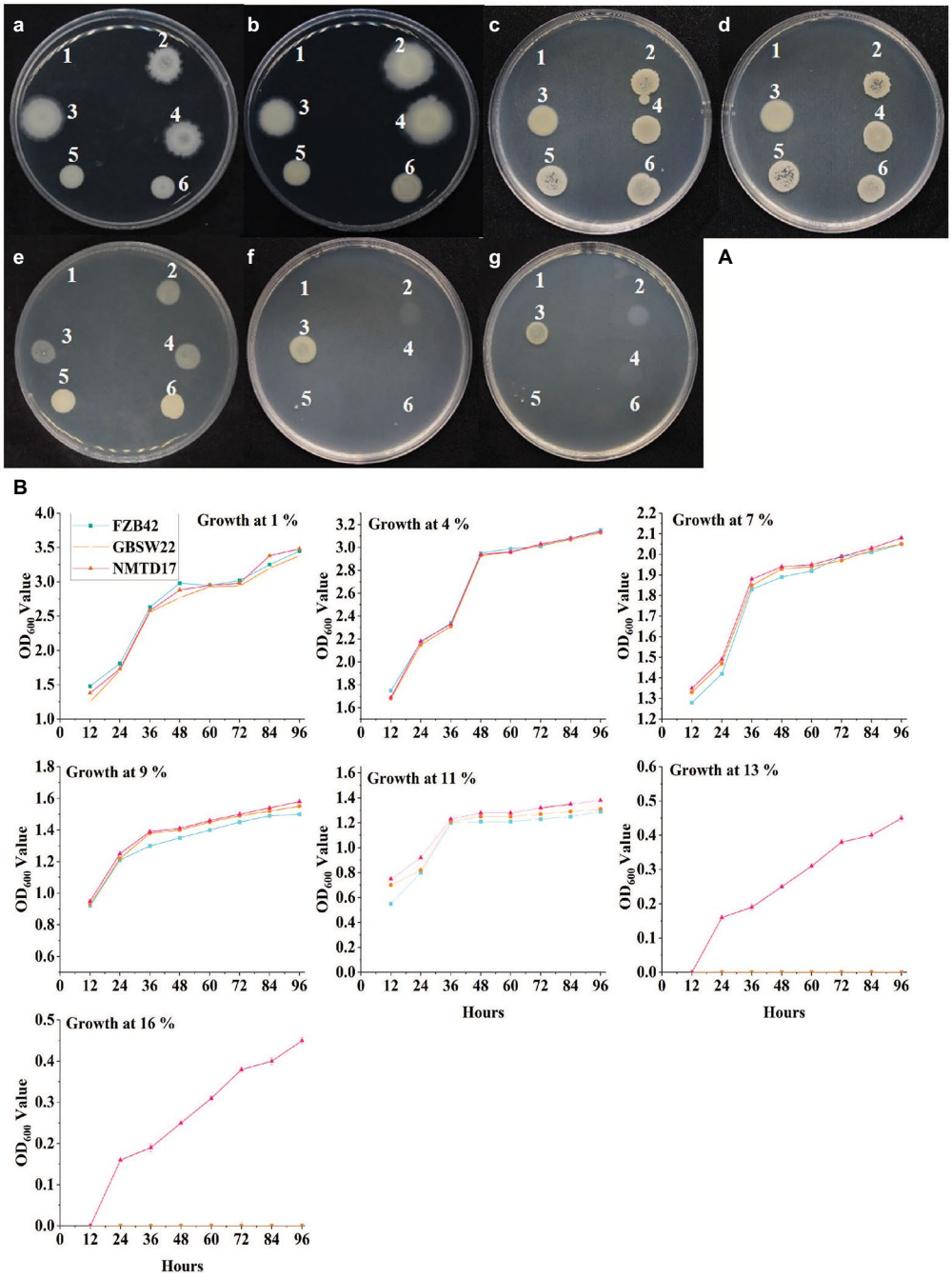

FIGURE 1
The *Bacillus* spp. grown on LB media with salt stress incubated for 96h at 30°C. **(A)** The growth of strains on solid LB media with different salt concentrations (a-g represent 1, 4, 7, 9, 11, 13, and 16%, respectively). Each number showing *Bacillus* strain: (1) CK, (2) FZB42, (3) NMTD17, (4) GBSW22, (5) NMSW10 and (6) GBSW11. **(B)** The graphical representation of the optical density of each strain at the same salt concentrations (1 to 16%) at different time intervals measured by spectrophotometer.

Biofilm formation assay under salt stress and ROS production

The results of the three strains' biofilm-forming capabilities under various saline environments (1, 4, 7, 9, 11, 13, and 16%) at 37°C with multiple time intervals up to 96h exhibited that all three strains were able to form the finest biofilm structure up to 11% salt concentration. However, the potential of FZB42 to make biofilm at 11% was reduced and finished under high saline conditions of 13–16% up to 96h (Figure 2A). NMTD17 was observed to be the strong strain to form biofilm continuously up to 16% and enclosed the full well surface at 96h after inoculation, followed by GBSW22. The strains FZB42 and GBSW22 were unable to generate appreciable biofilm structure at 16% salt

concentration at 96 h after inoculation. In addition, selected strains were grown in 16% LB media at 37°C for 4 days to determine their ROS levels. The data showed that salt-tolerant strains NMTD17 and GBSW22 sustained lower levels of ROS-stained cells observed under the microscope. Whereas the strain FZB42 exhibited a considerable rise in the amount of ROS production when grown in the same conditions (Figure 2B).

Relative expression profiling of predicted genes through qPCR

The expression profile of important genes involved in salt resistance was studied in NMTD17, GBSW22 and FZB42 grown in various salt treatments (1, 7, 11, 13, and 16%) for 4 days. The results showed a linear up-regulation in the expression of salt-resistant genes in NMTD17 and GBSW22 as compared with control. The relative expression of salt-resistant genes in FZB42 was observed up to 11% salt treatment. However, by increasing saline conditions, i.e., 13 and 16%, FZB42 was unable to exhibit the expression of salt-resistant genes (Figure 3). The high expression of selected salt-resistant genes was noticed in NMTD17 followed by GBSW22 in linear order by increasing salt treatment from "11% to 13 and 16%." The genes (*DegU* and *DegS*) involved in the signal transduction pathway mitigating stress response also revealed elevated expression levels for NMTD17 and GBSW22 strains. The responsible superoxide dismutase genes (*SodA* and *SodB*) were noticed to be highly expressed in respective treatments under saline conditions. The glycine betaine genes (*OpuAC* and *OpuD*) responsible for osmotic stress were

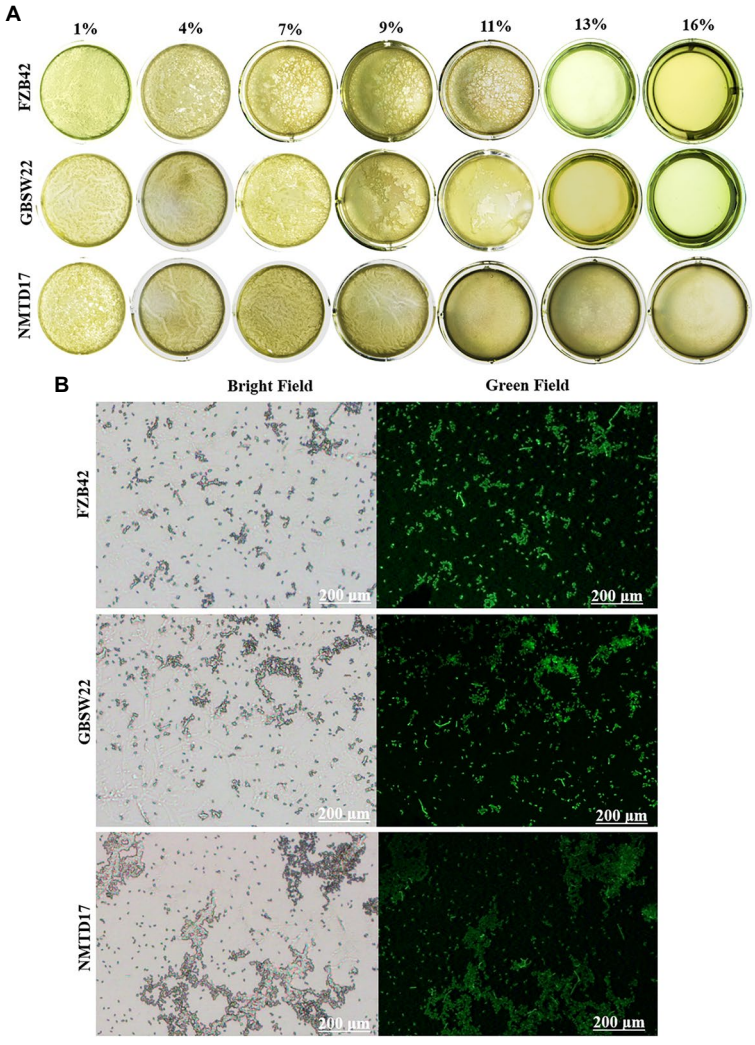

FIGURE 2
The biofilm formation of *Bacillus* strains grown under different salt conditions (1, 4, 7, 9, 11, 13, and 16%) up to 96h at 37°C. The biofilm formation ability was observed in selected *Bacillus* strains **(A)**. The higher amount of green fluorescence in the FZB42 strain cultured for 4days at 37°C indicates a higher quantity of reactive oxygen species (ROS). When compared to GBSW22 and FZB42, the reduced fluorescence indicates that NMTD17 cells produce less ROS **(B)**.

10.3389/fpls.2022.994902

also increased in NMTD17, followed by GBSW22 under salt conditions. The *HPII* gene playing an important role in catalase regulation under saline conditions, was observed to be highly expressed in NMTD17. The high expression of the *ComA* gene involved in quorum-sensing regulation, was also observed in NMTD17 and GBSW22. The overall results exhibited that all the selected salt-resistant genes showed a significant relative expression level in high salt-resistant strains, as shown in Figure 3.

Seedling growth and root morphological parameters

The inoculation of selected strains promoted seedling development and root morphological factors under different saline conditions (0, 100, 150, and 200 mmol). The seedling growth in vigor index (VI), which is a measure of total germination (%) and total length of seedlings, which was found to be highest in rice seedlings treated with NMTD17

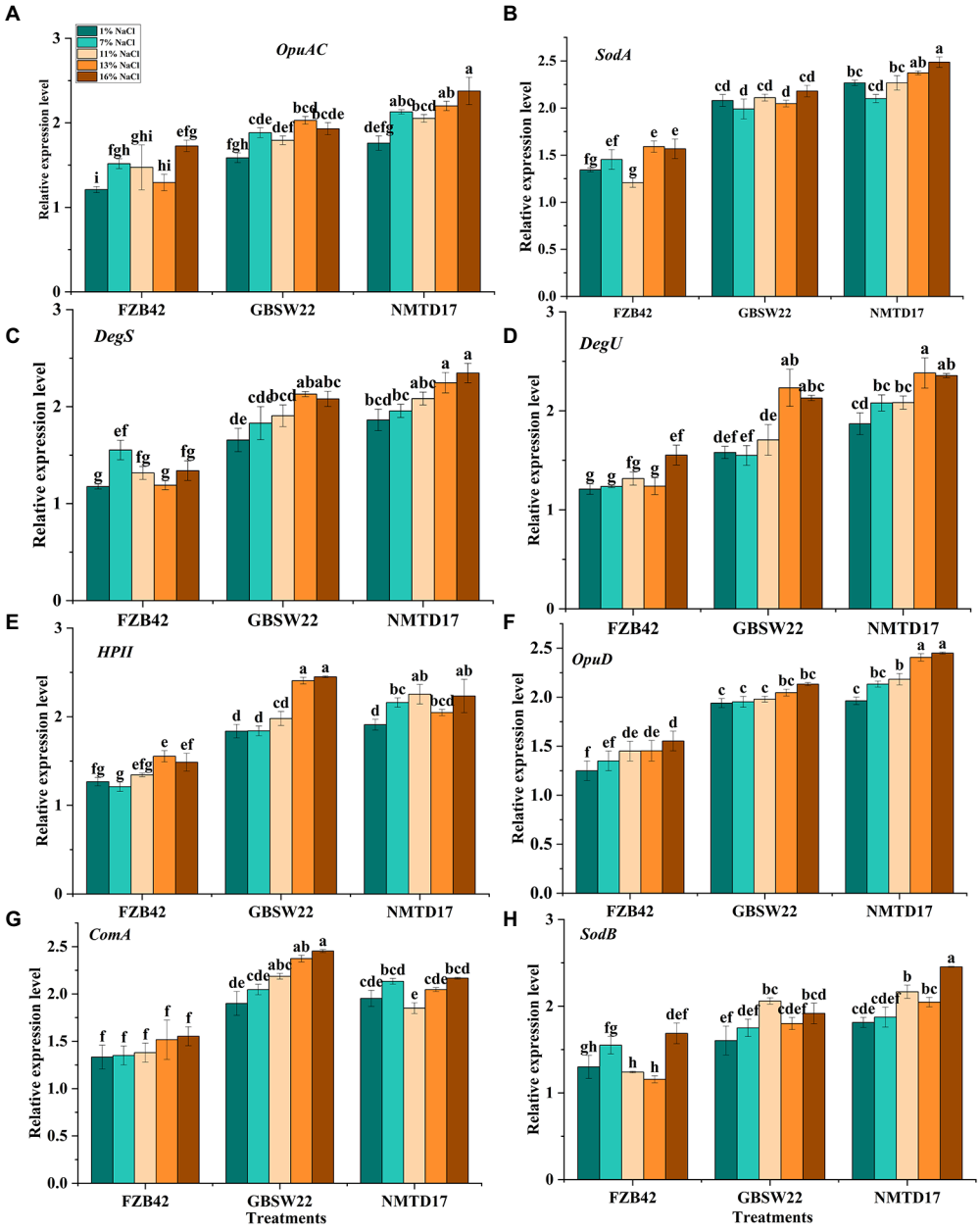

FIGURE 3
Relative expression levels of various *Bacillus* strains grown under salt and normal conditions for 96h. **(A)** *OpuAC,* **(B)** *SodB,* **(C)** *DegS,* **(D)** *DegU,* **(E)** *HPII,* **(F)** *OpuD,* **(G)** *ComA,* and **(H)** *SodA*. Vertical bars on graphs indicate the standard deviation of the mean (n=3). Tuckey's HSD test was used to recognize a significant difference at $p \leq 0.05$ between the treatments.

(VI = 1,210) under high saline conditions (200 mmol) that was significantly greater than control, as well as GBSW22 and FZB42 treatments as shown in Supplementary Figure S1. Seedlings inoculated with GBSW22 showed moderate VI (VI = 1,157) growth under 200 mmol saline conditions. At normal condition (0 mmol), the rice seedlings inoculated with all selected *Bacillus* strains NMTD17, GBSW22, and FZB42 demonstrated the significant VI (VI = 1,211, 1,157, and 1,153 respectively) as compared to control (Supplementary Figure S1).

Furthermore, root morphological analysis revealed that the root morphological parameters were significantly improved under control and salt stress treatments when inoculated with selected strains. However, NMTD17 exhibited the highest impact on seedling root morphology, such as root volume, area, length, diameter, and number of root tips under high salt stress (200 mmol) compared to control seedlings grown under the same condition. When compared to the control under normal conditions (0 mmol), seedlings treated with all three bacterial strains significantly improved root morphological factors (Supplementary Figure S2).

Furthermore, the seedling and plant root morphology, including total root length, root tips, volume, diameter, and surface area were analyzed. PGPR strain NMTD17 increased plant root morphological parameters by 2–3-fold as compared to controls plants. Root diameter, surface area, and tips were increased significantly in the case of NMTD17-inoculated plants, followed by the plants inoculated with GBSW22 and FZB42 (Supplementary Figure S3). Thus, the strain NMTD17 was found to be more effective at reducing the risk of high salt stress treatment (200 mmol) compared to GBSW22 and FZB42.

The growth of rice plants under salt stress

The plant growth promotion characteristics showed significant improvements under both normal and salt stress conditions when inoculated with PGPR strains. As mentioned in above findings, the strain NMTD17 exerted the highest impact on plant growth parameters, i.e., plant shoot length and fresh and dry weight were significantly increased by NMTD17 under salt stress compared to control plants (Supplementary Figure S4). Plants inoculated with GBSW22 showed substantial growth improvement as well, whereas FZB42-inoculated plants were unable to tolerate high salt stress (200 mmol). In normal conditions, i.e., 0 mmol, the selected strains significantly enhanced shoot length and fresh and dry weight of rice plants in comparison to the control. Whereas no significant difference was found among the selected strains for different growth-promoting factors. Moreover, the increase in salt stress condition, i.e., 100–200 mmol negatively affected the growth of un-inoculated rice plants. The NMTD17 presented the most beneficial effect on rice seedlings by alleviating the negative effect of increased saline condition. The overall data showed that the loss caused by salt toxicity in rice plants was observed to be alleviated in the presence of selected strains NMTD17 and GBSW22 (Supplementary Figure S4).

Antioxidant enzymes activity under salt stress in rice plants

The increased soil salinity effectively modulates the microbial community, plant enzyme activity, and soil health. Thus, the antioxidant activity of different enzymes (POD, CAT, SOD, and APX) was examined in rice plants grown under different salt concentrations. The bacterial-inoculated rice plants had higher POD activity than the control plants under salt treatment. The POD activity increased by 20.22, 45.35, and 50.45% with FZB42, GBSW22, and NMTD17, respectively, in salt-stressed plants. It increased 10.45, 15.39, and 20.85% with FZB42, GBSW22, and NMTD17, respectively, in the control plants, as shown in Supplementary Figure S5a. The inoculated plants exhibited higher SOD activity as compared to control plants. Compared to control, the SOD activity was increased by 25.75, 45.46, and 52.68% in inoculated plants under salt stress, followed by 12.25, 20.65, and 35.34% with FZB42, GBSW22, and NMTD17, respectively, in control plants without salt stress (Supplementary Figure S5c). The activity of CAT was increased due to salt stress in rice plants, and it was greater under the salt condition as compared to the control. The plants inoculated with FZB42, GBSW22, and NMTD17 showed higher CAT activity 25.36, 35.75, and 55.57%, respectively, as compared to control plants followed by 15.65, 18.36, 20.45%, respectively, compared to control plants as shown in Supplementary Figure S5b. Similarly, the activity of APX increased due to salt stress in rice plants, where the inoculated plants showed higher APX activity as compared to control plants under salt stress. The APX activity was increased by 45.25, 50.63, and 58.35% in inoculated plants and 13.36, 15.45, and 19.68% in control plants for FZB42, GBSW22, and NMTD17, respectively (Supplementary Figure S5d). In general, the results revealed that as the salt concertation was increased in rice plants, the antioxidant activity was significantly enhanced with bacterial inoculation as compared to control conditions (Supplementary Figure S5).

Relative gene expression analysis

The relative expression profiling of various differentially expressed genes (DEGs) related to salt stress, including *Ossamdc2*, *Osdreb1f*, *Oserebp2*, *Oslea3-1*, *Oserf104*, and *Oscyp89g1* was observed to be highly stimulated in inoculated rice plants under salt stress. We observed that DEG expression levels under various salt circumstances were not the same as that of the control rice plants. After salt treatment, the plants treated with the highly halophilic strain NMTD17 showed the highest up-regulation of all the six salt stress-responsive genes, followed by GBSW22 and FZB42 compared to control plants (Figure 4). The 4–5-fold up-regulation of these genes was found in rice plants inoculated

with NMTD17 grown under high salt stress conditions as compared to control plants. In addition, GBSW22 exhibited the higher expression of these genes, followed by FZB42. It was observed that the rice plants inoculated with halophilic strains NMTD17 and GBSW22 showed higher expression of salt stress-related DEGs under saline conditions, which might play important roles in rice tolerance to high salinity.

Microbial community associated with rice rhizosphere

The relative abundance of the dominant bacterial community in inoculated and non-inoculated rice rhizosphere was determined using Illumina sequencing and the 16S ribosomal-RNA (rRNA) sequencing method. At the phylum level, the classification of the high-quality fragments revealed changes in bacterial communities among the selected treatments (Figure 5). A total of 28 bacterial phyla were found across all samples: the twelve with a relative abundance > 1.0%, as shown in Figure 5A. *Proteobacteria* was the most prevalent phylum in all treatments, with a relative abundance of 78.26%, *Actinobacteriota* 25.94%, *Bacteroidetes* 7.65%, *Firmicutes* 30.22%, and *Armatimonadetes* 2.33%. Both the inoculated and un-inoculated rice rhizosphere soils showed that *Proteobacteria* was the dominant phylum among all bacterial communities. In addition, the heatmap was constructed, which revealed significant differences in relative abundances of taxa among rice rhizosphere soil samples (Figure 5B). The analysis at the genus level exhibited that the genera *Enhydrobacter*, *Bacillus*, *Hydrocarboniphaga*, *Brenneria*, *Macrococcus*, *Sorangium*, and *Caldicellulosiruptor* were highly abundant in control. Whereas the genera *Burkholderia*, *Luteibacter*, *Bosea*, *Shimia*, *Pseudoclavibacter*, *Nocardiopsis*, *Mesorhizobium*, *Cryocola*, *Rhodococcus*, and *Actintobacter* had a high abundance in inoculated followed by *Streptococcus*, *Paenibacillus*, *Emiticicia*, *Niastella*, and *Propionispora* in un-inoculated soil. The data revealed that a high abundance of genera was found in inoculated and un-inoculated rice rhizosphere soil under salt stress as compared to control.

Diversity matrix of bacterial community

The evaluation of the α-diversity of rhizosphere bacterial community among each treatment showed significant differences in microbial diversity. The alpha-diversity and beta-diversity, such as Observed index, Shannon index, Simpson index, Chao1 index, and ACE diversity of the microbial community in rhizosphere soil isolated from inoculated and un-inoculated treatments were observed. The outcomes revealed a significant difference in the microbial community in inoculated, un-inoculated, and control rhizosphere soils (Figures 6A–E). Significant variances were also observed for the rhizobacterial community from rice rhizosphere soil treated with different salt concentrations. These findings suggested that the rhizospheric bacterial community diversity and relative abundance of the bacterial microbiomes within the rhizosphere might be influenced by salt stress. Besides, in inoculated rhizosphere soil, the bacterial community increased due to *Bacillus* strain NMTD17, which is highly resistant to salt stress. To validate these outcomes, the Venn diagram was used to compare and contrast the bacterial communities of all treatments based on operational taxonomic units (OUTs; Figure 6F). The overall number of common OTUs was 276, accounting for 48.25% of all OTUs detected (i.e., 1,375). The shared OTUs indicated that microbial community existed in all respective treatments.

Principal coordinate analysis (PCoA) and correlation of bacterial communities with plant growth promotion

To understand more details, we conducted the Bray–Curtis distance metrics using principal coordinate analysis (PCoA), which indicated the differences in microbial communities of inoculated and un-inoculated rice rhizosphere soil (Figure 7A). The inoculated and un-inoculated rhizosphere soil in rice showed a similar microbial community structure. However, the inoculated rhizosphere soil was separated according to salt concentration level. The results demonstrated that the samples with an inoculated and un-inoculated rhizosphere soil were separated as compared to control due to salt stress, indicating that microbial communities and structural sequence were different in inoculated and un-inoculated rhizosphere soil.

The relative abundances of dominating bacteria at the genus levels were calculated using Spearman's correlation coefficients, and growth promotion parameters were identified at the jointing stage. The dominating bacteria, rice growth and antioxidant activity displayed a general positive or negative correlation. In inoculated and un-inoculated rice rhizosphere soil, relative abundances of *Streptococcus*, *Paenibacillus*, *Propionispora*, *Rhizobium Couchioplanes*, and *Niastella* at the genus level were positively correlated ($p < 0.05$) with rice growth promotion and enzymatic activity (Figure 7B).

Discussion

Salinity stress is one of the important abiotic factors affecting growth and production of crops, including rice, which necessitates appropriate sustainable agricultural management (Akram et al., 2019; Kumar et al., 2021). Many plant growth-promoting rhizosphere bacteria are known to mitigate the hazardous effects of abiotic stresses, including salinity and heavy metals through a variety of direct and indirect processes and eventually enhance crop development and yield (Choudhary, 2012; Hussain et al., 2019). However, the effectiveness of PGPR in reducing plant salt stress in plants has yet to be completely investigated. Therefore, in the present study, the *Bacillus* strains were screened for salt tolerance *in vitro* and the prospective salt-tolerant PGPR strains

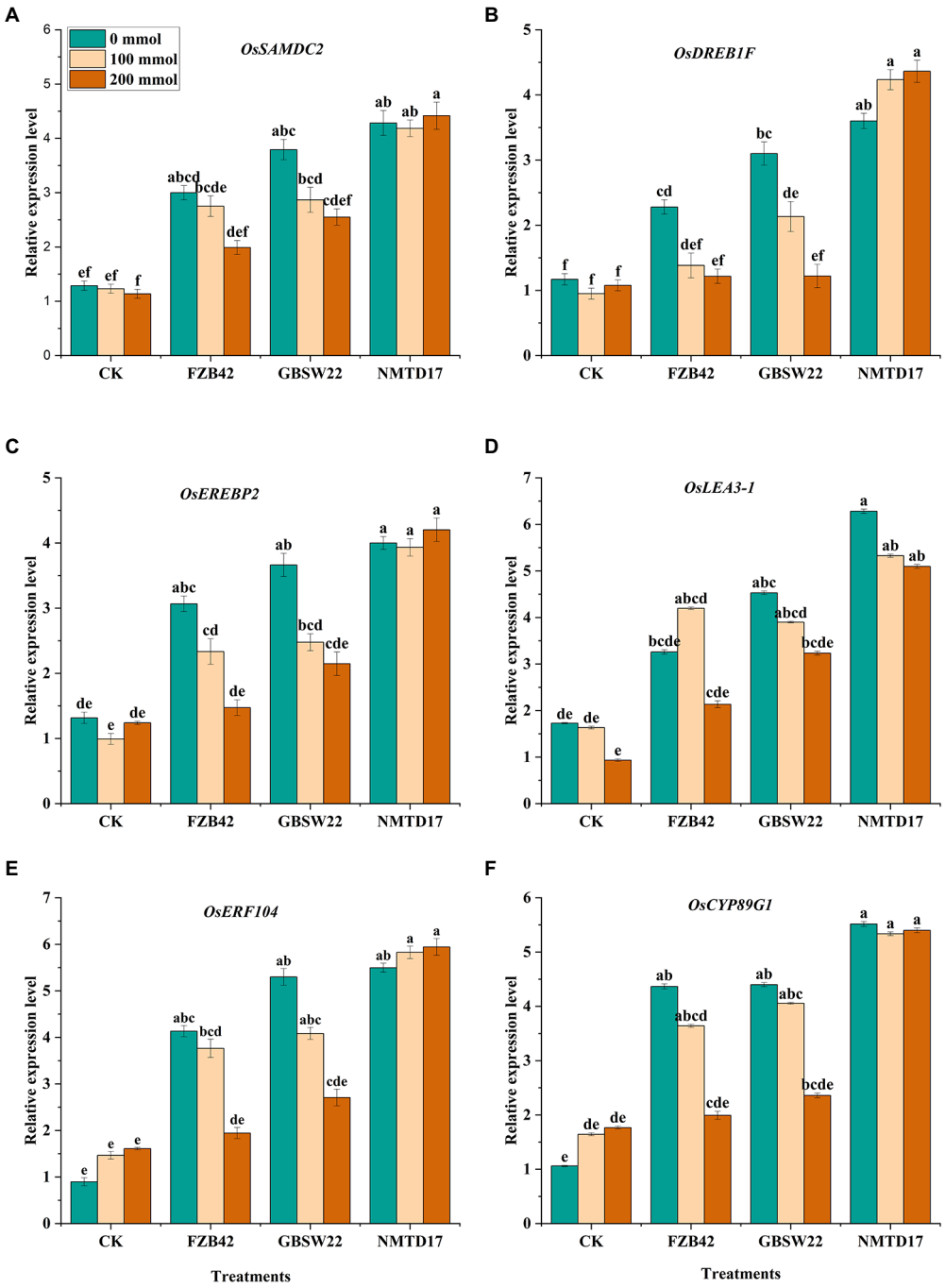

FIGURE 4
Relative expression levels of six possible DEGs in inoculated and un-inoculated rice plants under salt stress and control conditions **(A)** *Ossamdc2,* **(B)** *Osdreb1f,* **(C)** *Oserebp2,* **(D)** *Oslea3-1* **(E)** *Oserf104,* **(F)** *Oscyp89g1*. The rice plants were subjected to different treatments. Vertical bars on graphs indicate the standard deviation of the mean (n=3). Tuckey's HSD test was used to recognize a significant difference at $p \leq 0.05$ between the treatments.

with desired traits were then employed in soil–plant systems under salt stress conditions. The growth curves at different time intervals up to 96 h of growth indicate the high potential of these strains against salt stress (Figure 1). Among these, the NMTD17 strain exhibited a higher potential to grow at a high salt concentration (16%) as compared to GBSW22 and FZB42. Previously reported PGPR strain FZB42 was also used that could effectively grow up to 11% at salt stress conditions but failed to grow as the concentration was increased from 13 to 16% (Wu et al., 2019).

The role of PGPR in biofilm formation in rhizosphere soil and root surface colonization is being increasingly recognized as a key

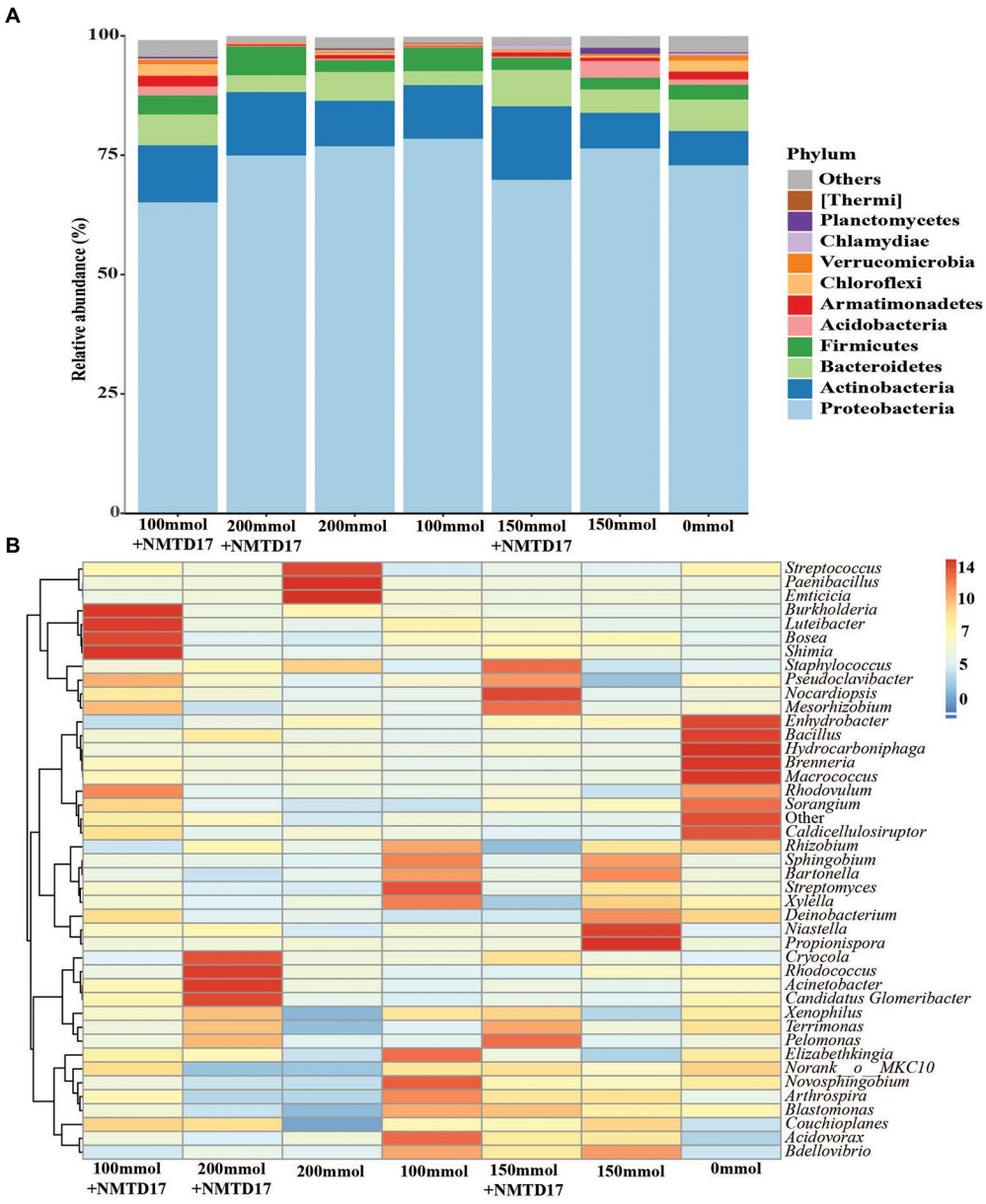

FIGURE 5
Taxonomic composition of the microbial communities in different inoculated and un-inoculated rice rhizosphere soils. **(A)** Microbial compositions at the phylum level. **(B)** Heatmap of compositions showing 43 microbial communities at the genus level.

feature for successful survival mechanisms (Ansari and Ahmad, 2018; Abbas et al., 2019). Biofilm is a collection of bacteria in a self-secreted environment that allows bacterial colonies to exist and produce secondary metabolites in extreme environments (Marsden et al., 2017). After 4 days' inoculation in LB media, the maximum biofilm formation was found in NMTD17 under salt stress, whereas GBSW22 and FZB42 developed biofilm structures up to 11% saline condition, and it lost biofilm ability as the salt concentration was raised from 13 to 16% (Figure 2A). Research has reported that bacterial biofilm structures are distorted under stress (Feldman et al., 2016), but there is very little evidence of biofilm development under severe salt stress conditions. The halophilic PGPR strains employed in the present study exhibited a unique biofilm-forming ability that allows them to persist and generate the essential metabolites under salt stress. This characteristic is related to the bacterial ability to colonize plant roots and help them cope with salt stress. In addition, ROS are dominant free oxy-radicals that can be generated in response to biotic and abiotic stresses (Ramu et al., 2016; Ayaz et al., 2021). The selected bacterial strains were cultured under salt conditions for 96 h. The salt-sensitive strain FZB42 produced the high ROS, as demonstrated by green fluorescence emitted by the bacterial cells, showing a higher level of cellular disruption (Figure 2). In contrast, the NMTD17 and GBSW22 strains produced the least

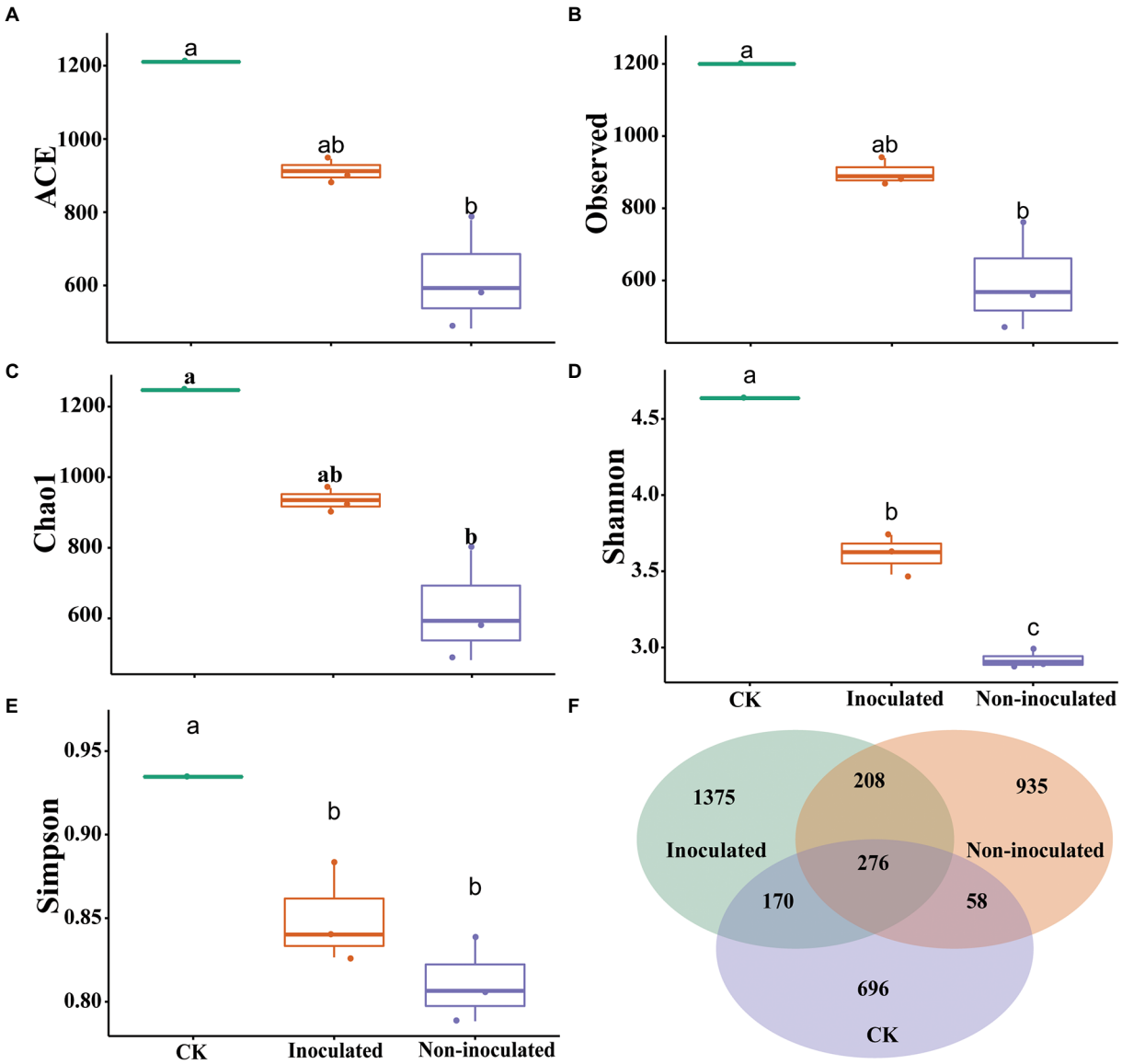

FIGURE 6
Analysis of the bacterial communities in various inoculated and un-inoculated rice rhizosphere soils. The box diagram of alpha- and beta-diversity of the inoculated and un-inoculated rice rhizosphere soil in groups **(A)** ACE, **(B)** Observed value, **(C)** Chao1 index, **(D)** Shannon index, **(E)** Simpson index, **(F)** Venn diagram of bacterial communities of different inoculated and inoculated rice rhizosphere soils in groups based on OTUs.

ROS labeled cells, showing that these strains can withstand salt stress agreeing to (Zubair et al., 2019).

Furthermore, important genes involved in membrane transport, lipid metabolism, fatty acid regulation, and cell signaling, as well as those involved in combating salt stress were analyzed to compare their expression in FZB42, GBSW22, and NMTD17. The following genetic characteristics have a significant influence on abiotic stress tolerance in bacteria that have already been examined (Allen et al., 2009; Zubair et al., 2019). Under salt treatments, the expression level of genes associated with salt stress tolerance in all three *Bacillus* strains revealed an up-regulation of selected genes in PGPR strain NMTD17 and GBSW22, which might be a key cause of growth capacity to survive in high salinity conditions. The expression of all these genes decreased in FZB42 as salt concentration was increased, which might be the reason for its inability to survive in high salt concentrations. The expression level of the quorum-sensing regulator gene *ComA*, which acts as a transcriptional activator for several significant physiological responses in bacteria, also helps salt-tolerant strains survive under salt stress conditions (Dogsa et al., 2014). The signal transduction pathway genes (*DesS* and *DegU*) had higher expression levels in NMTD17 and GBSW22, suggesting that these genes can change the response to abiotic stress or a changing environment. This is consistent with the previous finding that these genes play a significant role in the

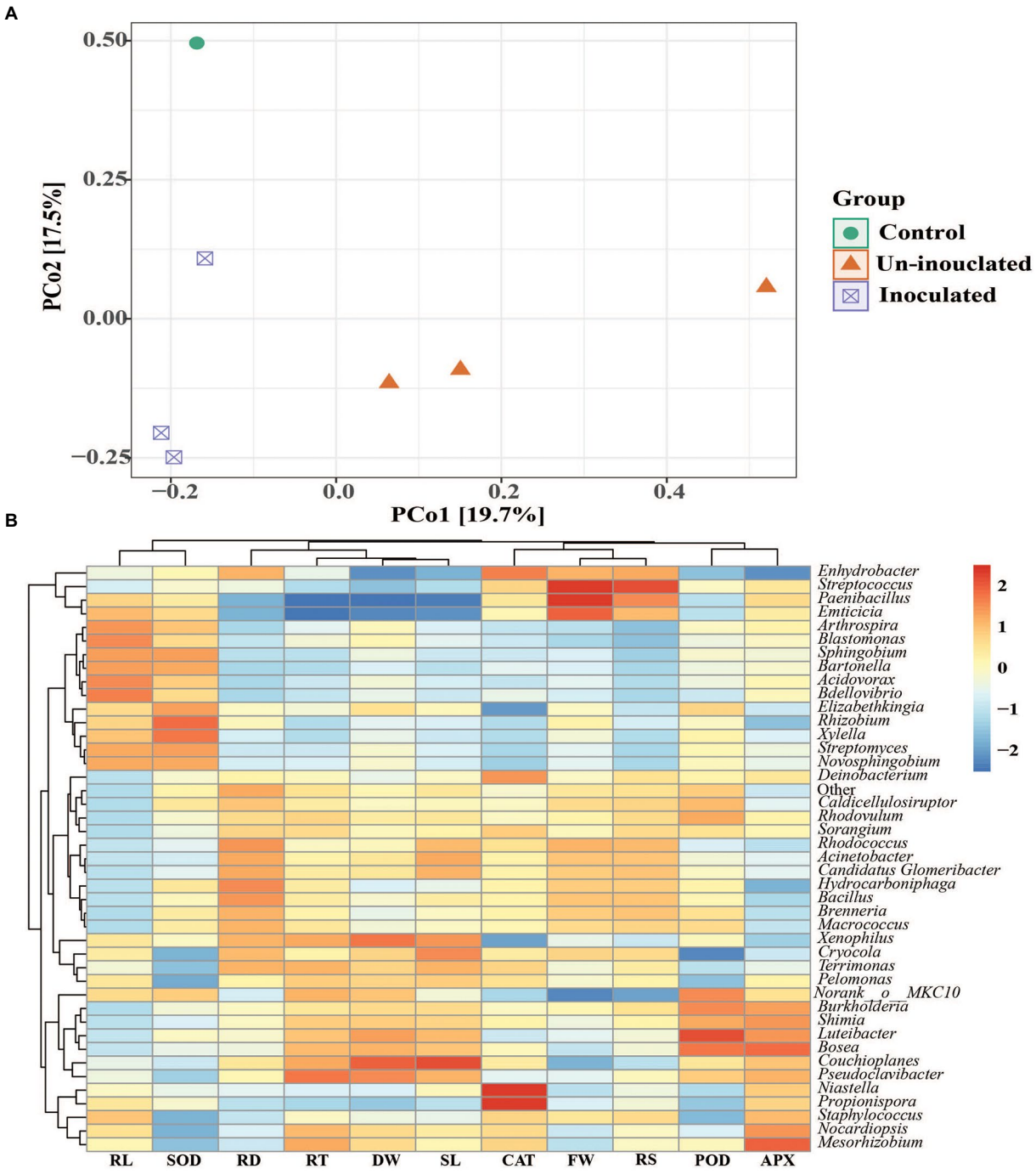

FIGURE 7
(A) The Principal coordinate analysis (PCoA) ordinations of bacterial community composition based on total OTUs using the Bray–Curtis matrix from the rhizosphere of rice under inoculated and un-inoculated plants. **(B)** Spearman's correlation coefficients between the relative abundance of dominant bacterial community at genera level with plant growth and antioxidant activity parameters. Root length (RL), superoxide dismutase (SOD), Root diameter (RD), Root tips (RT), Dry weight (DW), Shoot length (SL), catalase (CAT), Fresh weight (FW), Root surface (RS), Peroxidase (POD), ascorbate peroxidase (APX).

Bacillus Pumilus 7P strain under salt stress (Helmann et al., 2003). When these genes are overexpressed in NMTD17 and GBSW22, the strains are better able to perceive and detect the salt stress signal, but FZB42 only minimally increases the expression of these genes growing under high salt stress conditions. Glycine betaine encoding genes (*OpuD* and *OpuAC*) are key osmo-protectants and are involved in osmotic stress management. In NMTD17, the *OpuAC* gene revealed the greatest expression level (4-fold), followed by GBSW22 (Figure 3). Our results are agreeing by the fact that these

transcription features are active in response to abiotic stress (Helmann et al., 2003).

We also analyzed different plant growth attributes, such as root length, dry weight, fresh weight, height, antioxidant enzymes, and microbial quantity. In general, plant growth characteristics reduced as the salt concentration in control plants was increased. However, compared with the control, the plant growth attributes of the inoculated plants were significantly enhanced (Supplementary Figure S4), as supported by (Zhang et al., 2018; Ansari et al., 2019). Salt stress has been linked to an imbalance in plant nutrition and osmosis, resulting in lower growth and photosynthesis (Khan et al., 2019). The application of the *Bacillus* NMTD17 strain proved that it could restore normal physiological characteristics more effectively, followed by GBSW22 and FZB42 as compared to control in rice plants under salt stress. Similarly, Zhang et al. (2018) described the restoration of plant physiological functions through bacterial inoculation.

The use of PGPR to enhance plant development has received much attention because PGPR can help plants grow better under stress conditions (Etesami and Maheshwari, 2018; Li et al., 2020). Inoculating *Pseudomonas* sp. into pea plants under drought stress has been observed to promote the development of pea plants (Sarkar et al., 2018). Similarly, in the present study, the PGPR *Bacillus* strains NMTD17 and GBSW22 improved rice plant development under salt stress *via* increasing seed vigor index (Supplementary Figures S1, S2). Under normal conditions, the selected PGPR strains showed the highest results for all seedling growth promotion factors, but this is the first report of the FZB42 strain having no significant effect on plant development when exposed to high salt (200 mmol). However, it is well proven that *Pseudomonas* and *Bacillus* strains have a favorable influence on seedling and young plant vigor index and root morphological characteristics (Rasul et al., 2019; Kumar et al., 2021). However, we found a significant difference in the root morphological and vigor index factors of rice seedlings and rice plants under salt stress after inoculation with highly halophilic *Bacillus* strains NMTD17 and GBSW22. The fresh and dry weight of root and shoot length of inoculated plants increased significantly under salt stress when compared to control plants (Supplementary Figure S3), which is in accordance with (Ansari and Ahmad, 2018; Abbas et al., 2019).

The outcomes of this investigation clearly reveal that plants treated with *Bacillus* strains have significantly increased the activity of antioxidant enzymes (Supplementary Figure S5). Under salinity stress, the studies have discovered that bacterially inoculated plants have higher antioxidant enzyme activity (CAT, SOD, POD, and APX) than control plants (Narayanasamy et al., 2020; Kumar et al., 2021). The findings of this study demonstrate that as the concentration of NaCl in rice plants increased, antioxidative enzyme activities like CAT and SOD were also increased (Numan et al., 2018; Mubeen et al., 2022). Increased NaCl content was closely associated with higher antioxidant enzyme activity in rice (Khan et al., 2017; Numan et al., 2018). Plants have evolved an enzymatic defense mechanism to alleviate the effects of salt stress. The findings imply that at greater NaCl doses, increased antioxidant activity is necessary to protect plants from oxidative stress caused by salt stress (Li et al., 2020).

Furthermore, stress-related genes were also studied to explain the improved resistance to salt stress. Using qRT-PCR, we confirmed the expression levels of six genes, including *Ossamdc2*, *Osdreb1f*, *Oserebp2*, *Oslea3-1*, *Oserf104*, and *Oscyp89g1* (Figure 4). The NMTD17 and GSW22 strains upregulated the expression levels of *Oscyp89g1* and *Oserf104* genes, which are members of the *CPY* and *ERF* families and may be crucial in stress-related responses (Yao et al., 2018; Yu et al., 2018; Zhang et al., 2020). Through binding to the DRE/CRT element (G/ACCGAC), the transcription factor gene *Osdreb1f* has been found to increase rice salt tolerance by promoting the expression of many stress-related genes (Wang et al., 2008). A transcription factor that regulates a receptor-like kinase gene *Oserebp2*, which is a negative regulator of the NaCl stress response, was found to be involved in rice NaCl tolerance (Serra et al., 2013). S-adenosylmethionine decarboxylase and stress-induced protein kinase genes were encoded by *Ossamdc2*. The ROS scavenging pathway of these genes was postulated to be implicated in rice salt tolerance (Ouyang et al., 2010; Shah et al., 2021). The relative expression level further supports our findings that *Bacillus* strains have the ability to regulate the genes mentioned above under salt stress. We confirm that the *Bacillus* strains NMTD17 and GSW22 can alleviate salt toxicity in rice by owning genes that also improve growth and regulate the expression level of stress-responsive genes and improve plant development under salt stress.

Numerous studies have shown that the PGPR application can strongly impact the bacterial community (Song et al., 2021). In the current study, the *Proteobacteria*, *Actinobacteriota*, *Bacteroidetes*, *Firmicutes*, *Armatimonadetes*, *Chloroflexi*, and *Acidobacteriia* were the dominant microbial communities in the rice rhizosphere soil (Figure 5), which is consistent with earlier findings (Chen et al., 2021a,b). Our findings revealed that PGPR inoculation could change the rhizobacterial communities (Figure 6), which agree with the previous study (Hu et al., 2020). The rhizobacterial populations were changed after the inoculation of PGPR. The differences in rhizobacterial communities between the inoculated and non-inoculated treatments as well as control, were correlated to growth promotion in a linear method (Figure 7). As a result, the PGPR effect on rhizobacterial populations was typically beneficial to plants, as demonstrated by earlier investigations (Li et al., 2021; Taye et al., 2022). At the genus level, *Streptococcus*, *Paenibacillus*, *Propionispora Rhizobium Couchioplanes*, and *Niastella* showed higher abundance following PGPR inoculation. According to previous research, these taxa were favorably correlated with growth traits and antioxidant activities (Chen et al., 2021b). These bacterial communities are common in plant rhizosphere soil and have the ability to improve plant growth (Kielak et al., 2016; Gu et al., 2020; Chen et al., 2021a). *Bacillus* is the most common member of the *Bacilli* class that has long been employed in microbial fertilizers to boost crop growth and disease resistance (Ali et al., 2021c). Plants have been

shown to be protected from abiotic conditions (including cold, salt, and drought) and to have improved nutrition, vigor, and yield when inoculated with *Arthrobacter* and *Bacillus* (Krishnan et al., 2016; Zubair et al., 2019). These findings imply that PGPR inoculation can lead to rhizosphere communities with other beneficial microorganisms (Li et al., 2021).

Conclusion

The current study discovered that biofilm-forming *Bacillus* strains are resistant to salt stress and have a variety of biological and physiological features that help them cope with salt stress. In comparison to control plants, those treated with bacteria (*Bacillus* strains NMTD17 and GBSW22) demonstrated higher rice plant growth and antioxidant enzyme activity. Biochemical and physiological characteristics were also discovered to play a significant role as a marker of salt stress and can be utilized to determine the efficacy of new bacterial inoculants. Furthermore, inoculation of PGPR strain NMTD17 improved species richness and rhizobacterial abundance, as well as enriched the relative abundances of beneficial bacteria in rice rhizosphere soil. Furthermore, the beneficial effects of *Bacillus* strains in saline environments must be tested in large-scale field trials before they can be used in sustainable agriculture.

Data availability statement

The datasets generated for this study can be found in NCBI public database. All sequences of 16S *rRNA* genes can be found in Sequence Read Archive (SRA) under BioSample accession no. PRJNA862745.

Author contributions

QA: conceptualization, investigation, methodology, formal analysis, writing—original draft, and validation. QY, YX and CY: methodology and formal analysis. GM, QG, and HW: validation, investigation, and writing—review and editing. MA, AH, and HM: validation, methodology, and formal analysis. XG: conceptualization, supervision, validation, project administration, and writing—review and editing. All authors contributed to the article and approved the submitted version.

Funding

This work was supported by the Guidance Foundation of the Sanya Institute of Nanjing Agricultural University (NAUSY-MS18), Fundamental Research Funds for the Central Universities (KYZZ2022001), and the Key Project of NSFC regional innovation and development joint fund (U20A2039).

Conflict of interest

GM was employed by Shenzhen Batian Ecotypic Engineering Co., Ltd.

The remaining authors declare that the research was conducted in the absence of any commercial or financial relationships that could be construed as a potential conflict of interest.

Publisher's note

Supplementary material

The Supplementary material for this article can be found online at: https://www.frontiersin.org/articles/10.3389/fpls.2022.994902/full#supplementary-material

References

Abbas, R., Rasul, S., Aslam, K., Baber, M., Shahid, M., Mubeen, F., et al. (2019). Halotolerant PGPR: a hope for cultivation of saline soils. *J. King Saud Univ.* 31, 1195–1201. doi: 10.1016/j.jksus.2019.02.019

Akram, W., Aslam, H., Ahmad, S. R., Anjum, T., Yasin, N. A., Khan, W. U., et al. (2019). Bacillus megaterium strain A12 ameliorates salinity stress in tomato plants through multiple mechanisms. *J. Plant Interact.* 14, 506–518. doi: 10.1080/17429145.2019.1662497

Ali, M., Ahmad, Z., Ashraf, M. F., and Dong, W. (2021a). Maize endophytic microbial-communities revealed by removing PCR and 16S rRNA sequencing and their synthetic applications to suppress maize banded leaf and sheath blight. *Microbiol. Res.* 242:126639. doi: 10.1016/j.micres.2020.126639

Ali, Q., Ahmar, S., Sohail, M. A., Kamran, M., Ali, M., Saleem, M. H., et al. (2021c). Research advances and applications of biosensing technology for the diagnosis of pathogens in sustainable agriculture. *Environ. Sci. Pollut. Res.* 28, 9002–9019. doi: 10.1007/s11356-021-12419-6

Ali, M., Ali, Q., Sohail, M. A., Ashraf, M. F., Saleem, M. H., Hussain, S., et al. (2021b). Diversity and taxonomic distribution of Endophytic bacterial Community in the Rice Plant and its Prospective. *Int. J. Mol. Sci.* 22:10165. doi: 10.3390/ijms221810165

Ali, Q., Ayaz, M., Yu, C., Wang, Y., Gu, Q., Wu, H., et al. (2022). Cadmium tolerant microbial strains possess different mechanisms for cadmium biosorption and immobilization in rice seedlings. *Chemosphere* 303:135206. doi: 10.1016/j.chemosphere.2022.135206

Allen, M. A., Lauro, F. M., Williams, T. J., Burg, D., Siddiqui, K. S., De Francisci, D., et al. (2009). The genome sequence of the psychrophilic archaeon, *Methanococcoides burtonii*: the role of genome evolution in cold adaptation. *ISME J.* 3, 1012–1035. doi: 10.1038/ismej.2009.45

Ansari, F. A., and Ahmad, I. (2018). Plant growth promoting attributes and alleviation of salinity stress to wheat by biofilm forming *Brevibacterium* sp. FAB3 isolated from rhizospheric soil. *Saudi J. Biol. Sci.* doi: 10.1016/j.sjbs.2018.08.003

Ansari, F. A., Ahmad, I., and Pichtel, J. (2019). Growth stimulation and alleviation of salinity stress to wheat by the biofilm forming Bacillus pumilus strain FAB10. *Appl. Soil Ecol.* 143, 45–54. doi: 10.1016/j.apsoil.2019.05.023

Ayaz, M., Ali, Q., Farzand, A., Khan, A. R., Ling, H., and Gao, X. (2021). Nematicidal volatiles from bacillus atrophaeus gbsc56 promote growth and stimulate induced systemic resistance in tomato against meloidogyne incognita. *Int. J. Mol. Sci.* 22:5049. doi: 10.3390/ijms22095049

Barnawal, D., Bharti, N., Maji, D., Chanotiya, C. S., and Kalra, A. (2014). ACC deaminase-containing Arthrobacter protophormiae induces NaCl stress tolerance through reduced ACC oxidase activity and ethylene production resulting in improved nodulation and mycorrhization in *Pisum sativum*. *J. Plant Physiol.* 171, 884–894. doi: 10.1016/j.jplph.2014.03.007

Bistgani, Z. E., Hashemi, M., DaCosta, M., Craker, L., Maggi, F., and Morshedloo, M. R. (2019). Effect of salinity stress on the physiological characteristics, phenolic compounds and antioxidant activity of *Thymus vulgaris* L. and thymus daenensis Celak. *Ind. Crop. Prod.* 135, 311–320. doi: 10.1016/j.indcrop.2019.04.055

Chaves, S., Longo, M., López, A. G., del V Loto, F., Mechetti, M., and Romero, C. M. (2020). Control of microbial biofilm formation as an approach for biomaterials synthesis. *Colloids Surf.* 194:111201. doi: 10.1016/j.colsurfb.2020.111201

Chen, L., Hao, Z., Li, K., Sha, Y., Wang, E., Sui, X., et al. (2021a). Effects of growth-promoting rhizobacteria on maize growth and rhizosphere microbial community under conservation tillage in Northeast China. *Microb. Biotechnol.* 14, 535–550. doi: 10.1111/1751-7915.13693

Chen, L., Li, K., Shang, J., Wu, Y., Chen, T., Wanyan, Y., et al. (2021b). Plant growth–promoting bacteria improve maize growth through reshaping the rhizobacterial community in low-nitrogen and low-phosphorus soil. *Biol. Fertil. Soils* 57, 1075–1088. doi: 10.1007/s00374-021-01598-6

Choudhary, D. K. (2012). Microbial rescue to plant under habitat-imposed abiotic and biotic stresses. *Appl. Microbiol. Biotechnol.* 96, 1137–1155. doi: 10.1007/s00253-012-4429-x

Compant, S., Samad, A., Faist, H., and Sessitsch, A. (2019). A review on the plant microbiome: ecology, functions, and emerging trends in microbial application. *J. Adv. Res.* 19, 29–37. doi: 10.1016/j.jare.2019.03.004

Daliakopoulos, I. N., Tsanis, I. K., Koutroulis, A., Kourgialas, N. N., Varouchakis, A. E., Karatzas, G. P., et al. (2016). The threat of soil salinity: a European scale review. *Sci. Total Environ.* 573, 727–739. doi: 10.1016/j.scitotenv.2016.08.177

Dogsa, I., Choudhary, K. S., Marsetic, Z., Hudaiberdiev, S., Vera, R., Pongor, S., et al. (2014). ComQXPA quorum sensing systems may not be unique to Bacillus subtilis: a census in prokaryotic genomes. *PLoS One* 9:e96122. doi: 10.1371/journal.pone.0096122

Dubey, A., Kumar, A., Abd-Allah, E. F., Hashem, A., and Khan, M. L. (2019). Growing more with less: breeding and developing drought resilient soybean to improve food security. *Ecol. Indic.* 105, 425–437. doi: 10.1016/j.ecolind.2018.03.003

Etesami, H., and Glick, B. R. (2020). Halotolerant plant growth–promoting bacteria: prospects for alleviating salinity stress in plants. *Environ. Exp. Bot.* 178:104124. doi: 10.1016/j.envexpbot.2020.104124

Etesami, H., and Maheshwari, D. K. (2018). Use of plant growth promoting rhizobacteria (PGPRs) with multiple plant growth promoting traits in stress agriculture: action mechanisms and future prospects. *Ecotoxicol. Environ. Saf.* 156, 225–246. doi: 10.1016/j.ecoenv.2018.03.013

Feldman, M., Ginsburg, I., Al-Quntar, A., and Steinberg, D. (2016). Thiazolidinedione-8 alters symbiotic relationship in *C. albicans*-S. mutans dual species biofilm. *Front. Microbiol.* 7:140. doi: 10.3389/fmicb.2016.00140

Gu, Y., Dong, K., Geisen, S., Yang, W., Yan, Y., Gu, D., et al. (2020). The effect of microbial inoculant origin on the rhizosphere bacterial community composition and plant growth-promotion. *Plant Soil* 452, 105–117. doi: 10.1007/s11104-020-04545-w

Han, Q., Ma, Q., Chen, Y., Tian, B., Xu, L., Bai, Y., et al. (2020). Variation in rhizosphere microbial communities and its association with the symbiotic efficiency of rhizobia in soybean. *ISME J.* 14, 1915–1928. doi: 10.1038/s41396-020-0648-9

Hassan, A., Amjad, S. F., Saleem, M. H., Yasmin, H., Imran, M., Riaz, M., et al. (2021). Foliar application of ascorbic acid enhances salinity stress tolerance in barley (*Hordeum vulgare* L.) through modulation of morpho-physio-biochemical attributes, ions uptake, osmo-protectants and stress response genes expression. Saudi. *J. Biol. Sci.* 28, 4276–4290. doi: 10.1016/j.sjbs.2021.03.045

Helmann, J. D., Wu, M. F. W., Gaballa, A., Kobel, P. A., Morshedi, M. M., Fawcett, P., et al. (2003). The global transcriptional response of Bacillus subtilis to peroxide stress is coordinated by three transcription factors. *J. Bacteriol.* 185, 243–253. doi: 10.1128/JB.185.1.243-253.2003

Hu, D., Li, S., Li, Y., Peng, J., Wei, X., Ma, J., et al. (2020). Streptomyces sp. strain TOR3209: a rhizosphere bacterium promoting growth of tomato by affecting the rhizosphere microbial community. *Sci. Rep.* 10, 1–15. doi: 10.1038/s41598-020-76887-5

Hubbard, C. J., Li, B., McMinn, R., Brock, M. T., Maignien, L., Ewers, B. E., et al. (2019). The effect of rhizosphere microbes outweighs host plant genetics in reducing insect herbivory. *Mol. Ecol.* 28, 1801–1811. doi: 10.1111/mec.14989

Hussain, A., Amna, K. M. A., Javed, M. T., Hayat, K., Farooq, M. A., Ali, N., et al. (2019). Individual and combinatorial application of *Kocuria rhizophila* and citric acid on phytoextraction of multi-metal contaminated soils by Glycine max L. *Environ. Exp. Bot.* 159, 23–33. doi: 10.1016/j.envexpbot.2018.12.006

Ke, J., Wang, B., and Yoshikuni, Y. (2020). Microbiome engineering: synthetic biology of plant-associated microbiomes in sustainable agriculture. *Trends Biotechnol.* 39, 244–261. doi: 10.1016/j.tibtech.2020.07.008

Khan, M. A., Asaf, S., Khan, A. L., Adhikari, A., Jan, R., Ali, S., et al. (2019). Halotolerant rhizobacterial strains mitigate the adverse effects of NaCl stress in soybean seedlings. *Biomed. Res. Int.* 2019, 1–15. doi: 10.1155/2019/9530963

Khan, W. U., Yasin, N. A., Ahmad, S. R., Ali, A., Ahmed, S., and Ahmad, A. (2017). Role of Ni-tolerant bacillus spp. and *Althea rosea* L. in the phytoremediation of Ni-contaminated soils. *Int. J. Phytoremediation* 19, 470–477. doi: 10.1080/15226514.2016.1244167

Kielak, A. M., Cipriano, M. A. P., and Kuramae, E. E. (2016). Acidobacteria strains from subdivision 1 act as plant growth-promoting bacteria. *Arch. Microbiol.* 198, 987–993. doi: 10.1007/s00203-016-1260-2

Kong, M., Sheng, T., Liang, J., Ali, Q., Gu, Q., Wu, H., et al. (2021). Melatonin and its homologs induce immune responses via receptors trP47363-trP13076 in *Nicotiana benthamiana*. *Front. Plant Sci.* 12:691835. doi: 10.3389/fpls.2021.691835

Korenblum, E., Dong, Y., Szymanski, J., Panda, S., Jozwiak, A., Massalha, H., et al. (2020). Rhizosphere microbiome mediates systemic root metabolite exudation by root-to-root signaling. *Proc. Natl. Acad. Sci.* 117, 3874–3883. doi: 10.1073/pnas.1912130117

Krishnan, R., Menon, R. R., Tanaka, N., Busse, H.-J., Krishnamurthi, S., and Rameshkumar, N. (2016). *Arthrobacter pokkalii* sp nov, a novel plant associated actinobacterium with plant beneficial properties, isolated from saline tolerant pokkali rice, Kerala, India. *PLoS One* 11:e0150322. doi: 10.1371/journal.pone.0150322

Kumar, V., Kumar, P., and Khan, A. (2020b). Optimization of PGPR and silicon fertilization using response surface methodology for enhanced growth, yield and biochemical parameters of French bean (*Phaseolus vulgaris* L.) under saline stress. *Biocatal. Agric. Biotechnol.* 23:101463. doi: 10.1016/j.bcab.2019.101463

Kumar, A., Singh, S., Gaurav, A. K., and Srivastava, S. (2020a). Plant growth-promoting bacteria: biological tools for the mitigation of salinity stress in plants. *Front. Microbiol.* 11:1216. doi: 10.3389/fmicb.2020.01216

Kumar, A., Singh, S., Mukherjee, A., Rastogi, R. P., and Verma, J. P. (2021). Salt-tolerant plant growth-promoting Bacillus pumilus strain JPVS11 to enhance plant growth attributes of rice and improve soil health under salinity stress. *Microbiol. Res.* 242:126616. doi: 10.1016/j.micres.2020.126616

Kumar, A., and Verma, J. P. (2018). Does plant—microbe interaction confer stress tolerance in plants: a review? *Microbiol. Res.* 207, 41–52. doi: 10.1016/j.micres.2017.11.004

Kumar, A., and Verma, J. P. (2019). "The role of microbes to improve crop productivity and soil health," in *Ecological Wisdom Inspired Restoration Engineering*. eds. V. Achal and A. Mukherjee (Berlin: Springer), 249–265.

Kumar, A., Vyas, P., Malla, M. A., and Dubey, A. (2019). Taxonomic and functional annotation of termite degraded (lam.) Kuntze (flame of the Forest). *Open Microbiol. J.* 13, 154–163. doi: 10.2174/1874285801913010154

Li, X., Sun, P., Zhang, Y., Jin, C., and Guan, C. (2020). A novel PGPR strain Kocuria rhizophila Y1 enhances salt stress tolerance in maize by regulating phytohormone levels, nutrient acquisition, redox potential, ion homeostasis, photosynthetic capacity and stress-responsive genes expression. *Environ. Exp. Bot.* 174:104023. doi: 10.1016/j.envexpbot.2020.104023

Li, Y., Wang, M., and Chen, S. (2021). Application of N2-fixing Paenibacillus triticisoli BJ-18 changes the compositions and functions of the bacterial, diazotrophic, and fungal microbiomes in the rhizosphere and root/shoot endosphere of wheat under field conditions. *Biol. Fertil. Soils* 57, 347–362. doi: 10.1007/s00374-020-01528-y

Liang, Z., Ali, Q., Wang, Y., Mu, G., Kan, X., Ren, Y., et al. (2022). Toxicity of *Bacillus thuringiensis* strains derived from the novel crystal protein Cry31Aa with high nematicidal activity against rice parasitic nematode *Aphelenchoides besseyi*. *Int. J. Mol. Sci.* 23:8189. doi: 10.3390/ijms23158189

Liu, H., Brettell, L. E., Qiu, Z., and Singh, B. K. (2020). Microbiome-mediated stress resistance in plants. *Trends Plant Sci.* 25, 733–743. doi: 10.1016/j.tplants.2020.03.014

Manghwar, H., Hussain, A., Ali, Q., and Liu, F. (2022). Brassinosteroids (BRs) role in plant development and coping with different stresses. *Int. J. Mol. Sci.* 23:1012. doi: 10.3390/ijms23031012

Marsden, A. E., Grudzinski, K., Ondrey, J. M., DeLoney-Marino, C. R., and Visick, K. L. (2017). Impact of salt and nutrient content on biofilm formation by Vibrio fischeri. *PLoS One* 12:e0169521. doi: 10.1371/journal.pone.0169521

Mengistu, A. A. (2020). Endophytes: colonization, behaviour, and their role in defense mechanism. *Int. J. Microbiol.* 2020, 1–8. doi: 10.1155/2020/6927219

Mubeen, S., Shahzadi, I., Akram, W., Saeed, W., Yasin, N. A., Ahmad, A., et al. (2022). Calcium nanoparticles impregnated with benzenedicarboxylic acid: a new approach to alleviate combined stress of ddt and cadmium in brassica alboglabra by modulating bioacummulation, antioxidative machinery and osmoregulators. *Front. Plant Sci.* 13:825829. doi: 10.3389/fpls.2022.825829

Mukherjee, A., Gaurav, A. K., Singh, S., Chouhan, G. K., Kumar, A., and Das, S. (2019). Role of potassium (K) Solubilising microbes (KSM) in growth and induction of resistance against biotic and abiotic stress in plant: a book review. *Clim. Chang. Environ. Sustain.* 7, 212–214.

Mukherjee, A., Singh, B. K., and Verma, J. P. (2020). Harnessing chickpea (Cicer arietinum L.) seed endophytes for enhancing plant growth attributes and bio-controlling against *Fusarium* sp. *Microbiol. Res.* 237:126469. doi: 10.1016/j.micres.2020.126469

Narayanasamy, S., Thangappan, S., and Uthandi, S. (2020). Plant growth-promoting bacillus sp. cahoots moisture stress alleviation in rice genotypes by triggering antioxidant defense system. *Microbiol. Res.* 239:126518. doi: 10.1016/j.micres.2020.126518

Numan, M., Bashir, S., Khan, Y., Mumtaz, R., Shinwari, Z. K., Khan, A. L., et al. (2018). Plant growth promoting bacteria as an alternative strategy for salt tolerance in plants: a review. *Microbiol. Res.* 209, 21–32. doi: 10.1016/j.micres.2018.02.003

Ouyang, S., Liu, Y., Liu, P., Lei, G., He, S., Ma, B., et al. (2010). Receptor-like kinase OsSIK1 improves drought and salt stress tolerance in rice (*Oryza sativa*) plants. *Plant J.* 62, 316–329. doi: 10.1111/j.1365-313X.2010.04146.x

Ramu, V. S., Paramanantham, A., Ramegowda, V., Mohan-Raju, B., Udayakumar, M., and Senthil-Kumar, M. (2016). Transcriptome analysis of sunflower genotypes with contrasting oxidative stress tolerance reveals individual- and combined-biotic and abiotic stress tolerance mechanisms. *PLoS One* 11:e0157522. doi: 10.1371/journal.pone.0157522

Rasul, M., Yasmin, S., Zubair, M., Mahreen, N., Yousaf, S., Arif, M., et al. (2019). Phosphate solubilizers as antagonists for bacterial leaf blight with improved rice growth in phosphorus deficit soil. *Biol. Control* 136:103997. doi: 10.1016/j.biocontrol.2019.05.016

Sarkar, A., Ghosh, P. K., Pramanik, K., Mitra, S., Soren, T., Pandey, S., et al. (2018). A halotolerant *Enterobacter* sp. displaying ACC deaminase activity promotes rice seedling growth under salt stress. *Res. Microbiol.* 169, 20–32. doi: 10.1016/j.resmic.2017.08.005

Serra, T. S., Figueiredo, D. D., Cordeiro, A. M., Almeida, D. M., Lourenço, T., Abreu, I. A., et al. (2013). OsRMC, a negative regulator of salt stress response in rice, is regulated by two AP2/ERF transcription factors. *Plant Mol. Biol.* 82, 439–455. doi: 10.1007/s11103-013-0073-9

Shah, A. A., Aslam, S., Akbar, M., Ahmad, A., Khan, W. U., Yasin, N. A., et al. (2021). Combined effect of Bacillus fortis IAGS 223 and zinc oxide nanoparticles to alleviate cadmium phytotoxicity in Cucumis melo. *Plant Physiol. Biochem.* 158, 1–12. doi: 10.1016/j.plaphy.2020.11.011

Singh, B. K., Trivedi, P., Egidi, E., Macdonald, C. A., and Delgado-Baquerizo, M. (2020). Crop microbiome and sustainable agriculture. *Nat. Rev. Microbiol.* 18, 601–602. doi: 10.1038/s41579-020-00446-y

Solangi, Z. A., Ali, Q., Soomro, Z. A., Saleem, M. H., and Rattar, T. M. (2021). Effects of drought stress on morphological, physiological traits of wheat (TriticumAestivumL.) cultivars in Pakistan. *J Plant Physiol Pathol* 93:2.

Song, J., Kong, Z. Q., Zhang, D. D., Chen, J. Y., Dai, X. F., and Li, R. (2021). Rhizosphere microbiomes of potato cultivated under *Bacillus subtilis* treatment influence the quality of potato tubers. *Int. J. Mol. Sci.* 22:12065. doi: 10.3390/ijms222112065

Stassen, M. J. J., Hsu, S.-H., Pieterse, C. M. J., and Stringlis, I. A. (2020). Coumarin communication along the microbiome–root–shoot axis. *Trends Plant Sci.* 26, 169–183. doi: 10.1016/j.tplants.2020.09.008

Sun, A., Jiao, X.-Y., Chen, Q., Wu, A.-L., Zheng, Y., Lin, Y.-X., et al. (2021). Microbial communities in crop phyllosphere and root endosphere are more resistant than soil microbiota to fertilization. *Soil Biol. Biochem.* 153:108113. doi: 10.1016/j.soilbio.2020.108113

Taye, Z. M., Noble, K., Siciliano, S. D., Helgason, B. L., and Lamb, E. G. (2022). Root growth dynamics, dominant Rhizosphere bacteria, and correlation between dominant bacterial genera and root traits through *Brassica napus* development. *Plant Soil* 473, 441–456. doi: 10.1007/s11104-022-05296-6

Trivedi, P., Leach, J. E., Tringe, S. G., Sa, T., and Singh, B. K. (2020). Plant–microbiome interactions: from community assembly to plant health. *Nat. Rev. Microbiol.* 18, 607–621. doi: 10.1038/s41579-020-0412-1

Wang, Q., Guan, Y., Wu, Y., Chen, H., Chen, F., and Chu, C. (2008). Overexpression of a rice OsDREB1F gene increases salt, drought, and low temperature tolerance in both Arabidopsis and rice. *Plant Mol. Biol.* 67, 589–602. doi: 10.1007/s11103-008-9340-6

Wang, Q., Kang, L., Lin, C., Song, Z., Tao, C., Liu, W., et al. (2019). Transcriptomic evaluation of Miscanthus photosynthetic traits to salinity stress. *Biomass Bioenergy* 125, 123–130. doi: 10.1016/j.biombioe.2019.03.005

Wu, H., Gu, Q., Xie, Y., Lou, Z., Xue, P., Fang, L., et al. (2019). Cold-adapted Bacilli isolated from the Qinghai–Tibetan plateau are able to promote plant growth in extreme environments. *Environ. Microbiol.* 21, 3505–3526. doi: 10.1111/1462-2920.14722

Yao, L., Cheng, X., Gu, Z., Huang, W., Li, S., Wang, L., et al. (2018). The AWPM-19 family protein OsPM1 mediates abscisic acid influx and drought response in rice. *Plant Cell* 30, 1258–1276. doi: 10.1105/tpc.17.00770

Yu, S., Huang, A., Li, J., Gao, L., Feng, Y., Pemberton, E., et al. (2018). OsNAC45 plays complex roles by mediating POD activity and the expression of development-related genes under various abiotic stresses in rice root. *Plant Growth Regul.* 84, 519–531. doi: 10.1007/s10725-017-0358-0

Zhang, S., Fan, C., Wang, Y., Xia, Y., Xiao, W., and Cui, X. (2018). Salt-tolerant and plant-growth-promoting bacteria isolated from high-yield paddy soil. *Can. J. Microbiol.* 64, 968–978. doi: 10.1139/cjm-2017-0571

Zhang, X., Long, Y., Huang, J., and Xia, J. (2020). OsNAC45 is involved in ABA response and salt tolerance in rice. *Rice* 13, 1–13. doi: 10.1186/s12284-020-00440-1

Zubair, M., Hanif, A., Farzand, A., Majid, T., and Sheikh, M. (2019). Genetic screening and expression analysis of psychrophilic bacillus spp. Reveal Their Potential to Alleviate Cold Stress and Modulate Phytohormones in Wheat. *Microorganisms* 7:337. doi: 10.3390/microorganisms7090337

frontiers | Frontiers in Plant Science

TYPE Original Research
PUBLISHED 06 September 2022
DOI 10.3389/fpls.2022.982668

OPEN ACCESS

EDITED BY
Aqeel Ahmad,
University of Florida,
United States

REVIEWED BY
Mohammad Faizan,
Maulana Azad National Urdu University,
India
Gholamreza Abdi,
Persian Gulf University,
Iran
Kashif Hayat,
Shanghai Jiao Tong University, China

*CORRESPONDENCE:
Yushuang Guo
yshguo@126.com
Imran Haider Shamsi
drimran@zju.edu.cn

SPECIALTY SECTION
This article was submitted to Plant Symbiotic Interactions, a section of the journal Frontiers in Plant Science

RECEIVED 30 June 2022
ACCEPTED 27 July 2022
PUBLISHED 06 September 2022

CITATION
Sehar S, Feng Q, Adil MF, Sahito FS, Ibrahim Z, Baloch DM, Ullah N, Ouyang Y, Guo Y and Shamsi IH (2022) Tandem application of endophytic fungus *Serendipita indica* and phosphorus synergistically recuperate arsenic induced stress in rice.
Front. Plant Sci. 13:982668.
doi: 10.3389/fpls.2022.982668

Tandem application of endophytic fungus *Serendipita indica* and phosphorus synergistically recuperate arsenic induced stress in rice

Shafaque Sehar[1], Qidong Feng[1], Muhammad Faheem Adil[1], Falak Sehar Sahito[2], Zakir Ibrahim[1,3], Dost Muhammad Baloch[3], Najeeb Ullah[4], Younan Ouyang[5], Yushuang Guo[6]*and Imran Haider Shamsi[1]*

[1]Zhejiang Key Laboratory of Crop Germplasm Resource, Department of Agronomy, College of Agriculture and Biotechnology, Zhejiang University, Hangzhou, China, [2]Dow International Medical College, Dow University of Health Sciences, Karachi, Pakistan, [3]Faculty of Agriculture, Lasbela University of Agriculture, Water and Marine Sciences, Uthal, Pakistan, [4]Faculty of Science, Universiti Brunei Darussalam, Bandar Seri Begawan, Brunei, [5]China National Rice Research Institute (CNRRI), Fuyang, China, [6]Guizhou Academy of Tobacco Science, Guizhou, China

In the context of eco-sustainable acquisition of food security, arsenic (As) acts as a deterring factor, which easily infiltrates our food chain *via* plant uptake. Therefore, devising climate-smart strategies becomes exigent for minimizing the imposed risks. Pertinently, *Serendipita indica* (*S. indica*) is well reputed for its post-symbiotic stress alleviatory and phyto-promotive potential. Management of phosphorus (P) is acclaimed for mitigating arsenic toxicity in plants by inhibiting the uptake of As molecules due to the competitive cationic exchange in the rhizosphere. The current study was designed to investigate the tandem effects of *S. indica* and P in combating As toxicity employing two rice genotypes, i.e., Guodao-6 (GD-6; As-sensitive genotype) and Zhongzhe You-1 (ZZY-1; As-tolerant genotype). After successful fungal colonization, alone and combined arsenic (10 μM L^{-1}) and phosphorus (50 μM L^{-1}) treatments were applied. Results displayed that the recuperating effects of combined *S. indica* and P treatment were indeed much profound than their alone treatments; however, most of the beneficial influences were harnessed by ZZY-1 in comparison with GD-6. Distinct genotypic differences were observed for antioxidant enzyme activities, which were induced slightly higher in *S. indica*-colonized ZZY-1 plants, with or without additional P, as compared to GD-6. Ultrastructure images of root and shoot exhibited ravages of As in the form of chloroplasts-, nuclei-and cell wall-damage with enlarged vacuole area, mellowed mostly by the combined treatment of *S. indica* and P in both genotypes. Gene expression of PHTs family transporters was regulated at different levels in almost all treatments across genotypes. Conclusively, the results of this study validated the promising role of *S. indica* and additional P in mitigating As stress, albeit corroborated that the extent of relevant benefit exploitation is highly genotype-dependent. Verily, unlocking the potential of

nature-friendly solutions will mend the anthropogenic damage already been done to our environment.

KEYWORDS

arsenic toxicity, endophytic fungus, phosphorous nutrition, *Oryza sativa*, antioxidant enzymes, gene expression analysis

Introduction

Rice (*Oryza sativa* L.) stands out among the cereals as the 3rd most commonly cultivated crop across the globe with a production of 211 million metric tons in 2020, spreading across 164.19 m ha (FAOSTAT, 2021). Most concerning, the World Population Prospects report, promulgated by the Department of Economic and Social Affairs (UNDESA, 2019), presents an extensive review of the future global demographic trends/prospects, according to which the world population is expected to reach 9.8 billion in 2050 and the statistical ascension of population size is projected to persist. Unfortunately, the available arable land is actually reducing in size and rice production is under threat due to the heavy metal (HM) pollution (e.g., cadmium, arsenic, lead, etc.), brought about by human activities (Adil et al., 2020a). As a matter of fact, about 1/3rd of the world's cultivable land has been lost due to these reasons in past 4 decades with potentially devastating consequences on the horizon as the global food demand rises exponentially (Ahmad et al., 2014; Delang, 2018). Arsenic toxicity is prevalent in rice production due to the considerable amount of water required for a production cycle (Nagajyoti et al., 2010). Arsenic is an exceptionally harmful and ubiquitous metalloid in the environment that not only has adverse effects on agricultural production, but also on human health. Arsenate (As^{5+}) is the abundant form of arsenic in aerobic environments and promotes plant cell damage *via* oxygen species (ROS) signaling pathways (Zvobgo et al., 2018). Acceptable levels of arsenic set by United States Environmental Protection Agency (USEPA) in soil range from 0.39 to 39 ppm (ATSDR, 2007). Although, the concentration of soil As varies with geographical regions, the global average is about 5 mg kg^{-1}; however, the concentration could reach hundreds or thousands of mg kg^{-1} in contaminated environments (Zhao et al., 2010). Soil samples collected across China's arable soils in 2011 and 2016 revealed that the median As concentration in surface soils was 9.7 mg kg^{-1}; moreover, the total arsenic in the Chinese agricultural surface soils was inventoried to be 3.7×10^6 tons (Zhou et al., 2018). Due to the increasing reports of contamination of As in the soil and water and its potential downstream health risks (Shahzadi et al., 2022), it is reasonable to investigate how As toxicity could be counterbalanced. Therefore, crop scientists have been working round the clock to help find alternatives, researching on sustainable and productivity boosting aspects of agricultural crops around the world (Shah et al., 2021; Ulhassan et al., 2022).

Fortunately, there are some ways to help plants manage As stress; these ways include beneficial microorganisms' interaction with plants and one of the great illustration is *S. indica*, an endophytic fungus with exceptional abilities to promote plant growth indices even in stressful scenarios such as arsenic exposure (Unnikumar et al., 2013). Classified under a rather new fungal family *Sebacinaceae* and new order *Sebacinales* under the phylum *Glomeromycota* (Varma et al., 1999), *S. indica*, (previously known as *Piriformospora indica*), can colonize a wide range of crop and non-crop plants, including but not limited to rice, maize, wheat and barley (Gill et al., 2016). Ever since its discovery, *S. indica* has been the cynosure of many scientific investigations because of its phenomenal potential; Singhal et al. (2017) and Bakshi et al. (2017) have thoroughly reviewed the magnificent features hidden in the fungus, such as bio-protection, growth promotion and enhancement of plants' defense mechanisms against abiotic and biotic stresses. Mohd et al. (2017) explored the *S. indica* colonization-mediated response of *Oryza sativa* to As toxicity and revealed that host root-fungal symbiosis promoted the rescue of total biomass, chlorophyll and root damage caused by As toxicity. *S. indica* was able to achieve this by immobilizing soluble As and restrict its infiltration to the roots, with only a small amount of As gaining access to the shoots. Its colonization led to a change in the cells' redox status by manipulation of the antioxidative framework, thereby defending the photosynthetic apparatus of the plant from As stress (Mohd et al., 2017). As reported by Ghorbani et al. (2021), *S. indica*-colonized seedlings displayed significant reductions in malondialdehyde and methylglyoxal levels by modulating AsA, glyoxalase system and GSH homeostasis. Evidence provided by Bertolazi et al. (2019) substantiate the claim of crop growth promotion and a higher performance by means of symbiotic interactions, as they witnessed similar growth responses in their investigation with the wild-type rice plants set against H + -PPase gene overexpressing transgenic plants.

Another way to cope with arsenic toxicity is through nutrient management such as P, which can specifically interact with As due to the anionic structural similarity (Zvobgo et al., 2018). Phosphorus makes about 0.2% of a plant's dry weight and is among the three macronutrients most essential to plants' existence, as it partakes in many key metabolic pathways, enzymatic reactions and is the chief constituent of biological molecules such as phospholipids, nucleic acids and adenosine triphosphate. It is notable that enzymes that utilize P, have the same binding mode and kinetic parameters as As^{5+}, therefore

plants incur toxicity when As^{5+} substitutes P in metabolic reactions (Kamiya et al., 2013). Phosphorus has been registered as an alleviant of stress specifically As stress in plants, as P and As share common transporters (Ye et al., 2017). Rice plants lack inherently evolved As transporters (Ghorbani et al., 2021), yet arsenic manages to get easily transported across the plasma lemma by PHT proteins (Ye et al., 2017). The function and characteristics of all plant PHTs, and their roles in *Arabidopsis* and rice have been discussed in depth by Młodzińska and Zboińska (2016). A research on *Salix* spp. revealed that the expression of PHT 1; 3 and PHT 1; 12 in the absence of P, was up-regulated immediately upon As exposure (Puckett et al., 2012); moreover, some PHTs have been identified in plants that show strong association with mycorrhizal symbiosis, such as PHT11 and PHT13 (Ye et al., 2017). Previous studies attribute *S. indica*-mediated promotion of plant development to phosphate transfer, as impairment in growth resulted from plant's inoculation with its phosphate transfer (PiPT) knock-out strains (Kumar et al., 2011). According to an experiment conducted by Ngwene et al. (2016), P utilization is increased by the endophytic root symbiont *S. indica*, particularly when the source is inorganic; moreover, the resultant symbiosis could reprogram gene expression but may not necessarily compensate for phosphate limitation (Bakshi et al., 2017), therefore an additional P supply would certainly help.

To further comprehend the role of *S. indica* in plant As toxicity amelioration, it is paramount to discern first how *S. indica* utilizes P for counteracting As toxicity, and second its capability to work together with the innate genotypic potential of the crop in question. Based on the above facts, the current study was designed with the salient objectives: (i) to study the physio-biochemical responses of rice to arsenic stress under the combined treatment of *S. indica* and phosphorus, (ii) to investigate the possible mechanism involved in the combined treatment of *S. indica* with phosphorus in alleviating arsenic stress in rice, and (iii) to explore the ultrastructural configurations of root and leaf tissues and relative gene expression involved in As-stress mitigation.

Materials and methods

Plant material, *Serendipita indica* culture preparation and inoculation

Healthy seeds of two rice genotypes, Guodao-6 (high As accumulator) and Zhongzhe You-1 (low As accumulator), were disinfected using 3% perhydroxic acid for about 15 min, then rinsed 3 times with ddH_2O. Thereafter, the seeds of each genotype were soaked in a labeled germination box overnight at room temperature (25°C). Afterward, the well moist seeds were placed for germination in a rice growth chamber at 29°C ± 1°C during the day (12 h) and 26°C ± 1°C at night. A hydroponic setup was arranged and 10 days old, uniform sized seedlings were transferred to half strength nutrient solution (slightly modified from Zeng et al., 2008) for 3 days followed by full strength solution for 4 days before fungal inoculation. Nutrient solution comprised of the following chemicals (L^{-1}): 2.9 mM NH_4NO_3, 1.7 mM $MgSO_4{\cdot}7H_2O$, 1.0 mM K_2SO_4, 1.0 mM $CaCl_2$, 0.125 mM $NaH_2PO_4.2H_2O$, 36 μM EDTAFeNa, 18 μM H_3BO_3, 9.1 μM $MnCl_2{\cdot}4H_2O$, 0.52 μM $(NH_4)_6Mo_7O_{24}{\cdot}4H_2O$, 0.16 μM $CuSO_4{\cdot}5H_2O$, and 0.15 μM $ZnSO_4{\cdot}7H_2O$. *Serendipita indica* was first grown on agar Petri plates with Aspergillus medium; circular agar disks (5 mm in diameter) inclosing active spores of *S. indica* (Hill and Kafer, 2001), were placed on solidified medium and kept in absolute dark for 7 days at 30°C ± 1°C. For inoculation, *S. indica* was grown in a liquid Käfer medium from previously inoculated Petri plates; a small circular section of about 1 mm diameter of the inoculated fungus was introduced into a 500 ml glass flask and then incubated for 12 days at 30°C ± 1°C in a shaking incubator (200 rpm). Thereafter, the liquid containing active spores was filtered through sterile muslin cloth then used for plant inoculation by root soaking method (Chadha et al., 2015).

Confirmation of *Serendipita indica* root colonization and treatment application

Seven-day post-inoculation, successful colonization was confirmed by microscope visualization of *S. indica* spores in the root cortical tissues of the host plant. Inoculated plant roots were first gathered and rinsed thoroughly with water before cutting them into 1 cm long pieces and then immersed in KOH solution (10%) overnight at room temperature (25°C; Chadha et al., 2015). The roots were thereafter, washed three times with ddH_2O and then immersed again, this time with 1% HCl for about 3 min prior to trypan blue (0.05%) staining for microscopic visualization as seen in Figure 1. Followed by successful colonization, plants were kept either as positive control (*S.i*) or treated with alone 10 μM As L^{-1} (As + *S. indica*), 50 μM P L^{-1} (P + *S. indica*) and their combination (As + P + *S. indica*). A set of un-inoculated plants were also treated with either alone or combined As and P treatments (As, P, and As + P), meanwhile seedlings without any treatment were designated as control (CK). Arsenic was provided as $Na_2HAsO_4.7H_2O$ (0.0078 g L^{-1}), whereas for 50 μM phosphorus, 0.25 mM $NaH_2PO_4.2H_2O$ (0.039 g L^{-1}) was added (stock solutions).

Evaluation of phenotypic and photosynthetic attributes

Measurement process and methods used were identical for both genotypes; growth indices including shoot height (SH) and root length (RL), fresh (FW) and dry weights (DW) were measured upon harvest (15-day post-treatment) taking two seedlings from each of the three biological replicates. Dried mass was measured after drying the roots and shoots separately in labeled paper bags at 75°C ± 2°C for 72 h using a hot air oven. Measurements of net photosynthetic capability (A_{max}), stomatal conductance (*Gs*), transpiration rate (*Tr*), and intercellular CO_2

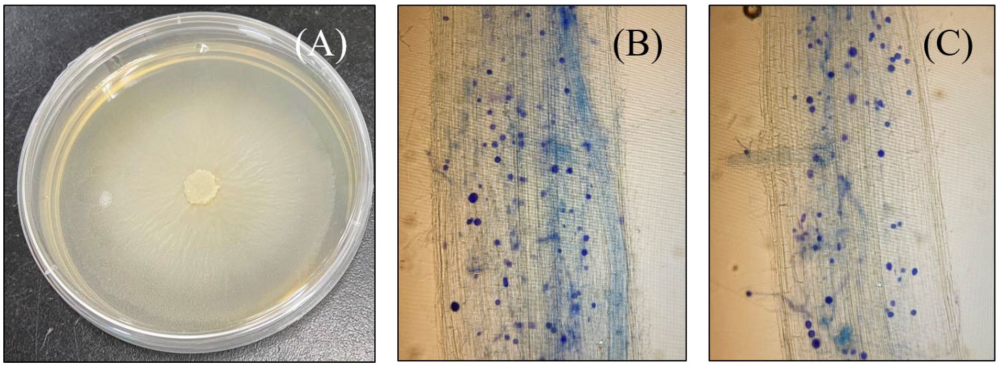

FIGURE 1
Photograph of a petri plate growing culture of *Serendipita indica* **(A)**, and microscopic images of both rice genotypes successfully colonized with *S. indica* spores; Roots of ZZY-1 genotype **(B)** and, GD-6 genotype **(C)**.

concentration (*Ci*), were performed on second fully expanded leaves 24 h before harvest at day 14 post-treatment, using an infrared analyzer (LI-6400 System, Li-COR Company, United States). All measurements were performed between 9 am and 12 pm, with relative humidity of 50%–70%, CO_2 concentration of 400 µmol mol^{-1}, air temperature of 25°C to 28°C and photosynthetic photon flux density of 1,000 µmol m^{-2} s^{-1}.

Electron microscopic imaging

Ultrastructural study was performed on root and shoot of both genotypes, the samples were examined using only a tiny portion of the plant tissues, about 1 mm^2 sections of fresh root tips and fully expanded uppermost leaves of the plants. The samples were fixed in a 1:1 mixture of 2.5% glutardialdehyde and 0.1 M phosphate buffer (PBS; pH 7.0) for 6 h and post-fixed in a 1:1 mixture of 2% $OsSO_4$ and 0.1 M PBS (pH 7.0) for 2 h. A series of graded ethanol (75%, 80%, 90%, and 95%) was used to dehydrate the samples with a subsequent pure acetone wash (Mapodzeke et al., 2021). Later, the samples were infiltrated with successive combinations of Spur resin and acetone, followed by embedding in Spur resin overnight. The samples were then polymerized at 70°C for 9 h. Ultrathin sections of the samples were made and stained in uranyl acetate ($C_4H_6O_6U$), and later by lead citrate ($C_{12}H_{12}O_{14}Pb_2$). Shoot and root ultra-structures were examined and photographed under a Hitachi H7650 transmission electron microscope.

Determination of elemental concentration and translocation factor

Dried root and shoot samples of the two genotypes were collected (0.1 g) and placed in digestion glass tubes with high heat resistance according to their labels, then 3 mL of nitric acid (HNO_3) were added to each sample tube and processed in a microwave (Mars 6, CEM Technologies, United States) at 120°C for 1 h 30 min. Macro-, meso- and micro-elements were then detected using an inductively coupled plasma–optical emission spectrometer (ICP-OES; Optima 8000DV; Perkin Elmer). The translocation factor (%TF) was calculated by the ratio of As total accumulation in the shoot with As total accumulation in the root as presented by Zvobgo et al. (2018).

Antioxidant enzyme activity and estimation of lipid peroxidation

About 0.2 g of leaf tissue was homogenized with 4 mL cold 5 mM PBS (pH 7.8) and centrifuged (Eppendorf 5810R; Hamburg, Germany) at 4°C for 15 min at 12,000 rpm. The activities of SOD (EC 1.15.1.1), CAT (EC 1.11.1.6), and POD (EC 1.11.1.7) were assayed according to Wu et al. (2003). By measuring the MDA content (Murphy et al., 2014), lipid peroxidation levels were calculated; the reaction solution comprised of 5% trichloroethanoic acid solution, 2.5 g of thiobarbituric acid and enzyme extract. The final mixture was heated for 15 min at 95°C, followed by immersion in an ice water bath to halt the reaction and subsequently centrifuged for 10 min at 4,800 rpm. Lastly, the supernatant was read spectrophotometrically (BMG Labtech—SPECTROstar® Nano; Offenburg, Germany) at 532 nm (Zhang et al., 2005). Quantification of H_2O_2 in crude extracts was performed using the colorimetric H_2O_2 assay kit (A064-1), as per the manufacturer's protocol (Nanjing Jiancheng Bioengineering Institute NJBI). Quantification of O_2^- was performed using crude extracts following the method of Jiang and Zhang (2001). Frozen root/shoot tissues (0.1 g) were homogenized with 1 mL of 65 mM PBS (pH 7.8) and centrifuged for 10 min at 5,000×*g*. The incubation solution contained 65 mM PBS (pH 7.8; 0.9 mL), 10 mM hydroxylamine hydrochloride (0.1 mL), and supernatant (1 mL). Incubation at 25°C for 20 min ensued both before and after the addition of 17 mM sulfanilamide and 7 mM α-naphthylamine. Ethyl ether (4 mL) was added followed by centrifugation at 1,500×*g* for 5 min. The upper organic layer was removed and absorbance in the

10.3389/fpls.2022.982668

TABLE 1 List of *Oryza sativa* specific primer sequences used in this study.

Gene name	Primer pair sequence (5–3`)	Length (bp)	Product length
OsPHT4-1F	ATCGAAAGGGAAGTCGCTGG	20	
OsPHT4-1R	ACCATCTCAACTCCGGACGA	20	109
OsFe-SOD1-1F	GCCAGAAGGTGGTGGGTCA	19	
OsFe-SOD1-1R	AGCCAGACCCCAAAAGTGATA	21	122
OsMn-SOD1-1F	CCGCACGCTGGCCTC	15	
OsMn-SOD1-1R	CGACGGTCGTCACACCC	17	147
OsPHT1-1F	GTGATGCTGCAAGCTCTTCG	20	
OsPHT1-1R	CCAGGTCGAGAAGTACGCAA	20	107
OsHMA2-F	ATTACACACCTGCGGTCGTT	20	
OsHMA2-R	GGGTGTGGACAGTACCAGTG	20	146
OsHMA3-F	GCAAGTCAAGCCACCCAATG	20	
OsHMA3-R	CCCACATTTTCCGGGTTTGG	20	86
OsAPX-F	CTAGGGCCAGTGTGAACCAG	20	
OsAPX-R	GCAGCATTGCAGTTGAGCAT	20	127
OsCAT-F	CTCCGTGGCATCTGGATCTC	20	
OsCAT-R	TTCCTCCTGGCCGATCTACA	20	108
OsCu-ZnSOD-F	CAGATTCCTCTGAGTGGCCC	20	
OsCu-ZnSOD-R	AACAACACCGCATGCAAGTC	20	141
OsActin-1F	AGGCCCCTTTGAACCCAAAA	20	
OsActin-1R	ATAGCGACGTACATGGCAGG	20	106

lower aqueous layer was read (at 530 nm). In order to calculate the production rate of O_2^- from the chemical reaction of O_2^- and hydroxylamine, a standard curve with NO_2^- was used.

RNA extraction, synthesis of cDNA, and qRT-PCR assay

Total RNA was extracted from 100 mg of root and shoot samples from each treatment employing TaKaRa MiniBEST Universal RNA Extraction Kit (catalog # 9767) as per the manufacturer's instructions. Titertek-Berthold nanospectrometer (Pforzheim, Germany) was used for RNA concentration check, whereas for quality assessment, the samples were electrophoresed in 1% agarose gel running with 1X TAE buffer. To obtain cDNA, TaKaRa Prime script RT reagent Kit (catalog # RR037A) was used. The cDNA samples were assayed by quantitative real time PCR (qRT-PCR) in the Roche Light Cycler® 480 Instrument II Real Time PCR System using the TB Green® Premix Ex Taq™ II Clontech (catalog # RR820A; Takara). To calculate threshold cycle values, software provided with the qRT-PCR system was used; consequently, the quantification of mRNA levels was performed employing Schmittgen and Livak (2008) method. Ten primers were designed including the reference gene for *Oryza sativa* with genes of interest and are listed in Table 1. The genes were blasted from NCBI primer blast and designed choosing the most promising output among which phosphate transporters from PHTs families were chosen for expression across treatments. Other genes related to antioxidant activities were also selected and designed for expression to check correlation with antioxidant and ROS enzyme assays, performed through enzyme extraction and different reagent solutions.

Statistical analysis

A completely randomized experiment was designed with 3 biological replicates for each treatment administrated and the statistical analysis (one-way ANOVA) was performed by SPSS-10 statistical software (SPSS Inc., Chicago, IL, United States) using Duncan's Multiple Range test (DMRT) at $p < 0.05$ (Goodall, 1991). OriginPro 2019 (Origin Lab Corporation, Wellesley Hills, Wellesley, MA, United States) was employed for PCA analysis and graphs, whereas the tables were made in Microsoft Excel 2019.

Results

Growth responses and photosynthetic indices

The phenotypic differences across the two rice genotypes are presented in Table 2. Growth attributes of both genotypes, i.e., fresh (FW) and dry biomass (DW) or length of roots (RL)/height of shoots (SH), were severely affected by arsenic toxicity. It is interesting to note that symbiosis of *S. indica*, in the absence of any other treatment, had a burgeoning effect on the growth of plants, although not statistically significant from their respective controls in some cases, with 15.6% and 18% increase in SFW, 16.8% and 13.7% in RFW, 16% and 14.8% in RDW, as well as 3.8% and 5.9% in RL, for ZZY-1 and GD-6 genotype, respectively; whereas, a significant difference in SDW (30.7%) was observed with *S. indica* colonization for ZZY-1, and in SH (18% and 14.6%) for both ZZY-1 and GD-6, respectively, as compared to their control plants. The combined treatment of P and *S. indica* also had a positive impact on all the growth indices except for SFW in As-stressed ZZY-1. When the ameliorative treatments were compared for their efficacy, *S.i* + As displayed 41.4% and 2.34% improvement in RL against As alone treatment, As + P showed 27% and 17.5%, whereas *S.i* + As + P had 27% and 33.4% better root growth in ZZY-1 and GD-6, respectively. Moreover, in terms of SL, ZZY-1, and GD-6 indicated a 21.9% and 17.7%, 3.8% and 3.5%, along with 0.52% and 30.3% recovery under *S.i* + As, As + P, and *S.i* + As + P treatments, respectively. A noteworthy 2.3- and 2.7-fold improvement in RDW was observed for ZZY-1 under combined *S. indica* treatments with As and As + P than alone As treatment. Moreover, GD-6 plants benefited the most from *S.i* + As + P with 66.5% lesser reduction in comparison with their alone As treated counterparts. While recording the data for shoot dry weight, it was observed that *S.i* + As brought forth a better shoot

10.3389/fpls.2022.982668

TABLE 2 Growth indices of rice plants differing in arsenic accruing tendency following alone and combined interactions of *Serendipita indica* symbiosis and phosphorus against arsenic stress.

Genotype	Treatment	Shoot FW (g)	Root FW (g)	Shoot DW (g)	Root DW (g)	Shoot length (cm)	Root length (cm)
ZZY-1	CK	6.04 ± 0.71 ab	1.25 ± 0.08 a	0.673 ± 0.022 b	0.119 ± 0.03 ab	80.5 ± 4.2 b	21.3 ± 0.45 a
	As	1.24 ± 0.32 d	0.409 ± 0.09 b	0.225 ± 0.015 d	0.03 ± 0.005 d	51.9 ± 3.1 c	11.8 ± 1.7 c
	S.i	6.99 ± 0.95 a	1.46 ± 0.21 a	0.78 ± 0.031 a	0.138 ± 0.01 a	95 ± 2.5 a	22.1 ± 2.3 a
	P	5.58 ± 0.84 b	1.15 ± 0.34 a	0.732 ± 0.024 ab	0.118 ± 0.07 b	77.2 ± 3.8 b	19.3 ± 1.5 ab
	S.i + As	1.78 ± 0.23 d	0.43 ± 0.07 b	0.51 ± 0.011 c	0.097 ± 0.02 bc	63.3 ± 4.23 c	16.7 ± 0.9 b
	As + P	1.55 ± 0.11 d	0.41 ± 0.01 b	0.29 ± 0.016 d	0.041 ± 0.006 d	53.9 ± 1.9 c	15.1 ± 1.25 bc
	S.i + P	4.92 ± 0.45 bc	1.69 ± 0.25 a	0.685 ± 0.042 b	0.137 ± 0.04 a	83.9 ± 4.9 ab	20.7 ± 2.1 a
	S.i + As+ P	4.17 ± 0.21 c	1.02 ± 0.41 ab	0.275 ± 0.001 d	0.11 ± 0.055 bc	52.2 ± 5.62 c	15 ± 2.4 bc
GD-6	CK	4.19 ± 0.52 a	1.23 ± 0.25 b	0.58 ± 0.065 abc	0.117 ± 0.04 b	62 ± 2.8 b	16.3 ± 1.7 a
	As	1.12 ± 0.34 c	0.592 ± 0.06 c	0.32 ± 0.028 e	0.056 ± 0.01 d	47.6 ± 2.3 d	12.8 ± 0.95 c
	S.i	4.94 ± 0.61 a	1.42 ± 0.34 ab	0.671 ± 0.11 ab	0.134 ± 0.012 ab	69.4 ± 1.78 a	17.3 ± 1.1 a
	P	3.97 ± 0.74 ab	1 ± 0.08 bc	0.54 ± 0.02 c	0.107 ± 0.06 bc	55.8 ± 3.5 bc	17 ± 0.89 ab
	Si + As	2.2 ± 0.15 bc	0.735 ± 0.02 c	0.363 ± 0.041 de	0.069 ± 0.003 cd	56 ± 1.2 bc	13.1 ± 1.02 c
	As + P	2.22 ± 0.46 bc	0.669 ± 0.07 c	0.372 ± 0.023 de	0.059 ± 0.017 d	49.2 ± 2.7 cd	15 ± 0.11 b
	S.i + P	5.1 ± 0.82 a	1.14 ± 0.09 b	0.756 ± 0.09 a	0.167 ± 0.028 a	68.9 ± 1.14 a	16.2 ± 1.5 a
	S.i + As+ P	3.41 ± 0.69 ab	1.75 ± 0.38 a	0.472 ± 0.02 cde	0.094 ± 0.003 c	60.5 ± 1.69 b	15.9 ± 1.13 a

All values are means of three replications (±SE). Different letters represent significant difference among the treatments within each genotype at $p \leq 0.05$ probability level by applying Duncan's multiple range test. CK, control; S.i, *Serendipita indica*.

dry weight than As + P and *S.i* + As + P application (4.7- and 3.4-fold, respectively), when compared to As treated ZZY-1 plants; however, *S.i* + As + P showed a 2.5- and 2-fold higher SDW preservation compared to *S.i* + As and As + P, respectively. Against arsenic treated plants, root fresh weights were restored significantly under *S.i* + As + P application than *S.i* + As and As + P, while an opposing trend was seen in SFW values, where both *S.i* + As and As + P treatments presented higher FW (43% and 24.7% for ZZY-1, 97% and 99% for GD-6) against 2.35% and 2% under *S.i* + As + P, respectively.

The effects of all treatments across rice genotypes on A_{max}, *Gs*, *Ci*, and *Tr* under As stress are illustrated in Figure 2. Arsenic stress, as expected significantly reduced net A_{max} (66% and 58%), stomatal conductance (93% and 77%), and transpiration rate (66% and 71%) compared to control plants in ZZY-1 and GD genotypes, respectively. Furthermore, the combined treatment of *S. indica* and phosphorus under As stress showed much improvement in net photosynthetic rate (41%) when compared to *S.i* + As and As + P, in ZZY-1 genotype. However, GD-6 plants took advantage of *S. indica* alone (*S.i* + As; 22.7%) and in combination with phosphorus (*S.i* + As + P; 37.8% improvement), when compared with their As treated counterparts. The results indicated better performance of GD-6 under *S.i* + As + P (values closer to control) in terms of *Gs* in contrast to ZZY-1 genotype (48% revival). Although, As stress caused an elevation in intercellular CO_2 concentrations, ZZY-1 experienced a recuperative effect under As + P (116%), *S.i* + As + P (91%), and *S.i* + As (49%); while for GD-6 plants, *S.i* + As + P tended to ameliorate the most (109%). It was interesting to note that transpiration rate was highly improved under *S.i* + As + P, and *S.i* + As treatment (41.3% and 15.4% higher compared to As treated plants, respectively) for ZZY-1 genotype, whereas for GD-6, arsenic

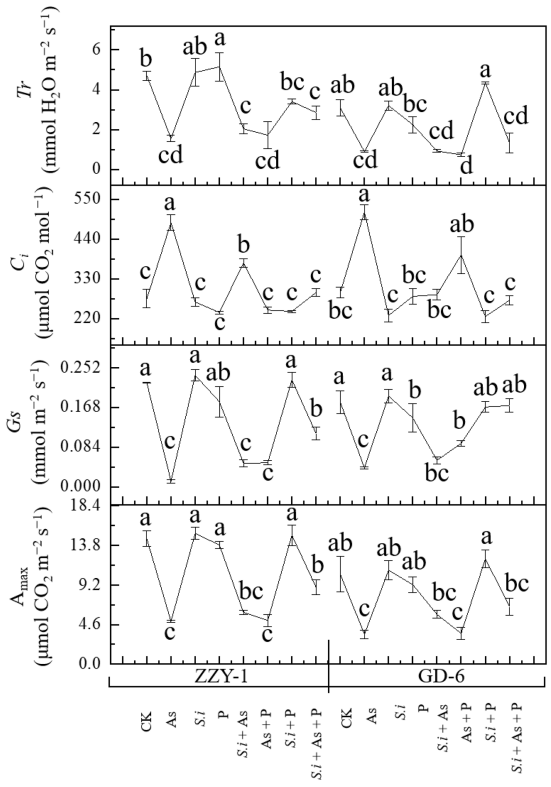

FIGURE 2
Photosynthetic attributes of two rice genotypes differing in As accumulation tendency following alone and combined interactions of *Serendipita indica* symbiosis and phosphorus against As stress. Error bars represent standard errors (n=3). Different letters represent significant difference ($p \leq 0.05$) among the treatments within each genotype.

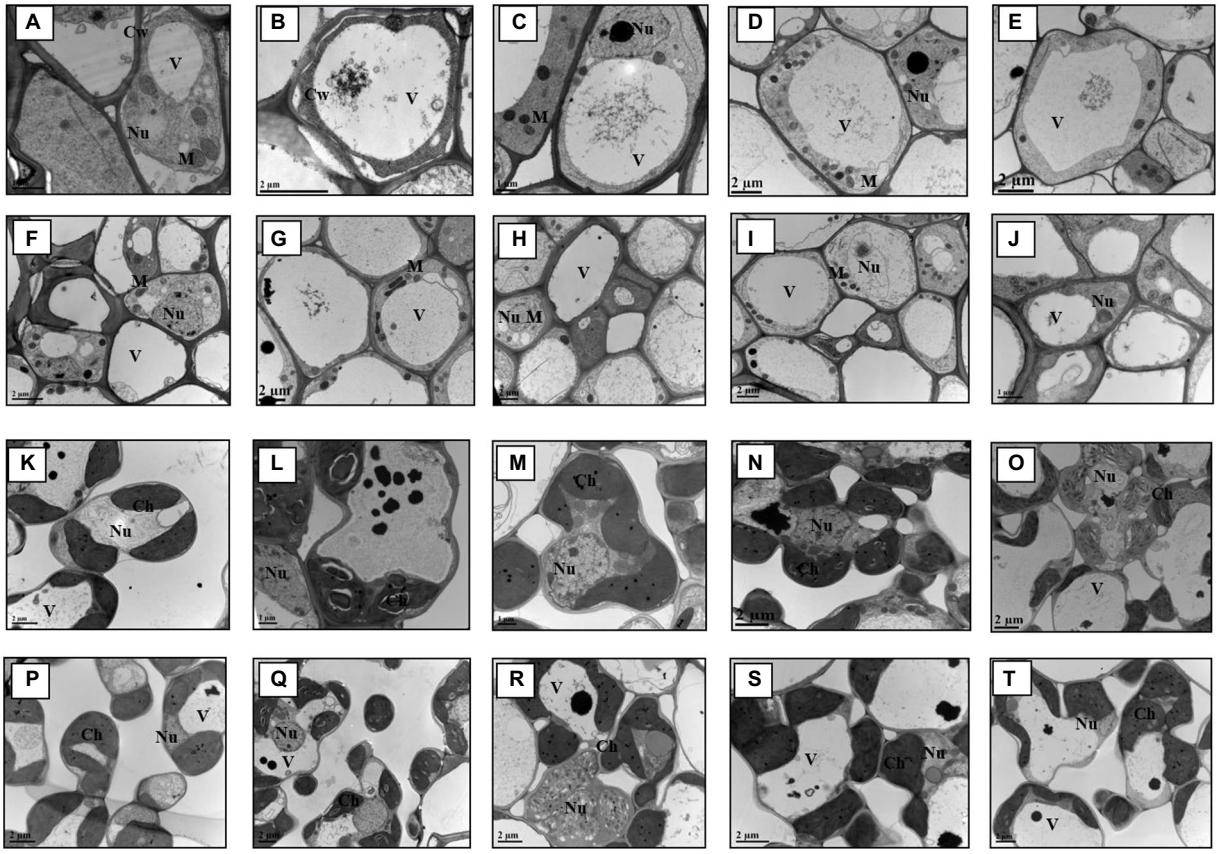

FIGURE 3
Transmission electron micrographs of root and leaf cells. Key: **(A–J)**=Root; GD-6: A=Control; B=As; C= *Serendipita indica*+ As; D = *S. indica*+As + Phosphorus; E=As + Phosphorus; ZZY-1: F=Control; G=As; H=*S. indica*+ As; I=D=*S. indica*+As + Phosphorus; J=As + Phosphorus. **(K–T)**=Leaves; GD-6: K=Control; L=As; M=*S. indica*+ As; N=*S. indica*+As + Phosphorus; O=As + Phosphorus. ZZY-1: P=Control; Q=As; R=*S. indica*+ As; S=*S. indica*+As + Phosphorus; T=As + Phosphorus.

stressed plants benefited mostly under *S. indica* symbiosis combined with phosphorus (i.e., *S.i* + As + P; 20% improvement).

Effects of the treatments on root and leaf cell ultrastructural fingerprints

The ultrastructure images of the root and shoot tissues present noticeable differences on cellular structure level among the treatments and across genotypes (Figure 3). It is apparent that most cellular organelles, such as mitochondria, chloroplast etc. in the control plant tissues, both in root and shoot, present normal morphology. However, other treatments in combination with As showed negative impact on plant cell organelles structures with the most damaging effect being in the cells of GD-6 genotype. Furthermore, the combined treatment of *S. indica* and P in addition to As, in particular showed greater phenotypic difference in GD-6 genotype (As-sensitive) and less damaging effect in ZZY-1. Arsenic deposition in vacuole is also visible in most of the ultrastructure images across treatments with increased vacuole area and in some, complete cell destruction.

Concentration of macro, meso, and micronutrients

Mineral concentrations of root and shoot As, zinc (Zn), iron (Fe), calcium (Ca), potassium (K), phosphorus (P) and magnesium (Mg) were measured and the effects of all treatments applied to both rice genotypes are shown in Figure 4A, whereas percentage of arsenic translocation is also depicted alongside (Figure 4B). In shoots of ZZY-1, the ameliorative treatments, i.e., *S.i* + As, As + P and *S.i* + As + P, instigated a reduction of 42%, 24.7%, and 62.8% of arsenic concentration as compared to As alone stress, whereas for GD-6, 56.5%, 42.2%, and 68.7% decrease was observed, respectively. Roots of ZZY-1, displayed a decline of 28%, 12.6%, and 39.8% in comparison with its respective As treated counterparts, while GD-6 roots also exhibited an attenuative trend to a lesser extent (20.2%, 14.6%, and 22.4% under *S.i* + As, As + P and *S.i* + As + P, respectively). Regardless of the genotype, symbiosis of *S. indica* alone and in combination with phosphorus, tended to increase the concentration of Zn, Fe, Ca, Mg, and K, predominantly in shoots than the roots. The concentration of Zn in ZZY-1 and GD-6 shoots reduced

A

Genotypes	Treatments	Shoot							Root						
		As (mg/g)	Zn (µg/g)	Fe (µg/g)	Ca (mg/g)	K (mg/g)	P (mg/g)	Mg (mg/g)	As (mg/g)	Zn (µg/g)	Fe (µg/g)	Ca (mg/g)	K (mg/g)	P (mg/g)	Mg (mg/g)
ZZY-1	Ck	0 ± 0 e	16.8 ± 0.63 ab	81.8 ± 1.6 c	1.7 ± 0.015 b	13.5 ± 0.24 b	1.48 ± 0.06 b	2.76 ± 0.28 ab	0 ± 0 e	2.97 ± 0.6 a	297 ± 1.5 c	0.595 ± 0.032 bc	2.08 ± 0.16 ab	0.262 ± 0.001 ab	0.488 ± 0.025 ab
	As	0.00781 ± 0.0004 a	6.56 ± 0.84 d	42.1 ± 1.08 f	1.18 ± 0.1 d	5.7 ± 0.11 d	0.769 ± 0.026 d	1.13 ± 0.11 c	0.515 ± 0.02 a	1.41 ± 0.19 bc	91.9 ± 0.97 h	0.449 ± 0.07 d	0.923 ± 0.05 c	0.115 ± 0.002 c	0.123 ± 0.006 c
	S.i	0 ± 0 e	18.5 ± 0.4 a	184.9 ± 2.68 a	1.92 ± 0.022 ab	15.5 ± 0.72 a	1.57 ± 0.064 ab	3.2 ± 0.12 a	0 ± 0 e	3.54 ± 0.74 a	425 ± 3.1 a	0.75 ± 0.03 a	2.42 ± 0.3 a	0.304 ± 0.053 a	0.566 ± 0.015 a
	P	0 ± 0 e	15.7 ± 0.76 b	75.2 ± 0.47 g	1.57 ± 0.06 bc	12.8 ± 0.68 b	1.72 ± 0.027 a	2.6 ± 0.07 ab	0 ± 0 e	2.9 ± 0.4 a	305 ± 2.4 b	0.59 ± 0.064 bc	2.07 ± 0.39 ab	0.297 ± 0.04 a	0.484 ± 0.07 ab
	S.i + As	0.00453 ± 0.0001 c	12.6 ± 0.55 c	85 ± 1.1 c	2.09 ± 0.22 a	11 ± 0.63 c	1.09 ± 0.04 c	2.15 ± 0.58 b	0.37 ± 0.01 c	2.42 ± 0.3 ab	224 ± 1.9 e	0.485 ± 0.011 cd	1.7 ± 0.2 b	0.113 ± 0.08 c	0.398 ± 0.01 b
	As + P	0.00588 ± 0.0002 b	10.9 ± 0.57 c	70.7 ± 0.2 e	1.32 ± 0.03 cd	5.78 ± 0.09 d	1.21 ± 0.17 c	1.2 ± 0.036 c	0.45 ± 0.04 b	1.02 ± 0.05 c	153 ± 1.2 g	0.454 ± 0.008 d	0.714 ± 0.06 c	0.15 ± 0.01 bc	0.167 ± 0.032 c
	S.i + P	0 ± 0 e	17.1 ± 0.64 ab	128.2 ± 1.15 b	1.74 ± 0.17 ab	13.7 ± 0.98 b	1.5 ± 0.035 ab	2.81 ± 0.049 ab	0 ± 0 e	3.41 ± 0.2 a	248 ± 4 d	0.673 ± 0.013 ab	2.39 ± 0.05 a	0.301 ± 0.023 a	0.561 ± 0.013 a
	S.i +As+ P	0.0029 ± 0.0003 d	11.6 ± 0.017 c	81.9 ± 1.2 c	1.33 ± 0.11 cd	10.75 ± 0.15 c	1.43 ± 0.02 b	2.23 ± 0.03 b	0.31 ± 0.01 d	2.74 ± 0.16 a	210 ± 1.6 f	0.54 ± 0.021 cd	1.92 ± 0.21 ab	0.142 ± 0.055 bc	0.448 ± 0.01 b
GD-6	Ck	0 ± 0 e	14.5 ± 0.43 c	77.3 ± 1.87 cd	1.46 ± 0.15 b	11.6 ± 0.59 b	1.28 ± 0.055 c	2.38 ± 0.16 bc	0 ± 0 d	2.71 ± 0.19 bc	233 ± 1.08 b	0.583 ± 0.03 bc	2.04 ± 0.015 bc	0.257 ± 0.012 ab	0.45 ± 0.008 bc
	As	0.0736 ± 0.0001 a	8.01 ± 0.53 e	61.8 ± 2.65 f	0.809 ± 0.02 e	6.98 ± 0.3 d	0.59 ± 0.03 e	1.32 ± 0.02 d	0.89 ± 0.01 a	0.75 ± 0.06 d	98.5 ± 0.95 g	0.282 ± 0.06 ef	0.588 ± 0.04 d	0.136 ± 0.011 b	0.231 ± 0.012 d
	S.i	0 ± 0 e	16.3 ± 0.23 b	160.9 ± 3.02 a	1.81 ± 0.29 ab	13.4 ± 0.43 a	1.48 ± 0.052 b	2.75 ± 0.14 ab	0 ± 0 d	3.2 ± 0.45 b	215 ± 2.1 d	0.67 ± 0.017 b	2.72 ± 0.034 a	0.295 ± 0.06 ab	0.549 ± 0.04 b
	P	0 ± 0 e	13.6 ± 0.57 c	78.6 ± 0.21 bc	1.36 ± 0.12 b	10.8 ± 0.23 b	1.39 ± 0.011 bc	2.21 ± 0.51 bc	0 ± 0 d	2.61 ± 0.22 bc	274 ± 1.12 a	0.535 ± 0.037 bc	1.87 ± 0.39 bc	0.235 ± 0.043 ab	0.439 ± 0.08 bc
	S.i + As	0.0325 ± 0.005 c	9.09 ± 0.61 e	84.7 ± 1.69 b	1.08 ± 0.19 c	8.94 ± 0.26 c	0.695 ± 0.01 e	1.49 ± 0.018 d	0.71 ± 0.03 c	1.37 ± 0.06 d	169.2 ± 1.5 e	0.395 ± 0.038 de	0.961 ± 0.05 d	0.154 ± 0.05 b	0.235 ± 0.06 d
	As + P	0.0425 ± 0.001 b	9.26 ± 0.21 e	65.8 ± 1.08 e	0.961 ± 0.064 e	7.3 ± 0.17 d	0.91 ± 0.02 d	1.52 ± 0.017 d	0.76 ± 0.01 b	0.77 ± 0.08 d	105.1 ± 1.58 f	0.254 ± 0.055 f	0.54 ± 0.032 d	0.14 ± 0.09 b	0.127 ± 0.029 d
	S.i + P	0 ± 0 e	18.6 ± 0.57 a	85.6 ± 3.71 b	1.98 ± 0.41 a	13.7 ± 0.59 a	1.66 ± 0.12 a	3.1 ± 0.13 a	0 ± 0 d	4.2 ± 0.13 a	235 ± 2.33 b	0.836 ± 0.029 a	2.24 ± 0.13 ab	0.368 ± 0.052 a	0.685 ± 0.01 a
	S.i +As+ P	0.023 ± 0.002 d	11.8 ± 0.16 d	71.2 ± 2.02 de	1.17 ± 0.02 bc	9.44 ± 0.28 c	0.92 ± 0.03 d	1.94 ± 0.032 cd	0.69 ± 0.02 c	2.35 ± 0.27 c	225 ± 1.15 c	0.46 ± 0.06 cd	1.64 ± 0.27 c	0.141 ± 0.01 b	0.379 ± 0.05 c

B

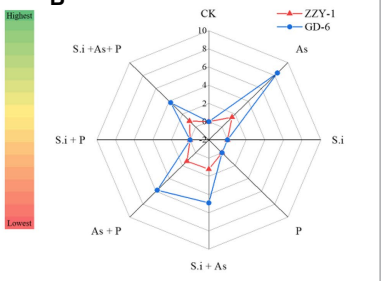

FIGURE 4
Macro-, meso-, and micro-element concentration **(A)**; green in color scale displays higher values and red shows lower values. Radar chart representing % As translocation factor **(B)**. Different letters represent significant difference ($p \leq 0.05$) among the treatments within each genotype.

significantly under As stress (30.8% and 18.6%, respectively), however *S.i* + As + P treatment rescued both genotypes (49.4% and 58% improvement, respectively) when compared to their respective As alone treated counterparts, while *S.i* + As and As + P proved to be more promising for ZZY-1 (58.5% and 42.6% recovery, respectively) than GD-6 (16.5% and 19.2%, respectively). In case of roots, although not much assistance was provided by the additional supplementation of phosphorus against As, the symbiosis of *S. indica* (*S.i* + As + P) remarkably improved the Zn contents in ZZY-1 and GD-6 roots (85.2% and 81.6%, respectively), followed by *S.i* + As with 64.7% and 31.7% recovery for the former and later genotype, respectively.

The calculations regarding percent translocation factor of arsenic revealed a higher reduction in GD-6 than ZZY-1; lowest As TF was observed under *S.i* + As + P (38.3% reduction) followed by *S.i* + As (19.3%) and As + P (13.8%) in ZZY-1 plants, whereas for GD-6, *S.i* + As + P was highly effective (59.7% reduction) compared to *S.i* + As (45.5%) and As + P (33.3%). Iron concentration reduced drastically under As stress for both genotypes irrespective of the tissue analyzed. It is, rather impressive to observe that treatments with *S. indica* brought about much improvement, and in few cases, higher than control Fe concentration values when compared to phosphorus amended treatments. Meanwhile, the concentration of phosphorus was higher under the treatments with augmented phosphorus as well as under *S. indica* inoculated plants and the beneficial impact was much pronounced in GD-6 shoots than ZZY-1 with 15.6% and 30% increment under *S.i* and *S.i* + P, respectively. Roots accumulated more phosphorus under alone and combined *S.i* and P treatments in both genotypes, whereas the inhibitory effect of As against phosphorus was counteracted prominently by As + P (23.8%) and *S.i* + As + P (18% improvement) in ZZY-1 compared to its As treated counterparts when set against GD-6 roots (with only 14.9% and 4.5% retrieval, respectively). A significant elevation in the concentration of shoot Ca was displayed by ZZY-1 plants under *S.i* (1.92%) and *S.i* + As (22.8% increase), whereas for GD-6, it was observed for *S.i* (23.9%) and *S.i* + P treated plants (35.3% increase). When arsenic treatment was compared with control, a 30.4% and 44.6% reduction was recorded for ZZY-1 and GD-6 shoots, while roots exhibited 24.5% and 51.6% decline in Ca content, respectively. Among the ameliorative treatments, *S.i* + As + P offered a 28% and 55.4% as well as 62.3% and 59% improved Ca accumulation in ZZY-1 and GD-6 shoots and roots, respectively. Unfortunately, in terms of K concentration restoration, As + P failed to deliver, not only in shoots but also roots of both genotypes. Concentration of Mg saw a sharp decline under As stress, where a 59.2% and 44.7% drop was observed in shoots and 74.8% and 48.6% in roots of ZZY-1 and GD-6, respectively. Shoots of ZZY-1 experienced much improvement in Mg content under *S.i* + As (62.9%) and *S.i* + As + P (67.5%) than As + P (only 4.5%), albeit GD-6 shoots were able to benefit mainly from *S.i* + As + P (58.2% recovery) as *S.i* + As and As + P did not yield much improvement (16.4% and 19%, respectively); almost a similar pattern was observed for root Mg concentration in both genotypes.

Construing the activities of reactive oxygen species scavenging enzymes

An increase of 5.3- and 2.6-fold was observed for catalase enzyme activity under As stress in ZZY-1 shoot and root, respectively (Figure 5); ameliorative treatments also brought forth significantly high levels of CAT activity, i.e., 5.5-, 1.45-, and 4.2-fold increase in shoots and 7.2-, 2.3-, and 2.8-fold in roots under *S.i* + As, As + P and *S.i* + As + P, respectively. Contrariwise, the *S.i* and P alone and combined treatments in the absence of As produced a downregulatory response in the activity of aforementioned enzyme, which was true for the ZZY-1 shoot but not completely for its roots, as *S. indica* symbiosis indeed raised the enzymic levels of CAT up to 2-fold; additionally, a 3.48- and 2.4-fold spike was also witnessed for GD-6 shoots and roots, respectively. Arsenic treatment triggered the activity of guaiacol peroxidase significantly in shoots and roots of both genotypes; moreover, the alleviatory treatments, predominantly *S.i* + As, also played their part in enhancing the POD levels in shoots (184% and 87.4% for ZZY-1 and GD-6, respectively), although the combined treatment (*S.i* + As + P) showed a comparatively lower increment

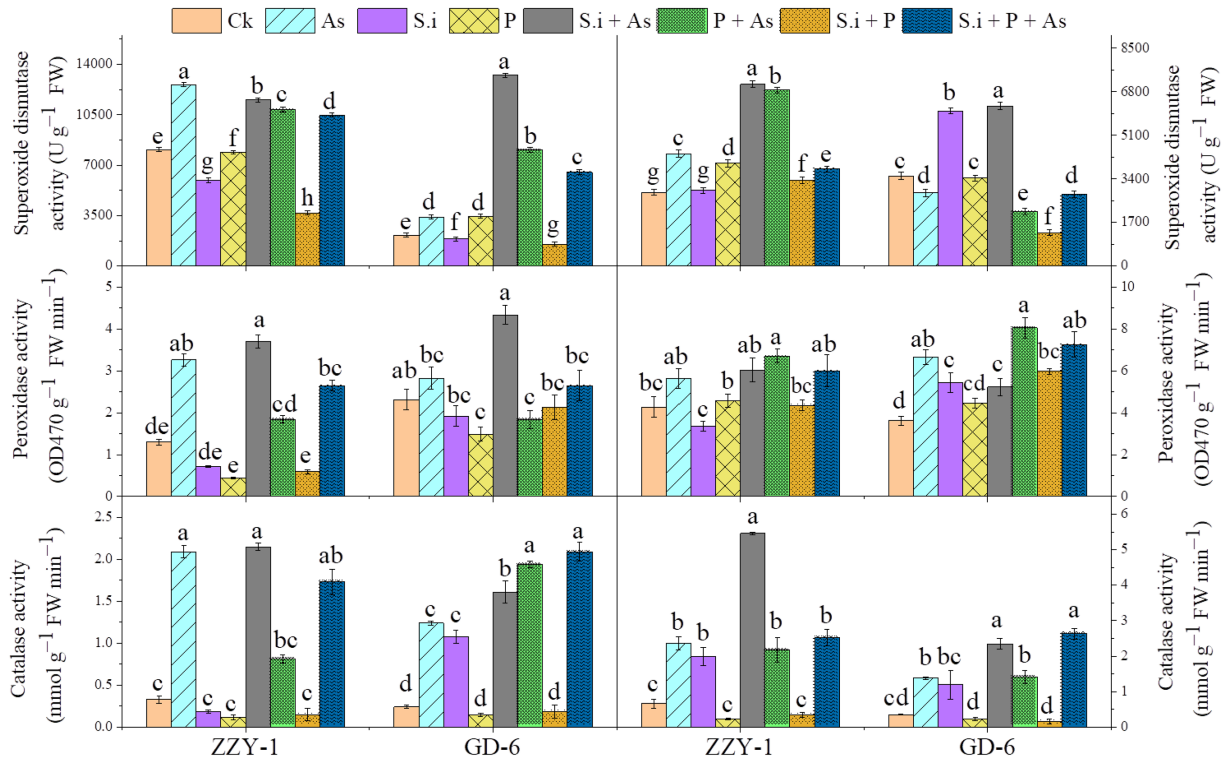

FIGURE 5
Levels of ROS scavenging enzymes in two rice genotypes differing in As accumulation tendency following alone and combined interactions of *Serendipita indica* symbiosis and phosphorus application against As stress. Right panel represent root and left shows analysis of antioxidant enzymic activities in leaves. Vertical bars represent the means of three independent replicates (±SE). Different letters represent significant difference ($p \leq 0.05$) among the treatments within each genotype.

both in shoots and roots of ZZY-1. Additionally, roots of both genotypes exhibited an increased level of POD activity under As + P (56% and 122.4% for ZZY-1 and GD-6, respectively). Compared to control, regardless of the treatment and plant tissue analyzed, the enzyme activity of superoxide dismutase increased with highest values obtained under *S.i* + As (42.3% and 147% in ZZY-1; 513% and 76.7% in GD-6, shoot and root, respectively) among the mitigatory treatments.

Reactive oxygen species and malondialdehyde levels

As presented in Figure 6, all the treatments except for As + P treatment assisted in reducing the lipid peroxidation caused by As toxicity in both above and below ground parts of ZZY-1 and GD-6 genotype. Of note, a 31%, 22.3%, and 49.6% drop in hydrogen peroxide content was observed for ZZY-1 shoots, meanwhile for GD-6, a 71%, 13.2%, and 93.9% decrease was recorded under *S.i* + As, As + P and *S.i* + As + P, respectively. In regard to roots, the abovementioned ameliorating treatments rendered a higher percentage of reduction in H_2O_2 content for both genotypes when compared to their As-stressed counterparts. Furthermore, across the genotypes both in shoot and root, a decline in the superoxide ($O_2^{\cdot-}$) was detected (ZZY-1: 36.8%, 19.7%, and 47.4% in shoots, 22%, 3.9%, and 34% in roots; GD-6: 23.5%, 85.3%, and 97% in shoots, 33.3%, 69.4%, and 50% in roots) when plants under *S.i* + As, As + P and *S.i* + As + P were compared with their respective As-treatments, respectively. Reasonably, there was a strong correlation among A2, A5, A6, B2, B5, and B6 when analyzed through principal component analysis (Figure 7), then among A1, A3, A4, A7, B1, B3, B4, and B7, while A8 and B8 had inter-correlation with the two aforementioned groups.

Relative gene expression pattern

The heat map of genes expressed differentially is presented in Figure 8. Different colors indicate different gene expressions, with light blue being the most up-regulated genes and yellow, the ones least expressed or downregulated. For GD-6 (Figure 8A) and ZZY-1 (Figure 8B) genotypes, relative expression of genes was determined based on the calculated value from the reference gene with up-regulated genes being ≥1 and downregulated genes being <1, with control plants having relative gene expression value equal to 1. A downregulatory trend in the phosphate transporters was observed with the onset of As stress in ZZY-1 genotype shoot as well as roots, in contrast with GD-6 root and shoot tissues where more than 2-fold increase was witnessed for *OsPHT1* gene expression levels. Alone and combined application of *S. indica* and

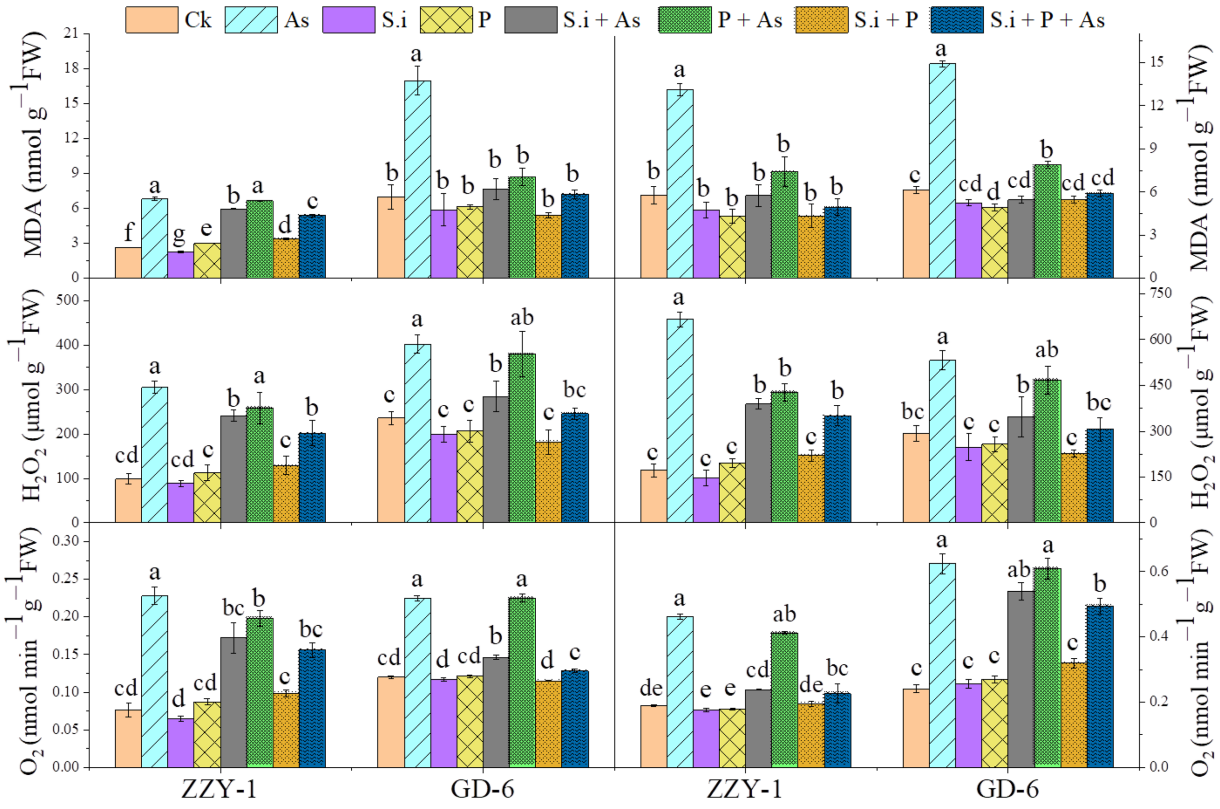

FIGURE 6
Arsenic stress-mediated oxidative burst amelioration through alone and combined interactions of *Serendipita indica* symbiosis and phosphorus application in two rice genotypes differing in As accumulation tendency. Right panel represent root and left shows analysis of ROS levels in leaves. Vertical bars represent the means of three independent replicates (±SE). Different letters represent significant difference ($p \leq 0.05$) among the treatments within each genotype.

phosphorus enhanced the expression of the phosphate transporters as well. In GD-6 shoots, a higher expression of *OsPHT4* was recorded for both *S.i* + As and P + As treatments (4.1- and 4.8-fold increase), while in roots it was mostly in the later treatment (4.2-fold). Regarding ZZY-1 plants, the elevation in the expression of phosphate transporters was mainly observed in roots under treatments with phosphorus supplementation with (2.7-fold increment) or without As treatment (2.3-fold increase). Considering the antioxidative capacity, there was a surge of relative expression in *OsFe-SOD*, *OsMn-SOD*, *OsCu-ZnSOD*, *OsAPX*, and *OsCAT* in both roots and shoots of ZZY-1 under *S.i* + As, P + As and *S.i* + As + P treatments. Whereas for GD-6, As combined with *S.i* or with *S.i* + P yielded the most augmentation in both the tested tissues, particularly the expression levels of *OsMn-SOD* and *OsCAT* with 15.5- and 11.8-fold increase in roots under *S.i* + As, respectively. Note-worthily, a fold change of 8.2 and 3.6 was exhibited by the roots of ZZY-1 under As stress, while the shoots presented a 1.7- and 3.4-fold increase in the expressions of *OsMn-SOD* and *OsCAT* genes as opposed to the control plants, respectively. Moreover, the expression of *OsHMA2* and *OsHMA3* was pronounced in As + P (4.5- and 1.97-fold increase, respectively) and *S.i* + As + P treatments (2.95- and 2-fold, respectively) in leaves, albeit roots displayed a 2.8-fold increase under *S.i* + As, and 1.5- and 3.2-fold as well as 1.2- and 2.3-fold relative increase of *OsHMA2* and *OsHMA3* gene expression under *S.i* + P and *S.i* + As + P, respectively. Arsenic treatment impacted the *OsHMA2* and *OsHMA3* genes in almost all the treatments in GD-6 roots and leaves. Of note, a 4.7- and 3.8-fold increase under As stress was observed in roots along with 3.9- and 2.7-fold increase under phosphorus alone treatment; a similar impact extended toward leaves as well with 2- and 2.9-fold elevation in expression of *OsHMA2* and *OsHMA3* under As stress, while 4.9- and 2.1-fold increase was seen under phosphorus fortification.

Discussion

Most biotechnologists display a great deal of interest in the use of genetically engineered plants with superior yields and improved traits in agriculture considering it safe. However, the public abhorrence of transgenic plants and the fragmentary knowledge regarding post-consumption hazards calls for substitutes that are eco-friendly and, at the same time, cost-effective (Faiz et al., 2022). Interestingly, genotype-dependent alterations became apparent with the onset of As stress as a downregulatory trend in relative expression of phosphate

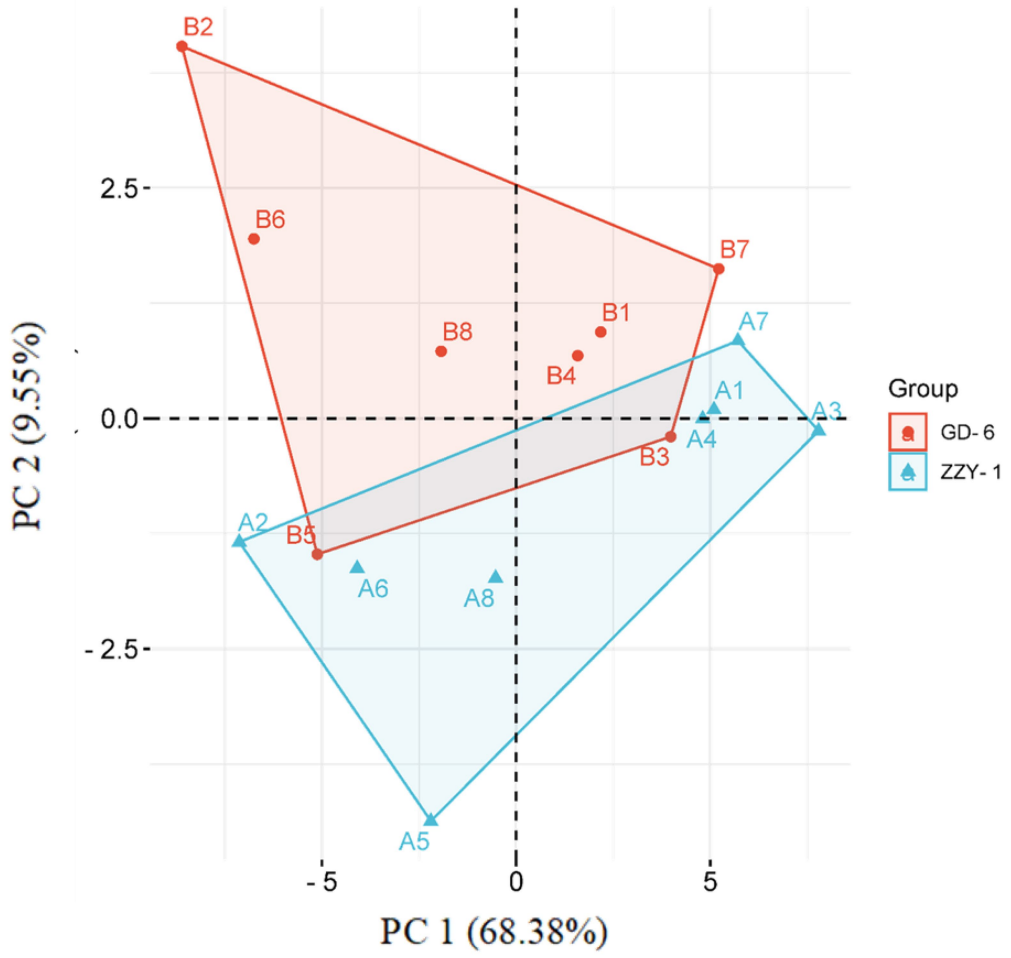

FIGURE 7
A PCA-contingent biplot of measured physio-biochemical parameters under alone and combined *Serendipita indica* symbiosis and phosphorus application. Key: A=ZZY-1 genotype; B= GD-6; numbers 1 to 8 correspond with CK, As, *S.i*, P, *S.i*+As, P+As, *S.i*+P, and *S.i*+P+As, respectively. Sh, Shoot/leaves; R, Root.

transporter genes was displayed by ZZY-1 (Figure 8), more so than GD-6, which explains the reduction in phosphorus concentration in the plants exposed to As toxicity. Arsenic utilizes phosphate transporters to enter the plant's system, for that reason, less As accumulating genotype (i.e., ZZY-1), tended to adopt an avoidance strategy by reducing the expression levels of such genes (Kumar et al., 2011; Ghorbani et al., 2021), even though its development was interfered considerably but the plant still managed to survive and grow slowly, which was the absolute reverse effect observed for GD-6 genotype. Contrariwise, *Serendipita indica*-mediated burgeoning of ZZY-1 and GD-6 plants was predicated on an increased uptake of macro and micro nutrient, particularly P, very much compatible with the upregulation of phosphate transporters in roots such as PHT1-1 and PHT1-5, as described previously for *Arabidopsis* and rice (Johnson et al., 2014). Bajaj et al. (2018) declared a significant increase in the nitrogen, phosphorus and potassium concentration in aboveground tissues of *S. indica*-colonized soybean plants, along with some other vital nutrients, such as manganese, zinc, calcium, magnesium, and especially iron. It has also been confirmed that in symbiosis with roots, *S. indica* acts as a shield or immobilize/sequesters HMs in its vacuoles, and our results regarding As translocation factor (Figure 3) correspond well with those of previous studies (Mohd et al., 2017). By immobilizing As in the roots, *S. indica* prevents its translocation to the aerial parts and subsequent dysfunction of photosynthetic organs, which might, otherwise, lead to reduced chlorophyll biosynthesis, distorted chloroplast membranes and reduced photosynthetic rate (Gusman et al., 2013). Improvement of *Gs* by *S. indica* has also been documented in different plants under various stresses (Saddique et al., 2018; Bertolazi et al., 2019). During its colonization (at early symbiotic stages), extracellular adenosine 5′-triphosphate (eATP) accrues in the apoplast, which is known to promote stomatal opening and helps regulate plant's growth and development along with the biotic and abiotic stress responses (Nizam et al., 2019).

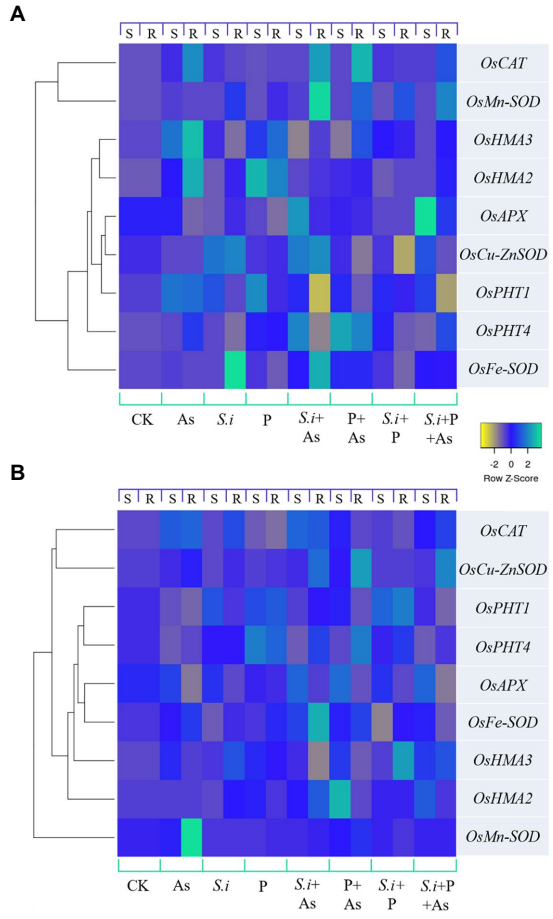

FIGURE 8
Expression levels of certain antioxidant enzymes, phosphate and heavy metal transporter genes under alone and combined *Serendipita indica* symbiosis and phosphorus application in two rice genotypes displaying different As accumulation tendencies. Color scale shows Z values, where yellow depicts downregulatory and light blue shows upregulatory trend. **(A)** GD-6 genotype and **(B)** ZZY-1; S, Shoot; R, Root.

Nam et al. (2021) provided evidence regarding Fe deficiency induced ROS generation as well as chlorosis that becomes more pronounced in the presence of phosphorus rather than its absence, which explains the improved photosynthetic capability and overall growth of plants in this study under *S.i* + As + P treatment as As hinders the uptake of Fe (Mousavi et al., 2020); neither the availability of P alone compensate for Fe deficit, nor does it represent a guarantee of counterbalancing As toxicity (Begum et al., 2008; Abbasi et al., 2021). Availability of P is, tacitly assumed to be, crucial for the concentrations of elements that are imperative for metabolic processes associated with photosynthesis, biomass growth and yield formation, such as Mg (Weih et al., 2021); plants colonized by *S. indica* combined with As and P benefitted much more than the ones without its symbiosis (i.e., As + P), not only in terms of nutrient uptake but also in the element concentration of Mg, which is indispensable for the formation of chlorophyll molecule (Weih et al., 2021). From this perspective, the augmented P proved rather inefficacious, when accompanied by As, for the studied genotypes. The ravaging effects of As on the physiological growth of plants has been delineated extensively in literature (Sharma et al., 2017; Li et al., 2018; Mousavi et al., 2020). Generally, the consensus is that As significantly reduces plant development and root/shoot biomass (Ghorbani et al., 2021). A parallel trend was observed in current study (Table 2; Figure 2), which validates the phytotoxicity of As on rice plants. Arsenic (AsV) vies with PO_4^{3-} in ATP synthesis and replaces it, forming an unstable adenosine diphosphate-As (V), causing disruptions in cellular energy flow (Ye et al., 2017).

Even though plant inoculation with this endophytic symbiont results in phyto-promotion, the inoculation itself exerts a moderate biotic stress that activates defense mechanisms and induces systemic resistance (ISR) in plants (Gill et al., 2016; Shrivastava et al., 2018; Xu et al., 2018). Previous studies explain *S. indica*-mediated root protection through the stimulation of antioxidant system under stress, which likewise prompts developmental reprograming in response to the redox state of the roots and environmental cues (Vadassery et al., 2009; Harrach et al., 2013; Bakshi et al., 2017). It initially colonizes living cells *via* invagination of the cell-membrane, keeping the organelles intact but this biotrophic phase soon progresses into a cell-death related colonization phase (Qiang et al., 2012), rendering dominance of this endophyte over plant's root (Sagonda et al., 2021; Ulhassan et al., 2022). Consequently, a characteristic corollary of *S. indica* symbiosis is an improved plant water homeostasis through an improved root system induction and access of mycelium to water, otherwise outside the reach of the root system, which contributes to higher A_{max} and gaseous exchange (Porcel et al., 2015). The present study results confirmed once again the effectiveness of *S. indica* in alleviating HM toxicity in rice plants concurring with numerous previous studies (Gill et al., 2016; Mohd et al., 2017; Sagonda et al., 2021). Ghorbani et al. (2021) proved in his study that *S. indica* can endow resistance against As toxicity to its host plant by a numbers of mechanisms, a very few of which have been understood by scientists, and among these, is the stimulation of enzymic activities within the plant cells and therefore regulation of stress by the plant natural defense mechanism; the same trends have been recorded in this study apropos of the stimulation of CAT, POD, and SOD in plants colonized by *S. indica*. In addition, other genes of interest, across the treatments and between genotypes, such as *OsMn-SOD*, *OsFe-SOD*, and *OsCu-ZnSOD* were also upregulated between genotypes and across treatments, indicating the relative induction of their activities and highly correlated with the elemental concentrations and the enzymic analysis witnessed across the treatments. The results gave us a new prospective, as we have noticed that the combined effects of the treatments perhaps can be more promising in the As-sensitive genotypes. Heavy metal ATPases, i.e., HMA2 and HMA3 partake in xylem transportation and vacuolar sequestration of HMs, respectively (Adil et al., 2020a). However, their association is not limited to Cd and Zn translocation only as the involvement, of HMA3 in particular, reportedly encompasses stress response,

senescence as well as Fe-deficiency (Zeshan et al., 2021). Current study also showed upregulation in the expressions of both HMAs, especially under treatments with As, which validates the role of these genes in metal homeostasis.

Results from the ROS determination (Figure 6) gave us new perspectives to understand and explain the differential responses of the two rice genotypes and corroborate previous studies done by Karuppanapandian et al. (2011), Ghorbani et al. (2021) and Mohd et al. (2017), all supporting the fact that in stressful conditions, ROS production increases significantly ($p < 0.05$) and this consequently leads to systematic observation of poor growth parameters and bad performances of the plant. Symbiosis of *S. indica* does not induce oxidative burst rather represses it by triggering different enzymes that scavenge ROS (Vadassery et al., 2009). The acquired oxidative burst data correlated with growth parameters and ultrastructure images. The electron imaging of both genotypes tissues cells, revealed the important damaging effects caused by the different treatments on different scales, it was however, noted that the combined treatment effect was greater on root and shoot cellular organelles of GD-6 genotype as shown in Figure 3; these results correlate with the growth parameters discussed above. Taken together, data from this study implied the higher impact of treatments in GD-6 (As-sensitive genotype), surpassing ZZY-1 (As-tolerant genotype). The complex root-fungi cellular interactions necessitate constant recognition/signal exchange (Bonfante and Requena, 2011). Consistent with the fact that *S. indica* is a root colonizing endophyte, its cell wall extracts have been previously reported to induce sequential cytoplasmic and nuclear Ca^{2+}elevations, preferably in the roots and marginally in the shoots (Vadassery et al., 2009). Inferentially, Ca^{2+} ions function as a second messenger in plant-signaling pathways to create a link between extracellular stimuli and intracellular responses (Adil et al., 2020b), thereby facilitating an improved plant performance. A comparatively higher concentration of calcium in both shoots and roots of *S. indica* inoculated plants with or without As stress imply toward the remarkable tendency of this fungus in forearming the plants to the anticipated agricultural challenges.

Conclusion

In current study, the augmented provision of P assisted the susceptible genotype much more than the tolerant one. Moreover, the *S. indica* colonization without additional P was sufficient enough to support growth and photosynthetic aspects of less As accumulating genotype (ZZY-1). The *S. indica* symbiosis serves as a lynchpin by enabling plants to take up and utilize the available resources to their fullest and contributing to an increased P nutrition, improved plant growth and amelioration of As toxicity. High-P contents facilitated by the association of this endophyte convey enough energy to plants for their survival and produce enough biomass to produce a dilution effect. Albeit, for an in-depth assessment of the regulatory pathways that underlie the symbiotic association of *S. indica* with P amended arsenic stressed rice plants, further studies encompassing proteomic or metabolic approaches are imperative. The evidence gathered here portrays the significance of *S. indica* combined with P application as a model approach for integration in sustainable agriculture and the improvement of crop productivity in farmlands polluted with arsenic.

Data availability statement

The original contributions presented in the study are included in the article/supplementary material, further inquiries can be directed to the corresponding author.

Author contributions

SS and MFA: Experimental work, Methodology, Data analysis and Writing—original draft. QF and ZI: Methodology, Formal analyses and Software. FSS, DMB, NU and YO: Writing - review & editing. YG: Conceptualization, Funding acquisition and Writing—review & editing and IHS: Conceptualization, Supervision, Funding acquisition, Correspondence and Writing—review & editing. All authors have read and agreed to the published version of the manuscript.

Funding

This research work was financially supported by the Sino-Pakistan Project NSFC (grant no. 31961143008), National Natural Science Foundation of China, International (Regional) Cooperation and Exchange Program, Research fund for International young scientists (grant no. 31750110462), Jiangsu Collaborative Innovation Center for Modern Crop Production (JCIC-MCP), China and Guizhou Provincial Academician Workstation of Microbiology and Health, Project Number: Guizhou Kehe Platform Talents[2020]4004.

Acknowledgments

The authors gratefully acknowledge China National Rice Research Institute (CNRRI) Fuyang, Zhejiang, China for providing the rice germplasm used in our experiments and J. M. Xu for the technical support regarding this research.

Conflict of interest

The authors declare that the research was conducted in the absence of any commercial or financial relationships that could be construed as a potential conflict of interest.

Publisher's note

References

Abbasi, S., Lamb, D., Rahman, M. A., Naidu, R., and Megharaj, M. (2021). Response of phosphorus sensitive plants to arsenate. *Environ. Technol. Innov.* 24:102008. doi: 10.1016/j.eti.2021.102008

Adil, M. F., Sehar, S., Chen, G., Chen, Z. H., Jilani, G., Chaudhry, A. N., et al. (2020a). Cadmium-zinc cross-talk delineates toxicity tolerance in rice via differential genes expression and physiological/ultrastructural adjustments. *Ecotoxicol. Environ. Saf.* 190:110076. doi: 10.1016/j.ecoenv.2019.110076

Adil, M. F., Sehar, S., Han, Z., Lwalaba, L. W. J., Jilani, G., Zeng, F., et al. (2020b). Zinc alleviates cadmium toxicity by modulating photosynthesis, ROS homeostasis, and cation flux kinetics in rice. *Environ. Pollut.* 265:114979. doi: 10.1016/j.envpol.2020.114979

Ahmad, A., Shafique, S., and Shafique, S. (2014). Intracellular interactions involved in induced systemic resistance in tomato. *Sci. Hortic.* 176, 127–133. doi: 10.1016/j.scienta.2014.07.004

ATSDR. (2007). *Agency for Toxic Substances and Disease Registry. Toxicological Profile for Arsenic*. Atlanta, GA: U.S. Department of Health and Human Services, Public Health Service.

Bajaj, R., Huang, Y., Gebrechristos, S., Mikolajczyk, B., Brown, H., Prasad, R., et al. (2018). Transcriptional responses of soybean roots to colonization with the root endophytic fungus *Piriformospora indica* reveals altered phenylpropanoid and secondary metabolism. *Sci. Rep.* 8:10227. doi: 10.1038/s41598-018-26809-3

Bakshi, M., Sherameti, I., Meichsner, D., Thürich, J., Varma, A., Johri, A. K., et al. (2017). *Piriformospora indica* reprograms gene expression in *Arabidopsis* phosphate metabolism mutants but does not compensate for phosphate limitation. *Front. Microbiol.* 8:1262. doi: 10.3389/fmicb.2017.01262

Begum, M., Akter, J., Jahiruddin, M., and Islam, M. R. (2008). Effects of arsenic and its interaction with phosphorus on yield and arsenic accumulation in rice. *J. Bangladesh Agril. Univ.* 6, 277–284. doi: 10.3329/jbau.v6i2.4822

Bertolazi, A. A., de Souza, S. B., Ruas, K. F., Campostrini, E., de Rezende, C. E., Cruz, C., et al. (2019). Inoculation with Piriformospora indica is more efficient in wild-type rice than in transgenic rice over-expressing the vacuolar H^+-PPase. *Front. Microbiol.* 10:1087. doi: 10.3389/fmicb.2019.01087

Bonfante, P., and Requena, N. (2011). Dating in the dark: how roots respond to fungal signals to establish arbuscular mycorrhizal symbiosis. *Curr. Opin. Plant Biol.* 14, 451–457. doi: 10.1016/j.pbi.2011.03.014

Chadha, N., Mishra, M., Rajpal, K., and Bajaj, R. (2015). An ecological role of fungal endophytes to ameliorate plants under biotic stress. *Arch. Microbiol.* 197, 869–881. doi: 10.1007/s00203-015-1130-3

Delang, C. O. (2018). Causes and distribution of soil pollution in China. *Environ. Socio. Econ. Stud.* 5, 1–17. doi: 10.1515/environ-2017-0016

Faiz, S., Yasin, N. A., Khan, W. U., Shah, A. A., Akram, W., Ahmad, A., et al. (2022). Role of magnesium oxide nanoparticles in the mitigation of lead-induced stress in Daucus carota: modulation in polyamines and antioxidant enzymes. *Int. J. Phytoremediation* 24, 364–372. doi: 10.1080/15226514.2021.1949263

FAOSTAT. (2021). *World Food and Agriculture: Statistical Yearbook 2021*. Rome: FAOSTAT.

Ghorbani, A., Tafteh, M., Roudbari, N., Pishkar, L., Zhang, W., and Wu, C. (2021). *Piriformospora indica* augments arsenic tolerance in rice (*Oryza sativa*) by immobilizing arsenic in roots and improving iron translocation to shoots. *Ecotoxicol. Environ. Saf.* 209:111793. doi: 10.1016/j.ecoenv.2020.111793

Gill, S. S., Gill, R., Trivedi, D. K., Anjum, N. A., Sharma, K. K., Ansari, M. W., et al. (2016). *Piriformospora indica*: potential and significance in plant stress tolerance. *Front. Microbiol.* 7, 1–20. doi: 10.3389/fmicb.2016.00332

Goodall, C. (1991). Procrustes methods in the statistical analysis of shape. *J. R. Stat. Soc. Series B* 53, 285–321. doi: 10.1111/j.2517-6161.1991.tb01825.x

Gusman, G. S., Oliveira, J. A., Farnese, F. S., and Cambraia, J. (2013). Arsenate and arsenite: the toxic effects on photosynthesis and growth of lettuce plants. *Acta Physiol. Plant.* 35, 1201–1209. doi: 10.1007/s11738-012-1159-8

Harrach, B. D., Baltruschat, H., Barna, B., Fodor, J. K., and Ogel, K. H. (2013). The mutualistic fungus *Piriformospora indica* protects barley roots from a loss of antioxidant capacity caused by the necrotrophic pathogen *Fusarium culmorum*. *Mol. Plant Microbe Interact.* 26, 599–605. doi: 10.1094/MPMI-09-12-0216-R

Hill, T. W., and Kafer, E. (2001). Improved protocols for Aspergillus minimal medium: trace element and minimal medium salt stock solutions. *Fungal Genet. Rep.* 48, 20–21. doi: 10.4148/1941-4765.1173

Jiang, M., and Zhang, J. (2001). Effect of abscisic acid on active oxygen species, antioxidative defense system and oxidative damage in leaves of maize seedlings. *Plant Cell Physiol.* 42, 1265–1273. doi: 10.1093/pcp/pce162

Johnson, J. M., Alex, T., and Oelmüller, R. (2014). *Piriformospora indica*: the versatile and multifunctional root endophytic fungus for enhanced yield and tolerance to biotic and abiotic stress in crop plants. *J. Trop. Agric.* 52, 103–122.

Kamiya, T., Islam, R., Duan, G., Uraguchi, S., and Fujiwara, T. (2013). Phosphate deficiency signaling pathway is a target of arsenate and phosphate transporter, *OsPT1*, is involved in as accumulation in shoots of rice. *Soil Sci. Plant Nutr.* 59, 580–590. doi: 10.1080/00380768.2013.804390

Karuppanapandian, T., Moon, J. C., Kim, C., Manoharan, K., and Kim, W. (2011). Reactive oxygen species in plants: their generation, signal transduction, and scavenging mechanisms. *Aust. J. Crop. Sci.* 5, 709–725. doi: 10.3316/informit.282079847301776

Kumar, M., Yadav, V., Kumar, H., Sharma, R., Singh, A., Tuteja, N., et al. (2011). *Piriformospora indica* enhances plant growth by transferring phosphate. *Plant Signal. Behav.* 6, 723–725. doi: 10.4161/psb.6.5.15106

Li, J., Sun, Y., Jiang, X., Chen, B., and Zhang, X. (2018). Arbuscular mycorrhizal fungi alleviate arsenic toxicity to *Medicago sativa* by influencing arsenic speciation and partitioning. *Ecotoxicol. Environ. Saf.* 157, 235–243. doi: 10.1016/j.ecoenv.2018.03.073

Mapodzeke, J. M., Adil, M. F., Wei, D., Joan, H. I., Ouyang, Y., and Shamsi, I. H. (2021). Article modulation of key physio-biochemical and ultrastructural attributes after synergistic application of zinc and silicon on rice under cadmium stress. *Plan. Theory* 10, 1–20. doi: 10.3390/plants10010087

Młodzińska, E., and Zboińska, M. (2016). Phosphate uptake and allocation - A closer look at *Arabidopsis thaliana* L. and *Oryza sativa* L. *Front. Plant Sci.* 7:1198. doi: 10.3389/fpls.2016.01198

Mohd, S., Shukla, J., Kushwaha, A. S., and Mandrah, K. (2017). Endophytic fungi *Piriformospora indica* mediated pprotection of host from arsenic toxicity. *Front. Microbiol.* 8, 1–14. doi: 10.3389/fmicb.2017.00754

Mousavi, S. R., Niknejad, Y., Fallah, H., and Barari-Tari, D. (2020). Methyl jasmonate alleviates arsenic toxicity in rice. *Plant Cell Rep.* 39, 1041–1060. doi: 10.1007/s00299-020-02547-7

Murphy, B. R., Doohan, F. M., and Hodkinson, T. R. (2014). Yield increase induced by the fungal root endophyte *Piriformospora indica* in barley grown at low temperature is nutrient limited. *Symbiosis* 62, 29–39. doi: 10.1007/s13199-014-0268-0

Nagajyoti, P. C., Lee, K. D., and Sreekanth, T. V. M. (2010). Heavy metals, occurrence and toxicity for plants: A review. *Environ. Chem. Lett.* 8, 199–216. doi: 10.1007/s10311-010-0297-8

Nam, H. I., Shahzad, Z., Dorone, Y., Clowez, S., Zhao, K., Bouain, N., et al. (2021). Interdependent iron and phosphorus availability controls photosynthesis through retrograde signaling. *Nat. Commun.* 12:7211. doi: 10.1038/s41467-021-27548-2

Ngwene, B., Boukail, S., Söllner, L., Franken, P., and Andrade-Linares, D. R. (2016). Phosphate utilization by the fungal root endophyte *Piriformospora indica*. *Plant and Soil* 405, 231–241. doi: 10.1007/s11104-015-2779-8

Nizam, S., Qiang, X., Wawra, S., Nostadt, R., Getzke, F., Schwanke, F., et al. (2019). *Serendipita indica* E5'NT modulates extracellular nucleotide levels in the plant apoplast and affects fungal colonization. *EMBO Rep.* 20:e47430. doi: 10.15252/embr.201847430

Porcel, R., Redondo-Gómez, S., Mateos-Naranjo, E., Aroca, R., Garcia, R., and Ruiz-Lozano, J. M. (2015). Arbuscular mycorrhizal symbiosis ameliorates the optimum quantum yield of photosystem II and reduces non-photochemical quenching in rice plants subjected to salt stress. *J. Plant Physiol.* 185, 75–83. doi: 10.1016/j.jplph.2015.07.006

Puckett, E. E., Serapiglia, M. J., Deleon, A. M., Long, S., Minocha, R., and Smart, L. B. (2012). Differential expression of genes encoding phosphate transporters

contributes to arsenic tolerance and accumulation in shrub willow (*Salix* spp.). *Environ. Exp. Bot.* 75, 248–257. doi: 10.1016/j.envexpbot.2011.07.008

Qiang, X., Zechmann, B., Reitz, M. U., Kogel, K. H., and Schafer, P. (2012). The mutualistic fungus *Piriformospora indica* colonizes *Arabidopsis* roots by inducing an endoplasmic reticulum stress-triggered caspase-dependent cell death. *Plant Cell* 24, 794–809. doi: 10.1105/tpc.111.093260

Saddique, M. A. B., Ali, Z., Khan, A. S., Rana, I. A., and Shamsi, I. H. (2018). Inoculation with the endophyte Piriformospora indica significantly affects mechanisms involved in osmotic stress in rice. *Rice* 11:34. doi: 10.1186/s12284-018-0226-1

Sagonda, T., Adil, M. F., Sehar, S., Rasheed, A., Joan, H. I., Ouyang, Y. N., et al. (2021). Physio-ultrastructural footprints and iTRAQ-based proteomic approach unravel the role of *Piriformospora indica*-colonization in counteracting cadmium toxicity in rice. *Ecotoxicol. Environ. Saf.* 220:112390. doi: 10.1016/j.ecoenv.2021.112390

Schmittgen, T. D., and Livak, K. J. (2008). Analyzing real-time PCR data by the comparative CT method. *Nat. Protoc.* 3, 1101–1108. doi: 10.1038/nprot.2008.73

Shah, A. A., Aslam, S., Akbar, M., Ahmad, A., Khan, W. U., Yasin, N. A., et al. (2021). Combined effect of *Bacillus fortis* IAGS 223 and zinc oxide nanoparticles to alleviate cadmium phytotoxicity in *Cucumis melo*. *Plant Physiol. Biochem.* 158, 1–12. doi: 10.1016/j.plaphy.2020.11.011

Shahzadi, I., Khan, Z. H., Akram, W., Khan, W. U., Ahmad, A., Yasin, N. A., et al. (2022). Heavy metal and organic pollutants removal from water using bilayered polydopamine composite of sandwiched graphene Nanosheets: one solution for two obstacles. *Sep. Purif. Technol.* 280:119711. doi: 10.1016/j.seppur.2021.119711

Sharma, S., Anand, G., Singh, N., and Kapoor, R. (2017). Arbuscular mycorrhiza augments arsenic tolerance in wheat (*Triticum aestivum* L.) by strengthening antioxidant defense system and thiol metabolism. *Front. Plant Sci.* 8:906. doi: 10.3389/fpls.2017.00906

Shrivastava, N., Jiang, L., Li, P., Sharma, A. K., Luo, X., Wu, S., et al. (2018). Proteomic approach to understand the molecular physiology of symbiotic interaction between *Piriformospora indica* and *Brassica napus*. *Sci. Rep.* 8:5773. doi: 10.1038/s41598-018-23994-z

Singhal, U., Prasad, R., and Varma, A. (2017). "*Piriformospora indica* (*Serendipita indica*): The novel Symbiont," in *Mycorrhiza-Function, Diversity*. eds. A. Varma, R. Prasad and N. Tuteja (Cham: State of the Art. Springer), 349–364.

Ulhassan, Z., Bhat, J. A., Zhou, W., Senan, A. M., Alam, P., and Ahmad, P. (2022). Attenuation mechanisms of arsenic induced toxicity and its accumulation in plants by engineered nanoparticles: a review. *Environ. Pollut.* 302:119038. doi: 10.1016/j.envpol.2022.119038

UNDESA, (2019). World population prospects 2019: data booklet. ST/ESA/SER.A/424. Available at: https://population.un.org/wpp/Publications/Files/WPP2019_DataBooklet.pdf

Unnikumar, K. R., Sree, K. S., and Varma, A. (2013). *Piriformospora indica*: a versatile root endophytic Symbiont. *Symbiosis* 60, 107–113. doi: 10.1007/s13199-013-0246-y

Vadassery, J., Ranf, S., Drzewiecki, C., Mithöfer, A., Mazars, C., Scheel, D., et al. (2009). A cell wall extract from the endophytic fungus *Piriformospora indica* promotes growth of *Arabidopsis* seedlings and induces intracellular calcium elevation in roots. *Plant J.* 59, 193–206. doi: 10.1111/j.1365-313X.2009.03867.x

Varma, A., Verma, S., Sahay, N. S., Butehorn, B., and Franken, P. (1999). *Piriformospora indica*, a cultivable plant-growth-promoting root endophyte. *Appl. Environ. Microbiol.* 65, 2741–2744. doi: 10.1128/AEM.65.6.2741-2744.1999

Weih, M., Liu, H., Colombi, T., Keller, T., Jäck, O., Vallenback, P., et al. (2021). Evidence for magnesium–phosphorus synergism and co-limitation of grain yield in wheat agriculture. *Sci. Rep.* 11:9012. doi: 10.1038/s41598-021-88588-8

Wu, F., Zhang, G. P., and Dominy, P. (2003). Four barley genotypes respond differently to cadmium: lipid peroxidation and activities of antioxidant capacity. *Environ. Exp. Bot.* 50, 67–78. doi: 10.1016/S0098-8472(02)00113-2

Xu, L., Wu, C., Oelmüller, R., and Zhang, W. (2018). Role of phytohormones in *Piriformospora indica*-induced growth promotion and stress tolerance in plants: more questions than answers. *Front. Microbiol.* 9:1646. doi: 10.3389/fmicb.2018.01646

Ye, Y., Li, P., Xu, T., Zeng, L., Cheng, D., Yang, M., et al. (2017). *OsPT4* contributes to arsenate uptake and transport in rice. *Front. Plant Sci.* 8, 1–12. doi: 10.3389/fpls.2017.02197

Zeng, F. R., Chen, S., Miao, Y., Wu, F. B., and Zhang, G. P. (2008). Changes of organic acid exudation and rhizosphere pH in the rice plants under chromium stress. *Environ. Pollut.* 155, 284–289. doi: 10.1016/j.envpol.2007.11.019

Zeshan, A., Abdullah, M., Adil, M. F., Wei, D. M., Noman, M., Ahmed, T., et al. (2021). Improvement of morpho-physiological, ultrastructural and nutritional profiles in wheat seedlings through astaxanthin nanoparticles alleviating the cadmium toxicity. *J. Hazard. Mater.* 424:126511. doi: 10.1016/j.jhazmat.2021.126511

Zhang, H. Y., Jiang, Y. N., He, Z. Y., and Ma, M. (2005). Cadmium accumulation and oxidative stress burst in garlic (*Allium sativum*). *J. Plant Physiol.* 162, 977–984. doi: 10.1016/j.jplph.2004.10.001

Zhao, F. J., McGrath, S. P., and Meharg, A. A. (2010). Arsenic as a food chain contaminant: mechanisms of plant uptake and metabolism and mitigation strategies. *Annu. Rev. Plant Biol.* 61, 535–559. doi: 10.1146/annurev-arplant-042809-112152

Zhou, Y., Niu, L., Liu, K., Yin, S., and Liu, W. (2018). Arsenic in agricultural soils across China: distribution pattern, accumulation trend, influencing factors, and risk assessment. *Sci. Total Environ.* 616-617, 156–163. doi: 10.1016/j.scitotenv.2017.10.232

Zvobgo, G., Lwalaba, W. L. J., Sagonda, T., Mapodzeke, J. M., Muhammad, N., Shamsi, H. I., et al. (2018). Phosphate alleviates arsenate toxicity by altering expression of phosphate transporters in the tolerant barley genotypes. *Ecotoxicol. Environ. Saf.* 147, 832–839. doi: 10.1016/j.ecoenv.2017.09.043

frontiers | Frontiers in Plant Science

TYPE Original Research
PUBLISHED 13 September 2022
DOI 10.3389/fpls.2022.1001427

OPEN ACCESS

EDITED BY
Waheed Akram,
University of the Punjab, Pakistan

REVIEWED BY
Muhammad Furqan Ashraf,
UiT The Arctic University of Norway, Norway
Iqra Shahzadi,
Wuhan University, China

*CORRESPONDENCE
Zhongjian Liu
zjliu@fafu.edu.cn
Donghui Peng
fjpdh@126.com

SPECIALTY SECTION
This article was submitted to Plant Symbiotic Interactions, a section of the journal Frontiers in Plant Science

RECEIVED 23 July 2022
ACCEPTED 16 August 2022
PUBLISHED 13 September 2022

CITATION
Ahmad S, Chen G, Huang J, Yang K, Hao Y, Zhou Y, Zhao K, Lan S, Liu Z and Peng D (2022) Beauty and the pathogens: A leaf-less control presents a better image of Cymbidium orchids defense strategy. *Front. Plant Sci.* 13:1001427. doi: 10.3389/fpls.2022.1001427

Beauty and the pathogens: A leaf-less control presents a better image of Cymbidium orchids defense strategy

Sagheer Ahmad[1], Guizhen Chen[1], Jie Huang[1], Kang Yang[1], Yang Hao[1], Yuzhen Zhou[1], Kai Zhao[1,2], Siren Lan[1], Zhongjian Liu[1]* and Donghui Peng[1]*

[1]Key Laboratory of National Forestry and Grassland Administration for Orchid Conservation and Utilization at College of Landscape Architecture, Fujian Agriculture and Forestry University, Fuzhou, China, [2]College of Life Sciences, Fujian Normal University, Fuzhou, China

Biological control is a safe way of combating plant diseases using the living organisms. For the precise use of microbial biological control agents, the genetic information on the hypersensitive response (HR), and defense-related gene induction pathways of plants are necessary. Orchids are the most prominent stakeholders of floriculture industry, and owing to their long-awaited flowering pattern, disease control is imperative to allow healthy vegetative growth that spans more than 2 years in most of the orchids. We observed leaf-less flowering in three orchid species (*Cymbidium ensifolium*, *C. goeringii* and *C. sinense*). Using these materials as reference, we performed transcriptome profiling for healthy leaves from non-infected plants to identify genes specifically involved in plant-pathogen interaction pathway. For this pathway, a total of 253 differentially expressed genes (DEGs) were identified in *C. ensifolium*, 189 DEGs were identified in *C. goeringii* and 119 DEGs were found in *C. sinense*. These DEGs were mainly related to bacterial secretion systems, FLS2, CNGCs and EFR, regulating HR, stomatal closure and defense-related gene induction. FLS2 (LRR receptor-like serine/threonine kinase) contained the highest number of DEGs among three orchid species, followed by calmodulin. Highly upregulated gene sets were found in *C. sinense* as compared to other species. The great deal of DEGs, mainly the FLS2 and EFR families, related to defense and immunity responses can effectively direct the future of biological control of diseases for orchids.

KEYWORDS

leaf-less control, orchids, pathogens, biological control, immunity, defense

Introduction

Plants have developed a multi-layered defense system to resist the invasion of pathogens (Kaur et al., 2022). In the primary response, plants recognize pathogens by using PTI (PAMP-triggered immunity) which uses cell-surface pattern-recognition receptors (PRRs). Defense-related genes are activated to produce antimicrobial compounds through MAPK signaling pathway triggered by FLS2 and EFR (Nishad et al., 2020). The increase in the

concentration of Ca^{2+} in the cytosol regulates the production of ROS (reactive oxygen species) and HR (hypersensitive response)/ programmed cell death. The secondary response is called ETI (effector-triggered immunity). In this response, pathogens use secretion systems to inject effector proteins into the plant cells to suppress PTI. Pathogens also invade the immunity of the host plants by manipulating their hormone signaling pathways. In response to pathogen effectors, plants use intracellular surveillance proteins called R proteins to monitor the presence of the virulence proteins from pathogens. The ETI arrests pathogen growth by localized programmed cell death, which causes cultivar-specific disease resistance (Nishad et al., 2020).

FLAGELLIN SENSING 2 (FLS2) is an important regulator of plant immunity against pathogenic bacteria (Zipfel et al., 2004). It acts as a PRR (pattern recognition receptor) for flagellin, which is the building block of bacterial flagellum and is perceived as PAMP (pathogen-associated molecular pattern) protein in animals and plants (Gómez-Gómez and Boller, 2000; Hayashi et al., 2001). PRRs proteins contain single transmembrane bearing N-terminal receptor-like domain that recognizes ligands. FLS2 is the first PRR identified in plants and belongs to a large family of receptor kinases (Robatzek and Wirthmueller, 2013). It can recognize a conserved 22-amino acid peptide called flg22 in the N-terminus of flagellin (Felix et al., 1999; Bauer et al., 2001; Chinchilla et al., 2006). In Arabidopsis, other PRRs include EFR (EF-Tu receptor) that identifies the elf18 peptide corresponding to the N-terminus of the bacterial EF-Tu, and CERK1 (chitin elicitor receptor kinase 1) that recognizes the chitin of fungi and the bacterial peptidoglycans (Zipfel et al., 2006; Miya et al., 2007; Petutschnig et al., 2010; Shafique et al., 2011; Willmann et al., 2011). In rice, chitin-elicitor-binding protein, a receptor protein, functions together with *OsCERK1* for chitin perception (Shimizu et al., 2010). The receptor kinase XA21 uses the XA21 peptide sensing to create resistance against *Xanthomonas oryzae* bacteria (Lee et al., 2009). Tomato receptor proteins LeEix1/2 confer the perception of xylanase from fungi in the ethylene-induction pathway (Ron and Avni, 2004). Moreover, PRRs can perform heterologous functions (Monaghan and Zipfel, 2012). For example, *Ve1* is a PRR in tomato and mediates immunity against *Verticillium* fungus, while it can also provide resistance against *Verticillium* in Arabidopsis (Fradin et al., 2011; De Jonge et al., 2012).

FLS2 regulates the ROS (reactive oxygen species) production, the defense-related hormones (salicylic acid and ethylene), deposition of secondary compounds (e.g., callose) and the transcriptional reprogramming involving WRKY TFs (Boller and Felix, 2009), thereby establishing plant immunity. FLS2 makes a stable complex with BRI-associated kinase 1 (BAK1) in a flg22-dependent manner (Robatzek and Wirthmueller, 2013). BAK1 is a regulatory transmembrane receptor kinase and a member of SERK (somatic embryo receptor kinase) family; it involves brassinosteroid signaling and flg22-activated multiple immune responses (Li et al., 2002; Chinchilla et al., 2007; Heese et al., 2007; Roux et al., 2011; Schwessinger et al., 2011). BAK1 and FLS2 interact with BIK1 (botrytis-induced kinase 1) and its homologs (PBL1, PBL2, and PBS1); while BIK1 is receptor-like cytoplasmic kinase (Robatzek and Wirthmueller, 2013). MAPK (mitogen-activated protein kinase) cascades work downstream of FLS2-BAK1 complex in response to flg22 (Asai et al., 2002; Ichimura et al., 2006). Moreover, FLS2-BAK1 dimerization activates CDPK (calcium dependent protein kinase) signaling pathways (Boudsocq et al., 2010).

Calcium signaling plays important roles in symbiotic and pathogenic plant-microbe interactions (Zipfel and Oldroyd, 2017; Mubeen et al., 2022; Rhodes et al., 2022). PRRs trigger a transiently rapid influx in the cytoplasmic calcium, depending upon the PRR complex and downstream RLCKs (receptor-like cytoplasmic kinases; Ranf et al., 2012, 2014; Li et al., 2014; Monaghan et al., 2015; Ahmad et al., 2018). Recently, a number of calcium channels have been implicated, such as CNGCs (cyclic nucleotide-gated channels; Rhodes et al., 2022). The NRL-triggered cell death, known as HR (hypersensitive response), depends on calcium (Bashir et al., 2013). Treatment with calcium channel blockers and calcium chelators can inhibit cell death (Levine et al., 1996; Grant et al., 2000; Ali et al., 2007).

Perception of PAMP by PRRs instigates a defense response called PTI (pattern-triggered immunity) to inhibit pathogenic infections (Macho and Zipfel, 2014). Against it, pathogens use effector molecules to suppress PTI (Wang et al., 2022) and plants have evolved intracellular receptors to counter effector molecules. These receptors are called NLR (nucleotide-binding, leucine-rich repeats) proteins which activate ETI (effector-triggered immunity; Ngou et al., 2022). PTI and ETI have been considered as two independent pathway layers regulating plant immune system (Rhodes et al., 2022). PRR activation also triggers the phosphorylation of MAPK cascades. MAP kinase kinase kinase (MAPKKK/MEKK) activation triggers the downstream MAP kinase kinase (MAPKK/MKK), which stimulates the downstream MAPK/MPK (Asai et al., 2002; Ichimura et al., 2002; Akram et al., 2014; He et al., 2018; Komis et al., 2018).

The Orchidaceae falls among the largest and the highly evolved monocot plant families (Roberts and Dixon, 2008). Approximately, 70,000 orchid species have been cultivated worldwide as medicinal and ornamental plants (Wong, 2002). The Cymbidium orchids are best known for their ideal characteristics and aesthetic appeal around the world (Cribb, 2014). However, there are a number of biotic (viral, bacterial and fungal diseases) and abiotic (salinity and drought stress) factors that seriously affect the quality and production of orchids (Tuhid et al., 2012; Akram et al., 2019; Ren et al., 2020). For example, Tobamovirus and CymMV (Cymbidium mosaic virus) are the lethal viral pathogens causing necrosis, chlorosis and dwarfism in orchids, which causes huge ornamental and economic losses to orchids (Koh et al., 2014). A little information is available on the immunity mechanism of orchids, although their long vegetative phase requires a strong defense strategy to cope with pathogens. Such studies indicate the orchid immunity and defense responses for some specific diseases. A

transcriptome-wide analysis for multiple orchid species has not been described, especially the Cymbidium orchids. Moreover, a leaf-less control has not been discussed before, that can produce much more genetic information on immunity regulation in the healthy leaves. For an effective biological control, the understanding of orchids defense machinery is a demanding area of research. Therefore, this study identifies an ideal leaf-less control to study the genetic makeup of immunity responses for Cymbidium orchids. Three ideal Cymbidium orchids, *C. ensifolium*, *C. goeringii* and *C. sinense* were used to perform reference-based transcriptome analysis and then genes related to plant-pathogen interaction pathway and MAPK-signaling pathways were ascertained. This study provides a broader image of orchid defense mechanism and maximizes the immunity information than ever before. The outcomes, thus, suggest the effective immunity mechanism to devise biological control strategy for orchids and other floriculture crops.

Materials and methods

Induction of leafless protocorm growth

Three orchid species (*C. ensifolium*, *C. goeringii*, and *C. sinense*) were grown through protocorms in long jars with special media containing 6-BA (8.0 mg L^{-1}), NAA (0.5 mg L^{-1}), sugar (35 g L^{-1}), activated carbon (1.5 g L^{-1}) and agar (7.0 g L^{-1}). The chamber temperature was set to 26 ± 2 °C with a photoperiod of 12 h/day and light intensity of 2,500–3,000 Lx.

Two types of protocorms were obtained for each species; at an age of 6 months, the leaf-less plants which produced flowers without vegetative growth and the normal plants with leaf and root growth. Three replicates were obtained for each pattern of each species for RNA Sequencing.

RNA-seq library preparation and sequencing

A total of 18 (6 tissues in 3 replicates) tissues were obtained from 6 month old plants to extract RNA suing the TaKaRa kit. The total RNA was used to prepare cDNA libraries. The mRNA was obtained with Oligotex Midi Kit for mRNA (Qiagen, Germany) and the quality assessment was done with Nano-Drop spectrophotometer (Thermo Fisher Scientific, United States). The cDNA libraries were prepared by using Illumina protocol. The library product evaluation was made through Agilent 2,200 TapeStation and Qubit®2.0 (Life Technologies, United States), followed by product dilution to 10 pM to generate *in situ* clusters on HiSeq2500 pair-end flow cells and pair-end sequencing (2 × 100). Finally, the reference-based transcriptome sequencing was performed using the reference genomes of each species. Gene expression was measures as FPKM (fragments per kilobase per transcript per million mapped reads).

Functional annotation

The assembled genes were mapped to publically available databases, such as NR (non-redundant), GO (Gene Ontology), KEGG (Kyoto Encyclopedia of Genes and Genomes) and KO (KEGG ortholog) databases using the BLASTX program with a threshold E-value ≤10-5. The GO and KEGG annotations were further classified into functional categories and pathways using the phyper function in R software. The corrected *p*-value was obtained by FDR and the terms with functional *Q*-value ≤0.05 were considered as significantly enriched (Ahmad et al., 2021).

Differentially expressed genes

The Bowtie2 program (v2.4.4, Johns Hopkins University) was used to align clean reads to genomic sequences and the expression level of each sample was calculated using RSEM (v1.2.8) with default parameters. Then the DEGseq package (1.10.1) was used in R software to obtain DEGs. The DEGs were sorted at a threshold value of $p < 0.001$ and the log2FC > 1 (Ahmad et al., 2022).

Plant defense related gene identification

From the DEGs, we filtered the genes related to two key pathways that play important roles in the regulation of defense responses and plant immunity against pathogens. These pathways included Plant-pathogen interaction pathway (ko04626) and MAPK signaling pathway (ko04016). The genes for each pathway were divided into different categories according to their up- and down-regulated trends.

Common interaction network for three species

The common gene names were obtained for defense-related genes for three species and their protein sequences were run on online string facility[1] to generate a network. The network annotation was shown as GO biological processes for all the genes.

Highly upregulated and downregulated genes and pathogen stress pathway

The top five highly upregulated and highly downregulated genes were identified for each species in plant-pathogen interaction pathway. Their expression intensities were drawn as

1 https://string-db.org/cgi/input?sessionId=HofWDb4VJD8K (Accessed August 21, 2022).

heatmap using TBtools.[2] Finally, the pathway integrators were shown for pathogen stress in a combined form for three species.

Results

Expression analysis and pairwise comparison of DEGs

The expression patterns for leaf and leaf-less flowers were observed for each species using the empirical cutoff values of genes with positive expressions. The boxplots in Figure 1 shows the expression distribution of the FPKM values of genes. The boxplots curtail the uniform distribution of median and quartile values of DEGs among samples of each species.

The DEGs were compared between leaf-less flowers and leaf samples within each species separately (Figure 2). The highest number of up- and down-regulated genes (4089) can be seen for *C. goeringii* (Figure 2B), followed by *C. ensifolium* (3414; Figure 2A) and *C. sinense* (2807; Figure 2C). *C. ensifolium* showed the highest number of leaf-specific upregulated genes (2167) as compared to *C. goeringii* (1827) and *C. sinense* (1442). Interestingly, the highest numbers of downregulated genes were observed in the leaves of *C. goeringii* (2262), which was significantly different from *C. ensifolium* (1247) and *C. sinense* (1365).

2 https://github.com/CJ-Chen/TBtools/releases (Accessed August 21, 2022).

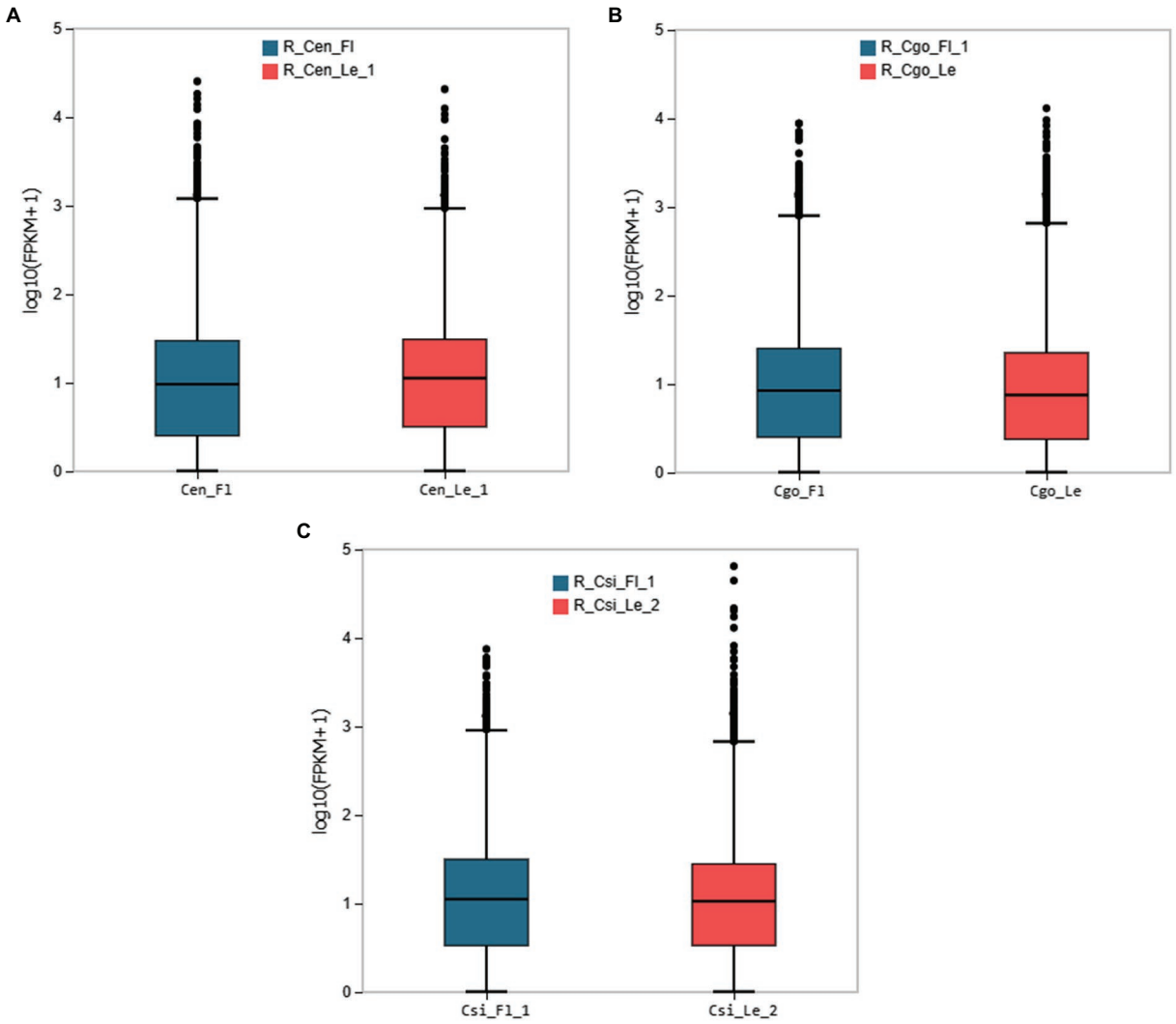

FIGURE 1
The boxplot distribution of gene expression from the two tissues of each species; **(A)** *C. ensifolium*, **(B)** *C. goeringii*, **(C)** *C. sinense*. The X-axis shows the sample name; the Y-axis represents log10(FPKM+1). The boxplot of each area shows five statistics (from top to bottom are the upper limit, upper quartile, median, and lower quartile, respectively).

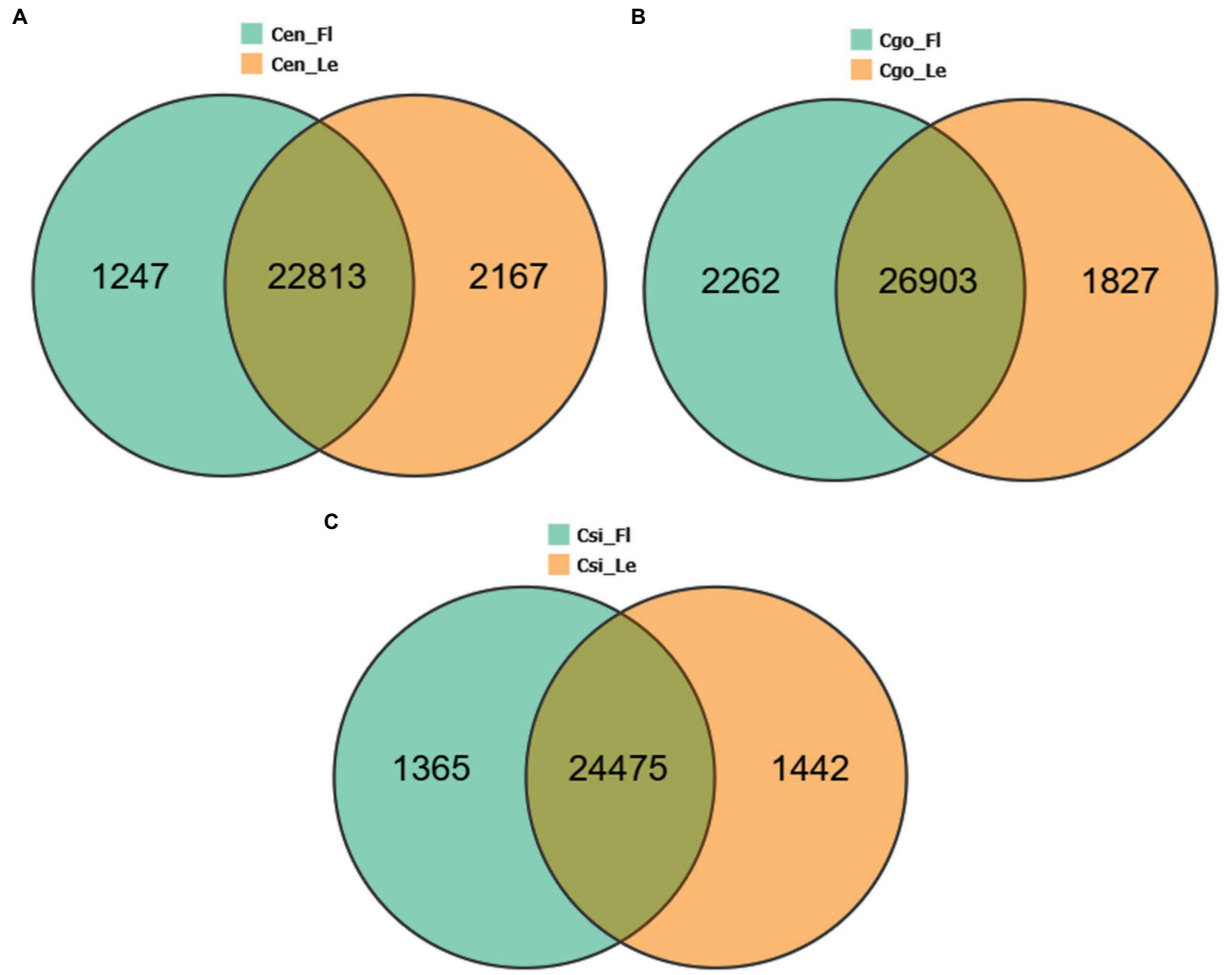

FIGURE 2
Individual species tissue-specific and common DEGs among the leaf-less control and leaf samples of *C. ensifolium* **(A)**, *C. goeringii* **(B)**, and *C. sinense* **(C)**.

GO and KEGG annotation analysis

The GO annotation was obtained for individual species (Figure 3). For *C. ensifolium* the maximum number of genes was related to cellular process and metabolic process in the GO biological process category (Figure 3A). For the cellular component category, the highest number of genes was enriched for cellular anatomical entities followed by intracellular components. The major molecular functions were related to catalytic activity and binding (Figure 3A). In the case of *C. goeringii* (Figure 3B), the GO annotations were similar to *C. ensifolium*. Although similar GO enrichments were observed for *C. sinense* (Figure 3C), however, the number of genes were less than other two species.

The plant-pathogen interaction pathway (ko04626) was counted among the most enriched KEGG pathways in the three orchid species (Figure 4). Highly enriched number of genes for this pathway were found in *C. ensifolium* (Figure 4A), followed by *C. goeringii* (Figure 4B) and *C. sinense* (Figure 4C). MAPK signaling pathway was prominent among the other pathways in *C. ensifolium* and *C. goeringii*, however, it was not prominent in *C. sinense*. The other major pathways with significant gene enrichment included plant hormone signal transduction, phenylpropanoid biosynthesis, and starch and sucrose metabolism, which may indirectly play roles in plant defense and immunity responses.

Defense responses for each species

A number of plant-pathogen interaction response pathways were observed in the three orchid species (Figure 5). All the routes were converged to the three key responses, i.e., defense related gene induction, stomatal closure and hypersensitive response. The stimulation originates from the cell membrane and the final responses are shown in the cytoplasm of plant cells. Four key response generators were observed in the three species, including CNGCs, FLS2, EFR and bacterial secretion system

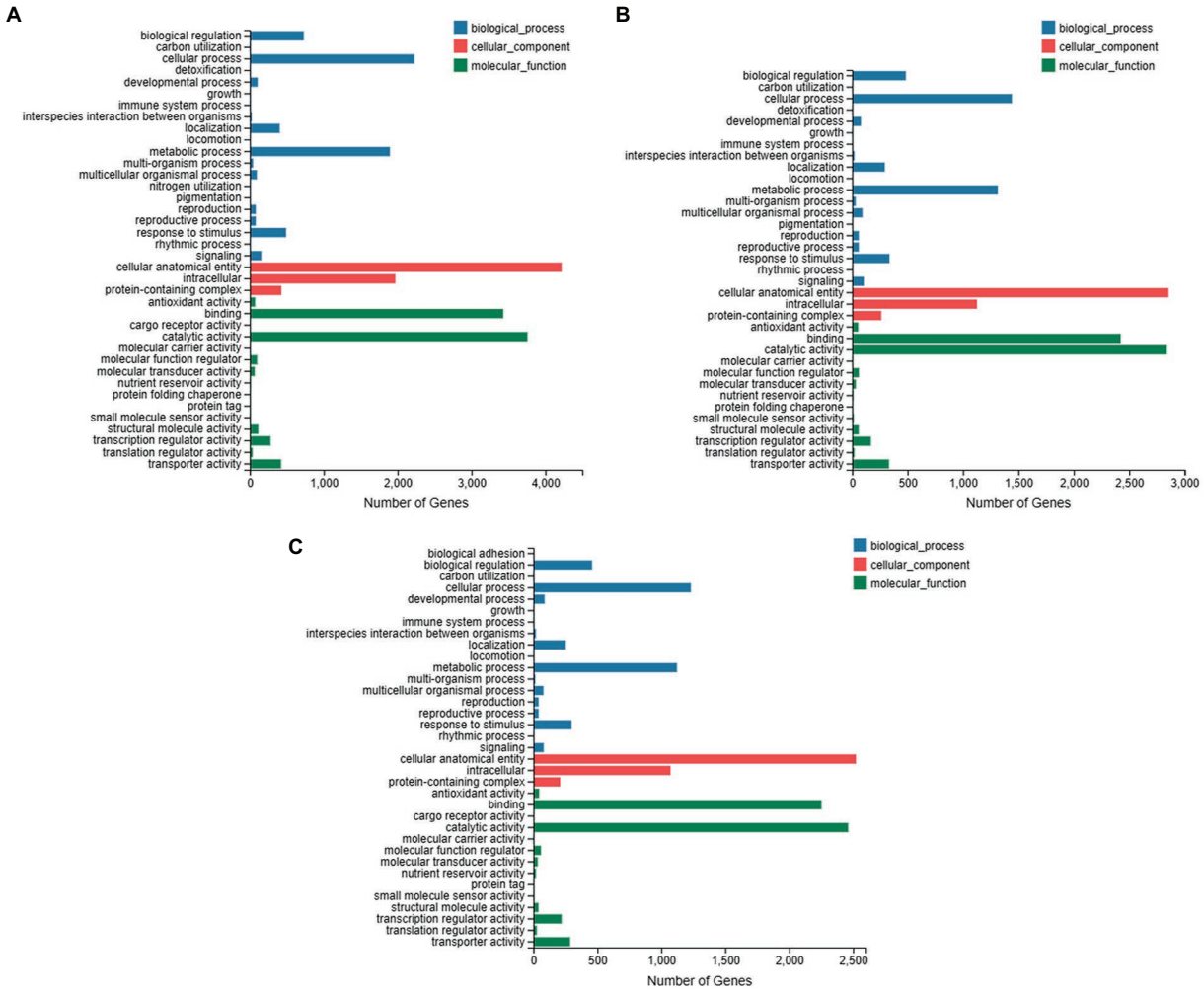

FIGURE 3
Overview of GO enrichments for *C. ensifolium* **(A)**, *C. goeringii* **(B)**, and *C. sinense* **(C)**. The DEGs enrichment is shown in three GO categories, including biological process, cellular component and molecular function. The y-axis shows the GO category and the x-axis shows the number of genes enriched to each category.

(Supplementary Tables 1–3). In *C. ensifolium*, the genes related to CNGCs were upregulated in leaves as compared to leaf-less flowers (Figure 5A). Contrarily, the EFR related genes were downregulated in the leaves. The FLS2 contained both upregulated and downregulated genes. The other solely upregulated genes were related to Rboh in the CNGCs routes, MEKK1 in the FLS2 route and *Pti1* in the bacterial secretion route. All other regulators contained both upregulated and downregulated genes (Figure 5B). Higher number of downregulated genes were observed in *C. ensifolium* leaves than upregulated genes among the 27 expressed pathway stimulators (Figure 5B). Moreover, *NHO1* was the only defense-related gene downregulated in the leaves of three species.

Contrary to *C. ensifolium* the EFR contained both upregulated and downregulated genes in *C. goeringii* (Figure 5C). Moreover, the *MEKK1* and *Pti1* were completely downregulated, while Pti6 was upregulated as compared to *C. ensifolium*. In the bacterial secretion route, the *RPM1* and *RPS2* were completed downregulated in the *C. goeringii* leaves as compared to *C. ensifolium* (Figure 5C). Similar to *C. ensifolium*, *NHO1* was the only defense related gene downregulated in the leaves of *C. goeringii*. Moreover, the number of downregulated genes was higher than the upregulated genes (Figure 5D).

The defense-related genetic map of *C. sinense* was much different than other two species (Figures 5E,F). In the CNGCs rout, Rboh genes were completely upregulated in the leaves. In the FLS2 route, *MKK4/5* and *WRKY22* and *WRKY29* were also upregulated. In the bacterial secretion route, the *RIN4*, *RPS2* and *PBS1* were upregulated, while, the *RAR1* and *HSP90* were completely downregulated. Three defense-related genes were induced in *C. sinense* as compared to other two species. Here, the *FRK1* and *PR1* were upregulate and *NHO1* was downregulated. Most of the genes were upregulated in *C. sinense* contrary to other two species, while a few were downregulated (Figure 5F).

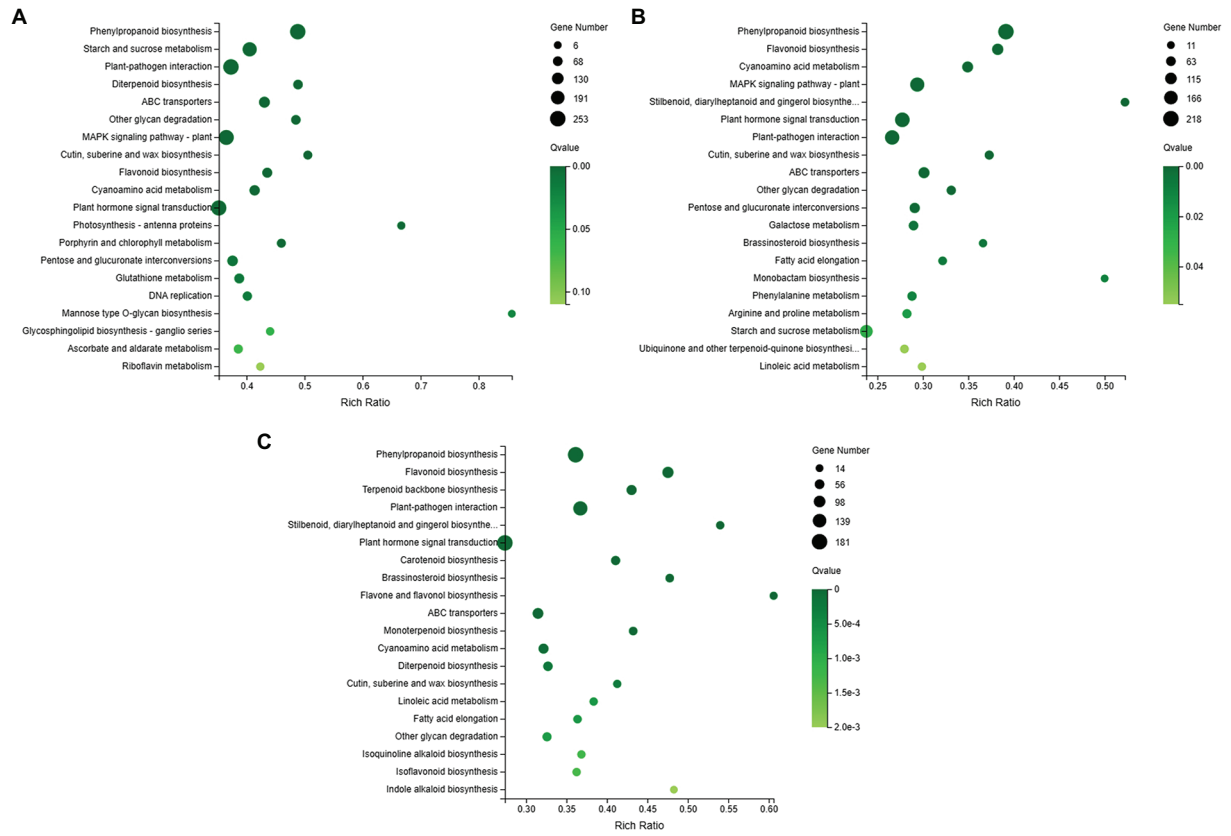

FIGURE 4
Overview of KEGG enrichments for *C. ensifolium* **(A)**, *C. goeringii* **(B)**, and *C. sinense* **(C)**. The y-axis shows the KEGG pathway names and the x-axis shows the pathway-richness ratio. The size of the black circles shows the number of genes enriched to each pathway; bigger the circle size more is the number of genes.

Interaction networks by defense proteins

The protein sequences of plant-pathogen interaction and MAPK signaling pathway genes were run on the online string database to see their interaction patterns (Figure 6A). All the important regulators of plant defense and immunity were interconnected. The interconnected proteins were mainly involved in calcium mediated signaling (GO:0019722), cellular macromolecule metabolic process (GO:0044260), defense responses (GO:0006952), defense response to bacteria (GO:0042742), hormone-mediated signaling (GO:0009755), immune system process (GO:0002376), and JA-mediated signaling (GO:2000022; Figure 6C).

Up-and down-regulation profiles were compared for both the pathways (Figure 6B). For plant-pathogen interaction pathway the number of downregulated genes was higher than the number of upregulated genes in *C. ensifolium* and *C. goeringii* as compared to *C. sinense*, where the number of downregulated genes (40) was significantly lower than the number of upregulated genes (79; Figure 6B). For MAPK signaling pathway, the number of upregulated genes was higher than that of downregulated genes in *C. ensifolium* and *C. sinense*. However, the number of upregulated genes (77) was significantly lower than the number of downregulated genes (104) in *C. goeringii*.

Highly tissue-specific gene sets

The leaf-less controls provides the best control to study the defense and immunity mechanism in the leaf (Figure 7A). Using this control, we found the top 5 highly upregulated and highly downregulated genes in the leaves of three orchid species (Figure 7B). In *C. ensifolium*, the downregulated genes included calmodulin, three EFRs and one FLS2, while the upregulated genes included three FLS2s, *CDPK* and *WRKY2*. In *C. goeringii*, the downregulated genes included FLS2, MAPK4, rhamnogalacturonan endolyase, Pti1-like and HtpG, while the upregulated genes included three disulfide isomerases, MAPK4/5 and ULK4. In the case of *C. sinense*, the downregulated genes included two *WRKY2*, FLS2, calmodulin and rhamnogalacturonan endolyase, while the upregulated genes were *CML41*, *FLS2*, *CML30*, *WRKY72*, and *RPM1* (Figure 7B).

In the orchid species, the defense-related responses are induced by four key routes, including bacterial secretion system,

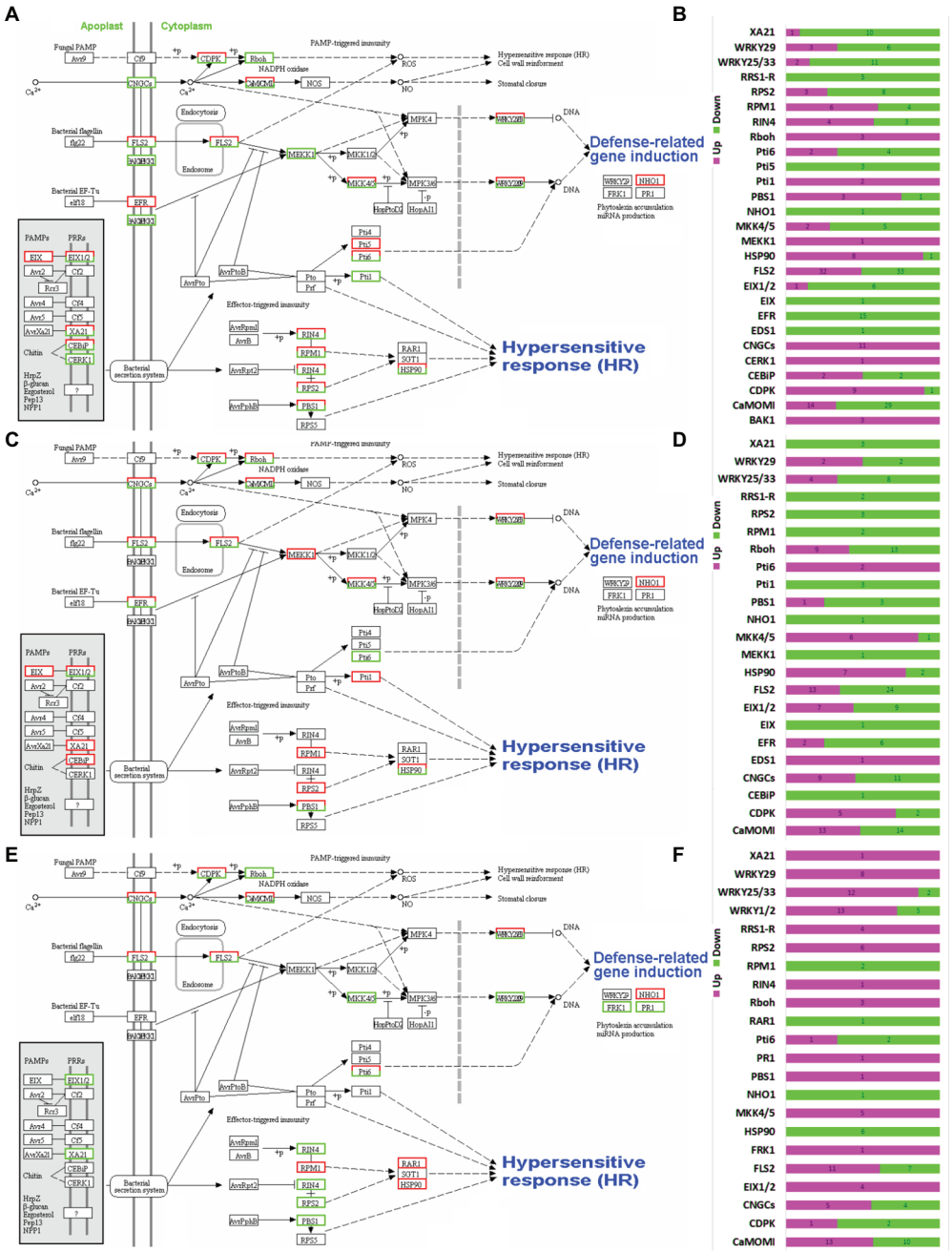

FIGURE 5
Overview of defense response pathway and the distribution of up- and downregulated pathway integrators for *C. ensifolium* **(A,B)**, *C. goeringii* **(C,D)**, and *C. sinense* **(E,F)**.

FLS2, CNCGs, and EFR (Figure 7C). The bacterial secretion system stimulates four proteins in orchids, such as RIN4, RPS2, RPM1 and PBS1. RIN4 was not expressed in *C. goeringii*, while the remaining three were expressed in all the three species. These proteins ultimately instigate hypersensitive response (HR) through the stimulation of *RAR1* and *HSP90*. *RAR1* was only downregulated in *C. sinense*, while it was not expressed in other two species. *HSP90* was downregulated in *C. sinense* and showed both up- and down-regulation in *C. ensifolium* and *C. goeringii*. FLS2 also triggers HR through reactive oxygen species (ROS). Both up- and downregulation profiles were found for FLS2 in the three orchid species. The CNGCs use calcium signaling to induce CaM, which then cause HR and stomatal closure through NOS and NO signals. Both up- and downregulation profiles were found for CNGCs and CaM in the three orchid species.

The EFR routes works differently than the previous three routes and cause the induction of defense-related genes. It

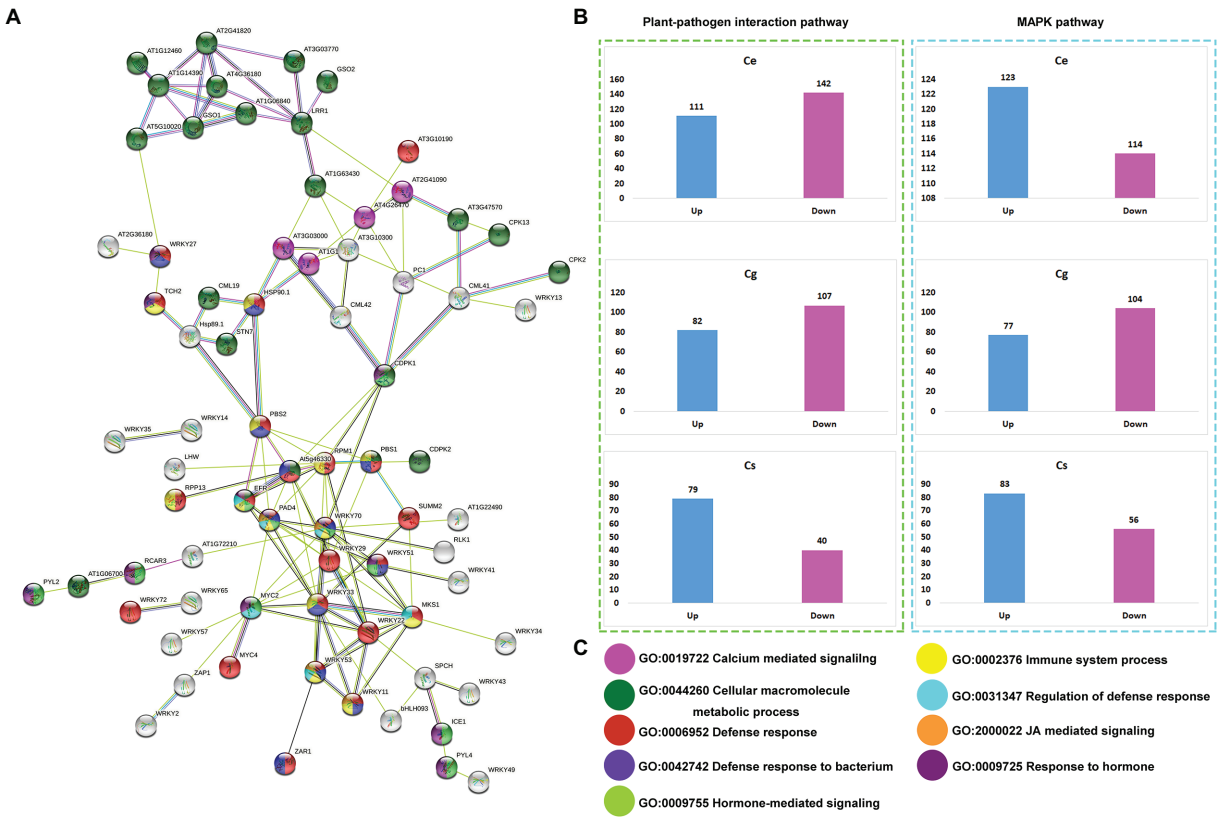

FIGURE 6
Identification string-based interaction network for all the genes expressed in three orchid species **(A)**, up- and downregulated genes for plant-pathogen interaction pathway and MAPK signaling pathway for three orchid species **(B)**, and the representation of major biological process enriched in the interaction network **(C)**.

involves multiple regulatory before the final response. These regulators include *MEKK1*, *MKK4/5*, *MPK* and *WRKY*, which finally induce defense-related genes, such as *NHO1*, *FRK1* and *PR1*. EFR and MEKK1 genes were not expressed in *C. sinense*, while MPK genes were not expressed in any of the species. The *MKK4/5* and *WRKY* were expressed in all the species. Among the defense-related genes, the *NHO1* was expressed in all the species, while the *FRK1* and *PR1* were expressed only in *C. sinense* (Figure 7C).

Discussion

Orchids share a huge portion of floriculture industry. Obtaining virus free orchids through meristem culturing has been used to control the spread of diseases (Panattoni et al., 2013). However, tissue culturing of orchids is very costly and time-consuming and their long vegetative phase (2–3 years) requires a permanent solution against pathogens. The mechanisms of plant defense and immunity against pathogens have been documented in numerous model plants. However, limited genomic information has been presented on the orchids, especially the Cymbidium orchids. A detailed and genome-wide searching of defense-related genes would facilitate the future breeding programs for disease-resistance in Orchidaceae.

Reference-based transcriptome sequencing produced significantly upregulated and downregulated gene profiles for leaf-less control and leaf samples for each of three orchid species, *C. ensifolium*, *C. goeringii* and *C. sinense* (Figure 2). Cellular and metabolic process were the most enriched GO biological processes, mainly involving catalytic and binding activities in the cellular anatomical entities (Figure 3). Plant-pathogen interaction and MAPK signaling pathways were highly enriched KEGG terms in the three orchid species (Figure 4) among the other pathways including, mainly, plant hormone signal transduction and phenylpropanoid biosynthesis pathways. The data enrichment suggests the significance of plant defense and immunity responses of orchids.

Highly upregulated and downregulated transcripts associated with plant-pathogen interaction were induced for the leaves of three orchid species. For example, LRR receptor kinases encoding transcripts were highly expressed in the leaves as compared to leaf-less controls. EFR and FLS2, LRR receptor-like kinases, are the primary response elements and act to recognize bacterial epitopes elf18 and flg22

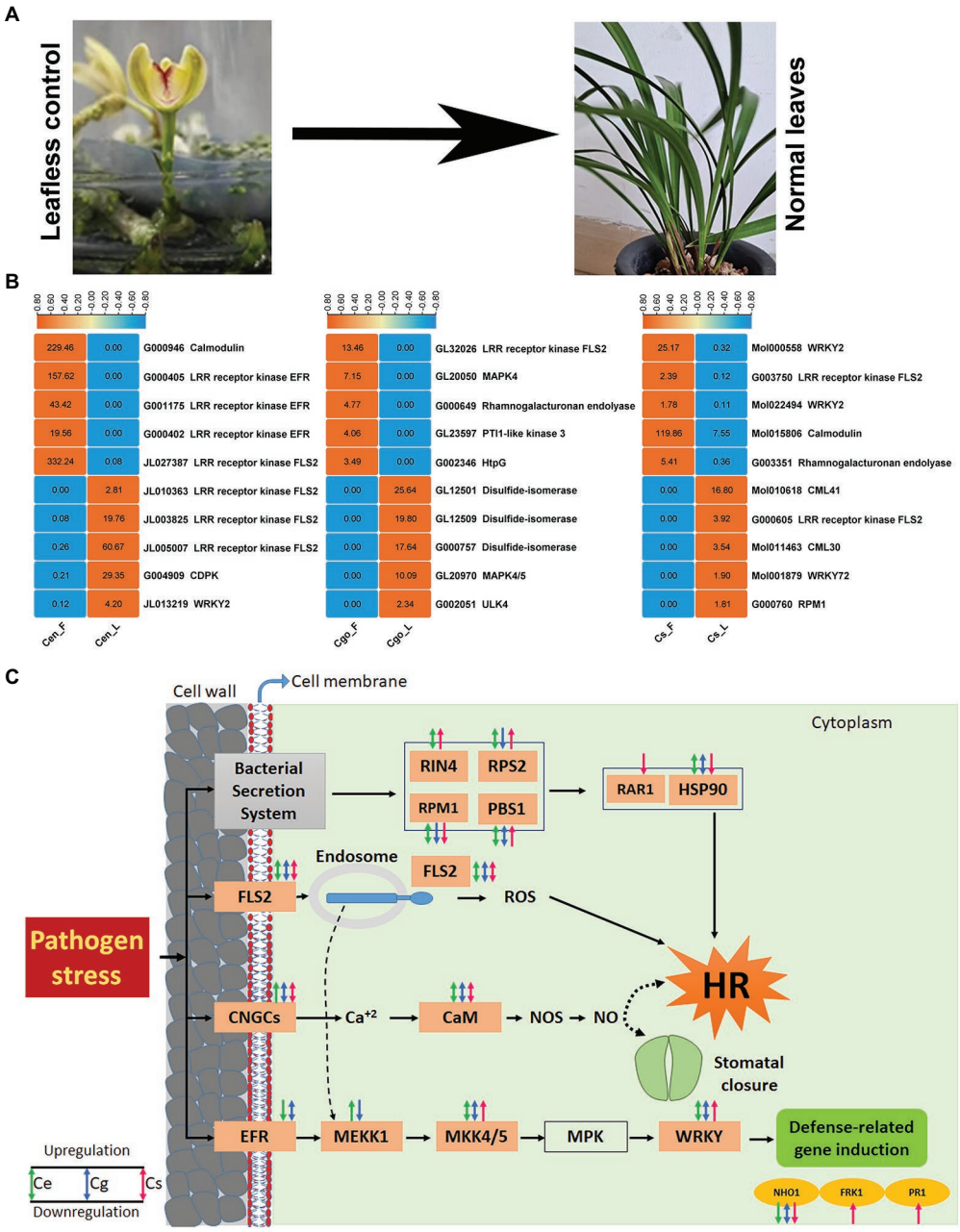

FIGURE 7
Leaf-less control and the healthy leaf samples used for sequencing analysis **(A)**, top 5 highly upregulated and highly downregulated defense-related DEGs **(B)**, and the final pathway of pathogen stress showed by three orchid species **(C)**. The orange boxes show the genes expressed in either of the species.

(Figures 5A,C,E; Saijo et al., 2009; Ahmad et al., 2014). A total of 65 FLS2-related transcripts (32 upregulated and 33 downregulated) were found in the leaves of *C. ensifolium* (Figure 5D), while 15 EFRs were found, which were all downregulated. In *C. goeringii*, 37 FLS2s were found (13 upregulated and 24 downregulated; Figure 5F), while there were 8 EFRs (2 upregulated and 6 downregulated). *C. sinense* contained 18 FLS2s (11 upregulated and 7 downregulated) and no EFR expressed here (Figure 5F).

CML and CaM are calcium sensors and play pivotal roles in calmodulin signaling pathways involving oxidative burst and cell death regulation in the infected plants enduring HR (Harding et al., 1997; Harding and Roberts, 1998; Poovaiah et al., 2013). A total of 43 CaM transcripts were identified in *C. ensifolium* (14 upregulated and 29 downregulated; Figure 5B), 27 in *C. goeringii* (13 upregulated and 14 downregulated; Figure 5D), and 23 CaMs were identified in *C. sinense* (13 upregulated and 10 downregulated; Figure 5F).

Plants use specific pattern recognizing receptors to identify microbes. These receptors are activated by MAMPs (microbe associated molecular patterns), which results into MTI (MAMP-triggered immunity). However, clever pathogens bypass MTI using virulence effectors, thereby causing pathogen proliferation. In the resistant genotypes, intracellular immune receptors detect these effectors and start defense responses called ETI (effector triggered immunity), including HR and transcriptional reprogramming in order to halt the growth of pathogens. *Pseudomonas syringae* secretes AvrRpm1 effector into the host cell to induce virulence. *RIN4* negatively regulates MTI and its modification in the presence of effectors like ArvRpm1. The *RPM1* and *RPS2* are a nucleotide binding leucine-rich repeat sensors. *RPM1* perceives the perturbation of *RIN4* in disease resistance, which also activates the *RPS2*, causing an enhanced immune response (Cherkis et al., 2012). Heat shock proteins (HSP90) involve detoxification and stress responses (Azaiez et al., 2009). The AvrB effector of *P. syringae* suppresses PTI by using RAR1, an HSP90 cochaperone required for ETI, indicating that RAR1 is a negative regulator of PTI (Shang et al., 2006). Our data included all the components responding to ETI, including *RIN4*, *RPS2*, *RPM1*, *PBS1*, *HSP90*, which were expressed in all the species, except *RAR1* which was only expressed but downregulated in the leaves of *C. sinense* (Figure 7C), suggesting the immunity level of Cymbidium orchids against RAR-mediated pathogenic attack.

Among the highly expressed genes, EFRs were downregulated in the leaves of *C. ensifolium*, while FLS2s were upregulated. A number of WRKY transcription factors were differentially expressed, such as *WRKY25*, *WRKY29*, and *WRKY33* (Figures 5B,D,F). WRKY TFs have admitted role in the regulation of plant defense responses (Eulgem, 2006; Knoth et al., 2007; Azaiez et al., 2009; Faiz et al., 2022). *WRKY2* represses the basal immunity of barley by directly targeting PAMP recognition receptor genes (Yu et al., 2022). It was upregulated in the leaves of *C. ensifolium*, while downregulated in the leaves of *C. sinense* (Figure 7), suggesting that orchids may differ in their immunity responses even within the same genus. Similarly FLS2 has also dual roles with both upregulated and downregulated genes in the three species.

Previous studies show that flg22 triggers MAP kinases, such as MEKK1, MKK4/5 and MPK (Nuhse et al., 2000; Asai et al., 2002). Three flg22-inducible genes, including *NHO1*, *FRK1*, and *WRKY29* (An and Mou, 2012), are induced by this cascade of kinases in the EFR pathway. We found up- and downregulated transcripts for *EFR*, *MEKK1*, *MKK4/5*, and defense-related genes, such as *NHO1*, *FRK1*, and *PR1* (Figure 7C). *NHO1* was expressed in all the species, while *FRK1* and *PR1* were upregulated only in *C. sinense*. Our study, thus, presents a general comparison among three orchid species for a transcriptome-wide mining of defense related genes. This information can be used to plant biological control strategies for orchids and floriculture crops.

Conclusion

This is the first study that uses leaf-less control to mine the defense and immunity related gene profiles in three Cymbidium orchids. A number of upregulated and downregulated genes were identified in four major routes of pathogen stress, including bacterial secretion system, FLS2, CNGCs and EFR. These routes mainly regulate three processes, namely, hypersensitive response (HR), stomata closure and defense-related gene induction. The regulation of immunity response was a little different in *C. sinense* as compared to *C. ensifolium* and *C. goeringii*. For example, two of the defense related genes (*FRK1* and *PR1*) were upregulated only in *C. sinense*, while they did not express in other two species. Overall, the results present a broad picture of defense machinery of Cymbidium orchids, which can be used to ameliorate pathogen affliction through biological control.

Data availability statement

The transcriptome sequences described in this article have been submitted to The National Genomics Data Center (NGDC, https://ngdc.cncb.ac.cn) under accession number PRJCA009885.

Author contributions

SA: conceptualization and writing—original draft. GC: data curation and software. JH: investigation. KY: data curation. YH: software. YZ: visualization, investigation, and editing. KZ: data curation and editing. SL: software and editing. ZL: supervision, conceptualization, and funding acquisition. DP: supervision, conceptualization, funding acquisition, and writing—reviewing and editing. All authors contributed to the article and approved the submitted version.

Funding

This work was supported by The National Natural Science Foundation of China (no. 32071815); The National Key Research and Development Program of China (2019YFD1001000); The National Key Research and Development Program of China (2018YFD1000401); The Innovation and Application Engineering Technology Research Center of Ornamental Plant Germplasm Resources in Fujian Province (115-PTJH16005); and National Natural Science Foundation of China (no. 32101583).

Acknowledgments

We are thankful to funding agencies for funding support.

Conflict of interest

The authors declare that the research was conducted in the absence of any commercial or financial relationships that could be construed as a potential conflict of interest.

Publisher's note

All claims expressed in this article are solely those of the authors and do not necessarily represent those of their affiliated organizations, or those of the publisher, the editors and the reviewers. Any product that may be evaluated in this article, or claim that may be made by its manufacturer, is not guaranteed or endorsed by the publisher.

Supplementary material

The Supplementary material for this article can be found online at: https://www.frontiersin.org/articles/10.3389/fpls.2022.1001427/full#supplementary-material

References

Ahmad, A., Shafique, S., and Shafique, S. (2014). Intracellular interactions involved in induced systemic resistance in tomato. *Sci. Hortic.* 176, 127–133. doi: 10.1016/j.scienta.2014.07.004

Ahmad, A., Yasin, N. A., Ibrahim, A., Shahzadi, I., Gohar, M., Bashir, Z., et al. (2018). Modelling of cotton leaf curl viral infection in Pakistan and its correlation with meteorological factors up to 2015. *Clim. Dev.* 10, 520–525. doi: 10.1080/17565529.2017.1318738

Ahmad, S., Chen, J., Chen, G., Huang, J., Hao, Y., Shi, X., et al. (2022). Transcriptional proposition for uniquely developed protocorm flowering in three orchid species: resources for innovative breeding. *Front. Plant Sci.* 13:942591. doi: 10.3389/fpls.2022.942591

Ahmad, S., Lu, C., Gao, J., Ren, R., Wei, Y., Wu, J., et al. (2021). Genetic insights into the regulatory pathways for continuous flowering in a unique orchid Arundina graminifolia. *BMC Plant Biol.* 21:587. doi: 10.1186/s12870-021-03350-6

Akram, W., Anjum, T., Ahmad, A., and Moeen, R. (2014). First report of Curvularia lunata causing leaf spots on Sorghum bicolor from Pakistan. *Plant Dis.* 98:1007. doi: 10.1094/PDIS-12-13-1291-PDN

Akram, W., Aslam, H., Ahmad, S. R., Anjum, T., Yasin, N. A., Khan, W. U., et al. (2019). Bacillus megaterium strain A12 ameliorates salinity stress in tomato plants through multiple mechanisms. *J. Plant Interact.* 14, 506–518. doi: 10.1080/17429145.2019.1662497

Ali, R., Ma, W., Lemtiri-Chlieh, F., Tsaltas, D., Leng, Q., Von Bodman, S., et al. (2007). Death don't have no mercy and neither does calcium: Arabidopsis CYCLIC NUCLEOTIDE GATED CHANNEL2 and innate immunity. *Plant Cell* 19, 1081–1095. doi: 10.1105/tpc.106.045096

An, C., and Mou, Z. (2012). Non-host defense response in a novel Arabidopsis-Xanthomonas citri subsp. citri pathosystem. *PLoS One* 7:e31130. doi: 10.1371/journal.pone.0031130

Asai, T., Tena, G., Plotnikova, J., Willmann, M. R., Chiu, W.-L., Gomez-Gomez, L., et al. (2002). MAP kinase signalling cascade in Arabidopsis innate immunity. *Nature* 415, 977–983. doi: 10.1038/415977a

Azaiez, A., Boyle, B., Levée, V., and Séguin, A. (2009). Transcriptome profiling in hybrid poplar following interactions with Melampsora rust fungi. *Mol. Plant-Microbe Interact.* 22, 190–200. doi: 10.1094/MPMI-22-2-0190

Bashir, Z., Ahmad, A., Shafique, S., Anjum, T., Shafique, S., and Akram, W. (2013). Hypersensitive response—a biophysical phenomenon of producers. *Eur. J. Microbiol. Immunol.* 3, 105–110. doi: 10.1556/EuJMI.3.2013.2.3

Bauer, Z., Gómez-Gómez, L., Boller, T., and Felix, G. (2001). Sensitivity of different ecotypes and mutants of Arabidopsis thaliana toward the bacterial elicitor flagellin correlates with the presence of receptor-binding sites. *J. Biol. Chem.* 276, 45669–45676. doi: 10.1074/jbc.M102390200

Boller, T., and Felix, G. (2009). A renaissance of elicitors: perception of microbe–associated molecular patterns and danger signals by pattern-recognition. *Ann. Rev. Plant Biol* 60, 379–406. doi: 10.1146/annurev.arplant.57.032905.105346

Boudsocq, M., Willmann, M. R., Mccormack, M., Lee, H., Shan, L., He, P., et al. (2010). Differential innate immune signalling via $Ca2^+$ sensor protein kinases. *Nature* 464, 418–422. doi: 10.1038/nature08794

Cherkis, K. A., Temple, B. R., Chung, E.-H., Sondek, J., and Dangl, J. L. (2012). AvrRpm1 missense mutations weakly activate RPS2-mediated immune response in Arabidopsis thaliana. *PLoS One* 7:e42633. doi: 10.1371/journal.pone.0042633

Chinchilla, D., Bauer, Z., Regenass, M., Boller, T., and Felix, G. (2006). The Arabidopsis receptor kinase FLS2 binds flg22 and determines the specificity of flagellin perception. *Plant Cell* 18, 465–476. doi: 10.1105/tpc.105.036574

Chinchilla, D., Zipfel, C., Robatzek, S., Kemmerling, B., Nürnberger, T., Jones, J. D., et al. (2007). A flagellin-induced complex of the receptor FLS2 and BAK1 initiates plant defence. *Nature* 448, 497–500. doi: 10.1038/nature05999

Cribb, P. (2014). Subtribe Polystachyinae, Taxonomic notes. *Gen. Orchid.* 6:544.

De Jonge, R., Peter Van Esse, H., Maruthachalam, K., Bolton, M. D., Santhanam, P., Saber, M. K., et al. (2012). Tomato immune receptor Ve1 recognizes effector of multiple fungal pathogens uncovered by genome and RNA sequencing. *Proc. Natl. Acad. Sci.* 109, 5110–5115. doi: 10.1073/pnas.1119623109

Eulgem, T. (2006). Dissecting the WRKY web of plant defense regulators. *PLoS Pathog.* 2:e126. doi: 10.1371/journal.ppat.0020126

Faiz, S., Yasin, N. A., Khan, W. U., Shah, A. A., Akram, W., Ahmad, A., et al. (2022). Role of magnesium oxide nanoparticles in the mitigation of lead-induced stress in Daucus carota: modulation in polyamines and antioxidant enzymes. *Int. J. Phytoremediation* 24, 364–372. doi: 10.1080/15226514.2021.1949263

Felix, G., Duran, J. D., Volko, S., and Boller, T. (1999). Plants have a sensitive perception system for the most conserved domain of bacterial flagellin. *Plant J.* 18, 265–276. doi: 10.1046/j.1365-313X.1999.00265.x

Fradin, E. F., Abd-El-Haliem, A., Masini, L., Van Den Berg, G. C., Joosten, M. H., and Thomma, B. P. (2011). Interfamily transfer of tomato Ve1 mediates Verticillium resistance in Arabidopsis. *Plant Physiol.* 156, 2255–2265. doi: 10.1104/pp.111.180067

Gómez-Gómez, L., and Boller, T. (2000). FLS2: an LRR receptor–like kinase involved in the perception of the bacterial elicitor flagellin in Arabidopsis. *Mol. Cell* 5, 1003–1011. doi: 10.1016/S1097-2765(00)80265-8

Grant, M., Brown, I., Adams, S., Knight, M., Ainslie, A., and Mansfield, J. (2000). The RPM1 plant disease resistance gene facilitates a rapid and sustained increase in cytosolic calcium that is necessary for the oxidative burst and hypersensitive cell death. *Plant J.* 23, 441–450. doi: 10.1046/j.1365-313x.2000.00804.x

Harding, S. A., Oh, S.-H., and Roberts, D. M. (1997). Transgenic tobacco expressing a foreign calmodulin gene shows an enhanced production of active oxygen species. *EMBO J.* 16, 1137–1144. doi: 10.1093/emboj/16.6.1137

Harding, S. A., and Roberts, D. M. (1998). Incompatible pathogen infection results in enhanced reactive oxygen and cell death responses in transgenic tobacco expressing a hyperactive mutant calmodulin. *Planta* 206, 253–258. doi: 10.1007/s004250050397

Hayashi, F., Smith, K. D., Ozinsky, A., Hawn, T. R., Yi, E. C., Goodlett, D. R., et al. (2001). The innate immune response to bacterial flagellin is mediated by toll-like receptor 5. *Nature* 410, 1099–1103. doi: 10.1038/35074106

He, Y., Zhou, J., Shan, L., and Meng, X. (2018). Plant cell surface receptor-mediated signaling: a common theme amid diversity. *J. Cell Sci.* 131:jcs209353. doi: 10.1242/jcs.209353

Heese, A., Hann, D. R., Gimenez-Ibanez, S., Jones, A. M., He, K., Li, J., et al. (2007). The receptor-like kinase SERK3/BAK1 is a central regulator of innate immunity in plants. *Proc. Natl. Acad. Sci.* 104, 12217–12222. doi: 10.1073/pnas.0705306104

Ichimura, K., Casais, C., Peck, S. C., Shinozaki, K., and Shirasu, K. (2006). MEKK1 is required for MPK4 activation and regulates tissue-specific and temperature-dependent cell death in Arabidopsis. *J. Biol. Chem.* 281, 36969–36976. doi: 10.1074/jbc.M605319200

Ichimura, K., Shinozaki, K., Tena, G., Sheen, J., Henry, Y., Champion, A., et al. (2002). Mitogen-activated protein kinase cascades in plants: a new nomenclature. *Trends Plant Sci.* 7, 301–308. doi: 10.1016/S1360-1385(02)02302-6

Kaur, S., Samota, M. K., Choudhary, M., Choudhary, M., Pandey, A. K., Sharma, A., et al. (2022). How do plants defend themselves against pathogens-

biochemical mechanisms and genetic interventions. *Physiol. Mol. Biol. Plants* 28, 485–504. doi: 10.1007/s12298-022-01146-y

Knoth, C., Ringler, J., Dangl, J. L., and Eulgem, T. (2007). Arabidopsis WRKY70 is required for full RPP4-mediated disease resistance and basal defense against Hyaloperonospora parasitica. *Mol. Plant-Microbe Interact.* 20, 120–128. doi: 10.1094/MPMI-20-2-0120

Koh, K. W., Lu, H.-C., and Chan, M.-T. (2014). Virus resistance in orchids. *Plant Sci.* 228, 26–38. doi: 10.1016/j.plantsci.2014.04.015

Komis, G., Šamajová, O., Ovečka, M., and Šamaj, J. (2018). Cell and developmental biology of plant mitogen-activated protein kinases. *Annu. Rev. Plant Biol.* 69, 237–265. doi: 10.1146/annurev-arplant-042817-040314

Lee, S.-W., Han, S.-W., Sririyanum, M., Park, C.-J., Seo, Y.-S., and Ronald, P. C. (2009). A type I–secreted, sulfated peptide triggers XA21-mediated innate immunity. *Science* 326, 850–853. doi: 10.1126/science.1173438

Levine, A., Pennell, R. I., Alvarez, M. E., Palmer, R., and Lamb, C. (1996). Calcium-mediated apoptosis in a plant hypersensitive disease resistance response. *Curr. Biol.* 6, 427–437. doi: 10.1016/S0960-9822(02)00510-9

Li, J., Wen, J., Lease, K. A., Doke, J. T., Tax, F. E., and Walker, J. C. (2002). BAK1, an Arabidopsis LRR receptor-like protein kinase, interacts with BRI1 and modulates brassinosteroid signaling. *Cell* 110, 213–222. doi: 10.1016/S0092-8674(02)00812-7

Li, L., Li, M., Yu, L., Zhou, Z., Liang, X., Liu, Z., et al. (2014). The FLS2-associated kinase BIK1 directly phosphorylates the NADPH oxidase RbohD to control plant immunity. *Cell Host Microbe* 15, 329–338. doi: 10.1016/j.chom.2014.02.009

Macho, A. P., and Zipfel, C. (2014). Plant PRRs and the activation of innate immune signaling. *Mol. Cell* 54, 263–272. doi: 10.1016/j.molcel.2014.03.028

Miya, A., Albert, P., Shinya, T., Desaki, Y., Ichimura, K., Shirasu, K., et al. (2007). CERK1, a LysM receptor kinase, is essential for chitin elicitor signaling in Arabidopsis. *Proc. Natl. Acad. Sci.* 104, 19613–19618. doi: 10.1073/pnas.0705147104

Monaghan, J., Matschi, S., Romeis, T., and Zipfel, C. (2015). The calcium-dependent protein kinase CPK28 negatively regulates the BIK1-mediated PAMP-induced calcium burst. *Plant Signal. Behav.* 10:e1018497. doi: 10.1080/15592324.2015.1018497

Monaghan, J., and Zipfel, C. (2012). Plant pattern recognition receptor complexes at the plasma membrane. *Curr. Opin. Plant Biol.* 15, 349–357. doi: 10.1016/j.pbi.2012.05.006

Mubeen, S., Shahzadi, I., Akram, W., Saeed, W., Yasin, N. A., Ahmad, A., et al. (2022). Calcium nanoparticles impregnated With Benzenedicarboxylic acid: a new approach to alleviate combined stress of DDT and cadmium in Brassica alboglabra by modulating bioacummulation, antioxidative machinery and osmoregulators. *Front. Plant Sci.* 13, –825829. doi: 10.3389/fpls.2022.825829

Ngou, B. P. M., Ding, P., and Jones, J. D. (2022). Thirty years of resistance: zig-zag through the plant immune system. *Plant Cell* 34, 1447–1478. doi: 10.1093/plcell/koac041

Nishad, R., Ahmed, T., Rahman, V. J., and Kareem, A. (2020). Modulation of plant defense system in response to microbial interactions. *Front. Microbiol.* 11:1298. doi: 10.3389/fmicb.2020.01298

Nuhse, T. S., Peck, S. C., Hirt, H., and Boller, T. (2000). Microbial elicitors induce activation and dual phosphorylation of the Arabidopsis thaliana MAPK 6. *J. Biol. Chem.* 275, 7521–7526. doi: 10.1074/jbc.275.11.7521

Panattoni, A., Luvisi, A., and Triolo, E. (2013). Elimination of viruses in plants: twenty years of progress. *Span. J. Agric. Res.* 11, 173–188. doi: 10.5424/sjar/2013111-3201

Petutschnig, E. K., Jones, A. M., Serazetdinova, L., Lipka, U., and Lipka, V. (2010). The lysin motif receptor-like kinase (LysM-RLK) CERK1 is a major chitin-binding protein in Arabidopsis thaliana and subject to chitin-induced phosphorylation. *J. Biol. Chem.* 285, 28902–28911. doi: 10.1074/jbc.M110.116657

Poovaiah, B., Du, L., Wang, H., and Yang, T. (2013). Recent advances in calcium/calmodulin-mediated signaling with an emphasis on plant-microbe interactions. *Plant Physiol.* 163, 531–542. doi: 10.1104/pp.113.220780

Ranf, S., Eschen-Lippold, L., Fröhlich, K., Westphal, L., Scheel, D., and Lee, J. (2014). Microbe-associated molecular pattern-induced calcium signaling requires the receptor-like cytoplasmic kinases, PBL1 and BIK1. *BMC Plant Biol.* 14, 1–15. doi: 10.1186/s12870-014-0374-4

Ranf, S., Grimmer, J., Pöschl, Y., Pecher, P., Chinchilla, D., Scheel, D., et al. (2012). Defense-related calcium signaling mutants uncovered via a quantitative high-throughput screen in Arabidopsis thaliana. *Mol. Plant* 5, 115–130. doi: 10.1093/mp/ssr064

Ren, R., Wei, Y., Ahmad, S., Jin, J., Gao, J., Lu, C., et al. (2020). Identification and characterization of NPR1 and PR1 homologs in Cymbidium orchids in response to multiple hormones, salinity and viral stresses. *Int. J. Mol. Sci.* 21:1977. doi: 10.3390/ijms21061977

Rhodes, J., Zipfel, C., Jones, J. D., and Ngou, B. P. M. (2022). Concerted actions of PRR-and NLR-mediated immunity. *Essays Biochem.* doi: 10.1042/EBC20220067

Robatzek, S., and Wirthmueller, L. (2013). Mapping FLS2 function to structure: LRRs, kinase and its working bits. *Protoplasma* 250, 671–681. doi: 10.1007/s00709-012-0459-6

Roberts, D. L., and Dixon, K. W. (2008). Orchids. *Curr. Biol.* 18, R325–R329. doi: 10.1016/j.cub.2008.02.026

Ron, M., and Avni, A. (2004). The receptor for the fungal elicitor ethylene-inducing xylanase is a member of a resistance-like gene family in tomato. *Plant Cell* 16, 1604–1615. doi: 10.1105/tpc.022475

Roux, M., Schwessinger, B., Albrecht, C., Chinchilla, D., Jones, A., Holton, N., et al. (2011). The Arabidopsis leucine-rich repeat receptor–like kinases BAK1/SERK3 and BKK1/SERK4 are required for innate immunity to hemibiotrophic and biotrophic pathogens. *Plant Cell* 23, 2440–2455. doi: 10.1105/tpc.111.084301

Saijo, Y., Tintor, N., Lu, X., Rauf, P., Pajerowska-Mukhtar, K., Häweker, H., et al. (2009). Receptor quality control in the endoplasmic reticulum for plant innate immunity. *EMBO J.* 28, 3439–3449. doi: 10.1038/emboj.2009.263

Schwessinger, B., Roux, M., Kadota, Y., Ntoukakis, V., Sklenar, J., Jones, A., et al. (2011). Phosphorylation-dependent differential regulation of plant growth, cell death, and innate immunity by the regulatory receptor-like kinase BAK1. *PLoS Genet.* 7:e1002046. doi: 10.1371/journal.pgen.1002046

Shafique, S., Anjum, T., Shafique, S., Ahmad, A., Akram, W., and Bashir, Z. (2011). Induction of systemic defenses in plants under the activity of dynamic inducers. *Mycopathologia* 9, 95–104.

Shang, Y., Li, X., Cui, H., He, P., Thilmony, R., Chintamanani, S., et al. (2006). RAR1, a central player in plant immunity, is targeted by pseudomonas syringae effector AvrB. *Proc. Natl. Acad. Sci.* 103, 19200–19205. doi: 10.1073/pnas.0607279103

Shimizu, T., Nakano, T., Takamizawa, D., Desaki, Y., Ishii-Minami, N., Nishizawa, Y., et al. (2010). Two LysM receptor molecules, CEBiP and OsCERK1, cooperatively regulate chitin elicitor signaling in rice. *Plant J.* 64, 204–214. doi: 10.1111/j.1365-313X.2010.04324.x

Tuhid, N.H., Abdullah, N.E., Khairi, N., Saaid, M., Shahrizam, M., and Hashim, H. (2012). "A statistical approach for orchid disease identification using RGB color," in 2012 IEEE control and system graduate research colloquium: IEEE, 382–385.

Wang, Y., Pruitt, R. N., Nürnberger, T., and Wang, Y. (2022). Evasion of plant immunity by microbial pathogens. *Nat. Rev. Microbiol.* 20, 449–464. doi: 10.1038/s41579-022-00710-3

Willmann, R., Lajunen, H. M., Erbs, G., Newman, M.-A., Kolb, D., Tsuda, K., et al. (2011). Arabidopsis lysin-motif proteins LYM1 LYM3 CERK1 mediate bacterial peptidoglycan sensing and immunity to bacterial infection. *Proc. Natl. Acad. Sci.* 108, 19824–19829. doi: 10.1073/pnas.1112862108

Wong, S. (2002). Orchid viruses: a compendium. *Orchid Biology: Reviews and Perspectives*. 8, 505–546.

Yu, D., Fan, R., Zhang, L., Xue, P., Liao, L., Hu, M., et al. (2022). HvWRKY2 acts as an immunity suppressor and targets HvCEBiP to regulate powdery mildew resistance in barley. *Crop J.*, in press. doi: 10.1016/j.cj.2022.05.010

Zipfel, C., Kunze, G., Chinchilla, D., Caniard, A., Jones, J. D., Boller, T., et al. (2006). Perception of the bacterial PAMP EF-Tu by the receptor EFR restricts agrobacterium-mediated transformation. *Cell* 125, 749–760. doi: 10.1016/j.cell.2006.03.037

Zipfel, C., and Oldroyd, G. E. (2017). Plant signalling in symbiosis and immunity. *Nature* 543, 328–336. doi: 10.1038/nature22009

Zipfel, C., Robatzek, S., Navarro, L., Oakeley, E. J., Jones, J. D., Felix, G., et al. (2004). Bacterial disease resistance in Arabidopsis through flagellin perception. *Nature* 428, 764–767. doi: 10.1038/nature02485

frontiers | Frontiers in Plant Science

TYPE Original Research
PUBLISHED 28 September 2022
DOI 10.3389/fpls.2022.984483

OPEN ACCESS

EDITED BY
Waheed Akram,
University of the Punjab, Pakistan

REVIEWED BY
Shihong Luo,
Shenyang Agricultural University, China
Bartholomew Saanu Adeleke,
Ondo State University of Science and Technology, Nigeria

*CORRESPONDENCE
Qinwan Huang
huangqinwan@cdutcm.edu.cn
Jin Wang
wangjin0816@126.com

†These authors share first authorship

SPECIALTY SECTION
This article was submitted to Plant Symbiotic Interactions, a section of the journal Frontiers in Plant Science

RECEIVED 02 July 2022
ACCEPTED 18 August 2022
PUBLISHED 28 September 2022

CITATION
Zhang X, Lv H, Tian M, Dong Z, Fu Q, Sun J, Huang Q and Wang J (2022) Colonization characteristics of fungi in *Polygonum hydropipe* L. and *Polygonum lapathifolium* L. and its effect on the content of active ingredients.
Front. Plant Sci. 13:984483.
doi: 10.3389/fpls.2022.984483

Colonization characteristics of fungi in *Polygonum hydropipe* L. and *Polygonum lapathifolium* L. and its effect on the content of active ingredients

Xiaorui Zhang[1,2†], Hongyang Lv[1,2†], Maoying Tian[1,2], Zhaowei Dong[1,2], Qinwen Fu[1,2], Jilin Sun[3], Qinwan Huang[1,2*] and Jin Wang[1,2*]

[1]State Key Laboratory of Characteristic Chinese Medicine Resources in Southwest China, Chengdu University of Traditional Chinese Medicine, Chengdu, China, [2]Pharmacy College, Chengdu University of Traditional Chinese Medicine, Chengdu, China, [3]Sichuan Fuzheng Pharmaceutical Co., Ltd., Chengdu, China

Polygonum hydropiper, is a plant of the Persicaria genus, which is commonly used to treat various diseases, including gastrointestinal disorders, neurological disorders, inflammation, and diarrhea. However, because of different local standards of *P. hydropiper*, people often confuse it with *Polygonum lapathifolium* L. and other closely related plants. This poses a serious threat to the safety and efficacy of the clinical use of *P. hydropiper*. This study aims to determine the six active ingredients of *P. hydropiper* and *P. lapathifolium*. Then the endophytic fungi and rhizosphere soil of the two species were sequenced by Illumina Miseq PE300. The results show significant differences between the community composition of the leaves, stems, and roots of the *P. hydropiper* and the *P. lapathifolium* in the same soil environment. Of the six secondary metabolites detected, five had significant differences between *P. hydropiper* and *P. lapathifolium*. Then, we evaluated the composition of the significantly different communities between *P. hydropiper* and *P. lapathifolium*. In the *P. hydropiper*, the relative abundance of differential communities in the leaves was highest, of which *Cercospora* dominated the differential communities in the leaves and stem; in the *P. lapathifolium*, the relative abundance of differential community in the stem was highest, and *Cladosporium* dominated the differential communities in the three compartments. By constructing the interaction network of *P. hydropiper* and *P. lapathifolium* and analyzing the network nodes, we found that the core community in *P. hydropiper* accounted for 87.59% of the total community, dominated by *Cercospora*; the core community of *P. lapathifolium* accounted for 19.81% of the total community, dominated by *Sarocladium*. Of these core communities, 23 were significantly associated with active ingredient content. Therefore, we believe that the community from *Cercospora* significantly interferes with recruiting fungal communities in *P. hydropiper* and affects the accumulation of secondary metabolites in the host plant. These results provide an essential foundation for the large-scale production of *P. hydropiper*. They indicate that by colonizing

specific fungal communities, secondary metabolic characteristics of host plants can be helped to be shaped, which is an essential means for developing new medicinal plants.

KEYWORDS

***Polygonum hydropiper* L., endophytic fungi, community assembly process, flavonoids, core community**

Introduction

Polygonum hydropiper is a plant of the *Persicaria* genus in the family *Polygonaceae*. The whole plant of *P. hydropiper* is commonly used to treat various diseases, including gastrointestinal disorders, neurological disorders, inflammation, and diarrhea (Xiang and Ming, 2020). Due to the low requirements for growth conditions, it has abundant wild plant resources what is more, it is widely distributed in China in Sichuan, Guangdong, Guangxi, and other places (Hong and Hanshen, 2013). Many studies have shown that *P. hydropiper* is rich in various chemical components, including flavonoids, terpenes, and organic acids, with antimicrobial, antioxidant, antiviral, insecticidal, and other biological activities (Rahman et al., 2002; Ayaz et al., 2014; Sharif et al., 2014; Shahed-Al-Mahmud and Lina, 2017). Due to different local standards, the large-scale commercial cultivation of *P. hydropiper* has not yet been achieved. People are often confused by plants, such as *Polygonum lapathifolium* and *P. orientale* (Hong et al., 2019). This poses a serious threat to the safety and efficacy of the clinical use of *P. hydropiper*. Therefore, clarifying the differences between *P. hydropiper* and other obfuscated species is crucial to developing and improving the production of *P. hydropiper*.

Our preliminary research found that as one of the drugs for the treatment of enteritis, the role of flavonoids in it cannot be ignored (Zhang et al., 2021). Quercetin, kaempferol, isorhamnetin, hyperoside, catechins, and chlorogenic acid are the main active ingredients of *P. hydropiper* in treating enteritis (Yue, 2005; Wei et al., 2021). It is worth noting that Tian et al. (2014) found the potential of flavonoids to act as signaling molecules between endophytic fungi and plants. Meanwhile, Tang et al. (2020) found that the endophyte isolated from Conyza blinii H. Lév could produce flavonoids with high yield and excellent biological activity. Endophytic fungi are present in all plants and, together with host plants, determine the production of secondary metabolites (Waqas et al., 2012; Adeleke and Babalola, 2021). With the development of next-generation sequencing, there is increasing evidence that the compositional pattern of endophytic fungi is related to the production of specific secondary metabolites (Lunardelli Negreiros de Carvalho et al., 2016; Dang et al., 2021; Ribeiro et al., 2021). In some crops and medicinal plants, it is also recognized that the specific community composition pattern can reflect the quality and yield of the host plant (Song et al., 2010; Vergara et al., 2018; Cao et al., 2021; Martins et al., 2021).

There are abundant researches of chemical composition and pharmacological effect research of *P. hydropiper* (Hong and Hanshen, 2013). However, its endophytic fungi research is still blank. Thus, this experiment uses Illumina Miseq PE300 sequencing technology to sequence the endophytic fungi of *P. hydropiper* and *P. lapathifolium*. At the same time, we measured the content of 6 flavonoids of two species to reveal the relationship between the endophytic fungal community composition and the accumulation of active ingredients. Furthermore, determining the composition of the core microbiota related to active ingredients to improve the production of *P. hydropiper* provides key fundamental data.

Methods

Sampling

In July 2021, the whole plant and rhizosphere soil of *P. hydropiper* (ZP) and *P. lapathifolium* (WP) were sampled from Huoba Village in Jianyang City, China. At each sample point, four repeats of the whole plant and three repeats of the rhizosphere soil were collected. The rhizosphere soil was collected by the jitter root method. The plant residue and gravel were selected and discarded, and the samples were collected by the quartering method and loaded into sterile centrifuge tubes. To ensure the representativeness of the samples and avoid edge effects, we set the sample point away from the field ridge at least 25 m and each sample point interval at least 2 m. Samples are frozen with liquid nitrogen after on-site sampling and quickly transported back to the laboratory on dry ice for preservation at −80°C (Table 1).

Determination of active ingredients content

Chemicals and reagents

Six commercial standards of HPLC grade, including catechins, chlorogenic acid, hyperoside, quercetin, kaempferol,

10.3389/fpls.2022.984483

TABLE 1 Samples information.

Samples	Type	Date	Site
ZY-1	Leaf	2020/7/6	Huoba Village in Jianyang City, China
ZY-2	Leaf	2020/7/6	Huoba Village in Jianyang City, China
ZY-3	Leaf	2020/7/6	Huoba Village in Jianyang City, China
ZY-4	Leaf	2020/7/6	Huoba Village in Jianyang City, China
ZJ-1	Stem	2020/7/6	Huoba Village in Jianyang City, China
ZJ-2	Stem	2020/7/6	Huoba Village in Jianyang City, China
ZJ-3	Stem	2020/7/6	Huoba Village in Jianyang City, China
ZJ-4	Stem	2020/7/6	Huoba Village in Jianyang City, China
ZG-1	Root	2020/7/6	Huoba Village in Jianyang City, China
ZG-2	Root	2020/7/6	Huoba Village in Jianyang City, China
ZG-3	Root	2020/7/6	Huoba Village in Jianyang City, China
ZG-4	Root	2020/7/6	Huoba Village in Jianyang City, China
WY-1	Leaf	2020/7/6	Huoba Village in Jianyang City, China
WY-2	Leaf	2020/7/6	Huoba Village in Jianyang City, China
WY-3	Leaf	2020/7/6	Huoba Village in Jianyang City, China
WY-4	Leaf	2020/7/6	Huoba Village in Jianyang City, China
WJ-1	Stem	2020/7/6	Huoba Village in Jianyang City, China
WJ-2	Stem	2020/7/6	Huoba Village in Jianyang City, China
WJ-3	Stem	2020/7/6	Huoba Village in Jianyang City, China
WJ-4	Stem	2020/7/6	Huoba Village in Jianyang City, China
WG-1	Root	2020/7/6	Huoba Village in Jianyang City, China
WG-2	Root	2020/7/6	Huoba Village in Jianyang City, China
WG-3	Root	2020/7/6	Huoba Village in Jianyang City, China
WG-4	Root	2020/7/6	Huoba Village in Jianyang City, China
ZT-1	Rhizosphere soil	2020/7/6	Huoba Village in Jianyang City, China
ZT-2	Rhizosphere soil	2020/7/6	Huoba Village in Jianyang City, China
ZT-3	Rhizosphere soil	2020/7/6	Huoba Village in Jianyang City, China
WT-1	Rhizosphere soil	2020/7/6	Huoba Village in Jianyang City, China
WT-2	Rhizosphere soil	2020/7/6	Huoba Village in Jianyang City, China
WT-3	Rhizosphere soil	2020/7/6	Huoba Village in Jianyang City, China

and isorhamnetin, were purchased from Chengdu Pufei De Biotech Co., Ltd. (China). Other HPLC grade reagents used were acetonitrile and methanol from Thermo Fisher Scientific Co., Ltd. (USA). The Watsons distilled water was applied to prepare for samples and the mobile phase. All other reagents were just met for an analytical grade.

Sample preparation

We precisely weighed 0.1 g of PL sample, added it to 15 mL of 60% ethanol in an Erlenmeyer flask, and dissolved it by sonication at 50°C for 30 min. Then filtering the sample, and evaporated the filtrate. The methanol was added to the residue until the volume to 5 mL, and the solution was filtered with a microporous filter membrane of 0.22 μm.

UPLC-QQQ-MS/MS analysis

Ultra performance liquid chromatograph LC-20A and triple quadrupole mass spectrometer LCMS-8045 were purchased from Shimadzu Co., Ltd. (Japan). A Shim-pack Velox C18 column (2.1 × 1,000 mm, 2.7 μm) was employed at a column temperature of 30°C. The mobile phase consisted of 0.3% carboxylic acid in water (A) and methanol (B), and the flow rate was 0.2 mL/min. The gradient elution parameters were set as follows: 0–6 min, 15% B; 6–15 min, 15–45% B; 15–20 min, 45%–47% B; 20–22 min, 47%−50% B; 22–25 min, 50%−15% B. The injection volume was 2 μL.

Ionization method: Electrospray ion source (ESI); Multi-reaction monitoring mode (MRM); Curtain Gas (CUR) flow rate: 40 $L{\cdot}min^{-1}$; Atomized Gas (GS1) flow rate: 55 $L{\cdot}min^{-1}$; Auxiliary gas (GS2) flow rate: 55 $L{\cdot}min^{-1}$; ionization temperature (TEM): 550°C; Spray voltage (IS): 4,500 V in positive ion mode, −4,500 V in negative ion mode. The optimized MS/MS parameters of ZP are shown in Table 1.

Method validation

The six reference standards were weighed accurately and dissolved with methanol comparable to sample extracts. Calibration curves were constructed by measuring the signal intensity (peak area) of MRM transitions for at least six appropriate concentrations of each compound. Intra-day and inter-day precisions were evaluated by calculating the relative standard deviations (RSDs) of retention time and signal intensity during a single day and on three successive days, respectively. Repeatability was evaluated by calculating the RSDs of retention time and signal intensity of six tested solutions made from the same sample on a single day. Stability was evaluated by calculating the RSDs of retention time and signal intensity of the same tested solution during a single day at 0, 2, 4, 8, 12, and 24 h. Recovery experiments were done by spiking authentic standards into samples directly.

DNA extraction and library construction

Plants and soil samples were finely ground to powder in liquid nitrogen using a tissue grinder separately, and 0.5 g was taken for DNA extraction using the FastDNA®SPIN Kit (MP Biomedicals, US). Three repeats per sample were required. The DNA bands, concentration, and purity of the extract were detected using a 1% agarose gel electrophoresis and an accounting analyzer, and samples with a concentration of ≥20 ng/μL were selected and sent to Shanghai Majorbio Bio-pharm Technology Co., Ltd for Polymerase Chain Reaction (PCR) amplification, DNA sequencing, and library construction. Fungal ITSregion was amplified using the forward primer ITS1F (CTTGGTCATTTAGAGGAAGTAA) and reverse primer ITS2R (GCTGCGTCTTCATCGATGCGC). The PCR reaction

mixture, including 2 μL 10 × buffer, 2 μL 2.5 mM dNTPs, 0.8 μL each primer (5 μM), 0.2 μL rTaq polymerase, 0.2 μL BSA, 10 ng of template DNA, and ddH_2O to a final volume of 20 μL. PCR amplification cycling conditions were as follows: initial denaturation at 95°C for 3 min, followed by 35 cycles of denaturing at 95°C for 30 s, annealing at 55°C for 30 s and extension at 72°C for 45 s, and single extension at 72°C for 10 min, and end at 4°C. All samples were amplified in triplicate. The PCR product was extracted from a 2% agarose gel and purified using the AxyPrep DNA Gel Extraction Kit (Axygen Biosciences, Union City, CA, USA) according to the manufacturer's instructions and quantified using Quantus™ Fluorometer (Promega, USA). Purified amplicons were pooled in equimolar amounts and paired-end sequenced on an Illumina MiSeq PE300 platform (Illumina, San Diego, USA) according to the standard protocols by Majorbio Bio-Pharm Technology Co. Ltd. (Shanghai, China). The data presented in the study are deposited in the NCBI Sequence Read Archive (SRA) database repository, accession number SRR20897189-SRR20897218.

Data processing

Clean reads were obtained by filtering the raw sequences using a microbial ecological quantitative analysis pipeline (QIIME, version 1.9.1, USAU). Low-quality sequences (such as uncertain nucleotide sequences, three nucleotides with a *Q*-value of <20, and unmatched barcode sequences) were removed. The QIIME v1.9.0 was used for quality control to obtain valid data, and the Uchime algorithm and gold database were used to remove delusion. These sequences were grouped into operational taxonomic units (OTUs) based on 97% sequence identity using UPARSE (V7.0.1090). Each row was annotated by comparing the Ribosomal Database Project (RDP) classifier (V2.11) against the unite8.0 database using a comparison threshold of 70%. Resampling was carried out with the smallest amount of data in the sample as the standard to make the uniform treatment for each sample. Mothur (version 1.30.2) 1 was used for diversity analysis. R 3.6.0 was used to perform various data conversions. Fungi Functional Guild (FUNGuild) was used for function prediction.

Statistical analysis

All statistical analyses were performed in R (v4.0.3) (Team, 2020). Hellinger transformation was first used to convert microbiota data. The Alpha diversity and Principal Component Analysis (PCA) analysis were generated by the vegan package in R (Oksanen et al., 2013) and plotted by ggplot2 (Wickham, 2011). The ternary diagram was drawn using the ggtern in R (Hamilton and Ferry, 2018). The significant difference between the functional composition of ZP and WP were detected by the Wilcoxon test. The significant different taxa between ZP and WP were detected by the MetagenomeSeq package (Wickham, 2011). Then, we performed the Pearson correlation analysis between the core community and the ingredients. Draw the heatmap of the correlation analysis using the Pheatmap package (Kolde and Kolde, 2015), and remove the community not significantly.

Interaction network analysis

We first use the iGraph package (Csardi and Nepusz, 2006) to analyze the network structure of the endophytic fungi community of *P. hydropiper* and *P. lapathifolium*. Then we use the weighted gene co-expression network analysis (WGCNA) package (Langfelder and Horvath, 2008) to calculate the correlation and *P*-values. And use the false discovery rates (FDR) to correct the *P*-values. The interaction network was generated by retaining the edges of $R \geq \pm 0.4$ and $P \leq 0.05$. Then we import the interaction network into Cytoscape (Shannon et al., 2003) to analyze the module. We choose the fast greedy algorithm to calculate the module, and use the GuImerà Amaral NeTwork (GIANT) package (Cumbo et al., 2014) to analyze the module's connectivity and the connectivity between modules. Finally, we use the ggplot2 package to plot the results.

Results

Determination of active ingredient content

Method validation

A preliminary optimization of the UPLC method (flow rate, gradient, injection volume, etc.) successfully achieved a well-separated peak for every standard compound, as shown in Figure 1. Moreover, the performance validation of the method was evaluated, including linearity, precision, reproducibility, stability, and recovery (Table 2). The linearity of the method was measured by analyzing standards over a linear range suitable for quantifying the corresponding analytes. Good linearity between concentration and signal intensity was obtained, and correlation coefficients of all compounds were calculated to be more than 0.999. Additionally, good reproducibility, stability, and precision were revealed in the results.

The above results suggest that the established method is sensitive, rapid, and reliable in identifying and quantifying phenolic compounds. The MRM mode of the UPLC-QQQ-MS/MS system is an effective and efficient tool for natural product analysis in complex matrices.

Sample content determination

The content determination results of catechins, chlorogenic acid, hyperoside, quercetin, kaempferol, and isorhamnetin are

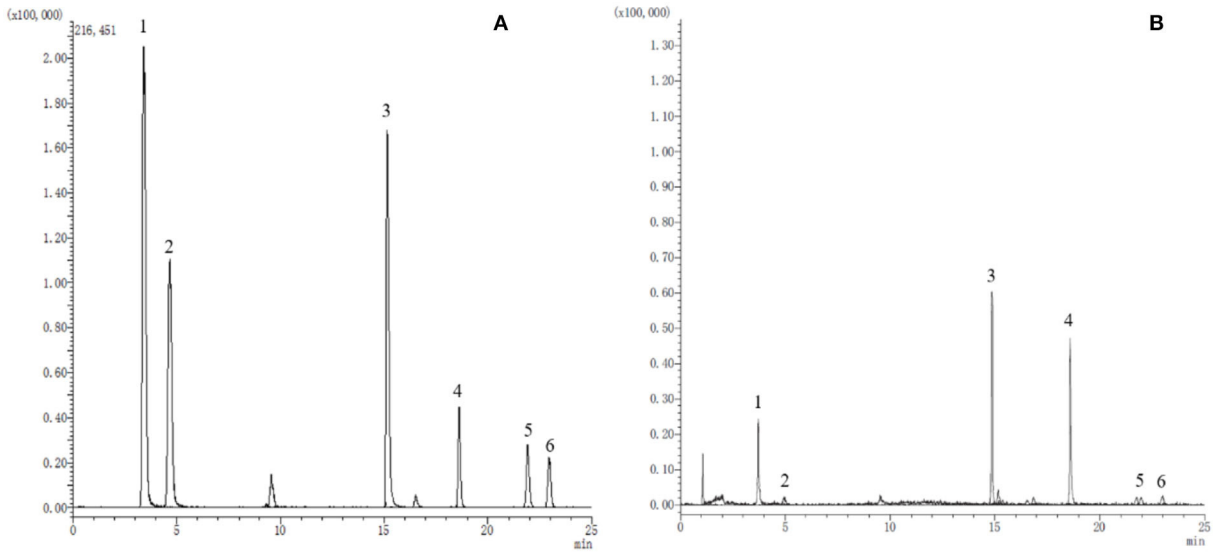

FIGURE 1
The extracted ion chromatograms (EICs) of reference substances **(A)** and sample **(B)**. 1. Catechin; 2. Chlorogenic acid; 3. Hyperoside; 4. Quercetin; 5. Kaempferol; 6. Isorhamnetin.

TABLE 2 Liner equations, precision, repeatability, stability, and average recovery rates of quantification of six components.

Compound	Liner equations	*R*	Precision (RSD/%)		Repeatability RSD/%	Stability RSD/%	Recovery	
			Intra-day (n = 6)	Inter-day (n = 9)			Mean/%	RSD/%
Catechins	Y = 55091.2X + 1252.94	0.9991	2.5	2.59	2.96	1.86	92.02	2.14
Chlorogenic acid	Y = 17261.2X + 22440.6	0.9996	2.73	2.42	2.58	2.58	102.45	2.75
Hyperoside	Y = 2982.38X + 29865.3	0.9992	2.87	2.57	0.60	0.11	100.62	2.41
Quercetin	Y = 4467.8X + 11024.8	0.9995	2.72	2.66	2.17	1.53	102.47	2.65
Kaempferol	Y = 12145.9X + 18648.7	0.9993	2.15	2.20	2.04	1.35	97.37	2.96
Isorhamnetin	Y = 28372.1X + 13477.73	0.9993	1.43	2.76	1.88	2.02	97.52	2.06

shown in four batches of ZP and four batches of WP in Table 3. In addition, we used student's *t*-test to detect the significant difference between the content of the active compounds in the two groups of ZP and WP, and the results are shown in Table 4.

For ZP, the catechins content was between 16.7874 and 17.5247 $\mu g\ g^{-1}$, the chlorogenic acid content was between 2.5801 and 3.7231 $\mu g\ g^{-1}$, the content of hyperoside was between 501.1931 and 519.0559 $\mu g\ g^{-1}$, the quercetin content was between 334.8053 and 389.4847 $\mu g\ g^{-1}$, and the content of kaempferol was between 18.7093 and 30.9806 $\mu g\ g^{-1}$. The content of isorhamnetin was between 24.1923 and 25.9680 $\mu g\ g^{-1}$; for WP, the content of catechins was between 29.2366 and 37.6574 $\mu g\ g^{-1}$; the chlorogenic acid content was between 1.1047 and 1.3370 $\mu g\ g^{-1}$; the content of hyperoside was between 204.4158 and 234.7462 $\mu g\ g^{-1}$; the quercetin content as between 184.4371 and 197.7751 $\mu g\ g^{-1}$; the content of kaempferol was between 14.0855 and 23.6914 $\mu g\ g^{-1}$, and the content of isorhamnetin was between 7.8025 and 13.6166 $\mu g{\cdot}g^{-1}$.

Student's *t*-test results (Table 4) showed that the contents of chlorogenic acid, hyperoside, quercetin, and isorhamnetin in ZP were significantly higher than those in WP, and the catechins in WP were considerably higher than those in ZP, while there was no significant difference in kaempferol between the two species.

Statistics of ITS amplicon sequencing

We sequenced 30 plant and soil samples, and a total of 2,321,991 reads were obtained, with a total base number of 696,597,300 bp. After filtering, the clean reads were 2,321,991, the total number of bases was 540,788,432 bp, and the average

10.3389/fpls.2022.984483

TABLE 3 The content of the six compounds in ZP and WP.

	Catechins (μg·g−1)	Chlorogenic acid (μg·g−1)	Hyperoside (μg·g−1)	Quercetin (μg·g−1)	Kaempferol (μg·g−1)	Isorhamnetin (μg·g−1)
Z1	17.3281	3.5837	501.1931	366.8620	30.9806	24.3484
Z2	17.5247	3.7231	507.4762	389.4847	30.7550	25.9680
Z3	17.4783	2.7570	508.8720	361.1795	22.5175	25.7283
Z4	16.7874	2.5801	519.0559	334.8053	18.7093	24.1923
W1	29.2366	1.1047	225.8444	184.4371	15.9720	13.5882
W2	33.4035	1.1563	215.0943	190.2311	14.0855	10.4824
W3	36.5700	1.3370	234.7462	197.7751	23.6914	13.6166
W4	37.6574	1.2769	204.4158	184.9176	19.7679	7.8025

TABLE 4 Student's *t*-test of component content between ZP and WP.

Compounds	ZP		WP		*P*-value
	Mean	SD	Mean	SD	
Catechins	17.2796	0.3387	34.2169	3.7789	0.0028
Chlorogenic acid	3.1610	0.5760	1.2187	0.1069	0.0057
Hyperoside	509.1493	7.4009	220.0252	13.1471	0.0000
Quercetin	363.0829	22.4691	189.3402	6.2059	0.0003
Kaempferol	25.7406	6.1218	18.3792	4.2575	0.1016
Isorhamnetin	25.0593	0.9184	11.3724	2.7978	0.0012

length was 232 bp. The number of sequences assigned to each sample was 47,618–169,166, with a median of 75,882 (Table 5). Based on the minimum sample sequence size, 1,642 OTUs were obtained at a similarity of 97%. The rarefaction curve showed sufficient sequencing depth (Figure 2), and the Good's coverage also shows good taxa coverage for each sample (Table 5).

Analysis of the diversity and composition of the fungal communities

To compare the differences in fungal communities of two plants from a macroscopic perspective. First, we compared the difference in the alpha diversity index of all samples of the two species. As can be seen from Figure 3A, there are no significant differences in the ACE, Shannon, and Simpson indices between the two species. Then, the difference in the alpha diversity of the same compartment of the two species was compared, and it can be seen from Figure 3B that there is a significant difference in the ACE index between ZP and WP in the leaves.

If we look at the composition of all the communities of the two species, as can be seen from Figure 4A, both ZP and WP are dominated by *Ascomycota*, accounting for an average of 87.83% of the entire community. As the sampling compartment ranges from rhizosphere soil and rhizome to leaf, the relative abundance of Ascomycota in ZP and WP increases in quantity. The Adonis analysis of community composition in different parts of ZP and WP shows significant differences in leaves, stems, and roots (Figure 5).

Furthermore, we performed the ternary phase diagram analysis of the leaves, stems, and roots of two plants (Figure 4B) to determine the distribution of the community in various compartments. We found that a large amount of OUT was shared between stems and leaves. Compared to ZP, the three compartments of WP shared more OTUs, while shared OTUs in ZP tended to occupy a higher proportion of stems and leaves. Based on MetagenomeSeq, the leaves, stems, and roots of ZP and WP were analyzed (Figure 4C). A significant difference in OTUs was found (88) in leaves, 38 in stems, and 71 in roots. We observed the composition of these OTUs at the genus level. In ZP, *Cercospora* (15.34 and 22.11%), *Phaeosphaeria* (8.48, 7.45%), and *Cladosporium* (7.29 and 5.68%) dominate the leaf and stem community, while *Branch06* (30.69%) dominates the root community. In WP, *Cladosporium* (16.02, 20.68, and 8.04%) and *Stachybotryaceae* (17.02, 9.55, and 1.23%) dominate the community of leaves, stems, and roots. In addition, *Plectosphaerella* has a significantly higher abundance in WP than in ZP, especially in stems; 16.29% in WP, compared with only 0.44% in ZP.

Interaction network analysis of endophytic fungal communities

The interaction networks of ZP and WP fungal communities were constructed, respectively, and the results are shown in Figure 6. The overall module connectivity of the ZP network is 0.38, and the overall module connectivity of the WP network is 0.34. Still, the nodes of ZP show special aggregation characteristics, while the nodes of WP are more widely distributed, and there is no obvious aggregation. We performed characteristic annotations to the nodes in the network to determine the core community in the endophytic fungal community (Figure 7). This study defines the node annotated

10.3389/fpls.2022.984483

TABLE 5 Sequencing statistics.

	Compartment	No.	Sequence number	Sequence base number	Average length	Min length	Max Length	Coverage
ZP	Leaf	1	81671	18659755	228.47	150	514	99.98%
	Leaf	2	75151	17275810	229.88	149	514	99.96%
	Leaf	3	67298	15158745	225.25	144	473	99.98%
	Leaf	4	80201	18570459	231.55	152	524	99.97%
	Rhizosphere soil	1	52439	12505425	238.48	165	517	99.84%
	Rhizosphere soil	2	60256	13933186	231.23	143	518	99.83%
	Rhizosphere soil	3	54748	13127476	239.78	140	522	99.84%
	Stem	1	47618	11099330	233.09	164	515	99.99%
	Stem	2	69632	16378460	235.21	173	505	99.99%
	Stem	3	63497	14935152	235.21	171	523	99.99%
	Stem	4	57766	13408123	232.11	172	423	99.99%
	Root	1	64740	16161710	249.64	173	494	99.93%
	Root	2	57239	16812244	293.72	146	395	99.94%
	Root	3	76613	17766891	231.90	145	349	99.93%
	Root	4	169166	42516049	251.32	150	438	99.99%
WP	Leaf	1	69738	16457499	235.99	141	321	99.99%
	Leaf	2	91724	20805391	226.83	169	504	99.99%
	Leaf	3	80418	18451726	229.45	157	321	99.98%
	Leaf	4	88068	20608782	234.01	181	393	99.98%
	Rhizosphere soil	1	72261	16224948	224.53	142	525	99.77%
	Rhizosphere soil	2	66798	15601070	233.56	141	433	99.79%
	Rhizosphere soil	3	63371	14296112	225.59	141	528	99.76%
	Stem	1	94776	20978893	221.35	154	531	99.99%
	Stem	2	96825	21836843	225.53	169	526	99.99%
	Stem	3	82421	18990185	230.40	187	528	99.95%
	Stem	4	76992	17647509	229.21	191	522	99.96%
	Root	1	85574	19244983	224.89	155	498	99.98%
	Root	2	76856	17077185	222.20	177	366	99.98%
	Root	3	100743	22772037	226.04	168	529	99.99%
	Root	4	97391	21486454	220.62	169	507	99.99%

as the module node and the connectors as the core community. In ZP, three module hub nodes were identified, including OUT1551 (*Teratosphaeriaceae*), OUT1542 (*Phaeosphaeriaceae*), and OUT1374 (*Basidiomycota*), in addition to 32 connection nodes. In the WP, 74 connection nodes are identified. Observing the community composition at the genus level (Figure 8), the relative abundance of key communities in the three compartments in WP was close, accounting for 19.81% of the total community, dominated by *Sarocladium* in stems and roots and dominated by *Cercospora* in leaves. In ZP, the relative abundance of key communities in the three compartments was significantly different, accounting for 87.59% of the community. The relative abundance of community in stems is highest, dominated mainly by *Sarocladium* and *Cercospora*, in the leaves by *Cercospora*, and in the roots by *Zopfiella*.

Functional composition analysis of endophytic fungi

To detect the differences in function community composition in two plants, we used FUNGuild to perform the functional annotations. A total of 10 trophic types are annotated (Figure 9).

We found significant differences in the relative abundance of trophic types between ZP and WP, including pathogen-saprotroph-symbiotroph, pathotroph, pathotroph-saprotroph-saprotroph, pathotroph-saprotroph-symbiotroph, and saprotroph-symbiotroph. Further, a functional analysis of the core community (Figure 10) was performed. In the dominant functional community, saprotrophs and pathotroph-saprotrophs in ZP were significantly higher than in the WP group.

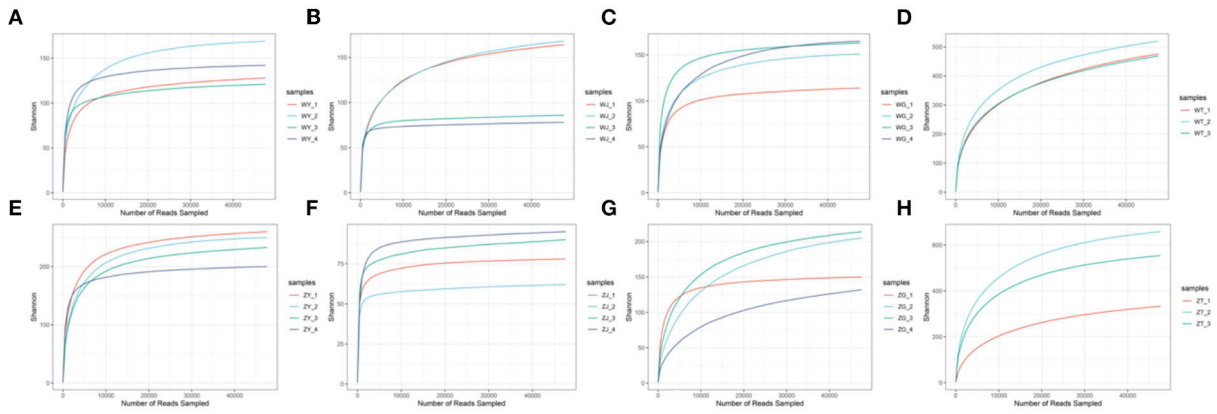

FIGURE 2
The rarefaction curve [**(A)** the leaf of WP; **(B)** the stem of WP; **(C)** the root of WP; **(D)** the rhizosphere soil of WP; **(E)** the leaf of ZP; **(F)** The stem of ZP; **(G)** the root of ZP; **(H)** the rhizosphere soil of ZP].

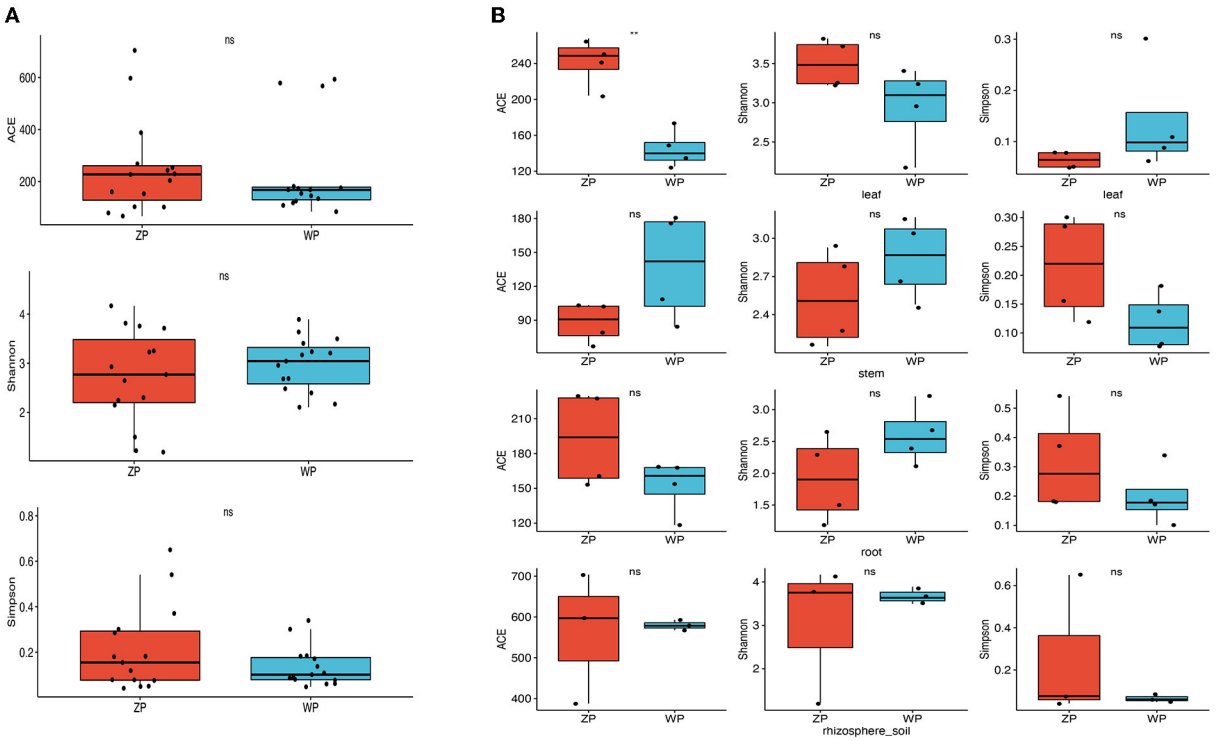

FIGURE 3
Alpha diversity of fungal communities; **(A)** Difference analysis between whole plant of two species; **(B)** Difference analysis between three compartments of two species. *Means P-value < 0.05, **means P-value <= 0.01, ***means p-value <= 0.001, ****means P-value <= 0.0001, ns mean P-value > 0.05.

Correlation analysis of fungal communities with active ingredients

The Pearson-related analysis of core community and active ingredient content in ZP and WP was performed. In the roots of ZP (Figure 10A), *Gibberella* and *Leptospora* were significantly positively correlated with chlorogenic acid and kaempferol. *Phaeosphaeria* was significantly inversely associated with hyperoside. In the stem of ZP (Figure 10B), *Tilletiopsis*, c_*Sordariomycetes*, *Pyrenochaetopsis*,

10.3389/fpls.2022.984483

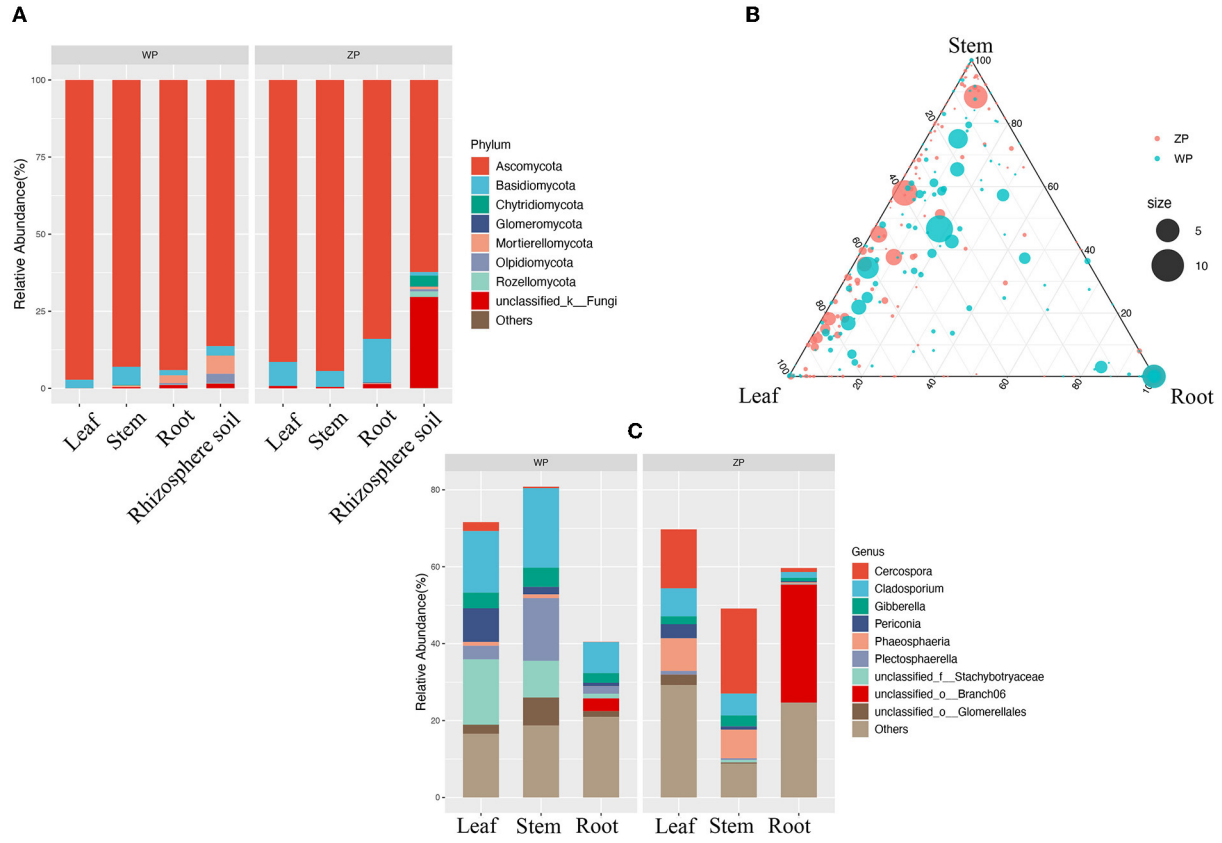

FIGURE 4
(A) The community composition of ZP and WP at the phylum level; **(B)** The ternary phase diagram of community in ZP and WP; **(C)** The significant differential communities between ZP and WP.

Cryptococcus_f_*Tremellacea*, and *Keissleriella* were significantly negatively correlated with catechins; *Cercospora* was significantly positively correlated with hyperoside; *Sarocladium* was significantly positively correlated with quercetin. In the leaves of ZP (Figure 10C), *Keissleriella*, *Phaeosphaeria*, *Sarocladium*, *Articulospora,* and c_*Sordariomycetes* were significantly negatively correlated with catechins; *Tilletiopsis* was significantly negatively correlated with chlorogenic acid and kaempferol; f_*Phaeosphaeriaceae* positively correlated with chlorogenic acid and kaempferol; *Leptospora* and *Rhodosporidiobolus* were positively correlated with hyperoside; *Keissleriella* was negatively correlated with quercetin; *Pyrenochaetopsis* and p_*Basidiomycota* were negatively correlated with Isorhamnetin significance.

In the roots of the WP (Figure 10D), *Mortierella*, *Symmetrospora*, and Taromyces were significantly positively correlated with kaempferol. *Mortierella* was *positively* correlated with quercetin; c_*Sordariomycetes* was significantly inextricably linked to catechins and chlorogenic acids; Verticillium was significantly inversely associated with Isorhamnetin. In the stem of WP (Figure 10E), *Botrytis* and *Sarocladium* were significantly positively correlated with kaempferol; *Sarocladium* was significantly positively correlated with chlorogenic acid; *Paraphoma* was significantly positively correlated with Hyperoside; *Cercospora* was significantly negatively correlated with Hyperoside and Isorhamnetin; *Pyrenochaetopsis* was significantly and negatively correlated with catechins. In the leaves of WP (Figure 10F), *Cercospora*, *Botrytis*, and *Keissleriella* were significantly positively correlated with chlorogenic acid; *Cercospora* was significantly positively correlated with catechins; *Cladosporium* was significantly negatively correlated with Isorhamnetin; *Hannaella* was significantly negatively correlated with hyperoside.

Discussion

The colonization of cercospora interferes with the assembly process of the endophytic fungi of *P. Hydropiper*

In this study, we found a high degree of overlap in the taxa and distribution areas of ZP and WP, and there was no significant difference in the overall alpha diversity between

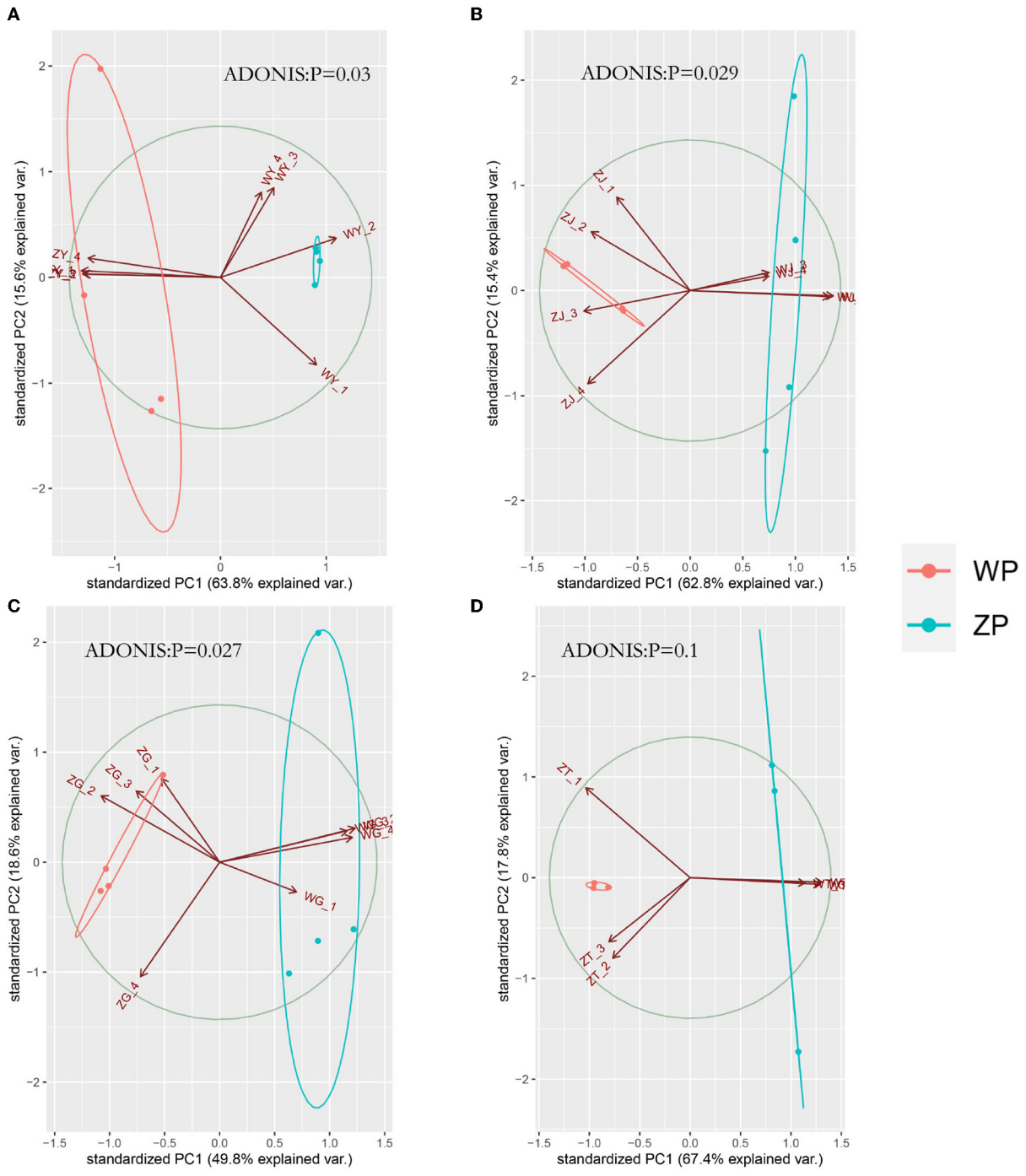

FIGURE 5
PCA analysis of three compartments between ZP and WP [**(A)** leaf, **(B)** stem, **(C)** root, **(D)** rhizosphere soil].

the two. The similarity of fungal communities in rhizosphere soil confirms that both acquire fungi from the same soil species pool. Moreover, the interaction network analysis shows that the connectivity of the endophytic fungi between ZP and WP is very close. These results indicate that the two plants are similar in their ability to shape the composition and structure of endophytic fungal communities. However, we also observed significant leaves, stems, and roots differences between the two plants. This suggests that the assembly process of fungal communities is the key factor influencing

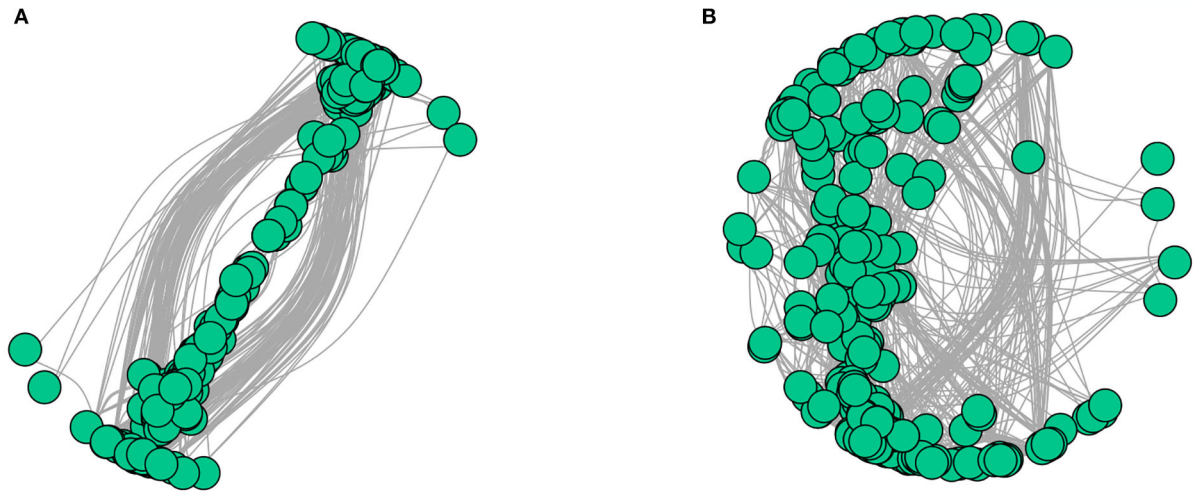

FIGURE 6
Interaction network diagram of ZP and WP [**(A)** ZP, **(B)** WP].

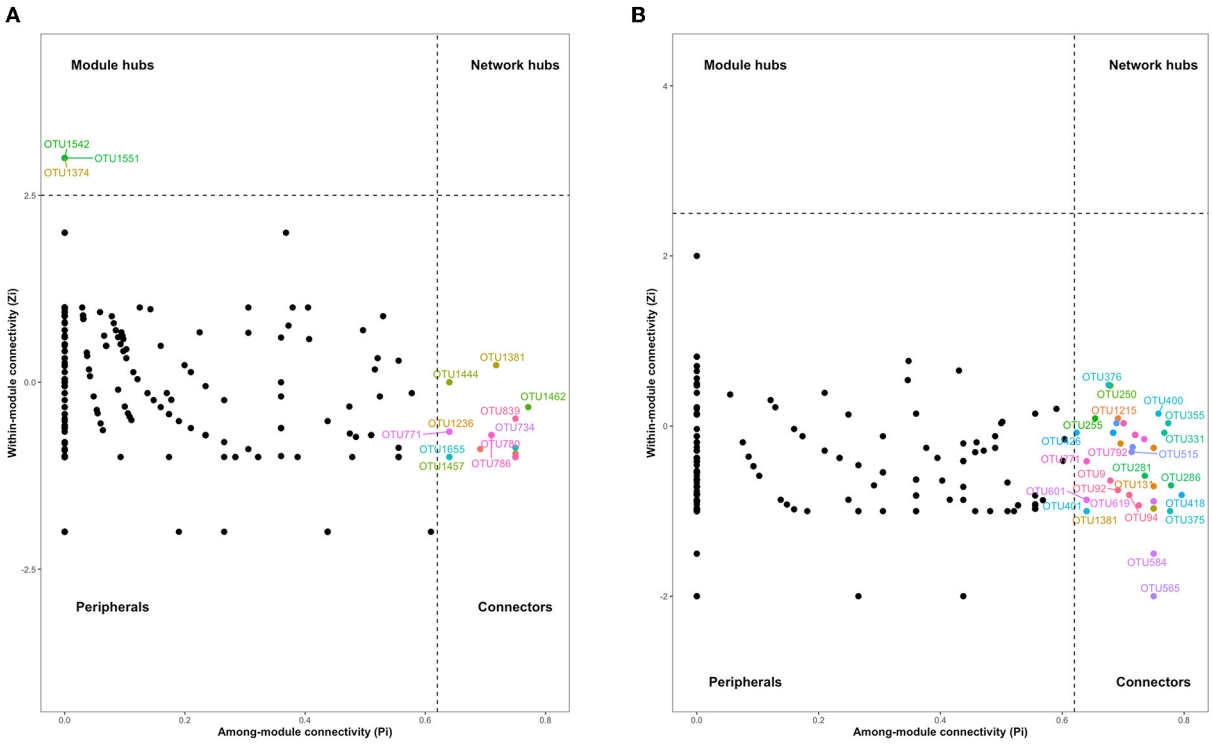

FIGURE 7
The characteristic annotation analysis of nodes in the interaction network. **(A)** ZP, **(B)** WP.

the composition of the community. Therefore, we compared the community composition of the three compartments in ZP and WP and assessed the community composition that differed significantly between the two. In ZP, the relative abundance of differential communities in leaves is highest, with *Cercospora* dominating the differential communities in

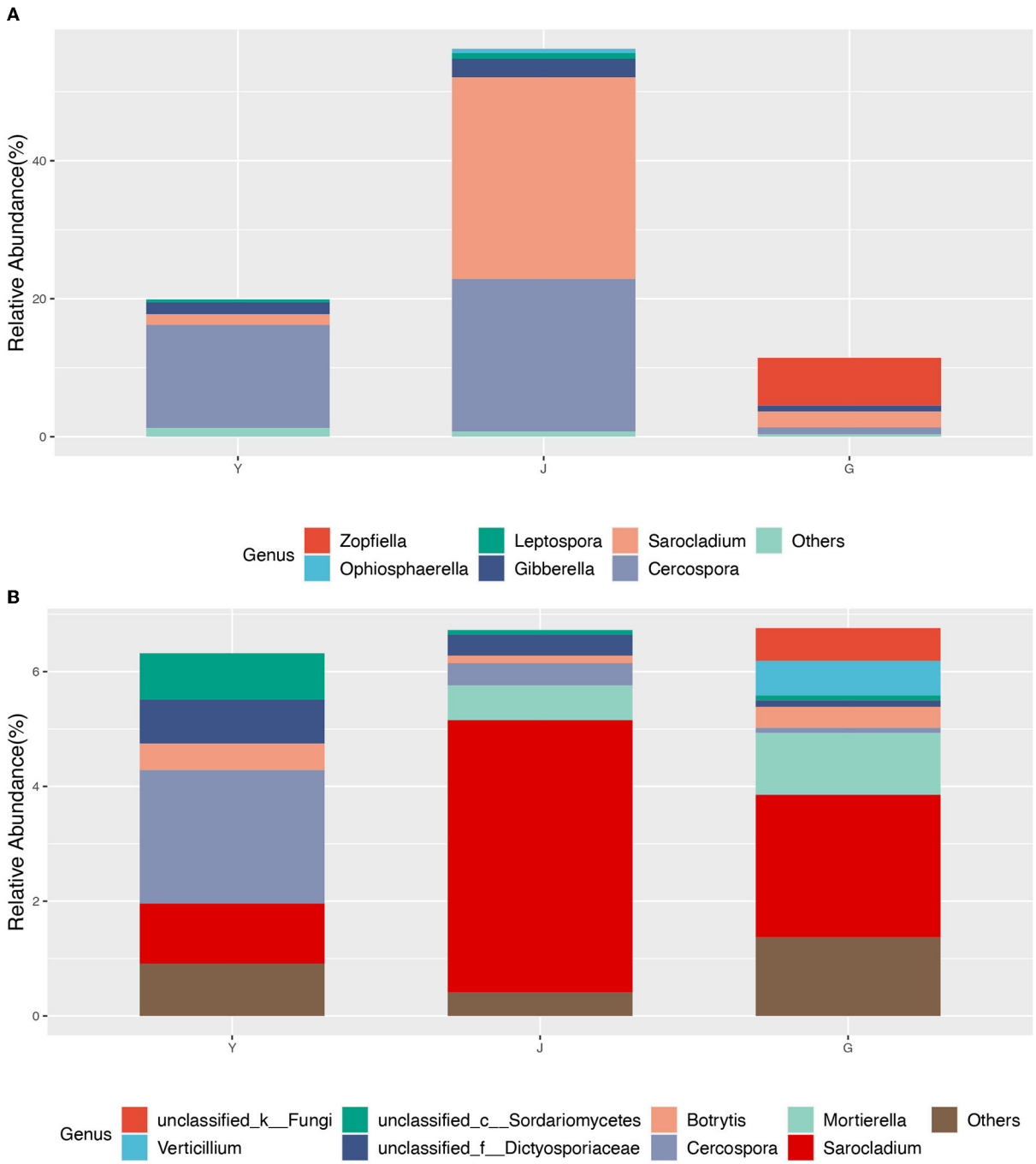

FIGURE 8
The core community composition at the genus level. **(A)** ZP, **(B)** WP.

stems and leaves. At the same time, the ACE index of the community in the leaves of ZP was significantly higher than that of WP, indicating a significant enrichment of the community in the leaves of ZP. Studies have shown that *Cercospora* usually colonizes leaves (Khan et al., 2008). Interestingly, the core community in ZP was also dominated by *Cercospora*, accounting for 38.12% of the total community. This suggests that after *Cercospora* colonizes the leaves of ZP, it significantly affects the assembly process of the endophytic fungi. In WP, the relative abundance of differential communities in stems was highest, and the differential community at all three compartments was dominated by *Cladosporium*, which is generally considered to

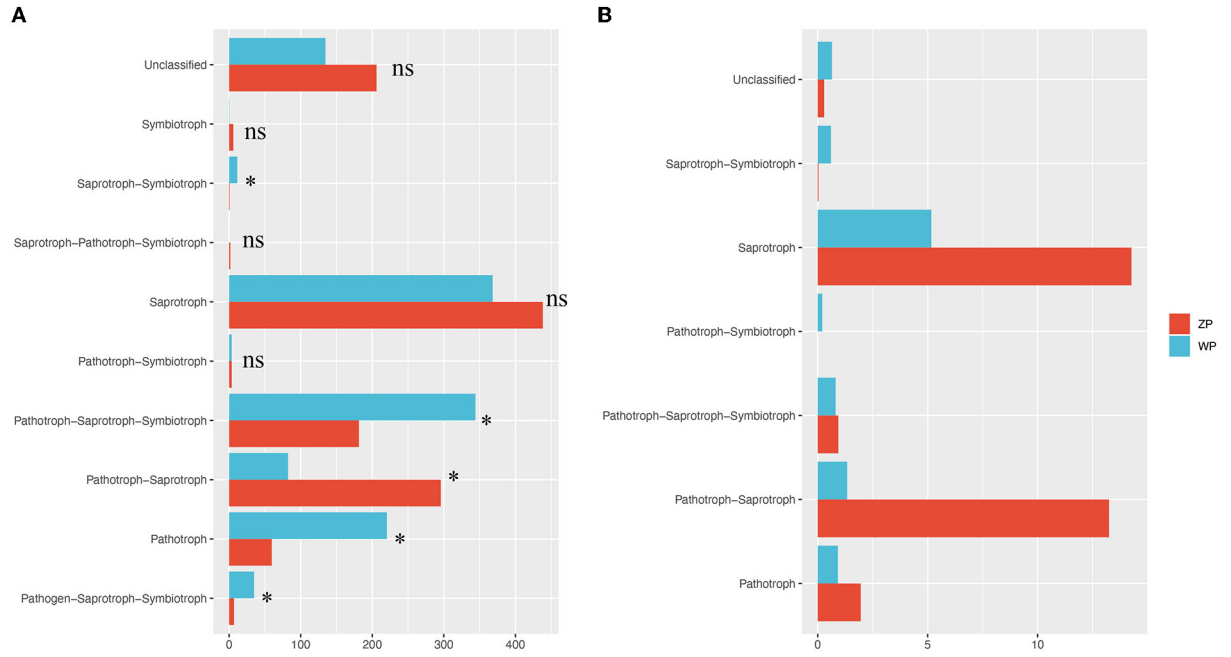

FIGURE 9
Functional community composition. **(A)** The functional composition of all compartments, **(B)** The functional composition of core community. *P-value < 0.05.

colonize the roots of plants (Hamayun et al., 2009; Chen et al., 2022); this suggests that the assembly process of endophytic fungal communities in WP is still dominated by fungi recruited in the soil.

Endophytic fungi communitites significantly affect host secondary metabolic processes

We found significantly different communities between ZP and WP, including *Cercospora*, *Phaeosphaeria*, *Branch06*, *Stachybotryaceae*, and *Plectosphaerella*. Most of the community from *Cercospora* is thought to be able to cause diseases in plants. Interestingly, Martínez et al. (2017) found that chlorogenic acid can effectively inhibit the growth of fungi such as *Cercospora*. In this study, the chlorogenic acid content of ZP was significantly higher than that of WP, and the relative abundance of this type of fungi in ZP was also considerably higher than WP, suggesting that it may be due to the extensive colonization of *Cercospora*, resulting in host stress producing more chlorogenic acid. For *Pheosphaeria*, there have been many studies that demonstrate it is rich in secondary metabolites, including polyketone derivatives, pyrazine alkaloids, isocoumarins, perylenequinonoid, anthraquinone, diterpenes, and cyclic peptides (El-Demerdash, 2018; Xiao et al., 2022). This may illustrate the reason that the content of secondary metabolites in ZP is significantly higher than in WP. Fungi, mainly plant pathogens or saprophytic, such as the widely studied *Cladosporium fulvum*, are considered to be the leading cause of moldy tomato leaves. However, many species have also been found in this genus that promotes plant growth, such as through the production of gibberellin (Hamayun et al., 2009, 2010), protein hydrolysates (Răut et al., 2021), and volatile substances (Paul and Park, 2013). In addition, some species from *Cladosporium* can also produce substances such as brefeldin A (Wang et al., 2007) and Cladosins LO (Pan et al., 2020) to play an anti-pathogenic fungus and bacterial activity. It is worth noting that after Ullah et al. (2019) found that the stem of *Poplars* was infected with *Plectosphaerella populi*, the content of catechins and proanthocyanidins increased significantly. In this experiment, the community of *Plectosphaerella* was observed in the stem of WP to be considerably higher than that of ZP. The catechin content of WP was also significantly higher than that of ZP, suggesting that *Plectosphaerella* is likely to be an essential potential community involved in or promoting catechin synthesis and indicating that the synthetic compartment of catechin in the plant may be the stem.

Moreover, we analyzed the functional composition of these communities. In ZP, it is dominated by saprotroph and pathotroph-saprotrophs. In WP, the community of pathotrophs, pathogen-saprotroph-symbiotrophs, and saprotroph-symbiotrophs. Moreover, the relative abundance of the ZP-led functional community was significantly higher

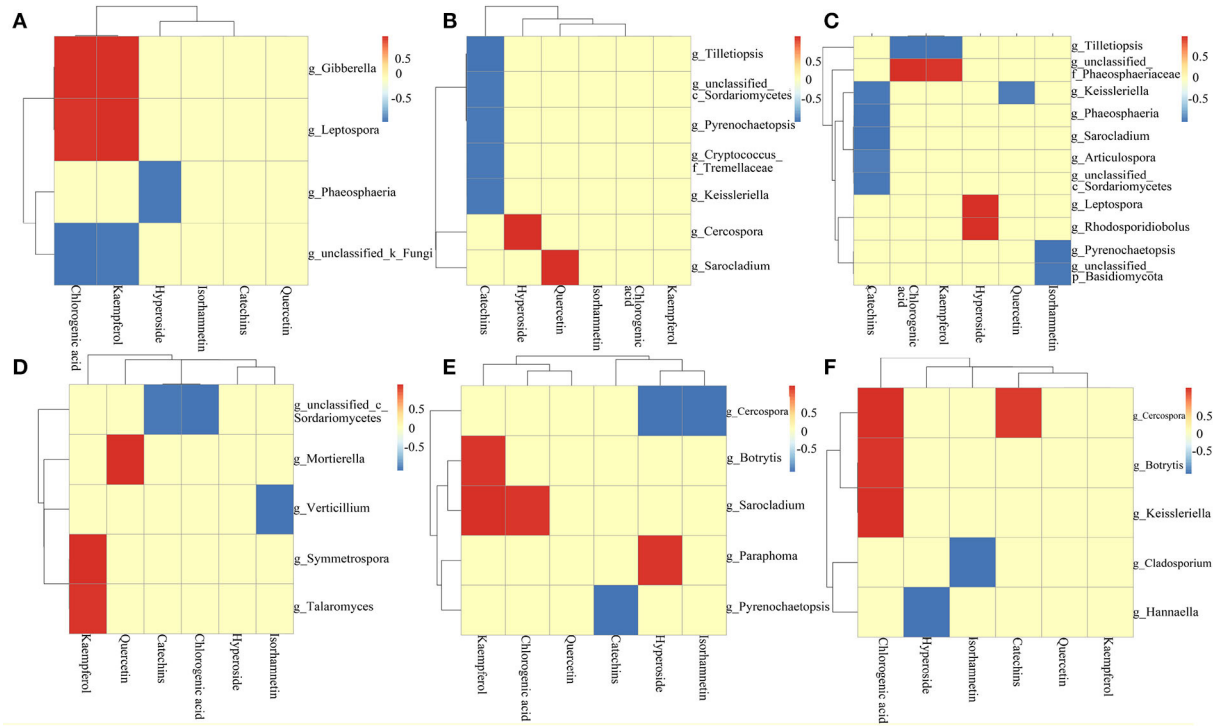

FIGURE 10
Analysis of the correlation between core community and active ingredient [**(A)** ZP root; **(B)** ZP stem; **(C)** ZP leaf; **(D)** WP root; **(E)** WP stem; **(F)** WP leaf].

than that of WP, and the relative abundance of the dominant community in WP was significantly higher than that of ZP. This indicates a significant difference in the functional community composition between the two. Further, in the functional composition analysis of the core community, it was also found that saprotroph and sathotroph-saprotrophs had significant differences between ZP and WP. These results suggest a difference in the status of endophytic fungi involved in the secondary metabolism of ZP and WP. Further research is needed on the function of these communities in plants.

The core communities are the essential members involved in the secondary metabolic processes of host plants

We constructed the interaction network of ZP and WP endophytic fungal communities, 3 module hub nodes and 35 connector nodes were found in ZP, and 74 connector nodes were found in WP. The two core communities present different compositions at the genus level, with ZP dominated by Cercospora and Zopfiella. In the WP, it is mainly dominated by Mortierella and *Cercospora*. Kemp et al. (2020) found that *Sarocladium* zeae from this genus acted as systemic endophytic fungi in wheat and as a biological control agent in the host. Since the *Cercospora* and *Sarocladium* play a dominant role in both ZP and WP, therefore, it may indicate that the *Cercospora* has a potential role in regulating the structure of the community. In addition, *Mortierella* is often thought to promote plant growth and increase biomass (Li, S. J. et al., 2018; Ozimek and Hanaka, 2020; Zhang et al., 2020). For *Zopfiella*, Sun et al. (2020) found that species from this genus are capable of producing sesquiterpenes and α-pyranone derivatives.

In the analysis of the correlation between the core community and the active ingredient, 23 distinctly associated communities were found, many of which were thought to promote plant growth and participate in secondary metabolic processes, including *Mortierella* (Li, F. et al., 2018; Ozimek and Hanaka, 2020; Zhang et al., 2020), *Talaromyces* (Naraghi et al., 2012; Lan and Wu, 2020), *Sordariomycetes* (Camarena-Pozos et al., 2021), *Verticillium* (You et al., 2009; Li, N., et al., 2018), *Sarocladium* (Kemp et al., 2020; Błaszczyk et al., 2021; Salvatore et al., 2021), *Gibberella* (Brian et al., 1954; Geng et al., 2014), *Tilletiopsis* (Klecan et al., 1990), and *Phaeosphaeriaceae* (Xiao et al., 2022; Xu et al., 2022), In addition, some plant pathogens are still present in these communities, including *Botrytis*, *Paraphoma*, *Cercospora*, and *Pyrenochaetopsis*. These communities potentially affect the secondary metabolic processes of the host, and it is necessary

to further identify these communities and their functions in subsequent studies. Therefore, these results demonstrate that the core community of the interaction network plays a vital role in the secondary metabolism of ZP and WP.

Conclusion

The results showed that the endophytic fungi community assembly processes of *P. hydropiper* and *P. lapathifolium* are significantly different. Since the two acquired fungi from the same soil species pool and have the same ability to shape the composition and structure of endophytic fungal communities, we believe that this difference was mainly due to the infestation of *Cercospora*. In addition, the results also found that the core community was an important member involved in the secondary metabolism of *P. hydropiper* and *P. lapathifolium*. The infection of *Cercospora* provided an opportunity to shape a specific core community. The infection process exerted selective pressure on recruiting other fungi, resulting in a higher proportion of the core community of *P. hydropiper* in the community as a whole than that of *P. lapathifolium*. This increases the odds of the host interacting with the core community. Therefore, it can enhance the communication between host plants and endophytic fungi, affecting the content of secondary metabolites of *P. hydropiper*. Although our study is limited to the two current species, more in-depth studies are needed to elucidate the mechanism by which *Cercospora* infestation affects the process of plant endophytic fungal community assembly. This study has important practical implications for inoculating specific communities in production to improve the yield of crops or medicinal plants. It also provides ideas for the study of the assembly process of other plant endophytic fungi.

Data availability statement

The data presented in the study are deposited in the NCBI Sequence Read Archive (SRA) database repository, https://www.ncbi.nlm.nih.gov/, accession number SRR20897189-SRR20897218.

Author contributions

XZ, HL, QH, and JW conceived and designed the study. XZ, HL, MT, ZD, and QF performed the experiments. XZ and HL processed the data and wrote the article. All authors read and approved the manuscript.

Funding

This work was financially supported by the Sichuan Science and Technology Department (2021ZYD0109 and 2022YFS0430). We are indebted to our alma mater, Chengdu University of Traditional Chinese Medicine, for the convenience of collecting documents and experiments. Thanks for all the help from everyone in our lab.

Conflict of interest

Author JS was employed by Sichuan Fuzheng Pharmaceutical Co., Ltd.

The remaining authors declare that the research was conducted in the absence of any commercial or financial relationships that could be construed as a potential conflict of interest.

Publisher's note

Supplementary material

The Supplementary Material for this article can be found online at: https://www.frontiersin.org/articles/10.3389/fpls.2022.984483/full#supplementary-material

References

Adeleke, B. S., and Babalola, O. O. (2021). The endosphere microbial communities, a great promise in agriculture. *Int. Microbiol.* 24, 1–17. doi: 10.1007/s10123-020-00140-2

Ayaz, M., Junaid, M., Subhan, F., Ullah, F., Sadiq, A., Ahmad, S., et al. (2014). Heavy metals analysis, phytochemical, phytotoxic and anthelmintic investigations of crude methanolic extract, subsequent fractions and crude saponins from *Polygonum hydropiper* L. *BMC Complem. Altern. Med.* 14, 1–9. doi: 10.1186/1472-6882-14-465

Błaszczyk, L., Waśkiewicz, A., Gromadzka, K., Mikołajczak, K., and Chełkowski, J. (2021). *Sarocladium* and *Lecanicillium* associated with maize seeds and their potential to form selected secondary metabolites. *Biomolcules* 11, 98. doi: 10.3390/biom11010098

Brian, P., Elson, G., Hemming, H., and Radley, M. (1954). The plant-growth-promoting properties of gibberellic acid, a metabolic product of the fungus *Gibberella fujikuroi*. *J. Sci. Food Agric.* 5, 602–612. doi: 10.1002/jsfa.2740051210

Camarena-Pozos, D. A., Flores-Núñez, V. M., López, M. G., and Partida-Martínez, L. P. (2021). Fungal volatiles emitted by members of the microbiome of desert plants are diverse and capable of promoting plant growth. *Environ. Microbiol.* 23, 2215–2229. doi: 10.1111/1462-2920.15395

Cao, J., Liu, B., Xu, X., Zhang, X., Zhu, C., Li, Y., et al. (2021). Plant endophytic fungus extract ZNC improved potato immunity, yield, and quality. *Front. Plant Sci.* 12, 707256. doi: 10.3389/fpls.2021.707256

Chen, H., Chen, J., Qi, Y., Chu, S., Ma, Y., Xu, L., et al. (2022). Endophytic fungus *Cladosporium* tenuissimum DF11, an efficient inducer of tanshinone biosynthesis in *Salvia miltiorrhiza* roots. *Phytochemistry* 194, 113021. doi: 10.1016/j.phytochem.2021.113021

Csardi, G., and Nepusz, T. (2006). The igraph software package for complex network research. *Int. J. Complex Syst.* 1695, 1–9.

Cumbo, F., Paci, P., Santoni, D., Di Paola, L., and Giuliani, A. (2014). GIANT: a cytoscape plugin for modular networks. *PLoS ONE.* 9, e105001–e105001. doi: 10.1371/journal.pone.0105001

Dang, H., Zhang, T., Wang, Z., Li, G., Zhao, W., Lv, X., et al. (2021). Succession of endophytic fungi and arbuscular mycorrhizal fungi associated with the growth of plant and their correlation with secondary metabolites in the roots of plants. *BMC Plant Biol.* 21, 1–16. doi: 10.1186/s12870-021-02942-6

El-Demerdash, A. (2018). Chemical diversity and biological activities of Phaeosphaeria fungi genus: a systematic review. *J. Fungi.* 4, 130. doi: 10.3390/jof4040130

Geng, Z., Zhu, W., Su, H., Zhao, Y., Zhang, K. Q., and Yang, J. (2014). Recent advances in genes involved in secondary metabolite synthesis, hyphal development, energy metabolism and pathogenicity in *Fusarium graminearum* (teleomorph *Gibberella zeae*). *Biotechnol. Adv.* 32, 390–402. doi: 10.1016/j.biotechadv.2013.12.007

Hamayun, M., Afzal Khan, S., Ahmad, N., Tang, D. S., Kang, S. M., Na, C. I., et al. (2009). *Cladosporium* sphaerospermum as a new plant growth-promoting endophyte from the roots of *Glycine max* (L.) Merr. *World J. Microbiol. Biotechnol.* 25, 627–632. doi: 10.1007/s11274-009-9982-9

Hamayun, M., Khan, S. A., Khan, A. L., Rehman, G., Kim, Y. H., Iqbal, I., et al. (2010). Gibberellin production and plant growth promotion from pure cultures of *Cladosporium* sp. MH-6 isolated from cucumber (*Cucumis sativus* L.). *Mycologia.* 102, 989–995. doi: 10.3852/09-261

Hamilton, N. E., and Ferry, M. (2018). ggtern: Ternary diagrams using ggplot2. *J. Stat. Softw.* 87, 1–17. doi: 10.18637/jss.v087.c03

Hong, H. H., and Hanshen, Z. (2013). Research progress of Chinese herbal medicine spicy indigo in recent years. *Chin. J. Ethnomed. Ethnoph.* 41, 38–40.

Hong, L. L., Wei, X., Long, W., and Kun, J. W. (2019). Analysis of *Polygonum hydropiper* and its promiscuous speceis in same genus. *Collections.* 8.

Kemp, N. D., Vaughan, M. M., McCormick, S. P., Brown, J. A., and Bakker, M. G. (2020). *Sarocladium* zeae is a systemic endophyte of wheat and an effective biocontrol agent against Fusarium head blight. *Biol. Control.* 149, 104329. doi: 10.1016/j.biocontrol.2020.104329

Khan, J., Rio, L. D., Nelson, R., Rivera-Varas, V., Secor, G. A., and Khan, M. F. R. (2008). Survival, dispersal, and primary infection site for *Cercospora* beticola in sugar beet. *Plant Dis.* 92, 741–745. doi: 10.1094/PDIS-92-5-0741

Klecan, A., Hippe, S., and Somerville, S. (1990). Reduced growth of *Erysiphe graminis* f. sp. hordei induced by *Tilletiopsis pallescens*. *Phytopathology* 80, 325–331. doi: 10.1094/Phyto-80-325

Kolde, R., and Kolde, M. R. (2015). Package "pheatmap". *R Package* 1, 790. doi: 10.1016/j.funeco.2018.04.004

Lan, D., and Wu, B. (2020). Chemistry and bioactivities of secondary metabolites from the Genus *Talaromyces*. *Chem. Biodivers.* 17, e2000229. doi: 10.1002/cbdv.202000229

Langfelder, P., and Horvath, S. (2008). WGCNA: an R package for weighted correlation network analysis. *BMC Bioinform.* 9, 559–559. doi: 10.1186/1471-2105-9-559

Li, F., Chen, L., Redmile-Gordon, M., Zhang, J., Zhang, C., Ning, Q., et al. (2018). Mortierella elongata 's roles in organic agriculture and crop growth promotion in a mineral soil. *Land Degrad. Dev.* 29, 1642–1651. doi: 10.1002/ldr.2965

Li, N., Wang, W., Bitas, V., Subbarao, K., Liu, X., and Kang, S. (2018). Volatile compounds emitted by diverse *Verticillium* species enhance plant growth by manipulating auxin signaling. *Mol. Plant Microbe Interact.* 31, 1021–1031. doi: 10.1094/MPMI-11-17-0263-R

Li, S. J., Zhang, X., Wang, X. H., and Zhao, C. Q. (2018). Novel natural compounds from endophytic fungi with anticancer activity. *Eur. J. Med. Chem.* 156, 316–343. doi: 10.1016/j.ejmech.2018.07.015

Lunardelli Negreiros de Carvalho, P., de Oliveira Silva, E., Aparecida Chagas-Paula, D., Honorata Hortolan Luiz, J., and Ikegaki, M. (2016). Importance and implications of the production of phenolic secondary metabolites by endophytic fungi: a mini-review. *Mini Rev. Med. Chem.* 16, 259–271. doi: 10.2174/1389557515666151016123923

Martínez, G., Regente, M., Jacobi, S., Rio, M. D., Pinedo, M., and Laura, D. (2017). Chlorogenic acid is a fungicide active against phytopathogenic fungi. *Pestic. Biochem. Physiol.* 140, 30–35. doi: 10.1016/j.pestbp.2017.05.012

Martins, F., Mina, D., Pereira, J. A., and Baptista, P. (2021). Endophytic fungal community structure in olive orchards with high and low incidence of olive anthracnose. *Sci. Rep.* 11, 1–11. doi: 10.1038/s41598-020-79962-z

Naraghi, L., Heydari, A., Rezaee, S., and Razavi, M. (2012). Biocontrol agent talaromyces flavus stimulates the growth of cotton and potato. *J. Plant Growth Regul.* 31, 471–477. doi: 10.1007/s00344-011-9256-2

Oksanen, J., Blanchet, F. G., Kindt, R., Legendre, P., Minchin, P. R., O'hara, R., et al. (2013). Package 'vegan'. *Commun. Ecol. Pack.* 2, 1–295.

Ozimek, E., and Hanaka, A. (2020). Mortierella species as the plant growth-promoting fungi present in the agricultural soils. *Agriculture* 11, 7. doi: 10.3390/agriculture11010007

Pan, F., El-Kashef, D. H., Kalscheuer, R., Müller, W. E. G., Lee, J., Feldbrügge, M., et al. (2020). Cladosins L–O, new hybrid polyketides from the endophytic fungus *Cladosporium* sphaerospermum WBS017. *Eur. J. Med. Chem.* 191, 112159. doi: 10.1016/j.ejmech.2020.112159

Paul, D., and Park, K. S. (2013). Identification of volatiles produced by *Cladosporium* cladosporioides CL-1, a fungal biocontrol agent that promotes plant growth. *Sens. Basel* 13, 13969–13977. doi: 10.3390/s131013969

R Core Team (2020). R: A language and environment for statistical computing. R Foundation for Statistical Computing, Vienna, Austria. Available online at: https://www.R-project.org/.

Rahman, E., Goni, S., Rahman, M., and Ahmed, M. (2002). Antinociceptive activity of *Polygonum hydropiper*. *Fitoterapia.* 73, 704–706. doi: 10.1016/S0367-326X(02)00239-3

Răut, I., Călin, M., Capră, L., Gurban, A. M., Doni, M., Radu, N., et al. (2021). *Cladosporium* sp. isolate as fungal plant growth promoting agent. *Agronomy* 11, 392. doi: 10.3390/agronomy11020392

Ribeiro, B. A., da Mata, T. B., Canuto, G. A., and Silva, E. O. (2021). Chemical diversity of secondary metabolites produced by Brazilian endophytic fungi. *Curr. Microbiol.* 78, 33–54. doi: 10.1007/s00284-020-02264-0

Salvatore, M. M., Andolfi, A., and Nicoletti, R. (2021). The genus *Cladosporium*: a rich source of diverse and bioactive natural compounds. *Molecules* 26, 3959. doi: 10.3390/molecules26133959

Shahed-Al-Mahmud, M., and Lina, S. M. M. (2017). Evaluation of sedative and anxiolytic activities of methanol extract of leaves of *Persicaria hydropiper* in mice. *Clin. Phytosci.* 3, 1–12. doi: 10.1186/s40816-017-0056-5

Shannon, P., Markiel, A., Ozier, O., Baliga, N. S., and Wang, J. T., Ramage, D., et al. (2003). Cytoscape: a software environment for integrated models of biomolecular interaction networks. *Genome Res.* 13, 2498–2504. doi: 10.1101/gr.1239303

Sharif, S., Ahmed, T., Haque, M. A., Bhuiyan, M., and Shahriar, M. (2014). Phytochemical screenings, thrombolytic activity, membrane stabilizing activity and cytotoxic properties of *Polygonum hydropiper*. *Res. J. Med. Plant.* 8, 92–98. doi: 10.3923/rjmp.2014.92.98

Song, W. L., Dai, C. C., Liu, X. Z., and Cai, X. Z. (2010). The effect of different endophytic fungi on *Chrysanthemum morifolium* output and quality. *J. Chin. Med. Mater.* 33, 4–7.

Sun, L. T., Chen, Y., Yang, H. X., Li, Z. H., Liu, J. K., Wang, G. K., et al. (2020). Bisabolane sesquiterpenes and α-pyrone derivative from endophytic fungus *Zopfiella* sp. *Phytochem. Lett.* 37, 29–32. doi: 10.1016/j.phytol.2020.03.008

Tang, Z., Wang, Y., Yang, J., Xiao, Y., Cai, Y., Wan, Y., et al. (2020). Isolation and identification of flavonoid-producing endophytic fungi from medicinal plant *Conyza blinii* H. Lév that exhibit higher antioxidant and antibacterial activities. *PeerJ.* 8, e8978. doi: 10.7717/peerj.8978

Tian, Y., Amand, S., Buisson, D., Kunz, C., Hachette, F., Dupont, J., et al. (2014). The fungal leaf endophyte Paraconiothyrium variabile specifically metabolizes the host-plant metabolome for its own benefit. *Phytochemistry* 108, 95–101. doi: 10.1016/j.phytochem.2014.09.021

Ullah, C., Unsicker, S. B., Reichelt, M., Gershenzon, J., and Hammerbacher, A. (2019). Accumulation of catechin and proanthocyanidins in black poplar stems after infection by *Plectosphaerella populi*: hormonal regulation, biosynthesis and antifungal activity. *Front. Plant Sci.* 10, 1441. doi: 10.3389/fpls.2019.01441

Vergara, C., Araujo, K. E., Urquiaga, S., Santa-Catarina, C., Schultz, N., da Silva Araújo, E., et al. (2018). Dark septate endophytic fungi increase green manure-15N recovery efficiency, N contents, and micronutrients in rice grains. *Front. Plant Sci.* 9, 613. doi: 10.3389/fpls.2018.00613

Wang, F., Jiao, R., Cheng, A., Tan, S., and Song, Y. (2007). Antimicrobial potentials of endophytic fungi residing in Quercus variabilis and brefeldin A obtained from *Cladosporium* sp. *World J. Microbiol. Biotechnol.* 23, 79–83. doi: 10.1007/s11274-006-9195-4

Waqas, M., Khan, A. L., Kamran, M., Hamayun, M., Kang, S. M., Kim, Y. H., et al. (2012). Endophytic fungi produce gibberellins and indoleacetic acid and promotes host-plant growth during stress. *Molecules* 17, 10754–10773. doi: 10.3390/molecules170910754

Wei, Y. H., Yu, L. Z., and Junru, L. (2021). Effects of 4 different TCM monomers on TNF-α, IL-1β, IL-6 levels and PKR/p-PKR in norovirus infectious enteritis mice. *J. Liaoning Univ. TCM* 23, 24–27.

Wickham, H. (2011). ggplot2. *Wiley Interdiscip. Rev. Comput. Stat.* 3, 180–185. doi: 10.1002/wics.147

Xiang, L., and Ming, L. (2020). Progression of pharmacological effects of *Polygonum hydropipe* L. *Int. J. Tradit. Chin. Med.* 40, 196–198.

Xiao, Y., Liang, W., Zhang, Z., Wang, Y., Zhang, S., Liu, J., et al. (2022). Polyketide derivatives from the endophytic fungus *Phaeosphaeria* sp. LF5 isolated from huperzia serrata and their acetylcholinesterase inhibitory activities. *J. Fungi* 8, 232. doi: 10.3390/jof8030232

Xu, Z. L., Yan, D. J., Tan, X. M., Niu, S. B., Yu, M., Sun, B. D., et al. (2022). Phaeosphspirone (1/1′), a pair of unique polyketide enantiomers with an unusual 6/5/5/6 tetracyclic ring from the desert plant endophytic fungus *Phaeosphaeriaceae* sp. *Phytochemistry* 194, 112969. doi: 10.1016/j.phytochem.2021.112969

You, F., Han, T., Wu, J., z., Huang, B., k., et al. (2009). Antifungal secondary metabolites from endophytic *Verticillium* sp. *Biochem. Syst. Ecol.* 37, 162–165. doi: 10.1016/j.bse.2009.03.008

Yue, Y. (2005). Ameliorating effect of green tea catechin on inflammatory bowel disease caused by trinitrobenzenesulfonic acid. *For. Med. Sci.* 27, 314–315.

Zhang, K., Bonito, G., Hsu, C. M., Hameed, K., Vilgalys, R., and Liao, H. L. (2020). Mortierella elongata increases plant biomass among non-leguminous crop species. *Agronomy* 10, 754. doi: 10.3390/agronomy10050754

Zhang, X. R., Ren, Y. Y., Zeng, Y. J., Li, T. L., Hong, Y. L., Ren, C. Y., et al. (2021). Characterization of the bioactive compounds with efficacy against enteritis in Polygonum hydropiper L. by UHPLC-Q-Orbitrap HRMS combined with network pharmacological analysis. *ChemistrySelect.* 6, 10336–47. doi: 10.1002/slct.202102886

frontiers | Frontiers in Plant Science

TYPE Original Research
PUBLISHED 10 November 2022
DOI 10.3389/fpls.2022.1040037

OPEN ACCESS

EDITED BY
Aqeel Ahmad,
University of Florida, United States

REVIEWED BY
Muhammad Riaz,
Shanghai Jiao Tong University, China
Umesh Pravin Dhuldhaj,
Banaras Hindu University, India

*CORRESPONDENCE
Guihua Li
liguihua@gdaas.cn

SPECIALTY SECTION
This article was submitted to Plant Symbiotic Interactions, a section of the journal Frontiers in Plant Science

RECEIVED 08 September 2022
ACCEPTED 21 October 2022
PUBLISHED 10 November 2022

CITATION
Mirza FS, Aftab Z-e-H, Ali MD, Aftab A, Anjum T, Rafiq H and Li G (2022) Green synthesis and application of GO nanoparticles to augment growth parameters and yield in mungbean (*Vigna radiata* L.). *Front. Plant Sci.* 13:1040037. doi: 10.3389/fpls.2022.1040037

Green synthesis and application of GO nanoparticles to augment growth parameters and yield in mungbean (*Vigna radiata* L.)

Faisal Shafiq Mirza[1,2], Zill-e-Huma Aftab[2], Muhammad Danish Ali[3], Arusa Aftab[4], Tehmina Anjum[2], Hamza Rafiq[2] and Guihua Li[1]*

[1]Guangdong Key Laboratory for New Technology Research of Vegetables/Vegetable Research Institute, Guangdong Academy of Agricultural Sciences, Guangzhou, China, [2]Department of Plant Pathology, Faculty of Agricultural Sciences, University of the Punjab, Lahore, Pakistan, [3]Department of Physics, University of the Punjab, Lahore, Pakistan, [4]Department of Botany, Lahore College for Women University, Lahore, Pakistan

Plant growth promotion has long been a challenge for growers all over the world. In this work, we devised a green nanomaterial-assisted approach to boost plant growth. It has been reported that carbon nanomaterials are toxic to plants because they can inhibit the uptake of nutrients if employed in higher concentrations, however this study shows that graphene oxide (GO) can be used as a regulator tool to improve plant growth and stability. Graphene oxide in different concentrations was added to the soil of mungbean. It is proved that when a suitable amount of graphene oxide was applied, it had a good influence on plant growth by enhancing the length of roots and shoots, number of leaves, number of root nodules per plant, number of pods, and seeds per pod. We presume that the use of bio-fabricated graphene oxide as a strategy would make it possible to boost both plant growth and the significant increase in the number of seeds produced by each plant.

KEYWORDS

graphene oxide, nanoparticles, physicochemical properties, nutrient uptake, *Vigna radiata*

Introduction

Mungbean [*Vigna radiata* (L.) R. Wilczek var. radiata] is a short-duration grain legume grown on 7 million hectares primarily in Asia but rapidly spreading to other parts of the world. Its seed has a protein content of 24% and is rich in antioxidants, fibre, and phytonutrients (Nair et al., 2019). It is the major summer pulse of Pakistan and is grown on 88% of the land in Punjab province, which produces 85% of the country's total output

(Ullah et al., 2020). Abiotic and biotic constraints, inadequate crop management methods, and lack of quality seeds of better varieties available to farmers all contribute to the low yield of mungbean (Chauhan13 et al., 2010; Pratap et al., 2019). The major biotic constraints of mungbean include diseases which are yellow mosaic, anthracnose, powdery mildew, Cercospora leaf spot, dry root rot, halo blight, bacterial leaf spot, and tan spot (Nair et al., 2019). The importance of effective food cultivation and food security has increased due to the world's rapid population expansion and climatic change. As a result, alternative ways are being recommended to meet the requirement of food production and crop protection under severe environmental conditions (Lesk et al., 2016; Ramankutty et al., 2018).

Nanomaterials (NMs) are molecules with a diameter of 1–100 nm that play an important role in plant development and production, especially in stressful situations. Moreover, these nanomaterials are used as fertilizers which reduce nutrient loss while also lowering fertilizer input. The graphene oxide nanoparticles (GO NPs) are being widely used in a variety of fields, including basic science, medical and energy (Aazami et al., 2022). Studies are being done utilizing carbon nanomaterials to solve problems in agriculture such as plant disease, pesticides, and stress (Vinković et al., 2017). Although GO NPs have the ability to control plant growth and development, its mechanism is unknown. Plant reaction to GO has been linked to the reactive oxygen species (ROS) pathway, according to research (Siddiqi and Husen, 2017).

Scientists are trying to minimize the negative impacts of nanoparticles which are synthesized using chemical processes, incorporating green synthesis of nanoparticles which is found to be very effective (Gur et al., 2022). The nanomaterials synthesized through chemical methods are not ecofriendly since the chemicals utilized in the process of chemical synthesis are often toxic and flammable (Jain et al., 2009). *N. sativa* belonging to family Ranunculaceae is a medicinal plant that is used all over the world. Because of its diverse potential, it is one of the most important medicinal plants and is commonly known as black seed. The black seeds are being used as natural food additions and have medical properties such as bronchodilator, insulinotropic, anticancer, antinociceptive, anti-inflammatory, hypoglycemic, hepatoprotective, neuroprotective, antihistamine, and antiulcer properties (Ahmad et al., 2013).

Graphene-based nanomaterial applications in agriculture have received a lot of attention. Researchers are employing GO NPs in agricultural crop enhancement. Soil-based graphene oxide treatment increased the physicochemical qualities of the soil (Shekari et al., 2017). On addition, a study in *Silybum marianum* found that using graphene-oxide improved chlorophyll content and relative water content (RWC), as well as improving plant growth and yield (Safikhan et al., 2018). GO at optimum concentrations improved *Arabidopsis thaliana* L. stability and growth, as shown by increases in root length, leaf area, leaf number, and flower bud production (Park et al., 2020). Under salt stress, graphene oxide was employed to improve the growth and yield of pearl millet (*Pennisetum glaucum* L.) and it gave ideal results at 20 mg/L concentration (Mahmoud and Abdelhameed, 2021).

In this research, we showed that low concentrations of graphene oxide nanoparticles (GO NPs) enhanced good plant development and stability, implying that this nanomaterial can have beneficial effects on plant growth and quality. Our findings offer insight into the logical design of an effective nanomaterial-assisted culture system that may be utilized to speed up both plant growth and fruit ripening.

Materials and methods

Chemicals and reagents

The graphite (90%), hydrogen peroxide (H_2O_2), potassium permanganate ($KMnO_4$), ferrous chloride ($FeCl_2.6H_2O$), ferric chloride ($FeCl_3.4H_2O$), and sulfuric acid (H_2SO_4) were purchased from Sigma-Aldrich. The chemicals were analytical grade. Seeds of *Nigella Sativa* were purchased from a local market in Lahore, Pakistan. The experiment was performed at the Experimental Station, Department of Plant Pathology (31°29'42.2664" N, 74°17'49.1316" E, 217 m altitude), Faculty of Agricultural Sciences, University of the Punjab in 2021-2022. A semi-arid climate (Köppen climatic classification BSh) with an average temperature of 40°C, 350 mm of annual precipitation, and a rainy season from July to September characterizes the area.

Preparation of *Nigella Sativa* seed extract

Nigella Sativa seeds (30 g) were washed, powdered, and boiled for 15 minutes in 150 mL of double-distilled water. The aqueous seed extract was then filtered through Whatman No. 1 filter paper and allowed to cool. The seed extract was kept in a sterile container at 4 °C for future use.

Synthesis of graphene oxide

Hummer's technique was used to prepare the GO (William et al., 1958). In the standard procedure, 3 g of graphite and 3 g of $NaNO_3$ were added to 150 mL of H_2SO_4 and the mixture was kept at 0 °C with constant stirring for 3 hours. Then, $KMnO_4$ was slowly added, and the suspension was constantly stirred for 2 hours. Then, 150 mL of distilled water was gently added, and the suspension was stirred for 30 minutes after. Then, H_2O_2 was added cautiously to the above suspension and stirred for 20 min. Finally, the suspension was transferred to a 1L beaker and multiple washings with double distilled water were performed until the neutral pH was achieved. Then, it was filtered and dried at 70°C. This resultant mixture was (GO).

Synthesis of graphene oxide nanoparticles

A mixture of 1g of GO and 70 mL of water was sonicated for 1.5 hours. The mixture was then given a 20-minute stir after the addition of 20 mL of *N. sativa* seed extract. Then, a solution of $FeCl_2.4H_2O$ (6.33 g) and $FeCl_3.6H_2O$ (16.22 g) was mixed separately in 200 mL of distilled water and stirred for 30 minutes, producing a dark green colour and mixed into the solution while constant stirring. Then, sodium hydroxide NaOH (2M) was mixed into the solution and stirred for 20 minutes. The resulting mixture was put to centrifuge at 4500 rpm for 15 minutes. After centrifugation, supernatant was discarded, and the pallet was dried in a hot air oven at 150°C. The powder was crushed in a mortar and pestle to produce the desired tiny graphene oxide nanoparticles. The graphene oxide nanoparticles were then transferred to a sterile falcon tube and used for additional optical and structural characterizations. Figure 1 depicts a schematic representation of the synthesis of graphene oxide nanoparticles.

Characterization of green synthesized graphene oxide nanoparticles

The X-ray diffraction studies of GO NPs were performed on a Rigaku 600Miniflex X-ray diffraction (XRD) instrument with Cu k-α radiation (λ= 1.5412) in the scanning range of 100 -800. UV–visible (UV–vis) spectrum was taken in the wavelength range of 200–600 nm using Agilent Technologies Cary 60 UV–vis to confirm the absorbance of GO NPs and to observe the changes in absorbance caused by variations in reaction conditions. Fourier transform infrared (FTIR) spectra of all samples were recorded in a range of 650–4000 cm−1 in order to identify the characteristic functional groups present on the surface of the GO. Morphological characterization of the green synthesized graphene oxide nanoparticles was performed using high-resolution scanning electron microscopy (HR-SEM).

In vivo application of graphene oxide nanoparticles

To create each GO NPs solution, GO NPs was disseminated in water using sonication. The soil was fumigated using and 10-12 kg soil per pot was filled in 12-inch earthen pots (having 0.264, 0.600 and 0.520 g urea, triple super phosphate and potash respectively in accordance with 40-60-40 kg N, P and K per hectare; half of the urea and other fertilizers applied before sowing and the rest was applied during the vegetative stage of the plants). The mungbean seeds were provided by the Nuclear Institute for Agriculture and Biology (NIAB), which is situated in Faisalabad, Pakistan. A mungbean variety NM-2011 was selected for pot experiment. In each pot, five holes (1cm depth) were drilled, and 3 seeds were planted in each hole. The treatments applied under *in vivo* trial are given in (Table 1). Every week, the pots were irrigated with 50 mL of an aqueous

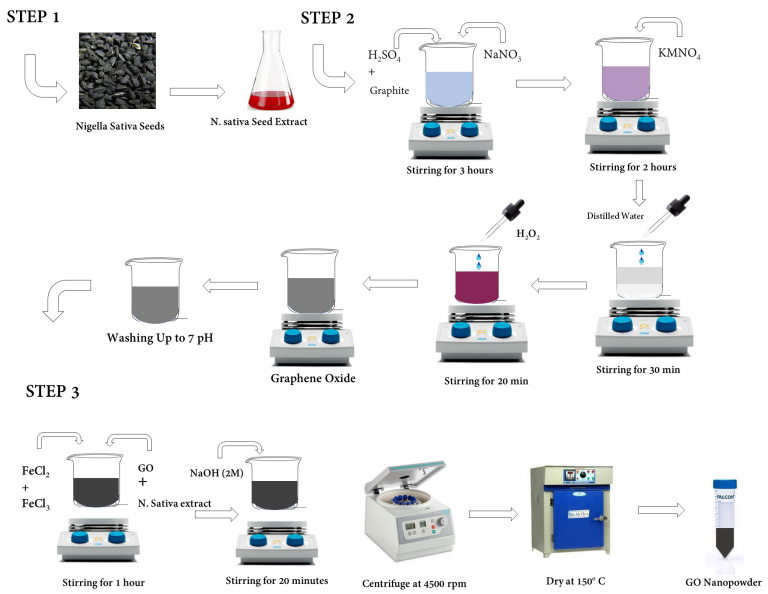

FIGURE 1
Schematic representation of the synthesis of graphene oxide nanoparticles.

TABLE 1 Treatments for evaluating the efficacy of green synthesized GO NPs to augment mungbean plant growth and yield *in vivo*.

Sr	Treatments	Label
1	Control (without GO treatment)	C
2	GO NPs solution (300 mg/L)	T1
3	GO NPs solution (600 mg/L)	T2
4	GO NPs solution (900 mg/L)	T3
5	GO NPs solution (1200 mg/L)	T4
6	GO NPs solution (1500 mg/L)	T5

solution of GO NPs in accordance with the treatments listed in Table 1, and the growth and germination were observed. The entire experiment was conducted in triplets. Every two days, the perimeter of the mungbean plant was checked.

Total chlorophyll and carotenoids measurements

The total Chl concentration was estimated by extracting from 0.05 g frozen leaf samples in the dark with 10 ml of 80% acetone for 24 hours (Gong et al., 2022). A spectrophotometer (UV-2550 Shimadzu, Japan) was used to measure the concentrations of Chl *a*, *b*, and total Chl (mg/L) in the supernatant. In each treatment, three plant samples were examined. Carotenoids were measured following (Alam et al., 2016), with minor adjustments. First, 2 g of dried sample was homogenized for 5 minutes in 40 mL acetone, 60 mL n-hexane, and 0.1 g $MgCO_3$ after which it was vacuum filtered. The filtrate was then washed twice in 25 mL acetone and once in 25 mL n-hexane. The filtrate was put into a separatory funnel and rinsed with 100 mL of distilled water five times. A spectrophotometer was used to determine the absorbance value of 436 nm. The absorbance levels were then quantified by comparing them to the β-carotene reference curve.

Estimation of total protein content

Total protein content of 2 g mungbean seeds from treated and non-treated plants was estimated by the following (Rizvi et al., 2022).

Measurement of enzymatic activity and malondialdehyde content

A total of 0.5 g of fresh mungbean leaves were crushed in 3 mL of a 50 mM ice-cold phosphate buffer (pH 7.0), centrifuged at 10,000 rpm for 20 min at 4 °C, and the supernatant was kept at 4 °C until an enzymatic activity assay.

The inhibition of nitrobluetetrazolium (NBT) reduction served to measure the superoxide dismutase (SOD) activity (Giannopolitis and Ries, 1977). Enzyme extract, phosphate buffer, Na2EDTA, NBT, methionine, and riboflavin were included in the reaction mixture. For 20 minutes, the mixture was exposed to 4000 lx of illumination. The reaction was terminated in complete darkness, and the absorbance at 560 nm was measured. One SOD unit indicates the enzyme concentration that inhibits NBT photochemical degradation by 50%.Peroxidase (POD) activity was measured by the guaiacol method (Omran, 1980). Enzyme extract was mixed with a solution containing phosphate buffer, H_2O_2, and guaiacol in 3 mL. The increase in absorbance was monitored at 470 nm.

The depletion of H_2O_2 at 240 nm was used to measure the catalase (CAT) activity (Aebi, 1984). Phosphate buffer, H_2O_2, and the enzyme extract made up the reaction mixture. At 240 nm, the absorbance decrease was seen. The amount of enzyme needed to break down 1 μmol of H_2O_2 per minute is described by a CAT unit.

Thiobarbituric acid (TBA) reaction was used to measure the amount of malondialdehyde (MDA) (De Vos et al., 1991). Trichloroacetic acid (5% w/v) was used to dissolve leaf samples and centrifuged for 10 min at 4000 rpm. The supernatant was then added to 2 mL of 0.67% (w/v) TBA, which was then heated for 15 minutes in a water bath. The liquid was immediately cooled, and then centrifuged once again for 10 min at 4000 rpm. By measuring the absorbance at 532, 60, 0, and 450 nm and converting it to μmol g^{-1} FW, the MDA content was calculated.

Nutrient analysis

After harvest, dried leaf samples (0.2 g) were processed with concentrated H_2SO_4 (98%) and H_2O_2 (30%), followed by the determination of nitrogen (N) using Nessler's colorimetry and the measurement of phosphorus (P) using molybdenum-antimony anti-spectrophotometry (Bao, 2000). The quantities of Cu, Zn, Fe, Mn, Mo, B, Si, and K were assessed by adding 0.2 g of dry leaves to a tube containing concentrated HNO_3 (67%) and H_2O_2 (30%) in a 3:1 (v/v) ratio. The samples were degraded at 120–150 °C on an electric hot plate until the solution was transparent. The samples were then digested at 120–150 °C on an electric hot plate until the solution was transparent. Deionized water was used to dilute the digest to a volume of 50 mL, and inductively coupled plasma mass spectrometry was used to quantify it (ICP-MS).

Data recording of growth parameters

Data on growth parameters were taken by following standard practices. Harvesting was done by pulling plants out

of the soil along with their roots. For later use, the samples were kept in polythene bags and labelled. The following parameters were recorded after harvesting the crop and during the growth period for each treatment.

Shoot and root length, number of leaves, number of pods, number of seeds per pod, pod size, fresh and dry weight of shoots, fresh and dry weight of roots, number of nodules per root, fresh and dry weight of pods.

Statistical analysis

The obtained data was statistically analyzed using the DSASTAT (Onofri, Italy). For average values, a one-way ANOVA variance analysis was performed and the significant differences among the values were determined using Tukey's Multiple Range test. For the applied variables, a significant value of $P \leq 0.05$ was achieved.

Results

X-ray diffraction

The X-ray diffractometry of the prepared sample was examined through diffractometer with wavelength of 1.5405 Å. The peaks of GO were detected at angle of diffraction 9.8 and 28.9 against planes of (001) and (002) as a result of oxygen based functional groups and graphite incomplete oxidation (Figure 2A). This incomplete oxidation observed due to graphite sheets that confirms that GO is formed (Ali et al., 2021). On the other hand, the extreme peak at 28.82 is detected as a result of disordered structure of carbon that is responsible of disordered assembling of graphene (Ali et al., 2022).

It was clearly obvious that the majority of oxygen-containing functional groups were eliminated throughout the reduction process. Nanocomposites exhibit intense diffraction peaks indexed to the (2 2 0), (3 1 1), (4 2 2), (5 1 1), and (4 4 0) planes which appear at 2θ = 11, 30, 35, 54, and 59 respectively, that are consistent with the standard XRD data from the JCPDS card (19-0629) to compare it with the face centered cubic (fcc) structure of Fe_3O_4 (Figure 2B) (Shen et al., 2012). The small size of magnetite nanoparticles is shown by the broadness of the diffraction peaks.

UV-vis spectroscopy

The UV absorption spectra of different Graphene oxide suspensions in DI water were observed to understand the transitions from the ground state to the excited states. Spectrum of UV-Vis. spectrum of GO was noticed at 217 and 327 nm (Ali et al., 2021, 2022). Some changes were observed during treatment of peaks and reduced values are shown in graph. It has been noticed that there are several defects observed in material due to the edge states, size and functional groups. Two peaks were observed in GO spectra. The first extreme peak is detected at 217 nm and the other peak is noticed at 327 nm (Figure 3A). Due to C-C bonding a peak of π to π^* transition was observed at 217 nm and because of n to π^* transition a shoulder peak was detected at 327 nm (Ali et al., 2021).

Figure 3B shows the UV-vis spectrum for GNS and exhibits a strong peak at around 231 nm and a wide shoulder peak at 287 nm. The peak noticed at 231 nm is because of the π- π^* transition of C-C bonds. Whereas the peak observed at 287 nm is because of the n-π^* transition and due to the presence of links that resemble epoxide (C-O-C) and peroxide (-O-O) in the structure of GNS. The absorption band of reduced GO from 231 nm to 287 nm could be because of the restoration of π electronic conjugation after reduction inside the graphene sheets. According to the absorption spectra of GNS nanocomposite, the peak at 231 nm indicates a red shift caused by a reduction in electronic conjugation of π electron, which increases the distance between HOMO and LUMO. This blue shift is also supported by the disappearance of the broad absorbance shoulder in GNS when compared to GO.

Fourier transform infrared spectroscopy

The functional groups were noticed due to the oxidation of graphite and response of these functional groups is detected in the form of peaks (Figure 4A). The peaks 1039, 1288, 1394, 1557, 1633, 1723, 2862, 2924, and 3390 (cm^{-1}) are noticed due to the presence of alkoxy C-O vibration, epoxy, C=O deformation, O-H bond, and O-H stretching. The peaks of absorbed water were detected at 2862, 2924, and 3390 cm^{-1} due to oxidation process and these peaks are attributed to O-H stretching. The skeleton vibration of graphite or Sp^2 vibration in graphite sheet was due to carbon and is noticed at 1633 cm^{-1}. By the presence of epoxide (C-O-C) and carboxyl (COOH) groups, the extremes were observed at 1039 and 1723 cm^{-1}.

According to the FTIR spectra observed, oxidized graphene contains several peaks which contain oxygen as functional group (Figure 4B). The spectra peaks show dissimilarity to pure graphene and C=O band expressing stretching vibration peak between 1700-2200 cm^{-1} and other oxygen bonds, i.e., C-O-C, C-O-H, and C-O, between 1546-1045 cm^{-1} (Golsheikh et al., 2013; Yan et al., 2014). The O-H bond expressing bending vibrational modes can be related to the wavenumbers 3271 cm^{-1} and 570 cm^{-1}. The significantly identified peaks of 3715 cm^{-1} and 715 cm^{-1} can be predicted to be for the stretching and bending vibrations of C-H bond (Hayyan et al., 2015). At 1747 cm^{-1} (Guo et al., 2009; Marcano et al., 2010), C=C from unoxidized sp^2 CC bonds was detected, whereas the peak at 2356cm^{-1} was brought on by CO_2 absorption from the atmosphere (Shen et al., 2012).

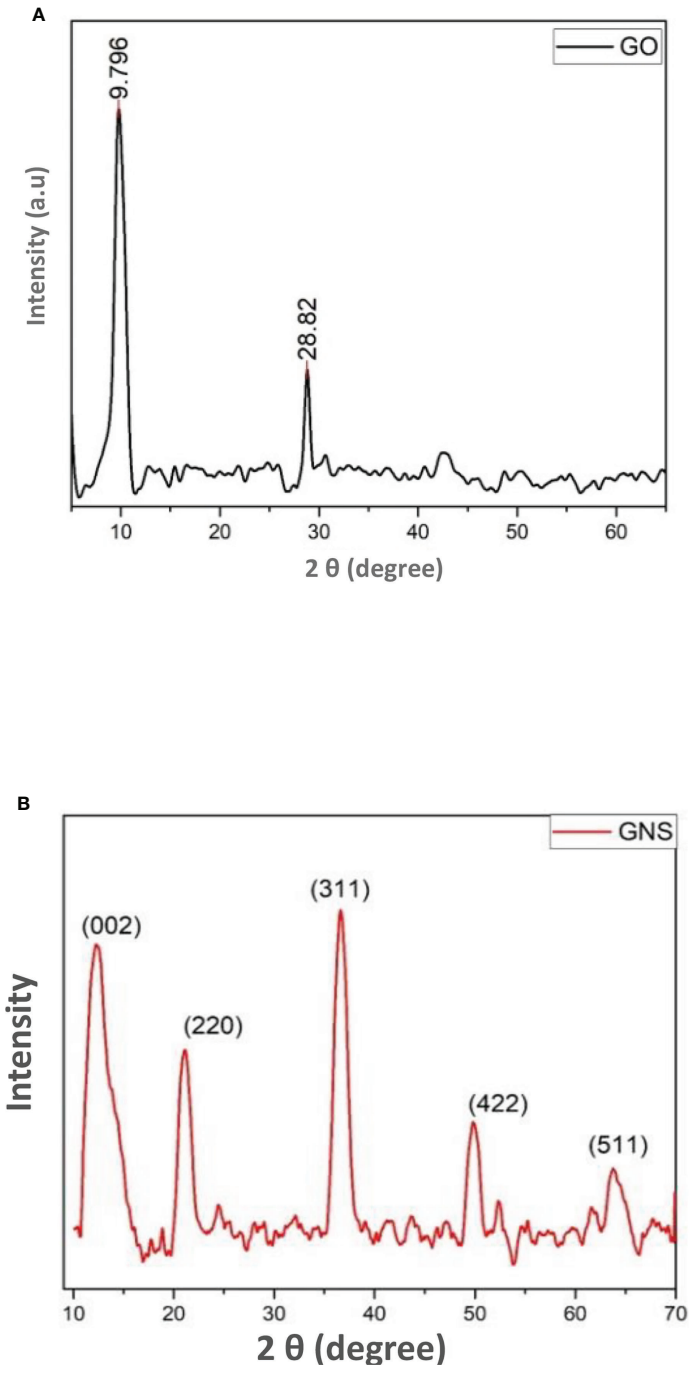

FIGURE 2
(A) = XRD pattern of synthesized graphene oxide; **(B)** = XRD pattern of green synthesized graphene oxide nanoparticles.

SEM analysis

Figure 5 depicts SEM images of GO NPs. From the images, it can be seen that the particles are homogenously distributed and in the form of a blob/fleck shape. The particle size is in the range of 10 nm to 100 μm. The distribution graph of particles presents the size range and in-homogeneity of the particles. It is suggested that the in-homogeneity of the particles was observed due to doping of Fe^{2+} and Fe^{3+} in GO. The distribution graphs show the distribution of particles on the sheets of GO (Figure 6).

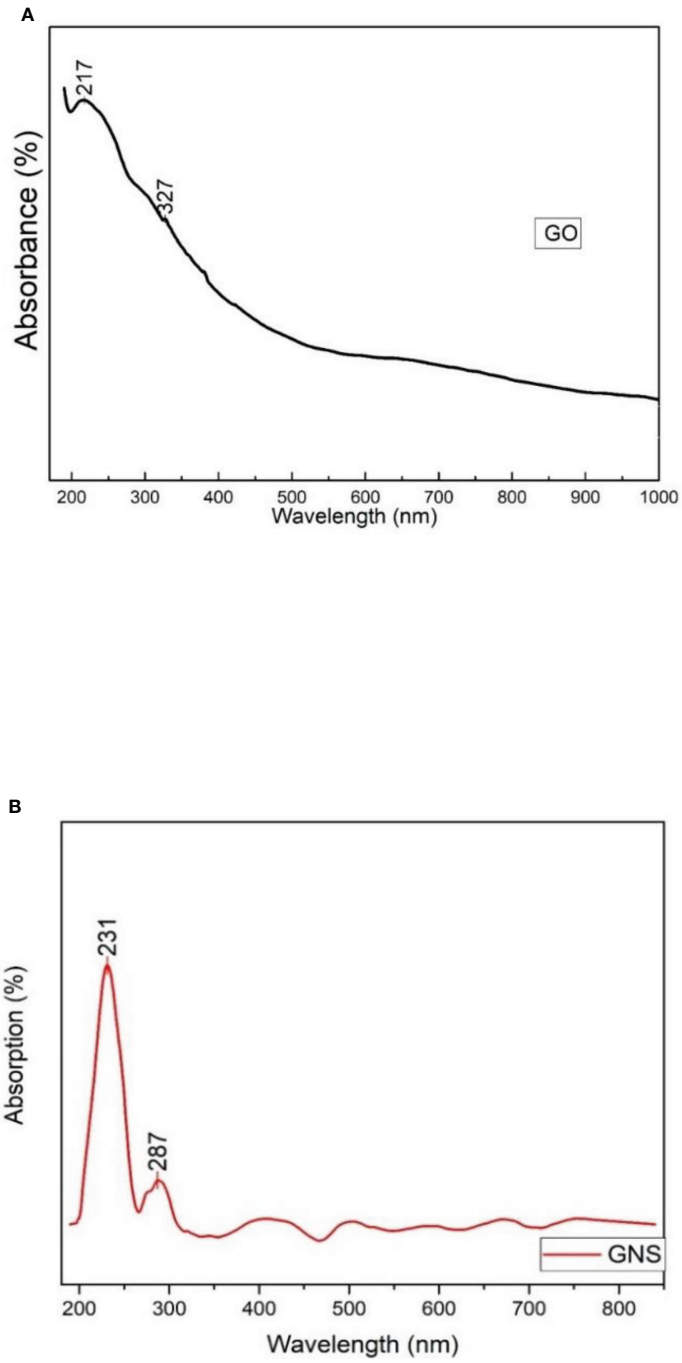

FIGURE 3
(A) = UV-vis analysis of synthesized graphene oxide; **(B)** = UV-vis analysis of green synthesized graphene oxide nanoparticles.

Chlorophyll contents

Chlorophyll contents were assessed in order to look into how the GO NPs affected the amount of photosynthetic pigments in the mungbean plants (Table 2). The mungbean plants performed positively in the applied treatments of GO NPs in terms of chlorophyll contents. In the current study, the contents of chlorophyll *a*, chlorophyll *b*, and total chlorophyll gradually increased as the concentration of GO NPs increased up to 1200 mg/L. When compared to the control, the amount of chlorophyll *a* increased by 61.83%, chlorophyll *b* increased by 69.21%, and the amount of total chlorophyll increased by 64.18% at 1200 mg/

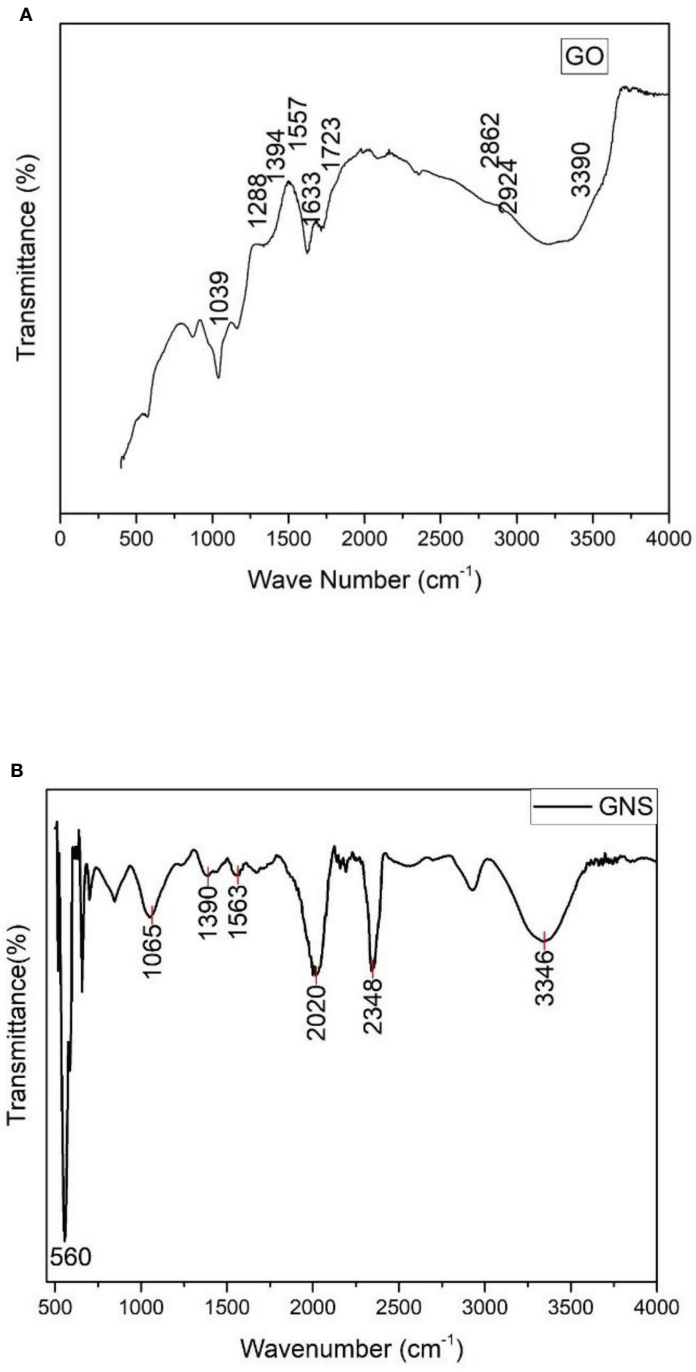

FIGURE 4
(A) = FTIR spectrum of synthesized graphene oxide; **(B)** = FTIR spectrum of green synthesized graphene oxide nanoparticles.

L concentration. But when these plants were exposed to a higher concentration of 1500 mg/L GO NPs, their photosynthetic contents were decreased. In comparison to the control plants, chlorophyll *a*, chlorophyll *b*, and total chlorophyll of mungbean plants all decreased by 7.90%, 9.87%, and 8.53%, respectively.

Total carotenoid content

In order to determine how the GO NPs affected the amount of photosynthetic pigments in the mungbean plants, the carotenoid content was assessed (Table 2). Treatment of GO

10.3389/fpls.2022.1040037

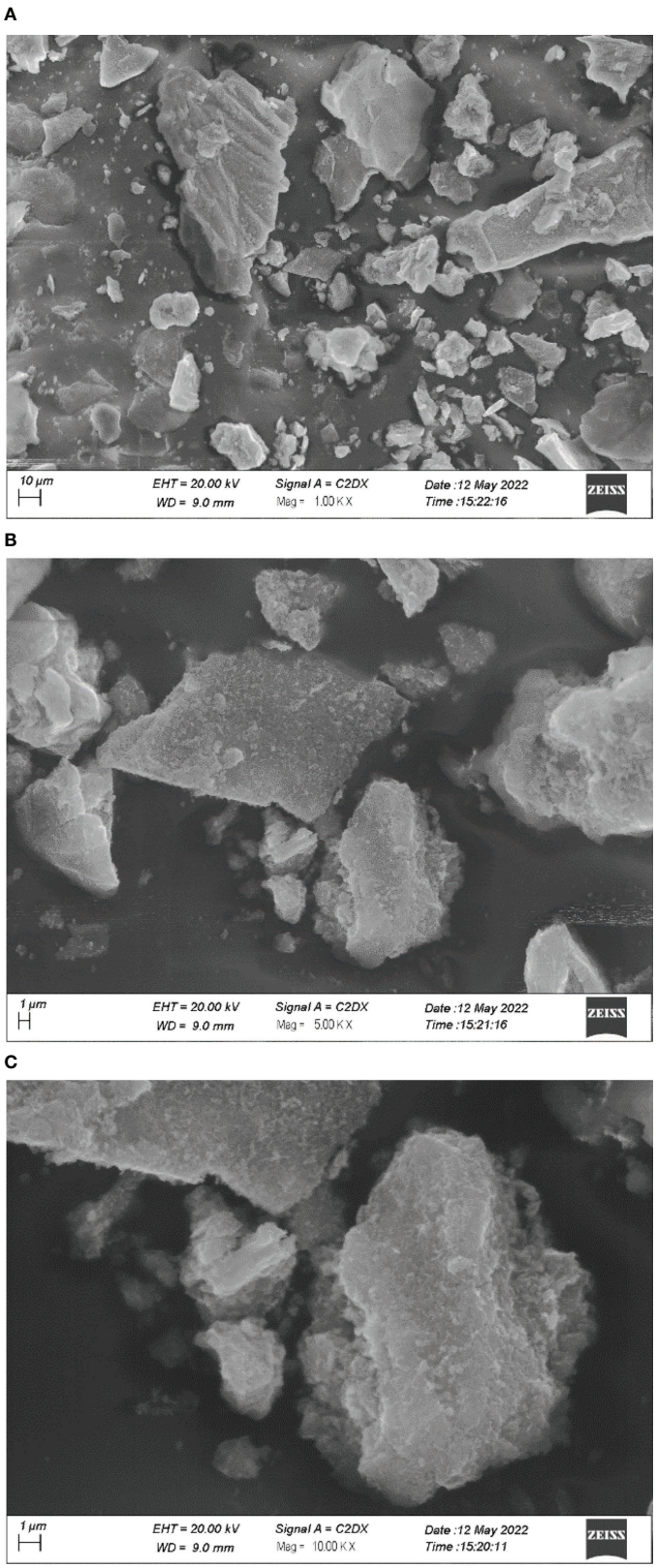

FIGURE 5
SEM images of graphene oxide nanoparticles under different magnifications **(A)** 1 KX; **(B)** 5KX; **(C)** 10KX.

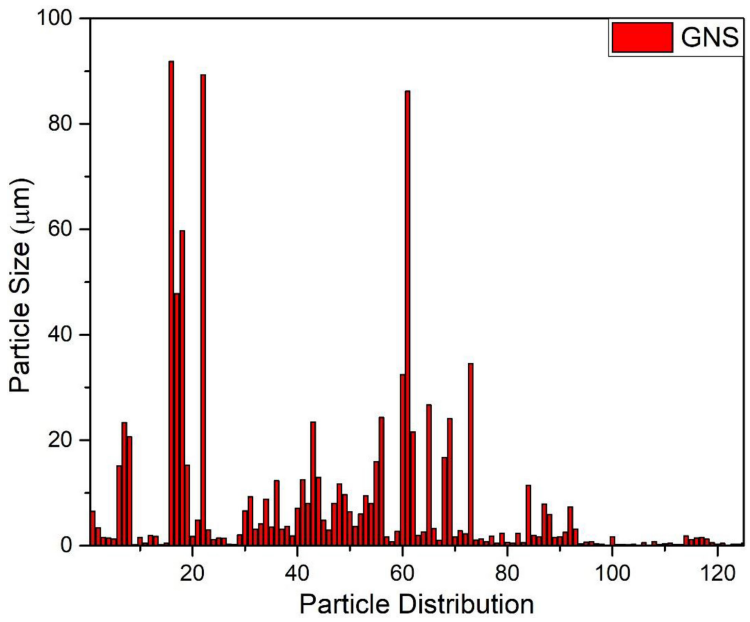

FIGURE 6
Graphical representation of particles distribution size of green synthesized graphene oxide nanoparticles.

NPs on mungbean plants resulted in an increase in carotenoid contents. The total carotenoid levels of mungbean seedlings were observed to increase in response to GO NPs (300-1200 mg/L). The carotenoid content increased by 59.34% at 1200 mg/L in comparison to the control. However, the carotenoid content was reduced when they were subjected to a greater concentration of 1500 mg/L. In the case of 1500 mg/L concentration, the carotenoid contents of mungbean plants were reduced by 9.02% as compared to the control plants.

Total protein content

The total protein content was determined in all the mungbean samples, and it was observed that the protein content increased with an increasing concentration of GO and showed a decline at concentration of 1500 mg/L (Table 2). The highest amount of protein (%) was found at a treatment of 1200 mg/L (3.96 %) and the lowest was at 1500 mg/L (1.24 %).

Enzymatic activity

Figure 7 shows that the CAT, POD and SOD activity significantly increased with increasing GO concentration except for T5 (1500 mg/L) GO. The peak values of CAT, POD and SOD activity occurred at T4 (1200 mg/L) GO, with an increase of 94.13%, 96% and 8.85%, respectively, compared with the control. While at T5 (1500 mg/L), the decreases in CAT, POD, and SOD were 17.98%, 21.84%, and 2.3%, respectively.

TABLE 2 Effects of different concentrations of green synthesized GO NPs on physio-biochemical parameters of mungbean plants.

GO Treatments (mg/L)	Chlorophyll *a*	Chlorophyll *b*	Total chlorophyll	Carotenoids	Total proteins
0	0.360 ± 0.009^{e}	0.168 ± 0.012^{c}	0.529 ± 0.013^{e}	13.699 ± 0.281^{d}	2.12 ± 0.009^{e}
300	0.407 ± 0.013^{d}	0.211 ± 0.003^{b}	0.619 ± 0.017^{d}	15.712 ± 0.213^{c}	2.25 ± 0.014^{d}
600	0.482 ± 0.008^{c}	0.225 ± 0.008^{b}	0.707 ± 0.017^{c}	18.775 ± 0.417^{b}	2.67 ± 0.008^{c}
900	0.538 ± 0.003^{b}	0.259 ± 0.005^{a}	0.798 ± 0.003^{b}	20.494 ± 0.577^{a}	3.47 ± 0.012^{b}
1200	0.583 ± 0.011^{a}	0.285 ± 0.008^{a}	0.868 ± 0.012^{a}	21.828 ± 0.333^{a}	3.96 ± 0.013^{a}
1500	0.331 ± 0.004^{e}	0.152 ± 0.005^{c}	0.483 ± 0.002^{e}	12.463 ± 0.577^{d}	1.24 ± 0.005^{f}

Data represent the mean ± standard error. Different letters denote statistically significant differences between treatments as evaluated by the Tukey's Multiple range test at the P<0.05 level. C= without GO NPs application (control; T1= 300 mg/L; T2= 600 mg/L; T3= 900 mg/L; T4= 1200 mg/L; T5= 1500 mg/L.

10.3389/fpls.2022.1040037

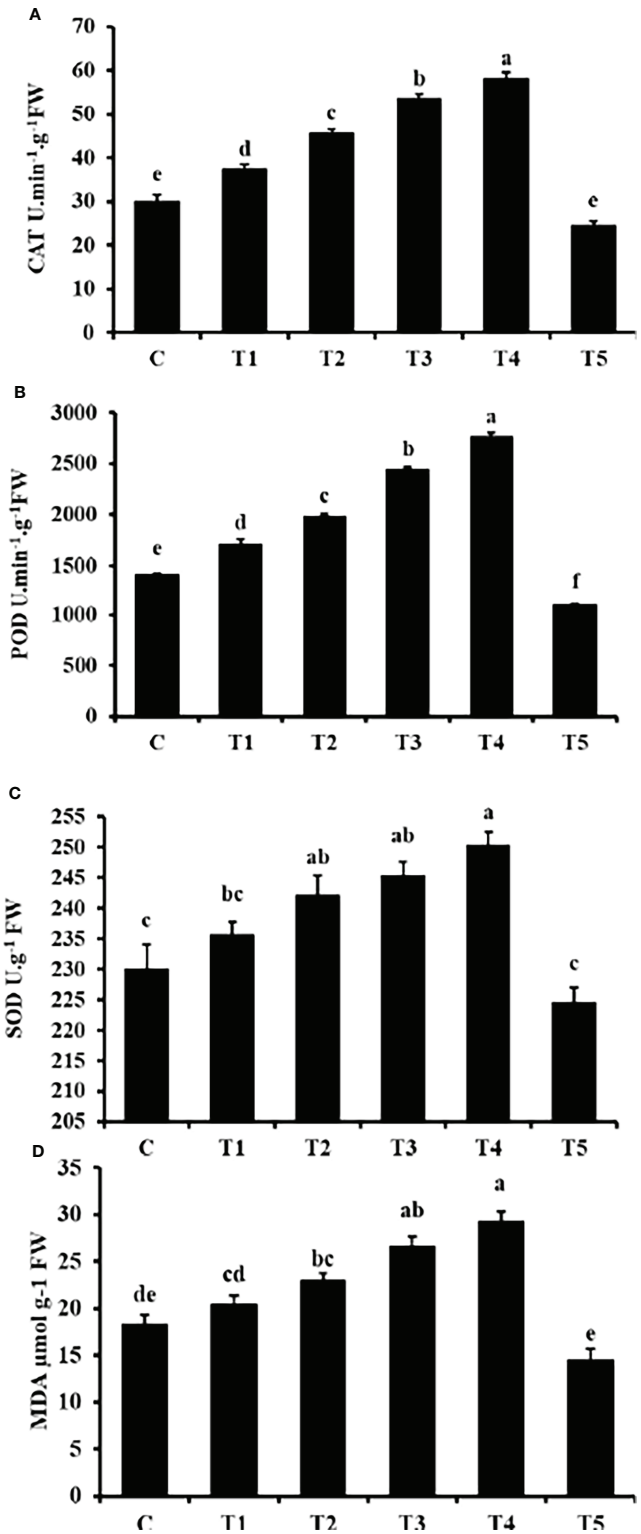

FIGURE 7
Effects of different GO NPs treatments on mungbean CAT **(A)**, POD **(B)**, SOD **(C)** activities and MDA **(D)** content. The error bars represent the standard error of means. Different letters denote statistically significant differences between treatments as evaluated by the Tukey's Multiple range test at the $P < 0.05$ level. C= without GO NPs application (control); T1= 300 mg/L; T2= 600 mg/L; T3= 900 mg/L; T4= 1200 mg/L; T5= 1500 mg/L.

Malondialdehyde content

The MDA content showed a consistent increase with increasing GO concentration except for T5 (1500 mg/L) (Figure 7D). Compared to the control, the MDA content in the T5 (1500 mg/L) GO treatment decreased by 20.56% and increased by 59.62% in the T4 (1200 mg/L) GO treatment. It was observed thar MDA content was enhanced in a concentration-related manner.

Nutrient uptake

Table 3 showed that in response to GO treatment concentrations, significant differences in the contents of nutrients were detected. The nutrient uptake increased with increasing GO concentration till T4 (1200 mg/L), while it was reduced in T5 (1500 mg/L). Moreover, the nutrient contents enhanced in a concentration-dependent manner. A significant decrease in content was found at T5 (1500 mg/L) GO, when compared to control.

Effect of graphene oxide nanoparticles on growth parameters of mungbean

GO NPs solution was applied to the root zone of mungbean plants over a concentration range of 300-1500 mg/L to examine the impact on plant growth in soil. Mungbean plants responded favourably to the GO NP concentrations. Their effects on different growth parameters are discussed briefly below.

Shoot and root length

As a result of the application of GO NPs to mungbean, plant height showed significant differences. With the exception of doses more than 1200 mg/L, mungbean plants consistently showed greater shoot and root length than control plants (Table 4). When compared to the control, maximum shoot and root lengths of 38.83 cm and 18.73 cm, respectively, were recorded at 1200 mg/L. In contrast, 1500 mg/L showed the minimum shoot and root lengths of 25.83 cm and 11.1 cm respectively. Mungbean plant shoot and root images are depicted in Figures 8, 9, respectively.

Number of leaves

With varying GO NPs concentrations, there was a noticeable difference in the number of leaves per plant (Table 4). The number of leaves of the mungbean plants increased significantly when the concentrations varied from 300 to 1200 mg/L. When compared to the control, 1200 mg/L yielded the most number of leaves, while 1500 mg/L yielded the fewest.

Number of pods per plant

The number of pods produced per plant differed statistically when compared to the control plant (Table 4). The application of GO NPs at 1200 mg/L resulted in an increase in the number of pods per plant by 49.92 %. While the higher concentration of 1500 mg/L resulted in decrease of number of pods by 30.13 %.

TABLE 3 Effects of different GO NPs treatments on nutrient uptake of mungbean.

GO NPs treatments(mg/L)	N (mg/g)	P (mg/g)	K (mg/g)	Cu (µg/g)	Zn (µg/g)	Fe (µg/g)	Mn (µg/g)	Mo (µg/g)	B (µg/g)	Si (µg/g)
0	43.38 ± 0.50^{c}	2.27 ± 0.02^{d}	21.75 ± 1.54^{bc}	51.21 ± 1.39^{cd}	43.85 ± 1.03^{ab}	537.33 ± 8.29^{cd}	57.03 ± 1.85^{bc}	2.80 ± 0.02^{de}	43.13 ± 1.01^{c}	260.12 ± 5.77^{d}
300	45.73 ± 0.80^{bc}	2.31 ± 0.01^{cd}	22.83 ± 0.93^{abc}	52.76 ± 1.11^{bc}	44.36 ± 1.27^{ab}	560.16 ± 11.69^{bcd}	59.96 ± 1.41^{abc}	2.91 ± 0.02^{cd}	44.56 ± 0.64^{bc}	278.63 ± 4.43^{c}
600	47.52 ± 0.60^{b}	2.36 ± 0.02^{bc}	25.10 ± 0.92^{ab}	53.66 ± 1.22^{bc}	46.31 ± 1.17^{a}	576.43 ± 7.81^{abc}	61.46 ± 1.12^{ab}	2.97 ± 0.03^{bc}	47.63 ± 0.59^{ab}	288.12 ± 3.78^{bc}
900	50.83 ± 0.63$_{a}$	2.42 ± 0.01^{ab}	26.11 ± 0.80^{ab}	55.34 ± 1.13^{ab}	47.80 ± 1.15^{a}	595.70 ± 8.60^{ab}	62.36 ± 1.09^{ab}	3.09 ± 0.04^{b}	48.20 ± 0.38^{a}	300.31 ± 4.56^{ab}
1200	53.30 ± 1.18^{a}	2.45 ± 0.02^{a}	27.26 ± 1.01^{a}	58.13 ± 1.29^{a}	49.52 ± 1.35^{a}	612.53 ± 10.68^{a}	65.52 ± 1.12^{a}	3.25 ± 0.05^{a}	50.36 ± 1.25^{a}	313.16 ± 5.29^{a}
1500	38.71 ± 0.51^{d}	2.34 ± 0.01^{d}	18.23 ± 1.06^{c}	47.69 ± 1.21^{d}	39.26 ± 1.35^{b}	519.58 ± 9.60^{d}	53.73 ± 1.47^{c}	2.71 ± 0.03^{e}	38.57 ± 0.93^{d}	251.33 ± 3.48^{d}

Data represent the mean ± standard error. Different letters denote statistically significant differences between treatments as evaluated by the Tukey's Multiple range test at the P<0.05 level. C= without GO NPs application (control); T1= 300 mg/L; T2= 600 mg/L; T3= 900 mg/L; T4= 1200 mg/L; T5= 1500 mg/L.

TABLE 4 Effect of different GO NPs treatment on growth parameters of mungbean at 75 days after sowing.

GO NPs treatments (mg/L)	Shoot length (cm)	Root length (cm)	Number of leaves (n)	Number of pods per plant (n)	No of seeds per pod (n)	Pod size (cm)	Shoot fresh weight (g)	Shoot dry weight (g)	Root fresh weight (g)	Root dry weight (g)	Root nodules (n)	Pod fresh weight	Pod dry weight
0	34.1 ± 0.72^{b}	14.0 ± 0.72^{bc}	22.0 ± 1.00^{b}	6.67 ± 0.33^{b}	7.67 ± 0.66^{c}	6.43 ± 0.21^{c}	12.9 ± 0.76^{bc}	4.1 ± 0.35^{b}	1.58 ± 0.06^{bc}	0.48 ± 0.02^{c}	10.6 ± 0.67^{cd}	1.10 ± 0.04^{e}	0.38 ± 0.02^{cd}
300	35.9 ± 0.95^{ab}	15.8 ± 0.95^{ab}	22.6 ± 0.88^{b}	7.33 ± 1.33^{b}	8.67 ± 0.33^{bc}	7.16 ± 0.12^{bc}	13.8 ± 0.62^{ab}	4.3 ± 0.24^{b}	1.7 ± 0.06^{b}	0.63 ± 0.02^{b}	11.6 ± 0.67^{bc}	1.25 ± 0.06^{d}	0.42 ± 0.02^{c}
600	37.1 ± 1.00^{a}	17.0 ± 1.00^{ab}	24.6 ± 0.66^{ab}	8.67 ± 0.66^{ab}	8.67 ± 0.33^{bc}	7.76 ± 0.14^{ab}	14.8 ± 0.78^{ab}	4.4 ± 0.48^{b}	1.8 ± 0.03^{b}	0.67 ± 0.03^{b}	14.0 ± 1.00^{abc}	1.47 ± 0.05^{c}	0.54 ± 0.03^{b}
900	38.4 ± 1.02^{a}	18.3 ± 1.02^{a}	27.3 ± 0.33^{a}	9.0 ± 0.57^{a}	10.0 ± 0.57^{ab}	7.86 ± 0.18^{ab}	16.1 ± 0.66^{a}	5.8 ± 0.23^{a}	2.2 ± 0.08^{a}	0.79 ± 0.03^{a}	15.0 ± 0.57^{ab}	1.67 ± 0.06^{b}	0.60 ± 0.02^{a}
1200	38.8 ± 0.83^{a}	18.7 ± 0.83^{a}	27.6 ± 0.66^{a}	10.0 ± 0.57^{a}	11.3 ± 0.33^{a}	8.57 ± 0.32^{a}	16.4 ± 0.66^{a}	6.1 ± 0.13^{a}	2.4 ± 0.05^{a}	0.84 ± 0.02^{a}	15.6 ± 1.20^{a}	1.84 ± 0.07^{a}	0.63 ± 0.04^{a}
1500	25.8 ± 1.54^{c}	11.1 ± 0.69^{c}	14.0 ± 1.00^{c}	5.0 ± 1.00^{c}	4.67 ± 0.33^{d}	4.93 ± 0.23^{d}	10.1 ± 0.54^{c}	3.2 ± 0.15^{b}	1.2 ± 0.06^{c}	0.36 ± 0.02^{c}	7.33 ± 0.88^{d}	1.01 ± 0.03^{e}	0.33 ± 0.02^{d}

Data represent the mean ± standard error. Different letters denote statistically significant differences between treatments as evaluated by the Tukey's Multiple range test at the P<0.05 level. C= without GO NPs application (control); T1= 300 mg/L; T2= 600 mg/L; T3= 900 mg/L; T4= 1200 mg/L; T5= 1500 mg/L.

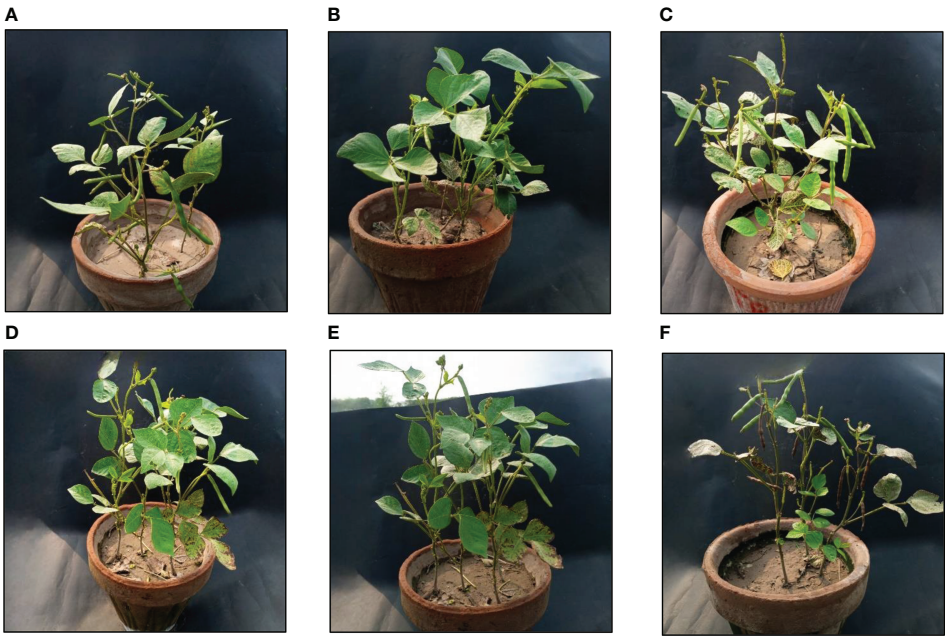

FIGURE 8
Effects of different GO NPs treatments on mungbean plants at harvesting stage. **(A)**= C= without GO NPs application (control); **(B)**= T1= 300 mg/L; **(C)**= T2= 600 mg/L; **(D)**= T3= 900 mg/L; **(E)**= T4= 1200 mg/L; **(F)**= T5= 1500 mg/L.

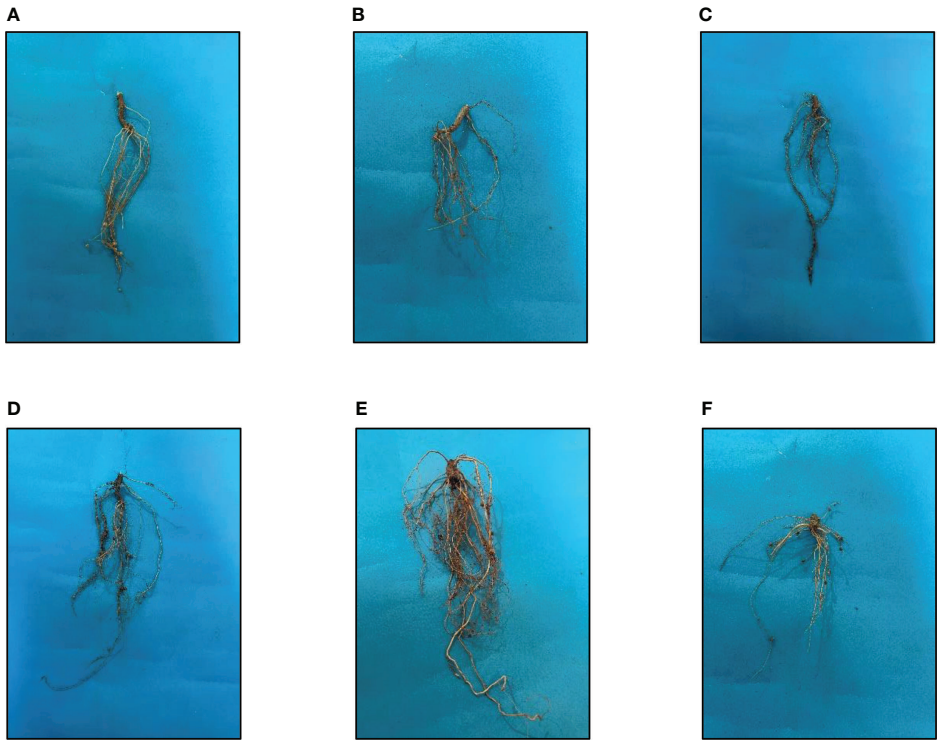

FIGURE 9
Effects of different GO NPs treatments on root lengths of mungbean. **(A)**= C= without GO NPs application (control); **(B)**= T1= 300 mg/L; **(C)**= T2= 600 mg/L; **(D)**= T3= 900 mg/L= **(E)**= T4= 1200 mg/L; **(F)**= T5= 1500 mg/L.

Pod size and number of seeds per pod

The size of the pods significantly changed as the concentration of GO NPs ranged from 300 to 1500 mg/L (Table 4). When the concentrations increased from 300 to 1500 mg/L, the size of the pods gradually increased, and it was highest at 1200 mg/L. While it was lowest at concentrations greater than 1200 mg/L. Effect of GO NPs on pod size can be seen in Figure 10.

Number of seeds per pod increased significantly with increasing concentration of GO except for T5 (1500mg/L) (Table 4). When compared to control, the quantity of seeds per pod increased by 47.51% in T4 (1200 mg/L) but it decreased by 39.16% in T5 (1500 mg/L).

Shoot fresh and dry weight

According to the preceding viewpoint, GO NPs applied to the soil resulted in a considerable increase in mungbean plant weights. The fresh and dry weight of shoots increased as the concentration increased over the range of 300-1200 mg/L (Table 4). While it decreased at a higher concentration of 1500 mg/L. Fresh and dried shoot weight increased by 27% and 49%, respectively at 1200 mg/L.

Root fresh and dry weight

GO NPs applied to the soil resulted in a significant rise in mungbean plant root weights. When compared to the control, the maximum fresh and dry root weight was obtained at 1200 mg/L, and it increased consistently as concentrations increased from 300 to 1200 mg/L. The percentage increase in 1200mg/L concentration for root fresh and dry weight was 51.89% and 75%, respectively. While the concentration of more than 1200mg/L decreased root weight. The percentage decrease in 1500 mg/L was 18.98% for root fresh weight and 25% for root dry weight (Table 4).

Root nodules

Mungbean can fix atmospheric nitrogen using bacteria found in its root nodules. The rate of nodulation is quite low

FIGURE 10
Effects of different GO NPs treatments on pod size of mungbean plants. **(A)**= C= without GO NPs application (control); **(B)**= T1= 300 mg/L; **(C)**= T2= 600 mg/L; **(D)**= T3= 900 mg/L; **(E)**= T4= 1200 mg/L; **(F)**= T5= 1500 mg/L.

in most of the mungbean growing areas in Pakistan. There are several causes, but one of them appears to be poor nutrient uptake. The application of GO NPs to the soil resulted in positive root nodulation results. When compared to the control, the number of root nodules increased as the concentration increased from 300 to 1200 mg/L (Table 4). When compared to the control plant, the percentage increase in 1200 mg/L was 46.76%. The effect of GO NPs on root nodulation is shown in Figure 11.

Pod fresh and dry weight

The application of GO NPs to the soil increased the pod weights of mungbean plants significantly. The maximum fresh and dry root weight was obtained at 1200 mg/L when compared to the control, and it rose consistently as concentrations increased from 300 to 1200 mg/L. For pod fresh and dry weight, the percentage increase in 1200mg/L concentration was 67% and 65%, respectively. While concentrations more than 1200mg/L reduced pod weight. The reduction in 1500 mg/L was 8.18 % for fresh pod weight and 13 % for dried pod weight, when compared to control (Table 4).

Discussion

Understanding how nanoparticles interact with living things is crucial for biosafety due to the rapid development of nanotechnology and the production of synthetic nanomaterials. The understanding of how nanomaterials interact with plants is fundamental for assessing ecological risks, but it is also essential for the advancement of nanotechnological applications in agriculture that will increase crop yields and minimize the use of agrochemicals. Although the impacts of nano-carbon compounds on seed germination and seedling development have been widely documented, less is known about how these materials affect plant growth and life cycles of mature plants, which may differ depending on the stage of development (Nel et al., 2006). The distinct variability of nanomaterials in terms of form, size, chemical composition, solubility, aggregation, surface structure and

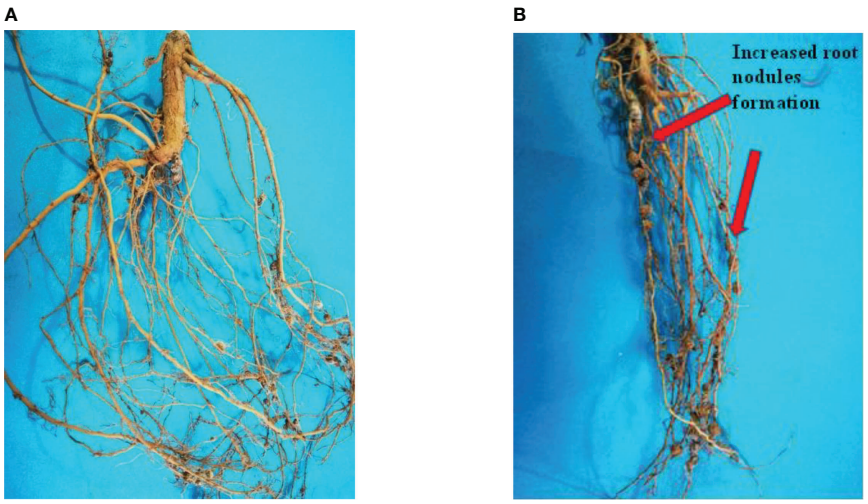

FIGURE 11
Effects of different GO NPs treatments on root nodules of mungbean plants. **(A)**= C= without GO NPs application (control); **(B)**= T4= 1200 mg/L.

application methods is a significant factor influencing the heterogeneity of plant responses (Petersen and Henry, 2012). The effects of graphene family nanoparticles (GFNs) on higher plants have been extensively studied, and for plants exposed to GFNs at different developmental stages, both promotion and inhibition in growth have been recorded (e.g., seed germination, root and shoot growth, and flowering). Numerous studies have shown that nanomaterials have beneficial impacts on plant development and stress tolerance when used in low doses (Mukherjee et al., 2016; Zhao et al., 2020). To determine its impact on various growth phases, we treated mungbean seedlings and matured plants with GO and it was found that exposure till 1200 mg/L GO increased plant height (root and shoot lengths), root fresh and dry weights, shoot fresh and dry weights, Number of leaves, Number of pods per plant and root nodules, but a larger dose of 1500 mg/L had a detrimental effect on seedling growth. The findings are in accordance with Song et al. (2020), which found that GN boosted seedling development at low doses but suppressed it at high doses For *Malus domestica*, 0.1 mg/L GO stimulated adventitious root development while 10 mg/L GO inhibited it (Li et al., 2018). Roots are a key organ of direct interaction between plants and soil and are crucial for plant growth due to their activities as anchors and absorbers. GO significantly influenced the development of plant roots, which may have had an impact on the growth and development of above-ground organs. According to Begum et al. (2011), graphene oxide at concentrations of 500, 1000, and 2000 mg/L was treated to the root surfaces of *Arabidopsis thaliana*, and as the concentration of graphene oxide was increased, the root length steadily declined, which ultimately effected all growth parameters. This outcome is due to the atomically thin layer of graphene oxide, which is principally a carbon-based material with a two-dimensional building block. This nanoparticle has a positive impact on plant growth (Mahmoud and Abdelhameed, 2021). Furthermore, because graphene oxide nanoparticles are smaller than cell walls, they can easily enter cell walls and perform as smart treatment-delivery systems for plant growth regulation. Graphene oxide nanomaterials influence both physiological and genetic processes in plants; as a result, it is utilized as a plant growth regulator (Chakravarty et al., 2015). Graphene oxide derivatives, like multiwalled carbon nanotubes (MWCNTs), can increase water and nutrient intake and promote plant development (Larue et al., 2012). Another factor which may have contributed to the enhanced growth in mungbean is nodules formation and development. In accordance with the previous research studies, GO NPs nanoparticles promoted root nodules and boosted the beneficial activity of soil microbiological processes (Abdallah et al., 2022). There is some evidence to support the minimal research that exists about the factors involved in the stimulatory impacts of nanoparticles on nodule formation and development. According to Burke et al. (2015), the increased nodule growth in soybean plants exposed to positively charged Fe_3O_4 nanoparticles was due to the availability of Fe, which is necessary for N2 fixing bacteria (Brear et al., 2013). The production of nodule factor (nodf) and genistein (a significant root-secreted isoflavone that triggers *Bradyrhizobium japonicum* nod YABC operon expression), were also found to be up-regulated by Fe_3O_4 NPs, which was suggested to be related to the enhanced nodulation seen in the symbiotic association between soybean plants and *Bradyrhizobium japonicum*. Photosynthesis allows plants to transform carbon dioxide into organic molecules, and pigments are required for plant growth and development (Taiz and Zeiger, 2010). A significant initial increase followed by a

decrease in pigment contents was observed in mung bean treated with GO in this study which is in accordance with Siddiqui et al. (2019). The impact of GO NPs on the electron transport and energy pathways within plant cells is thought to be the cause of the increase in chlorophyll content of treated plants (Van Aken, 2015). At high GO concentrations, chlorophyll content could be reduced due to chlorophyll synthesis inhibition or chloroplast death. Because GO may penetrate algal cells and destroy organelles, it can cause damage to the chloroplast structure. (Hu et al., 2014).

MDA is a result of lipid peroxidation, and its content is related directly to ROS production (Hossain et al., 2015). MDA content showed a similar increasing tendency to antioxidant enzyme activities, implying that increased amounts of GO encouraged the formation of free radicals. The SOD, POD, and CAT activities were all well correlated with MDA content also suggesting that at higher concentration The harmful effect of GO may be caused by oxidative stress *via* ROS production. This is comparable to how graphene nanoparticles affect higher plants (Begum et al., 2011; Anjum et al., 2014). All enzyme activity and MDA levels in leaf samples consistently interacted to GO. However, other markers, such as CAT activity and MDA content, were not very sensitive at low concentrations. GO at 1200 mg/L continued to significantly boost these three enzyme activities and MDA content in leaves, with SOD, POD, CAT, and MDA levels 8.8%, 96.2%, 94.1%, and 59.6% greater than the control, respectively.

Plant growth and development are closely related to nutrient uptake efficiency. The essential macronutrients N, P, and K are the limiting components for plant growth. The micronutrients (Cu, Zn, Fe, Mn, Mo, B, and Si) are also required and engaged in a variety of metabolic pathways. In this investigation, increasing the GO dose up to 1200 mg/L resulted in an increase in the levels of N, K, Fe, Zn, Mo, B, and Si. Researchers have represented some noteworthy aspects regarding this observation. GO may inhibit nitrate uptake and buildup in plant seedling roots at higher concentrations (Weng et al., 2020) and may impact the phytoavailability of N in soils, possibly by altering soil nitrification rates and/or organic N mineralization (Duncan and Owens, 2019). As a result, it has been suggested that nanoparticles may have coated the root surface, preventing water and mineral nutrients from entering the roots and destroying the production of root hairs, inhibiting nutrient uptake at higher concentration (Hu et al., 2014; Zhao et al., 2015; Zhang et al., 2016). GO has the potential to disrupt biological metabolic systems such as amino acid, glucose, lipid, and energy metabolism, resulting in reduced nutrient absorption.

Conclusion

Findings present in this study indicate the beneficial role of GO as plant growth promoter as well as yield enhancer within safe limits. GO formulations can be successfully incorporated in local agricuture system for better yield and profitability.

Data availability statement

The original contributions presented in the study are included in the article/Supplementary Material. Further inquiries can be directed to the corresponding author.

Author contributions

Conceived and designed the total experiments: Z-e-HA, TA. Performed the experiment: FM, MA, HR. Analyzed data: AA, GL. Manuscript writeup: FM. Funding procurement: GL. All authors contributed to the article and approved the submitted version.

Funding

This study was financially supported by the Guangdong Provincial special Fund for Modern Agriculture Industry Technology Innovation Teams (Project No: 2022KJ122 and 2023KJ122) and China Young Scientist Talent Program (Project No: QN2022030024L)

Conflict of interest

The authors declare that the research was conducted in the absence of any commercial or financial relationships that could be construed as a potential conflict of interest.

Publisher's note

All claims expressed in this article are solely those of the authors and do not necessarily represent those of their affiliated organizations, or those of the publisher, the editors and the reviewers. Any product that may be evaluated in this article, or claim that may be made by its manufacturer, is not guaranteed or endorsed by the publisher.

References

Aazami, M. A., Mehrabani, L. V., Hashemi, T., Hassanpouraghdam, M. B., and Rasouli, F. (2022). Soil-based nano-graphene oxide and foliar selenium and nano-fe influence physiological responses of'Sultana'grape under salinity. *Sci. Rep.* 12, 1–13. doi: 10.1038/s41598-022-08251-8

Abdallah, Y., Hussien, M., Omar, M. O. A., Elashmony, R., Alkhalifah, D. H. M., and Hozzein, W. N. (2022). Mung bean (*Vigna radiata*) treated with magnesium nanoparticles and its impact on soilborne *Fusarium solani* and *Fusarium oxysporum* in clay soil. *Plants* 11, 1514. doi: 10.3390/plants11111514

Aebi, H. (1984). Catalase *in vitro*. *Methods Enzimol.* 105, 121–126. doi: 10.1016/S0076-6879(84)05016-3

Ahmad, A., Husain, A., Mujeeb, M., Khan, S. A., Najmi, A. K., Siddique, N. A., et al. (2013). A review on therapeutic potential of *Nigella sativa*: A miracle herb. *Asian Pac. J. Trop. Biomed.* 3, 337–352. doi: 10.1016/S2221-1691(13)60075-1

Alam, M. K., Rana, Z. H., and Islam, S. N. (2016). Comparison of the proximate composition, total carotenoids and total polyphenol content of nine orange-fleshed sweet potato varieties grown in Bangladesh. *Foods* 5, 64. doi: 10.3390/foods5030064

Ali, M. D., Aslam, A., Zeeshan, T., Mubaraka, R., Bukhari, S. A., Shoaib, M., et al. (2022). Robust effectiveness behavior of synthesized cobalt doped Prussian blue graphene oxide ferrite against EMI shielding. *Inorg. Chem. Commun.* 137, 109204. doi: 10.1016/j.inoche.2022.109204

Ali, M. D., Majid, F., Aslam, A., Malik, A., Wahid, I., Dildar, S., et al. (2021). Dielectric and electrical properties of synthesized PBGO/Fe3O4 nanocomposite. *Ceram. Int.* 47, 26224–26232. doi: 10.1016/j.ceramint.2021.06.030

Anjum, N. A., Singh, N., Singh, M. K., Sayeed, I., Duarte, A. C., Pereira, E., et al. (2014). Single-bilayer graphene oxide sheet impacts and underlying potential mechanism assessment in germinating faba bean (Vicia faba l.). *Sci. Total Environ.* 472, 834–841. doi: 10.1016/j.scitotenv.2013.11.018

Bao, S. D. (2000). *Soil and agricultural chemistry analysis*. Beijing: China Agricultural Press.

Begum, P., Ikhtiari, R., and Fugetsu, B. (2011). Graphene phytotoxicity in the seedling stage of cabbage, tomato, red spinach, and lettuce. *Carbon. N. Y.* 49, 3907–3919. doi: 10.1016/j.carbon.2011.05.029

Brear, E. M., Day, D. A., and Smith, P. M. C. (2013). Iron: an essential micronutrient for the legume-rhizobium symbiosis. *Front. Plant Sci.* 4, 359. doi: 10.3389/fpls.2013.00359

Burke, D. J., Pietrasiak, N., Situ, S. F., Abenojar, E. C., Porche, M., Kraj, P., et al. (2015). Iron oxide and titanium dioxide nanoparticle effects on plant performance and root associated microbes. *Int. J. Mol. Sci.* 16, 23630–50.

Chakravarty, D., Erande, M. B., and Late, D. J. (2015). Graphene quantum dots as enhanced plant growth regulators: effects on coriander and garlic plants. *J. Sci. Food Agric.* 95, 2772–2778. doi: 10.1002/jsfa.7106

Chauhan13, Y. S., Douglas, C., Rachaputi, R. C. N., Agius, P., Martin, W., King, K., et al. (2010). Physiology of mungbean and development of the mungbean crop model in Proceedings of the 1st Australian Summer Grains Conference Australia, Gold Coast, QL 21–24.

De Vos, C. H. R., Schat, H., De Waal, M. A. M., Vooijs, R., and Ernst, W. H. O. (1991). Increased resistance to copper-induced damage of the root cell plasmalemma in copper tolerant *Silene cucubalus*. *Physiol. Plant* 82, 523–528. doi: 10.1111/j.1399-3054.1991.tb02942.x

Duncan, E., and Owens, G. (2019). Metal oxide nanomaterials used to remediate heavy metal contaminated soils have strong effects on nutrient and trace element phytoavailability. *Sci. Total Environ.* 678, 430–437. doi: 10.1016/j.scitotenv.2019.04.442

Giannopolitis, C. N., and Ries, S. K. (1977). Superoxide dismutases: I. occurrence in higher plants. *Plant Physiol.* 59, 309–314. doi: 10.1104/pp.59.2.309

Golsheikh, A. M., Huang, N. M., Lim, H. N., Chia, C. H., Harrison, I., and Muhamad, M. R. (2013). One-pot hydrothermal synthesis and characterization of FeS2 (pyrite)/graphene nanocomposite. *Chem. Eng. J.* 218, 276–284. doi: 10.1016/j.cej.2012.09.082

Gong, X., Liu, C., Dang, K., Wang, H., Du, W., Qi, H., et al. (2022). Mung bean (*Vigna radiata* l.) source leaf adaptation to shading stress affects not only photosynthetic physiology metabolism but also control of key gene expression. *Front. Plant Sci.* 36. doi: 10.3389/fpls.2022.753264

Guo, H.-L., Wang, X.-F., Qian, Q.-Y., Wang, F.-B., and Xia, X.-H. (2009). A green approach to the synthesis of graphene nanosheets. *ACS Nano* 3, 2653–2659. doi: 10.1021/nn900227d

Gur, T., Meydan, I., Seckin, H., Bekmezci, M., and Sen, F. (2022). Green synthesis, characterization and bioactivity of biogenic zinc oxide nanoparticles. *Environ. Res.* 204, 111897. doi: 10.1016/j.envres.2021.111897

Hayyan, M., Abo-Hamad, A., AlSaadi, M. A., and Hashim, M. A. (2015). Functionalization of graphene using deep eutectic solvents. *Nanoscale Res. Lett.* 10, 1–26. doi: 10.1186/s11671-015-1004-2

Hossain, Z., Mustafa, G., and Komatsu, S. (2015). Plant responses to nanoparticle stress. *Int. J. Mol. Sci.* 16, 26644–26653. doi: 10.3390/ijms161125980

Hu, X., Lu, K., Mu, L., Kang, J., and Zhou, Q. (2014). Interactions between graphene oxide and plant cells: Regulation of cell morphology, uptake, organelle damage, oxidative effects and metabolic disorders. *Carbon. N. Y.* 80, 665–676. doi: 10.1016/j.carbon.2014.09.010

Jain, D., Daima, H. K., Kachhwaha, S., and Kothari, S. L. (2009). Synthesis of plant-mediated silver nanoparticles using papaya fruit extract and evaluation of their anti microbial activities. *Dig. J. Nanomater. Bios.* 4, 557–563.

Larue, C., Pinault, M., Czarny, B., Georgin, D., Jaillard, D., Bendiab, N., et al. (2012). Quantitative evaluation of multi-walled carbon nanotube uptake in wheat and rapeseed. *J. Hazard. Mater.* 227, 155–163. doi: 10.1016/j.jhazmat.2012.05.033

Lesk, C., Rowhani, P., and Ramankutty, N. (2016). Influence of extreme weather disasters on global crop production. *Nature* 529, 84–87. doi: 10.1038/nature16467

Li, F., Sun, C., Li, X., Yu, X., Luo, C., Shen, Y., et al. (2018). The effect of graphene oxide on adventitious root formation and growth in apple. *Plant Physiol. Biochem.* 129, 122–129. doi: 10.1016/j.plaphy.2018.05.029

Mahmoud, N. E., and Abdelhameed, R. M. (2021). Superiority of modified graphene oxide for enhancing the growth, yield, and antioxidant potential of pearl millet (*Pennisetum glaucum* l.) under salt stress. *Plant Stress* 2, 100025. doi: 10.1016/j.stress.2021.100025

Marcano, D. C., Kosynkin, D. V., Berlin, J. M., Sinitskii, A., Sun, Z., Slesarev, A., et al. (2010). Improved synthesis of graphene oxide. *ACS Nano* 4, 4806–4814. doi: 10.1021/nn1006368

Mukherjee, A., Majumdar, S., Servin, A. D., Pagano, L., Dhankher, O. P., and White, J. C. (2016). Carbon nanomaterials in agriculture: a critical review. *Front. Plant Sci.* 7, 172. doi: 10.3389/fpls.2016.00172

Nair, R. M., Pandey, A. K., War, A. R., Hanumantharao, B., Shwe, T., Alam, A., et al. (2019). Biotic and abiotic constraints in mungbean production–progress in genetic improvement. *Front. Plant Sci.* 10, 1340. doi: 10.3389/fpls.2019.01340

Nel, A., Xia, T., Madler, L., and Li, N. (2006). Toxic potential of materials at the nanolevel. *Science* 311, 622–627. doi: 10.1126/science.1114397

Omran, R. G. (1980). Peroxide levels and the activities of catalase, peroxidase, and indoleacetic acid oxidase during and after chilling cucumber seedlings. *Plant Physiol.* 65, 407–408. doi: 10.1104/pp.65.2.407

Park, S., Choi, K. S., Kim, S., Gwon, Y., and Kim, J. (2020). Graphene oxide-assisted promotion of plant growth and stability. *Nanomaterials* 10, 758. doi: 10.3390/nano10040758

Petersen, E. J., and Henry, T. B. (2012). Methodological considerations for testing the ecotoxicity of carbon nanotubes and fullerenes. *Environ. Toxicol. Chem.* 31, 60–72. doi: 10.1002/etc.710

Pratap, A., Gupta, S., Basu, P. S., Tomar, R., Dubey, S., Rathore, M., et al. (2019). Towards development of climate smart mungbean: challenges and opportunities. *Genomic Des. Clim. Pulse Crop*, 235–264. doi: 10.1007/978-3-319-96932-9_5

Ramankutty, N., Mehrabi, Z., Waha, K., Jarvis, L., Kremen, C., Herrero, M., et al. (2018). Trends in global agricultural land use: implications for environmental health and food security. *Annu. Rev. Plant Biol.* 69, 789–815. doi: 10.1146/annurev-arplant-042817-040256

Rizvi, N. B., Aleem, S., Khan, M. R., Ashraf, S., and Busquets, R. (2022). Quantitative estimation of protein in sprouts of *vigna radiate* (Mung beans), lens culinaris (Lentils), and cicer arietinum (Chickpeas) by kjeldahl and lowry methods. *Molecules* 27, 814. doi: 10.3390/molecules27030814

Safikhan, S., Chaichi, M. R., Khoshbakht, K., Amini, A., and Motesharezadeh, B. (2018). Application of nanomaterial graphene oxide on biochemical traits of milk thistle (*Silybum marianum* l.) under salinity stress. *Aust. J. Crop Sci.* 12, 931–936. doi: 10.21475/ajcs.18.12.06.PNE972

Shekari, F., Abbasi, A., and Mustafavi, S. H. (2017). Effect of silicon and selenium on enzymatic changes and productivity of dill in saline condition. *J. Saudi Soc Agric. Sci.* 16, 367–374. doi: 10.1016/j.jssas.2015.11.006

Shen, J., Li, T., Long, Y., Shi, M., Li, N., and Ye, M. (2012). One-step solid state preparation of reduced graphene oxide. *Carbon. N. Y.* 50, 2134–2140. doi: 10.1016/j.carbon.2012.01.019

Siddiqi, K. S., and Husen, A. (2017). Plant response to engineered metal oxide nanoparticles. *Nanoscale Res. Lett.* 12, 1–18. doi: 10.1186/s11671-017-1861-y

Siddiqui, Z. A., Parveen, A., Ahmad, L., and Hashem, A. (2019). Effects of graphene oxide and zinc oxide nanoparticles on growth, chlorophyll, carotenoids, proline contents and diseases of carrot. *Sci. Hortic. (Amsterdam)* 249, 374–382. doi: 10.1016/j.scienta.2019.01.054

Song, J., Cao, K., Duan, C., Luo, N., and Cui, X. (2020). Effects of graphene on larix olgensis seedlings and soil properties of haplic cambisols in Northeast China. *Forests* 11, 258.

Taiz, L., and Zeiger, E. (2010). *Plant physiology* (Sunderland, MA: Sinauer Associates Inc).

Ullah, A., Shah, T. M., and Farooq, M. (2020). Pulses production in Pakistan: status, constraints and opportunities. *Int. J. Plant Prod.* 14, 549–569. doi: 10.1007/s42106-020-00108-2

Van Aken, B. (2015). Gene expression changes in plants and microorganisms exposed to nanomaterials. *Curr. Opin. Biotechnol.* 33, 206–219. doi: 10.1016/j.copbio.2015.03.005

Vinković, T., Novák, O., Strnad, M., Goessler, W., Jurašin, D. D., Parađiković, N., et al. (2017). Cytokinin response in pepper plants (*Capsicum annuum* l.) exposed to silver nanoparticles. *Environ. Res.* 156, 10–18. doi: 10.1016/j.envres.2017.03.015

Weng, Y., You, Y., Lu, Q., Zhong, A., Liu, S., Liu, H., et al. (2020). Graphene oxide exposure suppresses nitrate uptake by roots of wheat seedlings. *Environ. pollut.* 262, 114224. doi: 10.1016/j.envpol.2020.114224

William, S., Hummers, J. R., and Offeman, R. E. (1958). Preparation of graphitic oxide. *J. Am. Chem. Soc.* 80, 1339. doi: 10.1021/ja01539a017

Yan, H., Tao, X., Yang, Z., Li, K., Yang, H., Li, A., et al. (2014). Effects of the oxidation degree of graphene oxide on the adsorption of methylene blue. *J. Hazard. Mater.* 268, 191–198. doi: 10.1016/j.jhazmat.2014.01.015

Zhang, P., Zhang, R., Fang, X., Song, T., Cai, X., Liu, H., et al. (2016). Toxic effects of graphene on the growth and nutritional levels of wheat (*Triticum aestivum* l.): short-and long-term exposure studies. *J. Hazard. Mater.* 317, 543–551. doi: 10.1016/j.jhazmat.2016.06.019

Zhao, L., Lu, L., Wang, A., Zhang, H., Huang, M., Wu, H., et al. (2020). Nano-biotechnology in agriculture: use of nanomaterials to promote plant growth and stress tolerance. *J. Agric. Food Chem.* 68, 1935–1947. doi: 10.1021/acs.jafc.9b06615

Zhao, S., Wang, Q., Zhao, Y., Rui, Q., and Wang, D. (2015). Toxicity and translocation of graphene oxide in *Arabidopsis thaliana*. *Environ. Toxicol. Pharmacol.* 39, 145–156. doi: 10.1016/j.etap.2014.11.014

frontiers | Frontiers in Plant Science

TYPE Original Research
PUBLISHED 12 December 2022
DOI 10.3389/fpls.2022.1064710

OPEN ACCESS

EDITED BY
Waheed Akram,
University of the Punjab, Pakistan

REVIEWED BY
Hakim Manghwar,
Lushan Botanical Garden (CAS), China
Mohamed Hafez,
City of Scientific Research and Technological Applications, Egypt

*CORRESPONDENCE
Lamine Baba-Moussa
laminesaid@yahoo.fr

SPECIALTY SECTION
This article was submitted to Plant Symbiotic Interactions, a section of the journal Frontiers in Plant Science

RECEIVED 08 October 2022
ACCEPTED 25 November 2022
PUBLISHED 12 December 2022

CITATION
Adoko MY, Noumavo ADP, Agbodjato NA, Amogou O, Salami HA, Aguégué RM, Adjovi Ahoyo N, Adjanohoun A and Baba-Moussa L (2022) Effect of the application or coating of PGPR-based biostimulant on the growth, yield and nutritional status of maize in Benin. *Front. Plant Sci.* 13:1064710. doi: 10.3389/fpls.2022.1064710

Effect of the application or coating of PGPR-based biostimulant on the growth, yield and nutritional status of maize in Benin

Marcel Yévèdo Adoko[1], Agossou Damien Pacôme Noumavo[1,2], Nadège Adoukè Agbodjato[1], Olaréwadjou Amogou[1], Hafiz Adéwalé Salami[1], Ricardos Mèvognon Aguégué[1], Nestor Ahoyo Adjovi[3], Adolphe Adjanohoun[3] and Lamine Baba-Moussa[1]*

[1]Laboratoire de Biologie et Typage de Moléculaire en Microbiologie, Département de Biochimie et de Biologie Cellulaire, Faculté des Sciences et Technique, Université d'Abomey-Calavi, Cotonou, Benin, [2]Laboratoire de Microbiologie et de Technologie Alimentaire, Faculté des Sciences et Technique, Université d'Abomey-Calavi, Cotonou, Benin, [3]Institut National des Recherches Agricoles du Bénin (INRAB), Cotonou, Benin

Biotechnology proposes various ecological approaches to control climatic constraints, soil fertility and plant nutrition using biological products, such as biostimulants to achieve a healthy and environment-friendly agriculture. The aim of this study was to compare the effect of biostimulant-coated maize seed and biostimulant application on the growth, yield and nutritional status of maize in Benin. The trials were set up with 100 producers spread over the whole of Benin. The experimental design was a block of three treatments with 11 replicates per Research-Development (R-D) sites. The maize varieties 2000 SYNEE-W BENIN and TZL COMP 4-W BENIN were used. The best growth (height, stem diameter and leaf area) and yield performances (thousand grains weight and grains yield) were obtained by treatments T_2 (Application of biostimulant + ½ NPK-Urea) and T_3 (Seed coating with biostimulant + ½ NPK-Urea) compared to the farmers' practice (T_1). A significant difference was observed between the different treatments for height, leaf area, 1000 grains weight and maize-grain yield. From one Research-Development site to another, a significant difference was also observed for all parameters. The treatment- Research-Development site interaction was also significant in most areas. The applied or coated biostimulant improved the uptake of nitrogen, phosphorus and especially potassium with higher significant difference compared to the recommended dose of mineral fertilizer. The two techniques of using the biostimulant combined with the half-dose of mineral fertilizer gave the better growth, yield and nutritional status compared to the farmers'

practice in all areas study. This biostimulant can be used to ensure food security and sustainable agriculture in Benin.

KEYWORDS

biostimulant, maize, nutritional status, food security, sustainable agriculture

Introduction

Food security is the ability of a population to access and afford enough food to live a healthy life (Olanrewaju et al., 2022). Feeding the growing world population is one of the major challenges for agriculture. In Benin, soils are weakened and subject to deep disturbances, such as physical and chemical degradation, low microbial activity and this has resulted to the decline in the soil fertility with negative consequent to low productivity (Igué et al., 2013). For decades, the application of chemical fertilizers have played a crucial role worldwide to increase growth, crop yield and maintain an adequate food supply (Meena et al., 2017; Chaudhary et al., 2020). Several authors studied the long-term use of chemical fertilizers and their impacts on the agroecosystem (Chaudhary et al., 2017; Bishnoi, 2018). Their applications provide nutrients in high concentrations but with many drawbacks on soil health, water quality and safe environment (Vejan et al., 2016). The use of mineral fertilizers improve productivity, but also leaves undetermined effects on the ecosystem (Kumar and Shastri, 2017). These numerous environmental problems include groundwater pollution, soil acidification, eutrophication, low soil fertility, loss of biodiversity, high energy consumption in synthesis processes, and contamination of crop products (Agbodjato et al., 2016; Tomer et al., 2016; Mahanty et al., 2017; Ilangumaran and Smith, 2017; Kourgialas et al., 2017). To increase crop productivity in an environmentally friendly manner, the use of biostimulants, such as plant growth-promoting microorganisms remain the the most promising ways (De Pascale et al., 2017).

In the last decade, great efforts have been made to substitute chemical fertilizers with environmentally friendly biostimulants (Kamilova et al., 2015; Liu et al., 2018; Thomas and Singh, 2019; Amogou et al., 2021). The response to microbial biostimulants inoculation on different crops has been widely evaluated, thus showing significant increase in the growth and yields of agricultural crops (Babalola et al., 2020; Aguégué et al., 2021b; Adoko et al., 2021a).

Plant growth-promoting microorganisms play an important role in regulating the dynamics of various ecological processes, such as decomposition of organic matter and accessibility of different plant nutrients, such as iron magnesium, nitrogen, phosphorus and potassium (Priyanka et al., 2020). Microbial biostimulants are the main component of integrated nutrient management, thus leading to their sustainability. In addition, these biostimulants can be used as cost-effective biological inputs to increase crop productivity while reducing mineral fertilizer rates and ultimately harvesting more nutrients from the soil (Aguégué et al., 2021a). Biostimulants are sometimes composed of plant growth-promoting rhizobacteria (PGPR), a group of bacteria that actively colonise plant roots, that support plant growth and suppress plant pathogens (Khan et al., 2018). PGPR produce plant hormones (auxin, gibberellin and cytokinin), promote phosphate solubilisation, potassium mineralization and nitrogen fixation, which are important natural organic biostimulants (Rosier et al., 2018). PGPR based biostimulants, with their natures, can play important roles in maintaining soil fertility (Gamez et al., 2019).

Maize is a prevalent crop in Benin's cropping systems (Gogan et al., 2018). It is very sensitive to low availability of phosphorus and other mineral elements for growth (Postma and Lynch, 2011) and has been shown to be amenable to application of PGPR-based biostimulants (Agbodjato et al., 2021a). Over the last decades in Benin, a lot of work has been done on the use of different biostimulants on maize productivity These studies were carried out on the identification, biochemical characterization, formulation, inoculation and application of PGPR-based biostimulants to increase maize growth and yield (Adjanohoun et al., 2012; Agbodjato et al., 2021b; Adoko et al., 2021b). Nevertheless, studies on the PGPR-based biostimulant-coated maize seed in Benin are less documented. Therefore, the aim of this study was to compare the effect of biostimulant-coated maize seed and biostimulant application on growth, yield and nutritional status of maize in Benin.

Materials and methods

Study areas

Trials were set up at 100 farmers' sites in different villages of South, Center and North Benin (Figure 1). In South with 34 farmers, this includes 11 in Adakplamè (Kétou), 12 in Eglimey (Aplahoué) and 11 in Saharo-Nagot (Sakété). In

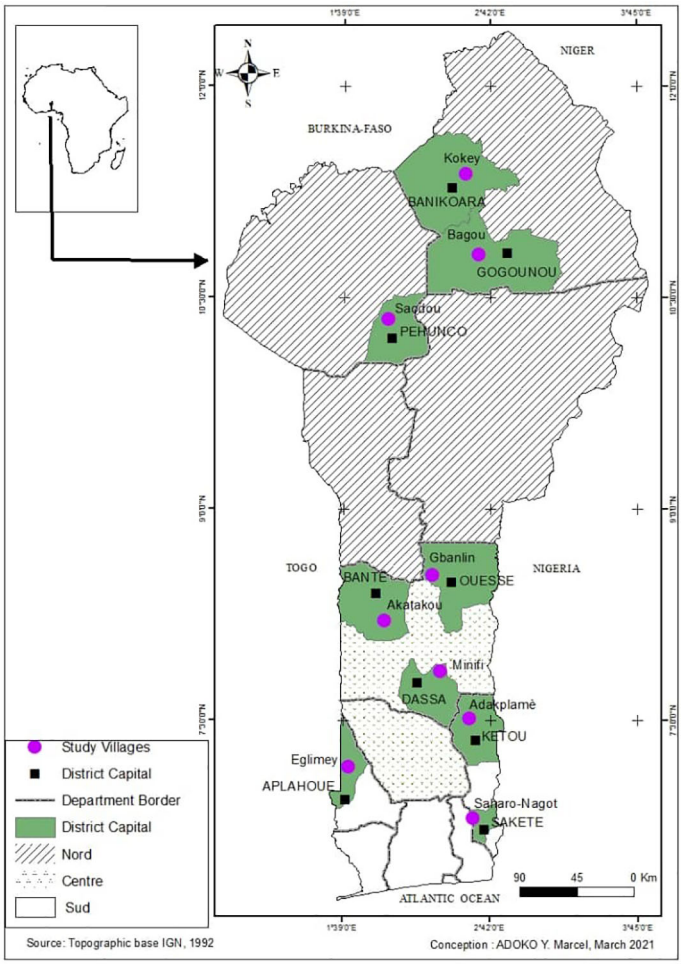

FIGURE 1
Study areas of the on farmers' trials in Benin.

Center with 33 producers, including 11 in Miniffi (Dassa-Zoumè), 11 in Gbanlin (Ouèssè) and 11 in Akatakou (Bantè). In North with 33 producers, this includes 11 in Soaodou (Péhuncho), 11 in Kokey (Banikoara) and 11 in Badou (Gogounou). Moreover, the selected sites were flat land with a maximum slope of 2%, and not flooded. The decline in the soil fertility was a major constraint. The experimental sites were at least 500 m apart.

Biostimulant formulation

Method adapted from Connick et al. (1991) was used. Maize flour, bacterial suspension (10^8 CFU/ml) of *Pseudomonas putida*, binder (Clay) and sucrose were used. These components were put into boxes and mixed with gloved hands until a soft paste was obtained. This was spread on aluminium foil for two days at a temperature of 25°C. After two days of drying, the resulting product was ground in a mortar and then sieved. The different activities were carried out under aseptic conditions. The strain of *P. putida* used in the study was isolated and characterised by Adjanohoun et al. (2011).

Characterization of maize seed

Maize variety 2000 SYNEE-W BENIN developed by the International Institute of Tropical Agriculture (IITA) and the Institut National des Recherches Agricoles du Bénin (INRAB) was used in the South. It is an extra-early variety of 75 days, with potential grains yield of 2.5t ha^{-1} in a farming environment. In Central and North, the maize variety TZL COMP 4-W BENIN was used. It is a 110-day composite variety with an average grain yield of 4t ha^{-1} on the farm (MAEP, 2016).

Experimental design

The experimental design was a block of three treatments with 11 replicates per R-D study site where each replicate represented one producer in each site. The treatments were defined as follows: T_1 = Farmer practice ($N_{13}P_{17}K_{17}S_6B_{0,5}Zn_{1,5}$ (200 Kgha^{-1}), Urea (100 Kgha^{-1}); T_2 = Biostimulant application + ½ dose of NPK-Urea (NPK (100 Kgha^{-1}), Urea (50 Kgha^{-1}); T_3 = Seed coated with biostimulant + ½ dose of NPK-Urea (NPK (100 Kgha^{-1}), Urea (50 Kgha^{-1}). Each elementary plot had an area of 40 m² and consisted of five lines of 10 m. The distance between plots was 5 m. The sowing was done at a spacing of 0.80 m x 0.40 m or a density of 31,250 plants ha^{-1} (Yallou et al., 2010).

Application of the recommended dose of $N_{13}P_{17}K_{17}S_6B_{0,5}Zn_{1,5}$-Urea

The half (½) dose of $N_{13}P_{17}K_{17}S_6B_{0,5}Zn_{1,5}$ was applied as a bottom dressing on the day of sowing on two biostimulants plots. It is only on the farmer's plot that NPK was applied on the 15th Day After Sowing (DAS). On the other hand, Urea was applied on the 45th DAS for all plots.

Application of biostimulant and half dose of $N_{13}P_{17}K_{17}S_6B_{0,5}Zn_{1,5}$-Urea

After opening three pits of about 5 cm deep with 2 cm apart, two maize seeds were placed into the central one. Then, 2 g of biostimulant + ½ $N_{13}P_{17}K_{17}S_6B_{0,5}Zn_{1,5}$ were applied separately in the other two pits on the day of sowing. The half dose of Urea was applied on the 45 DAS for all plots.

Coating of biostimulant and half dose of $N_{13}P_{17}K_{17}S_6B_{0,5}Zn_{1,5}$-Urea

The ratio of 1000 g of seed, 100 g of biostimulant and 100 ml sterile distilled water was used to coat maize seeds. The seeds were mixed and then dried at room temperature for 24 hours. After opening two pits about 5 cm deep and 2 cm apart, two maize seeds coated with biostimulant were placed in one pit and the half dose of $N_{13}P_{17}K_{17}S_6B_{0,5}Zn_{1,5}$ was applied separately in the second pit on the day of sowing. The half dose of Urea was applied on the 45 DAS for all plots.

Chemical analysis of the soil

Composite soil samples of 500 g were taken at a depth of 0-20 cm from the different sites in the South (Adakplamè, Eglimey, Saharo-Nagot), Center (Akatakou, Gbanlin, Miniffi) and North (Badou, Kokey, Soaodou) prior to the installation of the experimental device using an auger. Five sampling points were randomly selected. Four of the five sampling points were located on the four cardinal points (North-South-West-East). The fifth sampling point was located approximately at the junction of the four previous points (Adjanohoun et al., 2011). These samples were sent to the Laboratoire des Sciences du Sol, Eau et Environnement (LSSEE) of the Institut National des Recherches Agricoles du Bénin (INRAB) for analysis. These analyses consisted of determining the pH (water), (by glass electrode in a soil/water ratio of 1/2.5), organic matter and carbon (Walkley and Black, 1934), assimilable phosphorus (Bray and Kurtz, 1945), total nitrogen (Kjeldahl, 1883), and exchangeable bases by the Metson, (1956) method with ammonium acetate at a pH equal to 7.

Collection of growth and yield data

All growth parameters of the maize plants were measured at 60 DAS in South and 70 DAS in Center and North. Height was measured with a tape meter; stem diameter was measured with a calliper and leaf area was estimated by the product of length and width of leaves with the coefficient 0.75 (Ruget and Bonhomme Chartier, 1996). The ears of 10 maize plants located on central lines of each elementary plot were harvested at 80 DAS in South and at 120 DAS in Center and North. After shelling, total mass of maize grains was measured using a precision balance (Highland HCB 3001. Max: 3000 x 0.1 g) and the moisture content was taken using a moisture meter (LDS-1F). Grains yield was determined according to the formula described by Valdés et al. (2013): $R = \frac{(Px10.000) \quad x14}{(Sx1.000)xH}$

where: R = grains yield in t ha-1; P = mass of maize grains in kg; S = harvest area in m²; H = moisture percentage of maize grains in %.

After proper drying until moisture content stabilized (H = 14), the weight of 1000 maize grains were taken according to treatments and R-D sites.

Assessment of the nutritional status of maize plants

A representative 500 g sample of the dry biomass mixture was taken from each plot. Each sample was placed in a labelled bag. The packaged samples were sent to the Laboratoire des Sciences du Sol Eau et Environement (LSSEE) to determine the N, P, and K content. After dry mineralisation, the ash was dissolved with HCl (6N) and dissolved with HNO_3 (0.1N). Phosphorus (P) was determined by colorimetry, potassium (K) by atomic absorption spectrophotometry and nitrogen (N) was determined by the method of Kjeldahl (1883).

Statistical analysis

Effect of experimental area and applied treatments on plant growth and yield performance was assessed by means of a two-factor ANOVA test. Normality and homogeneity of variances of data were performed by ANOVA (Glèlè Kakaï et al., 2006). Thus, Shapiro-Wilk and Levene tests were performed, and type III ANOVA tests were adopted to analyse effect of zone and treatment factors on the parameters evaluated. Once the ANOVA test was significant, a *post hoc* test of pairwise comparisons using Tuckey *post hoc* test (Douglas and Michael, 1991) was carried out to assess statistical differences of the means. In addition, descriptive statistics were calculated per measured parameter. The various tests were performed in the R 4.0.2 software (R Core Team, 2020). These analyses require the use of dplyr and DescTools packages for calculation of descriptive statistics, ggplot2 and ggpur packages for creation of moustache boxes. Stats packages for shapiro test and levene test, the "car" packages for ANOVA and multcomp packages for *post hoc* pairwise comparison test. Significance level was at 5%.

Results

Soil chemical characteristics

The soil chemistry characteristics of the R-D sites were presented in Table 1. The recorded water pH values (5.78 to 6.80) indicated that the soils were moderately acidic. Cation Exchange Capacity (CEC) values of the soils at the different areas were very low, which ranges from 4.64 to 7.91 $cmol^{+}\ kg^{-1}$. The available phosphorus was between 4 and 14 mg kg^{-1}. The C/N ratio was relatively low and varied between 10.23 and 13.33. The sum of exchangeable bases varied between 3.48 to 9.23 $cmol^{+}\ kg^{-1}$ (Table 1).

Height of maize plants

The histogram in Figure 2 illustrates the variation in average height of maize plants per treatment and experimental site. In all R-D study sites in Benin, application of biostimulant + ½ NPK-Urea (T_2 = 196.57 cm) and the coating of biostimulant + ½ NPK-Urea (T_3 = 197.20 cm) gave the better performances. A respective increase of 17.65% (T_2) and 18.03% (T_3) compared to the farmers' practice (T_1 = 167.08 cm) was observed. ANOVA showed a significant difference in the effects of treatments (p = 0.001) and experimental sites (p< 0.001). Interaction between different treatments and different sites was also significant (p = 0.003) (Figure 2).

Stem diameter of maize plants

The histogram in Figure 3 shows the variation in the stem diameter of maize plants as a function of the experimental site and the histogram in Figure 4 shows Treatment and site effects on maize stem diameter. In all R-D sites, the three treatments had comparable effects on maize stalk diameter (T_2 = 3.22cm; T_3 = 3.17; T_1 = 3.08cm). The ANOVA revealed no significant difference between treatments in all R-D sites (P = 0.09) (Figure 4). However, a significant difference in the effects of the experimental site (p< 0.001) on the stem diameter of maize plants was found (Figure 3). The interaction between treatments and sites was also not significant (P = 0.71).

Leaf area of maize plants

The effect of biostimulants on leaf area of maize plant by experimental site was illustrated by the histogram in Figure 5. Across all study sites in Benin, the largest leaf area (578.36 cm^2) was obtained in South at Eglimey with farmer practice (T_1). In

TABLE 1 Chemical characteristics of the soils in different Research-Development site.

Research-Development site	Horizons 0 – 20 cm					
	pH water	OM (%)	P-ass (mg Kg^{-1})	C/N	Sum of exchangeable bases ($cmol^{+}\ kg^{-1}$)	CEC ($cmol^{+}\ kg^{-1}$)
Eglymè (Aplahoué)	6.30	1.49	9	10.23	9.23	7.91
Adakplamè (Kétou)	6.80	1.57	12	10.43	8	7.82
Saharo-Nagot (Sakété)	6.50	1.50	14	11.12	4.83	5.94
Miniffi (Dassa)	6.20	1.16	4.75	13.33	7.84	8
Gbanlin (Ouèssè)	5.78	1.01	5	12.52	4.22	4.64
Akatakou (Bantè)	5.95	0.55	4	10.80	3.48	6.50
Kokey (Banikoara)	6.30	1.29	5.03	11.88	5.46	5.87
Bagou (Gogounou)	6.08	1.39	5.20	11.57	6.03	7.63
Saodou (Péunko)	6.10	1.36	12.60	12.27	5.92	6.20

pH (water); OM, organic matter; P-ass,assimilable phosphorus; C, carbon; N, Nitrogen; CEC, cation exchange capacity.

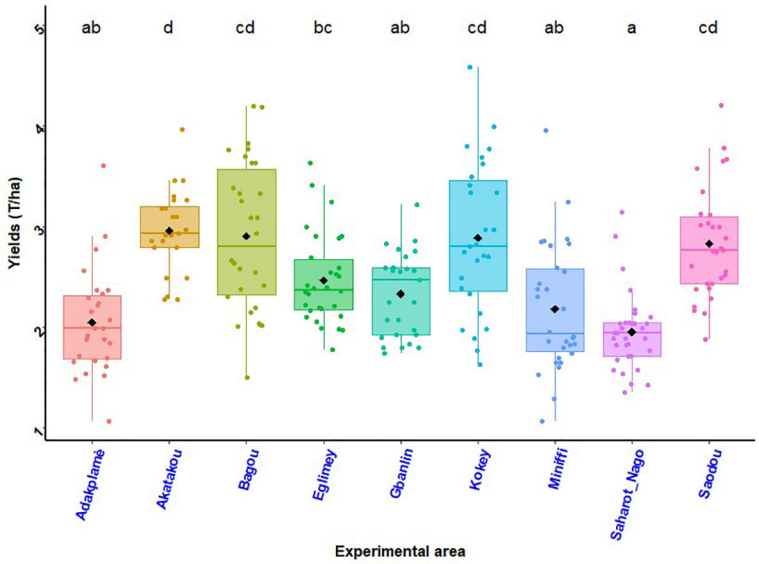

FIGURE 2
Average height of maize plants per treatment and experimental site. $p < 0.001$ (highly significant). In the same line, means marked with different letters [i,hi,gi,fgi,efgi etc ...]are significantly different at the 5% threshold. T_1: farmer practice (100% NPK-Urea), T_2: biostimulant application + ½ NPK-Urea, T_3: biostimulant coating + ½ NPK-Urea.

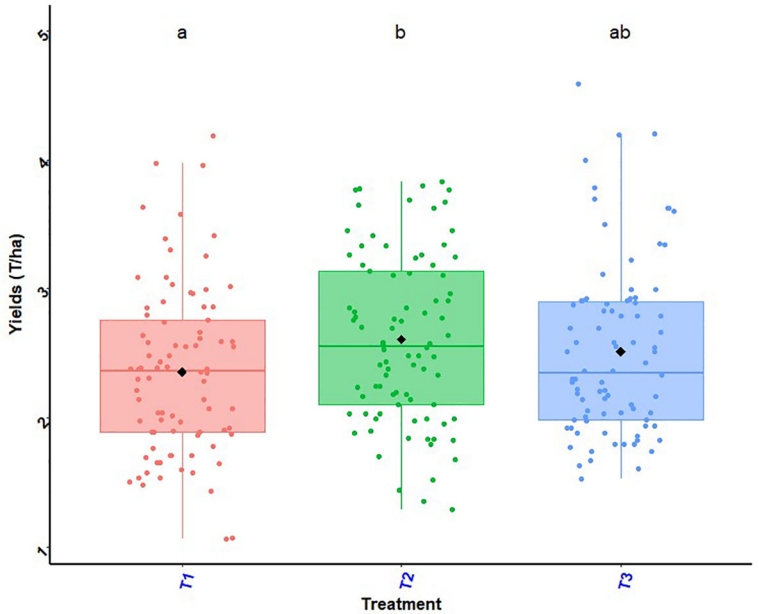

FIGURE 3
Stem diameter of maize plants by experimental site. $p < 0.001$ (highly significant). In the same line, means marked with different letters [f,ef,df,de,cd etc ...]are significantly different at the 5% threshold.

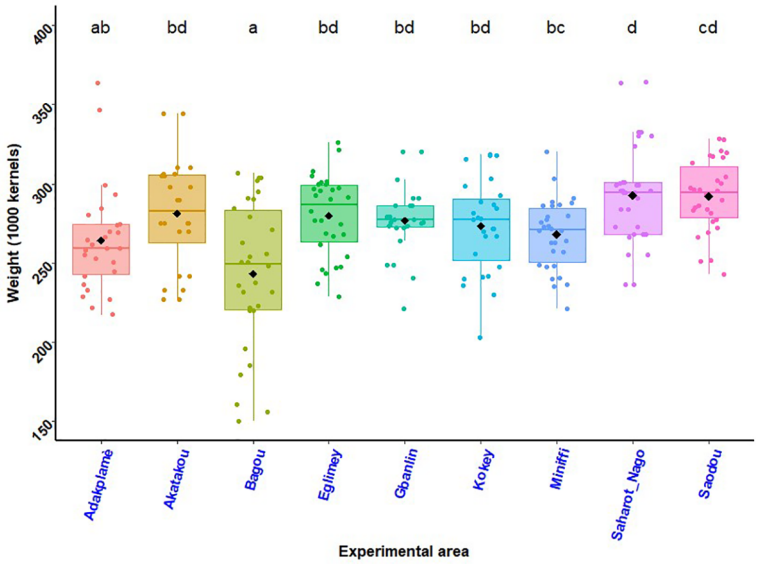

FIGURE 4
Treatment and site effects on maize stem diameter. $p > 0.05$ (not significant). In the same line, means marked with same letters [a,a,a]are not significantly different at the 5% threshold. T_1: farmer practice (100% NPK-Urea), T_2: biostimulant application + ½ NPK-Urea, T_3: biostimulant coating + ½ NPK-Urea.

Adakplamè, Saharo-Nagot and Soaodou the farmers' practice and the application of biostimulant + ½ NPK-Urea were better than the seed coating with biostimulant with a significant difference (p = 0.015). There was no significant difference between the treatments on leaf area in the R-D sites of Akatakou, Gbanlin, Miniffi, Badou and Kokey. Across experimental sites, the difference was significant (p< 0.001). From one experimental site to another, the difference was significant (p< 0.001). There was no significant difference between interactions of treatments and the different sites (p = 0.061).

Maize grains yield

Maize grain yields as a function of experimental site illustrated by the histogram in Figure 6 and the histogram in Figure 7 shows effects of treatments and site on maize grain yield. The best maize grain yield (T_2 = 2.48 t ha^{-1}) was obtained at Eglimey with the application of biostimulant + ½ NPK-Urea in South Benin. At Adakplamè the application of biostimulant + ½ NPK-Urea (T_2 = 2.23 t ha^{-1}) and seed coating with biostimulant + ½ NPK-Urea (T_3 = 2.17 t ha^{-1}) induced respective increases of 27.42% and 24.00%. In Saharo-Nagot, application of biostimulant + ½ NPK-Urea (T_2 = 2.10 t ha^{-1}) and seed coating with biostimulant + ½ NPK-Urea (T_3 = 2.00 t ha^{-1}) exceeded the farmers' practice by 20.00% and 14.28%, respectively with a significant difference (p< 0.001). In the Centre, the best yield was obtained by the application of biostimulant + ½ NPK-Urea (T_2 = 3.25 t ha^{-1}) at Akatakou. This treatment resulted in an increase of 12.06% compared to farmers' practice. In Gbanlin and Miniffi, no significant difference was observed between treatments. In the North, the best yield was obtained in Kokey with the application of biostimulant + ½ NPK-Urea (T_2 = 3.24 t ha^{-1}) which had an increase of 31.7%. At Badou, the same treatment was better (T_2 = 2.99 t ha^{-1}) with an increase of 6.03%. In Soaodou, seed coating with biostimulant + ½ NPK-Urea was better (T_3 = 3.04 t ha^{-1}) with an increase of 15.58% compared to the farmers' practice. The ANOVA results were significant between treatments (p< 0.001) and sites (P = 0.009) (Figures 6, 7). Interactions between treatments and sites were not significant (P = 0.61).

Maize 1000 grains weights

Maize 1000 grains weights as a function of experimental site illustrated by the histogram in Figure 8 and the histogram in Figure 9 shows effects of treatments and site on 1000 grains weights of maize. In the South, maize grains from the biostimulant + ½ NPK-Urea application had higher weights compared to the other treatments. The highest value of 1000 grains weight was recorded in Saharo-Nagot (T_2 = 324.60 g) with an increase of 18.44% compared to maize grains harvested with the farmer's practice. In the Centre, there was no significant difference between treatments. In the North, application of biostimulant + ½ NPK-

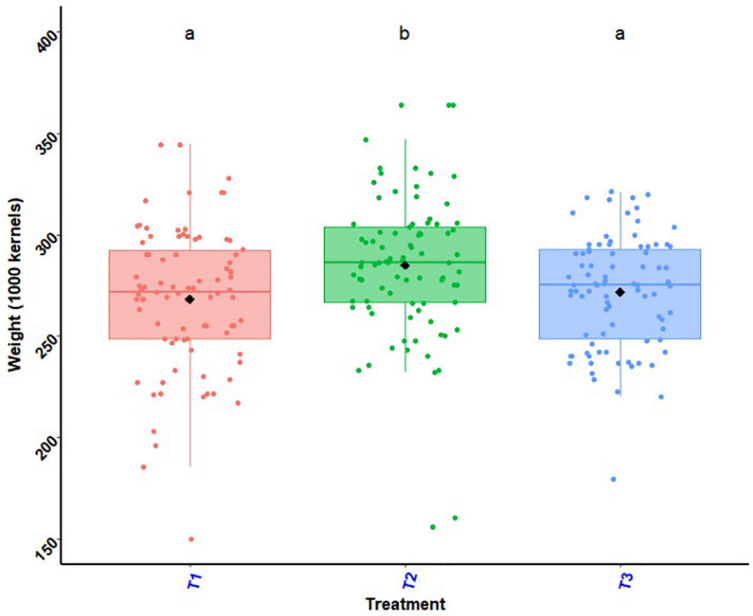

FIGURE 5
Maize plant leaf area by experimental site. $p < 0.001$ (highly significant). In the same line, means marked with different letters $^{e,d,cd,bd\ etc\ \ldots}$ are significantly different at the 5% threshold.

Urea (T_2) and seed coating with biostimulant + ½ NPK-Urea (T_3) were better. In Soaodou, the biostimulant treatments were better than the farmer practice (T_1 = 285.42 g, T_2 = 296.02 g and T_3 = 295.45 g). In all the R-D study sites, variance analysis's results showed a significant difference between the application of biostimulant + ½ NPK-Urea (T_2) and the others (T_1 and T_3). In addition, there was no significant difference between the farmer's practice (T_1) and the seed coating with biostimulant + ½ NPK-Urea (T_3) (Figure 9) Across sites, the difference was also significant (Figure 8).

Nutritional status of maize plants

The nutritional status of maize plants of the R-D sites are presented in Table 2. In a whole Benin, nitrogen status did not

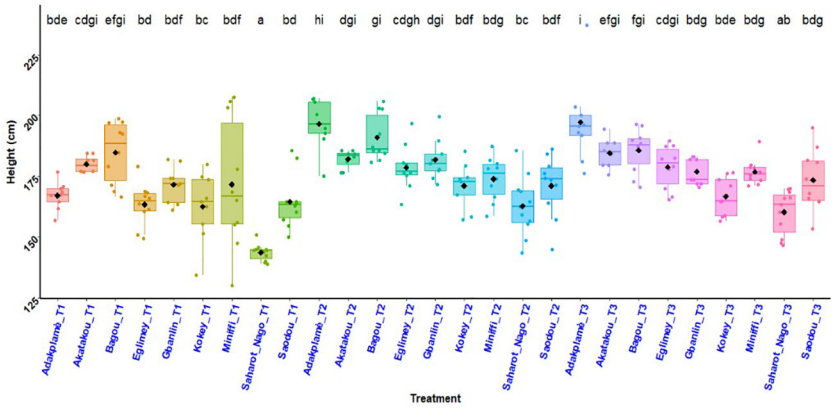

FIGURE 6
Maize grains yield by experimental site. $p < 0.001$ (highly significant). In the same line, means marked with different letters $^{d,cd,bc,ab\ etc\ \ldots}$ are significantly different at the 5% threshold.

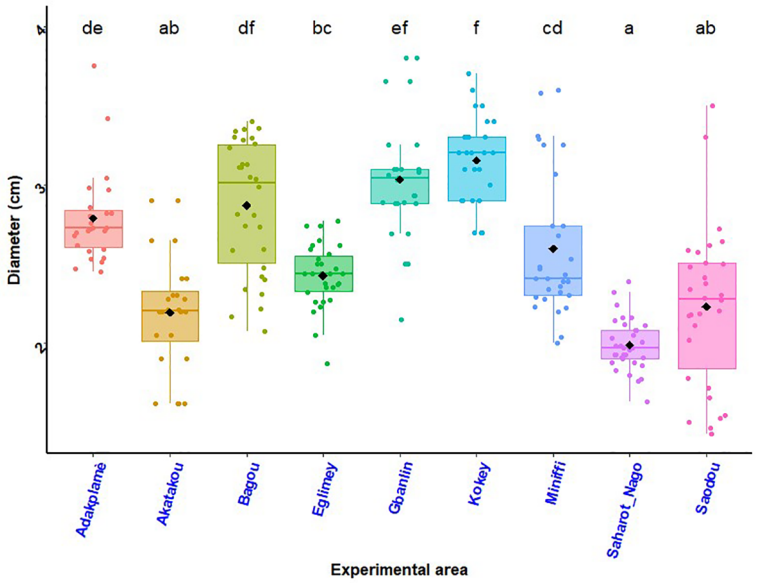

FIGURE 7
Effects of treatments and site on maize grain yield. $p < 0.001$ (highly significant). In the same line, means marked with different letters [b,ab,a] are significantly different at the 5% threshold.T_1: farmer practice (100% NPK-Urea), T_2: biostimulant application + ½ NPK-Urea, T_3: biostimulant coating + ½ NPK-Urea.

vary significantly with plants treated with 100% NPK-Urea and with application and coating of biostimulant + ½ NPK-Urea. All inoculated plants improved nitrogen content. For phosphorus, the same thing was observed. Mineral fertilizers, applied and coated biostimulants had practically the same nutritional status. Hence, no significant differences were recorded. The highest potassium levels were obtained with biostimulant + ½ NPK-Urea treatments with significant differences. This was observed

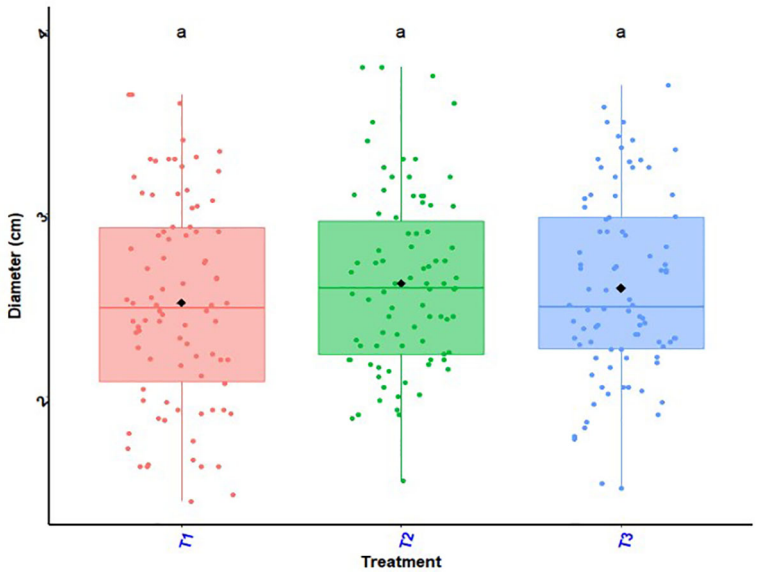

FIGURE 8
Weight of 1000 maize grains per experimental site.$p < 0.001$ (highly significant). In the same line, means marked with different letters [d,cd,bd,bc etc ···] are significantly different at the 5% threshold.

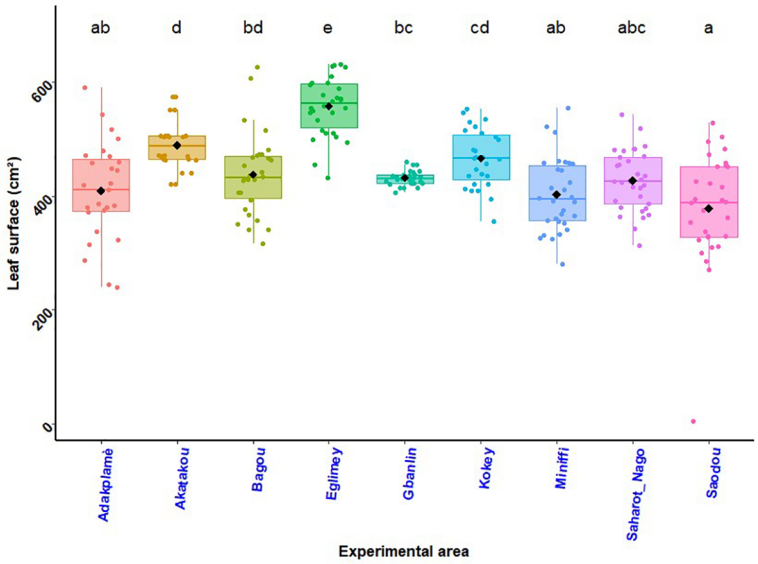

FIGURE 9
Effects of treatments and site on 1000 grains weights of maize. $p < 0.001$ (highly significant). In the same line, means marked with different letters [b,a,a]are significantly different at the 5% threshold.T_1: farmer practice (100% NPK-Urea), T_2: biostimulant application + ½ NPK-Urea, T_3: biostimulant coating + ½ NPK-Urea.

in all sites. ANOVA revealed a higher significant difference ($p< 0.001$) between treatments for potassium with no significance for nitrogen and phosphorus.

Discussion

The use of microbial biostimulants in agriculture to increase productivity is a natural and environmentally friendly alternative. Results of the initial chemical properties of experimental soils showed that they were slightly acidic. In addition, soils of different R-D sites had a low level of fertility characterised by a high C/N ratio in topsoil. Interaction between different chemical characteristics of soil, which leads to soil fertility classification, reveals that majority of soils in Benin have lost their agricultural potential (Igué et al., 2013). This might be due to very low nitrogen, phosphorus, potassium and cation exchange capacity in the soils. The pH of soil should be neutral to slightly acidic to favour assimilation of mineral elements. Only cation exchange capacity in all soils appears to be a severe to medium limitation regardless of farming system (Igué et al., 2013).

TABLE 2 Nutritional status of maize plants.

Zones	Traitements	Nitrogen (N)%		Phosphorus (P_2O_5)%		Potassium (K_2O)%	
		M	e	m	e	m	e
South Benin	T_1	1.956[a]	0.162	0.218[a]	0.031	0.389[a]	0.135
	T_2	1.897[a]	0.011	0.194[a]	0.088	0.886[a]	0.241
	T_3	1.873[a]	0.042	0.180[a]	0.083	1.587[b]	0.664
Centre-Bénin	T_1	1.864[a]	0.182	0.198[a]	0.071	0.889[a]	0.135
	T_2	1.904[a]	0.111	0.196[a]	0.078	1.486[b]	0.141
	T_3	1.876[a]	0.142	0.190[a]	0.082	1.587[b]	0.264
North Benin	T_1	1.926[a]	0.162	0.197[a]	0.076	0.489[a]	0.135
	T_2	1.987[a]	0.121	0.204[a]	0.068	1.586[b]	0.241
	T_3	1.983[a]	0.122	0.199[a]	0.086	1.587[b]	0.364
	Significance	ns		ns		***	

***= p< 0.001 (highly significant). ns= p > 0.05 (not significant). In the same column, means marked with different letters [b,a]are significantly different at the 5% threshold. m: mean. e: standard deviation; T_1: farmer practice (100% NPK-Urea), T_2: biostimulant application + ½ NPK-Urea, T_3: biostimulant coating + ½ NPK-Urea.

The best performance in height was obtained by coating the seeds with biostimulant, followed by the application of the biostimulant. Statistical analysis revealed in some R-D sites a significant difference in plant height between application and coating of the biostimulant. The difference between the biostimulant treatments can be explained by the seed coating carried out on the day one before sowing to allow a good adhesion of the PGPR contained in the formulation, which can be favourable to the height growth of the maize plants. It makes more PGPR and nutrients available to the plant for better height growth (Neufeld et al., 2017). An increase of 29.43% in the height of wheat plants was observed after the use of the biostimulant *Pseudomonas fluorescens* RRb-11 and talc (Jambhulkar and Sharma, 2013).

In all the study R-D sites, there was no significant difference between treatments on stem diameter of maize plants. However, from one site to another, the differences were significant. The same phenomenon was observed on the leaf area of maize plants in one South R-D site (Eglimey), in all Center R-D sites and in two North R-D sites. In the other two South R-D sites (Adakplamè and Saharo-Nagot) and the North (Soaodou) a significant difference was observed between treatments. These results were related to soil types (Bishnoi, 2015; Adoko et al., 2020; Agbodjato et al.,2021a) and also to maize varieties. Indeed, ferrallitic soils of South had a higher assimilable phosphorus rate (9-14) than ferruginous soils of Center (4-5) and North (5.03-12.6). In South, the 2000 SYNEE-W BENIN variety was used, in Center and North, the TZL COMP 4-W BENIN variety was used during the experiment. Similar results were recorded by Lin et al. (2019) who reported an increase in nitrogen and chlorophyll content throughout the growth stages of the plant that received the biostimulant in combination with mineral fertiliser. The biostimulant applied or coated to the seed makes more nitrogen available to the plant to achieve good photosynthesis for growth. Biostimulants were able to increase yield of cereals. Hassan and Bano (2015) shown that wheat yield was improved by 15-25% over controls with the use of *P. moraviensis* and *B. cereus*.

In all southern R-D sites, the highest maize grains yields were obtained with the application of biostimulant + ½ NPK-Urea, followed by the coating of maize seeds with biostimulant + ½ NPK-Urea. Farming practice gave the lowest yields in all R-D sites. In the majority of these sites, no significant difference was recorded between the application + ½ NPK-Urea and seed coating + ½ NPK-Urea. However, in very few R-D sites, there was a significant difference between the two biostimulant treatments (T_2 and T_3) and the farmers' practice. From one R-D site to another, the differences were significant. The results can be explained by the stimulating effect of a good yield of the rhizobacteria *P. putida* contained in the biostimulant used. This strain was able to produce indole acetic acid (IAA), solubilise certain nutrients, such as phosphate, potassium, make nitrogen (ammonia) and other micronutrients necessary for plant growth and yield enhancement (Noumavo et al., 2015; Agbodjato et al., 2018).

In the Southern R-D sites, maize grains from the application + ½ NPK-Urea had a higher weight than the other treatments. The highest weight of 1000 grains obtained was observed in Saharo-Nagot (324.60 g) with an increase of 18.44% compared to the farmers' practice. In the Center, there was no significant difference between treatments. In the North, the application + ½ NPK-Urea was also better. The ANOVA showed a significant difference between treatment T_2 and the others (T_1 and T_3) but there was no significant difference between treatments the farmers' practice (T_1) and the coating of maize seeds with biostimulant + ½ NPK-Urea (T_3). Across R-D sites, the differences were also significant. This effect can be due to the soil types, maize varieties and variation in the degree of fertility from one R-D site to another. The amount of biostimulant used for the application (2 g per hole) far exceeds that used for coating two maize seeds (0.1 g). These quantitative differences between application and coating can be the basis of our results. As the amount of biostimulant increases, there was more PGPR and binder (clay) available to the plant, which is favourable for good growth and grains yield and 1000 grains weight.

In all R-D sites, the application and seed coating of biostimulant gave the best results on all parameters (growth, yield and nutritional status) evaluated compared to the farmer practice. This allows us to say that the biostimulant + ½ of NPK-Urea was better than the recommended dose of NPK-Urea for maize cultivation in Benin. This biostimulant provided the plant with nutrients, such as nitrogen, phosphorus and especially potassium ($p< 0.001$) necessary for its growth and yield. Some soil nutrients can also be better absorbed by plants if microorganisms were added. The application of biostimulants was favourable to better increase the biodiversity of the soil microbial community (Ding et al., 2016), which justifies the results obtained in this study.

At some R-D sites in Benin, application and coating of biostimulant had comparable effects. This similarity can be explained by the intrinsic characteristics of *P. putida* known for their roles in promoting crop growth and development. Difference observed was believed to be due to the amount of biostimulant used in the two treatments (Adoko et al., 2021a). Indeed, 2 g of biostimulants applied per hole and less than one twentieth (0.1g) were used in seed coating. PGPR in biostimulants can help the host plant produce root exudates which, in turn, recruit beneficial bacterial communities, thereby increasing dissolved nutrient levels in the soil. Soil organic matter has previously shown to be the main substrate and energy source for microorganisms (Xu et al., 2013). Treatment of wheat seeds with the formulation of *P. fluorescens* RRb-11 in talc resulted in a significant increase in plant growth parameters and even increased the seed germination rate by 94% compared to controls (Jambhulkar and Sharma, 2013). Similarly, Jorjani et al. (2011) reported the efficacy of *P. fluorescens* bioformulation

on the fresh weight of sugar beets. Application of inoculated *P. putida* to maize seeds significantly increased the fresh and dry weight of the plants compared to the control at harvest (Khashei et al., 2020). Formulations of talc or peat and *Pseudomonas* spp. effectively controlled chickpea wilt disease in two field trials and increased its yield (Vidhyasekaran and Muthamilan, 1995).

Conclusion

Agricultural practices that reduce or eliminate chemical inputs through the use of biostimulants have been of paramount importance in recent years for sustainable and environmentally friendly agriculture. The application of biostimulants, such as PGPR in agriculture is one of the promising alternatives to combat abiotic stress and to ensure food security and environmental protection. This study revealed that the biostimulant formulated with *P. putida* and clay binder was effective on growth parameters, yield and nutritional status of maize in Benin. The best treatment was the application of biostimulant + ½ NPK-Urea, followed by the coating of maize seeds with biostimulant + ½ NPK-Urea. Both forms of biostimulant use combined with the recommended half-dose of mineral fertilizer were better than the recommended dose of mineral fertilizer in the majority of the Benin R-D study sites. Biostimulants formulated in Benin can be used to increase maize productivity while reducing the high use of mineral fertilizers. Coating maize seeds with the biostimulant require a small amount of biostimulant, less physical effort than applying the biostimulant, and is better than the recommended practice. However, the formulation process of the biostimulant deserves a slight improvement for a better adhesion of the biostimulant to the seed during coating. Nevertheless, the biostimulant formulated in Benin can be used as a seed coating for sustainable and environmentally friendly agriculture. It will be interesting to continue studies to see the acceptability of the technology by Beninese farmers and to evaluate its financial profitability.

Data availability statement

The raw data supporting the conclusions of this article will be made available by the authors, without undue reservation.

Author contributions

MA, AN, NaAA, OA, HS, and R.M.A, carried out the experimental work and analysis. MA, AN, NaAA, A.A., NeAA, and LB-M contributed to the designing, supervision, and interpretation of the results. MA, AN, A.A., NeAA, and LB-M, revised the final draft. LB-M, reviewed the final project. All authors contributed to the article and approved the submitted version.

Funding

This study (Projet CNS-Maïs—2020) was funded by Institut National des Recherches Agricoles du Bénin (INRAB).

Acknowledgments

The authors gratefully acknowledge the Centre de Recherches Agricoles-Sud (CRA-Sud) de l'Institut National des Recherches Agricoles du Bénin (INRAB) and the Laboratoire de Biologie et de Typage Moléculaire en Microbiologie (LBTMM).

Conflict of interest

The authors declare that the research was conducted in the absence of any commercial or financial relationships that could be construed as a potential conflict of interest.

Publisher's note

All claims expressed in this article are solely those of the authors and do not necessarily represent those of their affiliated organizations, or those of the publisher, the editors and the reviewers. Any product that may be evaluated in this article, or claim that may be made by its manufacturer, is not guaranteed or endorsed by the publisher.

References

Adjanohoun, A., Baba-Moussa, L., Glèlè kakaï, R., Allagbé, M., Yèhouénou, B., Gotoechan-Hodonou, H., et al. (2011). Caractérisation des rhizobactéries potentiellement promotrices de la croissance végétative du maïs dans différents agrosystèmes du sud-bénin. *Int. J. Biol. Chem. Sci.* 5, 433–444. doi: 10.4314/ijbcs.v5i2.72073

Adjanohoun, A., Noumavo, P. A., Sikirou, R., Allagbé, M., Gotoechan-Hodonou, H., Dossa, K. K., et al. (2012). Effets des rhizobactéries PGPR sur le rendement et les teneurs en macroéléments du maïs sur sol ferrallitique non dégradé au sud-bénin. *Int. J. Biol. Chem. Sci.* 6, 279–288. doi: 10.4314/ijbcs.v6i1.24

Adoko, M. Y., Agbodjato, N. A., Noumavo, A. P., Amogou, O., Adjanohoun, A., and Baba-Moussa, L. (2021b). Bioformulations based on plant growth promoting rhizobacteria for sustainable agriculture: Biofertilizer or biostimulant? *Afr. J. Agric. Res.* 17 (9), 1256–1260. doi: 10.5897/AJAR2021.15756

Adoko, M. Y., Agbodjato, N. A., Ouikoun, G. C., Amogou, O., Noumavo, P. A., Sina, H., et al. (2020). Inoculation of pseudomonas putida in farmer environment to improve growth and yield: Maize (Zea mays l.) trial in sothern, central and northern (Benin). *Int. J. Plant Soil Science.* 32, 9–21. doi: 10.9734/ijpss/2020/v32i630288

Adoko, M. Y., Sina, H., Amogou, O., Agbodjato, N. A., Noumavo, P. A., Aguégué, R. M., et al. (2021a). Potential of biostimulants based on PGPR rhizobacteria native to benin's soils on the growth and yield of maize (*Zea mays* l.) under greenhouse conditions. *Open J. Soil Science.* 11, 177–196. doi: 10.4236/ojss.2021.113010

Agbodjato, N. A., Adoko, M. Y., Babalola, O. O., Amogou, O., Badé, F. T., Noumavo, P. A., et al. (2021a). Efficacy of biostimulants formulated with *Pseudomonas putida* and clay, peat, clay-peat binders on maize productivity in a farming environment in south Benin. *Front. Sustain. Food Syst.* 5. doi: 10.3389/fsufs.2021.666718

Agbodjato, N. A., Amogou, O., Noumavo, P. A., Dagbenonbakin, G., Hafiz, A. S., Kamirou, R., et al. (2018). Biofertilising, plant-stimulating and biocontrol potentials of isolated PGPR rhizobacteria in central and north Benin. *Afr. J. Microbiol. Res.* 12, 664–672. doi: 10.5897/AJMR2018.8916

Agbodjato, N. A., Mikpon, T., Babalola, O. O., Dah-Nouvlessounon, D., Amogou, O., Lehmane, H., et al. (2021b). Use of plant growth promoting rhizobacteria in combination with chitosan on maize crop: Promising prospects for sustainable, environmentally friendly agriculture and against abiotic stress. *Agronomy*. 11, 2205. doi: 10.3390/agronomy11112205

Agbodjato, N. A., Noumavo, P. A., Adjanohoun, A., Agbessi, L., and Baba-Moussa, L. (2016). Synergistic effects of plant growth promoting rhizobacteria and chitosan on in vitro seeds germination, greenhouse growth, and nutrient uptake of maize (*Zea mays* l.). *Biotech. Res. Inter*. 2016, 7830182. doi: 10.1155/2016/7830182

Aguégué, M. R., Ahoyo Adjovi, N. R., Houédjofonon, E. M., Djinadou, K. A., Koda, D. A., Adoko, M. Y., et al. (2021a). Financial profitability of maize production with bio-fertilizer based on arbuscular mycorrhizal fungi native to Benin. *J. Dev. Agric. Economics.* 13 (1), 56–64. doi: 10.5897/JDAE2020.1221

Aguégué, R. M., Assogba, S. A., Salami, H. A. A., Koda, A. D., Agbodjato, N. A., Amogou, O., et al. (2021b). Organic fertilizer based on rhizophagus intraradices: Valorization in a farming environment for maize in the south, center and north of Benin. *Front. Sustain. Food Syst.* 5. doi: 10.3389/fsufs.2021.605610

Amogou, O., Noumavo, A. P., Agbodjato, N. A., Sina, H., Dagbénonbakin, G., Adoko, M. Y., et al. (2021). Rhizobacterial inoculation in combination with mineral fertilizer improves maize growth and yield in poor ferruginous soil in center of Benin. *BioTechnologia.* 102 (2), 141–155. doi: 10.5114/bta.2021.106520

Babalola, O. O., Fadiji, A. E., Enagbonma, B. J., Alori, E. T., Ayilara, M. S., and Ayangbenro, A. S. (2020). The nexus between plant and plant microbiome: Revelation of the networking strategies. *Front. Microbiol.* 11. doi: 10.3389/fmicb.2020.548037

Bishnoi, U. (2015). PGPR interaction: an ecofriendly approach promoting the sustainable agriculture system. *Adv. Bot. Res.* 75, 81–113. doi: 10.1016/bs.abr.2015.09.006

Bishnoi, U. (2018). Agriculture and the dark side of chemical fertilizers. *Environ. Anal. Ecol. Stud.* 3 (1), 552. doi: 10.31031/EAES.2018.03.000552

Bray, R. H., and Kurtz, L. T. (1945). Determination of total organic and available forms of phosphorus in soils. *Soil Sci.* 59, 39–45. doi: 10.1097/00010694-194501000-00006

Chaudhary, S., Dheri, G. S., and Brar, B. S. (2017). Long-term effects of NPK fertilizers and organic manures on carbon stabilization and management index under rice-wheat cropping system. *J.Soil Till.* 166, 59–66. doi: 10.1016/j.still.2016.10.005

Chaudhary, T., Dixit, M., Gera, R., Shukla, A. K., Prakash, A., Gupta, G., et al. (2020). Techniques for improving formulations of bioinoculants. *3 Biotech.* 10, 199. doi: 10.1007/s13205-020-02182-9

Connick, W. J., Boyette, C. D., and McAlpine, J. R. (1991). Formulation mycoherbicides using a pasta-like process. *Biol. Control.* 1, 281–287. doi: 10.1016/1049-9644(91)90079-F

De Pascale, S., Rouphael, Y., and Colla, G. (2017). Plant biostimulants: innovative tool for enhancing plant nutrition inorganic farming. *Eur. J. Hortic. Sci.* 82, 277–285. doi: 10.17660/eJHS.2017/82.6.2

Ding, J., Jiang, X., Ma, M., Zhou, B., Guan, D., Zhao, B., et al. (2016). Effect of 35 years inorganic fertilizer and manure amendment on structure of bacterial and archaeal communities in black soil of northeast China. *Appl. Soil ecology.* 105, 187–195. doi: 10.1016/j.apsoil.2016.04.010

Douglas, C. E., and Michael, F. A. (1991). On distribution-free multiple comparisons in the one-way analysis of variance. commun. statist. *Theory Methods* 20, 127–139. doi: 10.1080/03610929108830487

Gamez, R., Cardinale, M., Montesa, M., Ramirez, S., Schnell, S., and Rodriguez, F. (2019). Screening, plant growth promotion and root colonization pattern of two rhizobacteria (*Pseudomonas fluorescens* Ps006 and *Bacillus amyloliquefaciens* Bs006) on banana cv. williams (*Musa acuminata* colla). *Microbiol. Res.* 220, 12–20. doi: 10.1016/j.micres.2018.11.006

Glèlè Kakaï, R., Sodjinou, E., and Fonton, H. N. (2006). *Conditions d'Application des méthodes statistiques paramétriques : Application sur ordinateur* (Bénin: Bibliothèque Nationale), 86. Dépôt légal : N 378 du 8/09/006, 3ème trimestre.

Gogan, A. C., Montcho, P., Djivoh, H., and Houssou, C. (2018). *Programme national de développement de la filière maïs au bénin* (Cotonou, Bénin: Cabinet Golf Expertises), 142. BAI, B2A, MAEP.

Hassan, T. U. I., and Bano, A. (2015). The stimulatory effects of l-tryptophan and plant growth promoting rhizobacteria (PGPR) on soil health and physiology of wheat. *J. Soil Sci. Plant Nutr.* 15 (1), 190–201. doi: 10.4067/S0718-95162015005000016

Igué, A. M., Saidou, A., Adjanohoun, A., Ezui, G., Attiogbe, P., Kpagbin Gotoechan, H., et al. (2022). Evaluation de la fertilité des sols au sud et centre du Bénin. *Bull. Rech. Agron. Bénin, numèro spècial, Fertilisation du maïs*, 12–23. Available at : http://www.slire.net/download/1798/igue_et_al.evaluation_fertilit.pdf. (Accessed 12 August 12, 2022).

Ilangumaran, G., and Smith, D. L. (2017). Plant growth promoting rhizobacteria in amelioration of salinity stress: A systems biology perspective. *Front. Plant Sci.* 8. doi: 10.3389/fpls.2017.01768

Jambhulkar, P. P., and Sharma, P. (2013). Promotion of rice seedling growth characteristics by development and use of bioformulation of pseudomonas fluorescens. *Indian J. Agric. Sci.* 83, 136–142.

Jorjani, M., Heydari, A., Zamanizadeh, H. R., Rezaee, S., and Naraghi, L. (2011). Development of *Pseudomonas fluorescens* and *Bacillus coagulans* based bioformulations using organic and inorganic carriers and evaluation of their influence on growth parameters of sugar beet. *J. Biopesticides.* 4 (2), 180–185.

Kamilova, F., Okon, Y., de Weert, S., and Hora, K. (2015). "Commercialization of microbes: Manufacturing, inoculation, best practice for objective field testing, and registration," in *Principles of plant-microbe interactions*. Ed. B. Lugtenberg (Cham: Springer), 319–327. doi: 10.1007/978-3-319-08575-3_33

Khan, N., Martínez-Hidalgo, P., Ice, T. A., Maymon, M., Humm, E. A., Nejat, N., et al. (2018). Antifungal activity of bacillus species against fusarium and analysis of the potential mechanisms used in biocontrol. *Front. Microb.* 9. doi: 10.3389/fmicb.2018.02363

Khashei, S., Etemadifar, Z., and Rahmani, H. R. (2020). Multifunctional biofertilizer from *Pseudomonas putida* PT: A potential approach for simultaneous improving maize growth and bioremediation of cadmium-polluted soils. *BJM.* 8 (32), 117–129. doi: 10.22108/bjm.2019.115315.1181

Kjeldahl, J. (1883). A new method for the determination of nitrogen in organic matter. *Z. Anal. Chem.* 22, 366–382. doi: 10.1007/BF01338151

Kourgialas, N. N., Karatzas, G. P., and Koubouris, G. C. (2017). A GIS policy approach for assessing the effect of fertilizers on the quality of drinking and irrigation water and wellhead protection zones (Crete, Greece). *J. Env. Man.* 189, 150–159. doi: 10.1016/j.jenvman.2016.12.038

Kumar, R., and Shastri, B. (2017). "Role of phosphate-solubilising microorganisms in sustainable agricultural development," in *Agro-environmental sustainability*. Eds. J. Singh and G. Seneviratne (Cham: Springer). doi: 10.1007/978-3-319-49724-2_13

Lin, Y. R., Watts, D. B., Kloepper, J. W., Adesemoye, A. O., and Feng, Y. C. (2019). Effect of plant growth promoting rhizobacteria at various nitrogen rates on corn growth. *Agric. Sci.* 10, 1542–1565. doi: 10.4236/as.2019.1012114

Liu, K., McInroy, J. A., Hu, C. H., and Kloepper, J. W. (2018). Mixtures of plant-growth-promoting rhizobacteria enhance biological control of multiple plant diseases and plant-growth promotion in the presence of pathogens. *Plant Dis.* 102, 67–72. doi: 10.1094/PDIS-04-17-0478-RE

MAEP. (2016). Catalogue Béninois des Espèces et Variétés végétales (CaBEV), 2ème Edn. *Ministère de l'Agriculture de l'Elevage et de la Peche; INRAB/DPVPPAAO/ProCAD/MAEP & CORAF/WAAPP, Dépôt légal N° 8982 du 21 octobre 2016, Bibliothèque Nationale du Bénin, 4ème trimestre*, 12–23. Available at: http://inrab.org/wp-content/uploads/2018/01/CaBEV-interactif-2.pdf. (Accessed Jun 22, 2022).

Mahanty, T., Bhattacharjee, S., Goswami, M., Bhattacharyya, P., Das, B., Ghosh, A., et al. (2017). Biofertilizers: a potential approach for sustainable agriculture development. *Environ. Sci. pollut. Res.* 24, 3315–3335. doi: 10.1007/s11356-016-8104-0

Meena, K. K., Sorty, A. M., Bitla, U. M., Choudhary, K., Gupta, P., Pareek, A., et al. (2017). Abiotic stress responses and microbe-mediated mitigation in plants: the omics strategies. *Front. Plant Sci.* 8. doi: 10.3389/fpls.2017.00172

Metson, A. J. (1956). Methods of chemical analysis for soil survey samples. *N Z Soil Bur Bull.* 12, 208. doi: 10.2134/agronj1957.00021962004900040024x

Neufeld, K. R., Grayston, S. J., Bittman, S., Krzic, M., Hunt, D. E., and Smukler, S. M.. (2017). Long-term alternative dairy manure management approaches enhance microbial biomass and activity in perennial forage grass. *Biol. Fertil Soils.* 53, 613–626. doi: 10.1007/s00374-017-1204-2

Noumavo, A. P., Agbodjato, A. N., Gachomo, E. W., Salami, H. A., Baba-Moussa, F., Adjanohoun, A., et al. (2015). Metabolic and biofungicidal properties of

maize rhizobacteria for growth promotion and plant disease resistance. *Afr. J. Biotechnol.* 14 (9), 811–819. doi: 10.5897/AJB2014.14132

Olanrewaju, O. S., Oyatomi, O., Babalola, O. O., and Abberton, M. (2022). Breeding potentials of bambara groundnut for food and nutrition security in the face of climate change. *Front. Plant Sci.* 12. doi: 10.3389/fpls.2021.798993

Postma, J. A., and Lynch, J. P. (2011). Root cortical aerenchyma enhances the growth of maize on soils with suboptimal availability of nitrogen, phosphorus, and potassium. *Plant Physiol.* 156 (3), 1190–1201. doi: 10.1104/pp.111.175489

Priyanka, P., Mukherjee, S., and Malik, S. (2020). Plant growth promoting rhizobacteria role in agriculture biotechnology. *Adv. Biores.* 11 (2), 172–177. doi: 10.15515/abr.0976-4585.11.2.172177

R Core Team (2020). *A language and environment for statistical computing* (Vienna, Austria: R Foundation for Statistical Computing). Available at: http://www.r-project.org/index.html.

Rosier, A., Medeiros, F. H., and Bais, H. P. (2018). Defining plant growth promoting rhizobacteria molecular and biochemical networks in beneficial plant-microbe interactions. *Plant Soil.* 428, 35–55. doi: 10.1007/s11104-018-3679-5

Ruget, F., and Bonhomme Chartier, M. (1996). Estimation simple de la surface foliaire de plantes de maïs en croissance. *Agronomie.* 16, 553–562. doi: 10.1051/agro:19960903

Thomas, L., and Singh, I. (2019). "Microbial biofertilizers: Types and applications," in *Biofertilizers for sustainable agriculture and environment, soil biology*. Eds. B. Giri, R. Prasad, Q. S. Wu and A. Varma (Cham, Switzerland: Springer), 1–19. doi: 10.1007/978-3-030-18933-4_1(2020)

Tomer, S. K., Al Bitar, A., Sekhar, M., Zribi, M., Bandyopadhyay, S., and Kerr, Y. (2016). MAPSM: A spatio-temporal algorithm for merging soil moisture from active and passive microwave remote sensing. *Remote Sens.* 8, 990. doi: 10.3390/rs8120990

Valdés, E. M. F., González, E. C., Serrano, M. M., Labrada, H. R., Báez, E. M., Hernández, F. G., et al. (2013). Experiencias obtenidas en el desarrollo participativo de híbridos lineales simples de maíz (*Zea mays*, l.) en condiciónes de bajos insumos agrícolas. *Cultivos Tropicales.* 34 (2), 61–69. Available at: http://scielo.sld.cu/pdf/ctr/v34n2/ctr10213.pdf.

Vejan, P., Abdullah, R., Khadiran, T., Ismail, S., and Nasrulhaq Boyce, A. (2016). Role of plant growth promoting rhizobacteria in agricultural sustainability. a review. *Molecules.* 21, 573. doi: 10.3390/molecules21050573

Vidhyasekaran, P., and Muthamilan, M. (1995). Development of formulations of *Pseudomonas fluorescens* for control of chickpea wilt. *Plant Dis.* 79, 782–786. doi: 10.1094/PD-79-0782

Walkley, A., and Black, I. A. (1934). An examination of the degtjareff method for determining soil organic matter and a proposed modification of the chromic acid titration method. *Soil Sci.* 37, 29–38. doi: 10.1097/00010694-193401000-00003

Xu, X., Thornton, P. E., and Post, W. M. (2013). A global analysis of soil microbial biomass carbon, nitrogen and phosphorus in terrestrial ecosystems. *Global Ecol. Biogeography.* 22 (6), 737–749. doi: 10.1111/geb.12029

Yallou, C. G., Aïhou, K., Adjanohoun, A., Toukourou, M., Sanni, O.A., and Ali, D. (2010). Itinéraires Techniques de Production de Maïs au Bénin. Fiche technique. Dépôt légal N° 4922 du 3 Décembre, Bibliothèque Nationale du Bénin, 18.

frontiers | Frontiers in Plant Science

TYPE Original Research
PUBLISHED 19 January 2023
DOI 10.3389/fpls.2022.1098772

OPEN ACCESS

EDITED BY
Aqeel Ahmad,
University of Florida, United States

REVIEWED BY
Sagheer Ahmad,
Environmental Horticulture Research Institute, Guangdong Academy of Agricultural Sciences, China
Sami Ullah,
University of Sargodha, Pakistan
Hafiz Muhammad Rizwan,
Shenzhen University, China

*CORRESPONDENCE
Abdolkarim Cheheregani Rad
chehregani@basu.ac.ir

SPECIALTY SECTION
This article was submitted to Plant Symbiotic Interactions, a section of the journal Frontiers in Plant Science

RECEIVED 15 November 2022
ACCEPTED 23 December 2022
PUBLISHED 19 January 2023

CITATION
Salehi H, Cheheregani Rad A, Raza A, Djalovic I and Prasad PVV (2023) The comparative effects of manganese nanoparticles and their counterparts (bulk and ionic) in *Artemisia annua* plants *via* seed priming and foliar application.
Front. Plant Sci. 13:1098772.
doi: 10.3389/fpls.2022.1098772

The comparative effects of manganese nanoparticles and their counterparts (bulk and ionic) in *Artemisia annua* plants *via* seed priming and foliar application

Hajar Salehi [1], Abdolkarim Cheheregani Rad [1]*, Ali Raza [2], Ivica Djalovic [3] and P. V. Vara Prasad [4]

[1]Laboratory of Plant Cell Biology, Department of Biology, Bu-Ali Sina University, Hamedan, Iran, [2]College of Agriculture, Fujian Agriculture and Forestry University, Fuzhou, China, [3]Institute of Field and Vegetable Crops, National Institute of the Republic of Serbia, Novi Sad, Serbia, [4]Department of Agronomy, Kansas State University, Manhattan, KS, United States

The world has experienced an unprecedented boom in nanotechnology. Nanoparticles (NPs) are likely to act as biostimulants in various plants due to having high surface/volume value. However, understanding the actual effect of NPs is essential to discriminate them from other counterparts in terms of being applicable, safe and cost-effective. This study aimed to assay the impact of manganese(III) oxide (Mn_2O_3)-NPs *via* seed-priming (SP) and a combination of SP and foliar application (SP+F) on *Artemisia. annua* performance at several times intervals and comparison with other available manganese (Mn) forms. Our findings indicate that SP with $MnSO_4$ and Mn_2O_3-NPs stimulates the processes that occur prior to germination and thus reduces the time for radicle emergence. In both applications (i.e., SP and +F), none of the Mn treatments did show adverse phytotoxic on *A. annua* growth at morpho-physio and biochemical levels except for Mn_2O_3, which delayed germination and further plant growth, subsequently. Besides, from physio-biochemical data, it can be inferred that the general mechanism mode of action of Mn is mainly attributed to induce the photosynthetic processes, stimulate the superoxide dismutase (SOD) activity, and up-regulation of proline and phenolic compounds. Therefore, our results showed that both enzymatic and non-enzymatic antioxidants could be influenced by the application of Mn treatments in a type-dependent manner. In general, this study revealed that Mn_2O_3-NPs at the tested condition could be used as biostimulants to improve germination, seedling development and further plant growth. However, they are not as effective as $MnSO_4$ treatments. Nonetheless, these findings can be used to consider and develop Mn_2O_3-NPs priming in future studies to improve seed germination and seedling quality in plants

KEYWORDS

antioxidant compounds, biostimulants, germination index, nanotechnology, nutripriming, seed priming

1 Introduction

Nanotechnology is currently starting to govern various aspects of human life and getting to shape the near future of a number of disciplines, such as physics, biology, material science and so on. For the time being, some studies have displayed an optimistic side of this technology in plant science as well. Nanoparticles (NPs) have been explored as "multifunctional particles" carrying agrochemicals such as herbicides, fertilizers, and have been recently delivered genes, targeting the specific cell organelles (Das et al., 2009; Ahmar et al., 2021). Plants can benefit through the appropriate usage of nanomaterials at a lower amount as they have shown higher efficiency and probably lower contamination (Pérez-de-Luque, 2017). Although this scenario is something scientific society is willing to believe in, but it needs extra and persuadable work to prove it. Being used in the right place and at the right time with an effective method, nanoparticles can improve plant performance, particularly at the early stages of development. The expected effects have been reported to be increased germination, healthier seedlings and higher biomass in terms of growth indices (Szőllősi et al., 2020; Wu and Li, 2021). The NPs-induced alteration is highly influenced by many factors, such as the nature of NPs themselves, dosages, plant species and the application procedure (Khan et al., 2019; Salehi et al., 2021a; Salehi et al., 2021b). In this regard, studies are trying to provide evidence on how NPs work, but getting the whole overview is extremely complicated. Part of this complexity in plants is dealing with thousands of different plant species. Another reason is that most of the studies have been performed in some plant models or agricultural-related crops, and also the experiments have been limited to the early seedling stages (Pérez-de-Luque, 2017).

The application of oxide metal ions and metal NPs applied at lower dosages has been found to be eco-friendly, reduce oxidative stress, positively affect germination index, and promote biosynthesis of photosynthetic pigments, various enzymatic and non-enzymatic molecules, which is reflected in improved plant growth and development (Salehi et al., 2019; Kumari et al., 2022). Some studies have reported similar effects of NPs to their ionic and bulk counterparts (Jeevanandam et al., 2018; Pullagurala et al., 2018a; Pullagurala et al., 2018b); however, contrary results have been obtained by some others, indicating different effects of NPs due to their specific characteristics (Santiago et al., 2020; Kralova and Jampilek, 2021). On the other hand, it is not fully accepted that NPs forms have much more influence on plants. To achieve higher yield by NPs, it is vital to explore which kind of NPs and at which concentrations boost plant growth for individual plant species. Crop plants have been widely investigated to assay NPs effects from both negative and positive perspectives. However, how NPs affect medicinal plants is another key aspect of plant-NPs interactions, because it will affect the practical application of NPs.

Medicinal plants, considered as rich resources of ingredients either in pharmaceutical and food science, play not only an important role in medicine but also as phytochemical building blocks for the development of new drugs (Zahra et al., 2020). These valuable plants should generally not be cultivated in contaminated medium, and chemicals applied to promote their growth should be kept to a minimum in order to avoid showing toxic signs. Moreover, it is critical to introduce safe and favorable conditions for their germination and development. Regarding this, using NPs has recently been interested due to using a lower amount of active ingredient to obtain the biological results as similar to their bulk and ionic counterparts. To the best of the authors' knowledge, only a small number of researches on medicinal plants have been incorporating NPs. So far, several studies have shown the beneficial effects of NPs such as Ag, Cu, Fe, Zn and Ti on germination, seedling performance, and biochemical compounds in a limited number of medicinal plants like *Salvia officinalis* (Moazzami Farida et al., 2020), *Rosmarinus officinalis* (Hadi Soltanabad et al., 2020), *Mentha longifolia* (Talankova-Sereda et al., 2016), *Origanum vulgare* (Du et al., 2018), *Cuminum cyminum* (Sabet and Mortazaeinezhad, 2018), *Dracocephalum kotschyi* (Nourozi et al., 2019), *Tanacetum parthenium* (Shahhoseini et al., 2020), *Stevia rebaudiana* (Velázquez-Gamboa et al., 2021) and *Mentha piperita* (Ahmad et al., 2018). It has been reported that mild oxidative stress induced by NPs at the level of nontoxic concentrations can stimulate seed germination and enhance plant performance to achieve higher yields (Landa, 2021). In the case of medicinal plants, this event may boost the biosynthesis of valuable secondary compounds as well.

Manganese (Mn) is an essential micro-metalloid sustaining metabolic roles within cell compartments, which is led to plant growth and development. The metal has various roles in plant's metabolic processes, including being an important metalloenzyme cofactor in photosynthetic machinery, respiration, detoxification of reactive oxygen species (ROS), and hormone transduction signaling (Alejandro et al., 2020). Nanoscale Mn compared to conventional ionic and bulk Mn species found to be a better source of Mn and less phytotoxic, and thus more effective in minimizing internal and external stresses in plants (Ye et al., 2019). A recent study reported that watermelon seeds primed with MnO-NPs show less phytotoxicity compared to the bulk forms ($KMnO_4$ and Mn_2O_3). The findings indicated that MnO-NPs at 20 mg L^{-1} significantly affect the chlorophyll and antioxidant metabolites, while at ≤ 40 mg L^{-1}, phenolic and phytohormone profiles were altered (Kasote et al., 2021). Although there is evidence of promoting and alleviating the effect of different traditional types of Mn on plant growth, the unknown effects related to Mn_2O_3-NPs medicinal plant interaction need to be discovered.

Artemisia annua, an herbal plant, is the only commercially available resource for artemisinin biosynthesis, which has been applied to cure malaria for so long. Besides, the extracted compounds from *A. annua* have also been reported to have promising therapeutic effects for diabetes, tuberculosis, and,

recently corona virus (Shen et al., 2022). These findings further accelerate the global demand for huge amounts of *A. annua* plants and, therefore, their functional compounds. Taking this into account, the use of nutripriming could be an effective strategy to improve the growth and development of A. annua, thus providing higher yields. Since, soil application of Mn is often not effective due to its conversion to plant-unavailable Mn oxidase, in this study, we have used seed priming and foliar application of Mn_2O_3-NPs and their counterparts to assay and comparison their mode-of-action. Seed priming has been proven to be an effective method to stimulate seed germination rate and seedling emergence, leading to high-quality seedlings and improved plant growth (Adhikari et al., 2022). Nutri-seed-priming enhances water uptake into seeds, triggering starch metabolism and, therefore, faster seed germination (Nile et al., 2022). On the other hand, foliar application with NPs-based nutrients provides a faster and more efficient way to trap essential nutrients (Salehi et al., 2018; Salehi et al., 2021a). Based on these reports, we hypothesis that a combination of seed priming and foliar application has a better effect on plant growth.

2 Material and methods

2.1 Mn_2O_3 NPs preparation and characterization

Particulate Mn_2O_3-NPs with a size of 30 nm, 99.2% purity, surface area of 150 m^2 g^{-1}, and true density of ~0.35 g^{-1} cm^3 were obtained from NANOSANY Co. Ltd, Mashhad, Iran. Their physico-chemical properties, including scanning electron microscopy (SEM), transmission electron microscopy (TEM) and powder X-ray diffraction (XRD) have been presented in Figure S1. $MnSO_4$, $MnCl_2$ and Mn_2O_3 were also purchased from Sigma Aldrich (Germany).

2.2 Experimental design, phyto-safety of Mn_2O_3-NPs assay, and sample harvesting

Artemisia Annua seeds were obtained from Plant Bank, Iranian Biological Resource Center (IBRC, Tehran, Iran). This species has been recommended for high yields of bioactive compounds and, therefore, is applicable in clinical industry (Dogan et al., 2022). The experiment presented here was carried out using a completely randomized design in 2022 at Laboratory of Plant Cell Biology, Department of Biology, Bu-Ali Sina University, Hamedan, Iran. The Mn_2O_3-NPs concentration and time used in this experiment were determined after a phyto-safety germination test. Briefly, the sterilized seeds were primed with three different concentrations (25, 50, and 100 mg L^{-1}) of Mn_2O_3-NPs for 3 and 6 h and incubated in a germinator chamber for 10 days. The concentrations were selected according to available studies that highlight these levels cannot be considered phytotoxic in plants (Tian et al., 2018; Li et al., 2020; Kasote et al., 2021). The results of germination test showed that seed priming with 50 mg L^{-1} for 3 h causes a higher germination percentage (Figure S2). In this experiment, we used two applications (seed priming (SP) and a combination of seed priming+foliar spray (SP+F). The latter was done to evaluate the possible further improve plant growth under Mn treatments. Following germination, harvesting for analyses was carried out at several developmental stages including early vegetative (60 day), before flowering (90 day) and during flowering (120 day) stages. The schematic design of the experiment is shown in Figure 1A.

After selecting two factors (concentration and seed priming (SP) time), to assay seed germination, Mn_2O_3-NPs, $MnSO_4$, $MnCl_2$ and Mn_2O_3 suspensions were individually prepared in Milli-Q water and sonicated for 30 min before use to avoid aggregation. Ionic and bulk compounds were used as a positive control to assay the effect of different species of Mn on plant growth. *A. annua* seeds were presoaked in 2 mL of each priming solution for 3 h in a shaker to prime all seeds equally. Seeds soaked in Milli-Q water were used as hydro-primed control. After drying, primed seeds were divided into several groups and sown in a plug tray filled with coco perlite-vermiculite for germination and early seedling development. The germination-related parameters were measured after the whole germination for 10 days after sowing. After 30 days, the healthy seedlings from each treatment were transformed into growing pots (13 cm diameter and 15 cm height) containing 2 kg of local soil (pH=7.66, electrical conductivity =0.21ds/m, cation exchange capacity =28.17 meq/100g, $CaCO_3$ = 24.45%, organic matter=3.78%, and organic carbon=2.19%). Pots were then incubated in the environmental growth chamber (24 ± 5 temperature, 70% relative humidity and 12h photoperiod) for 120 days, till the flowering stage. These pots were already divided into two main groups (one for SP and other for SP+F). At least 50 seeds were used per group. The depth of the holes was 4 cm. The first group of plants was used to investigate the effect of Mn_2O_3-NPs SP method and then compared with other counterparts. The two-month-old plants grown in SP condition were selected for spray application (second group). Plants were sprayed with 5 mL suspensions at 75 and 105 days after planting (10 mL in total). During the foliar spray, an aluminum wrap was used to cover the soil surface to avoid contamination. Overall, samples were harvested three times at 60, 90 and 120 days after transplanting, which are determined as early vegetative seedlings, before and during flowering development stages. Samples were thoroughly washed with milli-Q water to remove Mn residues prior to freezing at -80°

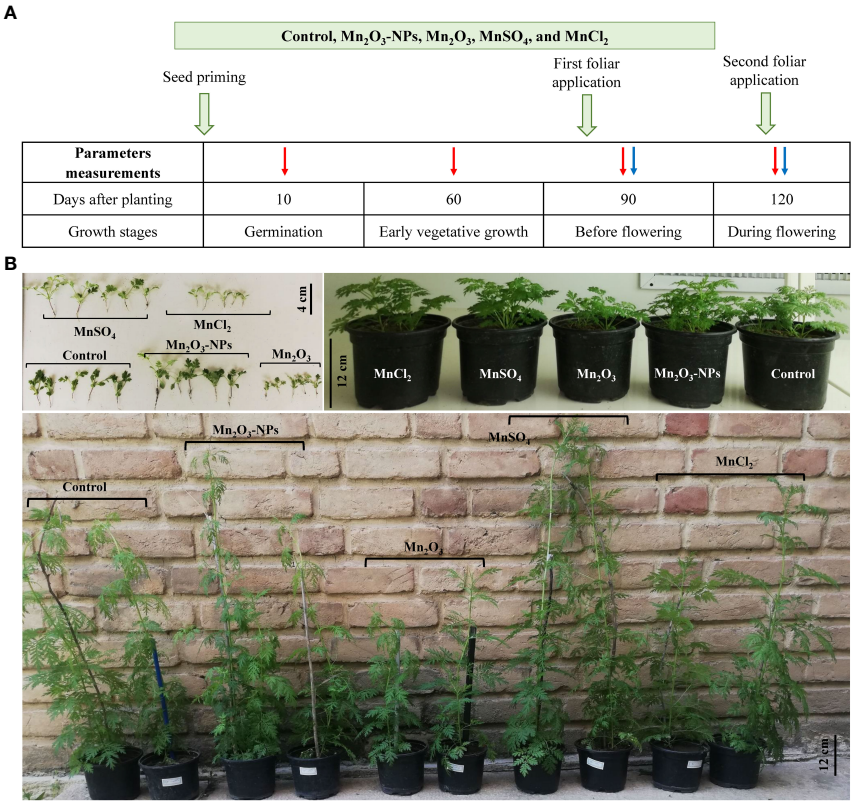

FIGURE 1
Schematic design of the treatments in the experiment **(A)**; the orange arrows indicate the time of treatments; the red and blue arrows show the parameters measured time-intervals in SP and SP+F conditions, respectively, to investigate the effects of Mn treatments in *A. annua*. Figure **(B)** is related to the plant growth at seedlings (top-left), 60 days (top-right) and 120 days (bottom) after planting. In the bottom figure, the post labeled in white are related to the SP condition.

C for further analysis. It is worth mentioning that plants were regularly watered to keep almost 60% of soil field capacity. In this experiment, no additional fertilizer was added. Five replicates (pots) were used for each treatment.

2.3 Germination and growth parameters analysis

Germination test was conducted in the dark at 25°C for 10 days. Sets of 20 primed seeds from each treatment were placed in Petri dishes and incubated in the germination chamber (25 ± 2° C, 80% humidity). Germination rates were assessed by counting the number of germinated seeds (1 mm radicle emergence) at every 24 h intervals. The germination and initial seedling growth-related variables including germination index (GI), germination percentage (GP), relative seed germination (RSG), and coefficient of the velocity of germination (CVG) were measured according to the previously reported formulas (Sobarzo-Bernal et al., 2021). At each developmental stage, plant height was measured per pot from the ground level to the panicle tip. In addition, dry weight was also measured at the end of the trial.

2.4 Determination of leaf relative water content and electrolyte leakage

Leaf relative water content (RWC), reflecting the balance between water supply and transpiration rate, was used to assay water status in *A. annua* plants after Mn treatments. In detail, two fully expanded and healthy leaves of three plants per replicate were cut, weighted and then floated in 20 mL distilled water for 24 h at room temperature for full hydration. The leaves were then blotted on a dry surface with filter paper. Following that, turgid and dry weights (at 70°C for 2 d) were measured. RWC was calculated following the equation: RWC = (FW-DW)/(TW-DW)×100. Where FW, DW, and TW are fresh weight, dry weight, and turgor weight, respectively.

Electrolyte leakage (EL), as cell membrane injury, was measured following the method of Lutts, 2004 (Lutts et al., 2004). Briefly, three fresh, mature and healthy leaves (the 4th leaf

from the tip) per plant were chosen, washed with distilled water until removing surface contamination and then cut into small pieces (1 cm). The leaf segments were placed in individual test tubes containing 15 mL of distilled water. After 24 h incubation at 25°C (room temperature), the electrical conductivity of the solution was read (EC_1). EC_2 was read after autoclaving (121°C for 15 min) and cooling down the solution to room temperature. The EL was calculated as the following equation: EL = (EC_1/EC_2)×100.

2.5 Determination of lipid peroxidation markers (MDA and H_2O_2content)

Hydrogen peroxidase (H_2O_2) and malondialdehyde (MDA) concentrations are the widely used method to analyze lipid peroxidation in plants. Potassium iodide (KI) was used to assay hydrogen peroxide (H_2O_2) level (Alexieva et al., 2001). Briefly, leaf tissues (0.5 g) were grinded in mortar and pestle with liquid nitrogen and thoroughly homogenized with 5 mL 0.1% (w/v) trichloroacetic acid (TCA). The homogenate mixture was centrifuged at 12000 revolutions per minute (rpm) at 4°C for 15 min. Reaction mixture consisted 0.5 mL extract supernatant, 0.5 mL 10 mM potassium phosphate buffer (pH 7.0) and 1 mL reagent (1 M KI w/v in fresh double-distilled water). The absorbance of reaction was measured at 390 nm and the content of H_2O_2 was calculated using a standard curve prepared with known concentrations of H_2O_2. The blank consisted of 0.1% TCA without leaf extract.

The same extract used for H_2O_2 measurement was also used for estimating the MDA level. To initiate the reaction, 225 µL of the extract was incubated with 1.5 mL of 20% TCA containing 0.5% thiobarbituric acid (TBA) for 40 min at 95 °C. The reaction was stopped by cooling it quickly in an ice bath, then centrifuged for 10 min at 6000 rpm to clear the reaction mixture. The absorbance of the supernatant was read at 532 nm and corrected for unspecific turbidity by subtracting the value from the absorbance at 600 nm. The MDA concentration was calculated using an extinction coefficient of 155 mM^{-1} cm^{-1} and expressed as mmol mg^{-1} fresh weight (Stewart and Bewley, 1980).

2.6 Chlorophylls and total carotenoid content

The spectral (Biowave II, England) determination of chlorophyll (Chl) a, b, and total, as well as total carotenoids of *A. annua* leaves (500 mg) was performed using 80% acetone (10 mL) according to the method of Arnon (Arnon, 1949). The related absorbance was taken at 663, 645 and 470 nm, respectively. The content of Chl a = 12.25 × A_{664}–2.55 × A_{645}, Chl b = 20.31 × A_{645}–6.91 × A_{664}, total Chl = 17.76 × A_{645} +7.37 × A_{664}, and carotenoids=A_{470}+(0.114×A_{663}) -(0.638×A_{645}) were then calculated and data were reported as mg pigments per g fresh weight.

2.7 Total phenolic and flavonoid content

To assay the total phenolic and total flavonoid content, the methanolic extract was prepared by grinding and homogenizing 300 mg of fresh tissues with 3 ml methanol 80% (0.1% formic acid). Then the mixture was centrifuged at 6000 rpm for 10 min at room temperature. The supernatant was used for further analyses.

The total phenolic content (TPC) was estimated by Folin-Ciocalteu (F-C) method (Chun et al., 2003) with a little modification. Briefly, 100 µL of the metabolic extract was mixed with 400 µL water and 500 µL F-C reagents (10 fold diluted with distilled water). The mixture was stand at room temperature for 5 min, and afterward, 1 mL of sodium carbonate (7.5%) was added to the mixture and then incubated in darkness for 2h. The absorbance of mixture was recorded at 765 nm. The TPC concentration was expressed in terms of gallic acid equivalent (mg gallic acid/g of fresh mass).

An aluminium chloride ($AlCl_3$) colorimetric assay was applied to measure the total flavonoid content (Zhishen et al., 1999). The mixture contained 500 µL methanolic extract, 2 mL distilled water, and 150 µL 5% sodium nitrate was left at room temperature for 10 min. Thereafter, 300 µL 10% $AlCl_3$ was added and incubated for another 15 min. The absorbance was read at 510 nm versus a blank. Total flavonoid content was expressed as mg catechin (CA) equivalents per g of fresh weight.

2.8 Proline content

The proline content was assayed to monitor the physiological status of *A. annua* with a standard ninhydrin-based method using a cuvette spectrophotometer (Bates et al., 1973). Briefly, fresh tissues (0.2 g) were homogenized in 5 mL of 3% aqueous sulfosalicylic acid and left for 1h to complete the extraction. The solution was centrifuged at 6000 rpm for 10 min. The mixture containing 2 mL of supernatant, 2 mL glacial acetic acid and 2 mL acidic ninhydrin was then boiled in a water bath for 60 min. The reaction was stopped by placing the mixture in an ice bath and afterward 4 mL of toluene was added and mixed vigorously using a vortex. After reaching room temperature the absorbance was read at 520 nm against toluene, as blank. The proline content was calculated using a standard curve from 20-100 µg/mL of L-proline.

2.9 Soluble protein content and enzyme assay

Crude enzyme extracts were prepared by grinding 500 mg of leaves tissue using liquid nitrogen and homogenized thoroughly

in 5 mL of potassium phosphate buffer (PPB) (100 mM, pH 7.8) containing 1 mM EDTA and 1% w/v polyvinylpyrrolidone (PVP). The homogenate was then centrifuged at 10000 rotations per min (rpm) at 4 °C for 15 min to remove debris. The supernatant was used for further analysis. Bradford dye-binding method was used to assay soluble proteins.

Catalase (CAT, EC 1.11.1.6) activity was assayed by estimating the initial rate of disappearance of H_2O_2 followed by Beers and Sizer method (Beers and Sizer, 1952). The reaction mixture contains 2.8 mL of 50 mM PPB, 0.1 mL of enzyme extract, and 30 µL of 15 mM H_2O_2. CAT activity was measured in 1 minute at 240 nm using a UV-visible spectrophotometer. One enzyme unit corresponds to the amount of enzyme required to break down one µM of H_2O_2 min^{-1} or mg^{-1} protein (extinction coefficient of 34 mM cm^{-1}).

Polyphenol oxidase (PPO, EC 1.14.18.1) activity was assayed by the method of Raymond et al. (Raymond et al., 1993). The enzyme was assayed by putting 2.5 mL of assay buffer (PBP 50 mM, pH 7) and 0.2 ml of pyrogallol (20 mM) in a cuvette of 5ml capacity. The assay reaction was initiated by adding 0.1 mL of enzyme extract, followed by recording the change in absorbance at 420 nm wavelength, simultaneously for 3 min. The enzyme activity was expressed as pyrogallol oxidized after 3 min per mg protein (unit mg^{-1} protein).

To assay ascorbate peroxidase (APX, EC 1.11.1.11) activity, a total reaction mixture containing 2.5 mL PPB (50 mM, pH 7), 30 µL H_2O_2 (0.1 mM), 300 µL ascorbic acid (0,5 mM), 30 µL EDTA (0.1 mM), and 150 µL enzyme extract was put into a cuvette. The decrease in absorbance was recorded at 290 nm for two min. Extinction coefficient of 2.8 mM cm^{-1} was used to calculate the amount of ascorbate oxidized (unit mg^{-1} protein) (Jebara et al., 2005).

Superoxide dismutase (SOD, EC 1.15.1.1) activity was measured by screening enzyme ability to inhibit the photochemical reduction of nitrotetrazolium blue (NBT), according to Fu and Huang protocol (2001). Briefly, each 3 mL of reaction mixture contained 50 µl of enzyme extract, 1 mL NBT (63 µM), 1 mL riboflavin 1.3 µM, 750 µL methionine (13 mM), and 250 µL EDTA (0.1 mM). Reaction was initiated by exposing the test tubes under fluorescent lamp for 10 min and stopped by switching off the lamp, anf then the absorbance was read at 560 nm. The blank reaction mixture was kept in the dark the whole time. SOD activity was expressed in units per min per mg protein. One unit of SOD was defined as the amount of enzyme that inhibits 50% of NBT photoreduction.

2.10 Statistical analysis

All estimated data were analyzed using the SPSS program (SPSS, Chicago, IL, USA). A one-way analysis of variance (ANOVA) and Duncan comparison test were performed to compare the mean values of the control plants verse the Mn-treated plants. Data are represented as mean ± standard error, and significant differences were determined at $P \leq 0.05$. A multivariate analysis, including a principal component analysis (PCA) and Pearson's moment-product correlations were further performed with individual values of all the parameters. A heatmap and cluster analysis was performed using ClustVis (www.biit.cs.ut.ee/clustvis/).

3 Results

3.1 The effect of different Mn forms on germination and plant growth

The results showed germination-related parameters, including CVG, RSG, GI, and GP showed significant differences between treatments (Table 1). Seeds treated with $MnSO_4$ and Mn_2O_3-NPs exhibited a mean value of GI and RSG parameters higher than 100%. In addition, the germination percentage in these two treatments were significantly higher than in others. These results represent a biostimulant effect of Mn_2O_3-NPs and particularly $MnSO_4$ on germination. However, seeds treated with $MnCl_2$ and Mn_2O_3 showed decreased mean

TABLE 1 Germination-related parameters of *A.annua* seeds primed with different Mn species.

Treatments	Germination Index	Relative Seed Germination (%)	Coefficient of Velocity of Germination	Germination Percentage (%)
Control	100.00 ± 00b	100.00 ± 0.00a	43.50 ± 4.41ab	81.11 ± 2.94a
Mn_2O_3-NPs	115.62 ± 7.03b	107.41 ± 7.41a	46.06 ± 2.49a	84.44 ± 1.11a
Mn_2O_3	21.31 ± 3.13c	48.48 ± 9.74b	29.93 ± 3.53c	32.22 ± 2.94c
$MnSO_4$	157.70 ± 23.12a	123.91 ± 12.94a	52.41 ± 2.88a	88.89 ± 2.94a
$MnCl_2$	51.27 ± 4.25c	69.61 ± 5.83b	34.71 ± 2.71bc	63.33 ± 3.85b
Sig	**	**	**	**

**means significant at $p \leq 0.005$.
Means ± SDs with different letters in each column indicate significant statistical differences (P≤, 0.05).

values in all parameters. Notably, Mn_2O_3, GI, RSG, and CVG parameters were decreased by 77%, 51%, and 31% compared to the control, respectively (Table 1). Additionally, Mn_2O_3 delayed the onset of germination by about 6-8 days. Figure 2 exhibits the shoot length and dry weight of *A. annua* plants after priming and foliar spraying of different Mn forms. At almost every developmental stage, shoot length was improved by $MnSO_4$ treatment compared with control and other treatments (Figures 1, 2). However, Mn_2O_3-NPs only had the inducing effect on shoot length at 30 days after planting (an increase of 24% compared to control), and after that, it was the same as the control condition.

Under Mn_2O_3 treatment, a significant decrease (42%) in plant growth was noted, as can be explained by lower and late germination. The comparison of plant growth after 120 days after planting in two application ways (i.e., SP and SP+F) showed the same trend, as $MnSO_4$ and Mn_2O_3 caused an increased and decreased, respectively. Analysis of variance showed that there is no significant difference between the two applications but treatments had significant effects ($P<0.005$) on plant growth. The RWC didnot show a remarkable difference between treatments and also applications (Figure 2D).

3.2 Changes in electrolyte leakage and cell injury indicators

The plants treated with Mn species were checked for electrolyte leakage (EL). The results showed that none of Mn treatments significantly affected EL in plants grown under SP conditions (Figure 3A). However, EL increased during plant growth, particularly at 120 days which could be due to the intrinsic changes of plant itself, like the senescence process. In SP +F application, at 90 days when foliar spray was done, EL increased slightly in Mn treatments compared to control. These changes at 120 days also showed significant differences between all Mn forms in which Mn_2O_3 induced higher EL, while NPs minimized it. Generally, a significant application-dependent change was observed in which EL was lower in SP +F compared to SP, indicating a mild alleviating effect of Mn foliar spray.

Furthermore, the MDA and H_2O_2 contents, known as cell injury indicators, were also monitored (Figures 3B, C). The content of MDA and H_2O_2 in almost all treatments in both applications was increased as plant grows, which originated from the internal metabolism. However, their content in Mn_2O_3 treatment in plants grown under SP conditions was lower compared to control and other treatments. This was expected because of the late germination and, thus, the stunned vegetative growth. Contrarily, a decreased MDA and H_2O_2 in some treatments like $MnSO_4$ and Mn_2O_3-NPs compared to control can be attributed to the positive effect of these Mn forms. Regarding SP+F application, the differences between treatments were not statistically significant. However, the first spray of Mn_2O_3-NPs and $MnCl_2$ treatments showed slightly decreased MDA and H_2O_2 content. The multivariate analysis showed no significant differences in MDA and H_2O_2 changes in two applications except for H_2O_2 at 120 days.

The increased proline accumulation at 60 days of plants grown in SP condition was observed mainly in Mn_2O_3 treatment

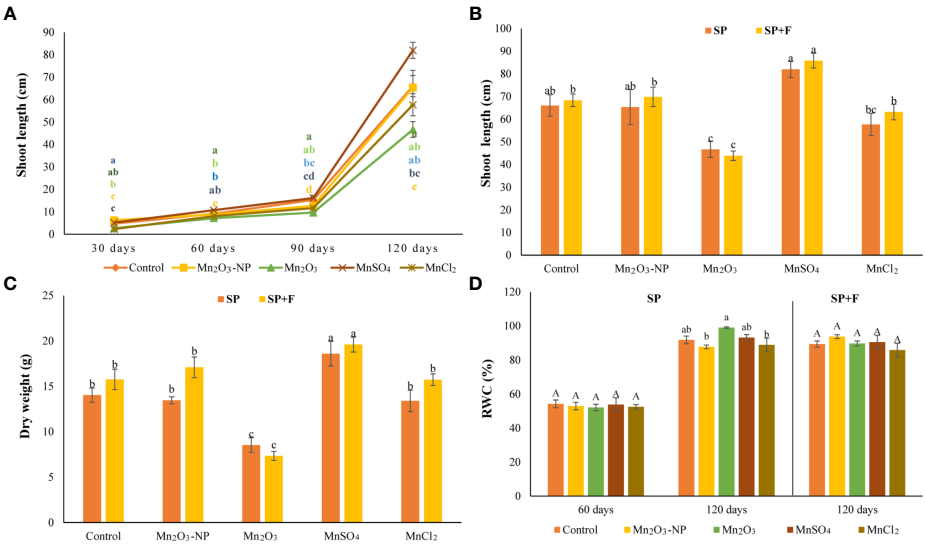

FIGURE 2
Shoot length of plants primed with different Mn forms (grown in SP condition) at different time intervals **(A)**; the comparison of shoot length **(B)** and dry weight **(C)** of plants grown in SP and SP+F condition at 120 days; relative water content **(D)**. Data points and error bars represent mean and S.E. (n = 3). Values with different letters indicate significant differences at the $P < 0.05$ level between different Mn forms.

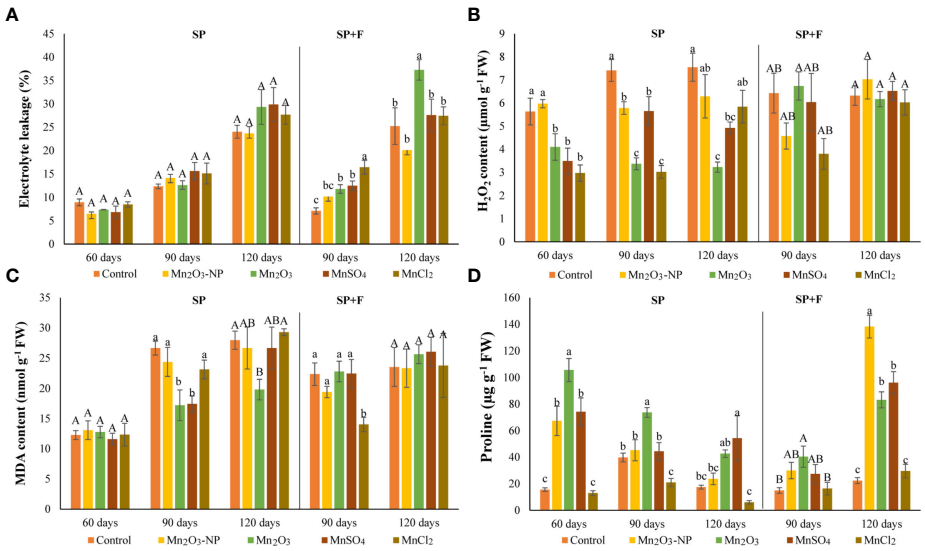

FIGURE 3
Electrolyte leakage **(A)**, H_2O_2 **(B)**, MDA **(C)**, and proline **(D)** contents in *A. annua* primed with different Mn forms at different durations. Data are mean ± SE (n=3). The different letters indicate statistically significant differences between Mn treatments within the same group at p<0.05. Capital letters represent no significant differences, statistically.

(+85%) (Figure 3D). It has also shown a significant increase with NPs and $MnSO_4$ treatments compared to control. However, a declining trend was observed over time at 90 and 120 days plants. Although the proline content was increased in all Mn forms (except $MnCl_2$) at 120 days, its level was lower than 60 days' treatments. Lower proline accumulation at 120 days after priming may be attributed to physiological adaptation. Moreover, a general decrease and increase were observed at 90 and 120 days' plants after foliar application of Mn forms, respectively. In detail, proline content was increased in Mn_2O_3-NPs (+83%) and $MnSO_4$ (+76%) treatments compared with control plants (Figure 3D). Accordingly, analysis of variance showed a significant application-dependent response of proline content in plants cultivated under SP and SP +F conditions.

3.3 Protein content and Antioxidant enzymes response

The protein content has also differed at tested time intervals, but the highest content was observed at 120 days' plants. In general, foliar application of Mn treatments at 90 days decreased protein content compared to the relevant treatments of SP only (Figure 4A). The oxidative status of the plants treated by different Mn forms grown in two conditions (SP and SP+F) was surveyed by measurement of CAT, PPO, APX, and SOD activities (Figures 4B-D). Each enzyme had a specific trend of changes based on the Mn form, application type and plant growth phase. For example, CAT activity did not show significant differences between all three developmental stages of plant growth in SP conditions over time. However, there was an Mn-dependent response as $MnSO_4$ and Mn_2O_3 treatments increased the activity of CAT at 60 and 90 days, respectively. Regarding SP+F application, spraying of Mn treatments (except for $MnCl_2$) and even water in control increased CAT activity at 90 days compared with their relevant treatments in SP (an average increase of 60%) (Figure 4B). Accordingly, the highest level of CAT activity was observed in Mn_2O_3 treatment (a 34% increase compared to the control).

PPO activity showed a general decrease in Mn treatments (except for $MnSO_4$) compared to control in 60 days' of plants grown in SP condition. However, an overall increase was observed over time as its activity was manifested by % 45 in 90 days' of plants treated with Mn_2O_3 (Figure 4C). At the same time, foliar application of NPs increased the PPO activity by 34% compared to its relevant treatment in plants grown only in SP conditions. The same trend of changes was also found for ionic forms of Mn but not Mn_2O_3. At 120 days' plants, all Mn forms increased PPO activity, but an overall decline was observed compared to 90 days' plants. A similar trend of increase was also observed for APX activity at 90 days' of plants grown under both SP and SP+F applications (Figure 4D). The highest level of APX activity was attributed to Mn_2O_3 treatment (a 44% increase compared with its relevant at 90 days in SP condition). At 120 days' plants, APX activity was decreased compared to 90 days' plants. Additionally, a general decline was observed for Mn_2O_3 and $MnCl_2$ treatments. An interesting trend of changes was observed for SOD activity, as its activity was upregulated in all Mn treatments (Figure 4E). In general, the results showed that

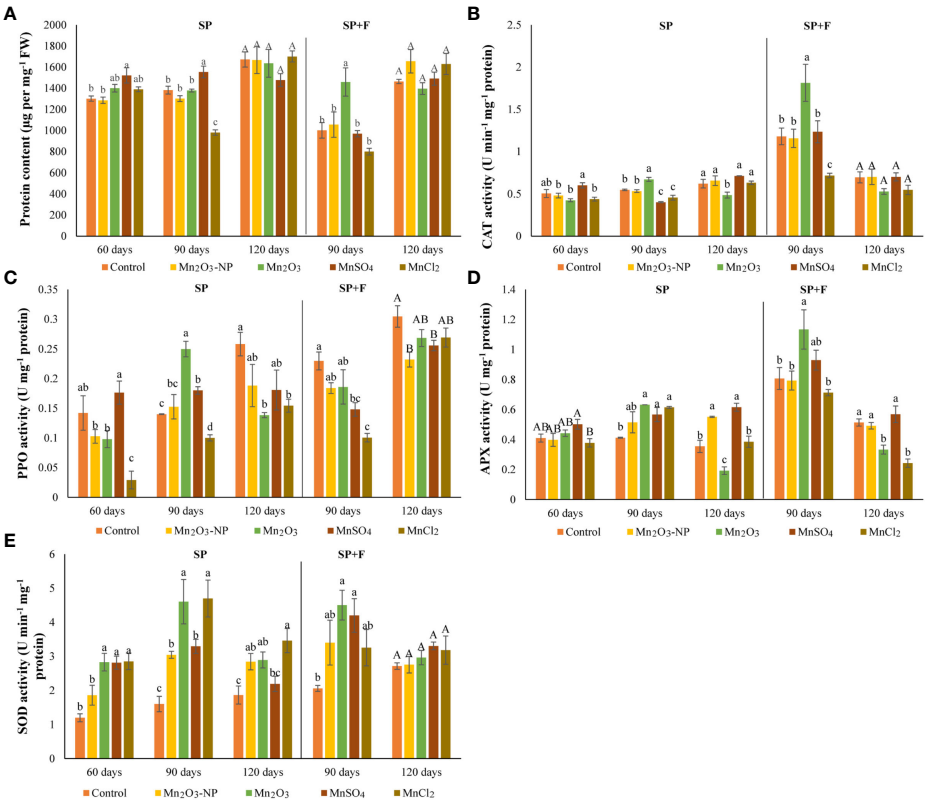

FIGURE 4
Protein content **(A)** and antioxidant enzymes (PPO **(B)**, APX **(C)**, SOD **(D)**, and CAT **(E)**) of *A. annua* under different Mn treatments using SP and a combination of SP+F at different time intervals.

SOD activity was significantly enhanced by Mn_2O_3 and $MnCl_2$ treatments. There was no remarkable alteration of SOD activity between SP and SP+F applications.

3.4 Photosynthetic pigments, total phenolic and flavonoid content

The Chl indices (Chla, b, total, a/b ratio, carotenoids, and Chlt/carotenoid ratio) have been represented in Table 1. A noticeable increase was observed in photosynthetic pigments, including Chl a, Chl b, total Chl, and carotenoids in both applications, especially at 90 days after planting. But their content was decreased in 120 days' plants compared to 90 days' plants which may be due to the senescence process in the plant. All Mn forms, particularly Mn_2O_3-NPs and Mn_2O_3, showed a positive effect on pigment synthesis. The multivariate analysis also showed a significant difference between applications, indicating a distinctive effect of seed priming and foliar spray on photosynthetic pigments. However, a general increase in Mn treatments was noticed at all developmental stages, even 120 days, highlighting the positive effect of Mn on pigments synthesis. Regarding the ratio of Chl a to Chl b, higher values were recorded for plants treated with Mn forms compared to control in SP condition, whereas the opposite trend was observed for SP+F condition. A general increase of Chl t/carotenoid ratio was mainly found in Mn treatments compared to control at 60 and 90 days' plants in both applications (Table 2). In total, it was found that all different Mn forms, regardless of the type, play an important role in improving photosynthetic pigments.

Total phenolic content was significantly altered by all three factors (i.e., application, Mn form and developmental stage) (Table 2). Briefly, the total phenolic content increased along with progressing the plant growth. Regarding SP condition, at the early (60 days) and mid (90 days) stages, the total phenolic content decreased by Mn treatments (except for $MnSO_4$) compared with control. However, the reduced trend was only observed in Mn_2O_3 treatment at 120 days, possibly due to its early developmental phase raising from late germination. Moreover, foliar application of Mn stimulated the synthesis of phenolic compounds mainly in $MnSO_4$ treatments (30%) compared to control and also its relevant treatment in SP condition (37%). However, $MnCl_2$, other ionic forms of Mn, decreased the total phenolic content by 30% compared to the control. Therefore, the highest content was recorded by foliar

10.3389/fpls.2022.1098772

TABLE 2 The effect of different forms of Mn on photosynthetic pigments, total phenol and total flavonoid content in *A. annua* plants at three different times using two applications (SP and SP+F).

	Chl a (mg g^{-1} FW)	Chl b (mg g^{-1} FW)	Chl t (mg g^{-1} FW)	Carotenoids (mg g^{-1} FW)	Chl a/Chl b ratio	Chl t/Car ratio	Total phenol (µg GAE g^{-1} FW)	Total flavonoids (mg CA g^{-1} FW)
SP								
60 day								
C	0.93 ± 0.18c	0.76 ± 0.09b	1.69 ± 0.27c	1.29 ± 0.05A	1.21 ± 0.11b	1.31 ± 0.22c	67.7 ± 8.8a	1.41 ± 0.03c
Mn_2O_3-NPs	1.01 ± 0.08c	0.77 ± 0.04b	1.78 ± 0.12c	1.32 ± 0.02A	1.31 ± 0.04b	1.34 ± 0.08c	36.0 ± 0.6b	1.37 ± 0.08a
Mn_2O_3	1.59 ± 0.10ab	1.04 ± 0.05ab	2.63 ± 0.15ab	1.46 ± 0.04A	1.53 ± 0.05a	1.80 ± 0.11ab	29.3 ± 4.4b	1.13 ± 0.07c
$MnSO_4$	1.33 ± 0.04bc	0.94 ± 0.02b	2.27 ± 0.06bc	1.49 ± 0.05A	1.42 ± 0.02ab	1.53 ± 0.08bc	61.7 ± 3.9a	1.79 ± 0.04ab
$MnCl_2$	1.90 ± 0.20a	1.35 ± 0.20a	3.26 ± 0. 4a	1.52 ± 0.14A	1.42 ± 0.06ab	2.13 ± 0.09a	30.7 ± 1.2b	1.38 ± 0.06bc
90 day								
C	1.71 ± 0.29b	1.28 ± 0.23b	2.99 ± 0.53b	1.68 ± 0.08B	1.34 ± 0.02A	1.75 ± 0.23A	106.0 ± 0.6b	2.34 ± 0.06b
Mn_2O_3-NPs	2.35 ± 0.04a	1.83 ± 0.05a	4.19 ± 0.09a	1.89 ± 0.01AB	1.28 ± 0.02A	2.21 ± 0.04A	78.1 ± 3.1c	1.95 ± 0.07c
Mn_2O_3	2.46 ± 0.02a	1.87 ± 0.10a	4.33 ± 0.08a	2.15 ± 0.21A	1.32 ± 0.09A	2.06 ± 0.24A	77.3 ± 3.2c	2.54 ± 0.04a
$MnSO_4$	2.20 ± 0.02a	1.57 ± 0.03ab	3.77 ± 0.05ab	1.76 ± 0.04B	1.41 ± 0.02A	2.15 ± 0.02A	157.9 ± 8.1a	2.31 ± 0.04b
$MnCl_2$	2.18 ± 0.02a	1.56 ± 0.04ab	3.76 ± 0.07ab	1.69 ± 0.03B	1.40 ± 0.02A	2.21 ± 0.01A	83.6 ± 7.4c	2.01 ± 0.06c
120 day								
C	1.59 ± 0.05A	1.08 ± 0.01A	2.67 ± 0.05A	1.76 ± 0.02A	1.46 ± 0.03c	1.52 ± 0.04B	199.5 ± 31.5b	1.92 ± 0.01B
Mn_2O_3-NPs	1.74 ± 0.10A	1.05 ± 0.05A	2.79 ± 0.16A	1.65 ± 0.02A	1.67 ± 0.01a	1.69 ± 0.07AB	276.0 ± 8.7a	1.87 ± 0.01B
Mn_2O_3	1.65 ± 0.11A	1.04 ± 0.08A	2.69 ± 0.20A	1.42 ± 0.29A	1.58 ± 0.02b	2.02 ± 0.30A	188.0 ± 38.7b	1.96 ± 0.02B
$MnSO_4$	1.70 ± 0.12A	1.09 ± 0.06A	2.79 ± 0.18A	1.73 ± 0.02A	1.56 ± 0.02b	1.61 ± 0.08AB	328.5 ± 2.6a	1.99 ± 0.03AB
$MnCl_2$	1.73 ± 0.11A	1.18 ± 0.07A	2.91 ± 0.18A	1.85 ± 0.07A	1.47 ± 0.01c	1.57 ± 0.04AB	312.0 ± 5.2a	2.22 ± 0.16A
SP+F								
90 day								
C	1.50 ± 0.23c	1.04 ± 0.18c	2.55 ± 0.40b	1.54 ± 0.12bc	1.46 ± 0.03AB	1.63 ± 0.14d	161.0 ± 6.4a	1.95 ± 0.03A
Mn_2O_3-NPs	2.12 ± 0.06ab	1.58 ± 0.08ab	3.69 ± 0.14a	1.81 ± 0.06a	1.34 ± 0.03AB	2.04 ± 0.01ab	119.2 ± 13.2b	2.35 ± 0.08A
Mn_2O_3	2.28 ± 0.02a	1.78 ± 0.06a	4.06 ± 0.08a	1.81 ± 0.05a	1.28 ± 0.03AB	2.24 ± 0.01a	104.3 ± 7.5b	1.92 ± 0.35A
$MnSO_4$	1.80 ± 0.05bc	1.23 ± 0.07c	3.03 ± 0.11b	1.73 ± 0.02ab	1.47 ± 0.04A	1.76 ± 0.09cd	163.6 ± 6.0a	2.26 ± 0.01A
$MnCl_2$	1.64 ± 0.07c	1.31 ± 0.06bc	2.96 ± 0.01b	1.50 ± 0.04c	1.26 ± 0.11B	1.98 ± 0.05bc	110.2 ± 22.4b	2.02 ± 0.05A
120 day								
C	1.45 ± 0.04A	0.79 ± 0.03B	2.23 ± 0.06B	1.41 ± 0.04B	1.84 ± 0.06A	1.58 ± 0.01ab	364.0 ± 53.0ab	1.69 ± 0.10c
Mn_2O_3-NPs	1.51 ± 0.07A	1.03 ± 0.04AB	2.54 ± 0.07AB	1.86 ± 0.04A	1.47 ± 0.11B	1.36 ± 0.01c	294.0 ± 49.0b	2.01 ± 0.05a
Mn_2O_3	1.65 ± 0.05A	1.26 ± 0.16A	2.92 ± 0.19A	1.79 ± 0.12AB	1.35 ± 0.15B	1.63 ± 0.06a	370.7 ± 63.8ab	1.66 ± 0.03c
$MnSO_4$	1.51 ± 0.13A	1.08 ± 0.03AB	2.59 ± 0.14AB	1.84 ± 0.04A	1.39 ± 0.11B	1.41 ± 0.07bc	522.7 ± 43.2a	1.95 ± 0.08ab
$MnCl_2$	1.40 ± 0.13A	0.98 ± 0.13AB	2.38 ± 0.24B	1.59 ± 0.23AB	1.46 ± 0.10B	1.52 ± 0.08abc	254.7 ± 27.5b	1.71 ± 0.11bc

Data are expressed as mean+standard error. Different letters show significant differences between treatments. Capital letters represent no statistical difference among treatments.

application of $MnSO_4$ at 120 days (Table 2). Similarly, total flavonoid content was differentially increased over time by treatments and applications as well. The data showed that the highest amount of total flavonoid is related to 90 day plants grown under SP conditions (Table 2). However, there were no remarkable differences between treatments (i.e., Mn forms and control). Notably, it is reasonable to infer that the synthesis of photosynthetic pigments and flavonoids might be slightly decreased during the flowering stage. Overall, despite not being significant, Mn_2O_3-NPs and $MnSO_4$ appear to have more influence on flavonoid content (Table 2).

3.5 Heatmap and principal component analysis analyses

The Pearson's correlation was performed on all targeted parameters, and outputs were analyzed using a heatmap (Figures 5, 3S). The heatmap related to 90 day's plants in SP (Figure 5A) and SP+F (Figure 5C) conditions showed that each application has specific responses based on the correlation between parameters. In detail, a positive correlation was somehow found between oxidative enzymes activity, protein content and proline accumulation as well as with photosynthetic pigments and total phenolic content in SP condition, but not with H_2O_2 and MDA content. However, in SP+F condition, both stress indicators and oxidative enzyme activity were positively correlated. The PCA plot for 90 days' of plants grown in SP condition accounted for 53.3% and 24.5% of the variance of PC1 and PC2 (Figure 5B), respectively, whereas the values of 50.4% and 32.1% were recorded for SP+F condition (Figure 5D). The PCA results also confirmed that the two applications impose some relatively different responses, but not entirely distinctive, in plants. This kind of difference was also observed in 60 and 120 days' of plants (Figure 3S). Interestingly, H_2O_2 and MDA were negatively correlated with almost all other parameters at 60 days' of plants, highlighting their competition to metabolize plant balance (Figures 3S, A). However, at the late developmental stage, the correlation coefficients were not highly significant, probably indicating plant adaptation status (Figures 3S; B, C). The relationships between growth, physiological and biochemical variables based on PCA plots (Figure 3S; D-F) were application and also developmental stage-dependent.

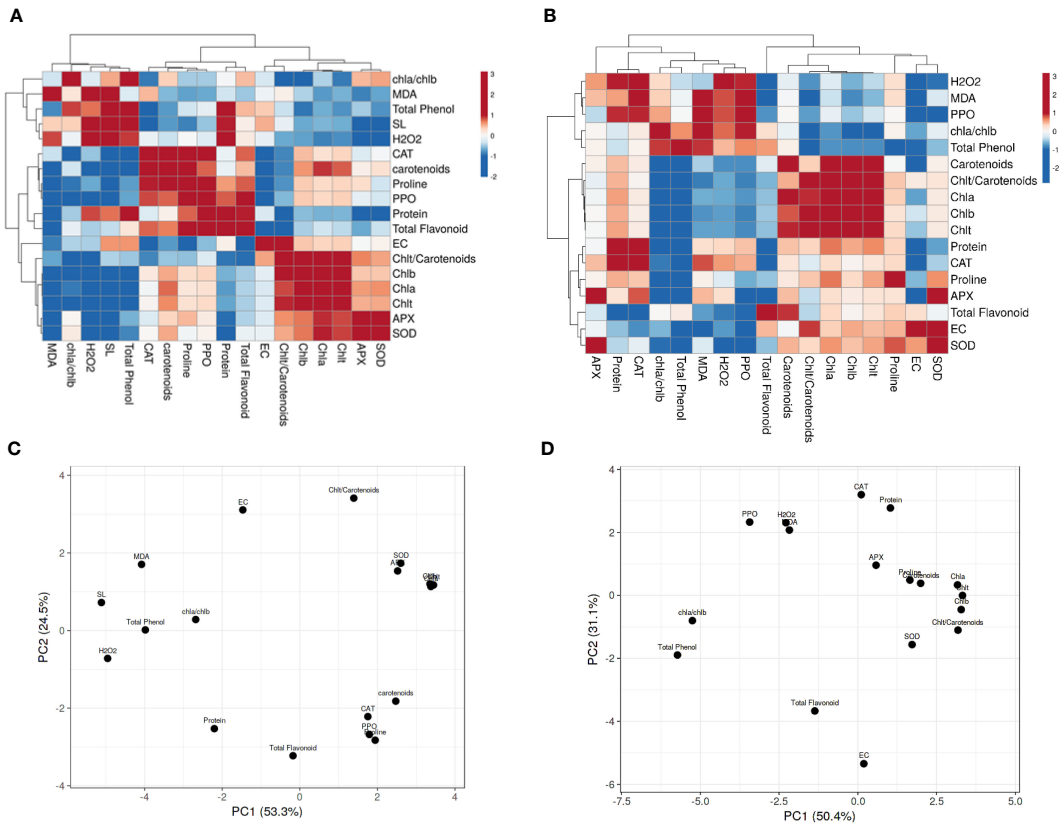

FIGURE 5
Heatmap and PCA analysis of Pearson's correlation for the targeted parameters in 90 days' plants in both SP **(A, C)** and SP+F **(B, D)** conditions. Pink and blue color represents positive and negative correlations, respectively.

4 Discussion

The use of metal NPs has revolutionized the agricultural sector to improve the production of crop products. This event is done to find more effective and eco-friendly stimulators contributing to a more sustainable future (Pokrajac et al., 2021). However, the effectiveness of NPs in terms of being positive, safe and economically efficient compared to other counterparts is still an open issue in the nanotechnology discipline. Here, we used two application methods (SP and SP +F) to investigate the effect of Mn_2O_3-NPs on *A. annua* performance and compare it with their bulk and ionic forms during short- to long-term intervals from the germination stage to maturation. Seed germination is one of the most vulnerable processes in plant's life cycle, supporting healthy and robust seedling development, which is largely affected by internal and external clues. Additionally, low crop productivity has been found to be linked with uneven seed germination. Research has proved that seed priming, a well-established method, can improve the quality of seeds and triggers seed germination efficiency and further plant growth (Adhikari et al., 2022; Thakur et al., 2022).

The findings presented in this study showed that SP with different Mn forms significantly alters the assayed attributes of germination and seedling growth (Table 1). Among Mn treatments, $MnSO_4$ and Mn_2O_3, respectively, improved and declined the germination-related parameters compared to the control. Mn_2O_3-NPs at the same concentration had a mild improving effect not as much different from control. Previous researches have reported that nano-priming significantly improves germination compared to ionic and hydropriming, mainly through accelerating water and nutrient uptake mediated by creating nanopores in seed coats (Mahakham et al., 2017; do Espirito Santo Pereira et al., 2021; Nile et al., 2022). Based on our results, however, this hypothesis was not proved for Mn_2O_3-NPs compared to $MnSO_4$. The plant length and dry mass of seedlings grown at seed priming conditions also demonstrated the effectiveness of Mn as $MnSO_4$>Mn_2O_3-NPs≥control>$MnCl_2$>Mn_2O_3.

It has been proved that hydropriming is highly cost-effective and environment friendly to better the emergence and establishment of seedlings (Thakur et al., 2022). However, our results showed that priming with suitable ionic and nano forms of Mn can remarkably prompt these processes. Previous studies have reported the effectiveness of nutripriming with $MnSO_4$ to accelerate germination rate (Munawar et al., 2013; Alejandro et al., 2020). On the other hand, a recent study showed that SP with MnO-NPs had comparatively less phytotoxicity than its bulk counterparts in watermelon seedlings (Kasote et al., 2021), which is in line with our results that nano forms of Mn are safer than their bulk. The mechanisms underlying the SP-induced modifications include the proper DNA conformation and reparation in embryos which is resulted in genome and protein integrity and, therefore, proceeding cell division (Thakur et al., 2022). In agreement, it is generally accepted that DNA polymerase conformational activation is mediated by a metal-based mechanism (Kirby et al., 2012), which can probably explain the Mn-induced germination.

The early responses of priming with Mn species were analyzed by germination-related parameters and the overall output confirms the critical role of seed-priming strategies (Devika et al., 2021). To further clarify the long-term responses of Mn-priming, the seedlings were grown for 120 days and then plant growth, physio-biochemical attributes were analyzed during this time. The plant growth at all tested times (60, 90, and 120, which are equal to specific developmental stages) followed the same trend as germination.

In other words, the higher growth rate in plants grown from seeds primed with $MnSO_4$, control, and Mn_2O_3-NPs can be ascribed to the early and faster germination by these treatments, highlighting the importance of seed germination and priming strategy for successful establishment and higher productivity of germinated seedlings (Carrera-Castaño et al., 2020). In the present experiment, no obvious toxic symptoms of plants such as leaf wilt, necrosis, and yellowish leaves was observed, even in Mn_2O_3 treatment, which caused germination delay and subsequently lower plant growth. Interestingly, when we applied Mn treatments through foliar spray, all treatments except for Mn_2O_3 increased the plant growth compared to seed priming only, indicating the higher efficiency of SP+F combination to improve plant productivity. In confirmation of this statement, the results showed that foliar application of $MnCl_2$ compensates the weak growth of seedlings developed from priming method. Foliar application of exogenous nutrients acts as a viable strategy to minimize nutrient efficiency in plants through fast delivery at the point of assimilation and therefore allows plant biofortification (Alshaal and El-Ramady, 2017; Dass et al., 2022).

Different processes involved in plant's life cycle, like photosynthesis, ROS scavenging, and signaling pathway, have been found to be Mn-dependent (Alejandro et al., 2020). The results presented here also showed that Mn-induced changes are mainly reflected in the synthesis of photosynthetic pigments, phenolic compounds and some specific antioxidant enzymes. For example, photosynthetic pigments were generally increased under Mn treatments, especially in SP conditions. It's worth mentioning that, it is difficult to determine which Mn form has the most influence on photosynthetic pigments since, at each time, different behavior was observed. However, it was reported that the optimum application of exogenous Mn can enhance photosynthetic efficiency under normal and stress conditions (Ahmad et al., 2019). Additionally, the Chl a/Chl b and total Chl/carotenoids ratios are considered to be vital parameters for photosynthesis efficiency (Jiménez-Lao et al., 2021). In the present study, an overall increased ratio of these parameters suggests a mild promotion of photosynthetic synthesis under Mn treatments. This could be due to improving the energy

generation and regeneration of Ribulose-1,5-Bisphosphate (RuBP) involved in Calvin cycle. The total phenolic content was also significantly affected by either Mn treatments (in particular $MnSO_4$) or application methods, highlighting the importance of Mn in phenylpropanoid pathways (Liu et al., 2019). Mn has been shown to serve as cofactor of the phenylalanine ammonia-lyase which is an important enzyme in the phenylpropanoid pathway to synthesize phenolic metabolites (Alejandro et al., 2020).

In accordance with our study, a recent study also showed that photosynthetic pigments, phenolic compounds and antioxidant profiles of watermelon seedlings were significantly affected by seed priming with 20 mg L^{-1}MnO-NPs (Kasote et al., 2021). However, there was no clear trend of changes regarding the antioxidant flavonoid content as it increased in some treatments but no changes in some others compared to the control. The foliar-sprayed $MnSO_4$ enhanced flavonoid content, which is in line with the results of Chen et al. (Li et al., 2020), reporting the increased flavonoid content in *Vitis vinifera* L treated by $MnSO_4$. Despite not being significant in some cases, the overall decline in H_2O_2 and MDA content under Mn treatments was observed, which indicates the key role of Mn in ROS-scavenger-induced compounds (Alejandro et al., 2020). This was also in line with generally increased SOD activity, which reflects the protective nature of Mn pre-treatments, specifically by Mn bulk and ionic ($MnCl_2$) forms. Increase SOD activity by metals such as Mn, Fe, and Zn has previously been reported, highlighting its key role as a cofactor of this enzyme (De Cuyper et al., 2017; Hu and Jinn, 2022). Declined oxidative markers, along with enhanced SOD activity, in this study, are mainly attributed to adaptive mechanism rather than defense system mechanism. Regarding other antioxidant enzymes, no clear trend of changes was found. However, an overall increase in PPO and APX activities was observed for $MnSO_4$ treatments. Considering that no adverse symptoms were observed in $MnSO_4$ treatments, up-regulated. Take this into account, the activation of antioxidant enzymes has been found to depend on Mn type, application method and finally, enzyme type, highlighting a diverse array of enzymatic responses exhibited by PCA analyses.

Antioxidant enzymes have been mainly reported to be the first line of defensive and protective mechanisms against any environmental factor such as abiotic stresses (Lei et al., 2022; Mittler et al., 2022; Najafi-Kakavand et al., 2022; Rahman et al., 2022; Raza et al., 2022a; Raza et al., 2022b; Shahid et al., 2022; Shaukat et al., 2022; Bhardwaj et al., 2023). At first, the superoxide radicals are converted to H_2O_2 by SOD activity which can be further decomposed into H_2O by CAT and peroxidases (Hasanuzzaman et al., 2020). In addition, proline was significantly increased in almost all Mn treatments, especially by foliar-sprayed Mn_2O_3-NPs. It has been accepted that proline, a non-essential amino acid, plays a vital role in the maintenance of cellular redox homeostasis and cell's energy status (Ghosh et al., 2022). Overall, the application of Mn treatments, except for its bulk form *via* both SP and foliar spray, improved *A. annua* performance by reducing H_2O_2 and MDA content. Mn is thought to scavenge free radicals itself or by increasing antioxidant enzyme activities, especially SOD and proline. Therefore, speaking generally, Mn as a micronutrient is involved in the scavenging of free radicals directly by itself or indirectly by activating various enzymes, top of them SOD (a primary antioxidative enzyme), and proline (Schmidt and Husted, 2019; Alejandro et al., 2020). On the other hand, different alteration of enzymes indicates the activation of specific antioxidant mechanisms by various forms of Mn, individually. Moreover, foliar application of Mn was only effective for a limited period after exposure since Mn is very little mobile in the plant and does not remobilize along plant organs. Considering the tested parameters, it is observed that the trend of changes was much more dynamic and significant at 90 days than 120 days, which also shows the adaptive status of plants at 120 days.

To sum up, comparing the effects of Mn_2O_3-NPs on *A.annua* performance in terms of morphological, and physio-biochemical attributes, our findings showed that NP form doesn't have a remarkable priority to induce distinctive effects on plants performance compared to their conventional forms and control. In other words, if one of the Mn forms is supposed to be used to improve plant growth, based on the results, $MnSO_4$ would be the best option.

5 Conclusion

Our study showed that SP with different Mn forms could improve seed germination attributes and further seedling development of *A. annua.* Among treatments, priming with $MnSO_4$, Mn_2O_3-NPs and water, respectively, resulted in the highest germination index and shortened the germination period. Similarly, vigorous and healthier seedlings were also observed in the mentioned treatments. On the other hand, foliar application of the mentioned Mn treatments helped in plant growth improvement even more. For instance, although SP with $MnCl_2$ decreased germination and early growth, its foliar application compensated the retarded seedlings, indicating the difference between the two applications. Although plant growth did not change in some of the Mn treatments (for example, Mn_2O_3-NPs and $MnCl_2$) compared to control, they all had their specific trend of changes in tested attributes. The biochemical analyses also suggest that each Mn form can activate different enzymatic and non-enzymatic antioxidants (Figure 6). However, the activation of SOD and proline can be considered a common Mn-induced response. After considering the overall attributes, including germination, morphological and physio-biochemical status, $MnSO_4$ is highly recommended to be used in triggering plant growth during the early phase and therefore is cost- and resource-effective. However, other forms, such as $MnCl_2$ and Mn_2O_3, which have more effect on the antioxidant defense systems, might be suitable under stress conditions. In addition, NPs, because of releasing more Mn^{+2} ions, are applicable to be

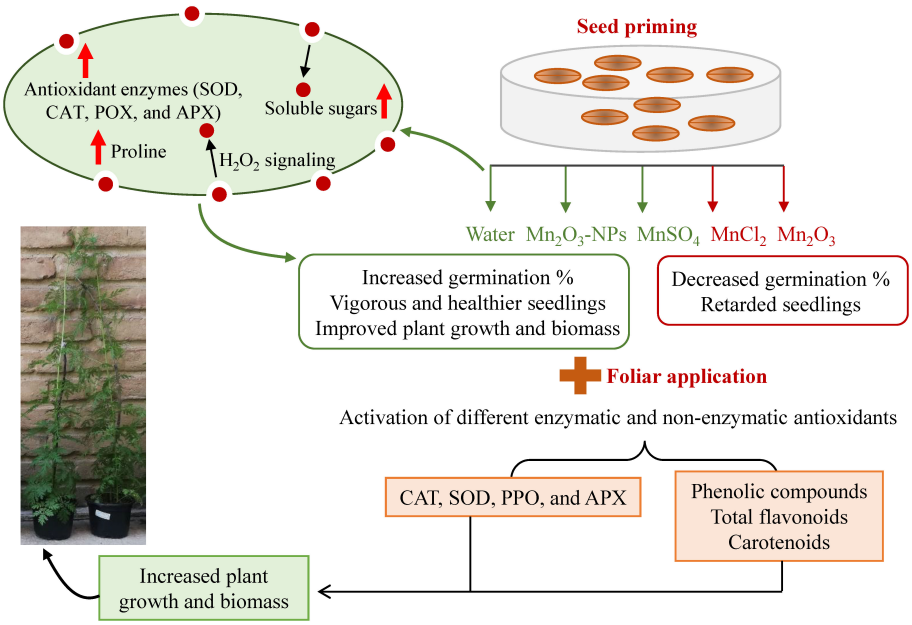

FIGURE 6
A schematic overview of the possible mechanism underlying improved plant growth and biomass based on different Mn application.

used in very small amounts. Overall, the exogenous application of specific Mn as combined seed and foliar pre-treatments is recommended to first accelerate germination and then improve further plant growth by modulating antioxidant enzymes. Future studies regarding the stimulating application should explore the optimal dose of Mn_2O_3-NPs at a very low amount and investigate their real efficiency to be cost-effective.

Data availability statement

The original contributions presented in the study are included in the article/Supplementary Material. Further inquiries can be directed to the corresponding author.

Author contributions

HS conceived the idea and conducted the formal analysis, data curation, writing- review and editing. ACR supervised the research work. HS, AR, ACR, ID, and PVVP proofread and edited the manuscript. All authors have read and approved the final version of the manuscript.

Funding

The research was supported by the Ministry of Science, Research and Technology (MSRT) and Bu-Ali Sina University. The research in this paper is part of the projects of NIO in 2022: 451-03-68/2022-14/200032 (to ID).

Conflict of interest

The authors declare that the research was conducted in the absence of any commercial or financial relationships that could be construed as a potential conflict of interest.

Publisher's note

Supplementary material

The Supplementary Material for this article can be found online at: https://www.frontiersin.org/articles/10.3389/fpls.2022.1098772/full#supplementary-material

References

Adhikari, B., Olorunwa, O. J., and Barickman, T. C. (2022). Seed priming enhances seed germination and morphological traits of lactuca sativa l. under salt stress. *Seeds* 1 (2), 74–86. doi: 10.3390/seeds1020007

Ahmad, I., Kamran, M., Yang, X., Meng, X., Ali, S., Ahmad, S., et al. (2019). Effects of applying uniconazole alone or combined with manganese on the photosynthetic efficiency, antioxidant defense system, and yield in wheat in semiarid regions. *Agric. Water Manage.* 216, 400–414. doi: 10.1016/j.agwat.2019.02.025

Ahmad, B., Shabbir, A., Jaleel, H., Khan, M. M. A., and Sadiq, Y. (2018). Efficacy of titanium dioxide nanoparticles in modulating photosynthesis, peltate glandular trichomes and essential oil production and quality in mentha piperita l. *Curr. Plant Biol.* 13, 6–15. doi: 10.1016/j.cpb.2018.04.002

Ahmar, S., Mahmood, T., Fiaz, S., Mora-Poblete, F., Shafique, M. S., Chattha, M. S., et al. (2021). Advantage of nanotechnology-based genome editing system and its application in crop improvement. *Front. Plant Sci.* 12. doi: 10.3389/fpls.2021.663849

Alejandro, S., Höller, S., Meier, B., and Peiter, E. (2020). Manganese in plants: from acquisition to subcellular allocation. *Front. Plant Sci.* 11, 300. doi: 10.3389/fpls.2020.00300

Alexieva, V., Sergiev, I., Mapelli, S., and Karanov, E. (2001). The effect of drought and ultraviolet radiation on growth and stress markers in pea and wheat. *Plant Cell Environ.* 24 (12), 1337–1344. doi: 10.1046/j.1365-3040.2001.00778.x

Alshaal, T., and El-Ramady, H. (2017). Foliar application: from plant nutrition to biofortification. *Environment Biodiversity Soil Secur.* 1 (2017), 71–83. doi: 10.21608/JENVBS.2017.1089.1006

Arnon, D. I. (1949). Copper enzymes in isolated chloroplasts. polyphenoloxidase in beta vulgaris. *Plant Physiol.* 24 (1), 1. doi: 10.1104/pp.24.1.1

Bates, L. S., Waldren, R. P., and Teare, I. (1973). Rapid determination of free proline for water-stress studies. *Plant Soil* 39 (1), 205–207. doi: 10.1007/BF00018060

Beers, R. F., and Sizer, I. W. (1952). A spectrophotometric method for measuring the breakdown of hydrogen peroxide by catalase. *J. Biol. Chem.* 195 (1), 133–140. doi: 10.1016/S0021-9258(19)50881-X

Bhardwaj, S., Verma, T., Raza, A., and Kapoor, D. (2023). Silicon and nitric oxide-mediated regulation of growth attributes, metabolites and antioxidant defense system of radish (*Raphanus sativus* l.) under arsenic stress. *Phyton-International J. Exp. Bot.* 92 (3), 763–782. doi: 10.32604/phyton.2023.025672

Carrera-Castaño, G., Calleja-Cabrera, J., Pernas, M., Gómez, L., and Oñate-Sánchez, L. (2020). An updated overview on the regulation of seed germination. *Plants* 9 (6), 703. doi: 10.3390/plants9060703

Chun, O. K., Kim, D.-O., and Lee, C. Y. (2003). Superoxide radical scavenging activity of the major polyphenols in fresh plums. *J. Agric. Food Chem.* 51 (27), 8067–8072. doi: 10.1021/jf034740d

Das, M., Saxena, N., and Dwivedi, P. D. (2009). Emerging trends of nanoparticles application in food technology: Safety paradigms. *Nanotoxicology* 3 (1), 10–18. doi: 10.1080/17435390802504237

Dass, A., Rajanna, G. A., Babu, S., Lal, S. K., Choudhary, A. K., Singh, R., et al. (2022). Foliar application of macro-and micronutrients improves the productivity, economic returns, and resource-use efficiency of soybean in a semiarid climate. *Sustainability* 14 (10), 5825. doi: 10.3390/su14105825

De Cuyper, C., Struk, S., Braem, L., Gevaert, K., De Jaeger, G., and Goormachtig, S. (2017). Strigolactones, karrikins and beyond. *Plant Cell Environ.* 40 (9), 1691–1703. doi: 10.1111/pce.12996

Devika, O. S., Singh, S., Sarkar, D., Barnwal, P., Suman, J., and Rakshit, A. (2021). Seed priming: a potential supplement in integrated resource management under fragile intensive ecosystems. *Front. Sustain. Food Syst.* 209. doi: 10.3389/fsufs.2021.654001

do Espirito Santo Pereira, A., Caixeta Oliveira, H., Fernandes Fraceto, L., and Santaella, C. (2021). Nanotechnology potential in seed priming for sustainable agriculture. *Nanomaterials* 11 (2), 267. doi: 10.3390/nano11020267

Dogan, K., Erol, E., Didem Orhan, M., Degirmenci, Z., Kan, T., Gungor, A., et al. (2022). Instant determination of the artemisinin from various artemisia annua l. extracts by LC-ESI-MS/MS and their in-silico modelling and *in vitro* antiviral activity studies against SARS-CoV-2. *Phytochemical Anal.* 33 (2), 303–319. doi: 10.1002/pca.3088

Du, W., Tan, W., Yin, Y., Ji, R., Peralta-Videa, J. R., Guo, H., et al. (2018). Differential effects of copper nanoparticles/microparticles in agronomic and physiological parameters of oregano (Origanum vulgare). *Sci. Total Environ.* 618, 306–312. doi: 10.1016/j.scitotenv.2017.11.042

Ghosh, U., Islam, M., Siddiqui, M., Cao, X., and Khan, M. (2022). Proline, a multifaceted signalling molecule in plant responses to abiotic stress: understanding the physiological mechanisms. *Plant Biol.* 24 (2), 227–239. doi: 10.1111/plb.13363

Hadi Soltanabad, M., Bagherieh-Najjar, M. B., and Mianabadi, M. (2020). Carnosic acid content increased by silver nanoparticle treatment in rosemary (Rosmarinus officinalis l.). *Appl. Biochem. Biotechnol.* 191 (2), 482–495. doi: 10.1007/s12010-019-03193-w

Hasanuzzaman, M., Bhuyan, M., Zulfiqar, F., Raza, A., Mohsin, S. M., Mahmud, J. A., et al. (2020). Reactive oxygen species and antioxidant defense in plants under abiotic stress: Revisiting the crucial role of a universal defense regulator. *Antioxidants* 9 (8), 681. doi: 10.3390/antiox9080681

Hu, S.-H., and Jinn, T.-L. (2022). Impacts of Mn, fe, and oxidative stressors on MnSOD activation by AtMTM1 and AtMTM2 in arabidopsis. *Plants* 11 (5), 619. doi: 10.3390/plants11050619

Jebara, S., Jebara, M., Limam, F., and Aouani, M. E. (2005). Changes in ascorbate peroxidase, catalase, guaiacol peroxidase and superoxide dismutase activities in common bean (Phaseolus vulgaris) nodules under salt stress. *J. Plant Physiol.* 162 (8), 929–936. doi: 10.1016/j.jplph.2004.10.005

Jeevanandam, J., Barhoum, A., Chan, Y. S., Dufresne, A., and Danquah, M. K. (2018). Review on nanoparticles and nanostructured materials: history, sources, toxicity and regulations. *Beilstein J. Nanotech.* 9 (1), 1050–1074. doi: 10.3762/bjnano.9.98

Jiménez-Lao, R., Garcia-Caparros, P., Pérez-Saiz, M., Llanderal, A., and Lao, M. T. (2021). Monitoring optical tool to determine the chlorophyll concentration in ornamental plants. *Agronomy* 11 (11), 2197. doi: 10.3390/agronomy11112197

Kasote, D. M., Lee, J. H., Jayaprakasha, G. K., and Patil, B. S. (2021). Manganese oxide nanoparticles as safer seed priming agent to improve chlorophyll and antioxidant profiles in watermelon seedlings. *Nanomaterials* 11 (4), 1016. doi: 10.3390/nano11041016

Khan, I., Saeed, K., and Khan, I. (2019). Nanoparticles: Properties, applications and toxicities. *Arabian J. Chem.* 12 (7), 908–931. doi: 10.1016/j.arabjc.2017.05.011

Kirby, T. W., DeRose, E. F., Cavanaugh, N. A., Beard, W. A., Shock, D. D., Mueller, G. A., et al. (2012). Metal-induced DNA translocation leads to DNA polymerase conformational activation. *Nucleic Acids Res.* 40 (7), 2974–2983. doi: 10.1093/nar/gkr1218

Kralova, K., and Jampilek, J. (2021). Responses of medicinal and aromatic plants to engineered nanoparticles. *Appl. Sci.* 11 (4), 1813. doi: 10.3390/app11041813

Kumari, S., Khanna, R. R., Nazir, F., Albaqami, M., Chhillar, H., Wahid, I., et al. (2022). Bio-synthesized nanoparticles in developing plant abiotic stress resilience: A new boon for sustainable approach. *Int. J. Mol. Sci.* 23 (8), 4452. doi: 10.3390/ijms23084452

Landa, P. (2021). Positive effects of metallic nanoparticles on plants: Overview of involved mechanisms. *Plant Physiol. Biochem.* 161, 12–24. doi: 10.1016/j.plaphy.2021.01.039

Lei, Y., He, H., Raza, A., Liu, Z., Xiaoyu, D., Guijuan, W., et al. (2022). Exogenous melatonin confers cold tolerance in rapeseed (Brassica napus l.) seedlings by improving antioxidants and genes expression. *Plant Signaling Behav.* 17 (1), 2129289. doi: 10.1080/15592324.2022.2129289

Li, W., Nguyen, K. H., Tran, C. D., Watanabe, Y., Tian, C., Yin, X., et al. (2020). Negative roles of strigolactone-related SMXL6, 7 and 8 proteins in drought resistance in arabidopsis. *Biomolecules* 10 (4), 607. doi: 10.3390/biom10040607

Liu, P., Huang, R., Hu, X., Jia, Y., Li, J., Luo, J., et al. (2019). Physiological responses and proteomic changes reveal insights into stylosanthes response to manganese toxicity. *BMC Plant Biol.* 19 (1), 1–21. doi: 10.1186/s12870-019-1822-y

Lutts, S., Almansouri, M., and Kinet, J.-M. (2004). Salinity and water stress have contrasting effects on the relationship between growth and cell viability during and after stress exposure in durum wheat callus. *Plant Sci.* 167 (1), 9–18. doi: 10.1016/j.plantsci.2004.02.014

Mahakham, W., Sarmah, A. K., Maensiri, S., and Theerakulpisut, P. (2017). Nanopriming technology for enhancing germination and starch metabolism of aged rice seeds using phytosynthesized silver nanoparticles. *Sci. Rep.* 7 (1), 1–21. doi: 10.1038/s41598-017-08669-5

Mittler, R., Zandalinas, S. I., Fichman, Y., and Van Breusegem, F. (2022). Reactive oxygen species signalling in plant stress responses. *Nat. Rev. Mol. Cell Biol.* 1-17. doi: 10.1038/s41580-022-00499-2

Moazzami Farida, S. H., Karamian, R., and Albrectsen, B. R. (2020). Silver nanoparticle pollutants activate oxidative stress responses and rosmarinic acid accumulation in sage. *Physiologia plantarum* 170 (3), 415–432. doi: 10.1111/ppl.13172

Munawar, M., Ikram, M., Iqbal, M., Raza, M. M., Habib, S., Hammad, G., et al. (2013). Effect of seed priming with zinc, boron and manganese on seedling health in carrot (DaucuscarotaL.). *Int. J. Agric. Crop Sci.* 5 (22), 2697.

Najafi-Kakavand, S., Karimi, N., Ghasempour, H.-R., Raza, A., Chaichi, M., and Modarresi, M. (2022). Role of jasmonic and salicylic acid on enzymatic changes in the root of two alyssum inflatum náyr. populations exposed to nickel toxicity. *J. Plant Growth Regul.*, 1–18. doi: 10.1007/s00344-022-10648-8

Nile, S. H., Thiruvengadam, M., Wang, Y., Samynathan, R., Shariati, M. A., Rebezov, M., et al. (2022). Nano-priming as emerging seed priming technology for sustainable agriculture–recent developments and future perspectives. *J. Nanobiotech.* 20 (1), 1–31. doi: 10.1186/s12951-022-01423-8

Nourozi, E., Hosseini, B., Maleki, R., and Abdollahi Mandoulakani, B. (2019). Iron oxide nanoparticles: a novel elicitor to enhance anticancer flavonoid production and gene expression in dracocephalum kotschyi hairy-root cultures. *J. Sci. Food Agric.* 99 (14), 6418–6430. doi: 10.1002/jsfa.9921

Pérez-de-Luque, A. (2017). Interaction of nanomaterials with plants: what do we need for real applications in agriculture? *Front. Environ. Sci.* 5, 12. doi: 10.3389/fenvs.2017.00012

Pokrajac, L., Abbas, A., Chrzanowski, W., Dias, G. M., Eggleton, B. J., Maguire, S., et al. (2021). *Nanotechnology for a sustainable future: Addressing global challenges with the international network4sustainable nanotechnology* (ACS Publications). doi: 10.1021/acsnano.1c10919

Pullagurala, V. L. R., Adisa, I. O., Rawat, S., Kalagara, S., Hernandez-Viezcas, J. A., Peralta-Videa, J. R., et al. (2018a). ZnO nanoparticles increase photosynthetic pigments and decrease lipid peroxidation in soil grown cilantro (Coriandrum sativum). *Plant Physiol. Biochem.* 132, 120–127. doi: 10.1016/j.plaphy.2018.08.037

Pullagurala, V. L. R., Adisa, I. O., Rawat, S., Kim, B., Barrios, A. C., Medina-Velo, I. A., et al. (2018b). Finding the conditions for the beneficial use of ZnO nanoparticles towards plants-a review. *Environ. pollut.* 241, 1175–1181. doi: 10.1016/j.envpol.2018.06.036

Rahman, M. A., Woo, J. H., Lee, S.-H., Park, H. S., Kabir, A. H., Raza, A., et al. (2022). Regulation of Na+/H+ exchangers, Na+/K+ transporters, and lignin biosynthesis genes, along with lignin accumulation, sodium extrusion, and antioxidant defense, confers salt tolerance in alfalfa. *Front. Plant Sci.* 13, 1041764–1041764. doi: 10.3389/fpls.2022.1041764

Raymond, J., Rakariyatham, N., and Azanza, J. (1993). Purification and some properties of polyphenoloxidase from sunflower seeds. *Phytochemistry* 34 (4), 927–931. doi: 10.1016/S0031-9422(00)90689-7

Raza, A., Charagh, S., García-Caparrós, P., Rahman, M. A., Ogwugwa, V. H., Saeed, F., et al. (2022a). Melatonin-mediated temperature stress tolerance in plants. *GM Crops Food* 13 (1), 196–217. doi: 10.1080/21645698.2022.2106111

Raza, A., Salehi, H., Rahman, M. A., Zahid, Z., Madadkar Haghjou, M., Najafi-Kakavand, S., et al. (2022b). Plant hormones and neurotransmitter interactions mediate antioxidant defenses under induced oxidative stress in plants. *Front. Plant Sci.* 13. doi: 10.3389/fpls.2022.961872

Sabet, H., and Mortazaeinezhad, F. (2018). Yield, growth and fe uptake of cumin (Cuminum cyminum l.) affected by fe-nano, fe-chelated and fe-siderophore fertilization in the calcareous soils. *J. Trace Elements Med. Biol.* 50, 154–160. doi: 10.1016/j.jtemb.2018.06.020

Salehi, H., Chehregani, A., Lucini, L., Majd, A., and Gholami, M. (2018). Morphological, proteomic and metabolomic insight into the effect of cerium dioxide nanoparticles to phaseolus vulgaris l. under soil or foliar application. *Sci. Total Environ.* 616, 1540–1551. doi: 10.1016/j.scitotenv.2017.10.159

Salehi, H., De Diego, N., Rad, A. C., Benjamin, J. J., Trevisan, M., and Lucini, L. (2021a). Exogenous application of ZnO nanoparticles and ZnSO4 distinctly influence the metabolic response in phaseolus vulgaris l. *Sci. Total Environ.* 778, 146331. doi: 10.1016/j.scitotenv.2021.146331

Salehi, H., Miras-Moreno, B.a., Chehregani Rad, A., Pii, Y., Mimmo, T., Cesco, S., et al. (2019). Relatively low dosages of CeO2 nanoparticles in the solid medium induce adjustments in the secondary metabolism and ionomic balance of bean (Phaseolus vulgaris l.) roots and leaves. *J. Agric. Food Chem.* 68 (1), 67–76. doi: 10.1021/acs.jafc.9b05107

Salehi, H., Rad, A. C., Sharifan, H., Raza, A., and Varshney, R. K. (2021b). Aerially applied zinc oxide nanoparticle affects reproductive components and seed quality in fully grown bean plants (Phaseolus vulgaris l.). *Front. Plant Sci.* 12. doi: 10.3389/fpls.2021.808141

Santiago, E. F., Pontes, M. S., Arruda, G. J., Caires, A. R., Colbeck, I., Maldonado-Rodriguez, R., et al. (2020). "Understanding the interaction of nanopesticides with plants,". *Nanopesticides Springer)*, 69–109. doi: 10.1007/978-3-030-44873-8_4

Schmidt, S. B., and Husted, S. (2019). The biochemical properties of manganese in plants. *Plants* 8 (10), 381. doi: 10.3390/plants8100381

Shahhoseini, R., Azizi, M., Asili, J., Moshtaghi, N., and Samiei, L. (2020). Effects of zinc oxide nanoelicitors on yield, secondary metabolites, zinc and iron absorption of feverfew (Tanacetum parthenium (L.) Schultz bip.). *Acta Physiologiae plantarum* 42 (4), 1–18. doi: 10.1007/s11738-020-03043-x

Shahid, S., Kausar, A., Zahra, N., Hafeez, M. B., Raza, A., and Ashraf, M. Y. (2022). Methionine-induced regulation of secondary metabolites and antioxidants in maize (Zea mays l.) subjected to salinity stress. *Gesunde Pflanzen*, 1–13. doi: 10.3390/plants9121745

Shaukat, K., Baksh, G., Zahra, N., Hafeez, M. B., Raza, A., Samad, A., et al. (2022). Foliar application of thiourea, salicylic acid, and kinetin alleviate salinity stress in maize grown under etiolated and de-etiolated conditions. *Discover Food* 2 (1), 1–14. doi: 10.3390/plants9121745

Shen, Q., Huang, H., Xie, L., Hao, X., Kayani, S., Liu, H., et al. (2022). Basic helix-Loop-Helix transcription factors AabHLH2 and AabHLH3 function antagonistically with AaMYC2 and are negative regulators in artemisinin biosynthesis. *Front. Plant Sci.* 13. doi: 10.3389/fpls.2022.885622

Sobarzo-Bernal, O., Gómez-Merino, F. C., Alcántar-González, G., Saucedo-Veloz, C., and Trejo-Téllez, L. I. (2021). Biostimulant effects of cerium on seed germination and initial growth of tomato seedlings. *Agronomy* 11 (8), 1525. doi: 10.3390/agronomy11081525

Stewart, R. R., and Bewley, J. D. (1980). Lipid peroxidation associated with accelerated aging of soybean axes. *Plant Physiol.* 65 (2), 245–248. doi: 10.1104/pp.65.2.245

Szőllősi, R., Molnár, Á., Kondak, S., and Kolbert, Z. (2020). Dual effect of nanomaterials on germination and seedling growth: Stimulation vs. phytotoxicity. *Plants* 9 (12), 1745. doi: 10.3390/plants9121745

Talankova-Sereda, T., Liapina, K., Shkopinskij, E., Ustinov, A., Kovalyova, A., Dulnev, P., et al. (2016). "The influence of Cu и Co nanoparticles on growth characteristics and biochemical structure of mentha longifolia in vitro," in *Nanophysics, nanophotonics, surface studies, and applications* (International Journal of Biosensors & Bioelectronics). : Springer), 427–436.

Thakur, M., Tiwari, S., Kataria, S., and Anand, A. (2022). Recent advances in seed priming strategies for enhancing planting value of vegetable seeds. *Scientia Hortic.* 305, 111355. doi: 10.1016/j.scienta.2022.111355

Tian, H., Ghorbanpour, M., and Kariman, K. (2018). Manganese oxide nanoparticle-induced changes in growth, redox reactions and elicitation of antioxidant metabolites in deadly nightshade (Atropa belladonna l.). *Ind. Crops Products* 126, 403–414. doi: 10.1016/j.indcrop.2018.10.042

Velázquez-Gamboa, M. C., Rodríguez-Hernández, L., Abud-Archila, M., Gutiérrez-Miceli, F. A., González-Mendoza, D., Valdez-Salas, B., et al. (2021). Agronomic biofortification of stevia rebaudiana with zinc oxide (ZnO) phytonanoparticles and antioxidant compounds. *Sugar Tech* 23 (2), 453–460. doi: 10.1007/s12355-020-00897-w

Wu, H., and Li, Z. (2021). Recent advances in nano-enabled agriculture for improving plant performance. *Crop J* 10(1)1–12. doi: 10.1016/j.cj.2021.06.002

Ye, Y., Medina-Velo, I. A., Cota-Ruiz, K., Moreno-Olivas, F., and Gardea-Torresdey, J. L. (2019). Can abiotic stresses in plants be alleviated by manganese nanoparticles or compounds? *Ecotoxicol. Environ. Saf.* 184, 109671. doi: 10.1016/j.ecoenv.2019.109671

Zahra, W., Rai, S. N., Birla, H., Singh, S. S., Rathore, A. S., Dilnashin, H., et al. (2020). "Economic importance of medicinal plants in Asian countries," in *Bioeconomy for sustainable development* (Bioeconomy for Sustainable Development; Springer), 359–377. doi: 10.1007/978-981-13-9431-7_19

Zhishen, J., Mengcheng, T., and Jianming, W. (1999). The determination of flavonoid contents in mulberry and their scavenging effects on superoxide radicals. *Food Chem.* 64 (4), 555–559. doi: 10.1016/S0308-8146(98)00102-2

frontiers | Frontiers in Plant Science

TYPE Original Research
PUBLISHED 08 May 2023
DOI 10.3389/fpls.2023.1146808

OPEN ACCESS

EDITED BY
Nasim Ahmad Yasin,
University of the Punjab, Pakistan

REVIEWED BY
Humaira Yasmin,
COMSATS University, Pakistan
Kotb Attia,
King Saud University, Saudi Arabia
Rehana Sardar,
University of the Punjab, Pakistan
Muhammad Akbar,
University of Gujrat, Pakistan

*CORRESPONDENCE
Marcelo Carvalho Minhoto Teixeira Filho
mcm.teixeira-filho@unesp.br

RECEIVED 17 January 2023
ACCEPTED 19 April 2023
PUBLISHED 08 May 2023

CITATION
Jalal A, Oliveira CEdS, Fernandes GC, da Silva EC, da Costa KN, de Souza JS, Leite GdS, Biagini ALC, Galindo FS and Teixeira Filho MCM (2023) Integrated use of plant growth-promoting bacteria and nano-zinc foliar spray is a sustainable approach for wheat biofortification, yield, and zinc use efficiency.
Front. Plant Sci. 14:1146808.
doi: 10.3389/fpls.2023.1146808

Integrated use of plant growth-promoting bacteria and nano-zinc foliar spray is a sustainable approach for wheat biofortification, yield, and zinc use efficiency

Arshad Jalal[1], Carlos Eduardo da Silva Oliveira[1], Guilherme Carlos Fernandes[1], Edson Cabral da Silva[1], Kaway Nunes da Costa[1], Jeferson Silva de Souza[1], Gabriel da Silva Leite[1], Antonio Leonardo Campos Biagini[1], Fernando Shintate Galindo[2] and Marcelo Carvalho Minhoto Teixeira Filho[1*]

[1]Department of Rural Engineering, Plant Health and Soils, São Paulo State University (UNESP), Ilha Solteira, Brazil, [2]Faculty of Agricultural Sciences and Technology, Department of Plant Production, São Paulo State University (UNESP), Dracena, Brazil

Introduction and aims: The intensive cropping system and imbalance use of chemical fertilizers to pursue high grain production and feed the fast-growing global population has disturbed agricultural sustainability and nutritional security. Understanding micronutrient fertilizer management especially zinc (Zn) through foliar application is a crucial agronomic approach that could improve agronomic biofortification of staple grain crops. The use of plant growth-promoting bacteria (PGPBs) is considered as one of the sustainable and safe strategies that could improve nutrient acquisition and uptake in edible tissues of wheat to combat Zn malnutrition and hidden hunger in humans. Therefore, the objective of this study was to evaluate the best-performing PGPB inoculants in combination with nano-Zn foliar application on the growth, grain yield, and concentration of Zn in shoots and grains, Zn use efficiencies, and estimated Zn intake under wheat cultivation in the tropical savannah of Brazil.

Methods: The treatments consisted of four PGPB inoculations (without inoculation, *Azospirillum brasilense, Bacillus subtilis*, and *Pseudomonas fluorescens*, applied by seeds) and five Zn doses (0, 0.75, 1.5, 3, and 6 kg ha^{-1}, applied from nano ZnO in two splits by leaf).

Results: Inoculation of *B. subtilis* and *P. fluorescens* in combination with 1.5 kg ha^{-1} foliar nano-Zn fertilization increased the concentration of Zn, nitrogen, and phosphorus in the shoot and grain of wheat in the 2019 and 2020 cropping seasons. Shoot dry matter was increased by 5.3% and 5.4% with the inoculation of *P. fluorescens*, which was statistically not different from the treatments with inoculation of *B. subtilis* as compared to control. The grain yield of wheat was

increased with increasing nano-Zn foliar application up to 5 kg Zn ha^{-1} with the inoculation of *A. brasilense* in 2019, and foliar nano-Zn up to a dose of 1.5 kg ha^{-1} along with the inoculation of *P. fluorescens* in the 2020 cropping season. The zinc partitioning index was increased with increasing nano Zn application up to 3 kg ha^{-1} along with the inoculation of *P. fluorescens*. Zinc use efficiency and applied Zn recovery were improved at low doses of nano-Zn application in combination with the inoculation of *A. brasilense, B. subtilis*, and *P. fluorescens*, respectively, as compared to control.

Discussion: Therefore, inoculation with *B. subtilis* and *P. fluorescens* along with foliar nano-Zn application is considered a sustainable and environmentally safe strategy to increase nutrition, growth, productivity, and Zn biofortification of wheat in tropical savannah.

KEYWORDS

***Triticum aestivum L.*, zinc fertilization, beneficial microorganisms, *Azospirillum brasilense*, *Bacillus subtilis*, *Pseudomonas fluorescens*, PGPBs**

1 Introduction

Zinc (Zn) malnutrition and deficiency is a persistent health and social concern that has affected approximately 17.5% of the global population (Bollinedi et al., 2020; Maxfield et al., 2023). Zinc deficiency is recognized as the 11th major health risk factor in the world and 5th in developing countries, and is declared as a "hidden hunger" (Bhatt et al., 2020; Poniedziałek et al., 2020). The high phytate–Zn ratio is another factor that can hinder Zn distribution into the edible tissues of cereal crops (Rehman et al., 2021). The prevalence of Zn malnutrition is most commonly seen in the population of wheat-consuming countries due to its cultivation on marginal and Zn-deficient soils (Chattha et al., 2017). In addition, several other factors including soil pH, bicarbonates, oxides, macronutrient concentration, and low mobility of Zn in soil solution affect Zn use efficiency and availability to the plants that can lead to crop failure, inadequate Zn accumulation in edible tissues, and human malnutrition (Bhatt et al., 2020; Zulfiqar et al., 2021; Penn et al., 2023). Therefore, to improve the quality and productivity of field crops, an alternative potential source of fertilizers is needed to replace conventional Zn fertilizers.

In recent years, the use of nano-Zn fertilizer is considered as an effective tool in the agricultural system because of its multiple impacts on plants and the environment (Aziz et al., 2019; Ahmad et al., 2020). The application of nano-Zn fertilizer can increase Zn mobility in phloem, increasing its bioavailability in the endosperm and contributing to protein synthesis and other biochemical traits of crop plants (Rossi et al., 2019; Ahmad et al., 2020). In addition, foliar nano-Zn application is considered as a less expensive and rapid strategy in comparison to soil Zn fertilization for better performance and agronomic biofortification of crop plants under different environmental conditions (Faizan et al., 2021; Jalal et al., 2022c). The application of nano-Zn in the early or late growth stages of crops can better define the effectiveness of agronomic biofortification under field conditions (Afshar et al., 2020; Jalal et al., 2022c). Nano-Zn application during tasseling and grain filling growth stages of wheat and maize could improve grain development and grain Zn concentration under field conditions (Jalal et al., 2022c; Jalal et al., 2023). However, foliar fertilization is limited by source, particulate size, and formulation (Fernández and Brown, 2013), which may cause toxicity in field crops and humans. Adopting sustainable agricultural practices to face the challenge of food and nutritional security in a sustainable manner is unprecedented.

The intervention of plant growth-promoting bacteria (PGPBs) in an agricultural system is a well-known sustainable strategy that could improve soil fertility, crop productivity, and nutrient bioavailability to deal with food and nutritional security (Akbar et al., 2019; Jalal et al., 2020c; Kumar et al., 2021). PGPBs can enhance Zn bioavailability and accumulation through solubilization, nitrogen fixation, synthesis of inorganic and organic acids, phyto-hormones, and chelators (Idayu et al., 2017; Khoshru et al., 2020). Inoculation with PGPBs could induce plant growth and performance by increasing nutrient use efficiency, improving water retention and synthesis of secondary metabolites, and protecting host plants against biotic and abiotic stresses (Jalal et al., 2021; Hungria et al., 2022; Ilyas et al., 2022; Yasmin et al., 2022). Among PGPBs, *Azospirillum brasilense, Bacillus subtilis*, and *Pseudomonas fluorescens* are the most studied inoculants in Brazil. The combined Zn fertilization and inoculation with *A. brasilense* can boost the productivity of tropical cereal crops by enhancing Zn absorption and use efficiency (Galindo et al., 2021). Additionally, *B. subtilis* and *P. fluorescens* are recently identified as the most effective inoculants for solubilizing Zn and phosphorus as well as for enhancing plant growth and performance under diverse environments (Ahmad et al., 2021; Jalal et al., 2021; Jalal et al., 2022a; Jalal et al., 2022b; Rosa et al., 2022).

Wheat has been recognized as a delicate cereal crop due to its naturally low grain Zn concentration (Zou et al., 2012). Wheat has a great agronomic relevance to food and nutritional security and its cultivation in tropical savannah can be considered as a promising approach towards achieving food security and sustainability (FAO. United Nations Food and Agricultural Organization, 2019; Galindo et al., 2022a). Wheat cultivation in tropical and marginal regions can be a diversified source of food to feed the increasing global population with optimal nutritional food (Galindo et al., 2022a). Therefore, inoculation with PGPBs in combination with Zn fertilizer could be considered as a sustainable strategy to improve nutrient use efficiency and wheat productivity (Galindo et al., 2021). However, there still exists a research gap on the combined application of PGPBs and foliar fertilizer of nano-Zn on the Zn use efficiency, nutritional status, and yield of wheat in tropical savannah. Hence, the present study hypothesized that the combined use of PGPBs and foliar fertilizer of nano-Zn would improve Zn use efficiencies and was assumed to be a sustainable strategy for increasing wheat productivity and biofortification. In the present scenario, the aim of the current study was to identify the best-performing PGPB inoculant in combination with nano-Zn foliar application on wheat growth, grain yield, biofortification, Zn use efficiencies, and estimated daily Zn intake in the tropical savannah of Brazil.

2 Materials and methods

2.1 Experimental area and location

A field experiment was performed with wheat crop for two consecutive cropping seasons (2019–2020) at the Extension and Research Farm of School of Engineering, São Paulo State University (UNESP) at Selvíria, State of Mato Grosso do Sul, Brazil. The experimental field is located at geographical coordinates of 20°22′ S latitude, 51°22′ W longitude, and an altitude of 335 m (Figure 1). The climate of the region was classified as Aw type (humid tropical with a dry winter and rainy summer) as per the classification of Köppen-Geiger. The daily rainfall and temperature data in both cropping seasons of wheat are summarized in Figure 2. The soil was classified as Dystrophic Rhodic Haplustox with a clayey texture (Soil Survey Staff, 2014). The experimental area was grown with

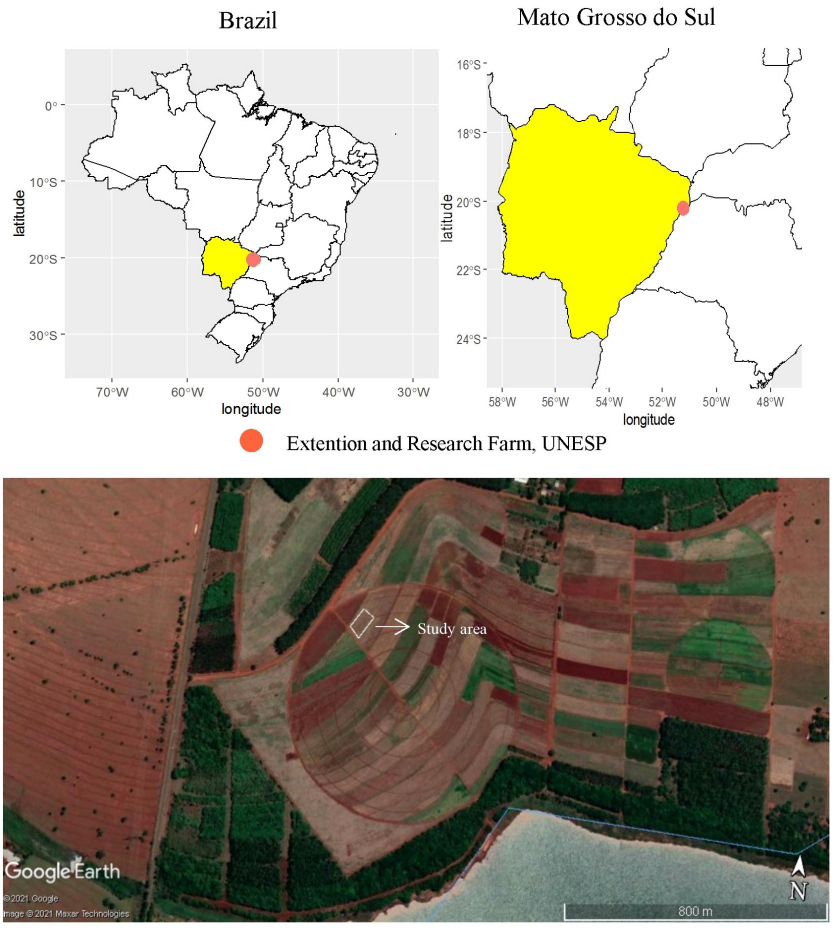

FIGURE 1
Experimental location at the Research and Extension Farm in Selvíria - Mato Grosso do Sul state, Brazil (20°22′S, 51°22′W, altitude of 335 m) in 2019 and 2020 crop seasons. The map was created using pacot, geobr, and ggplot with R software (R Development Core Team, 2015). Projection System WGS 84/ UTM 200DC [EPSG: 4326]. This image was taken from Google Earth program, Google Company (2021). Map data: Google, Maxar Technologies.

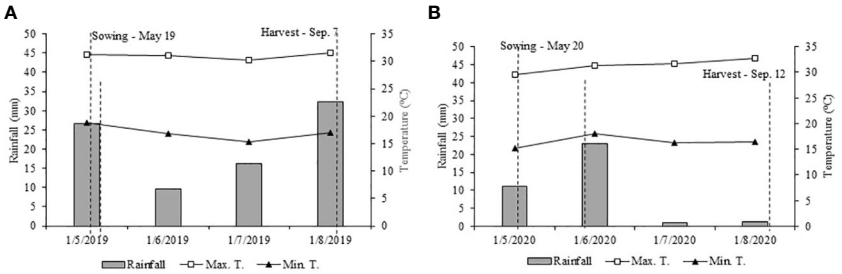

FIGURE 2
Meteorological data were acquired from the automatic weather station of Education and Research Farm during the wheat cultivation period from May to September 2019 **(A)** and May to September 2020 **(B)**.

annual cereal and legume crops for over 28 years, while for the past 13 years, the area is under a no-tillage system (Santos et al., 2018).

Before beginning the experiment, 20 randomly selected soil samples were collected from the location of the experiment using a cup-type auger at a soil depth of 0.0–0.20 m. The soil samples were mixed to make a composite sample and analyzed according to the procedure of Raij et al. (2001) for the following chemical properties: pH ($CaCl_2$) = 5.2; P (resin) = 37 mg dm^{-3}; S-SO_4^{-2} = 5 mg dm^{-3}, K^+ = 2.3 $mmol_c$ dm^{-3}; Ca^{2+}= 27 $mmol_c$ dm^{-3}; Mg^{2+}= 17 $mmol_c$ dm^{-3}; Al^{3+}= 0.01 $mmol_c$ dm^{-3}; H+Al = 35 $mmol_c$ dm^{-3}; cation exchange capacity = 69.1 $mmol_c$ dm^{-3}; base saturation = 52%; organic matter = 19 g kg^{-1}; B (hot water) 0.15 mg dm^{-3}. The pre-experiment soil analysis showed that diethylenetriaminepentaacetic acid (DTPA) extractable Zn content (0.7 mg dm^{-3}) was medium low, while Fe = 29 mg dm^{-3}, Mn = 41 mg dm^{-3}, and Cu = 4 mg dm^{-3}. A pre-experiment composite soil sample was also determined for the following granulometric attributes: clay (439 g kg^{-1}), sand (471 g kg^{-1}), and slit (90 g kg^{-1}) as per the methodology of Teixeira et al. (2017).

2.2 Experimental design and treatments

Experiments were carried out in a completely randomized block design with four replications, arranged in a 4 × 5 factorial scheme. The treatments consisting of four types of seed inoculations (no inoculation, *A. brasilense, B. subtilis*, and *P. fluorescens*) and five nano-Zn foliar doses (0, 0.75, 1.5, 3.0, and 6.0 kg Zn ha^{-1}) were applied 50% during tillering and 50% at the grain filling stage of wheat (Dhaliwal et al., 2019).

Seeds were manually inoculated in an individual plastic bag by mixing seeds with inoculant an hour before planting. Inoculation *via* seeds was performed using inoculants provided by the manufacturer (Biotrop®, Curitiba, Brazil). These inoculants are being commercially registered with the Ministry of Agriculture of Brazil with trade names of AzoTotal™ (*A. brasilense*), Vult™ (*B. subtilis*), and Audax™ (*P. fluorescens*). Wheat seeds were inoculated with *A. brasilense* strains Ab-V5 (CNPSo 2083) and Ab-V6 (CNPSo 2084) with a colony-forming unit (CFU) of 2×10^8 ml^{-1} at a dose of 200 ml of liquid inoculant per 24 kg of seeds. The genome sequences of *A. brasilense* described that both strains Ab-V5 and Ab-V6 carried *fix* and *nif* genes that could promote nutrient transportation, biological nitrogen fixation, and the production of phytohormones, and invigorate tolerance against abiotic stresses (Fukami et al., 2018; Hungria et al., 2018). Inoculations with a *B. subtilis* strain (CCTB04) at 1×10^8 CFU ml^{-1} and a *P. fluorescens* strain (CCTB03) at 2×10^8 CFU ml^{-1} were performed at a dose of 150 ml ha^{-1} per 24 kg of wheat seeds. *B. subtilis* is carrying a non-ribosomal peptide synthetase and beta-glucanase to prevent phyto-pathogen infestation, helping in the bioremediation of heavy metal and Zn transporter (*zntR*) that could promote plant growth (Chaoprasid et al., 2015; Rekha et al., 2017; Muñoz-Moreno et al., 2018). *P. fluorescens* produces antibiotics, gluconic acid, and volatile organic compounds to deter soil pathogens, solubilize nutrients, and help in biological N fixation (David et al., 2018; Jing et al., 2020).

Foliar application of nano-Zn was performed from a liquid source of Zn (Nano R1 Zinco™), obtained from Allplant® fertilizer industry, São Paulo, Brazil. The product is already registered with the Ministry of Agriculture, Brazil. Nano R1 zinc is characterized as a fluid suspension with 50% p/p Zn, 1,000 g L^{-1} solubility, 2.0 density, and 150-nm particle size, and is successfully used in previous studies to increase grain and plant Zn concentration (Nakao et al., 2018; Jalal et al., 2022c). Foliar application of nano-Zn was performed through a manual sprayer pump with a water capacity of 6.0 L (300 L ha^{-1} of volume application). Each foliar dose of nano-Zn was applied 50% during tillering and 50% at the grain filling stage of wheat (Dhaliwal et al., 2019). Spraying was carried out every morning. The field was visited soon after foliar spraying but no leaf damage was observed.

2.3 Plant materials

The experimental site was sprayed with herbicides [carfentrazone (40 g ha^{-1}), glyphosate (1,800 g ha^{-1}), and cletodim (240 g ha^{-1}) of active ingredient (a.i.)] approximately 15 days prior to experimental initiation to control weeds with narrow and broad leaves. Wheat seeds were chemically treated with Standak Top® [co-formulation of fungicides {thiram + carbendazim (105 g + 45 g of a.i.)} and insecticides {thiodicarb + imidacloprid (135 g + 45 g of a.i.)}] 100 kg^{-1} seeds, prior to inoculation and planting. Previous research reported that chemical treatment of cereal seeds before planting is a common agricultural practice in Brazil that

could prevent infestation of soil pathogen without any drastic effect on seed inoculation of the same nature as the current experiment (Cardillo et al., 2019; Galindo et al., 2021; Jalal et al., 2023).

Wheat genotype (TBIO SOSSEGO) of potential production and quality was planted in a no-tillage system on 11 May 2019 and 3 May 2020 in the first and second cropping seasons, respectively. Sowing was carried out with a drill sowing method at 80 seeds m^{-1} while seedlings emerged approximately 5 days after planting. A basal dose of 270 kg ha^{-1} was applied from 08-28-16 (32, 112 and 64 kg ha^{-1} of N, P_2O_5, and K_2O) at sowing on the basis of pre-experiment soil analysis and the recommendation of Boletim-100 for wheat crop (Cantarella et al., 1997). Each plot was composed of 13 rows, 5.0 m long and 0.17 m apart, for a total of 12.15 m^2. The recommended dose of 120 N kg ha^{-1} was manually applied using the fertilizer ammonium sulfate during tillering (decimal growth stage-GS21) (Zadoks et al., 1974). Crops were irrigated with a sprinkler central-pivot irrigation system (14 mm on average) on the same day as fertilizer application to achieve uniform distribution and incorporation in all treatments. The experimental area had boron (B) deficiency (Vale et al., 2008). Therefore, all the treatments were homogeneously applied with 1.0 kg ha^{-1} of B from the source of boric acid (18% of B) through a tractor sprayer machine on the basis of pre-experiment soil analysis and interpretation of Campinas Agronomic Institute- IAC (Raij et al., 2001). The wheat crop was manually harvested on 12 September 2019 (with a 125-day cycle) and 7 September 2020 (with a 128-day cycle).

2.4 Evaluation and analysis

2.4.1 Nutritional analysis

The plant materials (shoot and grain) were collected at physiological maturity in properly labeled paper bags and dried in an airtight oven at 60 ± 5°C for 72 h to measure nutritional analysis. The samples were ground in a stainless-steel Wiley knife mill by passing through a 10-mm-mesh sieve and stored in labeled plastic bags. Each sample was weighed (0.25 g), digested with nitroperchloric acid (HNO_3:$HClO_4$ solution), and quantified by atomic absorption spectrophotometry. The analysis was developed by following the methodology of Malavolta et al. (1997).

2.4.2 Growth and productivity attributes

Plant height at physiological maturity was manually measured with a meter rod from the ground surface to the upper apex of the plant. Shoot dry matter was determined after harvesting from four central lines. The plants harvested from four central lines and samples were kept in an oven for 72 h at 60 ± 5°C to measure shoot dry matter. Wheat spikes were harvested from five central rows of 5-m length in bags and desiccated in the shade for approximately 7 days. An electric thresher was used for threshing individual samples and processed grains were weighed for conversion into grain yield per hectare at 13% moisture content.

2.4.3 Zinc partitioning index, intake, and use efficiencies

The zinc partitioning index (ZPI) was derived from the fraction of grain-to-shoot Zn concentration following the methodology of Rengel and Graham (1996). Estimated daily Zn intake in Brazil with consumption of wheat grains on a daily basis was derived from the biofortified wheat grains in the present study, following the small modification in the study of Lessa et al. (2019). The consumption of wheat according to the Foreign Agricultural Service - United States Department of Agriculture (USDA. Foreign Agriculture Services, 2020) was 56.86 kg $person^{-1}$ per annum (156 g $person^{-1}$ per day) in Brazil. Following this information, the daily intake of biofortified wheat grains was calculated below in Eq. 1.

$$\text{Zn intake} = [\text{Grain Zn}] \times \text{C} \qquad \text{(Eq. 1)}$$

where Zn grain (g kg^{-1}) is the Zn concentration in biofortified grains in the present results and C (g $person^{-1}$ per day) is the mean grain consumption of wheat per capita per day in Brazil.

Zinc use efficiency (ZnUE) and recovery applied Zn (RAZn) were calculated from the fraction of shoot Zn uptake to shoot dry matter and grain Zn uptake to grain yield using the procedure of Fageria et al. (2009); Fageria et al. (2011), and Jalal et al. (2021).

$$\text{ZnUE} = \frac{\text{GY ZnF} - \text{GY ZnWF}}{\text{Zn applied dose (foliar)}} \qquad \text{(Eq. 2)}$$

$$\text{RAZn (\%)} = \frac{\text{ZnAF} - \text{ZnAWF}}{\text{Zn applied dose (foliar)}} \qquad \text{(Eq. 3)}$$

where GY ZnF = grain yield with Zn fertilization, GY ZnWF = grain yield without Zn fertilization, ZnAF = shoot + grain Zn accumulation in Zn fertilized plots, and ZnAWF = shoot + grain Zn accumulation in Zn-fertilized plots.

2.5 Statistical analysis

All data were initially tested for normality using Shapiro and Wilk test, which showed that data are normally distributed ($W \geq 0.90$). The data were submitted to analysis of variance (F test). Inoculations with PGPBs, Zn foliar doses, and their interactions were considered fixed effects in the model. When a main effect or interaction was significant by F test ($p \leq 0.05$), then Tukey test ($p \leq 0.05$) was used for the comparison of means of inoculations with PGPBs. In addition, regression analysis was performed for Zn foliar doses using R software (R Core Team, 2015).

The Pearson correlation analysis ($p \leq 0.05$) was performed using R software (R Development Core Team). To create a heatmap, the package of corrplot with "cor" and "cor.mtest" functions was used to calculate the coefficients and p-value matrices. The digits added to the heatmap cells identify the significant correlations.

10.3389/fpls.2023.1146808

TABLE 1 Shoot zinc (Zn), nitrogen (N), and phosphorus (P) concentrations of wheat as influenced by plant growth-promoting bacteria and foliar applied nano-Zn doses.

Treatments	Shoot Zn concentration		Shoot N concentration		Shoot P concentration	
	g kg^{-1}					
	2019	2020	2019	2020	2019	2020
Inoculations						
Without	29.5	32.9 b	5.4 b	5.2 b	1.17 b	1.15 b
A. brasilense	32.8	35.9 ab	5.5 b	5.9 ab	1.27 ab	1.27 ab
B. subtilis	35.3	37.1 a	6.7 a	6.4 a	1.26 ab	1.40 ab
P. fluorescens	33.6	39.0 a	6.3 ab	6.3 a	1.48 a	1.52 a
Foliar Zn application (kg ha^{-1})						
0	29.3	32.4	5.7	5.8	1.12	1.12
0.75	31.5	35.5	6.7	5.9	1.18	1.20
1.5	36.8	40.1	5.9	6.8	1.49	1.42
3	33.5	37.0	5.7	5.5	1.40	1.44
6	33.0	35.9	5.7	5.8	1.28	1.48
F-values						
Inoculation (I)	10.5**	8.9**	6.8**	7.2**	3.5*	5.5**
Foliar Zn (FZn)	10.8**	8.5**	2.9*	4.0**	3.7*	4.5**
I × FZn	2.06*	0.8 ns	0.9 ns	2.1*	1.7 ns	1.0 ns
CV (%)	10.23	10.5	16.7	15.6	23.9	22.7

Means in the column followed by different letters are significantly different (p-value ≤ 0.05); ** and * denote significant at p ≤ 0.01 and p ≤ 0.05, respectively, while ns indicates non-significant by F-test.

3 Results

3.1 Zinc, nitrogen, and phosphorus concentrations in wheat plant and grains

The concentrations of zinc (Zn), nitrogen (N), and phosphorus (P) in shoot and grains of wheat were significantly influenced by inoculation with PGPBs and nano-Zn spray. Inoculation with PGPBs and foliar fertilization with nano-Zn significantly enhanced shoot Zn concentration of wheat in the cropping seasons of 2019 and 2020 (Table 1). The interaction for shoot Zn concentration was only significant in the 2019 cropping season (Table 1). The graphical trend in the 2019 cropping season indicated that increasing nano-Zn foliar spray up to 3.6 and 3.2 kg ha^{-1} in combination with inoculation of *A. brasilense* and *B. subtilis* increased shoot Zn concentration, respectively, while further increase in foliar nano-Zn fertilization led to the reduction of shoot Zn concentration. The combination of inoculation with *P. fluorescens* and foliar nano-Zn application was observed to be non-significant (Figure 3A). In the 2020 wheat cropping season, shoot Zn concentration was increased by 18.5% with inoculation of *P. fluorescens*, which was statistically similar to the inoculation of *B. subtilis* and *A. brasilense* as compared to without inoculation treatments (Table 1). The quadratic equation of foliar nano-Zn application was adjusted to 3.38 kg ha^{-1} to increase shoot Zn concentration in the 2020 cropping season (Supplementary Table 1).

Shoot N concentration of wheat was positively increased with inoculation and foliar fertilization with nano-Zn in both cropping seasons (Table 1). Interaction of shoot N concentration was not significant in 2019 (Supplementary Table 1) and significant in the 2020 wheat cropping season (Figure 3B). Among inoculations, inoculation with *B. subtilis* enhanced shoot N concentration by 24% as compared to control treatments in first cropping season. Foliar application of nano-Zn at a dose of 1.5 kg ha^{-1} was observed with the highest shoot N concentration in the 2019 cropping season (Table 1). The shoot N concentration was adjusted to quadratic trend in the 2020 cropping season (Figure 3B). Shoot N concentration was enhanced with increasing foliar nano-Zn fertilization up to 3.11 kg ha^{-1} in combination with inoculation of *B. subtilis* while further increase in foliar nano-Zn doses led to the reduction of shoot N concentration of wheat (Figure 3B). In addition, the interactions of nano-Zn foliar doses with other inoculations were found to be non-significant (Figure 3B).

The interactions of inoculation with PGPBs and foliar fertilization with nano-Zn fertilization for shoot P concentration were not significant (Table 1). In addition, shoot P concentration of wheat was significantly enhanced with inoculation and foliar nano-Zn fertilization in the 2019 and 2020 cropping seasons (Table 1). Inoculation with *P. fluorescens* enhanced shoot concentration of P by 26.5% and 32.2% in the 2019 and 2020 cropping seasons, respectively, in comparison to the treatments without inoculation. The regression of foliar nano-Zn doses was adjusted to quadratic

10.3389/fpls.2023.1146808

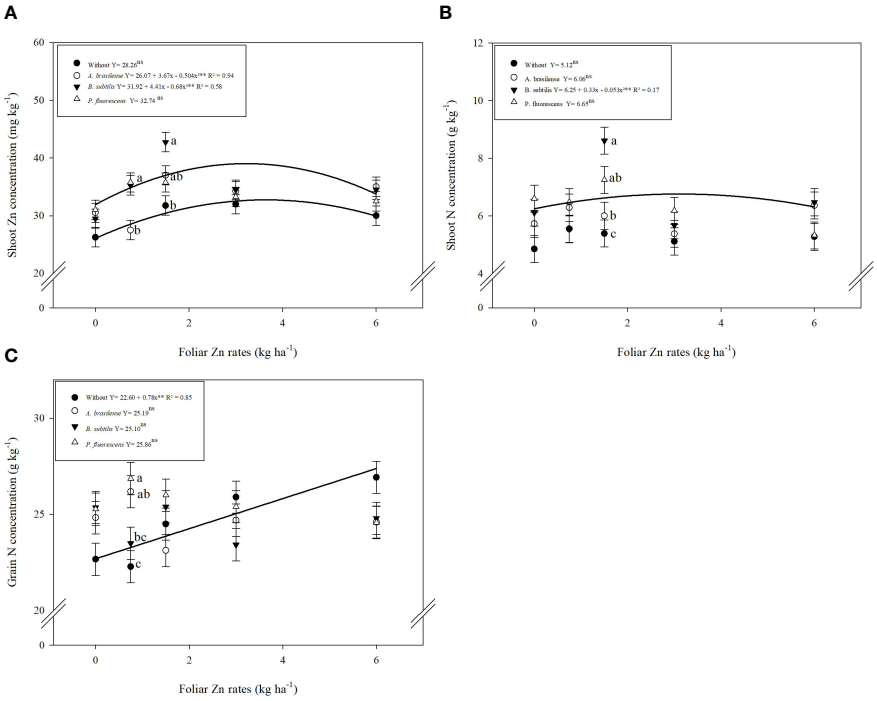

FIGURE 3
Influence of inoculation with PGPBs and nano-Zn foliar application on shoot Zn concentration in 2019 **(A)**, shoot N concentration in 2020 **(B)**, and grain N concentration in 2020 **(C)** of wheat. The different letters correspond to a significant difference at 5% probability level ($p \leq 0.05$). The identical letters do not differ from each other as analyzed by Tukey test (PGPBs inoculations; $p \leq 0.05$) and Regression (Foliar Zn rates; $p \leq 0.05$) tests for wheat cropping year 2019 and 2020, respectively. Error bars indicate the standard error of the mean (n = 4 replications). Selvíria, 2020. **: significant at $p \leq 0.01$.

TABLE 2 Grain zinc (Zn), nitrogen (N), and phosphorus (P) concentrations of wheat as a function of plant growth-promoting bacteria and foliar applied nano-Zn doses.

Treatments	Grain Zn concentration		Grain N concentration		Grain P concentration	
	——— mg kg^{-1} ———		——————————— g kg^{-1} ———————————			
	2019	2020	2019	2020	2019	2020
Inoculations						
Without	37.6 c	44.2 b	24.5	24.4	2.49 b	2.53 c
A. brasilense	42.6 b	49.6 a	24.6	24.7	2.79 b	2.82 cb
B. subtilis	45.6 ab	50.8 a	25.3	24.5	3.16 a	3.15 a
P. fluorescens	46.5 a	51.5 a	24.8	25.6	2.79 b	2.91 ab
Foliar Zn application (kg ha^{-1})						
0	40.3	45.5	23.5	24.5	2.68	2.63
0.75	41.8	47.0	24.3	24.7	2.69	2.91
1.5	45.9	54.0	26.1	24.7	3.16	3.05
3	43.8	50.0	25.3	24.8	2.74	2.96
6	43.3	48.6	24.9	25.2	2.77	2.71
F-values						
Inoculation (I)	16**	7.2**	0.7 ns	2.1 ns	9.1**	8.8**

(Continued)

10.3389/fpls.2023.1146808

TABLE 2 Continued

Treatments	Grain Zn concentration		Grain N concentration		Grain P concentration	
	——— mg kg^{-1} ———		———————— g kg^{-1} ————————			
	2019	2020	2019	2020	2019	2020
Foliar Zn (FZn)	3.6*	5.7**	3.8*	0.3 ns	3.7*	3.3*
I × FZn	1.3 ns	0.9 ns	1.1 ns	3.1**	1.6 ns	1.0 ns
CV (%)	10.2	11.2	7.87	6.7	14.4	13.5

Means in the column followed by different letters are significantly different (p-value ≤ 0.05); ** and * denote significant at p ≤ 0.01 and p ≤ 0.05, respectively, while ns indicates non-significant by F-test.

trend, where shoot P concentration was increased with a maximum estimated foliar nano-Zn dose of 5.0 and 4.4 kg ha^{-1} in 2019 and 2020, respectively (Supplementary Table 1). A further increase in foliar nano-Zn fertilization may cause reduction in shoot P concentration in the 2019 and 2020 cropping seasons.

The grain Zn concentration of wheat was positively influenced by inoculation and foliar nano-Zn fertilization in the 2019 and 2020 cropping seasons while their interactions were not significant in both studied cropping seasons (Table 2). Inoculation with *P. fluorescens* increased grain Zn concentration by 23.7% and 16.5%, which was statistically at par with inoculation of *B. subtilis* in 2019, and with inoculation of *B. subtilis* and *A. brasilense* as compared to without inoculation treatments in both seasons, respectively. The regression equation of nano-Zn foliar application was adjusted to a maximum estimated dose of 3.5 and 3.4 kg ha^{-1} for the higher grain Zn concentration of wheat in the 2019 and 2020 cropping seasons (Supplementary Table 1). These calculations indicated that a further increase of foliar nano-Zn fertilization may cause reduction in the grain Zn concentration of wheat.

Grain N concentration was not significantly enhanced by inoculations or the interaction of foliar nano-Zn × inoculations in 2019, while the interaction in 2020 was significant (Table 2). The regression of foliar nano-Zn application was adjusted to a quadratic equation with a maximum estimated dose of 3.5 kg ha^{-1} for the increasing grain N concentration in the 2019 cropping season (Supplementary Table 1). In addition, grain N concentration was linearly enhanced with increasing foliar nano-Zn fertilization regardless of the inoculation in the 2020 cropping season of wheat as indicated in the graph trend (Figure 3C).

Inoculation and foliar nano-Zn doses positively enhanced grain P concentration while their interactions were not significant in both the 2019 and 2020 cropping seasons (Table 2). Grain P concentration was increased by 26.9% and 24.5% with the inoculation of *B. subtilis* as compared to without inoculation in the first and second cropping seasons, respectively. The regression analysis indicated that foliar nano-Zn was adjusted to a quadratic equation, where increasing foliar nano-Zn doses up to 3.0 and 3.4 kg ha^{-1} could increase grain P concentration while a further increase may cause reduction in grain P concentration of wheat in 2019 and 2020, respectively (Supplementary Table 1).

3.2 Shoot dry matter, yield, and zinc partitioning

Shoot dry matter of wheat was significantly increased by inoculation with PGPBs and foliar fertilization of nano-Zn while the interactions in both 2019 and 2020 cropping seasons were not significant (Table 3). Shoot dry matter was increased by 5.3% with the inoculation of *P. fluorescens* in both cropping seasons, which was statistically similar to treatments with the inoculation of *B. subtilis* and *A. brasilense* as compared to without inoculation. The regression analysis of nano-Zn foliar application was adjusted to a quadratic equation with a maximum Zn dose of 3.0 and 3.2 kg ha^{-1} in the 2019 and 2020 cropping seasons, respectively (Supplementary Table 1). Any further increase in nano-Zn foliar application may lead to the reduction of wheat shoot dry matter.

The interactive effect of inoculation with PGPBs and foliar nano-Zn doses positively enhanced the grain yield of wheat in the first and second cropping seasons (Table 3). The graph trend of the interaction of inoculations and nano-Zn foliar doses for grain yield of wheat in the 2019 and 2020 cropping seasons was set to a quadratic function (Figures 4A, B). Increasing foliar application of nano-Zn to 5 kg ha^{-1} in combination with inoculation of *A. brasilense* increased grain yield in the 2019 cropping season (Figure 4A). In addition, a maximum calculated dose of foliar nano-Zn up to 1.5 kg ha^{-1} in combination with the inoculation of *P. fluorescens* increased grain yield of wheat in the 2020 cropping season (Figure 4B). A further increase in foliar application of nano-Zn fertilization after calculated doses in the presence of inoculation with *A. brasilense* and *P. fluorescens* caused reduction in grain yield of wheat.

ZPI improved with the inoculation and application of foliar nano-Zn doses (Table 3). The interactive effect of foliar nano-Zn application and inoculations for ZPI was not significant in 2019 whereas interaction for ZPI was significant in the 2020 cropping season. ZPI was increased by 20% with the inoculation of *P. fluorescens* (Table 3). Foliar nano-Zn doses adjusted to a quadratic trend with an increasing dose of up to 3 kg ha^{-1} increased ZPI in wheat grain (Supplementary Table 1). The interactive effect of inoculation and foliar nano-Zn doses for ZPI in the 2020 cropping season was also adjusted to a quadratic trend (Figure 4C). The graph trend of foliar nano-Zn doses indicated that

TABLE 3 Shoot dry matter, grain yield, and Zn partitioning index of wheat grains as a function of plant growth-promoting bacteria and foliar applied nano-Zn doses.

Treatments	Shoot dry matter		Grain yield		Zn partitioning index	
	———— kg ha^{-1} ————				—— % ——	
	2019	2020	2019	2020	2019	2020
Inoculations						
Without	4,843 b	4,909 b	3,436	3,341	70 b	131
A. brasilense	5,009 ab	5,095 a	3,508	3,705	75 b	139
B. subtilis	5,072 a	5,066 ab	3,582	3,731	78 ab	137
P. fluorescens	5,099 a	5,172 a	3,595	3,883	84 a	132
Foliar Zn application (kg ha^{-1})						
0	4,941	4,940	3,424	3,602	73	121
0.75	4,998	5,049	3,462	3,680	78	149
1.5	5,090	5,203	3,595	3,787	80	138
3	5,044	5,070	3,601	3,641	77	133
6	4,957	5,041	3,569	3,615	75	135
***F*-values**						
Inoculation (I)	6.5**	6.4**	1.4 ns	17**	6.2**	0.9 ns
Foliar Zn (FZ)	1.5 ns	3.7**	1.3 ns	1.4 ns	1.0 ns	5.1**
I × FZ	1.5 ns	0.8 ns	2.8**	2.9 **	0.8 ns	6.4**
CV (%)	4	3.8	7.8	6.7	13.2	13.2

Means in the column followed by different letters are significantly different (p-value ≤ 0.05); ** and * denote significant at p ≤ 0.01 and p ≤ 0.05, respectively; ns indicates non-significant, by F-test.

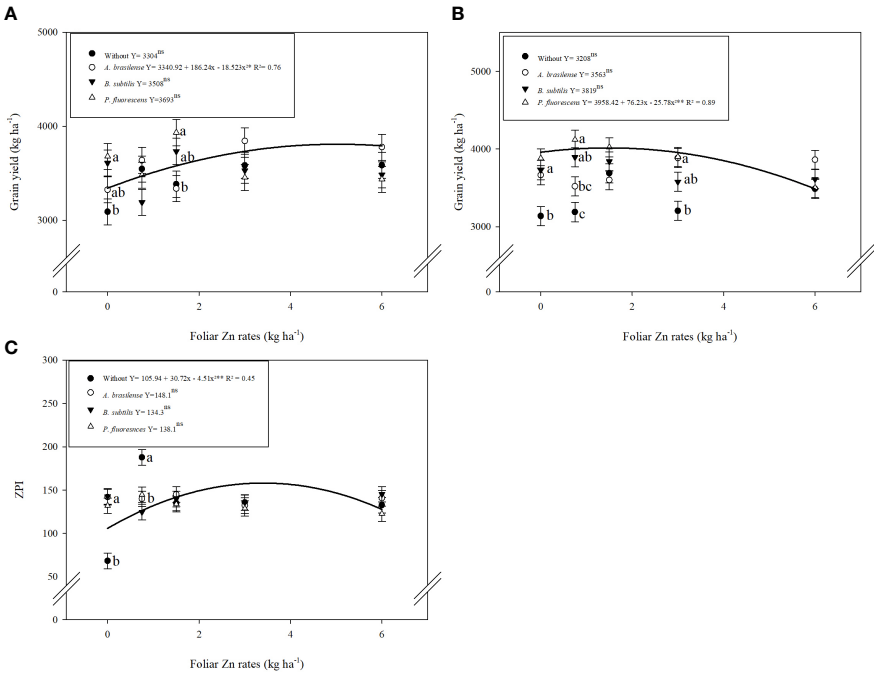

FIGURE 4
Influence of inoculation with PGPBs and nano-Zn foliar application on grain yield in 2019 **(A)** and 2020 **(B)**, and Zn partitioning index (ZPI) in 2020 **(C)** of wheat. The different letters correspond to a significant difference at 5% probability level ($p \leq 0.05$). The similar letters of different means showed no difference as analyzed by Tukey test (PGPBs inoculations; $p \leq 0.05$) and Regression (Nano-Zn foliar doses; $p \leq 0.05$) tests for the first and second wheat cropping year, respectively. Error bars indicate the standard error of the mean ($n = 4$ replications). Selvíria, 2020. **: significant at $p \leq 0.01$.

increasing nano-Zn application by up to 3.4 kg ha^{-1} regardless of inoculation increased ZPI in wheat grains (Figure 4C).

3.3 Zinc intake and Zn use efficiencies

The interactions of inoculation and nano-Zn foliar fertilization were not significant for the daily Zn intake with wheat consumption in both cropping seasons (Supplementary Table 2). Inoculation with *P. fluorescens* was observed with the maximum daily Zn intake from consumption of wheat in Brazil. Zinc intake was increased by 24% and 16% with the inoculation of *P. fluorescens* as compared to without inoculation in the 2019 and 2020 cropping seasons. The quadratic function for Zn intake described that increasing foliar nano-Zn application by up to 3.9 and 3.6 kg ha^{-1} improved the estimated daily Zn intake with wheat consumption in Brazil in the 2019 and 2020 cropping seasons, respectively (Supplementary Table 1). In both cases, a further increase in Zn-foliar doses may reduce estimated daily Zn intake in wheat grains.

The interactions between inoculations with PGPBs and foliar nano-Zn doses were significant for both Zn use efficiency (ZnUE) and applied Zn recovery (AZnR) (Supplementary Table 2). The graph trend indicated that ZnUE was linearly decreased with the inoculation of *A. brasilense* and *P. fluorescens* under increasing doses of nano-Zn foliar application in the first wheat cropping season. Zinc use efficiency with inoculation of *B. subtilis* was set to a quadratic trend with an increasing dose (1.8 kg ha^{-1}) of nano-Zn foliar application while a further increase may cause reduction under the same inoculation (Figure 5A). In 2020, ZnUE was also linearly decreased with increasing doses of foliar nano-Zn application along with the inoculation of *A. brasilense, B. subtilis*, and *P. fluorescens*, while the interaction of foliar nano-Zn doses and without inoculation was not significant (Figure 5B). In addition, applied Zn recovery was linearly decreased with increasing foliar nano-Zn doses in 2019 (Figure 5C) and 2020 (Figure 5D), regardless of inoculation.

3.4 Pearson's linear correlation

Pearson's linear correlations between most of the evaluated attributes of wheat were positive and significant in 2019 (Figure 6A) and 2020 (Figure 6B). There was a positive correlation between grain N concentration and all evaluated attributes except applied Zn recovery and Zn use efficiency, which was positive but not significant in wheat cultivation during the 2019 crop season (Figure 6A).

In addition, there was a positive correlation between grain N concentration and all the evaluated attributes of wheat, except shoot N concentration in the 2020 cropping season (Figure 6B).

4 Discussion

Wheat grains are inherently low in Zn, which may result in not meeting daily human Zn requirement, particularly in regions with

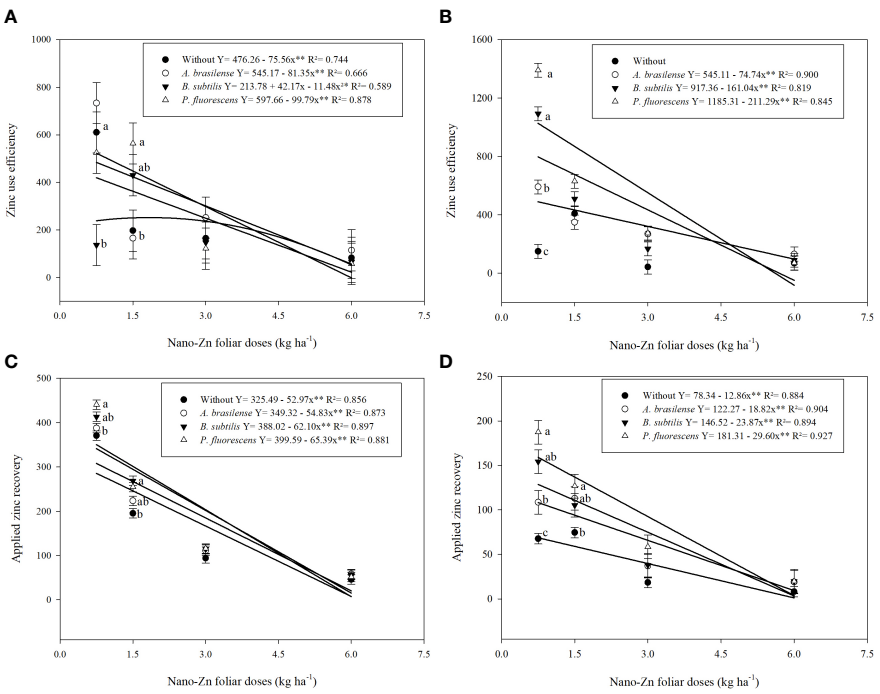

FIGURE 5
Influence of inoculation with PGPBs and nano-Zn foliar application on zinc use efficiency in 2019 **(A)** and 2020 **(B)**, and applied zinc recovery in 2019 **(C)** and 2020 **(D)** of wheat. The different letters correspond to a significant difference at 5% probability level ($p \leq 0.05$). The identical letters do not differ from each other as analyzed by Tukey test (PGPBs inoculations; $p \leq 0.05$) and Regression (Foliar Zn rates; $p \leq 0.05$) tests for wheat cropping year 2019 and 2020, respectively. Error bars represent the standard error of the mean (n = 4 replications). ** significant at $p \leq 0.01$.

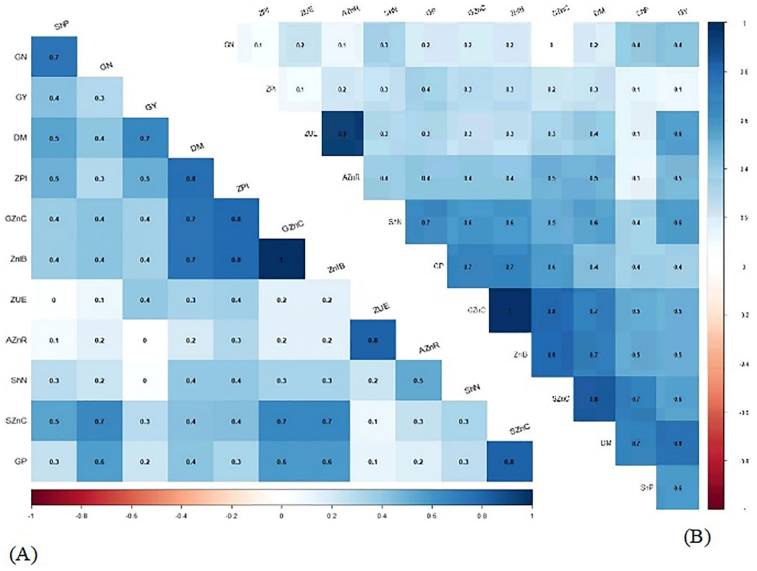

FIGURE 6
Heatmap color scale represented Pearson's correlation between the attributes of wheat in the function of plant growth-promoting bacteria and foliar nano ZnO applications in 2019 **(A)** and 2020 **(B)** cropping seasons. DM, shoot dry matter; ShN, shoot N concentration; ShP, shoot P concentration; SZnC, shoot Zn concentration; GN, grain N concentration; GP, grain P concentration; GZnC, grain Zn concentration; GY, grain yield; ZPI, zinc partitioning index; ZnIB, estimated Zn intake in Brazil; ZnUE, Zn use efficiency; and AZnR, applied Zn recovery.

Zn deficiency. Therefore, a potential and sustainable strategy is needed to improve grain Zn concentration for health purposes (Jalal et al., 2020a; Jalal et al., 2020b). The integrated use of Zn and PGPBs is one of the sustainable and easy adaptable strategies that can effectively eliminate plant and human Zn scarcity by improving nutrition and productivity of wheat (Jalal et al., 2020b; Jalal et al., 2022a; Jalal et al., 2023). In this sense, the current experiment revealed that nano-Zn foliar application in combination with inoculation of PGPBs has increased N, P, and Zn concentrations in shoots and grains of wheat under field conditions (Tables 1, 2). This might be due to the involvement of PGPBs in different soils and various mechanisms such as the production of phyto-hormones and enzymes, carboxylation, and biological fixation of nitrogen, which could help in the solubilization and availability of nutrients to plants for better absorption (Mitter et al., 2017; Rehman et al., 2021; Yasmin et al., 2022). In particular, it was reported that inoculation with *Pseudomonas* sp. could increase root architecture, branching, and proliferation, which will help host plants by improving their biochemical attributes and nutrient bioavailability to make plants healthy and for them to withstand harsh environmental conditions (Abadi et al., 2021; Yasmin et al., 2022). In addition, Zn is an important component and co-factor of several enzymes, cell division, and elongation, which help the plants maintain different biochemical activities for better crop growth, better physiology, more biofortified grains, and greater yield (Ullah et al., 2019; Jalal et al., 2020a; Faizan et al., 2021). In this sense, the present study demonstrated that inoculation with *B. subtilis* and *P. fluorescens* in combination with foliar fertilization of nano Zn increased the concentration of N, P and Zn in the shoot and grains of wheat (Tables 1, 2; Figure 3). The positive correlations between the treatments supported the hypothesis of the current study (Figure 6). Previous studies also supported our results in that inoculation with *A. brasilense, B. subtilis*, and *P. fluorescens* could promote nutrient uptake and plant growth of different cereals and sugarcane (Galindo et al., 2022b; Rosa et al., 2022).

The current study indicated that inoculation with *P. fluorescens* and *B. subtilis* in combination with foliar fertilization of nano-Zn enhanced shoot dry matter and grain yield of wheat (Table 3; Figure 4). It may be possible due to the role of these PGPBs in developing a root system and biomass of host plants that act as a gateway for better nutrient absorption for better plant performance and greater productivity (Moretti et al., 2020). Previously, inoculation with *Bacillus* sp. along with zinc oxide has been considered as one of the effective strategies to improve the different physiological and biochemical traits of maize, thus enhancing growth and grain yield with high nutritional values under field conditions (Jalal et al., 2023). Co-application of PBPBs and Zn increased Zn use efficiency under tropical soils that ultimately promoted plant growth and yield of the maize–wheat cropping system (Galindo et al., 2021). It was previously described that the combined use of PGPBs and nano-Zn can efficiently stimulate the defense system of plants by enhancing primary metabolites and photosystems, which may lead to greater plant growth and grain yield (Tanveer et al., 2022). In addition, Zn is one of the important nutrients for plant growth regulation, cell multiplication, and biochemical mechanisms; all these functions

together lead to higher dry matter and yield production (Doolette et al., 2020).

Wheat expansion to tropical and marginal regions is one of the best options to achieve food security; however, its inherent makeup of high ratio of phytic acid to Zn concentration in grains can cause malnutrition in Zn-deficient regions (Cakmak et al., 2010; Chattha et al., 2017). In this context, the current study indicated that foliar spray of nano-Zn along with the inoculation of *P. fluorescens* increased Zn partitioning and dietary intake of wheat grains (Table 3; Figure 4C). It has previously been stated that Zn-solubilizing bacteria such as *Bacillus* and *Pseudomonas* sp. strains stimulate several interactive mechanisms of soil and plant that convert the insoluble form of Zn into available Zn to enhance its uptake in plants for effective biofortification and higher yield (Hafeez et al., 2013; Singh et al., 2017; Jalal et al., 2021). Zinc-solubilizing bacteria could effectively increase bioavailability and assimilation of Zn in plants and grains by reducing phytic-P concentration, thus increasing these grains' consumption by humans (Mumtaz et al., 2017). Some previous studies reported that the application of foliar Zn is highly mobile in phloem, and quickly assimilated and redistributed into new generating grains of wheat (Doolette et al., 2020; Rehman et al., 2021). The redistribution and re-localization of Zn into grain tissues of wheat could better handle Zn malnutrition in humans (Firdous et al., 2020).

Zinc efficiencies are better defined by the ratio of grain Zn concentration to Zn-deficient soils, where Zn use efficiencies could decrease with increasing Zn fertilization. Hence, the present study showed that inoculation with *P. fluorescens* in combination with nano-Zn foliar application increased Zn use efficiency and applied Zn recovery under field cultivation of wheat (Figure 5). This might be due to the effectiveness of PGPBs in the dissolution of oxides, sulfides, and carbonates, thus increasing Zn bioavailability for better use of plants (Anuradha et al., 2015). Previous studies performed by Ullah et al. (2020) and Jalal et al. (2022a); Jalal et al. (2022b) reported that inoculation with PGPBs along with Zn fertilization could increase Zn use efficiencies *via* cultivation of different crops on soils with a low Zn content.

5 Conclusion

The combined use of foliar nano-Zn and PGPBs is among the rapid and sustainable alternative strategies for cereal production. It was verified from our results that inoculation with PGPBs in combination with nano-Zn foliar application increased plant and grain N, P and Zn concentrations, growth and yield of wheat. The inoculation with *B. subtilis* and *P. fluorescens* enhanced concentrations of nitrogen, phosphorus, and Zn in shoot and grain as well as provided greater shoot dry matter, grain yield and ZPI in wheat. The inoculation of *B. subtilis* and *P. fluorescens* along with the optimal calculated dose of foliar nano-Zn fertilizer, ranging from 3 to 3.5 kg ha^{-1}, increased most of the evaluated traits of wheat. Zinc intake from daily wheat consumption in Brazil, applied Zn recovery, and Zn use efficiency increased with the combined *P. fluorescens* and nano-Zn foliar application under field conditions. In this context, combined application of *P. fluorescens* and foliar nano-Zn under tropical savannah regions could be an effective strategy to improve plant nutrient acquisition and use efficiencies, particularly Zn, leading to sustainable production and biofortification of wheat. Prospective research should focus on the improvement of Zn use efficiency and recovery as well as the hormonal regulators produced as a result of inoculation and co-inoculation with PGPBs, and their influence on the performance, biofortification, and physiological traits of cereals to efficiently understand solubilization, assimilation, and partitioning of Zn under field conditions.

Data availability statement

The datasets presented in this study can be found in online repositories. The names of the repository/repositories and accession number(s) can be found below: http://hdl.handle.net/11449/238501.

Author contributions

Conceptualization and administration of the study: AJ and MF. Methodology, validation, and formal analysis: AJ, CO, GF and FG. Investigation, resources, and data curation: AJ, AB, KC, GL and JS. Writing—original draft preparation: AJ. Writing—review and editing: MF, ES and FG. Supervision, project administration, and funding acquisition: AJ and MF. All authors contributed to the article and approved the submitted version.

Funding

This project was funded by The World Academy of Science (TWAS) and Conselho Nacional de Desenvolvimento Científico e Tecnológico (CNPq) for the first author's doctoral fellowship (CNPq/TWAS grant number: 166331/2018-0), and productivity research grant (award number 311308/2020-1) for the corresponding author.

Acknowledgments

The authors thank São Paulo State University (UNESP) for providing technology and support as well as CNPq for financial support.

Conflict of interest

All the authors are aware of the manuscript publication and they have no financial, commercial, or other conflict of interest.

Publisher's note

All claims expressed in this article are solely those of the authors and do not necessarily represent those of their affiliated organizations, or those of the publisher, the editors and the reviewers. Any product that may be evaluated in this article, or claim that may be made by its manufacturer, is not guaranteed or endorsed by the publisher.

Supplementary material

The Supplementary Material for this article can be found online at: https://www.frontiersin.org/articles/10.3389/fpls.2023.1146808/full#supplementary-material

References

Abadi, V. A. J. M., Sepehri, M., Khatabi, B., and Rezaei, M. (2021). Alleviation of zinc deficiency in wheat inoculated with root endophytic fungus *Piriformospora indica* and rhizobacterium *Pseudomonas putida*. *Rhizosphere* 17, 100311. doi: 10.1016/j.rhisph.2021.100311

Afshar, R. K., Chen, C., Zhou, S., Etemadi, F., He, H., and Li, Z. (2020). Agronomic and economic response of bread wheat to foliar zinc application. *Agron. J.* 112 (5), 4045–4056. doi: 10.1002/agj2.20247

Ahmad, P., Alyemeni, M. N., Al-Huqail, A. A., Alqahtani, M. A., Wijaya, L., Ashraf, M., et al. (2020). Zinc oxide nanoparticles application alleviates arsenic (As) toxicity in soybean plants by restricting the uptake of as and modulating key biochemical attributes, antioxidant enzymes, ascorbate-glutathione cycle and glyoxalase system. *Plants* 9, 825. doi: 10.3390/plants9070825

Ahmad, H. T., Hussain, A., Aimen, A., Jamshaid, M. U., Ditta, A., Asghar, H. N., et al. (2021). Improving resilience against drought stress among crop plants through inoculation of plant growth-promoting rhizobacteria. In: A. Husen (eds) *Harsh Environ. Plant Resilience*. (Springer, Cham), 387–408. doi: 10.1007/978-3-030-65912-7_16

Akbar, M., Aslam, N., Khalil, T., Akhtar, S., Siddiqi, E. H., and Iqbal, M. ,. S. (2019). Effects of seed priming with plant growth-promoting rhizobacteria on wheat yield and soil properties under contrasting soils. *J. Plant Nutr.* 42 (17), 2080–2091. doi: 10.1080/01904167.2019.1655041

Anuradha, P., Syed, I., Swati, M., and Patil, V. D. (2015). Solubilization of insoluble zinc compounds by different microbial isolates *in vitro* condition. *Int. J. Trop. Agric.* 33 (2), 865–869.

Aziz, M. Z., Yaseen, M., Abbas, T., Naveed, M., Mustafa, A., Hamid, Y., et al. (2019). Foliar application of micronutrients enhances crop stand, yield and the biofortification essential for human health of different wheat cultivars. *J. Integ. Agric.* 18 (6), 1369–1378. doi: 10.1016/S2095-3119(18)62095-7

Bhatt, R., Hossain, A., and Sharma, P. (2020). Zinc biofortification as an innovative technology to alleviate the zinc deficiency in human health: a review. *Open Agric.* 5 (1), 176–187. doi: 10.1515/opag-2020-0018

Bollinedi, H., Yadav, A. K., Vinod, K. K., Gopala, K. S., Bhowmick, P. K., Nagarajan, M., et al. (2020). Genome-wide association study reveals novel marker-trait associations (MTAs) governing the localization of fe and zn in the rice grain. *Front. Genet.* 11. doi: 10.3389/fgene.2020.00213

Cakmak, I., Kalayci, M., Kaya, Y., Torun, A. A., Aydin, N., Wang, Y., et al. (2010). Biofortification and localization of zinc in wheat grain. *J. Agric. Food Chem.* 58 (16), 9092–9102. doi: 10.1021/jf101197h

Cantarella, H., van Raij, B., and Camargo, C. E. O. (1997). "Cereals. in 'Liming and fertilization recommendations for the state of são paulo'," in *Boletim técnico, 100*. Eds. B.v. Raij, H. Cantarella, J. A. Quaggio and A. M. C. Furlani (Campinas: Instituto Agronômico de Campinas), 285.

Cardillo, B. E. S., Oliveira, D. P., Soares, B. L., Martins, F. A. D., Rufini, M., Silva, J. S., et al. (2019). Nodulation and yields of common bean are not affected either by fungicides or by the method of inoculation. *Agron. J.* 111, 694–701. doi: 10.2134/agronj2018.06.0389

Chaoprasid, P., Nookabkaew, S., Sukchawalit, R., and Mongkolsuk, S. (2015). Roles of agrobacterium tumefaciens C58 ZntA and ZntB and the transcriptional regulator ZntR in controlling CD2+/Zn2+/Co2+ resistance and the peroxide stress response. *Microbiol.* 161, 1730–1740. doi: 10.1099/mic.0.000135

Chattha, M. U., Hassan, M. U., Khan, I., Chattha, M. B., Mahmood, A., Chattha, M. U., et al. (2017). Biofortification of wheat cultivars to combat zinc deficiency. *Front. Plant Sci.* 8. doi: 10.3389/fpls.2017.00281

David, B. V., Chandrasehar, G., and Selvam, P. N. (2018). "Pseudomonas fluorescens: a plant-growth-promoting rhizobacterium (PGPR) with potential role in biocontrol of pests of crops," in *Crop improvement through microbial biotechnology* (Amsterdam, Netherlands: Elsevier), 221–243. doi: 10.1016/B978-0-444-63987-5.00010-4

Dhaliwal, S. S., Ram, H., Shukla, A. K., and Mavi, G. S. (2019). Zinc biofortification of bread wheat, triticale, and durum wheat cultivars by foliar zinc fertilization. *J. Plant Nutr.* 42 (8), 813–822. doi: 10.1080/01904167.2019.1584218

Doolette, C. L., Read, T. L., Howell, N. R., Cresswell, T., and Lombi, E. (2020). Zinc from foliar-applied nanoparticle fertiliser is translocated to wheat grain: a65Zn radiolabelled translocation study comparing conventional and novel foliar fertilisers. *Sci. Total Environ.* 749, 142369. doi: 10.1016/j.scitotenv.2020.142369

Fageria, N. K., dos Santos, A. B., and Cobucci, T. (2011). Zinc nutrition of lowland rice. commun. *Soil Sci. Plant Anal.* 42, 1719–1727. doi: 10.1080/00103624.2011.584591

Fageria, N. K., Filho, M. B., Moreira, A., and Guimarães, C. M. (2009). Foliar fertilization of crop plants. *J. Plant Nutr.* 32 (6), 1044–1064. doi: 10.1080/01904160902872826

Faizan, M., Bhat, J. A., Chen, C., Alyemeni, M. N., Wijaya, L., Ahmad, P., et al. (2021). Zinc oxide nanoparticles (ZnO-NPs) induce salt tolerance by improving the antioxidant system and photosynthetic machinery in tomato. *Plant Physiol. Biochem. 161*, 122–130. doi: 10.1016/j.plaphy.2021.02.002

FAO. United Nations Food and Agricultural Organization. (2019). *Wheat yields global by country*. Available at: http://www.fao.org/faostat/en/#data (Accessed 20 Oct 2022).

Fernández, V., and Brown, P. H. (2013). From plant surface to plant metabolism: the uncertain fate of foliar-applied nutrients. *Front. Plant Sci.* 4. doi: 10.3389/fpls.2013.00289

Firdous, S., Agarwal, B. K., Chhabra, V., and Kumar, A. (2020). Zinc allocation and its re-translocation in wheat at different growth stages. *Plant Arch.* 20, 8653–8659.

Fukami, J., Abrantes, J. L. F., Del Cerro, P., Nogueira, M. A., Ollero, F. J., Megías, M., et al. (2018). Revealing different strategies of quorum sensing in azospirillum brasilense strains ab-V5 and ab-V6. *Arch. Microbiol.* 200, 47–56. doi: 10.1007/s00203-017-1422-x

Galindo, F. S., Bellotte, J. L. M., Santini, J. M. K., Buzetti, S., Rosa, P. A. L., Jalal, A., et al. (2021). Zinc use efficiency of maize-wheat cropping after inoculation with *Azospirillum brasilense*. *Nutr. Cycling Agroecosyst.* 120, 205–221. doi: 10.1007/s10705-021-10149-2

Galindo, F. S., Pagliari, P. H., Fernandes, G. C., Rodrigues, W. L., Boleta, E. H. M., Jalal, A., et al. (2022a). Improving sustainable field-grown wheat production with azospirillum brasilense under tropical conditions: a potential tool for improving nitrogen management. *Front. Environ. Sci.* 95. doi: 10.3389/fenvs.2022.821628

Galindo, F. S., Rodrigues, W. L., Fernandes, G. C., Boleta, E. H. M., Jalal, A., Rosa, P. A. L., et al. (2022b). Enhancing agronomic efficiency and maize grain yield with *Azospirillum brasilense* inoculation under Brazilian savannah conditions. *Europ. J. Agron.* 134, 126471. doi: 10.1016/j.eja.2022.126471

Hafeez, F. Y., Abaid-Ullah, M., and Hassan, M. N. (2013). "Plant growth-promoting rhizobacteria as zinc mobilizers: a promising approach for cereals biofortification," in *Bacteria in agrobiology: crop productivity* (Berlin, Heidelberg: Springer), 217–235. doi: 10.1007/978-3-642-37241-4_9

Hungria, M., Barbosa, J. Z., Rondina, A. B. L., and Nogueira, M. A. (2022). Improving maize sustainability with partial replacement of n fertilizers by inoculation with *Azospirillum brasilense*. *Agron. J.* 114 (5), 2969–2980. doi: 10.1002/agj2.21150

Hungria, M., Ribeiro, R. A., and Nogueira, M. A. (2018). Draft genome sequences of azospirillum brasilense strains ab-V5 and ab-V6, commercially used in inoculants for grasses and vegetables in Brazil. *Genome Announc.* 6, e00393–e00318. doi: 10.1128/genomeA.00393-18

Idayu, O., Maizatul, N., Radziah, O., Halimi, M., and Edaroyati, M. (2017). Inoculation of zinc-solubilizing bacteria with different zinc sources and rates for improved growth and zinc uptake in rice. *Int. J. Agric. Biol.* 19, 1137–1140. doi: 10.17957/IJAB/15.0396

Ilyas, N., Akhtar, N., Yasmin, H., Sahreen, S., Hasnain, Z., Kaushik, P., et al. (2022). Efficacy of citric acid chelate and bacillus sp. in amelioration of cadmium and chromium toxicity in wheat. *Chemos* 290, 133342. doi: 10.1016/j.chemosphere.2021.133342

Jalal, A., Azeem, K., Teixeira Filho, M. C. M., and Khan, A. (2020c). "Enhancing soil properties and maize yield through organic and inorganic nitrogen and diazotrophic bacteria," in *Sustainable crop production*. Eds. M. Hasanuzzaman, M. C. M. Teixeira Filho, M. Fujita and T. A. R. Nogueira (London: IntechOpen). doi: 10.5772/intechopen.92032

Jalal, A., Galindo, F. S., Boleta, E. H. M., Oliveira, C. E. D. S., Reis, A. R. D., Nogueira, T. A. R., et al. (2021). Common bean yield and zinc use efficiency in association with diazotrophic bacteria co-inoculations. *Agronomy* 11, 959. doi: 10.3390/agronomy11050959

Jalal, A., Galindo, F. S., Freitas, L. A., Oliveira, C. E., de Lima, B. H., Pereira, Í.T., et al. (2022c). Yield, zinc efficiencies and biofortification of wheat with zinc sulfate application in soil and foliar nanozinc fertilisation. *Crop Pasture Sci.* 73 (7-8), 749–759. doi: 10.1071/CP21458

Jalal, A., Oliveira, C. E. D. S., Bastos, A. C., et al. (2023). Nanozinc and plant growth-promoting bacteria improve biochemical and metabolic attributes of maize in tropical cerrado. *Front. Plant Sci.* 13. doi: 10.3389/fpls.2022.1046642

Jalal, A., Oliveira, C. E. D. S., Fernandes, H. B., Galindo, F. S., da Silva, E. C., Fernandes, G. C., et al. (2022b). Diazotrophic bacteria is an alternative strategy for increasing grain biofortification, yield and zinc use efficiency of maize. *Plants* 11 (9), 1125. doi: 10.3390/plants11091125

Jalal, A., Oliveira, C. E. D. S., Freitas, L. A., Galindo, F. S., Lima, B. H., Boleta, E. H. M., et al. (2022a). Agronomic biofortification and productivity of wheat with soil zinc and diazotrophic bacteria in tropical savannah. *Crop Pasture Sci.* 73 (7–8), 817–830. doi: 10.1071/CP21457

Jalal, A., Shah, S., Teixeira Filho, M. C. M., Khan, A., Shah, T., Hussain, M., et al. (2020a). Yield and phenological indices of wheat as affected by exogenous fertilization of zinc and iron. *Rev. Bras. Cienc. Agrar.* 15, e7730. doi: 10.5039/agraria.v15i1a7730

Jalal, A., Shah, S., Teixeira Filho, M. C. M., Khan, A., Shah, T., Ilyas, M., et al. (2020b). Agro-biofortification of zinc and iron in wheat grains. *Gesunde Pflanzen* 72 (3), 227–236. doi: 10.1007/s10343-020-00505-7

Jing, X., Cui, Q., Li, X., Yin, J., Ravichandran, V., Pan, D., et al. (2020). Engineering pseudomonas protens pf-5 to improve its antifungal activity and nitrogen fixation. *Microb. Biotechnol.* 13, 118–133. doi: 10.1111/1751-7915.13335

Khoshru, B., Mitra, D., Mahakur, B., Sarikhani, M. R., Mondal, R., Verma, D., et al. (2020). Role of soil rhizobacteria in utilization of an indispensable micronutrient zinc for plant growth promotion. *J. Crit. Rev.* 21, 4644–4654.

Kumar, S., Sindhu, S. S., and Kumar, R. (2021). Biofertilizers: an ecofriendly technology for nutrient recycling and environmental sustainability. *Curr. Res. Microbial Sci.* 3, 100094. doi: 10.1016/j.crmicr.2021.100094

Lessa, L. J. H., Araujo, A. M., Ferreira, L. A., da Silva Júnior, E. C., de Oliveira, C., Corguinha, A. P. B., et al. (2019). Agronomic biofortification of rice (*Oryza sativa* l.) with selenium and its effect on element distributions in biofortified grains. *Plant Soil* 444, 331–342. doi: 10.1007/s11104-019-04275-8

Malavolta, E., Vitti, G. C., and Oliveira, S. A. (1997). *Evaluation of the nutritional status of plants: principles and applications. 2nd edn* (Piracicaba: Associacao Brasileira para Pesquisa da Potaissio e do Fosfato).

Maxfield, L., Shukla, S., and Crane, J. S. (2023). Zinc deficiency. [Updated 2022 Nov 21]. In: *StatPearls* [Internet]. (Treasure Island (FL): StatPearls Publishing). Available from: https://www.ncbi.nlm.nih.gov/books/NBK493231/.

Mitter, B., Pfaffenbichler, N., Flavell, R., Compant, S., Antonielli, L., Petric, A., et al. (2017). A new approach to modify plant microbiomes and traits by introducing beneficial bacteria at flowering into progeny seeds. *Front. Microbiol.* 8. doi: 10.3389/fmicb.2017.00011

Moretti, L. G., Crusciol, C. A., Kuramae, E. E., Bossolani, J. W., Moreira, A., Costa, N. R., et al. (2020). Effects of growth-promoting bacteria on soybean root activity, plant development, and yield. *Agron. J.* 112 (1), 418–428. doi: 10.1002/agj2.20010

Mumtaz, M. Z., Ahmad, M., Jamil, M., and Hussain, T. (2017). Zinc solubilizing bacillus spp. potential candidates for biofortification in maize. *Microbiol. Res.* 202, 51–60. doi: 10.1016/j.micres.2017.06.001

Muñoz-Moreno, C. Y., de la Cruz-Rodríguez, Y., Vega-Arreguín, J., Alvarado-Rodríguez, M., Gómez-Soto, J. M., Alvarado-Gutiérrez, A., et al. (2018). Draft genome sequence of bacillus subtilis 2C-9B, a strain with biocontrol potential against chili pepper root pathogens and tolerance to Pb and zn. *Genome Announc.* 6, e01502–e01517. doi: 10.1128/genomeA.01502-17

Nakao, A. H., Costa, N. R., Andreotti, M., Souza, M. F. P., Dickmann, L., Centeno, D. C., et al. (2018). Agronomic characteristics and physiological quality of soybean seeds as a function of foliar fertilization with boron and zinc. *Cult. Agron.* 27 (3), 312–327. doi: 10.32929/2446-8355.2018v27n3p312-327

Penn, C. J., Camberato, J. J., and Wiethorn, M. A. (2023). How much phosphorus uptake is required for achieving maximum maize grain yield? part 1: luxury consumption and implications for yield. *Agronomy* 13 (1), 95. doi: 10.3390/agronomy13010095

Poniedziałek, B., Perkowska, K., and Rzymski, P. (2020). Food Fortification: What's in It for the Malnourished World?. In Noureddine Benkeblia ed 1. *Vitamins and minerals biofortification of edible plants*. New Jersey: Wiley Publishers, 27–44. doi: 10.1002/9781119511144.ch2

Raij, B., Andrade, J. C., Cantarella, H., and Quaggio, J. A. (2001). *Chemical analysis for fertility evaluation of tropical soils* (Campinas: IAC), 285.

R Core Team. (2015). *R: a language and environment for statistical computing* (Vienna, Austria: R Foundation for Statistical Computing). Available at: https://www.R-project.org/.

Rehman, R., Asif, M., Cakmak, I., and Ozturk, L. (2021). Differences in uptake and translocation of foliar-applied zn in maize and wheat. *Plant Soil.* 462 (1), 235–244. doi: 10.1007/s11104-021-04867-3

Rekha, K., Baskar, B., Srinath, S., and Usha, B. (2017). Plant-growth-promoting rhizobacteria bacillus subtilis RR4 isolated from rice rhizosphere induces malic acid biosynthesis in rice roots. *Can. J. Microbiol.* 18, 1–8. doi: 10.1139/cjm-2017-0409

Rengel, Z., and Graham, R. D. (1996). Uptake of zinc from chelate-buffered nutrient solutions by wheat genotypes differing in zinc efficiency. *J. Exp. Bot.* 47, 217–226. doi: 10.1093/jxb/47.2.217

Rosa, P. A. L., Galindo, F. S., Oliveira, C. E. D. S., Jalal, A., Mortinho, E. S., Fernandes, G. C., et al. (2022). Inoculation with plant growth-promoting bacteria to reduce phosphate fertilization requirement and enhance technological quality and yield of sugarcane. *Microorganisms* 10 (1), 192. doi: 10.3390/microorganisms10010192

Rossi, L., Fedenia, L. N., Sharifan, H., Ma, X., and Lombardini, L. (2019). Effects of foliar application of zinc sulfate and zinc nanoparticles in coffee (*Coffea arabica* l.) plants. *Plant Physiol. Biochem.* 135, 160–166. doi: 10.1016/j.plaphy.2018.12.005

Santos, H. G., Jacomine, P. K. T., Anjos, L. H. C., Oliveira, V. A., Lumbreras, J. F., Coelho, M. R., et al. (2018) *Brazilian System of soil classification* (Brasília: Embrapa solos). Available at: https://www.embrapa.br/en/busca-de-publicacoes/-/publicacao/1094001/brazilian-soil-classification-system (Accessed 18th June, 2022).

Singh, D., Rajawat, M. V. S., Kaushik, R., Prasanna, R., and Saxena, A. K. (2017). Beneficial role of endophytes in biofortification of zn in wheat genotypes varying in nutrient use efficiency grown in soils sufficient and deficient in zn. *Plant Soil* 416, 107–116. doi: 10.1007/s11104-017-3189-x

Soil Survey Staff (2014). *Keys to soil taxonomy* (Washington, DC, USA: United States Department of Agriculture and natural resources conservation service. Government Printing Office).

Tanveer, Y., Yasmin, H., Nosheen, A., Ali, S., and Ahmad, A. (2022). Ameliorative effects of plant growth promoting bacteria, zinc oxide nanoparticles and oxalic acid on *Luffa acutangula* grown on arsenic enriched soil. *Environ. Pollut.* 300, 118889. doi: 10.1016/j.envpol.2022.118889

Teixeira, P. C., Donagemma, G. K., Fontana, A., and Teixeira, W. G. (2017). *Manual of soil analysis methods* (Rio de Janeiro: Centro nacional de pesquisa de solos, Embrapa). doi: 10.1590/18069657rbcs20160574

Ullah, A., Farooq, M., Rehman, A., Hussain, M., and Siddique, K. H. (2020). Zinc nutrition in chickpea (*Cicer arietinum*): a review. *Crop Past Sci.* 71 (3), 199–218. doi: 10.1071/CP19357

Ullah, A., Romdhane, L., Rehman, A., and Farooq, M. (2019). Adequate zinc nutrition improves the tolerance against drought and heat stresses in chickpea. *Plant Physiol. Biochem.* 143, 11–18. doi: 10.1016/j.plaphy.2019.08.020

USDA. Foreign Agriculture Services (2020) *Brazil Grain and feed annual*. Available at: http://www.abitrigo.com.br/wp-content/uploads/2019/09/CONSUMO-MUNDIAL-DE-TRIGO-15_16-20_21.pdf (Accessed 29 May 2021).

Vale, F., Araujo, M. A. G., and Vitti, G. C. (2008). "Evaluation of nutritional status of micronutrients in areas with sugarcane = Avaliação do estado nutricional dos micronutrientes em áreas com cana-de-açúcar," in *FERTBIO*(Londrina). Embrapa-Soja/SBCS/IAPAR/UEL. Available at: https://repositorio.usp.br/result.php?filter[]=isPartOf.name:%22Desafios%20para%20o%20uso%20do%20solo%20com%20efici%C3%AAncia%20e%20qualidade%20ambiental%20-%20Anais%22.

Yasmin, H., Bano, A., Wilson, N. L., Nosheen, A., Naz, R., Hassan, M. N., et al. (2022). Drought-tolerant pseudomonas sp. showed differential expression of stress-responsive genes and induced drought tolerance in arabidopsis thaliana. *Physiol. Plant* 174 (1), e13497. doi: 10.1111/ppl.13497

Zadoks, J. C., Chang, T. T., and Konzak, C. F. (1974). A decimal code for the growth stages of cereals. *Weed Res.* 14, 415–421.

Zou, C. Q., Zhang, Y. Q., Rashid, A., Ram, H., Savasli, E., Arisoy, R. Z., et al. (2012). Biofortification of wheat with zinc through zinc fertilization in seven countries. *Plant Soil* 361 (1–2), 119–130. doi: 10.1007/s11104-012-1369-2

Zulfiqar, U., Hussain, S., Maqsood, M., Ishfaq, M., and Ali, N. (2021). Zinc nutrition to enhance rice productivity, zinc use efficiency, and grain biofortification under different production systems. *Crop Sci.* 61 (1), 739–749. doi: 10.1002/csc2.20381

frontiers | Frontiers in Plant Science

TYPE Original Research
PUBLISHED 24 October 2023
DOI 10.3389/fpls.2023.1233464

OPEN ACCESS

EDITED BY
Nasim Ahmad Yasin,
University of the Punjab, Pakistan

REVIEWED BY
Christopher Ngosong,
University of Buea, Cameroon
Krishan K. Verma,
Guangxi Academy of Agricultural Sciences, China

*CORRESPONDENCE
Jun Zhong
zhhjp@163.com
Yi He
zhhjp2005@126.com

†These authors have contributed equally to this work

RECEIVED 02 June 2023
ACCEPTED 09 October 2023
PUBLISHED 24 October 2023

CITATION
Zhou M, Sun C, Dai B, He Y and Zhong J (2023) Intercropping system modulated soil–microbe interactions that enhanced the growth and quality of flue-cured tobacco by improving rhizospheric soil nutrients, microbial structure, and enzymatic activities.
Front. Plant Sci. 14:1233464.
doi: 10.3389/fpls.2023.1233464

Intercropping system modulated soil–microbe interactions that enhanced the growth and quality of flue-cured tobacco by improving rhizospheric soil nutrients, microbial structure, and enzymatic activities

Muqiu Zhou[1†], Chenglin Sun[1†], Bin Dai[2], Yi He[2*] and Jun Zhong[1*]

[1]College of Agriculture, Hunan Agricultural University, Changsha, Hunan, China, [2]Technology center, Bijie Branch of Guizhou Tobacco Company, Bijie, Guizhou, China

As the promotive/complementary mechanism of the microbe–soil–tobacco (*Nicotiana tabacum* L.) interaction remains unclear and the contribution of this triple interaction to tobacco growth is not predictable, the effects of intercropping on soil nutrients, enzymatic activity, microbial community composition, plant growth, and plant quality were studied, and the regulatory mechanism of intercropping on plant productivity and soil microenvironment (fertility and microorganisms) were evaluated. The results showed that the soil organic matter (OM), available nitrogen (AN), available phosphorus (AP), available potassium (AK), the urease activity (UE) and sucrase activity (SC), the diversity, abundance, and total and unique operational taxonomic units (OTUs) of bacteria and fungi as well as plant biomass in T1 (intercropping onion), T2 (intercropping endive), and T3 (intercropping lettuce) treatments were significantly higher than those of the controls (monocropping tobacco). Although the dominant bacteria and fungi at the phylum level were the same for each treatment, LEfSe analysis showed that significant differences in community structure composition and the distribution proportion of each dominant community were different. Proteobacteria, Acidobacteria, and Firmicutes of bacteria and Ascomycota and Basidiomycetes of fungi in T1, T2, and T3 treatments were higher than those of the controls. Redundancy analysis (RDA) suggested a close relation between soil characteristic parameters and microbial taxa. The correlation analysis between the soil characteristic parameters and the plant showed that the plant biomass was closely related to soil characteristic parameters. In conclusion, the flue-cured tobacco intercropping not only increased plant biomass and improved chemical quality but also significantly increased rhizospheric soil nutrient and

enzymatic activities, optimizing the microbial community composition and diversity of rhizosphere soil. The current study highlighted the importance of microbe–soil–tobacco interactions in maintaining plant productivity and provided the potential fertilization practices in flue-cured tobacco production to maintain ecological sustainability.

KEYWORDS

flue-cured tobacco, intercropping, rhizospheric soil, soil nutrients, enzymatic activity, microbial community structure

1 Introduction

The growing demands for staple food and the limited arable land have resulted in flue-cured tobacco production with high cropping intensity and long monocropping periods (Chen et al., 2016; Fu et al., 2018; Li et al., 2022), but long-term monocropping may adversely affect the diversity and abundance of microbial community in the soil, thereby reducing soil quality, hindering the growth and development of tobacco plants, and ultimately affecting tobacco yield and quality (Wang, 2016; Gong et al., 2018; Ma et al., 2021).

However, intercropping, which simultaneously grows multiple crop species in a single field, has been widely practiced due to its economic, ecological, and environmental benefits (Martin-Guay et al., 2018; Dowling et al., 2021). Many researchers have shown that intercropping, in addition to affecting crop yield, may also cause functional and architectural alterations in the soil microbiota (Duchene et al., 2017; Yu et al., 2018). In the intercropping systems, the soil, microbes, and plants may interact with each other in various ways; e.g., microbes might influence soil nutrient turnover by decomposing soil organic matter (OM), which in turn influences soil enzymatic properties and secretion (Lauber et al., 2008; Peng et al., 2015). Soil enzymes facilitate the decomposition of soil microbes and plant debris, providing plants with nutrients to survive (Veres et al., 2015).

Different intercropping patterns may differentially affect soil physicochemical properties and microbial characteristics. Although previous studies have reported the tobacco–corn and tobacco–wheat (Zhou et al., 2015) intercropping systems, the effects of intercropping onion, endive, and lettuce with tobacco on soil nutrients, enzymatic activities, microbial community structure, and tobacco yield have been rarely reported. Therefore, we used high-throughput sequencing to investigate the impact of tobacco monocropping and intercropping systems on soil physio-biochemical and biological properties in Guizhou Province, which in turn affected tobacco productivity. The main objectives of the present study were as follows: 1) investigating the effects of tobacco intercropping with various other crops on the soil physio-biochemical properties, soil enzymatic activities, and tobacco yield; 2) comparing the differences in the microbial diversity and soil microflora composition between tobacco monocropping and intercropping; 3) determining the relationships among soil microbes, soil enzymatic activities, and physio-biochemical properties as well as flue-cured tobacco plants.

2 Materials and methods

2.1 Experimental design and sampling

The experiment was carried out in Weining County, Bijie City, Guizhou Province, China (103°80′E, 27°20′N, altitude 1,100 m) from April to October 2022, with the climate belonging to a humid subtropical monsoon and an average yearly temperature of 15.5°C, precipitation of 909 mm, and 1,812 hours of photoperiod. The prevailing soil composition in this geographical region primarily consists of clayey soil. The field has been continuously planted with tobacco for 10 years. The tested variety of flue-cured tobacco was the main local variety Yunyan 87, with a planting density of 16,500 plants/hectare at a row spacing of 1.2 m × 0.5 m.

Three treatments were used to intercrop the flue-cured tobacco: scallions (T1), endive (T2), and rapeseed (T3). A non-intercropped monoculture tobacco field was used as the control (CK). The total experimental area was 66.7 m^2. After transplanting tobacco seedlings in April 2022, the intercropping plants were respectively on both sides of the flue-cured tobacco, with 82,500 plants/hectare, 33,000 plants/hectare, and 16,500 plants/hectare planted for scallions, endive, and rapeseed, respectively.

Rhizospheric soil samples were collected in June by scooping the surface soil around the tobacco plants to a depth of 3 cm, followed by digging with a shovel approximately 25 cm away from the stem of the tobacco plant. After the rhizosphere of the tobacco plant was exposed, the soil was taken as a sample. The whole process was replicated three times. The collected soil samples were temporarily stored in a polyethylene box with an ice pack and then completely homogenized through a soil screen of 2 mm. Each soil sample was equally divided into two parts. The samples for biochemical analysis were air-dried for 1 week and kept at −20°C. Samples for microbial community analysis were kept at −80°C (Zhao et al., 2019).

Biomass analysis was conducted three times during the entire growth period of tobacco plants. The destructive sampling was carried out at 30 days, 60 days, and 90 days after transplanting. Three representative tobacco plants were selected from each

treatment with the roots, stems, and leaves dried for biomass measurement. After tobacco leaves were roasted, the contents of water-soluble sugar (including total sugar and reducing sugar), total alkali, total nitrogen, and potassium were determined with the tobacco industrial standards YC/T 159-2019, YC/T 160-2002, YC/T 33-1996, and YC/T 217-2007, respectively.

2.2 Soil properties and enzymatic activity

The available nitrogen (AN), available phosphorus (AP), available potassium (AK), and OM contents were measured following the instructions of the Kjeldahl method, the molybdenum antimony anti-chromogenic extraction method, inductively coupled plasma (ICP) spectrometer method, and the K2Cr2O7-H2SO4 oxidation approach (Zhao et al., 2020), respectively. Urease (UE), sucrase (SC), and peroxidase (POD) activities were measured using the phenol sodium hypochlorite colorimetric method, the 3,5-dinitrosalicylic acid colorimetric method, and spectrophotometry method (Jia, 2016), respectively.

2.3 Soil DNA extraction, PCR amplification, and sequencing

Total soil DNA was extracted from a 3-g soil sample using a Power Soil DNA Kit (MOBIO Inc., Carlsbad, CA, USA). PCR was performed to amplify the V3–V4 region of the bacterial 16S rRNA gene using primer pair 338F 5′-ACTCCTACGGGAGGCAGCA-3′ and 806R 5′-GGACTACHVGGGTWTCTAAT-3′. As for the fungal community, the ITS1 region of ITS gene was amplified using primer pair ITS1 5′-GGAAGTAAAAGTCGTAACAAGG-3′ and ITS2 5′-GCTGCGTTCTTCATCGATGC-3′. Finally, paired-end sequencing of the bacteria and fungi was performed on an Illumina MiSeq sequencer at Novogene Co., Ltd. (Beijing, China) (Wang, 2016).

2.4 Statistical analysis

The relative abundance of the rhizosphere soil microorganism community was analyzed by one-way ANOVA using SPSS 16.0 software. Uparse software was used to cluster Effective Tags into operational taxonomic units (OTUs) with a threshold value of 97% similarity, and the sequences with the largest number of OTUs were selected as the representative sequences of the OTUs for species annotation (citation). QIIME software was used to calculate the Alpha diversity index (citation). R language tool was used to make the composition of the community (citation). Circos software was used to analyze the composition proportion of the dominant community and its distribution proportion in samples (xxxx). LEfSe software was used to analyze soil communities with significant differences, and principal coordinate analysis (PCoA) in R was used to analyze the difference in community structure (xxxx). Tax4Fun and FUNGuild methods were used to compare the existing 16S rRNA and ITS gene sequencing data with the SILVA database used to compare the abundance differences of functional genes in biological metabolic pathways (xxxx). The “vegan” redundancy analysis R software (RDA) and Mantel test were used to analyze the relationship between soil nutrients, enzymatic activities, and microbial community (Tang et al., 2020).

3 Results

3.1 Effects of intercropping on soil nutrients and enzymatic activities in the rhizospheric soil of flue-cured tobacco

The OM, AN, AP, and AK contents in the soil of the intercropping treatment groups of flue-cured tobacco were significantly higher than those in CK (Table 1), in which T1 treatment reached the highest. Compared to the controls, T1, T2, and T3 increased OM content by 44.87%, 34.55%, and 40.32%, respectively; the AN contents were increased by 36.59%, 26.85%, and 33.12%, respectively; the AP contents were increased by 48.23%, 28.17%, and 36.84%, respectively; the AK contents were increased by 39.61%, 21.08%, and 30.59%, respectively. The enzymatic activity of the soil under intercropping treatments (T1, T2, and T3) decreased by 14.49%, 5.15%, and 7.30% in terms of POD contents, respectively. The UE contents were increased by 46.42%, 11.81%, and 34.48%, respectively, and the SC contents were increased by 40.92%, 17.94%, and 31.67%, respectively.

TABLE 1 Soil nutrients and enzymatic activity of the soil.

Treatment	Organic matter (g/kg)	Available nitrogen (mg/kg)	Available phosphorus (mg/kg)	Available potassium (mg/kg)	Peroxidase activity (U/g)	Urease activity (U/g)	Sucrase activity (U/g)
CK	14.73 ± 0.38c	62.49 ± 0.15b	127.39 ± 0.45c	56.92 ± 0.46b	38.64 ± 0.39c	65.86 ± 0.42c	188.31 ± 0.57b
T1	21.34 ± 0.22a	85.36 ± 0.26a	188.84 ± 0.37a	79.47 ± 0.38a	33.04 ± 0.31a	96.43 ± 0.28a	265.37 ± 0.46a
T2	19.82 ± 0.36b	79.27 ± 0.45ab	163.27 ± 0.33b	68.92 ± 0.43ab	36.65 ± 0.18b	73.64 ± 0.41b	222.09 ± 0.51ab
T3	20.67 ± 0.55ab	83.19 ± 0.39a	174.33 ± 0.28ab	74.33 ± 0.22a	35.82 ± 0.27a	88.57 ± 0.37ab	247.95 ± 0.37a

Different lowercase letters indicate significant differences ($p < 0.05$).

3.2 Effects of intercropping on microbial community diversity and structure in the rhizosphere soil of flue-cured tobacco

3.2.1 Microbial community diversity

The order of bacterial abundance was ranked as T1>T3>T2>CK, and the bacterial abundance in T1 was significantly higher than that in T2 and T3 treatments (Figure 1A) . Compared to the controls, the bacterial abundance in the T1, T2, and T3 treatments increased by 16.52%, 12.10%, and 6.28%, respectively. Among the Shannon, Ace, and Chao diversity indices of the T1, T2, and T3 treatments, only Ace indices between T1 and T2 treatments showed significant differences (Figure 1A). The PCoA showed (Figure 1C) that there was an obvious separation between the four treatments, with the X and Y axes explaining 49.72% and 21.08% of the overall variation of the bacterial population, respectively. The OTU analysis showed that the unique bacterial OTUs of CK, T1, T2, and T3 were 498, 852, 508, and 644, respectively (Figure 1E).

The changes in fungal abundance as well as the three Alpha diversity indices of Shannon, Ace, and Chao were ordered as T1>T3>T2>CK (Figure 1B). The differences between the T2 and the control were not significant, but both of them were significantly lower than the T1 and T3 treatments (Figure 1B). PCoA results indicated that the X and Y axes explained 38.63% and 25.69% of the overall variation of the fungal community, respectively (Figure 1D). The unique OTUs of the tobacco fungi in the rhizospheric soil were ranked as T1 (816)>T2 (784)>T3 (563)>CK (253) (Figure 1F).

3.2.2 Microbial community structure

Although the bacteria with relative abundance>3% at the phylum level were the same, Proteobacteria, Acidobacteria, Bacteroidota, Gemmatimonadetes, Firmicutes, and Actinobacteriota were the main bacterial communities. These were present in much higher quantities than other dominant bacterial groups and accounted for approximately 86.73% of the total bacterial groups (Figure 2A). However, the community structure composition from the phylum level to the genus level among different treatments was shown from the LEfSe analysis. Among them, nine groups in T1, seven groups in T2, three groups in T3, and two groups in CK were identified as differential bacterial communities (Figure 2B).

The top 100 fungi in each treatment group at the genus level belonged to six phyla, namely, Ascomycota, Basidiomycota, Chytridiomycota, Mortierellomycota, Mucormycota, and Glomeromycota, which accounted for 78.11%–95.32% of the total fungi (Figure 3A). However, the community structure composition

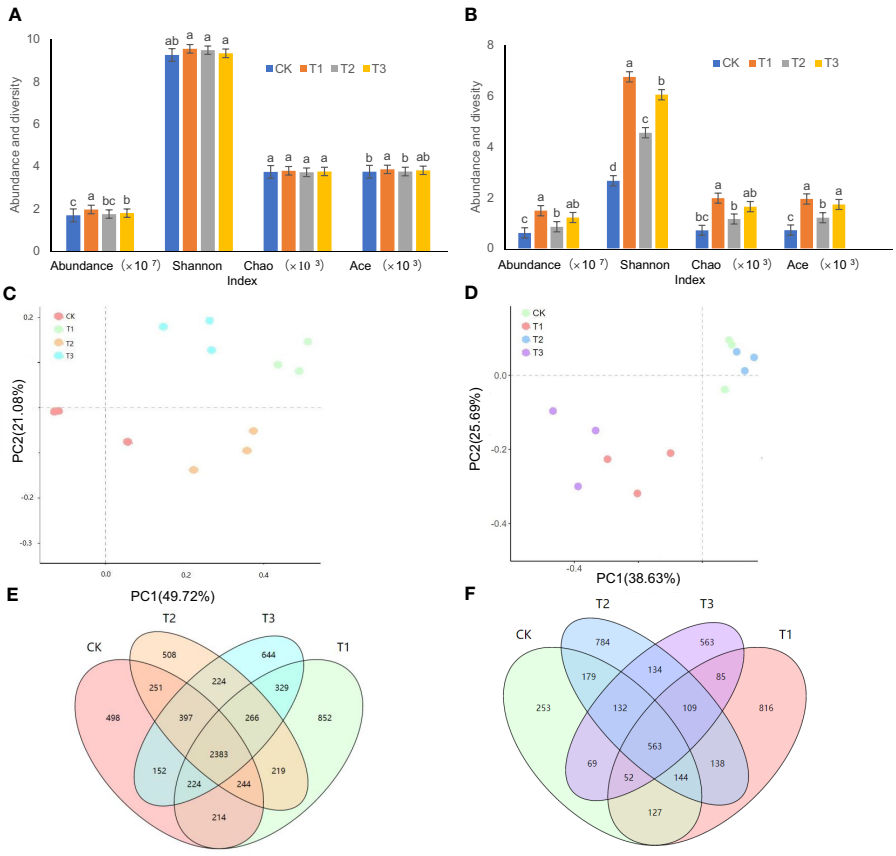

FIGURE 1
Microbial abundance and diversity in the rhizosphere soil of flue-cured tobacco under different intercropping treatments. **(A)** Abundance and diversity of bacteria; **(B)** Abundance and diversity of fungi; **(C)** PCoA analysis of bacteria; **(D)** PCoA analysis of fungi; **(E)** OTU analysis of bacteria; **(F)** OTU analysis of fungi. Different lowercase letters above the column indicate significant differences ($p<0.05$), the same as below.

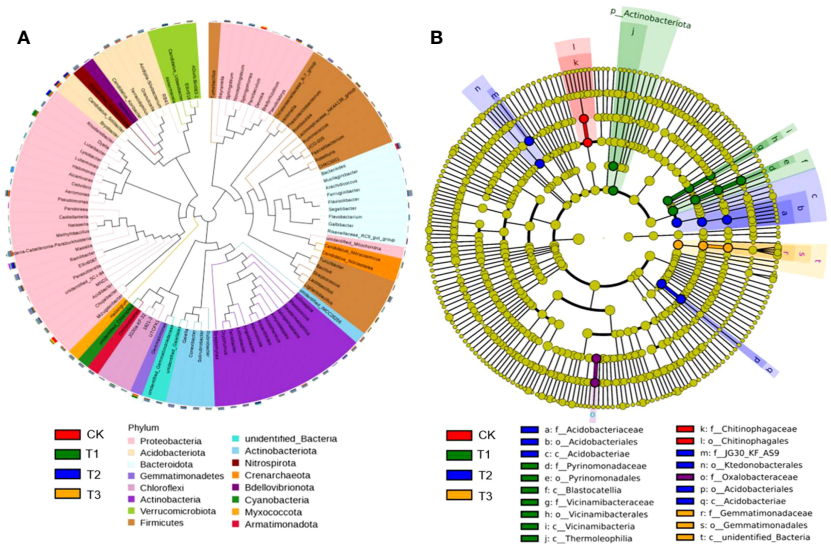

FIGURE 2
Bacterial dominant communities in the rhizosphere soil of flue-cured tobacco under different intercropping treatments. **(A)** Evolutionary map of phylum level of bacteria; **(B)** LEfSe analysis of differences in bacterial community structure composition.

among different treatments identified 22 groups in the T1 treatment, 16 groups in the T2 treatment, 15 groups in the T3 treatment, and 9 groups in the control as differential fungal communities (Figure 3B).

3.2.3 Effects of intercropping on the distribution of dominant microorganism communities

The Circos analysis showed the distributions of dominant bacteria3and fungi in different treatments (Figures 4A, 5A). Based on the phylum level of bacteria, the proportions were ranked as T1 (40%)>T3 (34%)>T2 (33%)>CK (28%) for Proteobacteria, T3 (15%)>T2 (14%)>T1 (12%)>CK (11%) for Acidobacteria, T1 (13%)>CK (12%)>T3 (11%)>T2 (10%) for Bacteroides, T2=CK (6%)>T3 (5%)>T1 (3%) for Gemmatimonadetes, T2 (15%)>CK (14%)>T3 (12%)>T1 (10%) for Actinobacteria, and T1 (14%)>T3 (12%)>T2=CK (11%) for Firmicutes (Figure 4B).

Based on the phylum level of fungi with the proportion larger than 1%, Ascomycota was distributed as T1 (97.22%)>T2 (80.89%)>CK (74.21%)>T3 (37.21%), Basidiomycetes as T3 (60.51%)>T2 (12.81%)>CK (11.77%)>T1 (1.26%), and *Mortierella* as CK (12.86%)>T2 (5.91%)>T3 (2.23%)>T1 (1.41%) (Figure 5B).

3.3 Effects of intercropping on growth and quality of flue-cured tobacco plants

Except for the biomass of tobacco root (Figure 6A), stem (Figure 6B), leaf (Figure 6C), or total biomass (Figure 6D) on the 30th day after transplanting, little differences were observed among the four treatments. However, on the 60th day after

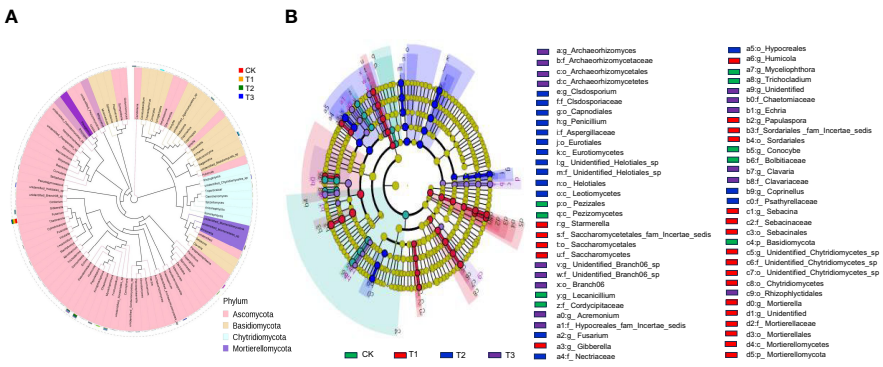

FIGURE 3
Fungal dominant communities in the rhizosphere soil of flue-cured tobacco under different intercropping treatments.**(A)** Evolutionary map of phylum level of fungi; **(B)** LEfSe analysis of differences in fungi community structure composition

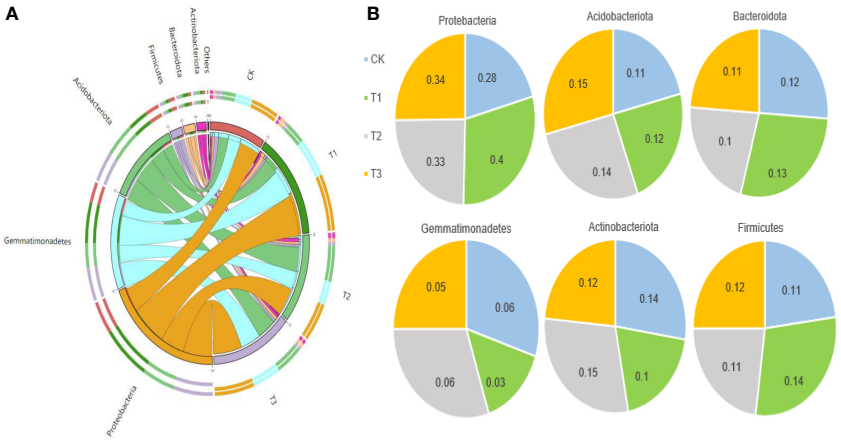

FIGURE 4
The distributions of bacterial dominant communities in the rhizosphere soil of flue-cured tobacco under different intercropping treatments. **(A)** Circos analysis of dominant fungal composition; **(B)** Distribution ratio of dominant fungi of phyla level in different treatments.

transplanting, there were slight differences in the root, stem, leaf, and total biomass of the four treatments, among which the T2 treatment was the largest and the CK treatment was the smallest. On the 90th day after transplanting, significant differences appeared in the total biomass of the roots, stems, and leaves among the four treatments, but they were still the largest in the T2 treatment and the smallest in the CK treatment.

When compared with the control, the tobacco leaves of the three intercropping systems were closer to the standard of high-quality tobacco leaves (Table 2).

3.4 Correlation analysis

3.4.1 Redundancy analysis between dominant microbial communities and soil nutrients

RDA showed that the contents of OM, AN, and AP were positively correlated with Proteobacteria, Acidobacteria, Gemmatimonadetes, Actinobacteriota, and Firmicutes but negatively correlated with Bacteroidota; the contents of AK, UE, and SC were positively correlated with Acidobacteria, Gemmatimonadetes, Actinobacteriota, and Firmicutes but

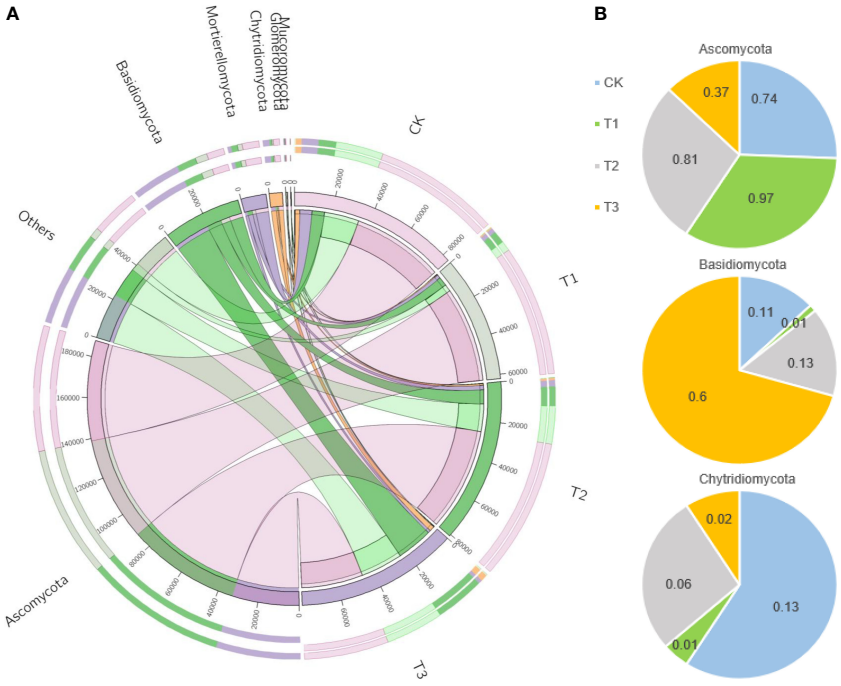

FIGURE 5
The distributions of fungal dominant communities in the rhizosphere soil of flue-cured tobacco under different intercropping treatments. **(A)** Circos analysis of dominant bacterial composition; **(B)** Distribution ratio of dominant bacteria of phyla level in different treatments.

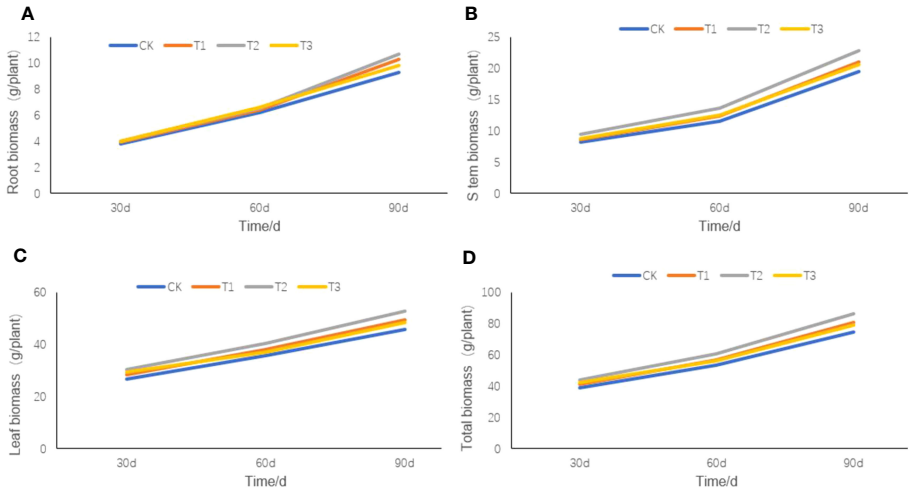

FIGURE 6
The root, stem, and leaf biomass of flue-cured tobacco under different intercropping treatments. **(A)** the root biomass of tobacco plant; **(B)** the stem biomass of tobacco plant; **(C)** the leaf biomass of tobacco plant; **(D)** the total biomass of tobacco plant.

negatively correlated with Proteobacteria and Bacteroidota. The POD activity was positively correlated with Gemmatimonadetes and Firmicutes but negatively correlated with Proteobacteria, Acidobacteria, Actinobacteriota, and Bacteroidobacteria (Figure 7A). Moreover, various soil nutrient contents (OM, AN, AP, and AK) and enzymatic activities (POD, UE, and SC) were positively correlated with Ascomycota and Basidiomycota but negatively correlated with Chytridiomycota, Mortierellomycota, Mucoromycota, and Glomeromycota (Figure 7B).

3.4.2 Correlation analysis between soil properties and flue-cured tobacco plants

According to the correlation analysis, the total biomass was positively correlated with all the soil nutrients and enzymatic activity. The total biomass after 60 days and 90 days of transplanting reached a significant level at $p < 0.01$, while the total biomass after 30 days of tobacco plant transplanting reached a significant level at $p < 0.05$. The contents of RS, TS, TN, and nicotine were significantly negatively correlated with all the soil nutrients and enzymatic activities (Figure 8).

4 Discussion

4.1 Soil nutrients and enzymatic activities in the intercropped tobacco fields

Intercropping has become increasingly popular over the past decade to maintain soil biodiversity and improve nutrient content (Dai et al., 2019). One of the biggest advantages of intercropping is to make use of the interaction among different plants to improve soil physio-biochemical properties and enzymatic activities as well as to promote crop growth and development (Gong et al., 2019). Previous studies have demonstrated that intercropping peanuts with maize changed the abundance of nitrogen-fixing microbes in the rhizosphere (Chen et al., 2018). Cassava–peanut intercropping enriched Actinomycetes in the soil rhizosphere and boosted the absorption of soil-available nutrients, thus increasing the peanut yield (Chen et al., 2020). The present study also verified that the nutrients of all flue-cured tobacco intercropping treatments were significantly higher than those of the controls (Table 1), suggesting that intercropping could contribute to elevating the levels of soil nutrients.

TABLE 2 Routine chemical composition of different intercropping treatments.

Treatment	Total sugar%	Reducing sugar%	Total nitrogen%	Nicotine%	Potassium%	Chlorine%
Contrast	23.67 ± 1.51a	23.12 ± 4.92a	3.03 ± 1.27a	2.80 ± 0.97a	1.65 ± 0.44b	0.31 ± 0.11a
T1	21.33 ± 0.74b	19.42 ± 3.17b	2.75 ± 1.19ab	2.60 ± 1.04b	1.76 ± 0.28ab	0.22 ± 0.06b
T2	20.86 ± 1.03bc	18.38 ± 2.46b	2.59 ± 2.22b	2.46 ± 1.37bc	1.89 ± 0.32a	0.17 ± 0.14b
T3	22.59 ± 0.95ab	20.27 ± 4.28ab	2.86 ± 1.68ab	2.68 ± 1.46ab	1.63 ± 0.47b	0.21 ± 0.25b
High-quality tobacco	18–24	16–22	1.–3.5	1.5–3.5	>2	<1

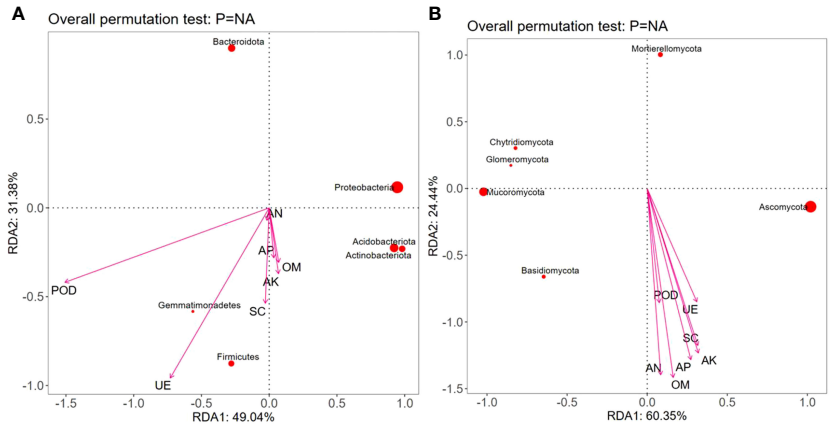

FIGURE 7
Redundancy analysis (RDA) between dominant microbial communities, nutrients, and enzymatic activity in the rhizospheric soil under different intercropping treatments. Note: OM, AN, AP, AK, UE, SC, and POD represent respectively organic matter, available nitrogen, available phosphorus, available potassium, urease, sucrase, and peroxidase. **(A)** Redundancy analysis of soil nutrients and bacterial communities; **(B)** Redundancy analysis of soil nutrients and fungal communities.

Soil enzymatic activity is a vital parameter indicating how organic matter is degraded and the nutrients are cycled in the soil (Nannipieri et al., 2012; Hussain et al., 2021). The soil enzymatic activity can be represented by the physio-biochemical traits and microbial communities (Gu et al., 2009). For example, sucrase hydrolyzes sucrose, which reflects the convertibility of the soil organic carbon, while urease impacts the metabolism of soil nitrogen through urea hydrolyzation (Cantarella et al., 2018). In this study, the intercropping soil systems (T1, T2, and T3) presented the highest UE and SC activities compared to the CK (Table 1). Likewise, Zhou et al. (2011) also reported elevation in the soil urease activity in the cucumber–garlic/onion intercropping system compared to the monocropping system. Peroxidase activity is considered a crucial predictor of the dynamics of soil organic matter (Tian and Shi, 2014).

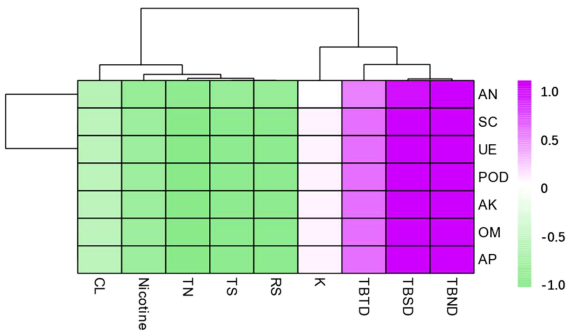

FIGURE 8
Correlation analysis between dominant microbial communities in the rhizosphere soil and total biomass, routine chemical composition under different intercropping treatments. TBTD, TBSD, TBND, TS, RS, and TN represent respectively total biomass of 30 days, total biomass of 60 days, total biomass of 90 days, total sugar, reducing sugar, and total nitrogen.

4.2 Effects of intercropping on the soil structure of microbial communities

The intercropping systems led to alterations in the soil physio-biochemical parameters and enzymatic activities, prompting the enrichment of a particular subset of functional bacteria and fungi, which was manifested as elevated diversities of both microbial types in the intercropped soil compared to the tea monoculture (Zhang et al., 2019; Bai et al., 2022; Jing et al., 2022). In agreement with this, an increase in the abundance and diversity of microbial communities in the rhizospheric soil of flue-tobacco plants was also observed under the three intercropping treatments (Figures 1A, B). This may be due to the fact that the plant root distribution in the top layer of the soil was expanded by intercropping. Thus, the permeability of the soil increased and the circulation of nutrient elements became more efficient, which provided a better microenvironment for the growth and propagation of microorganisms.

Intercropping may also influence soil microbiota composition differences (Bainard et al., 2012a; Floc'h et al., 2020) In this study, the PCoA of soil bacterial and fungal communities revealed a separation between the four treatments, indicating that the microbiota composition differed between the monoculture and intercropped plants (Figures 1C, D). The dominant microbial community in the rhizospheric soil of tobacco plants under four treatments was the same (Figures 4A, 5A), which is in agreement with previous studies (Zhang et al., 2017; De Vries et al., 2020), but the dominant community composition and their ratio were different (Figures 2, 3, 4B, 5B), which roughly corresponded to previous studies investigating agricultural soils (Li et al., 2011; Bai et al., 2020). Previous reports indicated that many members of Proteobacteria and Bacteroidetes of the soil bacteria community were closely associated with the carbon (C) and nitrogen (N) cycles (Leff et al., 2015; Pardon et al., 2017), while Ascomycota of the soil fungal community can rapidly metabolize organic substrates of rhizodeposition in rhizosphere soil (Bastida et al., 2013). As a

result, the intercropping systems might increase soil nutrient accumulation and nutrient utilization efficiency by promoting microbial growth that is closely associated with N fixation or other C–N processes. In this study, the abundance of Proteobacteria of bacteria and Ascomycota of fungi in the intercropping systems was significantly higher than the monocropping ones (Figures 4, 5), indicating the improved soil nutrient conditions after intercropping.

4.3 Effects of intercropping on tobacco growth and quality

Positive interactions occur in complex symbiotic systems that enhance the growth of crops, and these interactions are beneficial for improving soil fertility and yield (Hauggaard et al., 2001; Qian et al., 2018). In this study, intercropping can substantially increase the biomass (Figure 6) and improve the quality of routine chemical composition (Table 2) of tobacco plants. The growth and quality improvement results of the tobacco plants are consistent with previous research on *Aconitum carmichaeli*–rice intercropping systems (Ren et al., 2018). These results revealed that belowground interaction in intercropping can induce changes in soil microbial community structure, such as the increase in Acidobacteria abundance of bacteria can better degrade plant residue polymers and enhance photosynthesis, thereby increasing soil nutrients and plant biomass; the increase of plant residue polymers also promoted the increase of Ascomycota abundance of fungi, and the fungi can rapidly metabolize organic substrates of rhizodeposition in rhizosphere soil (Bastida et al., 2013). Therefore, we concluded that the increased microbial abundance of the tobacco intercropping system could accelerate the soil nutrients cycle, which in turn may have been beneficial to maintaining high soil fertility, growth, and quality of plants.

4.4 Soil–microbe–plant interaction

The direct and positive relationships between microbial diversity and soil nutrients in this study (Figure 1) coincide with the documented finding that soils with high microbial community diversity typically have increased nutrient availability (Zhang et al., 2021). This demonstrated that a diverse microbial community provides more nutrients for plants to absorb and less competition from microorganisms. Increased microbial diversity may promote the accumulation of available N and OM in the soil, all of which could increase overall plant productivity (Banerjee et al., 2018; Delgado-Baquerizo et al., 2020). Moreover, three intercropping treatments increased plant biomass (Figure 6) and improved the chemical composition of tobacco leaves (Table 2), which strongly suggests the potential role of intercropping on plant performance. Higher tobacco biomass and soil fertility of intercropping may depend on the regulating ability of belowground interactions since soils with high diversity also have higher plant productivity (Lan et al., 2023) and decomposition ability in organic matters (Liu et al., 2020b). In summary, intercropping could increase the abundance of soil microbes, which can promote the release of soil enzymes to catalyze various biochemical reactions such as mineralization of organic matter, synthesis of humus substances, and release of growth active substances, thus improving the overall growing environment and ultimately improving the biomass and quality of the flue-cured tobacco.

5 Conclusion

Our study suggested that intercropping flue-cured tobacco with other plants could increase the contents of soil AN, AP, AK, and OM and greatly improve soil nutrient status, thereby facilitating the improvement of the growth and quality of the flue-cured tobacco plants. Meanwhile, intercropping also altered the microbial community structure in the soil rhizosphere, while the microbial structure was closely related to the soil characteristics. Overall, intercropping may directly or indirectly increase plant productivity by regulating soil fertility and microbial dynamics in the rhizosphere of flue-cured tobacco. Therefore, soil–microbe–plant interactions should be promoted in arable systems to improve sustainable crop productivity.

Data availability statement

The data presented in the study are deposited in the BioSample database repository, accession number SAMN35711959, SAMN35711960, SAMN35711961, SAMN35711962.

Author contributions

MZ and CS performed the statistical analysis, and the preliminary manuscript was composed by JZ. BD and YH contributed to the conception and design of the study. MZ and CS are the co-authors, and JZ and YH are the co-corresponding authors. All authors contributed to the article and approved the submitted version.

Funding

This study was supported by the Guizhou Province Tobacco Company Bijie Company Project (2022520500240196).

Conflict of interest

The authors declare that the research was conducted in the absence of any commercial or financial relationships that could be construed as a potential conflict of interest.

Publisher's note

References

Bai, Y. C., Chang, Y. Y., Hussain, M., Lu, B., Zhang, J. P., Song, X. B., et al. (2020). Soil chemical and microbiological properties are changed by long-term chemical fertilizers that limit ecosystem functioning. *Microorganisms* 8, 694. doi: 10.3390/microorganisms8050694

Bai, Y. C., Li, B. X., Xu, C. Y., Raza, M., Wang, Q., Wang, Q. Z., et al. (2022). Intercropping walnut and tea: Effects on soil nutrients, enzyme activity, and microbial communities. *Front. Microbiol.* 13, 576–589. doi: 10.3389/fmicb.2022.852342

Bainard, L. D., Koch, A. M., Gordon, A. M., and Klironomos, J. N. (2012a). Growth response of crops to soil microbial communities from conventional monocropping and tree-based intercropping systems. *Plant Soil* 363, 345–356. doi: 10.1007/s11104-012-1321-5

Banerjee, S., Schlaeppi, K., and van der Heijden, M. G. A. (2018). Keystone taxa as drivers of microbiome structure and functioning. *Nat. Rev. Microbiol.* 16 (9), 567–576. doi: 10.1038/s41579-018-0024-1

Bastida, F., Hernández, T., Albaladejo, J., and García, C. (2013). Phylogenetic and functional changes in the microbial community of long–term restored soils under semiarid climate. *Soil Biol. Biochem.* 65, 12–21. doi: 10.1016/j.soilbio.2013.04.022

Cantarella, H., Otto, R., and Soares, J. R. (2018). Agronomic efficiency of NBPT as a urease inhibitor: A review. *J. Adv. Res.* 13, 19–27. doi: 10.1016/j.jare.2018.05.008

Chen, J., Arafat, Y., Wu, L. K., Xiao, Z. G., Li, Q. S., Khan, M. A., et al. (2018). Shifts in soil microbial community, soil enzymes and crop yield under peanut/maize intercropping with reduced nitrogen levels. *Appl. Soil Ecol.* 124, 327–334. doi: 10.1016/j.apsoil.2017.11.010

Chen, Y., Bonkowski, M., Shen, Y., Griffiths, B. S., Jiang, Y. J., Wang, X. Y., et al. (2020). Root ethylene mediates rhizosphere microbial community reconstruction when chemically detecting cyanide produced by neighbouring plants. *Microbiome* 8, 4. doi: 10.1186/s40168-019-0775-6

Chen, J. F., Sun, H., Xia, Y., Cai, K. X., Liu, H. Y., Zhao, S. H., et al. (2016). Changes in soil enzyme activity and nutrient content in tobacco fields under different continuous cropping years. *Henan Agric. Sci.* 45 (10), 60–64. doi: 10.15933/j.cnki.1004-3268.2016.10.014

Dai, J., Qiu, W., Wang, N., Wang, T., Nakanishi, H., and Zuo, Y. (2019). From Leguminosae/Gramineae intercropping systems to see benefits of intercropping on iron nutrition. *Front. Plant Sci.* 10. doi: 10.3389/fpls.2019.00605

Delgado-Baquerizo, M., Reich, P. B., Trivedi, C., Eldridge, D. J., Abades, S., Alfaro, F. D., et al. (2020). Multiple elements of soil biodiversity drive ecosystem functions across biomes. *Nat. Ecol. Evol.* 4 (2), 210–220. doi: 10.1038/s41559-019-1084-y

De Vries, F. T., Griffiths, R. I., Knight, C. G., Nicolitch, O., and Williams, A. (2020). Harnessing rhizosphere microbiomes for drought-resilient crop production. *Science* 368 (6488), 270–274.doi:10.1126/science.aaz5192. doi: 10.1126/science.aaz5192

Dowling, A., Sadras, O., Roberts, P., Doolette, A., Zhou, Y., and Denton, M. D. (2021). Legume-oilseed intercropping in mechanised broadacre agriculture – a review. *Field Crop Res.* 260, 107980. doi: 10.1016/j.fcr.2020.107980

Duchene, O., Vian, J. F., and Celette, F. (2017). Intercropping with legume for agroecological cropping systems: complementarity and facilitation processes and the importance of soil microorganisms. *A review. Agric. Ecosyst. Environ.* 240, 148–161. doi: 10.1016/j.agee.2017.02.019

Floc'h, J. B., Hamel, C., Harker, K., and Arnaud, M. (2020). Fungal communities of the canola rhizosphere: keystone species and substantial between-year variation of the rhizosphere microbiome. *Microbial Ecol.* 80 (4), 762–777. doi: 10.1007/s00248-019-01475-8

Fu, Z. Y., Zhang, X. Y., Zhang, X. F., Zhou, H. J., Qin, Y. H., Ma, J., et al. (2018). Effects of continuous cropping of tobacco on soil carbon pool and post-curing tobacco leaf quality. *J. Northwest A&F Univ. (Natural Sci. Edition)* 46 (08), 16–22. doi: 10.13207/j.cnki.jnwafu.2018.08.003

Gong, X., Liu, C., Li, J., Luo, Y., Yang, Q., Zhang, W., et al. (2019). Responses of rhizosphere soil properties, enzyme activities, and microbial diversity to intercropping patterns on the Loess Plateau of China. *Soil Tillage Res.* 195, 1022–1033. doi: 10.1016/j.still.2019.104355

Gong, Z. X., Ma, X. H., Ren, Z. G., Zhu, J. F., Huang, Y. J., Wang, M. M., et al. (2018). Analysis of bacterial community in rhizosphere soil of continuously cropped tobacco using 16S rDNA-PCR-DGGE. *China Agric. Sci. Technol. Tribune* 20 (2), 39–47. doi: 10.13304/j.nykjdb.2017.0231

Gu, Y., Wang, P., and Kong, C. H. (2009). Urease, invertase, dehydrogenase, and polyphenoloxidase activities in paddy soil influenced by allelopathic rice variety. *Eur. J. Soil Biol.* 45 (5), 436–441. doi: 10.1016/j.ejsobi.2009.06.003

Hauggaard, N. H., Ambus, P., and Jensen, E. S. (2001). Interspecific competition, N use and interference with weeds in pea–barley intercropping. *Field Crops Res.* 70, 101–109. doi: 10.1016/S0378-4290(01)00126-5

Hussain, S., Shafiq, I., Skalicky, M., Brestic, M., Rastogi, A., Mumtaz, M., et al. (2021). Titanium application increases phosphorus uptake through changes in Auxin content and later root formation in soybean. *Front. Plant Sci.* 12. doi: 10.3389/fpls.2021.743618

Jia, L. Q. (2016). Effects of soil leachate from leguminous plants on soil microbial community and enzyme activity in continuous cropping of potatoes. [Master's thesis (Gansu Agricultural University).

Jing, Y. Z., Guo, X. H., Wang, X. L., Niu, H. W., Han, D., and Xu, Z. C. (2022). Effects of ginger intercropping on yield and quality of flue-cured tobacco, soil bacterial population, and physicochemical properties. *Shandong Agric. Sci.* 54 (1), 86–94. doi: 10.14083/j.issn.1001-4942.2022.01.014

Lan, Y., Wang, S., Zhang, H., He, Y., Jiang, C., and Ye, S. (2023). Intercropping and nitrogen enhance eucalyptus productivity through the positive interaction between soil fertility factors and bacterial communities along with the maintenance of soil enzyme activities. *Land Degrad. Dev.* 4616, 1–15. doi: 10.1002/ldr.4616

Lauber, C. L., Strickland, M. S., Bradford, M. A., and Fierer, N. (2008). The influence of soil properties on the structure of bacterial and fungal communities across land-use types. *Soil Biol. Biochem.* 40 (9), 2407–2415. doi: 10.1016/j.soilbio.2008.05.021

Leff, J. W., Jones, S. E., Prober, S. M., Barberan, A., Borer, E. T., Firn, J. L., et al. (2015). Consistent responses of soil microbial communities to elevated nutrient inputs in grasslands across the globe. *Proc. Natl. Acad. Sci. U.S.A.* 112, 10967–10972. doi: 10.1073/pnas.1508382112

Li, Y., Lee, C. G., Watanabe, T., Murase, J., Asakawa, S., and Kimura, M. (2011). Identification of microbial communities that assimilate substrate from root cap cells in an aerobic soil using a DNA-SIP approach. *Soil Biol. Biochem.* 43, 1928–1935. doi: 10.1016/j.soilbio.2011.05.016

Li, Z. J., Zhu, W. Q., Huang, K., Ji, X. W., Wang, C., Zhao, T., et al. (2022). Effects of continuous cropping on agronomic traits, root morphology, and soil nutrients in tobacco. *J. Jiangsu Agric. Sci.* 50 (02), 67–72. doi: 10.15889/j.issn.1002-1302.2022.02.011

Liu, Z., Guo, Q., Feng, Z., Liu, Z., Li, H., Sun, Y., et al. (2020b). Long-term organic fertilization improves the productivity of kiwifruit (*Actinidia chinensis* Planch.) through increasing rhizosphere microbial diversity and network complexity. *Appl. Soil Ecol.* 147, 103426. doi: 10.1016/j.apsoil.2019.103426

Ma, W. F., Deng, X. P., Du, X. R., Dai, F.X., Li, J.Y., Zhao, Z.X., et al. (2021). Effects of continuous cropping years on soil chemical properties and tobacco leaf yield and quality. *J. Yunnan Agric. Univ. (Natural Science)* 36 (6), 993–999.

Martin-Guay, M.-O., Paquette, A., Dupras, J., and Rivest, D. (2018). The new green revolution: sustainable intensification of agriculture by intercropping. *Sci. Total Environ.* 615, 767–772. doi: 10.1016/j.scitotenv.2017.10.024

Nannipieri, P., Giagnoni, L., Renella, G., Puglisi, E., Ceccanti, B., Masciandaro, G., et al. (2012). Soil enzymology: classical and molecular approaches. *Biol. Fert. Soils* 48, 743–762. doi: 10.1007/s00374-012-0723-0

Pardon, P., Reubens, B., Reheul, D., Mertens, J., De Frenne, P., Coussement, T., et al. (2017). Trees increase soil organic carbon and nutrient availability in temperate agroforestry systems. *Agr. Ecosyst. Environ.* 247, 98–111. doi: 10.1016/j.agee.2017.06.018

Peng, X., Yan, X., Zhou, H., Zhang, Y. Z., and Sun, H. (2015). Assessing the contributions of sesquioxides and soil organic matter to aggregation in an Ultisol under long-term fertilization. *Soil Till. Res.* 146, 89–98. doi: 10.1016/j.still.2014.04.003

Qian, X., Zang, H., Xu, H., Hu, Y., Ren, C., Guo, L., et al. (2018). Relay strip intercropping of oat with maize, sunflower and mung bean in semi–arid regions of Northeast China: yield advantages and economic benefits. *Field Crops Res.* 223, 33–40. doi: 10.1016/j.fcr.2018.04.004

Ren, P., Huang, J., Chen, X., Yu, M., and Hou, D. (2018). Effects of relay intercropping of Chinese herbal medicine Aconitum carmichaelii debeaux and rice on soil properties and aconite yield. *J. Sichuan Agric. Uni.* 36 (3), 286–291. doi: 10.16036/j.issn.1000-2650.2018.03.002

Tang, X. M., Meng, X. Z., Jiang, J., Huang, Z.P., Wu, H.N., Liu, J., et al. (2020). Effects of intercropping sugarcane with peanuts on soil microecology in different soil layers. *Chin. J. Oil Crop Sci.* 42 (5), 713–722. doi: 10.19802/j.issn.1007-9084.2019318

Tian, L., and Shi, W. (2014). Soil peroxidase regulates organic matter decomposition through improving the accessibility of reducing sugars and amino acids. *Biol. Fertility Soils* 50 (5), 785–794. doi: 10.1007/s00374-014-0903-1

Veres, Z., Kotroczó, S., Fekete, I., Tóth, J. A., Lajtha, K., and Townsend, K. (2015). Soil extracellular enzyme activities are sensitive indicators of detrital inputs and carbon availability. *Appl. Soil Ecol.* 92, 18–23. doi: 10.1016/j.apsoil.2015. 03.006

Wang, M. M. (2016). *Study on the obstacles of continuous cropping of tobacco in the Luohe tobacco-growing area. [Dissertation]* (Zhengzhou: Henan Agricultural University). doi: 10.27117/d.cnki.ghenu.2016.000120

Yu, Z., Liu, J., Li, Y., Jin, J., Liu, X., and Wang, G. (2018). Impact of land use, fertilization and seasonal variation on the abundance and diversity of nirS-type denitrifying bacterial communities in a mollisol in northeast China. *Eur. J. Soil Biol.* 85, 4–11. doi: 10.1016/j.ejsobi.2017.12.001

Zhang, D., Li, D., Li, J. Y., Zeng, S. J., Xu, F. D., Ma, W. H., et al. (2021). Effects of planting modes on soil enzyme activity and photosynthetic characteristics of flue-cured tobacco. *Zhejiang Agric. Sci.* 62 (2), 50–52. doi: 10.16178/j.issn.0528-9017.20210203

Zhang, D. Y., Wang, J., Yang, S. P., Zhang, X., Liu, J., Zhao, J., et al. (2017). Effects of Codonopsis pilosula intercropping with tobacco on soil bacterial community structure. *Acta Prataculturae Sin.* 26 (6), 120–130.

Zhang, M., Wang, N., Zhang, J., Hu, Y., Cai, D., Guo, J., et al. (2019). Soil physicochemical properties and the rhizosphere soil fungal community in a mulberry (Morus alba L.)/Alfalfa (Medicago sativa l.) intercropping system. *Forests* 10 (2), 167. doi: 10.3390/f10020167

Zhao, J., Xie, H. J., and Zhang, J. (2020). Analysis of microbial diversity and physicochemical properties in the rhizosphere microenvironment of salt-alkaline soil in the Yellow River Delta. *Environ. Sci.* 41 (3), 1449–1455. doi: 10.13227/j.hjkx.201908044

Zhao, F., Zhao, M. Z., Wang, Y., Guan, L., and Pang, F. H.. (2019). Study on the structure and diversity of strawberry rhizosphere microbial community based on high-throughput sequencing. *Soils* 51 (1), 51–60. doi: 10.13758/j.cnki.tr.2019.01.008

Zhou, G., Yin, X., Li, Y., Zhao, Z., Xu, L., and Ding, J. (2015). Optimal planting timing for corn relay intercropped with flue-cured tobacco. *Crop Sci.* 55 (6), 2852–2862. doi: 10.2135/cropsci2014.05.0396

Zhou, X., Yu, G., and Wu, F. (2011). Effects of intercropping cucumber with onion or garlic on soil enzyme activities, microbial communities and cucumber yield. *Eur. J. Soil Biol.* 47 (5), 279–287. doi: 10.1016/j.ejsobi.2011.07.001

Frontiers in
Plant Science

Cultivates the science of plant biology and its applications

The most cited plant science journal, which advances our understanding of plant biology for sustainable food security, functional ecosystems and human health.

Discover the latest Research Topics

See more →

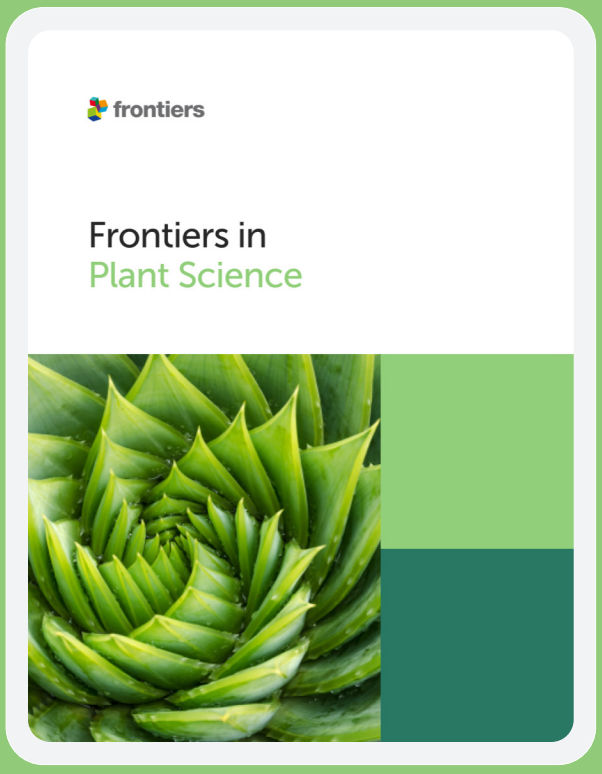

Frontiers

Avenue du Tribunal-Fédéral 34
1005 Lausanne, Switzerland
frontiersin.org

Contact us

+41 (0)21 510 17 00
frontiersin.org/about/contact